The interaction of the immune system with skeletal muscle during respiratory viral infection of the elderly

Johanna Sophie Sagawe

A thesis submitted to Imperial College London for the degree of Doctor of Philosophy

Respiratory Infections
National Heart and Lung Institute
Imperial College London
St Mary's Hospital Campus
Norfolk Place W2 1NY

2020

Abstract

The population of the world is ageing. Respiratory syncytial virus (RSV) is emerging as a leading cause of severe respiratory tract infection in the elderly. Loss of muscle mass occurs naturally with age, but can be exacerbated by inflammation, inactivity, or chronic disease, leading to increased risk of morbidity and mortality. If and how RSV infection promotes muscle wasting in the elderly is unknown. This study has developed an aged mouse model to investigate muscle wasting after RSV infection. 12-week-old and 80-week-old female C57BL/6 mice were infected with the same dose of RSV A2. Compared to young mice, elderly mice displayed enhanced RSV disease, including increased weight loss, viral load, and cellular airway infiltration. Elderly, but not young, mice displayed signs of muscle wasting following RSV infection, including decreased tibialis anterior muscle weight, increased expression of muscle atrophy-promoting enzymes, decreased muscle fibre size, and a failure to upregulate muscle protein synthesis. Elderly mice also displayed an impaired antibody response as evidenced by decreased anti-RSV IgG titres, but this was not due to reduced numbers of RSV-specific Tfh cells or germinal centre B cells. Blocking GDF-15, a TGF-β superfamily cytokine associated with muscle wasting and loss of appetite, which was produced in the elderly lung following RSV infection, unexpectedly led to signs of enhanced muscle wasting in elderly mice infected with RSV, suggesting a tissue-protective effect of GDF-15. Blocking IL-6R did not have consistent effects in elderly mice infected with RSV, potentially due to counteracting effects on systemic inflammation, the antibody response, and skeletal muscle. These results demonstrate that RSV infection promotes muscle wasting in an age-dependent manner, potentially regulated by GDF-15. This model is a useful tool for mechanistic studies and could be used in the future for the development of vaccines and treatments for RSV for the elderly.

Declaration of originality

I hereby declare that the work presented in this thesis is my own work, carried out at Imperial College London between 2015 and 2020, unless stated otherwise. The INFLAMMAGE study is conducted by Dr Chris Chiu of Imperial College London and INFLAMMAGE samples, demographic data, symptom scores and viral loads were provided by Dr Stephanie Ascough.

Copyright declaration

Acknowledgements

I would like to begin by thanking my supervisors, Fiona and Peter. It is fitting that PhD supervisors are called “Doktorvater” (“doctorate father”) and “Doktormutter” (“doctorate mother”) in German. You have been the Ying and Yang of my past four years, spurring me on or reining me in whenever I needed it. Peter, I will never grow tired of your stories from the department in the 80s and your big-picture thinking. Fiona, your guidance and support, especially in my darkest hours, has been invaluable to me. Thank you. Keep in touch. I also want to thank Paul Kemp. Although not technically my supervisor, your know-how in all things muscle was highly appreciated.

I am thankful to the many Masters and BSc students who have shared the bench with me: Lucy, Tasneem, Liv, Celia, and Richard; and other visitors to the lab: Chris Mason, Mike Vanden Oever, and Henning Jacobsen. I want to thank all members, past and present, of the Respiratory Infections Section, particularly Freja, David, Kate, and Inne. I’ll miss our office antics. And thank you to Myriam, who took me under her wing during my first rotation project when I really needed it.

No words can truly convey my thankfulness to my parents, whose hard work has given me the incredible privilege to pursue an academic career. Thank you to my mother and grandfather, who didn't live to see me complete this degree. I know you are proud of me no matter what. Thank you to Ulla, who has always supported me. I want to thank all my friends, who kept my spirits high, particularly Liam, who knows just when to say the magic words: “Everything will be alright in the end, and if it’s not alright, it’s not the end.”

Lastly, I would like to express my gratitude to the 334 mice who unknowingly gave their lives for this work. I strive to ensure their sacrifice was not in vain.

Table of contents

Table of figures

Chapter 1. Introduction

Chapter 2. Materials and Methods

Chapter 3. A mouse model of muscle wasting in the elderly after RSV infection

Chapter 4. The role of GDF-15 in the elderly during respiratory infection

Chapter 5. The role of IL-6 in the elderly during respiratory infection

Chapter 6. Discussion

List of tables

Chapter 1. Introduction

Chapter 2. Materials and Methods

Chapter 4. The role of GDF-15 in the elderly during respiratory infection

1.

Introduction

Chapter 1. Introduction

1.1. An ageing world

Advances in sanitation, nutrition, and medicine have led to vast increases in human life expectancy since the mid-1800s. Combined with slowing birth rates, this means the population of the UK – and the world – is ageing. By 2050, the number of people over the age of 60 on the planet is expected to more than double to over 2 billion (United Nations, 2017). An ageing population presents an opportunity, as older people can make significant contributions to society as experienced workers, caregivers, and volunteers. These benefits are highly dependent on the maintenance of good health in the ageing population. However, increases in life expectancy have not been matched by increases in healthy life expectancy, or *healthspan*, the number of years an individual can expect to live in good health (Kennedy *et al.*, 2014). Between 2009 and 2017, life expectancy in the UK at birth increased by seven months in men and four months in women (Office for National Statistics, 2018). *Healthy* life expectancy on the other hand increased by only five months in men, and even decreased by three months in women (Figure 1-1). On a population level, the incidence of almost all health problems increases with age, including susceptibility to infections, cardiovascular disease, cancers, and neurodegenerative diseases like dementia. A population that lives longer but spends more time in poor health presents a significant burden to economic, health and social care systems. To tackle these issues, there is an urgent need for scientific research into ageing. Firstly, there is a need for research into age-related diseases, such as cancer, cardiovascular disease, and neurodegenerative, since incidence will increase in step with the growth of the ageing population. Secondly, there is a need for research on the fundamental mechanisms underlying ageing itself, which are still incompletely understood.Since disease does not always accompany ageing, it is vital to understand which aspects of ageing cause it. Studying ageing inherently requires the passage of time. Due to our long lifespans and ethical considerations, human studies are expensive and may only yield results after

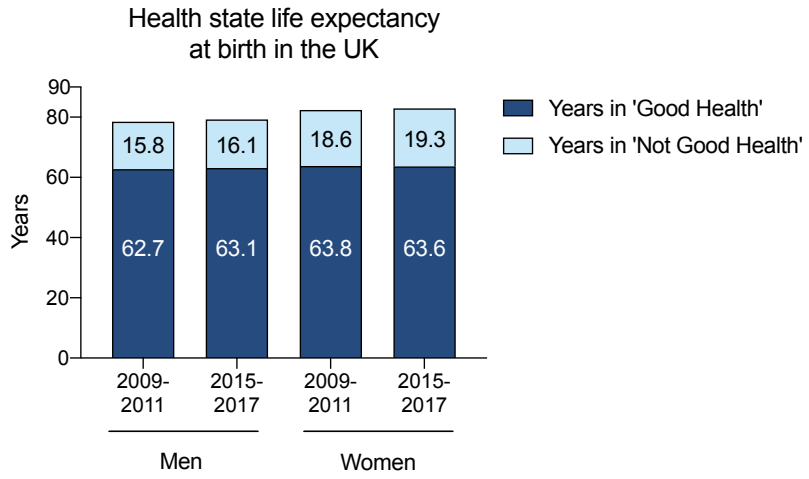

Figure 1-1 Lifespan and Healthspan at birth in the UK

Total life expectancy of men and women born in the UK in two different time frames, 2009-2011 and 2015-2017. Respondents to the Office for National Statistics' Annual Population Survey were asked about their general health, here divided into "Good Health" (Options "Very Good" or "Good") and "Not Good Health" (Options "Fair", "Bad", or "Very Bad"). Adapted from Office of National Statistics, Statistical Bulletin: Health state life expectancies, UK: 2015 to 2017 (2018), licensed under the Open Government Licence v3.0. (see Appendix).

many years. Hence, there is an urgent requirement to develop appropriate animal models, utilising the fact that the ageing process is evolutionarily highly conserved.

1.2. The biology of ageing

Ageing is difficult to define succinctly, but may be described as a progressive decline in physiological function of an organism, leading to an increase in mortality rate (Rose, 1991; Bronikowski & Flatt, 2010; Flatt, 2012). The decline in physiological function is attributable to the accumulation of damage to DNA, cells, tissues and organs, influenced by complex genetic and environmental factors. López-Otín and colleagues describe nine classical hallmarks of ageing: genomic instability, attrition of telomeres, epigenetic alterations, loss of proteostasis, deregulated nutrient sensing, mitochondrial dysfunction, cellular senescence, stem cell exhaustion, and altered intercellular communication (López-Otín *et al.*, 2013). The nine hallmarks of ageing are summarised briefly below.

1.2.1. Genome stability

Genomic stability is crucial for a cell to reproduce for maintenance or growth, and to be able to fulfill its tissue-specific functions via accurate transcription. Genetic damage can be caused by external factors, such as UV radiation, X-rays, or certain chemicals, or internally by reactive oxygen species, or replication errors. Numerous DNA repair mechanisms exist to repair this damage, such as homologous recombination between chromosomes, non-homologous end-joining, or mismatch repair (Lord & Ashworth, 2012). With increased age, DNA damage repair mechanisms become less effective and DNA damage accumulates (Moskalev *et al.*, 2013). Some conditions with symptoms of accelerated ageing, such as Werner syndrome and Cockayne syndrome, are caused by mutations in proteins belonging to DNA repair pathways (Burtner & Kennedy, 2010). However, these conditions do not recapitulate all aspects of ageing, suggesting that other factors also contribute.

1.2.2. Telomere attrition

Telomeres are sections of repetitive DNA capping the ends of chromosomes. Since replicative DNA polymerases are incapable of replicating the terminal ends of DNA strands, telomeres serve to protect protein-coding DNA from being eroded by repeated DNA replication (Blackburn, Greider & Szostak, 2006). As a consequence, progressive telomere shortening is observed in cells from both humans and mice with advancing age (Blasco, 2007). Telomere loss is an important cause of cell cycle arrest (See Cellular Senescence). Telomeres can be replicated and extended by a special DNA polymerase, telomerase, but its expression in adulthood is highly limited to male germ cells, some epidermal cells, haematopoietic stem cells, and activated T and B lymphocytes. Multiple diseases involving impaired tissue regeneration, such as pulmonary fibrosis, dyskeratosis congenita, and aplastic anaemia, have been associated with telomerase deficiency (Armanios & Blackburn, 2012). Genetically modified mice with shortened telomeres display reduced lifespans, whereas mice with artificially lengthened telomeres display extended lifespans (Rudolph *et al.,* 1999; Tomás-Loba *et al.,* 2008; Armanios *et al.*, 2009).

Moreover, the premature ageing observed in telomerase-deficient mice is reversible with reactivation of telomerase expression (Jaskelioff *et al.*, 2011). Even in naturally aged wild-type mice, increasing telomerase activity extends lifespan and alleviates symptoms of ageing such as insulin sensitivity and neuromuscular coordination, with no increased risk of cancer (Bernardes de Jesus *et al.*, 2012). These studies suggest that in the future, telomere attrition may be targeted clinically to prevent or ameliorate age-associated pathology.

1.2.3. Epigenetic changes

The epigenome comprises various alterations to chromatin, such as DNA methylation, post-translational histone acetylation and methylation, changes in chromatin conformation, and the enzymes that generate and maintain such modifications. Certain patterns of histone modification are characteristic of age-associated epigenetic changes, such as an increase in histone H4K16 acetylation and H3K4 trimethylation, and a decrease in H3K27 trimethylation (Fraga & Esteller, 2007; Han & Brunet, 2012). DNA methylation of certain loci, particularly those encoding tumour suppressors and Polycomb targets, increases with age, which may promote neoplasia (Maegawa *et al.*, 2010). Epigenetic alterations may affect ageing in multiple ways. Firstly, they may affect genomic stability and DNA repair mechanisms. Secondly, they may determine transcription and thus regulate cellular function, metabolism and inflammation.

Loss of function in enzymes maintainting epigenetic marks has been associated with either extended lifespan or accelerated ageing in animal models. For example, inhibition of a histone demethylase in *Caenorhabditis elegans* nematodes extends life span via loss of H3K27 trimethylation on genes in the insulin/IGF-1 signalling pathway (Jin *et al.*, 2011). Pharmacological inhibition of histone deacetylase can improve age-associated memory impairment in mice, and inhibition of histone acetyltransferases ameliorates symptoms and extends the lifespan of mice genetically modified to age prematurely (Peleg *et al.*, 2010; Krishnan *et al.*, 2011).

The sirtuin family contains a number of protein de-acetylases and ADP ribosyltransferas-

es that have various epigenetic roles. In mammals, overexpression of SIRT1 maintains health during ageing by improving genomic stability and metabolic efficiency, but does not increase lifespan (Herranz *et al.*, 2010; Nogueiras *et al.,* 2012). SIRT6 is a chromatin-associated protein important for base excision repair and the repair of double-stranded DNA breaks, with additional roles in Nuclear transcription factor kappa B (NF-κB signalling) and histone H3K9 deacetylation (Kawahara *et al.,* 2009; Kanfi *et al.*, 2010; Zhong *et al.*, 2010). SIRT6-deficient mice display symptoms of accelerated ageing (Mostoslavsky *et al.,* 2006), whereas SIRT6 overexpression prolongs the lifespan of male, but not female, mice (Kanfi *et al.,* 2012).

Levels of key chromatin remodelling proteins, such as heterochromatin protein 1α (HP1α), Polycomb group proteins, and NuRD complex, decrease with advancing age (Pegoraro *et al.*, 2009; Pollina & Brunet, 2011). This decline causes wide-reaching changes in chromatin architecture, such as loss and redistribution of heterochromatin, that is observed in both naturally and artificially aged cells (Oberdoerffer & Sinclair, 2007). Loss-of-function mutation of HP1α shortens the lifespan of *Drosophila* flies, whereas overexpression of HP1α extends lifespan and delays muscle wasting of flies, exemplifying the importance of chromatin changes in ageing (Larson *et al.*, 2012).

As a consequence of the above-mentioned epigenetic alterations, the transcriptome undergoes changes with advancing age. Cell-to-cell variation in gene expression is vastly increased with age (Bahar *et al.*, 2006), and mRNA splicing and maturation is dysregulated (Nicholas *et al.*, 2010; Harries *et al.*, 2011). Age-associated changes in the transcriptome typically include an upregulation of genes in inflammation, immune response, and lysosomal pathways, and a downregulation of genes involved in mitochondrial metabolism, apoptosis, and the cell cycle (de Magalhães, Curado & Church, 2009).

1.2.4. Loss of proteostasis

Proteostasis is the maintenance of a pool of correctly folded, functional proteins in a cell. It involves the stabilisation of correctly folded, functional proteins, and the removal and degradation of irreparably misfolded proteins. The family of heat shock proteins (HSP)

are the principal mediators of protein refolding, in concert with various chaperone proteins (Hartl, Bracher & Hayer-Hartl, 2011). Irreparably misfolded proteins can be targeted for degradation via either the ubiquitin-proteasome, or recognised by chaperones and imported into lysosomes for autophagic breakdown (Mizushima *et al.*, 2008). Larger proteins or organelles also undergo macro-autophagy by being sequestered into autophagosomes which fuse with lysosomes.

Ageing is associated with disturbed proteostasis, with sometimes profound proteotoxic effects (Koga, Kaushik & Cuervo, 2011). The accumulation of unfolded or misfolded proteins is characteristic of certain age-associated diseases, for example Alzheimer's disease and Parkinson's disease (Powers *et al.*, 2009). The transcription factor heat shock factor 1 (HSF-1) is the master regulator of the heat shock response. The overexpression of HSF-1 in *C. elegans* extends lifespan whereas reducing HSF-1 activity shortens lifespan and accelerates tissue ageing (Hsu, Murphy & Kenyon, 2003). In human cell culture, HSF-1 is a key target for deacetylation by SIRT1, leading to increased levels of heat shock proteins such as Hsp70 that refold proteins (Westerheide *et al.*, 2009). Mice genetically deficient in a co-chaperone interacting with Hsp70 have shortened lifespans and exhibit accelerated age-associated pathology (Min *et al.*, 2008). Pharmocological activation of the heat shock protein Hsp72 slows the progression of muscular decline in a mouse model of severe muscular dystrophy (Gehrig *et al.*, 2012).

The activity of both the ubiquitin-proteasome and the autophagy-lysosome systems for degrading misfolded proteins decline with age (Rubinsztein, Mariño & Kroemer, 2011; Tomaru *et al.*, 2012). Mice genetically engineered to have an additional copy of the autophagy receptor LAMP2a maintain their autophagy levels and liver function into old age (Zhang & Cuervo, 2008). Compounds which promote autophagy, such as rapamycin and spermidine, have been robustly associated with increased lifespan in yeast, nematodes, and flies (Eisenberg *et al.,* 2009; Rubinsztein, Mariño & Kroemer, 2011). Rapamycin can also extend lifespan in mice and ameliorates age-associated pathology, but its effects in mammals are not exclusively mediated through the induction of autophagy (Harrison *et*

al., 2009; Selman *et al.*, 2009; Wilkinson *et al.*, 2012). Increasing expression of parts of the ubiquitin-proteasome complex extends lifespan in *C. elegans*, and yeast strains with genetically increased proteasome activity display extended lifespan and higher tolerance of proteotoxic stress. These findings underscore the importance of correct protein clearance for healthy ageing.

1.2.5. Deregulated nutrient sensing

The most important cellular nutrient, glucose, is sensed by cells via insulin signalling. The intracellular signalling pathway of insulin is also activated by insulin-like growth factor 1 (IGF-1), which mediates the effects of growth hormone (GH). Targets of insulin/IGF-1 signalling include the FOXO transcription factor family and mTOR, forming a system that is evolutionarily highly conserved (Barzilai *et al.*, 2012). Experimentally inhibiting parts of the insulin/IGF-1 pathway extends lifespan in *C. elegans* worms, *Drosophila* flies, and laboratory mice (Kenyon, 2010). In different inbred mouse strains, systemic IGF-1 levels correlate inversely with lifespan (Yuan *et al.*, 2009).

Insulin/IGF-1 signalling pathway is a key mediator of the lifespan-enhancing effects of dietary restriction. Dietary restriction reduces circulating IGF-1 levels, and increases lifespan or healthspan in a variety of animal models, including non-human primates (Colman *et al.*, 2009; Mattison *et al.*, 2012). Since reduced IGF-1 signalling extends lifespan, one may assume that ageing is accompanied by increased IGF-1 levels. Paradoxically, the opposite is the case – levels of both GH and IGF-1 decline with age, and are low in progeroid mouse models (Schumacher *et al.*, 2008). This contradiction can be explained thus: GH, insulin, and IGF-1 signalling promote cell growth, metabolism, and turnover. This is beneficial for an organism in the short term, to attain maximum evolutionary fitness and ensure reproduction. However, in the long term, growth occurs at the expense of repair, and leads to the accumulation of molecular and cellular damage. Downregulation of insulin/IGF-1 signalling pathways with age is a mechanism of damage control in an attempt to prolong lifespan (Garinis *et al.*, 2008). Organisms with constitutively lower insulin/IGF-1 signalling on the other hand are longer lived because they experience

lower levels of cell growth and metabolism throughout life, and thus accumulate less damage. Unfortunately, the downregulation of the insulin/IGF-1 signalling pathways with ageing as a damage control response may further exacerbate symptoms of ageing in a downward spiral. For example, as will be discussed in Section 1.5, low levels of IGF-1 in ageing may contribute to muscle wasting.

The mTOR system is a key target of insulin/IGF-1 signalling and is a master regulator of anabolism. Attenuation of mTOR activity extends lifespan in yeast, *C. elegans* worms, *Drosophila* flies in a similar manner to dietary restriction (Laplante & Sabatini, 2012). Inhibition of mTOR activity with the drug rapamycin increases lifespan in mice and reverses obesity in mice caused by age-related increases in mTOR activity in hypothalamic neurons (Yang *et al.*, 2012). Other nutrient sensors, such as AMPK and SIRT1, signal nutrient scarcity and inhibit cell growth programmes. AMPK notably inhibits parts of the mTOR complex and may mediate the lifespan extension effects of metformin in *C. elegans* and mice (Onken & Driscoll, 2010; Anisimov *et al.*, 2011; Alers *et al.*, 2012).

1.2.6. Mitochondrial dysfunction

Mitochondria are crucial to energy generation in the cell. With advancing age, mitochondria become less efficient and generate less ATP (Short *et al.*, 2005). Respiratory chain capacity declines with age, and the number of mitochondria and mitochondrial protein content decreases, particularly in the liver (Bratic & Larsson, 2013). Mitochondrial dysfunction may promote ageing through multiple pathways:

Mitochondrial genome stability is essential to healthy ageing. Transgenic mice with impaired mtDNA polymerase function accumulate mutations in mitochondrial DNA and display reduced lifespan and premature symptoms of ageing such as sarcopenia (Trifunovic *et al.*, 2004; Vermulst *et al.*, 2008; Hiona *et al.*, 2010). Telomerase reactivation can partially reverse the decline in mitochondrial numbers observed in aged mice (Bernardes de Jesus *et al.*, 2012).

Mitochondria are key controllers of cell death by permeabilising their membranes, re-

leasing proteins that trigger apoptosis (Green, Galluzzi & Kroemer, 2011). Mitochondrial protein release can also promote the activation of inflammasomes. Dysfunctional, aged mitochondria may be more prone to initiate apoptosis or inflammation (Kroemer, Galluzzi & Brenner, 2007).

Damaged mitochondria are degraded in a specialised form of macro-autophagy termed "mitophagy". The accumulation of damaged macromolecules and organelles such as mitochondria during ageing has been proposed to be due to declining autophagy and mitophagy (Yen & Klionsky, 2008). *Drosophila* flies and *C. elegans* nematodes deficient in autophagy pathway genes exhibit accelerated ageing and shortened lifespans (Melén-dez *et al.*, 2003; Juhász *et al.*, 2007). Mitophagy is partially regulated by the sirtuin SIRT1, which also promotes the biogenesis of new mitochondria (In *et al.*, 2008). SIRT3 is the primary mitochondrial deacetylase and improves mitochondrial function (Giralt & Villar-roya, 2012). The combined effects of reduced mitochondrial biogenesis and reduced clearance of damaged mitochondria may contribute to ageing (Yen & Klionsky, 2008).

Hormesis is the concept that mildly toxic experiences can have beneficial effects by pro-moting compensatory responses that improve fitness beyond starting conditions (Cala-brese *et al.*, 2011). The theory of mitohormesis proposes that low levels of mitochondrial dysfunction may be beneficial to ageing. In support of this theory, some treatments that extend lifespan in animal models, such as metformin, are mildly toxic to mitochondria (Onken & Driscoll, 2010; Anisimov *et al.*, 2011). Moreover, lowering mitochondrial ATP generation by either pharmacologically or genetically induced mitochondrial uncou-pling also increases lifespan and reduced age-related disease in mice (Gates *et al.*, 2007; Caldeira Da Silva *et al.*, 2008).

Mitochondria naturally produce reactive oxygen species (ROS) as a byproduct of respi-ration. ROS can damage mtDNA and inhibit the electron transport chain. This has led to the free radical theory of ageing, proposing that age-related mitochondrial dysfunction is driven by increased ROS production, and conversely, inhibiting ROS should be beneficial

to ageing (Harman, 1965). Paradoxically, the opposite appears to be the case. Increased ROS extends lifespan in *C. elegans* worms, and neither increased mitochondrial ROS nor increased antioxidant responses affect ageing in mice (Doonan *et al.*, 2008; Pérez *et al.*, 2009; Zhang *et al.*, 2009). By contrast, ageing is accelerated in mice genetically altered to have impaired mitochondrial function without concomitantly increased ROS (Trifunovic *et al.*, 2004; Vermulst *et al.*, 2008; Hiona *et al.*, 2010). These findings sugggest that similarly to other features of ageing, ROS are a response to age-related accumulation of damage. In moderation, ROS can thus be beneficial to ageing, but in excess they may lead to a vicious cycle of ROS production and exacerbate age-related damage.

1.2.7. Cellular senescence

In 1961, Leonard Hayflick and Paul Moorhead observed that serially passaged human fibroblasts stopped proliferating after a 50-70 passages (Hayflick & Moorhead, 1961). The cells had become “senescent”, irreversibly arresting their cell cycle and developing characteristic phenotypic changes. This intrinsic replicative limit was termed the “Hayflick limit”. In Hayflick’s fibroblasts, the trigger for senescence was telomere attrition, but other age-related triggers contribute to senescence (Bodnar *et al.*, 1998).

Senescent cells accumulate with age, but senescence does not affect all cell and tissue types equally. In aged mice, some tissues, such as skin and lung, contain high levels of senescent cells, whereas others, such as heart and kidney, do not (Wang *et al.*, 2009).

Because of their age-related accumulation, senescence has been associated with the detrimental effects of ageing. However, in health, senescence is an important cellular mechanism to prevent the proliferation of damaged cells which may become cancerous (López-Otín *et al.*, 2013). But effective tissue rejuvenation requires both clearance of the senescent cells by the immune system and replacement via progenitor cells. The accumulation of senescent cells with age may reflect an increase in the generation of senescent cells, or a decrease in their clearance and replacement.

Senescent cells don’t just arrest their cell cycle, they also develop a characteristic altered

phenotype, the "senescence-associated secretory phenotype" (SASP). Senescent cells tend to secrete high levels of pro-inflammatory cytokines and matrix metalloproteinases that can damage the surrounding tissue and drive ageing (Basisty *et al.*, 2020).

Telomeric attrition is one driver of senescence, as in the case of Hayflick's fibroblasts, but another key driver of senescence is excessive mitogenic signalling. As described above, senescence is an important mechanism to limit the proliferation of potentially oncogenic cells. Excessive mitogenic signalling leads to excessive induction of senescence in an attempt to prevent oncogenesis. $p16^{INK4a}$ and $p19^{ARF}$ are tumour suppressors both encoded by the *INK4a/ARF* locus on chromosome 9 in humans and chromosome 4 in mice. Expression of the *INK4/ARF* locus is progressively derepressed with age, and levels of $p16^{INK4a}$ and $p19^{ARF}$ consistently correlate with chronological age in almost all tissues in mice and humans (Krishnamurthy *et al.*, 2004; Collado, Blasco & Serrano, 2007). Polymorphisms in this locus are associated with a large number of age-related diseases, including cardiovascular diseases, cancer, diabetes, and neurodegenerative diseases (Jeck, Siebold & Sharpless, 2012). This suggests that the *INK4a/ARF* locus is a key controller of ageing and age-related disease. Supporting this hypothesis, the age-related phenotypes of several progeroid mouse models can be ameliorated by the elimination of $p16^{INK4a}$ or p53 signalling, another key tumour suppressor (Cao *et al.*, 2003; Varela *et al.*, 2005; Baker *et al.*, 2011; Jeon *et al.*, 2017). Moreover, lifespan of mice can be extended and age-related pathology delayed by the removal of $p16^{INK4a}$ -positive cells (Baker *et al.*, 2016). However, there is also evidence that constitutive low-level increases in $p16^{INK4a}$, $p19^{ARF}$ or p53 extend lifespan in mice, more than would be expected by their effect on tumour suppression (Matheu *et al.*, 2007, 2009). This discrepancy can be explained in the same way as has been discussed for other mechanisms of ageing: Balance is everything. Senescence initiated by the *INK4a/ARF* locus is a fundamentally beneficial compensatory response to prevent the proliferation of damaged cells. However, in excess, or when the replenishing capacity of stem cells cannot keep pace, senescence may exacerbate age-related damage and accelerate ageing.

1.2.8. Stem cell exhaustion

Stem cells are required for the maintenance of all cell populations except the longest-lived ones. Age-related decline has been observed in almost all adult stem cell compartments, including the brain, bone, and muscle (Molofsky *et al.*, 2006; Gruber *et al.*, 2006; Conboy & Rando, 2012). In the bone marrow, haematopoiesis wanes with advancing age, resulting in a higher risk of anaemias and cancers of myeloid origins, and weakened immune responses to infection (Shaw *et al.*, 2010). Haematopoietic stem cells (HSCs) undergo fewer cell divisions and accumulate DNA damage (Rossi *et al.*, 2007).

Stem cell ageing is itself caused by a combination of the various mechanisms of ageing already discussed, particular telomere attrition and progressive upregulation of the senescence-controlling *INK4a/ARF* locus (Flores, Cayuela & Blasco, 2005). For example, aged HSCs overexpress $p16^{INK4a}$, and HSCs from *INK4a*$^{-/-}$ mice display increased cell cycle activity and better engraftment in an HSC transplant model (Janzen *et al.*, 2006).

Age-related alterations in stem cell behaviour may manifest both as a reduction in stem cell division, leading to difficulties in maintaining tissues, but also as an inappropriate increase in proliferation, accelerating stem cell exhaustion in the long term and increasing the risk of malignancy . For example, mice deficient in the cell cycle inhibitor $p21^{CIP1/WAF}$ display premature exhaustion of HSCs and neural stem cells and even premature death due to haematopoietic failure (Cheng *et al.*, 2000; Kippin, Martens & Van Der Kooy, 2005).

The exhaustion of stem cells is partially extrinsically determined. Dietary restriction increases gut and muscle stem functions, and transplanting muscle stem cells from young mice to prematurely aged mice extends their lifespan and improves age-related pathology (Cerletti *et al.*, 2012; Yilmaz *et al.*, 2012; Lavasani *et al.*, 2012). Moreover, insufficiently understood systemic factors may also maintain stem cell function, as evidenced by experiments demonstrating that bone marrow or plasma from young mice can rejuvenate the stem cell niches of aged mice (Conboy *et al.*, 2005; Katsimpardi *et al.*, 2014; Kang *et al.*, 2020).

Rapamycin, the mTOR inhibitor, has already been discussed in its capacity to delay or ameliorate ageing by multiple pathways, including boosting proteostasis and regulating nutrient sensing. Rapamycin may also improve stem cell function in various tissues, including the skin, gut, and haematopoietic system (Castilho *et al.*, 2009; Chen *et al.*, 2009; Yilmaz *et al.*, 2012). The effectiveness of rapamycin in targeting ageing through multiple pathways emphasises the high level of connectedness between the different mechanisms of ageing.

1.2.9. Altered intercellular communication

Many types of intercellular communication are dysregulated with age, including hormonal, neuronal, and inflammatory signalling. The age-related dysfunction of the insulin/IGF-1 pathway as an example of neuro-hormonal signalling has alread been mentioned. Elderly people often display "inflammageing", a state of chronic, low-level inflammation in the absence of any pathogenic threat, which indicates systemic dysregulation of immunity and intercellular communication (Franceschi *et al.*, 2006). The origins of inflammageing may be diverse and include failure of the aged immune system to clear pathogens and damaged cells, leading to prolonged inflammatory signalling, secretion of pro-inflammatory cytokines by senescent cells as part of the SASP, and dysfunctional autophagy (Green, Galluzzi & Kroemer, 2011; Salminen, Kaarniranta & Kauppinen, 2012). Dysregulated inflammation has been implicated in a number of age-related diseases, including obesity, type 2 diabetes, and atherosclerosis (Tabas, 2010; Barzilai *et al.*, 2012).

The NF-κB pathway is a key regulator of inflammation. Increased activity of NF-κB is characteristic of ageing (de Magalhães, Curado & Church, 2009). Inhibition of NF-κB activity by genetic or pharmacological means can rejuvenate tissues and delay age-associated pathologies in naturally aged and progeroid mice (Adler *et al.*, 2007; Osorio *et al.*, 2012; Tilstra *et al.*, 2012). Sirtuins have been discussed in their capacity to maintain genomic stability and promote mitochondrial biogenesis and function. Sirtuins may also have an effect on ageing by regulating inflammation. SIRT1, SIRT2, and SIRT6 can downregulate inflammatory signalling by deacetylating components of the NF-κB pathway (Xie, Zhang

& Zhang, 2013). SIRT6-deficient mice display shortened lifespan and accelerated ageing due to increased NF-κB signalling, and SIRT1 activation can prevent premature cellular senescence in mouse lung (Kawahara *et al.*, 2009; Yao *et al.*, 2012).

The importance of intercellular communication in ageing is evidenced by multiple studies suggesting that ageing can be "contagious". Senescent cells can trigger neighbouring cells to become senescent too via direct cell-cell contacts and ROS signalling, the microenvironment is a key factor in driving age-related dysfunction of $CD4^+$ T cells, and ageing is accelerated in young mice given a blood transfusion from old mice (Tomás-Loba *et al.*, 2008; Lavasani *et al.*, 2012; Conboy & Rando, 2012). Conversely, targeting age-related pathology in one tissue can simultaneously delay ageing in other tissues (Tomás-Loba *et al.*, 2008; Lavasani *et al.*, 2012).

1.2.10. Nature versus nurture in ageing

Healthspan and lifespan are determined by a combination of genetic and non-genetic factors (Passarino, De Rango & Montesanto, 2016). Disentangling the specific contributions of both genetic and non-genetic factors to ageing is crucial to the development of therapeutic and prophylactic treatments targeting the ageing process.

Numerous transgenic animal models have demonstrated that certain genes dramatically influence healthspan and lifespan. These sorts of genetic manipulations are of course impossible in humans. Twin studies have suggested that approximately 25% of the variation in human lifespan can be accounted for by genetic factors (Herskind *et al.*, 1996; Skytthe *et al.*, 2003). Genome-wide association studies have failed to identify universal genetic factors accounting for exceptional longevity, but polymorphisms in some genes, particularly those promoting genomic stability, telomere integrity, and mitochondrial function, may contribute (Sebastiani *et al.*, 2012; Soerensen *et al.*, 2012; Beekman *et al.*, 2013; Debrabant *et al.*, 2014; Deelen *et al.*, 2014; Raule *et al.*, 2014).

Caloric (dietary) restriction is the most robust intervention for prolonged health- and lifespan in almost all animal models tested. The various mechanisms through which die-

tary restriction promotes longevity have been discussed above. Human populations that engage in caloric restriction for cultural or religious reasons, such as communities of Seventh-Day Adventists in California or the indigenous inhabitants of the Okinawa islands in Japan, display remarkable longevity and vitality late into life (Willcox *et al.*, 2007; Orlich *et al.*, 2013; Poulain, Herm & Pes, 2014). The diets consumed by these populations are also predominantly plant-based and there is some evidence that the high protein content of animal products may promote the ageing process (Simpson & Raubenheimer, 2009; Nakagawa *et al.*, 2012). A randomised controlled trial of 25% dietary restriction in non-obese humans yielded the result that caloric restriction decreased cardiometabolic risk factors, improved insulin sensitivity, decreased systemic inflammation, and decreased biomarkers of ageing (Ravussin *et al.*, 2015; Belsky *et al.*, 2018; Kraus *et al.*, 2019).

Exercise is another extrinsic factor that can delay features of ageing. Highly active middle-aged amateur cyclists display lower levels of systemic inflammation and immunosenescence compared to less active peers (Duggal *et al.*, 2018). Resistance exercise training can also ameliorate a number of age-related features, such as improving mitochondrial function, preventing loss of muscle strength, improving cognitive function, and lowering blood pressure (Melov *et al.*, 2007; Pedersen & Saltin, 2015; Lazarus & Harridge, 2018; de Guia *et al.*, 2019).

Taken together, there is solid evidence that dietary and exercise lifestyle choices can have dramatic effects on the mechanisms of ageing, to delay age-associated disease and extend both healthspan and lifespan. Genetic factors still account for some proportion of the variation in longevity, but may be more difficult to target therapeutically than simple lifestyle interventions.

1.3. The ageing immune system

The immune system is affected by ageing. The overall decline in immune function is termed “immunosenescence” (Aw, Silva & Palmer, 2007). The section on stem cell exhaustion as a feature of ageing has already mentioned that the rate of haematopoiesis

declines with age. This fundamentally leads to lower numbers of many types of immune cell. However, many other aspects of immune cell physiology change with age.

1.3.1. Ageing of the innate immune response

Innate immunity presents the first response to invading pathogens or signs of danger. The innate immune response consists of a wide variety of cell types, including neutrophils, natural killer (NK) cells, NK T cells, monocytes, macrophages, and dendritic cells (DCs). All of these cell types exhibit age-related defects, including altered cell-cell communication, altered signal transduction and resultant impaired function, and dysregulated activity due to inflammageing (Shaw *et al.*, 2010). Together, these can combine to a paradoxical situation where immune responses are delayed and blunted with age, but other branches of the immune response are simultaneously hyperactive, with resultant excessive immunopathology.

1.3.1.1. Neutrophils

Neutrophils are one of the most rapidly recruited innate immune cells, combatting bacterial and fungal infections by phagocytosis, the release of microbicidal chemicals, and the deployment of neutrophil extracellular traps (NETs) (Brinkmann *et al.*, 2004). Neutrophil numbers are not reduced with age, as HSCs tend to skew towards myeloid lineages with age (Beerman *et al.*, 2010). Neutrophils from older human blood donors display impaired chemotaxis (Wenisch *et al.*, 2000). Since neutrophils secrete elastases and other proteases to migrate through tissue, inefficient chemotaxis is likely to cause bystander tissue damage. A burn injury model led to increased neutrophilia and delayed resolution of inflammation in aged compared to young mice, an effect which was mediated by dysregulated expression of chemokine receptors and adhesion molecules (Nomellini *et al.*, 2008, 2012). Data showing that statin administration and PI3K inhibition improve neutrophil function and clinical outcomes in pneumonia strongly suggest that both altered internal signalling and excessive inflammatory signalling in ageing contribute to detrimental neutrophil phenotypes (Sapey *et al.*, 2014, 2019; Wilson *et al.*, 2020)

1.3.1.2. NK cells and NK T cells

NK cells provide immune defence against viruses and certain cancers primarily via cell-cell cytotoxicity. The total number of NK cells increases with age, but the individual cell's capacity for cytotoxicity and the production of key NK cell cyto- and chemokines such as IL-8 and MIP1α decreases with age (Mocchegiani *et al.*, 2009). Mouse studies have also suggested that aged NK cells may contribute to B cell immunosenescence by interfering in early B cell development in the bone marrow (King *et al.*, 2009). NK T cells are innate-like lymphocytes that express both NK-typical cell surface markers and an invariant αβ T cell receptor recognising glycolipids presented by CD1d. Like NK cells, absolute NK T cell numbers increase with age, but in contrast to NK cells, NK T cells appear to become hyperactive with age. NK T cells from older mice are prolific producers of the pro-inflammatory cytokine IL-17A, and promote increased neutrophil migration, liver injury, and mortality during viral infection (Inui *et al.*, 2002; Stout-Delgado *et al.*, 2009). There is also evidence that NK T cells suppress T cell immunity in aged mice (Faunce *et al.*, 2005).

1.3.1.3. Monocytes/macrophages

Monocytes reside in the spleen and blood and differentiate into macrophages or dendritic cells in response to inflammation (Shaw *et al.*, 2010). Numbers of pro-inflammatory $CD16^+$ monocytes increase with age, but numbers of $CD16^-$ monocytes decrease with age (Nyugen *et al.*, 2010). Macrophage cytokine production in response to Toll-like receptor (TLR) activation is reduced in aged mice compared to young mice, especially IL-6, TNFα, and IL-1β (Renshaw *et al.*, 2002; Boehmer *et al.*, 2004, 2005; Chelvarajan *et al.*, 2005). Human aged macrophages may display a more pro-inflammatory phenotype at baseline, concordant with "inflamm-ageing", but tend to produce lower levels of cytokines when stimulated with TLR agonists (van Duin *et al.*, 2007a; Franceschi *et al.*, 2007; Nyugen *et al.*, 2010). TLR expression itself is also dysregulated on ages monocytes (van Duin *et al.*, 2007a). *In vivo*, dermal macrophages from elderly humans responded to antigen challenge with lower cytokine production than those of young controls, but the mac-

rophages from old individuals' skin were still capable of producing TNFα *ex vivo*, suggesting that macrophage dysfunction is partially dependent on extrinsic factors (Agius *et al.*, 2009). Aged human macrophages also display blunted upregulation of co-stimulatory factors such as CD80, which may impair vaccine responses (van Duin *et al.*, 2007b). Antigen presentation by macrophages is impaired with age in both mice and humans, mediated by overall lower levels of MHC class II and reduced expression of MHC class II in response to IFNγ (Villanueva *et al.*, 1990; Herrero *et al.*, 2001). Macrophage and monocyte cytotoxic function, such as phagocytosis and production of ROS, also declines with ageing (Solana *et al.*, 2012b).

1.3.1.4. Dendritic cells

Dendritic cells (DC) patrol the periphery, collecting antigens and presenting them to T cells. Plasmacytoid dendritic cells (pDC) classically produce IFN-α in response to viral infections. Myeloid dendritic cells (mDC) mainly recognise bacterial ligands and produce TNFα, IL-6, and IL-12 (Kadowaki, 2009). The number of pDCs has been reported to decline in humans with advancing age, whereas the number and cytokine production by mDCs is maintainted, except in frail older humans, where mDCs were dramatically reduced (Jing *et al.*, 2009). In mice, the migration and signal transduction of aged mDC is impaired (Grolleau-Julius *et al.*, 2006, 2008). Aged pDCs display lower IFN-α production both in a murine HSV-2 infection model and in human blood pDCs from healthy elderly donors (Stout-Delgado *et al.*, 2008; Jing *et al.*, 2009). Panda *et al.* observed an age-associated decline in TLR-induced cytokine production in human mDCs and pDCs, which correlated strongly with a protective antibody response to influenza A virus vaccination. Additionally, aged DCs were observed to have increased baseline levels of cytokine production, suggesting that additional TLR stimulation was unable to elicit a substantial increase in cytokine production (Panda *et al.*, 2010). Follicular dendritic cells (fDC) are specialised DC that orchestrate antibody affinity maturation in germinal centres. Aged fDC induce fewer germinal centres and generate fewer memory B cells (Aydar *et al.*, 2004; Brown *et al.*, 2009). These results together suggest that DCs are highly pleiotropic

mediators of innate immunity that are profoundly affected by ageing.

1.3.2. Ageing of the adaptive immune response

The adaptive immune response consists of T and B cells and confers long-lasting, pathogen-specific immunity. T cells are fundamentally divided into $CD4^+$ T cells, which promote and regulate the function of other immune cells, and $CD8^+$ T cells, which can have cytotoxic and memory function. Both the T cell and B cell compartments are profoundly impacted by ageing.

1.3.2.1. T cells

The total number of circulating T cells remains roughly constant with age, but the composition of the T cell compartment changes. The thymus involutes with age, leading to a declining output of naïve T cells, which results in a diminishing TCR repertoire (Fulop *et al.*, 2018). The decline in thymic output is compensated for by the expansion of different T cell populations, particularly $CD8^+$ memory T cells, and T cells lacking the co-stimulatory marker CD28 (Koch *et al.*, 2008; Goronzy *et al.*, 2015; Yanes *et al.*, 2017). Within $CD4^+$ T cells, the proportion of pro-inflammatory Th17 (IL-17A-producing T cells) and regulatory T cells (Tregs) increases with advancing age (van der Geest *et al.*, 2014). These changes in T cell composition has been considered the main reason for increased incidence of infections and cancers, and reduced vaccine efficacy, in the elderly (Pawelec, 2017). Ageing also entails an expansion of T cells of a certain clonality, particularly $CD8^+$ T cells reactive to the persistent herpesvirus cytomegalovirus (CMV) (Khan *et al.*, 2002). The overall effect of expanded CMV-reactive T cells on immunity is unclear. On the one hand, the constant antigenic stimulation may promote improved immune responses to other infections or vaccinations (Pawelec *et al.*, 2012). On the other hand, constant stimulation promotes T cell exhaustion, upregulation of inhibitory molecules such as CTLA-4, dysfunction, and eventually senescence (Pawelec, 2014; Tu & Rao, 2016). The SASP of CMV-specific aged T cells may also contribute to inflammageing (Akbar, Henson & Lanna, 2016). The degree of senescence or exhaustion of aged T cells is controversial, as they can usually still be stimulated back into fulfilling their physiological function (Solana

et al., 2012a; Daste *et al.*, 2017). T cell function is strongly dependent on cell metabolism, and there is evidence that T cell metabolism is dramatically altered in ageing (Weyand & Goronzy, 2016). Aged T cells exhibit an energy-deprived state and preferential use of the pentose phosphate pathway, which promotes an anabolic phenotype, but also leads to a higher production of ROS and suppressed TCR signalling by upregulated AMPK activity (Yu *et al.*, 2012; Li *et al.*, 2012). T cell signalling pathways are also impaired by ageing, for example by defective immune synapse formation and dysregulated translocation of transcription factors to the nucleus (Fulop *et al.*, 2014).

1.3.2.2. B cells

Similarly to T cells, the generation of new B cells declines with age in both mice and humans (Lin *et al.*, 2016; Yanes *et al.*, 2017). Mouse studies have attributed the reduced B cell output to age-related increases in inflammation in the bone marrow microenvironment (Stephan, Sanders & Witte, 1996; Henry *et al.*, 2015). Additionally, as discussed above, haematopoietic stem cells become dysregulated with age, skewing away from lymphoid commitment and towards myeloid fates, contributing to the decline in naïve B cell output (Pang *et al.*, 2011). As with T cells, memory B cells and B cells producing IgG/IgA (i.e. class-switched B cells) accumulate with age (Listì *et al.*, 2006; Colonna-Romano *et al.*, 2006; Bulati *et al.*, 2011). This impairs the ability to recognise novel antigens with increasing age. In terms of antibody secretion functionality, plasma cells are less abundant in the bone marrow of elderly people, aged memory B cells differentiate into plasma cells less readily, and aged memory B cells produce less antibody after antigen challenge (Howard, Gibson & Dunn-Walters, 2006; Pritz *et al.*, 2015). The most specific, high-affinity antibodies are produced by B cells undergoing class-switch recombination (CSR) and somatic hypermutation (SHM) in germinal centres. Both CSR and SHM are impaired in ageing, and are related to an age-associated decline in the expression of activation-induced cytidine deaminase (AID) (Frasca *et al.*, 2004; Blomberg & Frasca, 2013). AID activity correlates with antibody affinity after influenza A virus vaccination, highlighting the importance of proper CSR/SHM for B cell function in the elderly (Khu-

rana *et al.*, 2012). As a result of both dimished naïve B cell output and impaired germinal centre interactions, the diversity of the B cell repertoire also declines with age (Gibson *et al.*, 2009; Jiang *et al.*, 2013). The emergence of a unique subset of B cells, termed age-associated B cells (ABCs), has been reported in both mice and humans (Hao *et al.*, 2011; Rubtsov *et al.*, 2011; Jenks *et al.*, 2018). ABCs are described as mostly quiescent, but highly auto-inflammatory, secreting autoantibodies, and expand in the context of viral infections or auto-immune diseases (Rubtsova *et al.*, 2013; Knox *et al.*, 2017; Wang *et al.*, 2018a).

Taken together, the number, function, and microenvironment of adaptive immune cells is profoundly altered in ageing, resulting in blunted immune responses to infections and vaccinations, and a higher risk of auto-immunity.

1.4. Respiratory infections in the elderly

Elderly people are prone to more frequent and more severe infection, including respiratory infection. The airways are constantly exposed to air potentially containing pathogens, and as such are a common route of infection. In England and Wales in 2011, the over-65 age group accounted for 60% of hospitalisations (~200,000) for pneumonia or acute lower respiratory tract infection (LRTI), but crucially, almost 80% of bed days (~2.5 million) for pneumonia or acute LRTI (Snell *et al.,* 2016). As discussed above, the higher susceptibility to respiratory infection in elderly people is probably due to age-related quantitative and qualitative changes in the immune response, coupled with lower vaccine efficacy in elderly. Throughout the past decades, it has become increasingly evident that a major burden of respiratory infectious disease in the elderly population is due to Respiratory Syncytial Virus (RSV) infection (Nicholson, 1996; Cherukuri *et al.*, 2013; Lee *et al.,* 2017; Ackerson *et al.*, 2018). Severe RSV infection is considered to be a classical paediatric condition, particularly of very young children (<6 months), however, statistical models have been used to estimate that the majority (78%) of all RSV-associated deaths in the United States occur in those aged over 65 years (Thompson, 2003). Globally, this

may result in an annual number of deaths of elderly people from RSV infection in excess of 50,000 (Troeger *et al.*, 2017). It is also important to consider that the burden of RSV disease in elderly patients is probably underestimated, because it is frequently undiagnosed or misdiagnosed as other respiratory infections such as influenza virus infection or rhinovirus infection, based on its similar symptoms. There is currently no vaccine for RSV and treatment is predominantly supportive. The pathogenesis of RSV in the elderly is insufficiently understood, and infection is likely to interact with pre-existing health conditions, such as muscle weakness and chronic lung and heart disease, which are common in elderly people. The elderly are also more likely to have more than one pre-existing condition. The concept of "multi-morbidity", the co-existence of multiple factors influencing morbidity, is often insufficiently addressed in basic research particularly when using animal models (Figure 1-2). This thesis will investigate how aspects of ageing and

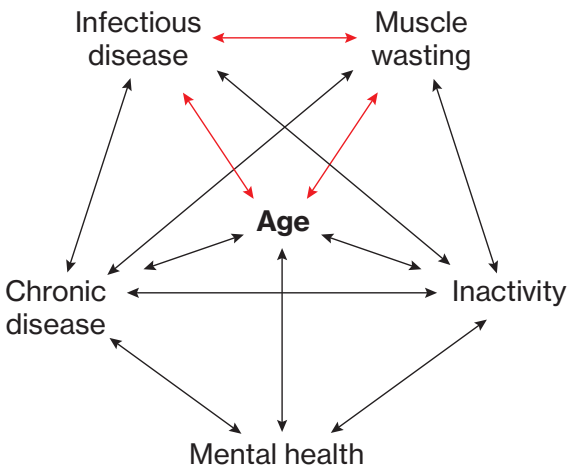

Figure 1-2 Factors in multimorbidity in the elderly

Diagram exemplifying how various aspects of ageing interact with one another. Age increases the susceptibility to both chronic and infectious disease. Age is associated with – but not necessarily causative of – lower levels of activity and poorer mental health. Age-associated muscle wasting (sarcopenia) is commonly observed, but can be prevented with exercise. These factors can interact, for example, the presence of chronic disease is likely to lead to inactivity and further muscle wasting, exacerbating the functional decline that constitutes ageing.

an age-related condition, muscle wasting, interact with RSV infection, using an elderly mouse model.

1.5. Respiratory Syncytial Virus (RSV)

1.5.1. The discovery of Respiratory Syncytial Virus

In 1956, a hitherto unknown pathogen was isolated from a chimpanzee with coryza (Morris, Blount & Savage, 1956). The pathogen, then named "Chimpanzee Coryza Agent" (CCA), was found to induce acute respiratory illness and a specific antibody response when cultured and administered to susceptible chimpanzees. Antibodies to CCA were also detected in the sera of a number of children and young adults, suggesting that the novel pathogen may be capable of infecting humans. This was quickly followed by pioneering work by Chanock and colleagues (Chanock & Finberg, 1957; Chanock, Roizman & Myers, 1957). Two novel viruses isolated from children with severe lower respiratory tract illness were found to be indistinguishable from CCA in terms of size, reactivity to complement-fixing and neutralising antibody, and cytopathogenic effects. Chanock and colleagues were also first to describe the virus' striking ability to induce the formation of large, multi-nucleated syncytia in cell cultures (Chanock, Roizman & Myers, 1957). Although at this point, the causal connection between infection and respiratory illness was tentative, it was noted that serum antibody to the new virus was so common (even in the control group of children without acute respiratory illness) as to imply almost ubiquitous infection. By the age of 4 years, 80% of children in the study had acquired neutralising antibodies (Chanock & Finberg, 1957). The pervasiveness of antibodies acquired at a young age may have implied protection and less frequent infection with the novel virus at older ages. However, almost a quarter of a different study population in their mid-twenties were also found to have antibodies to the new virus. Chanock and Finberg correctly predicted that reinfection with the novel virus was possible throughout life, perhaps due to waning antibody levels. Finally, it was suggested that Chimpanzee Coryza Agent be renamed "Respiratory Syncytial Virus" due to its proven ability to infect humans and the characteristic production of syncytia in cell culture (Chanock & Finberg, 1957).

1.5.2. The structure of Respiratory Syncytial Virus

Respiratory Syncytial Virus (RSV) was historically classed as a *Paramyxovirus* but is now considered part of the genus *Orthopneumovirus* of the family *Pneumoviridae* in the order *Mononegavirales* (Rima *et al.*, 2017). The RSV genome is a single strand of negative sense RNA, packaged into an enveloped virion studded with glycoproteins. The RSV virion was assumed to take a spherical shape like many other viruses, but electron microscopy has confirmed that RSV virions are highly heterogeneous and can take spherical, filamentous, or intermediate shapes (Liljeroos *et al.*, 2013). The 15.2kb RSV genome contains 10 genes encoding 11 known proteins (Figure 1-3). The genes, in order from the 3' end of the genome, are: NS1, NS2, N, P, M, SH, G, F, M2, and L. The M2 gene contains two open reading frames, yielding two proteins, M2-1 and M2-2 (Jin *et al.*, 2000). The F, G, and SH genes encode surface glycoproteins that stud the virion envelope, the F and G proteins mediate viral entry into host cells (Levine, Kaliaber-Franco & Paradiso, 1987; Krusat & Streckert, 1997; Fuentes *et al.*, 2007). The SH (small hydrophobic) protein forms pentameric ion channels thought to promote viral particle release (Gan *et al.*, 2008, 2012; Rixon *et al.*, 2004; Triantafilou *et al.*, 2013). The P and L genes encode the constituents of the viral RNA-dependent RNA polymerase. The genome is packaged with nucleoprotein (encoded by the N protein) to form helical ribonucleoprotein (RNP) complexes, which associate with P and L protein (Grosfeld, Hill & Collins, 1995). The M and M2 genes encode matrix proteins that provide virion stability and shape, and M2-1 protein additionally binds the RNP complexes (Tawar *et al.*, 2009; Kiss *et al.*, 2014). The M2-2 protein mediates switching from transcription to replication of the genome (Bermingham & Collins, 1999). The NS (non-structural) proteins have immune interfering roles such as inhibiting host cell apoptosis and interferon responses (Spann, Tran & Collins, 2005; Bitko *et al.,* 2007). Two antigenic types of RSV exist, RSV A and RSV B, which differ mainly in the mucin-like domains of the G protein (Anderson *et al.*, 1985; Mufson *et al.*, 1985). The A strain of RSV is more widespread and causes more severe infection (Hall *et al.*, 1990; Imaz *et al.*, 2000; Gilca *et al.*, 2006).

1.5.3. The lifecycle of RSV

RSV predominantly infects the ciliated epithelial cells of the upper respiratory tract, including the upper airways and small bronchioles (Zhang *et al.*, 2002a). Attachment of virions to the apical surface of host cells is known to be mediated by the G protein, but the cellular receptor that is bound by G protein is unclear (Levine, Kaliaber-Franco & Paradiso, 1987). A candidate cellular receptor is CX3CR1 (fractalkine receptor), which is expressed on the apical surface of ciliated epithelial cells. Mice deficient in fractalkine receptor are less susceptible to RSV infection (Johnson *et al.*, 2015). Fusion of the viral membrane and the host cell membrane is mediated by F protein, which is found in trimers on the viral envelope (Walsh & Hruska, 1983). The F protein trimer can exist in two conformations, an energetically labile pre-fusion (pre-F) state and a more robust post-fusion (post-F) state (McLellan *et al.*, 2011, 2013). F proteins in both conformations can be present on a virion surface at a given time (Liljeroos *et al.*, 2013). During viral entry, F protein in the pre-fusion conformation is inserted into the cell membrane. A conformational change to the post-fusion form creates a fusion pore, through which the viral genome is released into the cytoplasm of the target cell (McLellan *et al.*, 2011, 2013). In the host cell cytoplasm, the viral RNA-dependent RNA polymerase complex, consisting of L, P, and N proteins, transcribes and replicates the RSV genome (Fearns, Peeples & Collins, 2002). Viral mRNAs are then translated and processed by host cell machinery. RSV particle assembly occurs at the cell plasma membrane (Gower *et al.*, 2005; Ke *et al.*, 2018). F proteins in the cell membrane assemble into lipid rafts and recruit M proteins through interactions with their F cytoplasmic tails (Liljeroos *et al.*, 2013). The self-assembly of multiple M proteins into tubular helical sheets at the budding site drives the extrusion of a filamentous virion (Mitra *et al.*, 2012). A layer of M2-1 protein underneath the sheet of M protein recruits the viral RNP into the budding virion (Li *et al.*, 2008; Kiss *et al*., 2014). Finally, virions bud off, incorporating a variable amount of the cell plasma membrane. Redistribution of F protein on the virion surface and disassembly of the internal M protein layer may induce a shape change from filamentous to spherical (Liljeroos *et al.*, 2013).

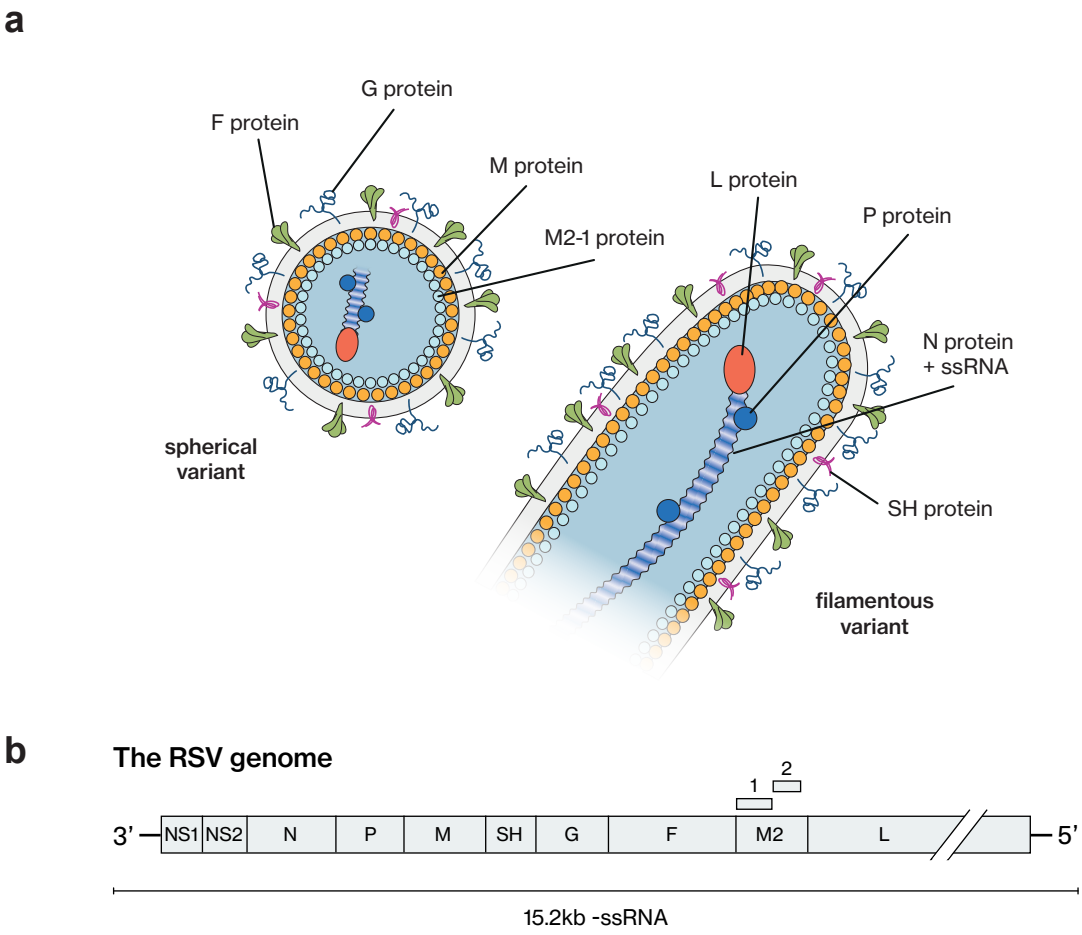

Figure 1-3 The structure and genome of RSV

a. Diagram of RSV virion particles (not to scale). RSV can take spherical, filamentous, or intermediate forms. The host-derived lipid bilayer envelope is studded with fusion (F) protein, attachment glycoprotein (G), and small hydrophobic (SH) protein. The inside of the virion is lined with matrix (M) protein and M2-1 protein. The genome associates with nucleoprotein (N) and is packed into helical filaments that associate with the large polymerase subunit (L) protein and phosphoprotein polymerase cofactor (P) protein, which make up the viral RNA-dependent RNA polymerase. **b.** Diagram of the genome of RSV. RSV encodes 10 genes in its 15.2kb single-stranded, negative sense RNA genome. The genes yield 11 protein products, because the M2 gene encodes both the M2-1 and M2-2 variants. Adapted by permission from Springer Nature: Nature Reviews Microbiology (Respiratory syncytial virus entry and how to block it, Battles & McLellan, 2019) (see Appendix).

Table 1-1 Proteins encoded by the RSV genome

The RSV genome contains 10 genes which encode 11 protein products. They are listed here in the order in which they are encoded from the 3' end to the 5' end.

Gene		Protein name	Protein function	Reference
NS1		Non-Structural protein 1	Inhibition of apoptosis and interferon responses	Spann, Tran & Collins, 2005; Bitko et al., 2007
NS2		Non-Structural protein 2	Inhibition of apoptosis and interferon responses	Spann, Tran & Collins, 2005; Bitko et al., 2007
N		Nucleoprotein	RNP stability, RNA protection	Grosfeld, Hill & Collins, 1995
P		Phosphoprotein polymerase cofactor	RNA-dependent RNA polymerase co-factor	Fearns, Peeples & Collins, 2002
M		Matrix protein	Virion structure and stability	Mitra et al., 2012
SH		Small Hydrophobic protein	Inhibition of TNFα signalling	Fuentes et al., 2007
G		Attachment Glycoprotein	Host cell attachment	Levine, Kaliaber-Franco & Paradiso, 1987
F		Fusion protein	Host cell and viral membrane fusion, syncytium formation	Walsh & Hruska, 1983
M2	M2-1	Matrix protein 2-1	Association between M and RNP	Li et al., 2008; Kiss et al., 2014
	M2-2	Matrix protein 2-2	Switch from transcription to translation	Bermingham & Collins, 1999
L		Large polymerase subunit	RNA-dependent RNA polymerase	Fearns, Peeples & Collins, 2002

1.6. RSV pathogenesis

RSV causes annual epidemics during the winter months (in the UK: November – March) (Shi *et al.*, 2017). In healthy, immunocompetent adults, RSV causes a self-resolving common-cold-like illness. However, at the extremes of age, RSV infection can induce severe illness including bronchiolitis and viral pneumonia (Hall *et al.*, 1990). RSV is a major cause of acute lower respiratory tract infection in children worldwide, and the most common cause of hospitalisation of infants in developed countries such as the UK (Shi *et al.*, 2017; Reeves *et al.*, 2019). It has been estimated that globally, RSV causes 33.1 million episodes of acute lower respiratory tract infection in children under the age of five years, of which 3.2 million (just under 10%) require hospitalization (Shi *et al.*, 2017). Symptoms of RSV

infection include coryza, rhinorrhoea, fever, tachypnoea, sneezing, and coughing. The lungs of children with severe RSV bronchiolitis contain a prominent infiltrate of immune cells, predominantly neutrophils, $CD8^+$ T cells, and $CD69^+$ monocytes (Johnson *et al.*, 2007). Immune cells are also commonly found in the airway lumen, where they caused airway obstruction in conjunction with mucus, oedema, and cellular debris caused by the infection. The airway fluids of children with severe RSV infection contain high levels of pro-inflammatory mediators such as TNFα, IL-6, IL8, CXCL10, CCL2, and CCL3 (McNamara *et al.*, 2004, 2005). The symptoms from RSV infection are thought to be due in a large part to an overexuberant immune response (immunopathology), particularly T cell activity (Varga *et al.*, 2001; Schmidt *et al.*, 2018). However, considering the fact that immunocompromised children are more likely to develop severe RSV disease, viral load may also play a role in determining severity (Hall *et al.*, 1986). This suggests that in response to RSV infection, the immune system can simultaneously fail to effectively control viral replication, and respond in an inappropriate manner that drives disease.

1.6.1. RSV is a significant pathogen of the elderly

The global burden of RSV disease in the elderly has been difficult to quantify. Firstly, data from Low and Middle Income Countries (LMIC), where the RSV burden in all age groups is suspected to be substantial, is scarce, since diagnosis and hospitalisation occurs less frequently than in resource-rich countries (Shi *et al.*, 2019). Secondly, as mentioned earlier, the RSV disease burden in the elderly is likely to be highly underestimated, as elderly patients with pneumonia or bronchitis are rarely tested for the causative agent, and RSV may be misdiagnosed as a similarly-presenting respiratory infection such as influenza or rhinovirus. Shi *et al.* (2019) estimated that there were 1.5 million episodes of acute RSV infection in elderly people in industrialised countries in 2015, of which approximately 14.5% required hospital admission. They further estimated that there were approximately 14,000 in-hospital deaths of elderly people from acute RSV infection globally. This contrasts with other studies that suggest the death toll from RSV infection in elderly people in the United States alone may lie between 11,000-14,000 annually (Thompson, 2003;

Falsey & Walsh, 2005). The reasons for a higher susceptibility of elderly people to severe RSV infection are not fully known, and likely include many factors, such as decreased lung elasticity, the barrier function of lung epithelia weakening, microbiome changes, and of course, changes in immune cell composition and function. RSV infection is also a major cause of exacerbation of underlying conditions such as COPD and asthma which are more common in the elderly, often requiring hospitalisation (Lee *et al.*, 2013).

1.6.2. The immune response to RSV infection

1.6.2.1. The innate immune response to RSV infection

The innate immune response plays an important role in detecting and fighting early RSV infection, and shapes the development of the adaptive immune response. Cells recognise components of RSV via three main types of pattern recognition receptors (PRRs): TLRs, RIG-I-like receptors (RLRs), and NOD-like receptors (NLRs) (Sun & López, 2017). Cell-external RSV envelope protein can be sensed by TLR2/6, and endosomal RSV RNA can be sensed by TLR3 and TLR7 (Rudd *et al.*, 2006; Murawski *et al.*, 2009; Lukacs *et al.*, 2010). These TLRs signal via myeloid differentiation primary response gene 88 (MyD88) and/or TIR-domain-containing adapter-inducing interferon-β (TRIF) to activate transcription factors, such as interferon regulatory factors (IRFs) and NF-κB. IRFs and NF-κB translocate to the nucleus and induce the expression of type I and III interferons and other pro-inflammatory cytokines. Interferons are secreted by the cell and subsequently signal in an autocrine or paracrine way to promote the expression of diverse antiviral interferon-stimulated genes (ISG) (López & Hermesh, 2011). Type I IFN signalling is crucial to the antiviral and inflammatory response to RSV in mice (Goritzka *et al.*, 2014). The cytosolic sensors Retinoic acid-inducible gene I (RIG-I) and melanoma differentiation-associated protein 5 (MDA5) are a major pathway for detection of RSV double-stranded RNA. RIG-I signalling also converges on promoting the type I IFN response (Liu *et al.*, 2007; Bhoj *et al.*, 2008; Gitlin *et al.*, 2010; Yoboua *et al.*, 2010; Grandvaux *et al.*, 2014; Kim *et al.*, 2014). Nucleotide-binding oligomerization domain containing 2 (NOD2), a NLR, is another cytosolic sensor that can detect RSV single-stranded RNA, which signals through the same

adaptor as RIG-I and MDA5, mitochondria antiviral-signaling protein (MAVS) (Sabbah *et al.*, 2009). Other NLRs, such as NLRP3, form multimeric inflammasome complexes in response to RSV detection by TLR2 (Segovia *et al.*, 2012; Triantafilou *et al.*, 2013). As described in a previous section RSV encodes gene products that interfere with the innate immune response. NS1 and NS2 associate with and promote the degradation of various innate immune components, including RIG-I and IRF3, to prevent the synthesis of type I interferons (Teng & Collins, 1999; Jin *et al.*, 2000b; Spann *et al.*, 2004; Swedan, Musiyenko & Barik, 2009). This highlights the importance of the innate immune system to RSV control. RSV infection causes different types of cell stress, including endoplasmic reticulum (ER) overloading with RSV glycoproteins that leads to activation of the unfolded protein response, transcriptional stress due to stalled RSV mRNAs, and oxidative stress, that promotes further inflammatory and antiviral transcriptional activation (Bitko & Barik, 2001; Lindquist *et al.*, 2010; Soucy-Faulkner *et al.*, 2010; Cervantes-Ortiz, Cuervo & Grandvaux, 2016). The detection of RSV in a cell can also induce apoptosis by both cell-extrinsic and cell-intrinsic pathways in an attempt to prevent further viral replication. The cell-extrinsic apoptosis is mediated by tumor necrosis factor-related apoptosis-inducing ligand (TRAIL) and death receptor 4 and 5 (DR4/5), and the cell-intrinsic apoptosis is mediated by proteins of the B-cell lymphoma 2 (Bcl-2) family localising to the mitochondria. Both of these pathways converge on the activation of caspase 3 that induces apoptosis (Kotelkin *et al.*, 2003; Nakamura-Lopez, Villegas-Sepúlveda & Gómez, 2015).

1.6.2.2. How is innate immunity to RSV altered in ageing?

The majority of our knowledge on the effect of ageing on the innate immune response to RSV comes from animal models. Pennings *et al.* found that the lung transcriptional profile of aged mice was characterised by dysregulation of the immune system and metabolic alterations (Pennings *et al.*, 2018). In addition, RSV infection induced stronger type I IFN pathway activation in the lungs of old mice than in young mice, in spite of exaggerated disease and higher viral load in the aged mice. This suggests that the increased susceptibility and severity of RSV in old age is not exclusively due to a failure to induce

strong innate immunity. Several studies have found that TLR expression is reduced with ageing (Dunston & Griffiths, 2010; Shaw *et al.*, 2011; Volkova *et al.*, 2012). This has not been specifically investigated in the context of RSV but may contribute to lower responsiveness of the aged innate immune system to RSV. Inflammageing has been associated with inhibition of TLR and downstream NF-κB signalling in the lungs, particularly alveolar macrophages, of aged mice (Hinojosa, Boyd & Orihuela, 2009; Hinojosa *et al.*, 2014). The infiltrating cells in the lungs of aged or progeroid RSV-infected mice and cotton rats are predominantly granulocytes, especially neutrophils (Curtis *et al.*, 2002; Liu & Kimura, 2007; Wong *et al.*, 2014). As discussed in an earlier section, the increased recruitment and less efficient chemotaxis of neutrophils with age may contribute to increased tissue damage. The production of type I and II interferons and TNFα, which are crucial for viral control, in response to RSV infection is decreased in the elderly, whereas the production of IL-1β and IL-4 is increased (Liu & Kimura, 2007; Boukhvalova *et al.*, 2007; Ditt *et al.*, 2011; Wong *et al.*, 2014). This is likely to hinder the ability of innate cells to induce T cell proliferation and functional $CD8^+$ T cell responses (Zhang *et al.*, 2002b; Fulton *et al.*, 2013). Studies using influenza A virus infection have shown that monocytes from aged mice have reduced interferon production, but intact inflammasome induction (Pillai *et al.*, 2016). This dysfunction in TLR signalling may impede the innate immune response to RSV with advancing age. NK cell cytotoxicity in response to RSV infection is also reduced with age in mice (Zhang *et al.*, 2002b; Liu & Kimura, 2007). A recent study has suggested dysregulation of DCs as the cause for overall suboptimal immunity to RSV infection (Le Nouën *et al.*, 2019). Compared to influenza A virus infection, RSV infection poorly stimulated the upregulation of maturation markers and cytokine production in monocyte-derived DCs from both cord blood and adult blood *in vitro*. This RSV-intrinsic impairment of DC activation and trafficking may be further exacerbated in ageing, since the migratory capacity of DCs decreases with age, for example the number of DCs recruited to the lymph nodes after RSV infection was significantly lower in elderly mice compared to young (Zhao *et al.*, 2011).

1.6.2.3. The antibody response to RSV infection

The adaptive immune response, and the generation of high-affinity, pathogen-specific antibodies, is important to the efficient defence against infectious disease. Dendritic cells carrying antigen migrate to secondary lymphoid tissues such as the lymph nodes or spleen to present antigen to B and T cells which circulate through these tissues (Nutt *et al.*, 2015). Upon encountering their cognate antigen, B cells are retained in secondary lymphoid organs such as spleen and lymph nodes and differentiate to highly proliferative B lymphoblasts which can perform class-switch recombination (CSR) to change the isotype of their secreted antibody. Lymphoblasts then take one of two paths. They may further differentiate into short-lived antibody-secreting plasmablasts, but because they do not undergo somatic hypermutation, their antibodies are of low affinity (Chiu & Openshaw, 2015). Alternatively, lymphoblasts can continue to interact with specialised dendritic cells called follicular dendritic cells (fDC) and specialised antigen-specific T cells, termed T follicular helper (Tfh) cells found in the lymphoid follicle and proliferate to form a germinal centre (Heesters, Myers & Carroll, 2014). Tfh cells are a subset of $CD4^+$ T helper cells specialised to provide survival and differentiation signals to B cells in germinal centres (Linterman, 2014). Germinal centres are highly specialised microenvironments in which B cells undergo somatic hypermutation and affinity maturation, being iteratively selected for high-affinity antibody production. The resultant B cells can differentiate to antibody-secreting plasma cells or long-lived memory B cells. In mice, the germinal centre microenvironment is known to become disorganised with age (Aw *et al.*, 2016), and germinal centres formed are smaller (Linterman, 2014; Thompson *et al.*, 2017). The lymph nodes of elderly mice exhibit less defined boundaries between T and B cell zones and signs of fibrosis, an altered lymph node architecture that impairs cell trafficking (Richner *et al.*, 2015; Becklund *et al.*, 2016). Together with lower numbers of naïve T cells as a result of age-related thymic atrophy, and increased senescence in protective memory T cells, this germinal centre dysfunction may help to explain why the elderly generally produce lower serum antibody titres after vaccination (Boraschi *et al.*, 2013).

1.6.2.4. Are RSV-specific antibodies protective?

As Chanock and Finberg discovered in the 1950s, serum antibodies to RSV are found in almost all humans tested from an early age onwards. In adults, there is some correlation between levels of RSV-specific antibody and protection from future infection, but protection is incomplete (Hall *et al.*, 1991). Further evidence that RSV antibodies can be protective comes from the fact that the best correlate of protection for RSV infection in infants is maternal antibody titre, and that an RSV-specific monoclonal antibody, palivizumab, can be used as a prophylactic to prevent RSV infection in infants (Glezen *et al.*, 1981; Ogilvie *et al.*, 1981; Stensballe *et al.*, 2009; Ochola *et al.*, 2009; Chu *et al.*, 2014). A key feature of RSV is that natural infection generates only a transient and weakly protective immunological memory response, a phenomenon termed "immunological amnesia" (Habibi *et al.*, 2015; Openshaw *et al.*, 2017). Even in immunocompetent adults, antibody titres return to baseline within a few months of RSV infection (Habibi *et al.*, 2015). This facilitates frequent reinfection throughout life, despite little antigenic variation in the virus (Hall *et al.*, 1991). The causes of this immunological amnesia are unknown but of crucial interest to the development of vaccines and treatments. Since high baseline levels of serum RSV-specific antibodies are to some extent protective, many vaccine studies use serum IgG as a correlate of protection. However, in a study of experimental RSV challenge in adult volunteers, RSV-specific nasal IgA correlated better with protection from RSV infection than baseline serum neutralizing antibody, but neither guaranteed complete protection even at high levels (Habibi *et al.*, 2015). This study also identified a striking impairment in the generation of IgA-producing RSV-specific memory B cells. Short-lived IgA-producing B cells were robustly induced, but long-lived RSV-specific memory B cells were almost undetectable both prior to challenge and one month after challenge. These results suggest that immunological amnesia may be due to RSV interfering with the proper generation of a protective mucosal IgA antibody response. This putative RSV immune evasion strategy combined with general age-associated impairment in germinal centre interactions may contribute to the higher susceptibility and repeated re-infection

of elderly people with RSV.

1.6.2.5. The role of RSV-specific antibody in the elderly

The role of RSV-specific circulating antibody in preventing RSV disease is unclear. One might assume that the humoral response wanes with age, predisposing the elderly to RSV infection. Indeed, low baseline serum levels of RSV-specific antibodies in elderly people have been associated with a higher risk of RSV infection and a more severe course of disease (Falsey & Walsh, 1998; Walsh, Peterson & Falsey, 2004). However, on average, there may be no difference in baseline serum neutralising titres between young and elderly people (Walsh & Falsey, 2004; Cherukuri *et al.*, 2013). Additionally, RSV infection induces a strong serum neutralising antibody response in elderly people, which may be due to higher viral loads or a stronger inflammatory response in elderly people (Agius *et al.*, 1990; Walsh & Falsey, 2004). The strong antibody response may imply there is no fundamental defect in the generation of an RSV-specific antibody response in the elderly. Another potential reason for a strong antibody response may be that elderly people are infected with RSV more frequently and a poor immune response ensures prolonged exposure to antigen.

1.6.2.6. The role of $CD8^+$ T cells during RSV infection

On the one hand, $CD8^+$ T cells have a key role in orchestrating the immune response, including secreting IFNγ and promoting the recruitment of other cells, particularly eosinophils and neutrophils (Schmidt & Varga, 2018). $CD8^+$ T cells are important for viral clearance during primary RSV infection, as depletion of $CD8^+$ T cells increases viral load (Graham *et al.*, 1991). Intranasal administration of recombinant IFNγ leads to faster RSV clearance in both adult and neonatal mice (Eichinger *et al.*, 2015, 2017). On the other hand, $CD8^+$ T cells may also contribute to immunopathology by promoting high levels of inflammation. Rodent models have shown that $CD8^+$ T cells are key drivers of RSV-associated weight loss, lung damage, eosinophilia and airway hyperresponsiveness, mostly due to their prolific production of IFNγ and TNFα (Schwarze *et al.*, 1999; Castilow *et al.*, 2008; Schmidt *et al.*, 2018). Depletion of $CD8^+$ T cells or inhibition of IFNγ was able to

prevent these effects. Concordant with this, IFNγ-knockout mice and mice treated with a monoclonal antibody to IFNγ develop develop stronger inflammation, but also exhibit less severe immunopathology (van Schaik *et al.*, 2000; Ostler, Davidson & Ehl, 2002). Excessive IFNγ signalling may also be detrimental to the antibody response, as depletion of IFNγ during RSV infection of neonatal mice significantly increased their RSV-specific antibody titre (Tregoning *et al.*, 2013).

The memory response of $CD8^+$ T cells in the tissue (T tissue-resident memory cells, Trm) has elicited particular interest due to the recurrent nature of RSV infection. The transfer of RSV-specific $CD8^+$ Trm cells into naïve mice reduces viral load and protects them from severe RSV disease (Kinnear *et al.*, 2018). In adults experimentally challenged with RSV, the abundance of pulmonary RSV-specific $CD8^+$ Trm cells at baseline correlates with reduced symptom severity and viral load (Jozwik *et al.*, 2015). These studies suggest that $CD8^+$ T cells, particularly tissue-resident memory $CD8^+$ Trm cells, contribute towards RSV clearance. However, the development of $CD8^+$ Trm cells from previous RSV infections may also poise the immune response to an overreaction to subsequent infections. For example, $CD8^+$ Trms developed after relatively mild neonatal RSV infection of mice drive enhanced disease in secondary infection, which can be attenuated by the depletion of $CD8^+$ T cells (Tregoning *et al.*, 2008). This finding emphasises that great caution must be taken in the development of future RSV vaccines that may aim to generate cellular immunity to RSV.

1.6.2.7. $CD8^+$ T cells and cytokine production during RSV infection of the elderly

Elderly humans have been reported to have various impairments in cellular immunity to RSV infection. The number of peripheral RSV-specific $CD8^+$ T cells declines with increasing age, despite more frequent RSV infection (de Bree *et al.*, 2005; Cusi *et al.*, 2010; Cherukuri *et al.*, 2013). Upon stimulation, the RSV-specific T cells of elderly people also display lower IFNγ production and higher IL-10 production compared to cells from young individuals, suggesting a switch away from cytotoxic activity and towards anti-inflamma-

tory activity (Looney *et al.*, 2002; Cusi *et al.*, 2010; Cherukuri *et al.*, 2013). However, many of these studies are based on *ex vivo* stimulation of PBMCs with RSV and are not necessarily representative of the aged immune response to RSV *in vivo*. These features are also seen in aged animal models. Lower levels of RSV-specific $CD8^+$ T cells are observed in elderly mice infected with RSV (Zhang *et al.*, 2002b; Fulton *et al.*, 2013). In one study, after primary RSV infection, fewer RSV-specific $CD8^+$ T cells in the lungs and airways of elderly mice produced IFNγ following *ex vivo* peptide challenge. However, during RSV re-challenge, the capacity of RSV-specific memory T cells to produce IFNγ was similar between young and elderly mice (Fulton *et al.*, 2013). Both elderly humans (Walsh *et al.*, 2013) and elderly mice (Zhang *et al.*, 2002b; Fulton *et al.*, 2013; Wong *et al.*, 2014) have higher viral titres after RSV infection and tend to shed virus longer than comparable young controls.

1.6.3. Treatment and prevention of RSV infection

Treatment for RSV is currently exclusively supportive. The NHS licenses the use of Palivizumab, a humanized monoclonal antibody against the RSV F protein, as prophylaxis for infants at high risk of severe RSV disease. However, the high cost of the drug and concerns about the timing of administration have so far prohibited more widespread use (Wang *et al.*, 2008; Ohler & Pham, 2013). A number of candidate vaccines against RSV are currently in trials (Higgins, Trujillo & Keech, 2016). Efforts to develop a vaccine against RSV have been slowed and overshadowed by the disastrous results of a vaccine trial using formalin-inactivated RSV in the 1960s (Kapikian *et al.*, 1969; Kim *et al.*, 1969). Subsequent natural RSV infection triggered an exaggerated severe immune response in a high proportion of participants given the formalin-inactivated RSV vaccine. Two children given the formalin-inactivated RSV vaccine died. Development of a vaccine for RSV is further complicated by the fact that vaccines tend to be less effective in the elderly, despite the elderly being an important target group due to their higher susceptibility and higher risk of severe disease (McElhaney *et al.*, 2012). Research and development into treatments and vaccines for RSV is urgently needed due to the high burden of disease

in both young children and the elderly, and must take into account the age-related differences in the immune response to RSV to ensure efficacy.

1.7. Skeletal muscle in ageing and disease

Early work by the Culley group had established that elderly mice lost more weight in response to RSV infection than young mice. It was hypothesised that part of the weight lost was skeletal muscle mass. Muscle mass is a key determinant of frailty, morbidity and mortality in old age (Wheeler *et al.*, 1998; Swallow *et al.*, 2007; Landi *et al.*, 2013; Arango-Lopera *et al.*, 2013), and increased muscle wasting is observed with repeated or chronic infections (Spruit *et al.*, 2003; Pitta *et al.*, 2006; Paton & Ng, 2006). Preliminary experiments in the group had additionally established that elderly mice produced large amounts of IL-6, a known "myokine" (muscle cytokine), in response to RSV infection (See also Section 1.7). It was hypothesised that RSV infection in the context of ageing may promote skeletal muscle wasting, with important clinical implications.

1.7.3.1. Skeletal muscle is a metabolically dynamic tissue

Skeletal muscle is what keeps our bodies upright and allows our bodies to generate force to interact with the outside world. Because muscle contraction requires the expenditure of large amounts of ATP, an organism's muscle mass must be tightly controlled to avoid the waste of precious energy. As a result, muscle exists in a constant balance between being built up (hypertrophy) and broken down (atrophy). A loss of muscle mass is due to a net imbalance between hypertrophy and atrophy, whether it be a decrease in hypertrophy, increase in atrophy, or a combination of both. Muscle mass is regulated by a plethora of local and circulating factors on either side of the balance. This section will describe a selection of these pathways. However, this is not exhaustive. Other factors and pathways that modulate muscle mass that will not be described here include insulin, growth hormone, testosterone, Activin A, IL-1β, and reactive oxygen species.

1.7.3.2. The structure of skeletal muscle

Skeletal muscle is a highly specialized tissue. It consists of many muscle fibres (myofibres) embedded in a network of connective tissue that is contiguous with the tendons

which are connected to the bones (Zammit, 2017). Each myofibre is a syncytial structure containing myofibrils and multiple post-mitotic myonuclei. Myofibrils are bundles of individual sarcomeres consisting of actin (thin filaments) and myosin (thick filaments). The ATP-dependent interaction of myosin and actin causes a shortening of the sarcomere, which generates physical force. The different isotypes of myosin heavy chain (MyHC) determine the contractile and metabolic characteristics of a muscle fibre. Four different types of MyHC are found in mammalian skeletal muscle, MyHC type I, type IIA, type IIB, and type IIX. Muscle fibres expressing MyHC type I, also known as "type I fibres" or "slow twitch" fibres have a slow contraction time and do not generate a lot of power, but they are highly resistant to fatigue (Schiaffino & Reggiani, 2011). Type I fibres have a high oxidative capacity but low glycolytic capacity which makes them suited to aerobic activities. The "fast twitch" fibres include those expressing MyHC type IIA, IIB, and IIX. These fibres generally produce more power than type I fibres but are more prone to fatigue. Type IIA fibres contract moderately fast, generate a moderate amount of power, and have a fairly high resistance to fatigue. They have both a high oxidative capacity and a high glycolytic capacity. Type IIB fibres by contrast contract very fast and can generate a large amount of power. However, the fibres fatigue quickly and the power can only be sustained for a very short amount of time. Type IIB fibres have a low oxidative capacity and a high glycolytic capacity which makes them suitable to short-term anaerobic activities that require quick bursts of power. Type IIX fibres have properties intermediate between type IIA and IIB.

The myonuclei found in skeletal muscle are post-mitotic and thus cannot contribute to muscle repair or regeneration. Novel muscle growth is derived from muscle stem cells, called satellite cells. Satellite cells are located between the plasmalemma and the basal lamina that encapsulate a myofibre (Biressi & Rando, 2010). Satellite cells are quiescent at steady state in adult muscle, but are readily activated in response to injury or hypertrophic signals. Satellite cells proliferate and differentiate into myoblasts, which then fuse into existing myofibres, or can fuse together to form myofibres *de novo* (Wright, Sassoon & Lin, 1989; Collins *et al.*, 2005) The nuclei of the former myoblasts then become the

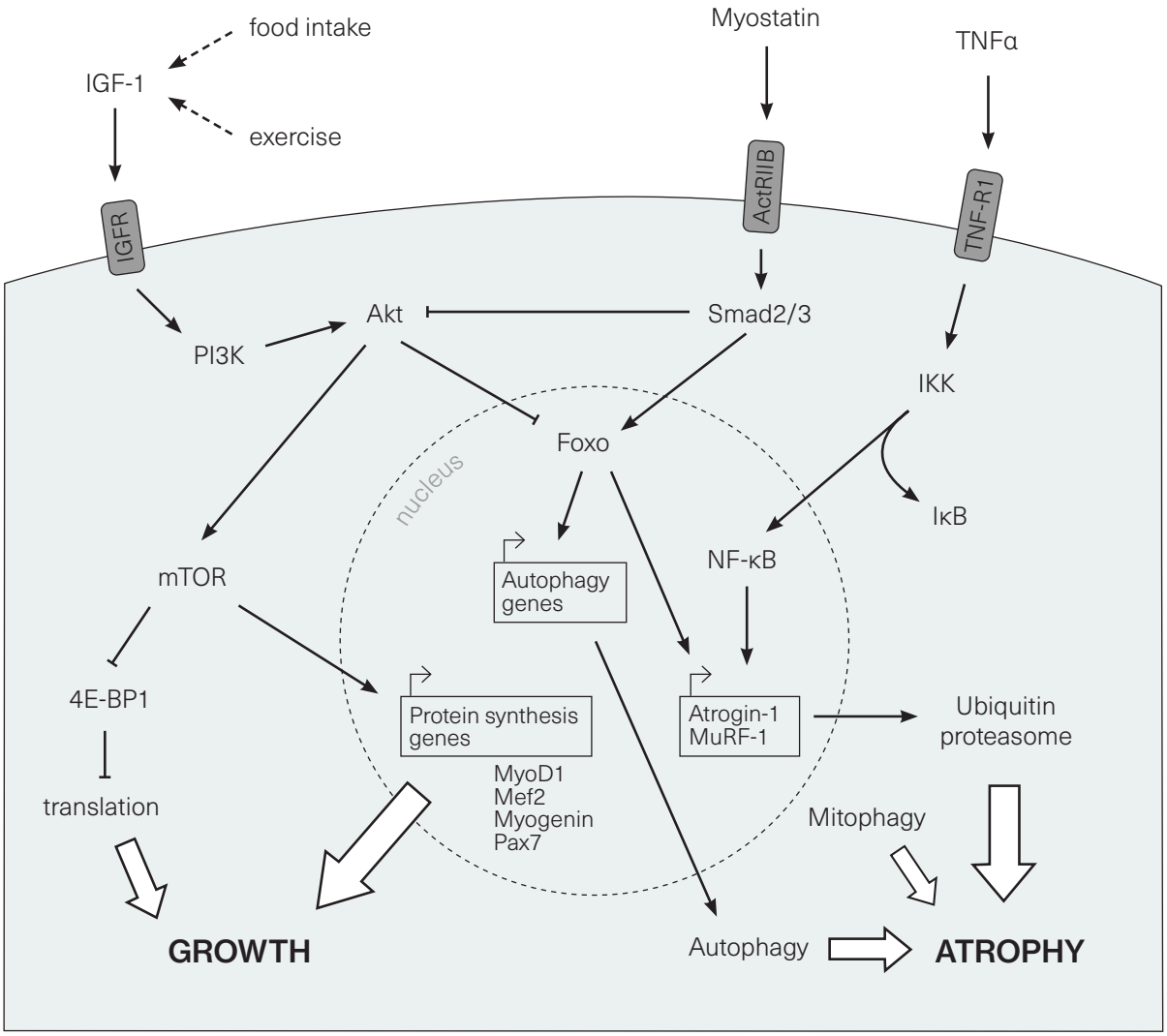

Figure 1-4 Factors governing growth and atrophy of skeletal muscle

Diagram of a selection of factors and pathways influencing the growth (left side) and atrophy (right side) of skeletal muscle. The IGF-1/Akt/mTOR axis is a major driver of cell growth, including muscle growth. mTOR signalling promotes the expression of genes involved in protein synthesis generally and genes promoting muscle growth and repair specifically (MyoD1, Mef2, Myogenin, Pax7). Myostatin promotes muscle atrophy via induction of Smad2/3, which leads to the expression of autophagy-promoting genes and the E3 ubiquitin ligases Atrogin-1 and MuRF-1. Atrogin-1 and MuRF-1 ubiquitinate a number of muscle-specific proteins, including actin, myosin, desmin, and MyoD1, causing their degradation in 26S proteasomes. Expression of Atrogin-1 and MuRF-1 is also upregulated by NF-κB signalling in response to various pro-inflammatory cytokines including TNFα. Adapted with permission of the American Thoracic Society. Copyright © 2020 American Thoracic Society. All rights reserved. Cite: Abdulai *et al.*: "Deterioration of Limb Muscle Function during Acute Exacerbation of Chronic Obstructive Pulmonary Disease" Am J Respir Crit Care Med Vol 197, Iss 4, pp 433–449, Feb 15, 2018. The American Journal of Respiratory and Critical Care Medicine is an official journal of the American Thoracic Society. Readers are encouraged to read the entire article for the correct context at https://doi.org/10.1164/rccm.201703-0615ci. The authors, editors, and The American Thoracic Society are not responsible for errors or omissions in adaptations.

myonuclei of the new or repaired myofibre.

1.7.1. Promoters of muscle growth

Muscle mass and muscle fibre size increase during development and in response to mechanical overload or anabolic steroid stimulation. Muscle growth is driven by increased rates of protein synthesis (transcription and translation), since the primary components of muscle, actin and myosin, are proteins.

1.7.1.1. Insulin-like growth factor 1 (IGF-1)

The insulin-like growth factor 1-phosphoinositide-3-kinase-Akt-mammalian target of rapamycin (IGF-1-PI3K/Akt-mTOR) axis positively regulates protein synthesis (Schiaffino *et al.*, 2013). Muscle produces IGF-1 in response to exercise. IGF-1 binds to the IGF-1 receptor, IGF-1R, on the surface of a myofibril. This activates both the MAPK/ERK pathway and the PI3K-Akt pathway. Only the PI3K-Akt pathway is necessary and sufficient for inducing muscle hypertrophy (Bodine *et al.*, 2001b; Pallafacchina *et al.*, 2002; Blaauw *et al.*, 2009). PI3K phosphorylates Akt. Akt in turn stimulates mTOR (mammalian target of Rapamycin) signalling (Bodine *et al.*, 2001b; Risson *et al.*, 2009). The kinase mTOR associates with a number of other proteins to form the mTOR complex, mTORC (either mTORC1 or mTORC2). mTORC is a master transcriptional regulator and a strong driver of cell growth. mTORC1 induces the displacement of the polycomb repressor complex, permitting the transcription of many growth-promoting genes. mTORC1 signalling also phosphorylates the translation inhibitor eukaryotic translation initiation factor 4E-binding protein 1 (4E-BP1), upregulates the synthesis of ribosomes and tRNAs, and activates transcription by all three nuclear RNA polymerases (Le Bacquer *et al.*, 2007; Risson *et al.*, 2009). mTOR gained its name from the drug which inhibits its action, Rapamycin. Rapamycin is a powerful inhibitor of muscle growth (Bodine *et al.*, 2001b; Pallafacchina *et al.*, 2002). Further evidence for the importance of IGF-1 signalling comes from transgenic studies. Mice which do not express IGF-1R in their muscles have impaired muscle growth with reduced muscle fibre number and size, while mice which overexpress IGF-1 in their muscles have larger muscles and preserve muscle mass with age (Mavalli *et al.*,

2010; Musarò *et al.*, 2001). In addition to stimulating protein synthesis, IGF-1 signalling also suppresses protein breakdown, for example by suppressing the expression of the atrophy-related ubiquitin ligases Atrogin-1 and MuRF-1 (see later section) (Rommel *et al.*, 2001; Sacheck *et al.*, 2004).

1.7.1.2. Myogenic differentiation 1 (MyoD1)

Myogenin, Myogenic differentiation 1 (MyoD1), Pax7 and Myocyte enhancer factor 2c (Mef2c) are important transcription factors during muscle development in embryogenesis, and also play a role during repair and regeneration of mature muscle. MyoD1 and myogenin are members of the family of myogenic regulatory factors (MRFs) (Weintraub *et al.*, 1991). MyoD1 directs embryonic progenitor cells to commit to the skeletal muscle lineage (Davis, Weintraub & Lassar, 1987; Sassoon *et al.*, 1989). MyoD1 protein and mRNA are very low in adult skeletal muscle, but higher in fast-twitch muscle than in slow-twitch muscle (Hughes *et al.*, 1993; Koishi *et al.*, 1995; Ekmark *et al.*, 2007). Overexpression or constitutive expression of MyoD1 promotes a switch to fast-twitch-type MyHCs in the muscles of rats and mice (Ekmark *et al.*, 2007). Depending on the genetic background, MyoD1-null mice have high perinatal mortality, but some viable animals can be generated (Megeney *et al.*, 1996). The muscles of these mice appear mostly normal, except for rare abnormalities such as forked myofibres (Cornelison *et al.*, 2000). MyoD1-null satellite cells enter the cell cycle normally but fail to differentiate into myotubes (Cornelison *et al.*, 2000). MyoD1 is likely to play a role in muscle regeneration, since its expression is upregulated in myofibres after a crush injury (Grounds *et al.*, 1992; Rantanen *et al.*, 1995). Additionally, the muscles of MyoD1-null mice regenerate poorly after crush injury and contain thinner myofibres (Megeney *et al.*, 1996). This is likely due to a reduced proliferation capacity of the satellite cells of MyoD1-null mice, which display delayed entry into the cell cycle and a lower number of cell divisions (Megeney *et al.*, 1996; Cornelison *et al.*, 2000). However, muscle regeneration in the absence of MyoD1 is not prevented entirely, just delayed, suggesting there are other factors that contribute to muscle regeneration (White *et al.*, 2000).

1.7.1.3. Myogenin

Myogenin drives the differentiation of committed muscle progenitor cells into myofibres (Wright, Sassoon & Lin, 1989). It is expressed early during embryonic myofiber formation, but downregulated in mature muscle fibres (Sassoon *et al.*, 1989; Hughes *et al.*, 1993). In adult rat muscle, myogenin protein and mRNA is found at higher levels in slow-twitch muscle than in fast-twitch muscle, the opposite of MyoD1 (Ekmark *et al.*, 2007). Myogenin-null mice have severely reduced skeletal muscle and die immediately after birth, suggesting that myogenin is essential for proper skeletal muscle development (Cusella-De Angelis *et al.*, 1992; Hasty *et al.*, 1993; Venuti *et al.*, 1995). Even though myogenin expression in mature muscle fibres is low, postnatal loss of myogenin results in smaller body size of mice, suggesting that myogenin still influences postnatal growth of muscles (Knapp *et al.*, 2006). Interestingly, overexpression of myogenin in mouse muscle shifts the metabolism of fast-twitch myofibres from glycolytic to more oxidative, and causes a reduction in fast-twitch fibre size (Hughes *et al.*, 1999). This result is consistent with myogenin-deleted mice having a higher exercise capacity due to more efficient glycolytic metabolism (Flynn *et al.*, 2010). Myogenin may also facilitate regeneration of damaged muscle, since its expression is upregulated in regenerating myofibres after muscle damage (Grounds *et al.*, 1992; Füchtbauer & Westphal, 1992; Rantanen *et al.*, 1995). However, others have found that in the context of a mouse model of muscular dystrophy, myogenin was not required for muscle regeneration (Meadows, Flynn & Klein, 2011).

1.7.1.4. Paired box 7 (Pax7)

The expression of *paired box 7* (*Pax7*) marks satellite cells in skeletal muscle beginning in embryogenesis, and continuing into adulthood (Kassar-Duchossoy *et al.*, 2005). Satellite cells are quiescent at steady state. Upon muscle damage, satellite cells are reactivated and begin to express *Pax7* along with other muscle factors like *MyoD1* and begin to differentiate into myoblasts (Biressi & Rando, 2010). As they differentiate, *Pax7* expression is lost and upregulation of *Myog* expression commits the cell to a myofibre fate. Satellite cells can also self-renew by undergoing asymmetric cell division, maintaining

Pax7 expression and downregulating *Myod1* again, to maintain the reservoir of satellite cells (Olguin & Olwin, 2004; Zammit *et al.*, 2006; Kuang *et al.*, 2007). Curiously, *Pax7*-deficient mice have no overt defects in muscle formation during embryogenesis, despite having no satellite cells (Seale *et al.*, 2000). This result suggest that the seeding of early muscle progenitors is partially distinct from the generation of satellite cells, and muscle is still formed due to the effect of other non-redundant factors such as Pax3. However, *Pax7*-deficient mice exhibit facial deformities and die shortly after weaning due to fatal progressive muscle wasting (Mansouri *et al.*, 1996; Kuang *et al.*, 2006). Apart from specifying satellite cell fate during embryogenesis, Pax7 has also been shown to be crucial to muscle regeneration in adult muscle. For example, the above mentioned *Pax7-null* mice are unable to regenerate muscle after cardiotoxin injury (Kuang *et al.*, 2006). Inducible genetic ablation of *Pax7*$^{+}$ satellite cells in adult mice likewise causes profound defects in muscle regeneration in response to injury (Lepper, Partridge & Fan, 2011; Murphy *et al.*, 2011; Sambasivan *et al.*, 2011; Von Maltzahn *et al.*, 2013). The muscles of *Pax7*$^{+}$-ablated mice also display dysregulation of fibroblasts, fibrosis, and infiltration of the muscle by inflammatory cells and adipocytes (Murphy *et al.*, 2011; Sambasivan *et al.*, 2011). The defect in muscle regeneration is likely due to premature differentiation of satellite cells, and could be rescued by transplantation of adult Pax7^{+} satellite cells (Sambasivan *et al.*, 2011; Von Maltzahn *et al.*, 2013).

1.7.1.5. Myocyte enhancer factor 2c (Mef2c)

The Myocyte enhancer factor 2 (Mef2) family of transcription factors has four members in vertebrates, termed Mef2a, b, c, and d (Yu *et al.*, 1992; Andres, Cervera & Mahdavi, 1995; Molkentin *et al.*, 1996). Mef2c is the only one that is highly and almost exclusively expressed in muscle (Martin, Schwarz & Olson, 1993). Mef2c does not have intrinsic myogenic activity, but acts synergistically with MRF family members (which includes MyoD1 and myogenin) to activate the transcription of muscle-specific genes (Molkentin *et al.*, 1995). For example, the *Myogenin* promoter contains a Mef2 binding element, which is bound and activated by Mef2c (Edmondson *et al.*, 1992; Buchberger, Ragge &

Arnold, 1994). The *Mef2c* gene itself is also positively regulated by MRF family factors and other Mef2 factors, inducing a positive feedback loop that amplifies and stabilises the myogenic commitment of a myoblast (Wang *et al.*, 2001). Mice with complete loss-of-function of Mef2c die at embryonic day 9.5 due to cardiovascular defects (Lin *et al.*, 1997, 1998). If Mef2c is conditionally deleted using Cre-lox beginning on embryonic day 8.5, pups survive to term and their muscles differentiate normally during embryogenesis. However, shortly after birth, sarcomeres become disorganised and myofiber structure deteriorates, resulting in high neonatal lethality from underdeveloped diaphragms (Potthoff *et al.*, 2007a). The expression of two genes encoding structural muscle proteins, myomesin and M protein, was dysregulated in these mice, suggesting that Mef2c is key to regulating proper gene transcription during postnatal maturation of muscle.

Mef2c also promotes a slow-twitch fibre phenotype, as demonstrated by the fact that the muscles of mice overexpressing Mef2c have an increased proportion of slow-twitch fibres, and muscle-specific deletion of Mef2c in mice (on a different genetic background to Potthoff *et al.*, 2007a, yielding viable pups) reduces the number of slow-twitch fibres (Potthoff *et al.*, 2007b). Overexpression of Mef2c can induce myofibre hypertrophy in some models, but this is not consistent in all models, potentially due to the different genetic backgrounds of the mice (Potthoff *et al.*, 2007; Moretti *et al.*, 2016). In some models, muscle wasting induced by denervation can be prevented by activation of Mef2c, suggesting a potential role for Mef2c in muscle regeneration (Moretti *et al.*, 2016). Conditional deletion of *Mef2a*, *c*, and *d*, but not any one gene individually, in satellite cells prevents regeneration of muscle in response to cardiotoxin injury because myoblasts derived from these satellite cells cannot differentiate (Liu *et al.,* 2014). Mef2c has also been implicated in muscle wasting by disuse, since its expression is strongly repressed in the skeletal muscle of humans after 21 days of bed rest (Rullman *et al.*, 2018).

1.7.2. Promoters of muscle wasting

During muscle atrophy, there is a net loss of proteins and cytoplasm, which causes myofibres to shrink. Factors that promote muscle atrophy broadly fall into two camps. First-

ly, negative regulators of protein synthesis, such as the myostatin-Smad2/3 axis, and secondly, proteasomal pathways that lead to the direct breakdown of muscle proteins (Schiaffino *et al.*, 2013). Proteasomal pathways can further be divided into ubiquitin-proteasomal pathways and autophagic-lysosomal pathways.

1.7.2.1. The myostatin-Smad2/3 axis

The myostatin-Smad2/3 axis is a negative regulator of protein synthesis. Myostatin is a member of the TGFβ superfamily that is produced by skeletal muscle (McPherron, Lawler & Lee, 1997). Loss-of-function mutations in myostatin lead to a characteristic "double-muscled" phenotype that has been described in many mammalian species, including dogs, sheep, cattle, and humans (McPherron & Lee, 1997; Schuelke *et al.*, 2004; Clop *et al.*, 2006; Mosher *et al.*, 2007). Recombinant myostatin inhibits protein synthesis and reduces fibre size in myotube cultures *in vitro*, and induces muscle atrophy in mice *in vivo* (McFarlane *et al.*, 2006). Myostatin binds to Activin RIIB (ActRIIB) receptors and its downstream effects are mediated by phosphorylation of the transcription factors Smad2 and Smad3 (Lee *et al.*, 2005; Sartori *et al.*, 2009; Trendelenburg *et al.*, 2009; Winbanks *et al.*, 2012). However, the transcriptional targets of Smad2 and 3 that result in muscle atrophy are not fully defined. Another potential mechanism of myostatin may be via interference with the IGF-1-Akt-mTOR pathway, since Smad3 is known to interact directly with Akt (Remy, Montmarquette & Michnick, 2004; Conery *et al.*, 2004).

1.7.2.2. The ubiquitin-proteasome system

Ubiquitylation is a common post-translational protein modification that generally designates a protein for transport to the 26S proteasome and subsequent breakdown. The addition of ubiquitin groups to proteins is catalysed by E3 ubiquitin ligase enzymes. The first two muscle-specific E3 ligases to be identified were Atrogin-1 (also referred to as MAFbx, encoded by the *Fbox32* gene) and Muscle RING Finger 1 (MuRF-1, encoded by the *Trim63* gene) (Bodine *et al.*, 2001a; Gomes *et al.*, 2001). Both are strongly upregulated in animal models of muscle wasting (Bodine *et al.*, 2001a). Furthermore, *Fbxo32/Trim63* double knockouts are resistant to muscle atrophy induced by denervation (Bodine *et al.*,

2001a).

Genetic knockdown of Atrogin-1 prevents muscle wasting during fasting (Cong *et al.*, 2011). The substrates of Atrogin-1 are poorly understood, but it is known to target MyoD1 and translation initiation factor eIF3-f (Tintignac *et al.*, 2005; Lagirand-Cantaloube *et al.*, 2008). Immunoprecipitation experiments have also identified interactions of Atrogin-1 with various structural muscle proteins, such as myosins, desmin and vimentin, and proteins involved in transcription, translation, and metabolism (Lokireddy *et al.*, 2011, 2012). However, it is unknown whether Atrogin-1 ubiquitinates and contributes to the degradation of these proteins *in vivo*.

MuRF-1 is known to ubiquitinate many structural muscle proteins, such as actin (Polge *et al.*, 2011), troponin I (Kedar *et al.*, 2004), myosin heavy chain proteins (Clarke *et al.*, 2007; Fielitz *et al.*, 2007; Cohen *et al.*, 2009), some myosin light chains, and myosin binding protein C (Cohen *et al.*, 2009). The degradation of the thin filament proteins actin and troponin is not entirely MuRF-1-dependent (Cohen *et al.*, 2009). However, while these targets can be ubiquitinylated by MuRF-1 *in vitro*, they may not be primary targets *in vivo*, or not during all types of atrophy conditions. MuRF-1 additionally may play a role in metabolic regulation. Contrary to expectations, mice overexpressing MuRF-1 had normal muscle weights, but expressed lower levels of a number of metabolic enzymes, notably those controlling glycolysis and glycogen metabolism (Hirner *et al.*, 2008). The mice also had high blood insulin levels and low hepatic glycogen. These results suggest that MuRF-1 signalling during stress conditions in skeletal muscle simultaneously works to preserve metabolites systemically.

There is some cross-talk between these different regulating systems. For example, addition of recombinant myostatin to myotube cultures induces the upregulation of both Atrogin-1 and MuRF-1 via Smad3 (McFarlane *et al.*, 2006; Lokireddy *et al.*, 2011), and transient overexpression of Smad3 in mouse muscles both promotes Atrogin-1 expression and inhibits Akt/mTOR signalling and protein synthesis (Goodman *et al.*, 2013).

1.7.2.3. The autophagic-lysosomal degradation pathway

Autophagy (Greek *autós* = self; *phageîn* = to eat) is a homeostatic process in which a cell digests its own components through the lysosomal pathway (Glick, Barth & Macleod, 2010). Many cellular components such as cytoplasm, proteins, and organelles can be broken down and "recycled" by autophagy. When mitochondria undergo autophagy, the process is named mitophagy. Mitochondria are primary producers of ATP in the cell, and as such their function is crucial to proper skeletal muscle function. After muscle atrophy induced by denervation or sepsis in mice, there is an increase in autophagy and decrease in mitochondrial content and mtDNA expression (Mofarrahi *et al.*, 2012; O'Leary *et al.*, 2013). Interestingly, the decrease in mitochondrial content and strong upregulation of autophagy proteins after denervation is not observed in aged mice (O'Leary *et al.*, 2013). The induction of autophagy is blunted in aged muscle, coupled with a strong induction of the unfolded protein response. This implies the accumulation of dysfunctional mitochondria in muscle with age. Conversely, impairment of autophagy, for example by muscle-specific mutation of autophagy-related genes such as *Atg7*, leads to muscle atrophy and loss of strength in mice, presumably due to the accumulation of damaged and dysfunctional mitochondria and other cell components (Raben *et al.*, 2008; Masiero *et al.*, 2009). Overexpression of the mitochondrial fission machinery, causing excessive numbers of mitochondria, also causes muscle atrophy in mice (Romanello *et al.*, 2010). This suggests that controlled levels of autophagy are crucial to maintain muscle mass and function.

1.7.3. Muscle wasting in the elderly

Muscle mass and strength is progressively lost with advancing age, a process named sarcopenia (from Greek *sark-* = muscle, flesh; *penia* = lack) (Cruz-Jentoft & Sayer, 2019). Relative skeletal muscle mass starts to decrease towards the end of the fifth decade of life (Janssen *et al.*, 2000). In elderly people, muscle loss is an important cause of frailty (Landi *et al.*, 2013; Arango-Lopera *et al.*, 2013). It negatively impacts the ability to perform daily tasks, decreases overall quality of life, and increases the risk of injury and all-cause

mortality (Wheeler *et al.*, 1998; Swallow *et al.*, 2007). Studies on cross-sections of the vastus lateralis (thigh) muscle in elderly humans have demonstrated that age-associated muscle wasting is accounted for both by a reduction in individual muscle fibre size and a reduction in the total number of muscle fibres (Lexell, 1995). The fibres that shrank with age were predominantly type 2 (fast-twitch) fibres, whereas type 1 (slow-twitch) fibres did not get significantly smaller with age. Lastly, limb circumference was not a reliable indicator of muscle wasting since muscle was commonly replaced by fat and connective tissue in aged individuals.

The role of the individual factors affecting muscle mass homeostasis outlined above in age-associated muscle wasting is controversial. Many are difficult to investigate in human subjects directly, or have not been specifically investigated in aged animal models. The expression of Atrogin-1 and MuRF-1 in aged mice has been found to be either decreased (Edström *et al.*, 2006), increased (Clavel *et al.*, 2006), or unchanged (Gaugler *et al.*, 2011; Hwee *et al.*, 2014). Aged MuRF-1 knockout mice display a significant increase in Atrogin-1 expression, perhaps as a compensatory mechanism. However, these mice maintain their muscle mass into old age, as well as their ability to hypertrophy in response to muscle overload (Hwee *et al.*, 2014). This was associated with stronger activation of the Akt/mTOR pathway, suggesting an increase in the rate of protein synthesis. These results suggest that MuRF-1 activity promotes age-associated wasting, potentially by lowering protein synthesis rates.

A number of medical conditions are associated with a loss of muscle mass, including respiratory infections, chronic infections, and chronic inflammatory conditions like chronic obstructive pulmonary disease (COPD) (Seymour *et al.*, 2010; Vilaró *et al.*, 2010; Jones *et al.*, 2015). Many of these conditions occur more frequently with age. Patients with TB have significantly reduced lean tissue in their limbs (Paton & Ng, 2006). In COPD, acute exacerbations, which are commonly caused by respiratory infections like RSV, cause deterioration of limb muscle function and cross-sectional area of quadriceps muscle (Spruit *et al.*, 2003; Pitta *et al.*, 2006). Moreover, muscle wasting as measured by quadriceps

strength is predictive of mortality in patients with moderate to severe COPD (Swallow *et al.*, 2007). Various aspects of an infection are likely to contribute to muscle wasting. Firstly, there is a well-known role for inflammation in promoting muscle atrophy. Secondly, an infection, particularly in elderly people where the infection is likely to be more severe, commonly leads to bedrest, causing muscle atrophy by disuse (muscle "unloading"). Influenced by both those factors, infection may also induce a systemic redistribution of resources, during which muscle is broken down to metabolites to fuel other processes deemed more essential.

1.7.3.1. The role of inflammation in muscle wasting

Inflammation is a strong inducer of muscle atrophy and cachexia (Peterson, Bakkar & Guttridge, 2011). Cachexia is defined as severe loss of bodyweight, loss of muscle and fat mass, and increased protein catabolism as a result of chronic disease, commonly cancer (Muscaritoli *et al.*, 2010). Nuclear transcription factor kappa B (NF-κB) is a master transcriptional regulator of inflammation. Under homeostatic conditions, NF-κB is sequestered in the cytoplasm by interaction with an inhibitor, IκB, which masks the nuclear localisation sequence of NF-κB. Inflammatory cytokines, particularly TNFα, induce a signalling cascade that activates IκB kinase (IKK) complex. IKK complex phosphorylates IκB, which leads to its removal and degradation, allowing NF-κB to translocate to the nucleus and promote transcription (Schütze *et al.*, 1992). NF-κB is expressed by skeletal muscle and has been implicated in muscle wasting (Schiaffino *et al.*, 2013). For example, mice which overexpress IKKβ, a component of the IKK complex, in their muscles (causing constitutive activation of NF-κB) display profound muscle wasting (Cai *et al.*, 2004). This effect was found to be mediated by MuRF-1, since crossing the mice with MuRF-1-deficient mice partially rescued the muscle wasting phenotype. Conversely, muscle-specific deletion of IKKβ in mice (inhibiting NF-κB activation) prevented muscle atrophy in response to denervation (Mourkioti *et al.*, 2006). Muscle force and fibre type distribution was maintained, along with increased protein synthesis and decreased protein degradation as evidenced by lower expression of MuRF-1. Notably, in response to muscle

damage, these mice exhibited enhanced satellite cell activation and improved muscle regeneration.

At the same time as promoting muscle atrophic factors like MuRF-1, NF-κB also inhibits factors promoting muscle growth. For example, NF-κB signalling has been found to suppress post-transcriptional processing of MyoD1 mRNA (Guttridge *et al.*, 2000). Inflammatory cytokines are also known to induce insulin resistance, i.e. the downregulation of insulin receptor expression. Insulin signalling, similarly to the IGF-1-Akt pathway, promotes protein synthesis, so insulin resistance is likely to play a role in muscle wasting (Monier, Le Cam & Le Marchand Brustel, 1983). TNFα and IFNγ have been found to cause insulin resistance in muscle (De Alvaro *et al.*, 2004; Sestan *et al.*, 2018). For example, Sestan *et al.* demonstrated that the IFNγ produced during viral infection of mice suppressed insulin receptor expression on skeletal muscle, which was sufficient to derail glycemic control in obese mice. Unfortunately, the aspect of muscle wasting was not specifically investigated in this study. The authors propose that insulin resistance during infection is a systemic response with the aim to increase glucose availability for immune cells, particularly $CD8^+$ T cells. In this case any potential muscle wasting due to suppressed insulin signalling would be an unintended side effect (Kotas & Medzhitov, 2015).

1.7.3.2. Inflammation-induced anorexia promotes muscle wasting indirectly

Inflammation is also an important regulator of appetite, which indirectly contributes to muscle wasting. Loss of appetite (anorexia) is a key component of sickness behaviour together with reduced physical activity. Administration of pro-inflammatory cytokines, such as IL-1β, or a potent stimulator of inflammation such as LPS or IL-6, induces anorexia and ablates exploratory behaviour in mice and rats (Langhans, Savoldelli & Weingarten, 1993; Kent *et al.*, 1996; Bret-Dibat *et al.*, 1995). This phenomenon is thought to conserve bodily resources for immune defence. Since food consumption and exercise promote muscle growth (primarily via the IGF-1 pathway), the absence of these signals can poise the balance of muscle homeostasis towards atrophy.

Pro-inflammatory cytokines and prostaglandins can act directly on the nervous system in

multiple ways to cause anorexia. Firstly, pro-inflammatory cytokines can stimulate peripheral sensory neurons. Vagal, spinal and trigeminal sensory neurons express receptors for IL-1β and prostaglandin E_2 (PGE2), and IL-1β in particular can cause depolarisation in vagal sensory neurons (Ek *et al.*, 1998; Gaigé *et al.*, 2004). This connection between inflammatory signalling and neural signalling has been evident since the finding that severing the vagus nerve (vagotomy) attenuated LPS-induced anorexia in rodents (Laye *et al.*, 1995; Bret-Dibat *et al.*, 1995; Kent *et al.*, 1996). The primary targets of vagal nerves are the nucleus of the solitary tract (NTS) and the area postrema (AP), which are located in the brain stem. The main neurotransmitter in the terminals of the NTS is glutamate, and the administration of a glutamate receptor antagonist can attenuate inflammation-induced anorexia (Weiland *et al.*, 2006). However, vagotomy does not completely abolish inflammation-induced anorexia, suggesting that there are other ways in which inflammation can cause anorexia (Schwartz, Plata-Salaman & Langhans, 1997; Wieczorek *et al.*, 2005).

Pro-inflammatory cytokines can also act directly on the *central* nervous system. Intracerebroventricular administration of LPS, IL-1β, TNFα or IL-6 induces anorexia in mice (Kent *et al.*, 1992; Yao *et al.*, 1999; Plata-Salamán, 1996; Plata-Salamán *et al.*, 1996). This is possible because some areas of the brain, including the AP, are devoid of the blood-brain-barrier, so are accessible to circulating inflammatory factors (Rivest, 2003). Additionally, IL-1β and LPS signalling in the endothelial cells that make up the blood-brain-barrier stimulates the production of PGE2 within the intracranial cavity (Rivest, 1999). PGE2 directly acts on neurons important for feeding. Inhibition or deletion of PGE2 synthesising enzymes attenuates anorexia after peripheral LPS or IL-1β (Johnson *et al.*, 2002; Elander *et al.*, 2007). PGE2 binds G protein-coupled receptors expressed in the hypothalamus and NTS (Zhang & Rivest, 1999). The NTS integrates neural signals (primarily vagal signals from the gut) and humoral signals (inflammatory factors from circulation) to regulate satiety and food aversion (Schwartz 2000). Activated NTS neurons relay signals to other areas of the brain, such as the central amygdala and the hypothalamus, which results in suppression of feeding through poorly understood mechanisms (Ferreira *et al.*,

2006; Gaykema, Chen & Goehler, 2007). As described previously in this chapter, some cytokines can also promote muscle wasting directly, for example, TNFα promotes the expression of Atrogin-1 and MuRF-1 via NF-κB signalling.

1.7.3.3. The role of disuse in muscle wasting

Muscle disuse through inactivity reduces the rate of protein synthesis and increases protein breakdown in muscle (Kortebein *et al.*, 2007; Tanner *et al.*, 2015). Elderly people are more prone to muscle wasting due to inactivity. For example, Tanner *et al.* found that as little as five days of bed rest significantly reduced leg muscle mass and strength in elderly, but not young, adults (Tanner *et al.*, 2015). The muscles of older adults displayed reduced rates of protein synthesis and increased markers of proteolysis. Muscle mass and strength could be restored in elderly individuals by an 8-week rehabilitation programme of resistance exercise. Hindlimb suspension is a common animal model of muscle atrophy by disuse. Disuse activates many similar pathways as inflammation. For example, Hunter & Kandarian found that hindlimb suspension of mice induced rapid muscle atrophy, particularly of fast-twitch fibres (Hunter & Kandarian, 2004). This process was show to be driven by NF-κB activation in the muscle. *Nfkb1*-deficient mice did not exhibit the unloading-induced activation of NF-κB and were protected from muscle atrophy induced by hindlimb suspension. Work by the same group later found that hindlimb suspension increased the expression of Atrogin-1 and accumulation of ubiquitinated proteins. Electroporating the muscle to express dominant negative IκB (inhibiting NF-κB signalling) caused partial resistance to muscle atrophy induced by hindlimb unloading and suppressed the expression of Atrogin-1 and the accumulation of ubiquitinated proteins (Judge *et al.*, 2007).

The factors that regulate the balance between muscle hypertrophy and atrophy and how they change with age are of significant interest to a rapidly ageing society. Investigation into these mechanisms may enable us to predict the individual risk of muscle wasting, and potentially even counteract it.

1.8. Growth Differentiation Factor 15 (GDF-15)

In vitro studies by collaborators at the Kemp lab at Imperial College London had suggested that the orphan cytokine GDF-15 could promote muscle wasting in cultured myotubes by upregulating the expression of atrophy-promoting genes like *Fbox32* (Bloch *et al.*, 2013; Patel *et al.*, 2016). Serum GDF-15 levels are also known to increase with age and in a number of acute and chronic medical conditions (Fujita *et al.*, 2017; Brown *et al.*, 2002). This suggests that GDF-15 may play a role in promoting muscle wasting in the elderly during viral infections such as RSV. The role of GDF-15 in viral infectious disease had not been previously investigated.

1.8.1. The discovery of GDF-15

In 1997, Bootcov *et al.* used a subtraction cloning method to identify a novel cytokine whose expression was associated with macrophage activation (Bootcov *et al.*, 1997). This novel cytokine was assigned to the TGFβ superfamily on the basis of its structural similarity, but it had no strong sequence homology to any existing member. The cytokine was named macrophage inhibitory cytokine 1 (MIC-1) because of its ability to inhibit TNFα production by macrophages that had been activated with LPS *in vitro*. Curiously, MIC-1 mRNA expression was upregulated in the macrophages themselves upon stimulation with various pro-inflammatory cytokines such as IL-1β, IL2, or TNFα (Fairlie *et al.*, 1999). As a consequence, it was suggested that MIC-1 functions as an autocrine regulator limiting excessive macrophage activation during inflammation. Two other groups simultaneously identified the same cytokine, and named it placenta bone morphogenic protein (PLAB) and placental transforming growth factor beta (PTGFB), respectively (Hromas *et al.*, 1997; Lawton *et al.*, 1997). MIC-1 was “rediscovered” multiple times in different contexts, leading to additional names including nonsteroidal anti-inflammatory drug-activated gene 1 (NAG-1), prostate-derived factor (PDF), and growth differentiation factor 15 (GDF-15) (Baek *et al.*, 2001; Paralkar *et al.*, 1998; Böttner *et al.*, 1999). Here, the term GDF-15 will be used throughout to refer to this cytokine.

1.8.2. Clinical associations between GDF-15 and disease

Most cells are capable of expressing GDF-15, but macrophages and epithelial cells express it most readily (Böttner *et al.*, 1999). The major tissue sources of GDF-15 are the liver, kidneys, prostate, pancreas, lung, and white adipose tissue (Fairlie *et al.*, 1999; Ding *et al.*, 2009). It is also highly expressed by placental trophoblasts, which leads to high serum levels of GDF-15 during pregnancy (Moore *et al.*, 2000; Marjono *et al.*, 2003). On a molecular level, the expression of GDF-15 is induced by p53 amongst other factors, but is independent of NF-κB signalling (Li *et al.*, 2000; Yang *et al.*, 2003; Yamaguchi *et al.*, 2004).

In healthy, non-pregnant humans, serum levels of GDF-15 are generally low. The reported range of normal levels of GDF-15 varies, from 200 - 1200 pg/ml (Brown *et al.*, 2002). With advancing age, GDF-15 levels rise, but are highly variable across individuals (Fujita *et al.*, 2017). Smoking and high body mass index are also associated with higher serum levels of GDF-15 (Dostálová *et al.*, 2009; Brown *et al.*, 2012). GDF-15 expression is robustly upregulated by tissue injury and inflammation *in vitro*, and it is now well-established that serum GDF-15 levels are elevated in a wide range of disease states. High circulating levels of GDF-15 are found in conditions as diverse as cancer (Brown *et al.*, 2003; Welsh *et al.*, 2003), cardiovascular disease (Brown *et al.*, 2002) including acute heart failure (Kempf & Wollert, 2009; Cotter *et al.*, 2015) and pulmonary arterial hypertension (Nickel *et al.*, 2008), renal disease (Breit *et al.*, 2012), rheumatoid arthritis (Brown *et al.*, 2007), anorexia nervosa (Dostálová *et al.*, 2010), COPD (Husebø *et al.*, 2017), and diabetes (Dostálová *et al.*, 2009; Carstensen *et al.*, 2010). In many of these disease states, high circulating levels of GDF-15 are predictive of a poor outcome, such as cardiac events, or even mortality. High serum GDF-15 is also associated with all-cause mortality (Wiklund *et al.*, 2010). Due to its clear elevation in many medical conditions, there has been plenty of speculation on the physiological function and mechanism of action of GDF-15.

1.8.3. GDF-15 as an anorectic agent

Soon after its discovery, work using rodent models suggested that GDF-15 signalling

was involved in appetite regulation, specifically, it was found to promote anorexia (loss of appetite, from Greek *a(n)*- = without; *orexis* = appetite). Anorexia is a key feature of cancer cachexia and contributes strongly to morbidity and mortality in cancer. Mice with tumor xenografts overexpressing GDF-15 were found to become anorexic and lost a substantial amount of body mass including muscle and fat (Johnen *et al.*, 2007). This effect could be reversed with the administration of antibodies to GDF-15. Administration of recombinant GDF-15 induced a decrease in body weight and food intake in both lean wild-type mice and mice with genetic and diet-induced obesity (Mullican *et al.*, 2017; Yang *et al.*, 2017; Tsai *et al.*, 2018). These results may suggest that excessive GDF-15, such as would occur in a constitutive overexpression model, would yield a detrimental phenotype in mice, perhaps characterised by pathological anorexia resulting in starvation. However, multiple different transgenic mouse models of constitutive GDF-15 overexpression showed that mice with high serum levels of GDF-15 from birth are healthy and develop a lean phenotype (Johnen *et al.*, 2007; Macia *et al.*, 2012; Wang *et al.*, 2014). Interestingly, mice with constitutive GDF-15 overexpression were also resistant to developing obesity when placed on a high-fat diet, less likely to develop intestinal neoplasia in response to carcinogens, and had a longer life span than wild-type mice (Macia *et al.*, 2012; Chrysovergis *et al.*, 2014; Baek *et al.*, 2006; Wang *et al.*, 2014). These results suggested a more protective role for GDF-15. The fairly mild phenotypes of knockout and overexpression models suggested that GDF-15 signalling may be less important at steady state, but a potent regulator of appetite during disease states. Modulation of GDF-15 signalling was quickly recognised to have potential therapeutic applications in both obesity and anorexia/cachexia syndromes, but was held back by uncertainty as to its mechanism of action and the resulting unknown risks or potential side effects.

1.8.4. The discovery of GFRAL, the GDF-15 receptor

Since appetite regulation is to a large extent controlled by the brain, studies investigated if GDF-15 might exert its anorectic effects via the brain. Tsai *et al.* found that surgical ablation of the area postrema and nucleus solitary tract in the brain stem caused mice to

become resistant to the anorectic effect of GDF-15, suggesting that the action of GDF-15 was mediated by specific neurons in this area (Tsai *et al.*, 2014). In 2017, four groups simultaneously identified the receptor for GDF-15 (Mullican *et al.*, 2017; Hsu *et al.*, 2017; Yang *et al.*, 2017; Emmerson *et al.*, 2017). Three of the groups carried out screens of human cell membrane-associated proteins and one carried out a screen of orphan members of the glial-derived neurotrophic factor (GDNF) receptor α family. The only target found to bind GDF-15 was GDNF family receptor α–like (GFRAL), an orphan receptor in the GDNF family. GFRAL expression is highly restricted to neurons in two areas of the brain stem, the area postrema and the nucleus of the solitary tract. This is consistent with the previous finding that this area of the hind brain is essential for the anorectic action of GDF-15 (Tsai *et al.*, 2014). GDF-15 and GFRAL were found to signal via the co-receptor Ret. After GDF-15 has bound GFRAL, the complex binds Ret. Ret is phosphorylated and induces a signalling cascade through Akt, Erk and PLC-γ1 (Mullican *et al.*, 2017; Hsu *et al.*, 2017; Yang *et al.*, 2017; Emmerson *et al.*, 2017). GDF-15 binding to GFRAL induced a strong anorectic effect in animal models. GFRAL-knockout mice did not reduce food intake or lose weight in response to exogenous GDF-15, confirming that GDF-15's anorectic effects are mediated through GFRAL signalling (Hsu *et al.*, 2017; Mullican *et al.*, 2017). GFRAL KO mice mostly had normal body weight and food intake when fed a standard diet, but a high-fat diet caused increased food intake, weight gain, and impaired glucose tolerance compared to wild-type littermates in two of the studies (Hsu *et al.*, 2017; Mullican *et al.*, 2017). Emmerson *et al.* on the other hand did not find that GFRAL-knockout mice increased in weight after a high-fat diet. Interestingly, much like GDF-15-knockout mice, GFRAL-knockout mice had very little overt phenotype at steady state, with mostly normal body weight and composition. This suggests the role of GDF-15 lies not in constant homeostasis, but in the systemic response to stress conditions.

These findings suggest that any loss of muscle mass observed concomitantly to GDF-15 signalling is likely not a direct effect on the muscle, but is secondary to an anorexia-induced negative energy balance. However, alternative mechanisms of action of GDF-15

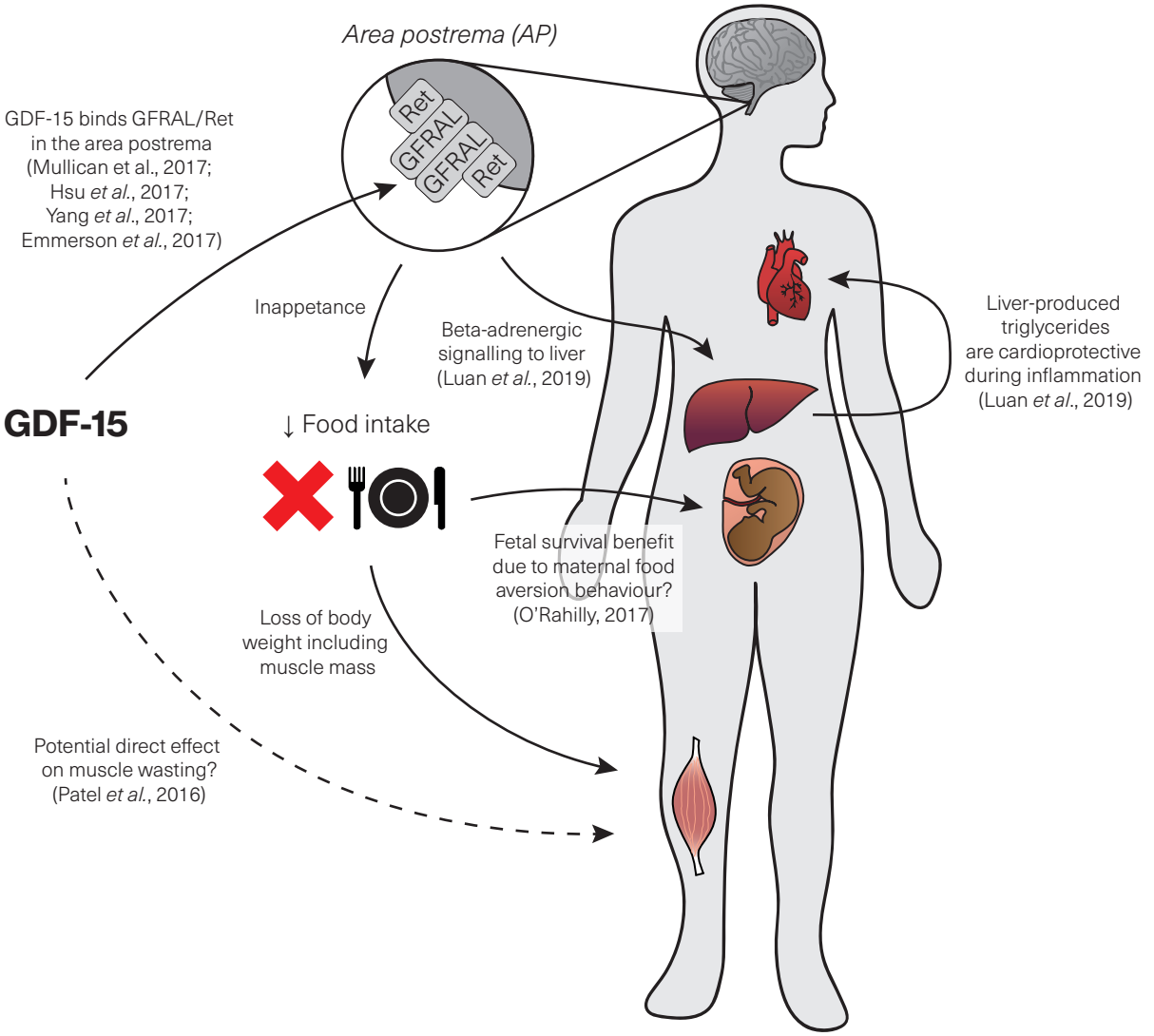

Figure 1-5 Our current understanding of GDF-15 signalling

Overview of our current understanding of GDF-15 signalling and effects. GDF-15 binds GFRAL/Ret complex in the area postrema (AP) in the hindbrain (Mullican *et al.*, 2017; Hsu *et al.*, 2017; Yang *et al.*, 2017; Emmerson *et al.*, 2017). Through poorly-understood mechanisms, this triggers a decrease in appetite and food intake, which can lead to the loss of body weight including muscle mass. It has been suggested that this food aversion behaviour is a protective mechanism that protects a fetus from noxious food stimuli during sensitive stages of development (O'Rahilly, 2017). GDF-15 binding GFRAL/Ret further induces beta-adrenergic signalling to the liver to stimulate release of triglycerides into the bloodstream (Luan *et al.,* 2019). These lipids are cardioprotective during acute inflammation such as viral and bacterial infections, suggesting a role for GDF-15 in promoting metabolic adaptation to systemic stress. Other signalling mechanisms of GDF-15 may exist, as suggested by Patel *et al.* (2016), but no other receptor for GDF-15 has been identified at this time.

have been suggested, as described in the following sections.

1.8.5. GDF-15 as an immunomodulator

GDF-15 has been implicated in various disease contexts where its action is not explained by its known role in appetite regulation or its interaction with GFRAL. For example, GDF-15-knockout mice are more susceptible to heart and kidney damage caused by an LPS model of sepsis, while overexpression of GDF-15 was protective (Abulizi *et al.*, 2017). In a mouse model of non-alcoholic fatty liver disease, GDF-15 deficiency exacerbated liver inflammation and fibrosis, whereas GDF-15 overexpression attenuated liver damage (Kim *et al.*, 2018). In GDF-15-knockout mice, there is excessive neutrophil recruitment to the infarcted heart, leading to increase risk of cardiac rupture. Recombinant GDF-15 led to downregulation of β2 integrins on neutrophils *in vitro*, thus preventing leukocyte adhesion and arrest on the endothelium (Kempf *et al.*, 2011). A similar mechanism was observed on platelets, with exogenous GDF-15 slowing thrombus formation and ameliorating pulmonary embolism in mice (Rossaint, Vestweber & Zarbock, 2013).

However, in other disease models, GDF-15 signalling was clearly detrimental. For example, in a mouse model of atherosclerosis, GDF-15-knockout mice had reduced macrophage infiltrates and decreased necrotic core formation in their sclerotic plaques, indicating better plaque stability. *In vitro*, GDF-15 promoted chemotaxis of macrophages by inducing CCR2 expression, suggesting that GDF-15 signalling drives atherosclerotic inflammation in a detrimental way (De Jager *et al.*, 2011). This stands in contrast to the original findings during the discovery of GDF-15 that it primarily inhibits macrophage function. In terms of infectious disease, in one study, GDF-15 overexpression in mice led to an exaggerated inflammatory response to human rhinovirus and increased viral load. The authors suggest this is caused by GDF-15-mediated suppression of interferon lambda in the lung (Wu *et al.*, 2018).

These studies are partially contradictory as to whether GDF-15 signalling is beneficial or detrimental, and its actions appear to be very context-dependent. Variability in results is probably also due to the use of different *in vitro* models, which may not reflect the sys-

temic activity of GDF-15, and different *in vivo* models, as it is known that different mouse strains can react very differently to the same stimulus. In conclusion, there is research still to be done on the immunomodulatory functions of GDF-15, if any are confirmed to be truly GDF-15-dependent.

1.8.6. GDF-15 as a protective mechanism against fetal toxicity

The location in the hindbrain where GFRAL is expressed, the area postrema, is also responsible for controlling emesis (vomiting). It is conceivable that GDF-15 signalling could contribute to food avoidance behaviour by causing nausea. O'Rahilly (2017) has suggested that the evolutionary purpose of the GDF-15/GFRAL axis is to be a fetal protection mechanism via the induction of food aversion. Serum GDF-15 levels rise rapidly in the first trimester of pregnancy, and remain elevated until delivery (Moore *et al.*, 2000; Marjono *et al.*, 2003). High circulating levels of GDF-15 during pregancy correlate to emesis, and a single nucleotide polymorphism (SNP) in the *Gdf15* gene is associated with hyperemesis gravidarum, a condition of severe nausea and emesis during pregnancy (Petry *et al.*, 2017; Fejzo *et al.*, 2018). O'Rahilly (2017) theorises that high GDF-15 levels decrease maternal food intake, limiting the exposure of the fetus to potentially toxic ingested substances. However, it is unclear whether the survival benefit to the fetus would be outweighed by the potentially severe restriction in nutrients.

1.8.7. The role of GDF-15 in skeletal muscle

The discovery of GFRAL as the receptor for GDF-15 and the further elucidation of its role as an appetite regulator are not consistent with GDF-15 having specific effects on skeletal muscle. No human or rodent cell line tested was found to endogenously express GFRAL, including L6 rat skeletal muscle cells, C2C12 mouse skeletal muscle cells, and primary human cardiac myocytes, challenging previous *in vitro* experiments claiming to have found brain-independent functions of GDF-15 (Mullican & Rangwala, 2018; Yang *et al.*, 2017). For example, Tsai *et al.* found that obese mice treated with GDF-15 lost more fat than muscle (Tsai *et al.*, 2018). Similarly, blocking GDF-15 in a cachexia model driven by GDF11 rescued appetite, but not loss of muscle mass (Jones *et al.*, 2018). These re-

sults suggest that GDF-15 does not specifically drive loss of muscle mass.

Two studies from the same group claim to have demonstrated that GDF-15 can directly promote muscle wasting. The authors propose that GDF-15 suppresses the expression of microRNA (miRNA) species that regulate muscle mass homeostasis, which in turn upregulates the expression of atrophy-promoting factors like Atrogin-1. Local overexpression of GDF-15 by electroporation into the tibialis anterior (TA) muscle (a large leg muscle in mice) caused a decrease in muscle fibre diameter (Patel *et al.*, 2016). No such change in muscle fibre size was observed in the other leg of each individual mouse, where the muscle was electroporated with an empty vehicle vector. This suggests that the expression of GDF-15 specifically, rather than the electroporation event, promoted muscle atrophy. TA muscles electroporated with GDF-15 were also significantly lighter than vehicle-electroporated muscles when normalised to the bodyweight of the mouse, but the raw muscle weight was not compared. Treatment of cultured myotubes with recombinant GDF-15 significantly upregulated the expression of muscle atrophy-promoting genes *Fbxo32* and *Trim63* (Atrogin-1 and MuRF-1) and downregulated the expression of miRNAs that positively regulate muscle mass by inhibiting Smad signalling (Bloch *et al.*, 2013). One of these miRNAs, miR-181a, suppressed TGFβ responses in myotubes. The authors hypothesise that GDF-15 may make muscles more sensitive to TGFβ-driven muscle wasting by inhibiting the expression of muscle-protective miRNAs like miR-181a.

These studies imply the existence of a GFRAL-independent, direct method of action of GDF-15 on muscle. However, it is still unclear how GDF-15 would signal into cells in this context. Additional research will be needed, for example, none of the experiments detailed above used GDF-15-blocking antibodies to test whether the results were indeed due to GDF-15 activity. Comparisons to other cytokines or positive controls were also not done. Recombinant GDF-15 has in some studies been found to activate the Smad pathway, which could promote muscle wasting similarly to myostatin signalling (Bloch *et al.*, 2015; Min *et al.*, 2016). However, this may not reflect true GDF-15 activity, since recombinant GDF-15 preparations from a major manufacturer were found to be contam-

inated with TGFβ. In these cases, Smad2 signalling could be ablated with anti-TGFβ antibodies, but not anti-GDF-15 antibodies (Okamura, 2015; Olsen *et al.*, 2017). Since TGFβ has a known atrogenic effect on muscle, many *in vitro* observations implicating GDF-15 in muscle wasting may in fact be due to TGF-β signalling.

Breit *et al.* suggest one potential alternative signalling mechanism for GDF-15 that is independent of brain stem signalling (Breit, Tsai & Brown, 2017). During characterisation of the GFRAL gene, an alternative transcript of GFRAL was identified, which lacks the transmembrane and cytoplasmic domain (Li *et al.*, 2005). If present at high enough levels, this truncated form may function as a soluble receptor, either mediating *trans* signalling on cells that do not express GFRAL themselves, or scavenging GDF-15 as a competitive inhibitor to brain stem signalling.

1.8.8. GDF-15 as a regulator of systemic stress responses

The role of GDF-15 in the context of infectious disease has not been extensively studied, but recent work by Luan *et al.* has suggested that GDF-15 may be a systemic regulator of responses to stressors such as infection (Luan *et al.*, 2019). Mice infected with influenza virus or with sepsis induced by cecal ligation and puncture had higher mortality when treated with a GDF-15-blocking antibody. However, blocking GDF-15 did not cause an increase in viral or bacterial load or inflammation, suggesting that GDF-15 was not directly involved with pathogen defence. Instead, the protective effects of GDF-15 were associated with neural signalling to the liver, stimulating triglyceride release into circulation. Maintenance of plasma triglycerides was required for cardiac function and maintenance of body temperature during infection, suggesting that GDF-15 regulates systemic metabolism in response to stress.

This is consistent with the various reports of metabolic disturbances in GDF-15 transgenic animals. For example, GDF-15-overexpressing mice have lower insulin levels, improved glucose tolerance, and increased oxidative metabolism (Wang *et al.*, 2014), whereas GFRAL-deficient mice displayed impaired glucose tolerance (Hsu *et al.*, 2017; Mullican *et al.*, 2017). The implication of body temperature maintenance had been pre-

viously investigated by Chrysovergis *et al.*, who found that GDF-15-overexpressing mice had increased expression of genes promoting thermogenesis and lipolysis in their white and brown adipose tissue (Chrysovergis *et al.*, 2014). The signalling downstream of GDF-15 binding GFRAL is still incompletely elucidated. Appetite regulation and systemic metabolic regulation may be the dominant effects, but others may well exist and be physiologically relevant.

1.9. Interleukin 6 (IL-6)

Preliminary experiments in the Culley group had shown that IL-6 protein was strongly elevated in the BAL fluid of elderly mice at the peak of RSV infection. Elevated IL-6 levels are also known to be a characteristic component of "inflammageing", the constitutive low-grade inflammation sometimes observed with ageing (Franceschi *et al.*, 2006). It was hypothesised that modulating IL-6 signalling may remove excess inflammation and thus improve the outcome of RSV infection in elderly mice. Simultaneously, IL-6 was known to affect both skeletal muscle mass and the germinal centre response, hence other effects of IL-6 modulation were also expected.

1.9.1. IL-6 signalling pathways

Interleukin 6 (IL-6) was originally described as a factor with the ability to promote the proliferation and activation of T cells, as well as the differentiation of B cells, primarily into antibody-secreting plasma cells (Klimpel, 1980; Yoshizaki *et al.*, 1984; Hirano *et al.*, 1986). Since then, many additional functions of IL-6 have been elucidated, yielding a picture of a complex, truly pleiotropic cytokine with both homeostatic, pro-inflammatory, and anti-inflammatory effects.

IL-6 is produced by almost all stromal cells and cells of the immune system (Hunter & Jones, 2015). IL-6 expression is induced by many different triggers, including IL-1β, TNF-α, TLR signalling, and prostaglandins, and its expression is controlled by a complex system of miRNAs, circadian factors, and RNAses (Viswanathan *et al.*, 2009; Masuda *et al.*, 2013; Sugimoto *et al.*, 2014). The receptor for IL-6 consists of a specific alpha-recep-

tor subunit (IL-6R) and the universal beta-receptor subunit gp130, which is responsible for signal transduction (Yamasaki *et al.*, 1988; Taga *et al.*, 1989; Hibi *et al.*, 1990). Gp130 is expressed ubiquitously on both immune and non-immune cells and also forms part of the receptor complexes for IL-11, IL-27, and a number of other cytokines (Yoshida *et al.*, 1996; Heinrich *et al.*, 2003). The expression of IL-6R is restricted to hepatocytes, neutrophils, monocytes, macrophages, and some lymphocytes (Kopf *et al.*, 1994; Jones *et al.*, 2010).

Multiple pathways can be activated downstream of IL-6 engagement of the IL-6R/gp130 complex. The best-characterised pathway activated by IL-6 signalling is the Jak/STAT pathway (Heinrich *et al.*, 2003). Gp130 dimerisation activates Jak kinases, which recruit and phosphorylate STAT1 and STAT3 transcription factors. The above describes 'classical' IL-6 signalling, where free IL-6 binds to the IL-6R/gp130 complex on the membrane of a cell. The classical signalling pathway is restricted to cells which express both IL-6R and gp130. However, it is known that IL-6 can also signal through the 'trans' signalling pathway. During trans-signalling, IL-6 complexes with a soluble form of the IL-6R (sIL-6R), which increases the half-life of IL-6 in circulation, and allows signalling through any cell that expresses gp130 (Peters *et al.*, 1996).

Classical IL-6 signalling is thought to be mainly responsible for the role of IL-6 in the acute phase response to infection, as well as homeostatic functions such as regulating glucose metabolism, hyperthermia, fatigue and appetite loss (Schöbitz *et al.*, 1995). IL-6 trans-signalling is involved in the recruitment and apoptosis of leukocytes, maintenance of T cell effector function, and the activation of stromal tissue during inflammation (Jones, 2005; Campbell *et al.*, 2014). sIL-6R is produced predominantly by monocytes and activated T cells (Atreya *et al.*, 2000; Nowell *et al.*, 2009; Briso, Dienz & Rincon, 2008; Jones *et al.*, 2010). The expression of IL-6R in $CD4^+$ T cells is mostly limited to naïve and central memory subsets (Briso, Dienz & Rincon, 2008; Jones *et al.*, 2010). sIL-6R is generated by proteolytic cleavage of membrane-bound IL-6R, catalysed by the proteases ADAM17 and ADAM10 in humans, and ADAM10 alone in mice (Garbers *et al.*, 2011;

Baran *et al.*, 2013). In humans, alternative splicing of *Il6ra* mRNA also contributes to sIL-6R production (Jones *et al.*, 2001). To complicate matters, gp130 also exists in a soluble form, sgp130, which can block trans-signalling by IL-6/sIL-6R complexes (Diamant *et al.*, 1997; Jostock *et al.*, 2001; Richards *et al.*, 2006).

Transgenic mouse models either removing a component or producing it in excess can shed light on the component's physiological function. Mouse strains which overexpress IL-6 are more prone to developing a host of disorders including multiple myeloma, neurological disorders, pulmonary fibrosis and hypertension (Suematsu *et al.*, 1989; Campbell *et al.*, 1993; DiCosmo *et al.*, 1994; Steiner *et al.*, 2009). Overexpression of IL-6 *in vivo* also inhibits the generation of inducible T regulatory cells (Tregs), but does not affect natural Tregs (Fujimoto *et al.*, 2011). IL-6- and IL-6R-knockout mice do not always display the same phenotype. For example, IL-6-deficient mice display a delay in wound healing, that IL-6R-deficient mice do not, but double-knockout mice display improved wound healing relative to IL-6-deficient mice (McFarland-Mancini *et al.*, 2010). Generally, IL-6- and IL-6R-deficient mice commonly display impairments in their response to infection, including a blunted antibody response and increased morbidity and mortality (Kopf *et al.*, 1994; Dienz *et al.*, 2012). IL-6R-deficient mice also display metabolic changes such as insulin resistance (Mauer *et al.*, 2014).

1.9.2. IL-6 in age

At steady state, serum levels of IL-6 in young, healthy humans are generally low, ranging from 1-5pg/ml. IL-6 levels rapidly rise in response to infection and can reach high levels in disease contexts like cancer, autoimmunity or septic shock (Waage *et al.*, 1989; Panichi *et al.*, 2004; Fraunberger *et al.*, 2006; Mroczko *et al.*, 2010). Serum levels of IL-6 increase with age and are a strong predictor of morbidity and mortality (Puzianowska-Kuźnicka *et al.*, 2016). This may be due to the process of "inflamm-ageing", a state of detrimental chronic inflammation sometimes observed with advancing age (Franceschi *et al.*, 2006). Since IL-6 can have strong pro-inflammatory effects, it is likely that IL-6 contributes to inflammageing.

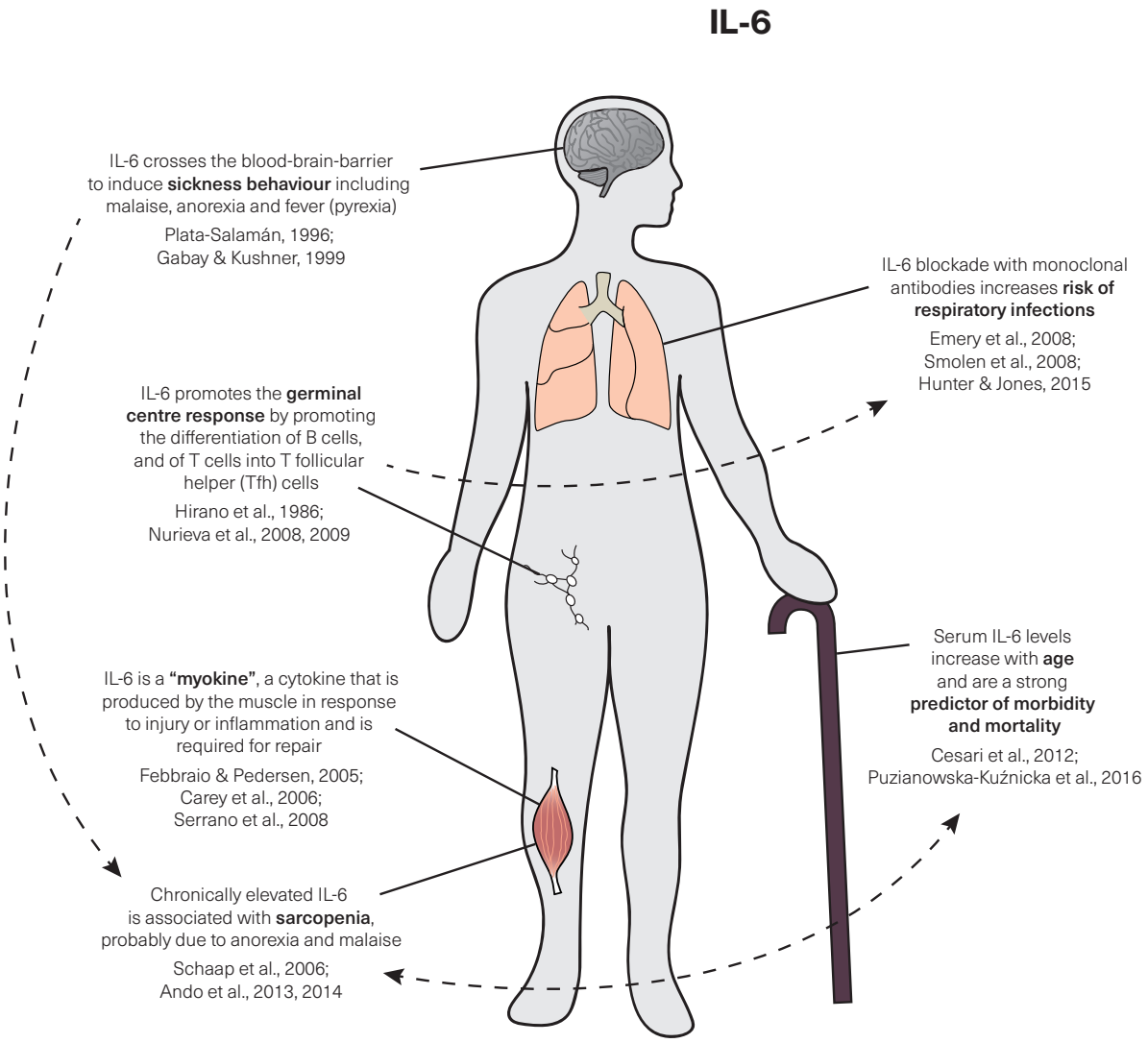

Figure 1-6 Overview of functions of IL-6

Overview of a selection of the effects of IL-6 signalling. IL-6 is a highly pleiotropic cytokine with disparate functions dependent on the biological context. Serum levels of IL-6 generally increase with age, and predict morbidity and mortality in the elderly (Cesari et al., 2012; Puzianowska-Kuźnicka et al., 2016). This increase in morbidity and mortality may in part be due to the effect of IL-6 on skeletal muscle. Chronically elevated IL-6 levels have been associated with sarcopenia and loss of muscle mass (Schaap et al., 2006; Ando et al., 2013, 2014). IL-6 may cause sarcopenia in various ways, including by inducing anorexia, fever, and malaise by signalling through the blood-brain-barrier to promote prostaglandin PGE2 production (Plata-Salamán, 1996; Gabay & Kushner, 1999). However, there is also evidence that IL-6 promotes muscle repair, since it is upregulated in response to exercise and injury and promotes the differentiation of satellite cells (Febbraio & Pedersen, 2005; Carey et al., 2006; Serrano et al., 2008). IL-6 is known to promote the germinal centre response by promoting the differentiation of B cells into antibody-secreting plasma cells and of T cells into T follicular helper (Tfh) cells (Hirano et al., 1986; Nurieva et al., 2008, 2009). This function may be the reason why therapeutic blockade of IL-6 signalling for other purposes has been associated with an increased risk of infections of the respiratory tract, gastro-intestinal tract, and urinary tract (Emery et al., 2008; Smolen et al., 2008; Hunter & Jones, 2015).

1.9.3. IL-6 in innate immunity

IL-6 is involved in the regulation of multiple aspects of the innate immune system, including haematopoiesis, granulopoiesis, and macrophage activity. IL-6 co-operates with granulocyte colony stimulating factor receptor (G-CSFR) to stimulate granulopoiesis, determining the production of neutrophils, eosinophils and basophils (Liu *et al.*, 1997).

IL-6 trans-signalling is a key regulator of immune cell recruitment during the innate immune response. Neutrophils express high levels of IL-6R, and readily shed IL-6R to create sIL-6R when activated (Modur *et al.*, 1997). High levels of sIL-6R activate neighbouring endothelial cells to produce cytokines including IL-6, adhesion molecules such as ICAM-1 and E-selectin, and CC and CXC chemokines which promote recruitment of mononuclear leukocytes (Modur *et al.*, 1997; Hurst *et al.*, 2001; McLoughlin *et al.*, 2004). Crucially, this trans-signalling appears to suppress the expression of the classical neutrophil recruitment chemokines CXCL1 and CXCL8, suggesting that IL-6 is crucial to support the transition from early neutrophil infiltration to later mononuclear leukocyte recruitment during inflammation (McLoughlin *et al.*, 2004). This is demonstrated by the fact that IL-6 KO mice display impaired leukocyte accumulation due to reduced chemokine production at the site of inflammation (Romano *et al.*, 1997).

IL-6 can promote macrophage differentiation and drive an alternatively activated phenotype associated with wound healing. IL-6 promotes the differentiation of monocytes into macrophages rather than dendritic cells (DCs) (Chomarat *et al.*, 2000; Bleier *et al.*, 2004). *In vitro*, IL-6 promotes the expression of macrophage colony stimulating factor (M-CSF) receptors on monocytes. This allows the monocytes to bind M-CSF (partially in an autocrine way) and promotes the macrophage lineage (Chomarat *et al.*, 2000). *In vitro*, IL-6-deficient bone marrow produces large amounts of dendritic cells when stimulated with GM-CSF, but *in vivo*, IL-6-deficient mice had equivalent numbers of DCs to WT mice (Bleier *et al.*, 2004). Mice whose myeloid cells are deficient in IL-6R are unable to generate alternately activated macrophages in response to IL4, suggesting that IL-6 together with IL4 is required for alternative polarization of macrophages, which have anti-inflammatory

and wound healing effects (Mauer *et al.*, 2014). Additionally, IL-6 can directly inhibit macrophage microbicidal activity and inhibit pro-inflammatory cytokine production (Silver *et al.*, 2011; Nagabhushanam *et al.*, 2003). IL-6 also has a role in barrier function and gut mucosal integrity. IL-6 produced by myeloid cells in the lamina propria protects intestinal epithelial cells (IECs) from apoptosis, which depending on the conditions can promote neoplastic growth and intestinal carcinomas, but also protects epithelial cells in models of acute colitis (Grivennikov *et al.*, 2009; Barkhausen *et al.*, 2011; Spehlmann *et al.*, 2013).

1.9.4. IL-6 in adaptive immunity

IL-6 is a key driver of multiple aspects of adaptive immunity. One of the earliest observations about IL-6 was that it was a strong inducer of antibody secretion by B cells (Yoshizaki *et al.*, 1984; Hirano *et al.*, 1986). IL-6 overexpression in mice leads to IgG1 plasmacytosis, and blockade of IL-6R with an antibody conversely inhibits plasmacytoma (Suematsu *et al.*, 1989; Coulie, Vink & Van Snick, 1990). IL-6-deficient mice mount weaker IgG and IgA responses, which can be rescued with recombinant IL-6 (Kopf *et al.*, 1994; Ramsay *et al.*, 1994). IL-6 promotes the survival, population expansion, and maturation of B cells, primarily to drive the plasmablast and plasma cell fates (Kawano *et al.*, 1995; Jourdan *et al.*, 2014). However, the beneficial effect of IL-6 on the humoral immune response may also in part be indirect, via the action of IL-6 on T follicular helper (Tfh) cells. IL-6 is required for the differentiation of T cells into Tfh cells. IL-6 controls the expression of IL-21 in T cells and upregulates the expression of Bcl6, which promotes commitment to a Tfh cell fate (Nurieva *et al.*, 2008, 2009; Dienz *et al.*, 2009; Harker *et al.*, 2011). Tfh cells in turn promote B cell proliferation and immunoglobulin class switching in lymphoid follicles in germinal centres. Thus IL-6 contributes to the generation of a functional antibody response in multiple ways.

IL-6 also plays a role in promoting the type-17 phenotype of T cells. This subset of T cells can be either $CD4^+$ (Th17 cells) or $CD8^+$ (Tc17 cells) and is characterised by the secretion of IL-17. Exposure of a naïve T cell to IL-6 and TGF-β activates STAT3 signalling and the transcription factor RORγt (Veldhoen *et al.*, 2006; Ivanov *et al.*, 2006; Zhou *et al.*, 2007).

This promotes expansion and the increased secretion of IL17. In humans, the differentiation of Th17 cells does not require TGF-β (Acosta-Rodriguez *et al.*, 2007). Th17 cells have physiological roles in the defence against fungal and bacterial diseases and promoting mucosal barrier functions, but can become pathogenic and cause local tissue damage in chronic inflammatory diseases such as rheumatoid arthritis (Langrish *et al.*, 2005; Bär *et al.*, 2014; Li, Casanova & Puel, 2018). This is evidenced by the fact that suppression of IL-17 or IL-6 improves experimental inflammatory conditions in mice, and that therapeutic targeting of IL-6 has some efficacy in treating rheumatoid arthritis (Langrish *et al.*, 2005; Nowell *et al.*, 2009; Jones, Scheller & Rose-John, 2011).

However, IL-6 can also promote anti-inflammatory responses. For example, IL-6 signalling promotes the production of the anti-inflammatory cytokine IL-10 by T cells. T helper type 1, 2, and 17 cells can be induced to produce IL-10 in this manner, which is dependent on STAT3 signalling (Stumhofer *et al.*, 2007; McGeachy *et al.*, 2007). This suggests that IL-6 also has a balancing role, in which it can both drive Th17 differentiation, but also restrain the pathogenic potential of this subset by inducing IL-10. Furthermore, IL-6 can inhibit Treg cell function in the presence of TLR signalling and prevents the conversion of T cells (particularly Th17) to Treg cells (Pasare & Medzhitov, 2003; Korn *et al.*, 2008). Overexpression of IL-6 *in vivo* inhibits the generation of inducible Tregs, but does not affect natural Tregs (Fujimoto *et al.*, 2011).

1.9.5. IL-6 in infectious disease

As described above, IL-6 has many and varied roles in the immune system. IL-6 can act as a pro-inflammatory cytokine and is elevated systemically in many infectious diseases.

IL-6-deficiency in mice generally correlates with a higher susceptibility to infection, emphasising its key role in pathogen defence. Mice deficient in IL-6 or IL-6R display increased susceptibility and mortality from influenza virus A (IAV) infection (Dienz *et al.*, 2012; Lauder *et al.*, 2013). This phenomenon was variably credited to impaired neutrophil-mediated viral clearance or impaired anti-viral T cell response in the absence of IL-6 signalling. IL-6-deficient mice also fail to control infection with vaccinia virus or *Listeria*

monocytogenes and mount an impaired IgG response to VSV (Kopf *et al.*, 1994). IL-6R-deficient mice are more susceptible to LPS endotoxemia than wild-type mice (Mauer *et al.*, 2014). Pyle *et al.* found that in young mice, IL-6 signalling early during RSV infection was essential to prevent excessive immunopathology (Pyle *et al.*, 2017). This mechanism was due to the induction of IL-27, which promotes Treg cells that dampen the immune response. This stands in contrast to the ability of excess IL-6 to prevent Treg differentiation, which may be due to differing inflammatory environments (Fujimoto *et al.*, 2011). The ability of IL-6 to prime Th17 may be counterproductive in a setting of viral infections since Th17 responses are anti-apoptotic, which might block the effects of cytotoxic T cells on virus-infected cells (Hou, Kang & Kim, 2009; Slaats *et al.*, 2016).

In humans, a number of naturally occurring mutations emphasise the importance of IL-6 signalling to pathogen defence. Children with autoantibodies to IL-6 develop recurrent staphylococcal infections and abscesses of the skin (Puel *et al.*, 2008). People with mutations in the gene that encodes STAT3, a transcription factor crucial for IL-6 signal transduction, have strongly impaired innate and adaptive immune responses and have recurrent skin, lung and gut infections that can be fatal (Freeman & Holland, 2010).

Due to its clear implication in detrimental inflammation, there have been attempts to block IL-6 signalling therapeutically in multiple disease contexts. Siltuximab is a monoclonal antibody against IL-6 itself, and Tocilizumab is a monoclonal antibody against IL-6R. Siltuximab is effective in the treatment of multicentric Castleman's disease, a condition characterised by systemic inflammation and excessive lymphoproliferation (Sarosiek, Shah & Munshi, 2016). Tocilizumab has shown effectiveness in treating inflammatory rheumatoid arthritis (Emery *et al.*, 2008; Smolen *et al.*, 2008). However, neither siltuximab nor tocilizumab have proven successful in the treatment of a number of other diseases, including cancers or inflammatory conditions such as psoriasis or Crohn's disease (Ito *et al.*, 2004; Jones, Scheller & Rose-John, 2011). Additionally, treatment with either siltuximab and tocilizumab has been consistently found to increase the susceptibility to infectious disease (Emery *et al.*, 2008; Smolen *et al.*, 2008). The types of infections

associated with IL-6-blockade treatment are predominantly infections of the respiratory, urinary and GI tracts, which may imply impaired barrier function in the absence of IL-6 signalling (Hunter & Jones, 2015). Treatment with Tocilizumab for rheumatoid arthritis was found to have side effects of serious bacterial infection, skin infections, soft tissue infections, and diverticulitis (Pawar *et al.*, 2019). A study evaluating Tocilizumab for the treatment of atopic dermatitis found it was effective but led to bacterial superinfection in some treated patients (Navarini, French & Hofbauer, 2011). These findings highlight that IL-6 plays a key role in the protection against infectious disease and that blockade of IL-6 signalling carries some risk.

1.9.6. IL-6 and muscle wasting

In response to exercise, skeletal muscle produces large amounts of IL-6 and releases them into circulation (Steensberg *et al.*, 2000). On this basis, IL-6 has been considered the prototypical "myokine", a cytokine produced by skeletal muscle (Febbraio & Pedersen, 2005). The effect of IL-6 signalling on skeletal muscle itself is controversial. Studies using IL-6-knockout mice have demonstrated that IL-6 has the potential to induce muscle hypertrophy by stimulating the proliferation of satellite cells (Serrano *et al.*, 2008). Myogenin expression is significantly reduced in the muscles of IL-6-deficient mice after muscle overload, suggesting impaired repair and growth in the absence of IL-6. IL-6 expression is also increased in myofibers and satellite cells during muscle overload, suggesting a role in hypertrophy (Serrano *et al.*, 2008). IL-6 produced by muscle during muscle overload also fulfils paracrine functions by regulating metabolism and stimulating glucose production. IL-6R-deficient mice display insulin resistance (Mauer *et al.*, 2014), and IL-6-deficient mice develop obesity and glucose intolerance (Matthews *et al.*, 2010; Wallenius *et al.*, 2002). Infusion of IL-6 stimulates glucose uptake in the muscles of humans, by a mechanism that was shown in myotubes to be due to the increased expression of GLUT4 on the plasma membrane (Carey *et al.*, 2006). IL-6 also causes lipolysis and fatty acid oxidation in skeletal muscle (Van Hall *et al.*, 2003; Wolsk *et al.*, 2010). By these mechanisms, IL-6 is able to promote muscle repair, growth and function.

However, the beneficial role of IL-6 in muscle may be restricted to short-term, acute IL-6 signalling, such as occurs during exercise-induced damage, which requires some amount of inflammation to adequately repair. Prolonged IL-6 signalling may represent an unphysiological state which leads to dysregulation of muscle homeostasis. Since IL-6 is commonly elevated in chronic inflammatory conditions which often involve muscle wasting, high IL-6 levels are frequently associated with muscle wasting, but may not be causative. For example, circulating IL-6 levels are inversely proportional to quadriceps strength of patients with acutely exacerbating COPD (Spruit *et al.*, 2003). Higher serum levels of IL-6 are predictive of decreased muscle strength, sarcopenia, disability, and mortality in older humans (Payette *et al.*, 2003; Schaap *et al.*, 2006; Cesari *et al.*, 2012). Mouse models provide some mechanistic evidence for a role of IL-6 in promoting muscle wasting. In cancer cachexia mouse models, blocking IL-6 suppresses cachexia, and transgenic mice overexpressing IL-6 display profound muscle wasting, a phenotype which can be reversed by blockade of IL-6R (Strassmann *et al.*, 1992; Tsujinaka *et al.*, 1995, 1996). Blockade of IL-6 signalling in humans can likewise ameliorate some types of muscle wasting. Siltuximab treatment increases lean and fat mass in multicentric Castleman's disease patients compared to placebo (Sawyer *et al.*, 2014), and tocilizumab increases appetite and ameliorates weight loss in both humans and mice with cancer cachexia (Ando *et al.*, 2013, 2014). A different anti-IL-6 monoclonal antibody, clazakizumab, ameliorated muscle wasting in a small study of cachectic lung cancer patients (Rigas *et al.*, 2010). However, the exact mechanism by which IL-6 promotes muscle wasting is unclear. Apart from direct, potentially autocrine effects on muscle, IL-6 may indirectly contribute to muscle wasting by generally promoting a pro-inflammatory, pro-catabolic environment (Muñoz-Cánoves *et al.*, 2013). High levels of inflammation promote sickness behaviour which often includes anorexia. Over longer time periods, anorexia leads to loss of lean and fat mass. IL-6-overexpressing mice or wild-type mice treated with IL-6 display growth defects and decreased IGF-1 levels, a phenotype which could be reversed with a monoclonal antibody to IL-6 (De Benedetti *et al.*, 1997). Crucially, there

was no difference in food intake between untreated mice and IL-6-overexpressing or IL-6-treated mice, suggesting that the effect of IL-6 on growth was independent of anorexia caused by systemic inflammation. IL-6 may contribute to muscle wasting including sarcopenia by inhibition of IGF-1 production and activity. In a cohort of elderly people, IGF-1 was independently associated with grip strength and muscle power only in subjects in the lowest tertile of plasma IL-6 levels, but not in those in the highest tertile (Barbieri *et al.*, 2003). This suggests that IL-6 negatively regulates the production of IGF-1 so as to induce muscle wasting. This effect was linked to the ability of IL-6 to stimulate hepatic expression of IGF-1 binding protein 4 (IGFBP-4) *in vitro*, a protein which binds and blocks IGF-1 activity (Fernández-Celemín & Thissen, 2001). IGF-1 production was also significantly decreased in mice treated with exogenous IL-6 (De Benedetti *et al.*, 1997).

A key cellular mediator of IL-6 signalling is the transcription factor STAT3. STAT3 has been suggested to promote muscle wasting because infusing muscles of rats with IL-6 induces muscle atrophy concomitantly with increased STAT3 phosphorylation, and decreased phosphorylation of ribosomal S6 kinase, which promotes protein synthesis (Haddad *et al.*, 2005). In this study, the expression of Atrogin-1 and MuRF-1 were not increased by IL-6 treatment, but IGF-1 mRNA was increased. This may be because the amounts of IL-6 delivered were very small, as may be produced during moderate exercise, and delivered directly into the muscle (500,000-fold lower than De Benedetti *et al.*, 1997). Muscle-specific knockout of *Stat3* was able to prevent muscle wasting in mouse models of chronic kidney disease or acute diabetes (Zhang *et al.*, 2013). Using myotubes, STAT3 was found to promote muscle wasting by stimulating the expression of myostatin.

There is also evidence that IL-6 stimulates proteolysis in the muscle, although the exact mechanism is unclear. It is possible that this is mediated by increased myostatin production as described above. Tsujinaka *et al.* in the earliest IL-6 overexpression models already found that IL-6 transgenic mice, which were atrophic, had increased mRNA and protein levels of the lysosomal cathepsins B and L in their muscles (Tsujinaka *et al.*, 1995, 1996). Increased activity of the 26S proteasome and cathepsin B and L was also

identified in myotube cultures treated with IL-6 (Ebisui *et al.*, 1995). In mice genetically predisposed to cachexia, IL-6 overexpression was associated with increased expression of Atrogin-1 and Atg5, a driver of autophagy, (White *et al.*, 2012). Although a direct link of IL-6 to muscle wasting is still elusive, the epidemiological evidence strongly suggests that IL-6 is a potent contributor to an atrogenic environment, particularly in the elderly. Any benefit from the blockade of IL-6 signalling however must be carefully balanced against the crucial role of IL-6 in the defence against pathogens.

1.10. Study rationale

Little is known as to why RSV causes more severe disease in the elderly population, but age-related changes in anti-viral immunity that drive excess inflammation are likely to contribute. Pro-inflammatory cytokines are known to promote muscle loss in humans and mice (Patel *et al.*, 2016; Peterson, Bakkar & Guttridge, 2011). These observations suggest that respiratory viral infections are important in promoting frailty in the elderly. Despite its clinical importance, the relationship between respiratory viral infection and muscle wasting, particularly in the elderly, is not well understood. This study aims to investigate muscle atrophy in a model of RSV infection in elderly mice. This model recapitulates the severe disease caused by RSV in elderly humans (Zhang *et al.*, 2002b). RSV infection in elderly mice leads to more severe illness than in young mice, including impaired viral clearance, enhanced cellular inflammation and tissue damage in the lungs, cytokine production, and delayed recovery compared to young mice. Furthermore, infection in elderly mice results not only in acute loss of body weight, but in a sustained weight deficit, long after recovery from the acute illness. This may correspond to a disproportionate loss of muscle mass. This study will develop multiple outputs for assessing the state of skeletal muscle in the elderly RSV mouse model, and correlate this to inflammatory responses. This will be the first detailed study of the potential mechanisms of muscle atrophy initiated during respiratory viral infection in the elderly. Understanding the pathways and mediators that promote muscle loss following respiratory infection could lead to new therapies that combat frailty in the elderly.

1.10.1. Hypotheses

- Elderly mice respond differently to RSV infection than young mice
- Increased inflammation during RSV infection drives loss of skeletal muscle mass in elderly mice

1.10.2. Aims

- Establish levels of muscle wasting in elderly mice with RSV infection
- Determine which pathways and/or mediators are altered during RSV infection in the elderly
- Block those mediators to attempt to stop wasting and identify therapeutic targets

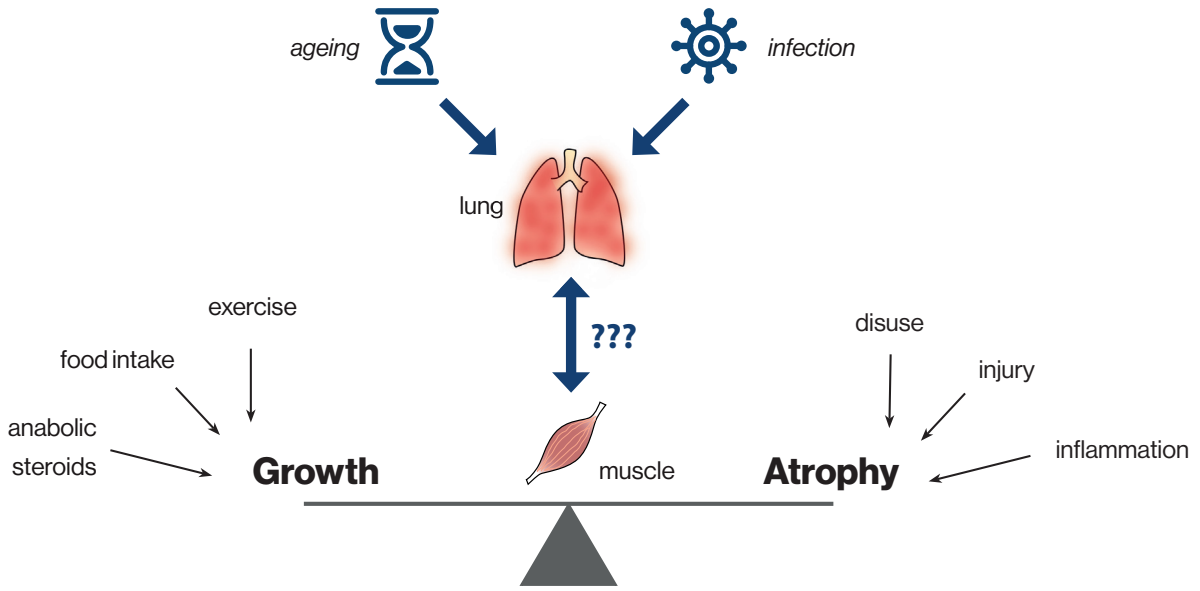

Figure 1-7 Summary diagram of hypothesis

Skeletal muscle exists in a balance between growth and atrophy. Muscle growth can be promoted by food intake, exercise, and anabolic steroids. Muscle atrophy can be caused by disuse (inactivity), injury of the muscle, or inflammation. This study aims to investigate how respiratory viral infection interacts with muscle wasting in the elderly.

2.

Materials and Methods

Chapter 2. Materials and Methods

2.1. Materials

2.1.1. Animals

All animals were purchased from Charles River Laboratories (Margate, United Kingdom). Female C57BL/6 mice were purchased either at age 8-10 weeks (hereafter called "young" mice) or 77+ weeks (~18 months; hereafter called "elderly" mice). Animals were housed in individually ventilated cages with food and water *ad libitum* at the animal facility of St Mary's Hospital (Imperial College London, UK). Animals were allowed to acclimatise for one week prior to any experimental procedures being conducted. All animal experiments were conducted in accordance with the United Kingdom's Home Office standards under the Animals (Scientific Procedures) Act, 1986 and were approved by the Animal Welfare and Ethical Review Board (AWERB) at Imperial College London.

2.1.2. Consumables

Table 2-1 Consumables

Product	Supplier
96-well round bottom plates	Corning, Corning, NY, USA
Axygen® Maxymum Recovery® filter pipette tips (1000µl)	Corning, Corning, NY, USA
Bijou 7ml sample containers	Thermo Fisher Scientific, Waltham, MA, USA
CELLSTAR® 175cm2/75cm2 cell culture flasks	Greiner Bio-One, Kremsmünster, AU
CELLSTAR® 96-well V-bottom/flat-bottom plates	Greiner Bio-One, Kremsmünster, AU
CELLSTAR® centrifuge tubes (15ml/50ml)	Greiner Bio-One, Kremsmünster, AU
CELLSTAR® serological pipettes	Greiner Bio-One, Kremsmünster, AU
Cryo.s™ freezing tubes ("cryotubes")	Greiner Bio-One, Kremsmünster, AU
DIAMOND Tipack filter pipette tips (10µl, 30µl, 100µl, 200µl)	Gilson, Middleton, WI, USA
DIAMOND Towerpack pipette tips (1000µl, 200µl)	Gilson, Middleton, WI, USA
EASYstrainer™ cell sieve (100µm)	Greiner Bio-One, Kremsmünster, AU
Microcentrifuge tubes (1.5ml)	Thermo Fisher Scientific, Waltham, MA, USA
gentleMACS C Tubes	Miltenyi Biotec, Bergisch Gladbach, Germany
MicroAmp™ Optical 96-Well Reaction Plate with Barcode	Applied Biosystems, Warrington, UK
MicroAmp™ Optical adhesive film	Applied Biosystems, Warrington, UK
Microlon™ 96-well ELISA microplates	Greiner Bio-One, Kremsmünster, AU
Natural thin-walled tubes (0.2ml)	BioQuote Limited, York, UK
Round-bottom (RB) tubes	QIAGEN, Hilden, Germany
Stainless steel beads (5mm diameter)	QIAGEN, Hilden, Germany

2.1.3. Reagents

Table 2-2 Reagents

Product	Supplier
1-bromo-3-chloropropane	Sigma-Aldrich, St Louis, MO, USA
7-AAD viability staining solution	BioLegend, London, UK
Anti-GDF-15 antibody	NGM Pharmaceuticals, San Francisco, CA, USA
Anti-IL-6-receptor antibody	Bio X Cell, West Lebanon, NH, USA
ArC Amine Reactive Compensation bead kit	Invitrogen, Carlsbad, CA, USA
BD CompBead Compensation bead kit	BD Biosciences, Franklin Lakes, NJ, USA
Bovine Serum Albumin (BSA)	Sigma-Aldrich, St Louis, MO, USA
Bradford reagent	Sigma-Aldrich, St Louis, MO, USA
Cell staining buffer	BioLegend, London, UK
Collagenase XI	Sigma-Aldrich, St Louis, MO, USA
cOmplete Mini EDTA-free protease inhibitor cocktail tablets	Roche, Welwyn Garden City, UK
Countbright absolute counting beads	Invitrogen, Carlsbad, CA, USA
Dulbecco's Modified Eagle's Medium (DMEM)	Sigma-Aldrich, St Louis, MO, USA
ELISA kits	R&D Systems, Minneapolis, MN, USA
Ethanol 96%	VWR, Radnor, PA, USA
ExtrAvidin-peroxidase	Sigma-Aldrich, St Louis, MO, USA
Foetal Calf Serum (FCS)	Gibco, Waltham, MA, USA
Foxp3 staining kit	eBioscience, San Diego, CA, USA
Foxp3 Transcription Factor staining buffer kit	Invitrogen, Carlsbad, CA, USA
GolgiStop™ protein transport inhibitor	BD Biosciences, Franklin Lakes, NJ, USA
High-Capacity RNA-to-cDNA kit	Applied Biosystems, Waltham, MA, USA
Hydrochloric acid	Thermo Fisher Scientific, Waltham, MA, USA
Isoflurane	Centaur Services, Castle Cary, UK
Isopropanol	Thermo Fisher Scientific, Waltham, MA, USA
Isotype antibody for anti-IL-6	Bio X Cell, West Lebanon, NH, USA
Isotype antibody for anti-GDF-15	NGM Pharmaceuticals, San Francisco, CA, USA
L-glutamine	Gibco, Waltham, MA, USA
Live/Dead Fixable Near-infrared stain	Life Technologies, Carlsbad, CA, USA
Mouse GAPDH control	Applied Biosystems, Waltham, MA, USA
Nuclease-free water	Promega, Madison, WI, USA
OCT cutting compound	VWR, Radnor, PA, USA
PBS tablets	Sigma-Aldrich, St Louis, MO, USA
Penicillin-Streptomycin (Pen-Strep)	Sigma-Aldrich, St Louis, MO, USA
Pentoject, Pentobarbitone Sodium 200 mg/ml	Animalcare, York, UK
Phosphate-buffered saline (PBS) 1x	Sigma-Aldrich, St Louis, MO, USA
ProLong Gold Antifade mountant	Life Technologies, Carlsbad, CA, USA
Puromycin dihydrochloride	Merck Millipore, Burlington, MA, USA
Rat IgG2b anti-mouse CD16/CD32 ("Fc block")	BD Biosciences, Franklin Lakes, NJ, USA
Roswell Park Memorial Institute (RPMI) medium	Sigma-Aldrich, St Louis, MO, USA
SIGMAFAST™ 3,3′-Diaminobenzidine tablets	Sigma-Aldrich, St Louis, MO, USA
Streptavidin-horseradish peroxidase	Sigma-Aldrich, St Louis, MO, USA
Taqman probes	Thermo Fisher Scientific, Waltham, MA, USA
Taqman Universal MasterMix II no UNG	Applied Biosystems, Waltham, MA, USA

Product	Supplier
TMB solution	Life Technologies, Carlsbad, CA, USA
TRI reagent	Life Technologies, Carlsbad, CA, USA
Triton X100	Sigma-Aldrich, St Louis, MO, USA
Trypsin-EDTA	Gibco, Waltham, MA, USA
TWEEN-20	Sigma-Aldrich, St Louis, MO, USA

2.1.4. Media and buffers

Media and buffers used “off-the-shelf” are listed in Table 2-2.

Table 2-3 Media and buffers

Name	Contents	Final concentration
ACK buffer	Distilled water	-
	$KHCO_3$	10mM
	EDTA	0.1mM
	NH_4Cl	154mM
BAL medium	PBS	1X
	EDTA	50mM
Complete DMEM	DMEM	1X
	FCS	10%
	L-glutamine	2mM
Complete RPMI	RPMI	1X
	FCS	10%
	L-glutamine	2mM
	Penicillin	100U/ml
	Streptomycin	100µg/ml
Coating buffer	Distilled water	-
	Sodium Bicarbonate	50mM
	adjusted to pH 9.6	

2.1.5. Instruments

Table 2-4 Instruments

Name	Supplier
BD LSRFortessa™	BD Biosciences, Franklin Lakes, NJ, USA
Heraeus Megafuge 40R	Thermo Fisher Scientific, Waltham, MA, USA
Sorvall Legend Micro 21 centrifuge	Thermo Fisher Scientific, Waltham, MA, USA
7500 Fast Real-Time PCR system	Applied Biosystems, Waltham, MA, USA
GentleMACS dissociator	Miltenyi Biotec, Bergisch Gladbach, Germany
Bright Cryostat microtome	Bright Instruments, Luton, UK
BioWizard Silver Line Biosafety cabinet	Kojair, Mänttä-Vilppula, Finland

Name	Supplier
mLINE® mechanical pipettes	Sartorius, Göttingen, Germany
NanoDrop 1000 Spectrophotometer	Thermo Fisher Scientific, Wilmington, DE, USA
Tissue culture incubator	Binder, Tuttlingen, Germany
Tissue lyser LT	QIAGEN, Hilden, Germany
Ultrasonic water bath	Ultrawave, Cardiff, South Wales, UK
Zeiss Axio Observer inverted Widefield microscope	Carl Zeiss Ltd, Cambridge, UK
SubAqua 18 Plus water bath	Grant Instruments, Royston, UK
FLUOStar Omega Microplate reader	BMG Labtech, Aylesbury, UK

2.1.6. Software

Table 2-5 Software

Name	Supplier
Adobe Illustrator CC 2019	Adobe Systems Europe Limited, Berkshire, UK
Adobe InDesign CC 2019	Adobe Systems Europe Limited, Berkshire, UK
BD FACSDiva™	BD Biosciences, Franklin Lakes, NJ, USA
7500 Fast Systems SDS v1.4	Applied Biosystems, Paisley, UK
Fiji v2	ImageJ, NIH, Bethesda, MD, USA
FlowJo v10	BD, Ashland, OR, USA
GraphPad Prism v8	GraphPad Software, San Diego, CA, USA
MARS Data Analysis v1.3	BMG Labtech, Aylesbury, UK
Microsoft Office 365	Microsoft, Redmond, WA, USA
Omega Reader Control	BMG Labtech, Aylesbury, UK

2.1.7. Antibodies

Antibodies used for flow cytometry staining are listed under Section 2.2.7.

Table 2-6 Primary antibodies for Immunohistochemistry

Target	Clone/Name	Supplier	Final concentration
Myosin Heavy Chain (MyHC) I	BA-D5	Developmental Studies Hybridoma Bank, Iowa City, IA, USA	0.35µg/ml
MyHC IIA	SC-71	Developmental Studies Hybridoma Bank	0.32µg/ml
MyHC IIB	BF-F3	Developmental Studies Hybridoma Bank	0.62µg/ml
Laminin	L9393	Sigma-Aldrich, Gillingham, UK	0.50µg/ml

Table 2-7 Secondary antibodies for Immunohistochemistry

Host specificity and isotype	Fluorophore	Supplier	Final concentration
Goat anti-Mouse IgG2b	Alexa Fluor 555	Invitrogen, Carlsbad, CA, USA	10µg/ml
Goat anti-Mouse IgG1	Alexa Fluor 350	Invitrogen, Carlsbad, CA, USA	10µg/ml
Goat anti-Mouse IgM Heavy Chain	Alexa Fluor 488	Invitrogen, Carlsbad, CA, USA	10µg/ml
F(ab')2-Goat anti-Rabbit IgG (H+L)	Alexa Fluor 647	Invitrogen, Carlsbad, CA, USA	10µg/ml

2.2. Methods

2.2.1. RSV stock propagation

RSV strain A2 (originally from ATCC, Old Town Manassas, VA, USA) was propagated in human epithelial type 2 (HEp-2, ATCC) cells and viral stock titre determined using an immunoplaque assay.

2.2.1.1. HEp-2 cell culture

HEp-2 cells were cultured in antibiotic-free complete DMEM in 175cm^2 flasks at 37°C with 5% CO_2 and passaged when almost confluent. Medium was removed and the cell monolayer washed with serum-free DMEM. 20ml of trypsin EDTA solution was added and incubated at room temperature for 5 minutes until the monolayer detached with gentle manual agitation. The trypsin was neutralised with an equal volume of complete DMEM. The contents of the flask were centrifuged and the supernatant was discarded. The cell pellet was resuspended in complete DMEM and seeded into new flasks at a density of 5 x 10^6 per flask.

2.2.1.2. Growing RSV

5 x 10^6 HEp-2 cells were seeded in a volume of 50ml of medium in a 175cm^2 flask. Cells were left to grow to approximately 50% confluence overnight at 37°C. The medium was removed and the cells gently washed with serum-free DMEM. Cells were infected with 0.1PFU RSV per cell, suspended in 3ml of serum-free DMEM, taking into account that cells had approximately doubled overnight. The flask was incubated at 37°C for two hours with gentle rocking, to achieve even distribution of infection and prevent drying out of the cell monolayer. After two hours, 30ml of complete DMEM was added and the flask incubated for 24 hours at 37°C. The serum content was reduced to 2% by removing 25ml of medium from the flask and replacing it with 25ml of serum-free DMEM. The flask was incubated for 24-48 hours and regularly assessed for the cytopathic effect of the infection. Once down to approximately 50% confluence, the medium was removed and the cells now containing virus were harvested with a cell scraper. Stocks were sonicated for 20 seconds in an ice cold water bath and centrifuged to remove cell debris. The super-

natant containing virus was aliquoted, snap frozen in liquid nitrogen and stored at -80°C.

2.2.1.3. RSV stock quantification

3 x 10^6 HEp-2 cells were seeded into a flat-bottom 96-well plate in complete DMEM and incubated at 37°C overnight. The next day, cells were washed with serum-free DMEM and infected with a serial dilution of viral stock (e.g. twofold dilution starting at 1:100). Each dilution was performed in triplicate. Cells were incubated for two hours at 37°C with gentle rocking. 150µl of complete DMEM was added to each well and plates incubated for 24 hours at 37°C. The next day, cells were washed with PBS and fixed with methanol and 2% hydrogen peroxide for 20 minutes at room temperature. Cells were washed twice with PBS 1% BSA. Cells were stained with biotinylated polyclonal goat anti-RSV antibody (1:500; Bio-Rad, Hercules, CA, USA) and incubated for one hour at room temperature. The plate was washed twice with PBS 1% BSA and incubated for 30 minutes with ExtrAvidin peroxidase (Sigma-Aldrich, St Louis, MO, USA) at room temperature. The plate was washed twice again and 50µl of 3,3'-diaminobenzidine (DAB) solution (Sigma-Aldrich, St Louis, MO, USA) added. Cells were incubated for approximately 20 minutes at room temperature, or until the desired level of colour change was achieved. The plate was washed with PBS to stop the reaction. Plaques were counted under a microscope and plaque-forming units (PFU) calculated with the following equation:

$$\text{pfu/ml} = \frac{\text{\# plaques counted x dilution of virus x 1000}}{\text{volume of virus dilution applied}}$$

2.2.2. RSV infection of animals

Mice were anaesthetised with isoflurane vapour and infected intranasally with 2.3-3 x 10^5 PFU of RSV suspended in 75µl phosphate-buffered saline (PBS). This dose caused weight loss in elderly, but not young mice. Age-matched control groups were not infected (referred to as "day 0"). Mice were weighed daily and monitored for signs of illness.

2.2.3. Antibody treatments

2.2.3.1. Anti-GDF-15 antibody

Anti-GDF-15 antibody and isotype control antibody against keyhole limpet hemocyanin

were kindly provided by Bernard Allan and Harding Luan (NGM Biopharmaceuticals, San Francisco, CA, USA). 250µg antibody or isotype control suspended in 100µl PBS was injected intraperitoneally one day pre-infection.

2.2.3.2. Anti-IL-6R antibody

Anti-IL-6R antibody (15A7) and isotype control antibody against keyhole limpet hemocyanin (LTF-2) were purchased from BioXCell (West Lebanon, NH, USA) (Coulie, Vink & Van Snick, 1990). 150µg antibody suspended in 200µl PBS was injected intraperitoneally one day before infection and every 5 days after that (i.e. day 4, 9, 14 post-infection) (Pyle *et al.*, 2017).

2.2.4. Tissue collection

Tissues were collected at three time points: from uninfected mice ("day 0"), 8 days post-infection, or 18 days post-infection. Mice were euthanised by intraperitoneal injection with an overdose of Pentoject (pentobarbitone sodium, 20% w/v; Animalcare, York, UK). Blood was obtained by cardiac puncture, serum extracted and stored at -80°C. The trachea was cannulated with polythene tubing and the lungs flushed three times with 1ml of 5mM EDTA/PBS to obtain bronchoalveolar lavage (BAL) fluid. The left lung was used for flow cytometric analysis as described below. Right lung lobes were retained and snap frozen for qPCR analysis. The tibialis anterior (TA) muscle was extracted from both legs. The right TA was snap frozen and later weighed and cut in half for qPCR and ELISA analysis. The left TA was weighed and embedded for immunohistochemistry as described below. The tibia bone was extracted from both legs, cleaned of muscle tissue, and length measured with calipers.

2.2.5. TA atrophy index

Relative muscle atrophy was calculated for each individual animal as follows:

$$\text{TA atrophy index} = \frac{1}{\left(\frac{\text{TA weight}}{\text{tibia length}^3}\right)}$$

This “TA atrophy index” was based on a previous method normalising TA weight to bodyweight (Patel *et al*., 2016). However, bodyweight of elderly mice was known to change over the course of RSV infection, distorting the index. Instead, TA weight was normalised to the length of the corresponding animal’s tibia. Tibia length should remain unchanged during infection. The length of the tibia was cubed to obtain a measure of the same dimension as weight. The reciprocal was taken so that larger values would indicate higher atrophy.

2.2.6. ELISA

2.2.6.1. Cytokines

Levels of IL-6, TNF-α, and GDF-15 were assayed using DuoSet ELISA kits (R&D Systems, Minneapolis, MN, USA) according to the manufacturer’s instructions.

2.2.6.2. RSV-specific serum IgG

Anti-RSV IgG levels in serum were assayed with a modified ELISA protocol. RSV was grown in HEp-2 cells as detailed in 2.2.1. Infected monolayers were harvested, centrifuged, and the supernatant discarded. The cell pellet was resuspended in 2ml cDMEM and sonicated in an ice bath for 10 minutes. This suspension was aliquoted and stored at –20°C. Mock-infected HEp-2 cells were prepared in the same way to measure background binding. Microlon ELISA plates were coated half with HEp-2 antigen and half with RSV antigen and incubated overnight at 4°C. Plates were washed with PBS + 0.05% TWEEN-20 and blocked with PBS + 1% BSA for 1 hour at 37°C. After three washes, serum was added in serial dilutions from 1:50 to 1:1,600 in PBS + 1% BSA and plates incubated for 2 hours at 37°C. After four washes, HRP-conjugated rabbit anti-mouse Ig (Sigma-Aldrich, St Louis, MO, USA) was added and plates incubated for another 2 hours at 37°C. Plates were washed five times and peroxidase TMB substrate (Life Technologies, Carlsbad, CA, USA) added. The reaction was stopped with 1N hydrochloric acid once colour had developed sufficiently. Plates were read at 450nm on an FluoStar Omega plate reader (BMG Labtech, Aylesbury, UK). The average optical density (OD) values of HEp-2-antigen-coated wells was subtracted from the average values for the correspond-

ing RSV-antigen-coated wells to obtain RSV-specific binding.

2.2.6.3. Puromycin

Puromycin content of muscle was assayed using a protocol adapted from one kindly provided by Paul Kemp (Schmidt *et al.*, 2009; Goodman & Hornberger, 2013). 30 minutes prior to euthanasia, mice were injected with 0.8µmol puromycin dihydrochloride (Sigma-Aldrich, St Louis, MO, USA) suspended in 100µl PBS. After euthanasia, the right tibialis anterior (TA) muscle was extracted and snap frozen. Later, the TA was thawed and cut in half. One half was used for qPCR and the other for this assay. The tissue was added to cOmplete protease inhibitor buffer in PBS (Roche, Welwyn Garden City, UK) and homogenised with a steel bead in a TissueLyser LT (Qiagen, Hilden, Germany) at 50Hz for 4 minutes. The samples were centrifuged and the protein-containing supernatant removed and assayed for protein content by Bradford assay. Plates were coated overnight with 100ng/µl protein supernatant in bicarbonate buffer (pH 9.6) at room temperature. The next day, plates were blocked with 5% BSA in PBS for 30 minutes at room temperature. Plates were incubated with 100ng/ml of puromycin antibody (12D10; Merck Millipore, Burlington, MA, USA) for one hour at room temperature. Plates were washed with PBS and incubated with the secondary antibody, AffiniPure peroxidase conjugated goat anti-mouse IgG2a (1:1,000; Jackson ImmunoResearch, Ely, UK), for one hour at room temperature. TMB substrate (Life Technologies, Carlsbad, CA, USA) was added and the reaction stopped with 1N HCl. Plates were read at 450nm on an FluoStar Omega plate reader (BMG Labtech, Aylesbury, UK).

2.2.7. Immunohistochemistry

2.2.7.1. Cryosectioning and histological staining

Left TA muscles were embedded in OCT compound (VWR, Radnor, PA, USA) and snap frozen in isopentane cooled with liquid nitrogen. Cryosections of 6µm thickness were cut using a cryostat microtome (Bright Instruments, Luton, UK). Cryosections were thawed, permeabilized with 0.5% Triton X-100 in PBS (Sigma-Aldrich, St Louis, MO, USA) for five minutes, and blocked in 2% goat serum in PBS for an hour. All antibodies were diluted

in 2% goat serum in PBS. Slides were incubated with primary antibodies at room temperature overnight or for three hours with gentle rocking. Slides were washed with PBS and secondary antibodies were applied for one hour. Finally, slides were washed and mounted in ProLong Gold mountant (Life Technologies, Carlsbad, CA, USA), and kept in the dark at 4°C until imaging. The panel used stains three different isoforms of myosin heavy chain (MyHC), the expression of which determines the contractile properties of a muscle fibril, and laminin, a primary component of the basal lamina, the extracellular matrix (ECM) in between individual muscle fibres. Primary antibodies against myosin heavy chain epitopes were obtained from the Developmental Studies Hybridoma Bank, created by The Eunice Kennedy Shriver National Institute of Child Health and Human Development of the National Institutes of Health and maintained at The University of Iowa, Department of Biology, Iowa City, IA, USA. The primary antibodies were used at concentrations described in Table 2-6. Secondary antibodies were purchased from Invitrogen (Carlsbad, CA, USA), at the concentrations described in Table 2-7.

2.2.7.2. Imaging and analysis

Slides were imaged on a Zeiss Axio Observer inverted Widefield microscope with a motorised stage at the Facility for Imaging by Light Microscopy (FILM) at Imperial College London. Images were acquired at 20x magnification and tiled to form a single image of the entire muscle cross section. Images were analysed using Fiji software (Schindelin *et al.*, 2012). A macro was written in order to automate analysis of the size of individual muscle fibres. In brief, an image of a laminin-stained section was converted to a binary black-and-white "thresholded" image, determining which parts of the image are ECM and which parts are individual muscle fibres. The minimum Feret's diameter of the individual muscle fibres thus detected was measured and recorded. Minimum Feret's diameter was chosen as the most appropriate measure of fibre size, since it is less prone to distortion by irregular cutting angles than maximum diameter or cross-sectional area (Patel *et al*., 2016; Guiraud & Davies, 2019). The minimum Feret's diameter is defined as the shortest possible distance between two parallel tangents of an object (here, a mus-

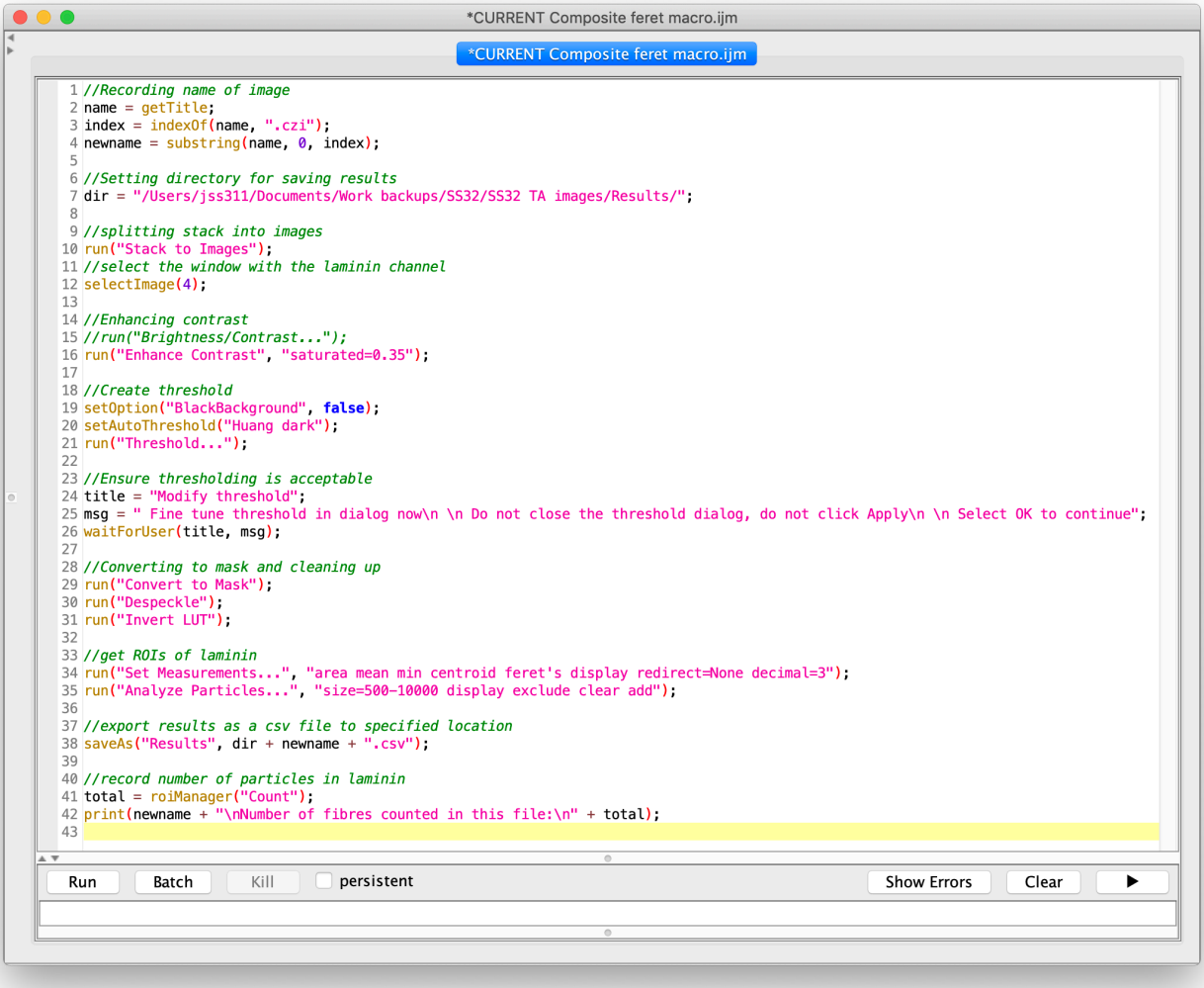

Figure 2-1 Macro for analysis of muscle fibre size

Macro written in the ImageJ macro language used for automatically detecting muscle fibres and measuring and recording minimum Feret's diameter. In brief, the macro records the name of the open image file. It determines the file directory in which results will be saved. The image file consisting of an overlay from multiple fluorescent channels is split into separate images each representing the signal from one stain. The image showing the laminin stain is selected and the contrast and brightness enhanced. The image is thresholded into a black-and-white image based on the intensity of the laminin staining. This distinguishes ECM from the individual muscle fibres. There is a manual approval step at this point. If approved, the image is converted to a mask that identifies each muscle fibre based on the threshold. Each fibre is then measured and the results saved to a spreadsheet.

cle fibre) (Briguet *et al*., 2004). Briefly, the minimum Feret's diameter is determined thus: An object is bordered by two parallel lines intersecting the opposite outermost edges of the object. The distance between the parallel lines is recorded. The object is rotated by a set number of degrees, here 5°, and the parallel lines adjusted to intersect the outermost edges of the object. The distance between the parallel lines is again recorded. This process is repeated until a full revolution of the object has been achieved. The minimum

Feret's diameter of the object is the shortest distance between the parallel lines recorded during any rotation. Areas of the image where sections were folded over or visibly distorted were excluded from analysis, as were fibres not derived from the TA. The code used in this analysis is shown in Figure 2-1. For an illustration of the steps of the macro see Figure 3-23.

2.2.8. Flow cytometry

2.2.8.1. Preparation of single-cell suspensions

Lungs were homogenised using a gentleMACS dissociator (Miltenyi Biotec, Bergisch Gladbach, Germany) and digested in 2.5 mL collagenase XI (Sigma-Aldrich, St Louis, MO, USA) at 37°C for 30 minutes. Red blood cells were lysed using filter sterilised ACK buffer (154mM ammonium chloride, 10mM potassium bicarbonate, 0.1mM EDTA), and single-cell suspensions obtained by filtering through 100µm filters. BAL fluid was centrifuged, and the supernatant removed and stored at -80°C. Red blood cells in the BAL cell pellet were lysed with ACK buffer as above. Final cell suspensions were in complete medium, consisting of RPMI 1640 (Thermo Fisher Scientific, Waltham, MA, USA) with 10% FCS, 100U/ml penicillin and 100µg/ml streptomycin.

2.2.8.2. Cell counting

The number of live cells in each sample was determined by flow cytometry. A small aliquot of single-cell suspensions was stained for dead cells with 7-AAD diluted 1:100 in PBS (BioLegend, London, UK) and combined with a known quantity of CountBright Absolute Counting Beads (Thermo Fisher Scientific, Waltham, MA, USA). 5,000 bead events were recorded on the flow cytometer. Dead cells staining for 7-AAD and doublets were excluded from analysis. The number of live single cells in the original sample was calculated based on the ratio of counting beads to cells acquired, with the following equation:

$$\text{live cells in sample} = \frac{\#\text{ live cells counted} \times \#\text{ beads added} \times \text{resuspension volume of original sample}}{\#\text{ beads counted} \times \text{volume of cells added}}$$

2.2.8.3. Surface epitope staining

For flow cytometric staining, 200µL of single-cell suspension was plated on a 96-well

Table 2-8 Antibodies used for flow cytometry surface staining

Antigen	Clone	Fluorophore	Isotype	Dilution	Manufacturer
CD3	AF700	17A2	Rat IgG2b	1:100	BioLegend
CD3	PE-eFluor610	145-2C11	American hamster IgG	1:400	eBioscience
CD4	BV510	RM4-5	Rat IgG2a	1:100	BioLegend
CD4	BV605	GK1.5	Rat IgG2b	1:200	BioLegend
CD4	FITC	RM4-5	Rat IgG2a	1:100	eBioscience
CD8	APC-H7	53-6.7	Rat IgG2a	1:100	BioLegend
CD8	BV785	53-6.7	Rat IgG2a	1:200	BioLegend
CD8	Pacific Blue	53-6.7	Rat IgG2a	1:100	BD Biosciences
CD19	BV605	6D5	Rat IgG2a	1:200	BioLegend
CD19	PerCP Cy5.5	6D5	Rat IgG2b	1:100	BioLegend
CD38	PE	90	Rat IgG2a	1:200	BD Biosciences
CD45	PE	30-F11	Rat IgG2b	1:400	BioLegend
CD95	PerCP Cy5.5	SA367H8	Mouse IgG1	1:100	BioLegend
CXCR5	BV421	L138D7	Rat IgG2b	1:50	BioLegend
GL7	AF488	GL7	Rat IgM	1:200	BioLegend
Gr1	BV510	RB6-8C5	Rat IgG2b	1:200	BioLegend
KLRG1	BV711	2F1/KLRG1	Syrian hamster IgG	1:100	BioLegend
NK1.1	PE-Cy7	PK136	Mouse IgG2a	1:100	BioLegend
PD1	PE-Cy7	RMP1-30	Rat IgG2b	1:200	BioLegend

Table 2-9 Antibodies used for flow cytometry intracellular cytokine staining

Antigen	Clone	Fluorophore	Isotype	Dilution	Manufacturer
IFNg	FITC	XMG1.2	Rat IgG1	1:100	BioLegend
IL-10	BV421	JES5-16E3	Rat IgG2b	1:100	BioLegend

v-bottomed plate. All staining was carried out in cell staining buffer (BioLegend, London, UK). Dead cells were stained using the Live/Dead® Fixable Near-Infrared stain kit (Life Technologies, Carlsbad, CA, USA) according to the manufacturer's instructions. Cells were incubated with Fc receptor block at 1:50 in staining buffer (BD Biosciences, Franklin Lakes, NJ, USA) on ice for 15 minutes to prevent non-specific antibody binding. Cells were then stained with antibodies at room temperature for one hour. Antibodies used are shown in Table 2-8. Cells were fixed with fixation buffer (BioLegend, London, UK) on

ice for 30 minutes, washed, and resuspended in FACS buffer. Plates were kept at 4°C until run on the flow cytometer. In addition to samples from individual mice, wells were prepared from a mixture of cells that were stained with all antibodies in the panel except for one (fluorescence minus one, FMO). The outcome of these FMO controls was used to determine gating strategies.

2.2.8.4. $CD4^+$ RSV tetramer staining

To assay RSV-specific $CD4^+$ responses, some samples were additionally stained with an MHC class II tetramer loaded with an RSV M2 peptide. This tetramer (I-A^b-$M2_{26-39}$-APC) and the CLIP loading control (I-A^b-hCLIP-APC) were a kind gift from James Harker. The tetramers were produced by the MHC tetramer core facility of the National Institute of Allergy and Infectious Diseases (Atlanta, Georgia). After dead cell staining and Fc receptor blockade as detailed above, cells were stained with tetramer in 1:100 dilution at room temperature for three hours. Cells were washed with staining buffer and surface epitope staining proceeded as above.

2.2.8.5. Intracellular cytokine staining

For intracellular cytokine staining, cell suspensions were prepared as above. After plating, cells were re-stimulated with 100ng/ml PMA and 1µg/ml ionomycin at 37°C for one hour. Then, 10µl Golgi Stop protein transport inhibitor (BD Biosciences, Franklin Lakes, NJ, USA) per well was added and cells were incubated for another two hours. Afterwards, staining steps for surface antibodies proceeded as above up to and including the final fixation and wash steps. The next day, cells were washed into Permeabilization Wash Buffer (BioLegend, London, UK) to permeabilise cell membranes and allow staining of intracellular epitopes. Non-specific binding of antibodies was prevented by incubation with Fc receptor block (BD Biosciences, Franklin Lakes, NJ, USA) on ice for 15 minutes. Cells were then stained with antibodies to intracellular cytokines at room temperature for 1 hour, washed, and analysed immediately on the flow cytometer. Antibodies used to intracellular cytokine staining are shown in Table 2-9.

2.2.8.6. Cell acquisition and analysis

Table 2-10 General qPCR probes

Name	Gene name	Catalogue number
Atrogin-1	*Fbxo32*	Mm00499523_m1
GDF-15	*Gdf15*	Mm00442228_m1
IFN-gamma	*Ifng*	Mm01168134_m1
IGF-1	*Igf1*	Mm00439560_m1
IL-1 beta	*Il1b*	Mm00434228_m1
IL-6	*Il6*	Mm00446190_m1
Mef2c	*Mef2c*	Mm01340842_m1
MuRF-1	*Trim63*	Mm01185221_m1
MyoD1	*Myod1*	Mm00440387_m1
Myogenin	*Myog*	Mm00446194_m1
Myostatin	*Mstn*	Mm01254559_m1
Pax7	*Pax7*	Mm01354484_m1
TNF-alpha	*Tnf*	Mm00443258_m1

Table 2-11 General qPCR reaction mix

Reagent	Volume (ul)
TaqMan Universal MasterMix II with no UNG	6.25
Target probe (FAM/MGB)	0.625
GAPDH mouse control (VIC/MGB)	0.625
Nuclease-free H_2O	4.00
Subtotal	11.5
+cDNA	1.00
Total reaction	12.5

Flow cytometry was carried out on an LSRFortessa™ Cell Analyzer (BD Biosciences, Franklin Lakes, NJ, USA) at the core Imperial College St Mary's Campus FACS facility. Data was acquired using BD FACSDiva™ software (BD Biosciences, Franklin Lakes, NJ, USA). Overlap in fluorescence spectra was compensated for using BD CompBeads (BD Biosciences, Franklin Lakes, NJ, USA) and ArC Amine reactive compensation beads (Thermo Fisher Scientific, Waltham, MA, USA). 50,000 live single-celled lymphocytes were acquired or as many as possible by acquiring the entire sample. Flow cytometric

Table 2-12 RSV L gene qPCR primers and probe

Name	Sequence (5'→3')	Supplier
L gene forward primer	GAACTCAGTGTAGGTAGAATGTTTGCA	Invitrogen, Carlsbad, CA, USA
L gene reverse primer	TTCAGCTATCATTTTCTCTGCCAAT	Invitrogen, Carlsbad, CA, USA
L gene probe (FAM)	TTTGAACCTGTCTGAACATTCCCGGTT	Invitrogen, Carlsbad, CA, USA

Table 2-13 RSV L gene qPCR reaction mix

Reagent	Volume (ul)
TaqMan Universal MasterMix II with no UNG	6.25
L gene forward primer (5µM)	2.25
L gene reverse primer (5µM)	0.75
L gene probe (FAM)	0.44
Nuclease-free H_2O	1.81
Subtotal	11.5
+cDNA	1.00
Total reaction	12.5

data was analysed with FlowJo software version 10.1 (BD, Ashland, OR, USA) and Microsoft Excel.

2.2.9. Quantitative polymerase chain reaction (PCR)

2.2.9.1. RNA extraction and cDNA conversion

Quantitative PCR (qPCR) was carried out to determine the mRNA expression levels of specific genes in lung and muscle at various times after RSV infection. Lung and TA muscle were homogenised in TRIzol (Thermo Fisher Scientific, Waltham, MA, USA) with a TissueLyser LT (Qiagen, Hilden, Germany). RNA was extracted with 1-Bromo-3-chloropropane (Sigma-Aldrich, St Louis, MO, USA) and precipitated with isopropanol. Pellets were washed with 75% ethanol, air dried, and resuspended in RNase-free water. RNA concentration was measured using a NanoDrop® ND-1000 spectrophotometer (Thermo Fisher Scientific, Waltham, MA, USA). cDNA was synthesised using a high-capacity RNA-to-cDNA kit (Applied Biosystems, Waltham, MA, USA) according to the manufacturer's instructions.

2.2.9.2. qPCR for relative gene expression

Probes used were purchased from Thermo-Fisher (Waltham, MA, USA) and are listed in Table 2-10. Probes were conjugated to a double dye with a FAM fluorophore and an MGB quencher. Simultaneously, the expression of the housekeeping gene GAPDH was measured using a probe conjugated to a VIC fluorophore with an MGB quencher (Applied Biosystems, Waltham, MA, USA). The reaction mix containing TaqMan Universal MasterMix II with no UNG (Applied Biosystems, Waltham, MA, USA), nuclease-free water, target probe, GAPDH probe, and cDNA was made up in the proportions shown in Table 2-11. Reactions were run on a 7500 Fast Real-Time PCR System machine (Applied Biosystems, Waltham, MA, USA). Samples underwent a two-minute hold phase at 50°C, a ten-minute hold phase at 95°C, followed by 40 cycles of 95°C for 15 seconds and 60°C for one minute. Results were analysed using the 7500 Fast Systems SDS software and Microsoft Excel. In brief, the C_T (cycle threshold) value of GAPDH was subtracted from the C_T value of the target gene, in order to eliminate differences in starting amount or enzymatic activity (obtaining the ΔC_T). This normalised mRNA expression level was then converted to the fold change in expression in relation to the average ΔC_T of young uninfected mice ($2^{-\Delta\Delta CT}$).

2.2.9.3. RSV L gene qPCR

The expression of RSV L gene was quantified absolutely using a DNA plasmid standard curve. Forward and reverse primers and a separate FAM-tagged probe for L gene were custom-made by Invitrogen (Carlsbad, CA, USA). The sequences of the probe and primers are shown in Table 2-12. The reaction mix consisting of TaqMan Universal MasterMix II with no UNG (Applied Biosystems, Waltham, MA, USA), nuclease-free water, L gene forward primer, L gene reverse primer, L gene probe, and cDNA was made up in the proportions shown in Table 2-13. Reactions were run on a 7500 Fast Real-Time PCR System machine (Applied Biosystems, Waltham, MA, USA). Samples underwent the same thermocycling protocol as above, but with 45 cycles to allow for detection of low levels of L gene. Results were fitted to the standard curve with the 7500 Fast Systems SDS software

and quantities of L gene per 0.1µg of RNA calculated.

2.2.10. Human RSV challenge samples

Plasma and BAL fluid samples were available from 10 participants of the INFLAMMAGE clinical study (trial registration NCT03728413). This study was conducted at the NIHR/ Wellcome Trust Imperial Clinical Research Facility (ICRF). The author was not involved in the design or execution of this study. The INFLAMMAGE study aims to systematically investigate the immune response of an elderly cohort to deliberate RSV inoculation challenge. In brief, healthy volunteers either "young" (18-55 years) or "elderly" (60-78 years) were recruited. Participants were challenged intranasally with 10^4 PFU RSV A strain Memphis 37 (Meridian Life Science, Memphis, TN, USA), quarantined for 10 days and monitored daily. Blood and nasal lavage were collected immediately prior to RSV inoculation ("day 0") and daily during the quarantine period. Participants returned for further blood and nasal sampling on days 14 and 28 and at a 6-month (day 180) follow-up. Participants were asked to complete a self-reported symptom diary every day, which was based on the Jackson score (Jackson *et al.,* 1958) to assess total, lower and upper respiratory tract symptoms. Symptoms were scored as follows; 0: absent, 1: mild (present but does not affect normal daily activities); 2: moderate (some interference with normal daily activities); 3: severe (prevents normal daily activities). Plasma samples from 7 elderly participants and 3 young participants, and BAL samples from 3 young and 2 elderly participants, were provided by Dr Stephanie Ascough and were assayed for GDF-15 with an ELISA kit following the manufacturer's instructions (R&D Systems, Minneapolis, MN, USA). Viral load data and symptom score data were provided by Dr Stephanie Ascough.

2.2.11. Statistical analysis

Data points shown represent individual mice unless otherwise indicated in the figure legend. Long bars represent the mean of a group and error bars shown are the standard error of the mean. Statistical significance of differences between groups was determined with unpaired, two-tailed Student's t-tests, or one- or two-way ANOVA, where appropriate. Bonferroni's post-test was applied to ANOVA analyses to correct for multiple

comparisons. Data were analysed with GraphPad Prism 8.0 software. Values of $p \leq 0.05$ were considered statistically significant. Stars shown in graphs represent the following levels of statistical certainty: *$p \leq 0.05$, **$p \leq 0.01$, ****$p \leq 0.001$, ****$p \leq 0.0001$.

3.

A mouse model of muscle wasting in the elderly after RSV infection

Chapter 3. A mouse model of muscle wasting in the elderly after RSV infection

3.1. Introduction

3.1.1. Background

The elderly are disproportionately at risk of both respiratory viral infections and muscle wasting. Loss of muscle mass and strength is common with advancing age (Holloszy, 2000), but can also be caused by other conditions such as respiratory infections, chronic infections, and COPD (Wanke *et al.*, 2000; Paton & Ng, 2006; Patel *et al.*, 2016). Muscle wasting is associated with frailty, increased mortality, and lower quality of life (Swallow *et al.*, 2007; Wheeler *et al.*, 1998). Respiratory syncytial virus (RSV) typically causes only mild illness in immunocompetent adults, but severe RSV disease can occur at the extremes of age (Falsey & Walsh, 2005). The elderly often display baseline inflammation ("inflamm-ageing") and inappropriate inflammatory responses to infection. Pro-inflammatory cytokines and factors such as IL-6 and TNF-α are known to promote muscle loss (Peterson, Bakkar & Guttridge, 2011). These observations suggest that respiratory viral infections are important in promoting frailty in the elderly. Despite its clinical importance, the relationship between respiratory viral infection and muscle wasting, particularly in the elderly, is not understood.

3.1.2. Purpose of chapter

This chapter aims to investigate if and how RSV infection affects skeletal muscle in a mouse model of RSV infection of the elderly. The chapter compares general features of the immune response to RSV between young and elderly mice, including markers of inflammation, cellular airway infiltration, viral load, and RSV-specific antibody generation. The chapter further develops a number of methodologies for determining the condition of skeletal muscle, including weight, fibre type composition, fibre size, protein turnover, and gene expression profile in order to demonstrate the effect of respiratory viral infection on the skeletal muscle.

3.1.3. Aims

- To establish a model of RSV infection in elderly mice
- To confirm age-related differences in general features of the immune response to RSV infection
- To establish outputs that describe the condition of skeletal muscle

3.2. Experimental Design

The results in this chapter describe a time course of RSV infection in young (±10 weeks) and elderly (±80 weeks) mice. Young and elderly mice were infected with the same dose (2.3x10^5 PFU) of RSV strain A2 and weighed daily. Tissues were collected at 8 days post-infection, 18 days post-infection, or from uninfected mice ("0 days") (Figure 3-1). Tissues collected were blood, BAL fluid, lung tissue, tibia, and tibialis anterior (TA) muscle. Flow cytometry of lung cells and BAL fluid cells was used to quantify cell numbers and determine changes in the frequency of various immune cell types. Copy number of RSV L gene was measured in lung tissue by qPCR. Cytokines were measured in BAL fluid by ELISA. Titres of RSV-specific IgG antibodies were measured in serum by ELISA. The

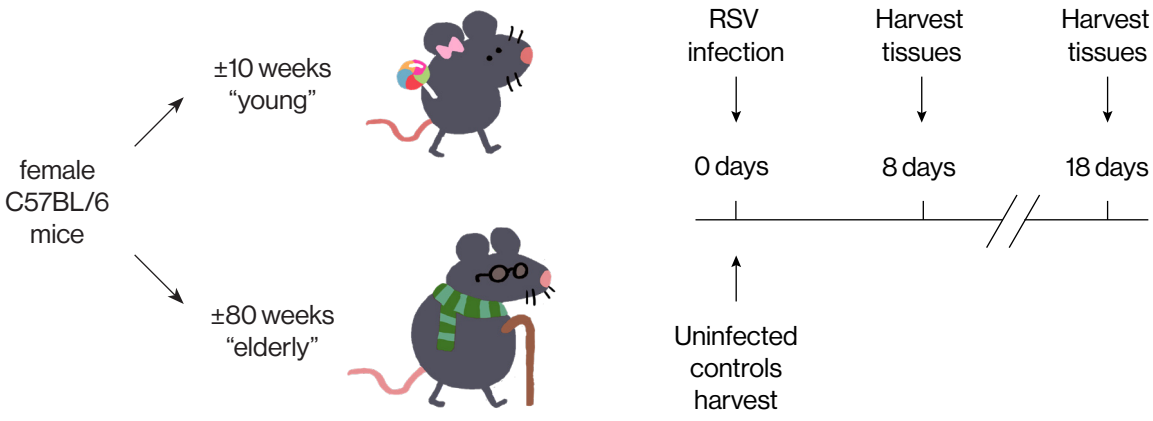

Figure 3-1 RSV infection of young and elderly mice

Timeline of RSV infection. Female C57BL/6 mice either ±10 weeks of age (from now on referred to as "young" mice) or ±80 weeks of age (from now on referred to as "elderly" mice) were intranasally inoculated with 2.3x10^5 PFU of RSV strain A2 in a volume of 75µl. Infected mice were euthanised and tissues harvested either 8 or 18 days post-infection. Age-matched groups of uninfected mice were also harvested and served as control groups ("day 0"). Illustration by Michael Barrett.

TA muscle was weighed and tibia length measured. The expression of various genes controlling muscle mass was determined by qPCR. Protein synthesis in the TA was determined with a novel assay measuring puromycin incorporation by ELISA technology. Muscle fibre size and fibre type composition was determined by immunohistochemistry of muscle cryosections.

3.3. Results

3.3.1. Elderly mice are heavier at baseline and display conserved signs of ageing

Elderly mice are not commonly used in infection research. Therefore, to establish baseline differences, elderly (18-month-old) mice were observed for differences in behaviour and appearance compared to young (10-12-week-old) mice. Elderly mice were heavier at baseline compared to young mice (mean 29.27g vs 19.71g) and displayed more variability in bodyweight (SD 3.35 vs SD 1.13) (Figure 3-2a). Elderly mice also displayed a remarkable degree of variability in general appearance. This variability manifested itself mainly in coat condition. Elderly mice commonly had greying fur, thinning fur, or bald patches (Figure 3-2b). These changes were particularly prominent on the neck and back. On the other hand, some elderly mice maintained a full, healthy coat. Rarely, elderly mice displayed blindness or spontaneous tumours. Mice with clearly visible tumours were excluded from analysis due to potential confounding interactions with experimental infection.

3.3.2. Elderly mice get more severe RSV disease than young mice

3.3.2.1. Elderly mice lose more weight during RSV infection

Before exploring the impact of infection on skeletal muscle, I determined how the aged immune system responded to RSV infection in this model using elderly mice. Young and elderly female C57BL/6 mice were infected intranasally with the same dose of RSV A2. Mice were culled 5, 8, or 18 days after infection, to represent early, acute, and recovery stages of the infection. Uninfected sets of young and elderly mice provided baseline measures. Elderly mice infected with RSV started losing weight approximately 6 days af-

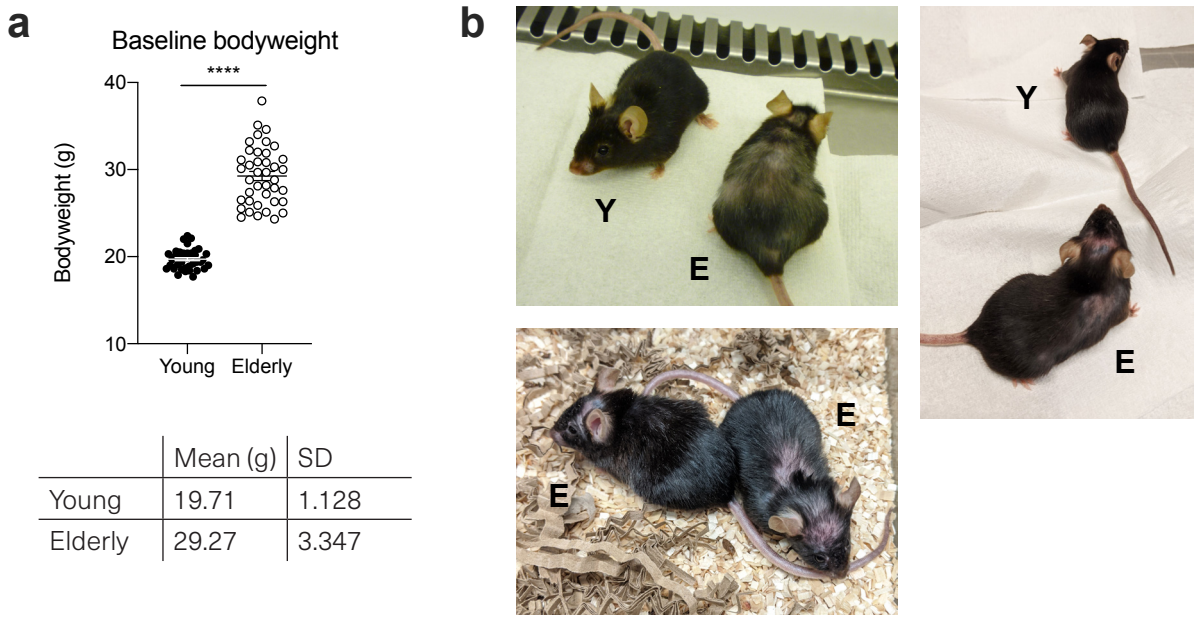

	Mean (g)	SD
Young	19.71	1.128
Elderly	29.27	3.347

Figure 3-2 Baseline weight and appearance of elderly mice

a. Bodyweight in grams of young (10-12 week-old) and elderly (18-month-old) mice at baseline before any infection. Student's unpaired two-tailed t test. Pooled from five independent experiments (n=5-10). **b.** Comparison of appearance of young and elderly mice. Young mice are marked "Y" and elderly mice "E". Note the greying and thinning fur, bald patches, and larger size of elderly mice compared to young.

ter infection (Figure 3-3a). Weight loss peaked 8 days after infection. At this point, elderly mice had lost an average of 14.46% (SD ±8.091) of their original bodyweight. By day 18, most elderly mice had still not returned to their baseline weight (average 96.81%, SD ±4.914). Young mice, despite being infected with the same dose of virus, did not lose weight, and in fact gained weight over 18 days. Percentage bodyweight was significantly different between young and elderly mice from day 3 to day 18 of infection (18 days being the longest any mice were followed up). Occasionally, transient weight loss (<5%) was observed in both young and elderly mice one day after infection. This may be attributable to the general anaesthesia the mice were placed under for the purpose of intranasal infection. The anaesthesia may have caused disorientation, loss of appetite, or general malaise leading to short-term weight loss not attributable to the RSV infection. This weight was generally recovered within an additional 24 hours (2 days after the infection).

To quantify the relative weight loss of young and elderly mice, the area under the curve (AUC) was calculated. Using the original bodyweight of each mouse as a baseline, this

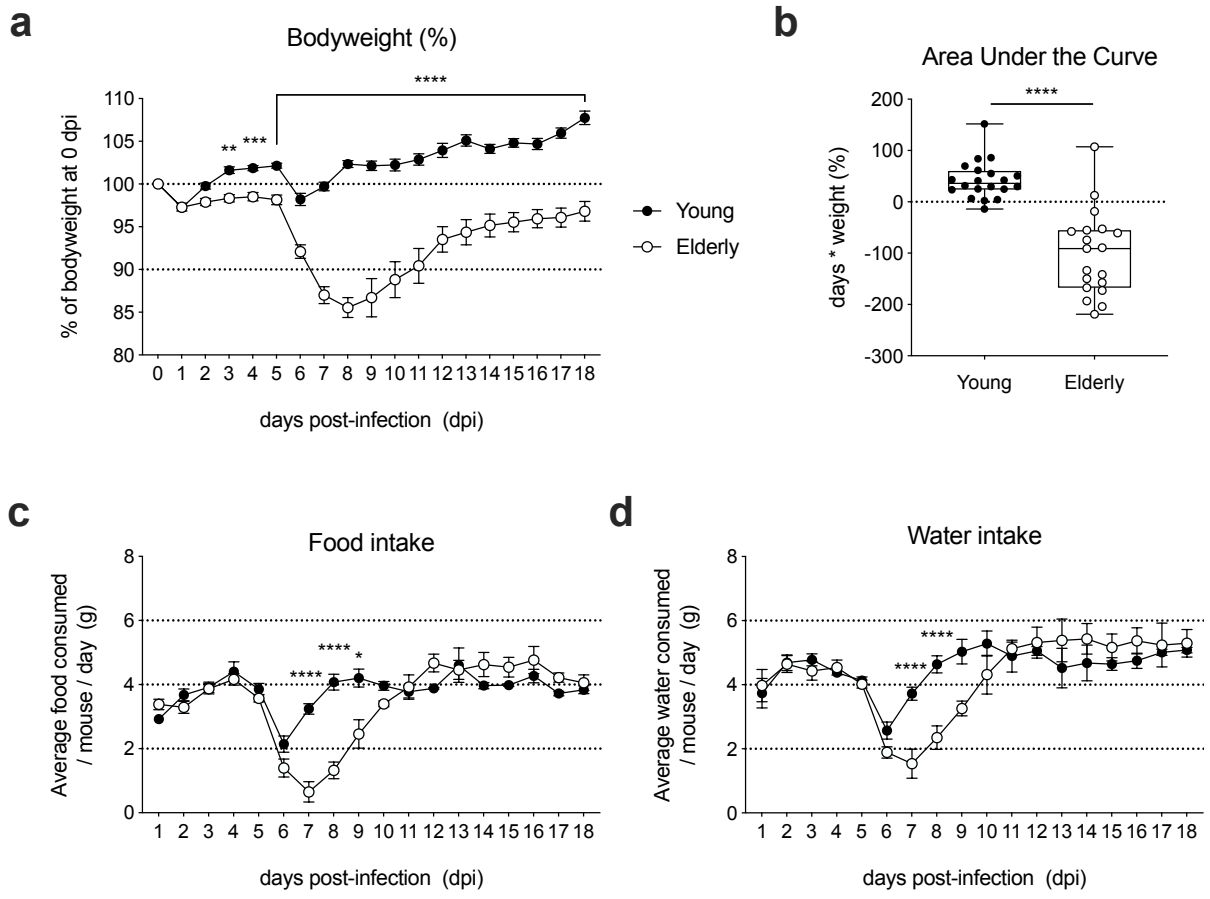

Figure 3-3 Weight loss, food and water intake of young and elderly mice after RSV infection

a. Bodyweight as a percentage of weight at day 0 (the day of infection). Shown are group means with the standard error of the mean. Pooled from nine independent experiments (one 5 dpi, four 8 dpi, four 18 dpi) n=5-10. **b.** Area under the curve of weight loss as a percentage of starting weight. Pooled from four independent experiments n=4-5. Student's two-tailed unpaired t test. **c.** and **d.** Food and water intake per mouse over the course of RSV infection. Pooled from seven experiments (one 5 dpi, three 8 dpi, three 18 dpi) n=5-10. All statistical analyses are 2-way ANOVA with Bonferroni's multiple comparisons test.

yields a value that represents the overall weight change over the 18 days of the infection. A negative value represents weight loss whereas a positive value represents weight gain. Elderly mice on average had a significantly lower AUC compared to young mice (Figure 3-3b). Using this technique it is clearly visible that almost all young mice cumulatively gained weight whereas almost all elderly mice cumulatively lost weight over 18 days of RSV infection. Weight loss during illness is often caused by anorexia (loss of appetite). To evaluate the contribution of anorexia to weight loss in this model, I measured food and water intake over the course of infection by weighing food hoppers and water bottles

every day. Daily food and water intake started to decrease in both young and elderly mice after day 5 post-infection (Figure 3-3c,d). In young mice, food and water intake reached its lowest on day 6, and increased back to baseline again by day 8. On the other hand, food and water intake of elderly mice continued to fall, reaching its lowest at day 7, and only slowly returned to baseline around day 10. Food intake was significantly lower in elderly mice compared to young mice for days 7, 8 and 9. Water intake was significantly lower in elderly mice for days 7 and 8.

3.3.2.2. Elderly mice display increased lung and airway inflammation

Bodyweight is a useful, but crude, measure of sickness. RSV infection causes a local inflammatory response that recruits immune cells into the airways. Counting the total number of live cells in the airways is a means of quantifying the amount of inflammation caused by RSV infection. Cells were counted in two types of samples, homogenised lung tissue and bronchoalveolar lavage (BAL) fluid. BAL fluid is obtained by cannulating the trachea of a euthanised mouse and repeatedly flushing the lungs with PBS + 5mM EDTA. This fluid contains mostly immune cells that were recruited into the airway lumen to combat the RSV infection of epithelial cells. Lung tissue was harvested and homogenised after BAL and thus contains both immune cells that are not removed by BAL (e.g. tissue-resident immune cells) as well as non-immune cells (e.g. structural cells). Cells in BAL fluid and lung tissue were counted by flow cytometry.

In both young and elderly mice, the number of cells in BAL fluid increased significantly from baseline to the peak of infection at day 8 (Figure 3-4a). At day 8, elderly mice had significantly more cells in their BAL fluid than young mice. From day 8 to day 18, cell numbers in the BAL fluid fell significantly in both young and elderly mice. At day 18, elderly mice still had significantly more cells in their BAL fluid than young mice, and cell numbers remained significantly higher compared to baseline.

Cell numbers in lung tissue also increased significantly from baseline to day 8 in both young and elderly mice (Figure 3-4b). At day 8, there were significantly more cells in the lung tissue of elderly mice compared to young mice. From day 8 to day 18, cell num-

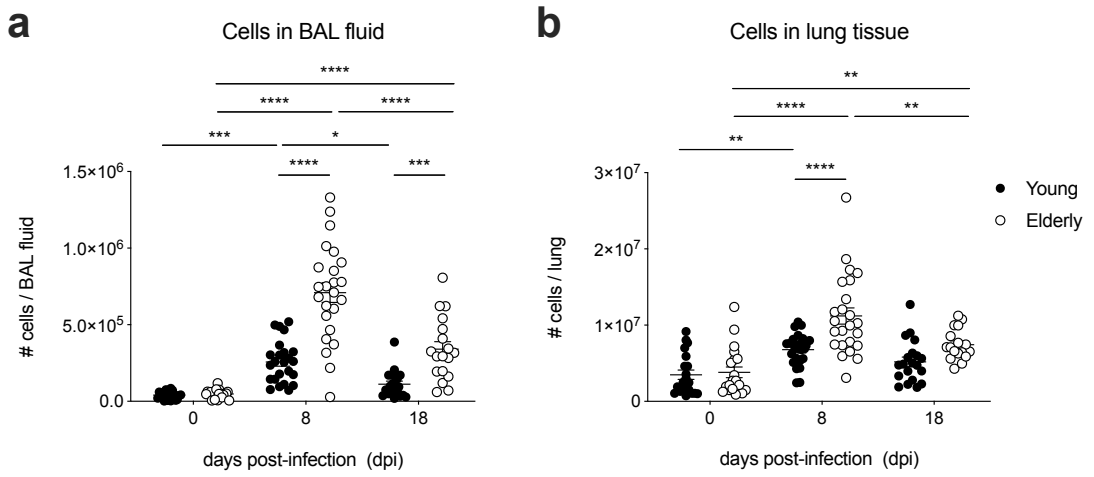

Figure 3-4 Cell counts in BAL fluid and lung tissue of young and elderly mice after RSV

a. Live cells in bronchoalveolar lavage (BAL) fluid of young and elderly mice infected with RSV. Pooled from 11 independent experiments (four 0 dpi, three 8 dpi, four 18 dpi) n=5-10. **b.** Live cells in homogenised lung tissue of young and elderly mice infected with RSV. Pooled from 11 independent experiments (four 0 dpi, three 8 dpi, four 18 dpi) n=5-10. All statistical analyses are 2-way ANOVA with Bonferroni's multiple comparisons test.

bers in lung tissue fell significantly in elderly mice but remained elevated compared to baseline. Cell numbers in lung tissue were not significantly different between young and elderly mice 18 days after infection.

3.3.2.3. Elderly mice have higher viral load but generate fewer RSV-specific antibodies

The higher weight loss and increased cellular infiltration of the lungs and airways observed in elderly mice are indicators of higher immunopathology. This immunopathology may be due in part to increased viral replication and in part to an overreaction of the immune response. To clarify the relative contributions of these two causes, viral replication in the lungs was measured. Additionally, antibodies responsive to RSV in the serum were measured to determine the ability of elderly mice to generate an RSV-specific immune response.

The copy number of RSV L gene, which encodes the viral polymerase, is used as a correlate of viral replication. RNA was extracted from homogenised lung tissue and the copy number of RSV L gene was quantified using quantitative PCR (qPCR) and an L gene plas-

mid standard. No L gene was detectable in the lungs of uninfected mice either young or elderly (not shown). At day 8, significantly more copies of L gene were detectable in the lungs of elderly mice compared to young mice (Figure 3-5a). L gene copy number was not significantly different between young and elderly at day 18, although there may be a trend towards elevated viral load in elderly mice. These results may suggest that more viral replication took place in the lungs of elderly mice, or that clearance of the virus was less efficient in elderly mice. The immune system of elderly mice may be less capable of mounting an anti-viral response, through a defect in either innate anti-viral responses or adaptive RSV-specific responses.

During a viral infection, the adaptive immune response generates antibodies specific to the virus. Levels of virus-specific antibodies can be used as an indicator of the functionality of the adaptive immune response. In clinical settings, levels of anti-RSV IgG in serum are used as a correlate of protection against RSV re-infection (Kulkarni *et al.*, 2018). As a measure of how well the adaptive immune system of RSV-infected mice had responded to the infection, levels of RSV-specific antibodies were quantified in serum. This work was carried out by Master's students Olivia Swann and Celia Diaz (data shown with permission). Serum samples taken from young and elderly mice 18 days post-infection were applied to plates coated with RSV antigen. Antibodies specific to RSV bound to the plate were then detected by ELISA. RSV-specific IgG titres were calculated from dilution curves using a cut-off point determined as the average blank well reading plus three standard deviations. Anti-RSV titres were significantly higher in young mice compared to elderly mice, suggesting a stronger RSV-specific antibody response in the young mice (Figure 3-5b,c). In the serum of elderly mice, anti-RSV IgG was very low even at the highest concentration of the dilution curve. In some samples from elderly mice, levels of RSV-specific IgG were below the limit of detection.

3.3.2.4. The adaptive immune response of elderly mice to RSV infection

Multicolour flow cytometry experiments were employed to identify different types of immune cells in the airways of infected mice. Cells from homogenised lung tissue and from

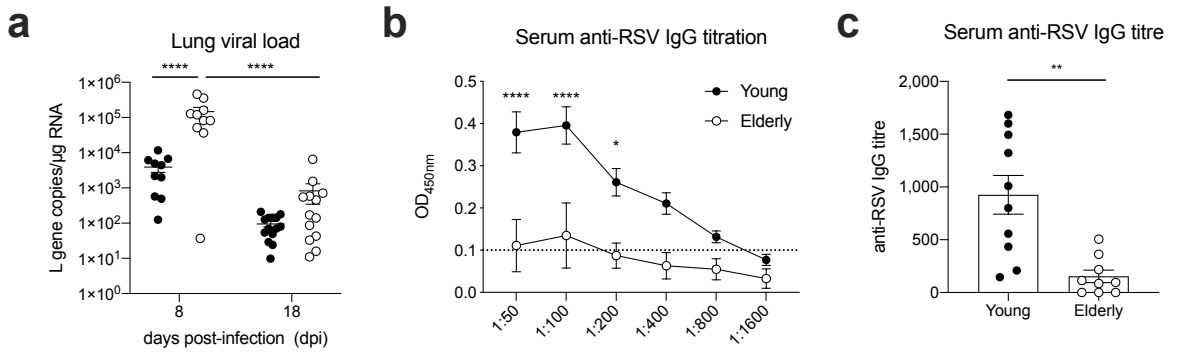

Figure 3-5 Lung viral load and RSV-specific antibody responses in young and elderly mice

a. Lung RSV viral load expressed as copies of RSV L gene detected per ug of RNA extracted from lung tissue. Pooled from five experiments (two 8 dpi, three 18 dpi) n=4-5. 2-way ANOVA with Bonferroni's multiple comparisons test. **b.+c.** The RSV-specific antibody response in serum of young and elderly RSV-infected mice. This work was carried out by Master's students Olivia Swann and Celia Diaz. Pooled from two experiments, n=5. **b.** Serum samples taken from young and elderly mice 18 days post-infection were applied in a dilution curve to RSV antigen-coated plates. Antibodies specific to RSV bound to the plate were then detected by ELISA methodology. Points represent group means, error bars represent standard error of the mean. 2-way ANOVA with Bonferroni's multiple comparisons test. **c.** RSV-specific IgG titres were calculated from dilution curves using a cut-off point determined as the average blank well reading plus three standard deviations (shown as dotted line). Student's unpaired two-tailed t test.

BAL fluid were stained for surface markers of Natural Killer (NK) cells, B cells, and T cells, including $CD4^+$ and $CD8^+$ subsets. Lung tissue contains predominantly resident immune cell populations, whereas BAL fluid contains mostly immune cells recruited into the airways due to the inflammation. The gating strategy used is shown in Figure 3-6. Lymphocytes were defined as live, singlet, $CD45^+$ cells that had characteristically low forward and side scatter. T cells were defined as $CD3^+$ lymphocytes. $CD4^+$ and $CD8^+$ T cells were defined as $CD3^+$ cells staining positive for $CD4^+$ and $CD8^+$, respectively. NK cells were defined as $CD3^-$ $NK1.1^+$ lymphocytes and B cells were defined as $CD19^+$ lymphocytes. Granulocytes were defined as $CD45^+$ $Gr1^+$ cells. Gates were set using FMO controls. This experiment was carried out at 8 dpi because that time point had proven the peak of weight loss and inflammation.

The proportion of lymphocytes found in lung tissue was not different between young and elderly mice, but the absolute number of lymphocytes was significantly higher in elderly mice, consistent with the higher number of cells in lung tissue, as established earlier

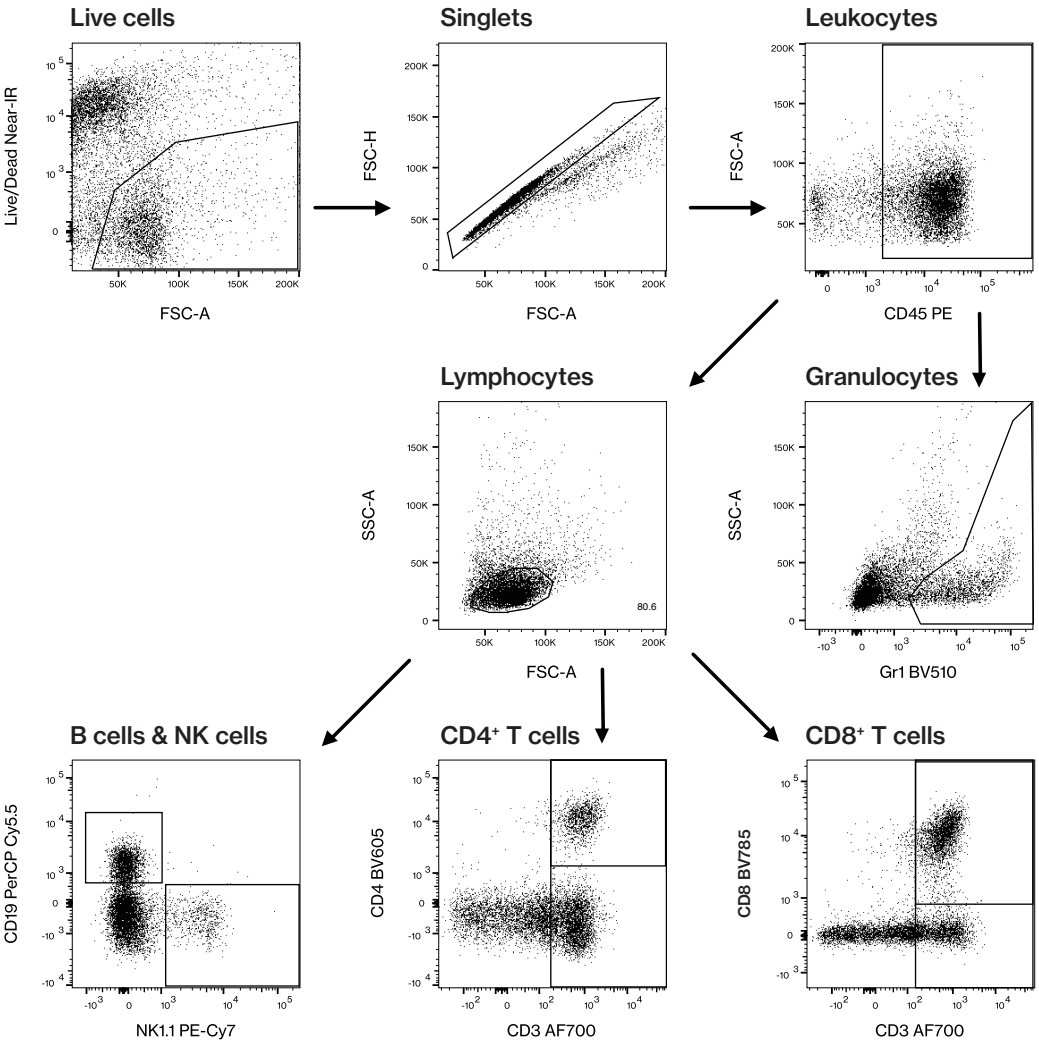

Figure 3-6 Gating strategy for immune response of young and elderly mice to RSV

Gating strategy shown as an example on a lung sample from an elderly mouse at 8 dpi. Lung and BAL cells were gated to remove debris and dead cells using Live/Dead fixable cell stain. Single cells were defined using forward scatter area and forward scatter height. Leukocytes were defined as $CD45^+$ cells and all other cell populations gated on it. Granulocytes were determined with Gr1 staining. Lymphocytes were identified using forward and side scatter area. Lymphocytes were then gated for B cells ($CD19^+$), NK cells ($NK1.1^+$), T cells ($CD3^+$) and $CD4^+$ and $CD8^+$ T cells.

(Figure 3-7a,b). Both the proportion of T cells out of lymphocytes and the total number of T cells in lung tissue was significantly higher in elderly mice compared to young (Figure 3-7c,d). The ratio of $CD4^+$ to $CD8^+$ T cells was different in elderly mice, since the proportion of $CD8^+$ T cells out of all T cells was significantly higher than in young mice (Figure 3-7g). Consistent with there being more T cells overall in the lung tissue of elderly mice, the absolute number of both $CD4^+$ and $CD8^+$ T cells was also significantly higher

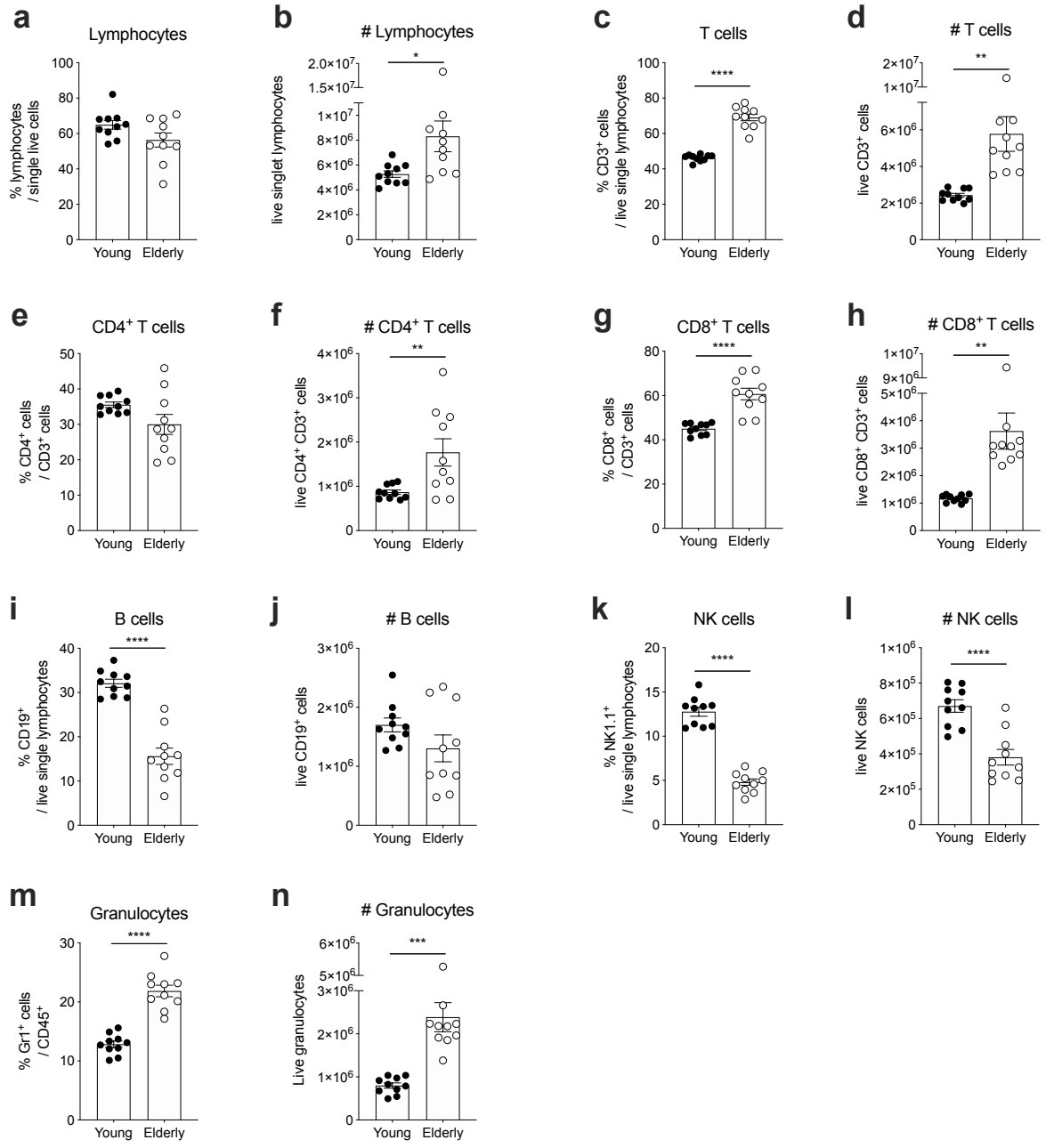

Figure 3-7 Immune responses to RSV in the lung tissue of young and elderly mice

Immune cell populations in lung tissue of young and elderly mice after 8 days of RSV infection. **a+b.** Lymphocytes. **c+d.** T cells. **e+f.** CD4+ T cells. **g+h.** CD8+ T cells. **i+j.** B cells. **k+l.** NK cells. **m+n.** Granulocytes. Student's unpaired two-tailed t-test . One experiment at n=10.

in elderly mice (Figure 3-7f,h). By contrast, the proportion of B cells and NK cells out of lymphocytes was significantly reduced in elderly mice compared to young mice (Figure 3-7i,k). The absolute number of NK cells in the lung tissue of elderly mice was significantly lower than in young mice, and there was an equivalent non-significant trend in B cells. Granulocytes accounted for a significantly larger proportion of leukocytes in the lung tissue of elderly mice, and there were significantly more granulocytes overall compared to in young mice (Figure 3-7m,n).

In BAL fluid, there was a similar effect on lymphocytes, T cells, and $CD4^+$ and $CD8^+$ subpopulations. The absolute number of lymphocytes, T cells, and $CD4^+$ and $CD8^+$ T cells was increased in elderly mice compared to young (Figure 3-8b,d,f,h). There was equally an increase in the proportion of $CD8^+$ T cells in elderly mice as there was in lung tissue (Figure 3-8g). There was no difference in the relative and absolute number of B cells in BAL cells between young and elderly mice (Figure 3-8i,j). In contrast to lung tissue, there was an increase in absolute NK cell numbers in the BAL cells of elderly mice (Figure 3-8l). This suggests that NK cells may be recruited out of lung tissue and into the airways in elderly mice during RSV infection. The proportion of granulocytes in BAL cells of elderly mice did not change, but in absolute terms granulocytes were more abundant among the BAL cells of elderly mice (Figure 3-8m,n). These results were not always consistent across experiments. There was a large variability in the response of elderly mice to infection. A separate experiment was conducted at 8 dpi (n=9-10) with a different flow cytometry staining panel (not shown). In this experiment, lung lymphocyte and $CD4^+$ T cell numbers were reduced in elderly mice compared to young, instead of elevated, and NK cells did not differ significantly between age groups. In BAL cells, the proportion of lymphocytes out of live single cells was lower in elderly mice rather than higher, but the total number of lymphocytes was still higher in elderly mice as in Figure 3-8b. In the repeated experiment, $CD4^+$ T cell numbers were not significantly different between young and elderly mice. These differences may in part be due to the different staining panel used, internal variability in virus batch, and elderly mice being inherently more variable. In sum-

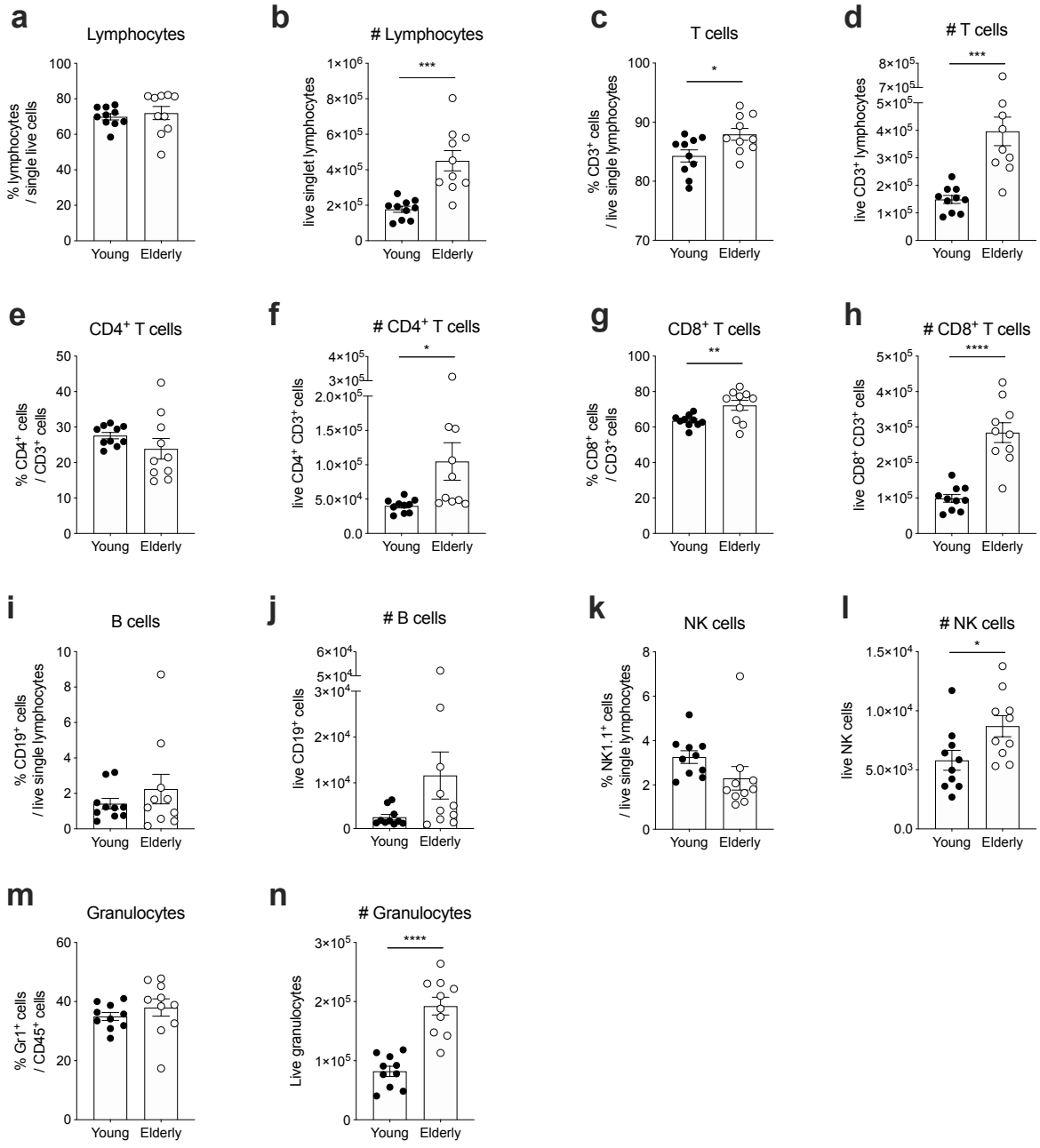

Figure 3-8 Immune responses to RSV in BAL cells of young and elderly mice

Immune cell populations in BAL fluid cells of young and elderly mice after 8 days of RSV infection. **a+b.** Lymphocytes. **c+d.** T cells. **e+f.** $CD4^+$ T cells. **g+h.** $CD8^+$ T cells. **i+j.** B cells. **k+l.** NK cells. **m+n.** Granulocytes. Student's unpaired two-tailed t-test . One experiment at n=10.

mary, elderly mice displayed a stronger inflammatory response to RSV infection in terms of a higher number of cells in the BAL fluid, of which the majority were lymphocytes.

3.3.2.5. RSV-specific immune responses of young and elderly mice

Not all adaptive immune cells found in infected mice will be specific to RSV. Hence, RSV-specific $CD4^+$ T cells were stained with an MHC class II tetramer presenting an RSV M2 peptide. $CD4^+$ T cells are instrumental in providing help to B cells during the germinal centre response. The germinal centre response describes the interaction of T cells, B cells, and dendritic cells in secondary lymphoid organs that leads to the generation of high affinity antibodies. In addition to the RSV tetramer, cells were stained for markers of the germinal centre response, to determine if elderly mice had a defect in generating this particular aspect of the RSV-specific antibody response. In addition to cells from lung tissue, cells from lymph nodes, and spleen tissue were stained, since the germinal centre response takes place in secondary lymphoid organs. The time points interrogated were day 0 (uninfected mice) and day 18, since the germinal centre response takes approximately two weeks from the start of infection to generate detectable levels of antibodies.

The gating strategy employed is shown in Figure 3-9. Germinal centre (GC) B cells were defined as $GL7^+$ $CD38^{lo}$ $CD19^+$ cells. T follicular helper (Tfh) cells were defined as $PD\text{-}1^+$ $CXCR5^+$ $CD4^+$ T cells. Tfh cells were further divided into Tfh “low” and Tfh “high” populations depending on the intensity of their staining for PD-1 and CXCR5. Positive staining of $CD4^+$ T cells with the RSV tetramer was determined by comparison to staining with a control tetramer that was ligated to the same fluorophore but loaded with CLIP, a fragment of the MHC class II invariant chain that should not be bound by murine $CD4^+$ T cells (Figure 3-10).

B cells and GC B cells were not significantly different between young and elderly in the lung (Figure 3-11a,d). This may be because no germinal centre responses should be taking place in the lung, except for rare induced bronchus-associated lymphoid tissues. The proportion of B cells out of lymphocytes increased significantly with infection in both young and elderly mice in lymph nodes and spleens (Figure 3-11b,c). At day 18, the lymph

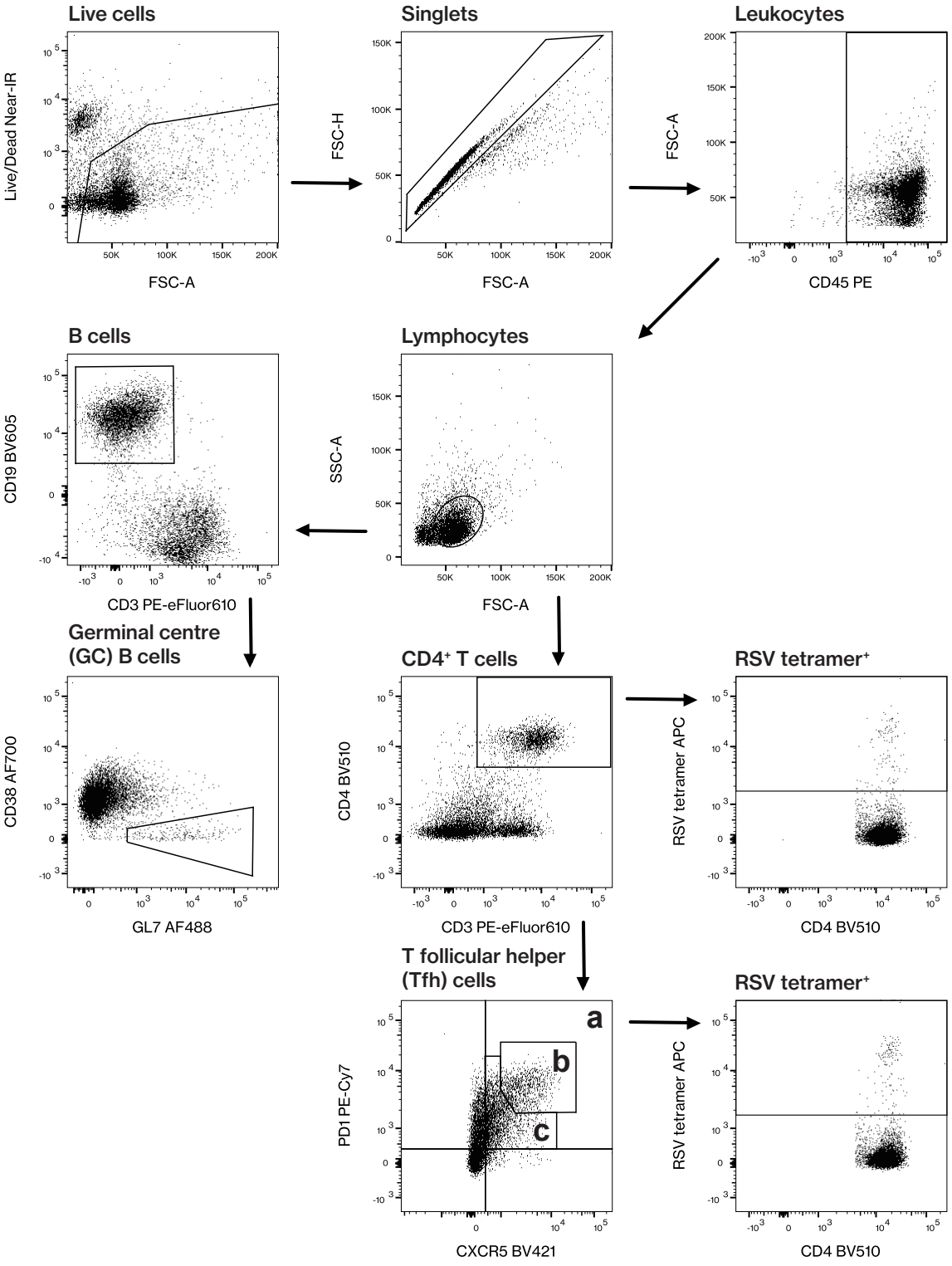

Figure 3-9 Gating strategy for germinal centre response of young and elderly mice with RSV

Gating strategy shown as an example on a lymph node sample from an elderly mouse at 18 dpi. **a.** All T follicular helper (Tfh) cells. **b.** "High" Tfh cells staining strongly for CXCR5 and PD1. **c.** "Low" Tfh cells staining less strongly for CXCR5 and PD1.

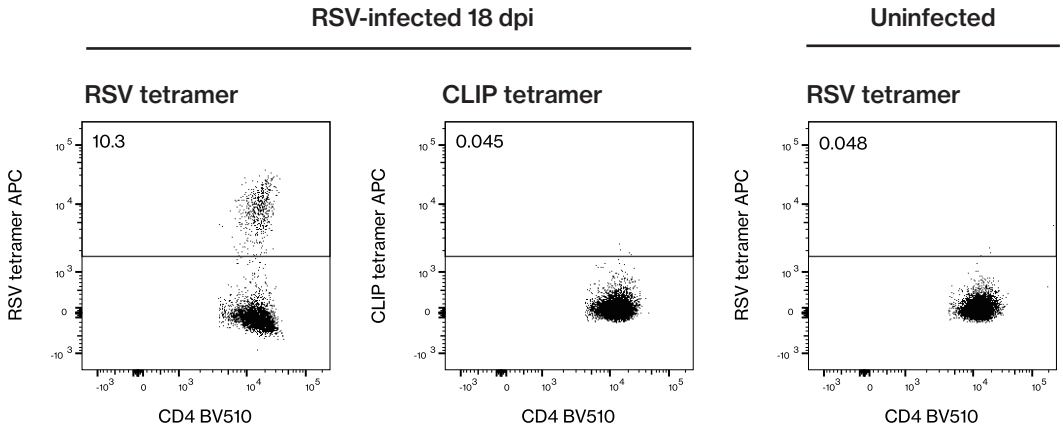

Figure 3-10 Comparison of RSV tetramer and CLIP tetramer staining

Staining of lung CD4⁺ T cells with RSV or CLIP tetramer. Gating was carried out as in Figure 3-10. Left and middle panel, staining of lung cells from RSV-infected mice with RSV tetramer (left) and CLIP control tetramer (middle). Right panel, staining of lung cells from uninfected mice with RSV tetramer.

nodes of elderly mice contained significantly more B cells than those of young mice. In the spleen, there was an opposite, non-significant trend. At baseline, the proportion of GC B cells out of all B cells in the lymph node was significantly higher in elderly mice compared to young, which may reflect a latent inflammatory state, or "inflammageing" (Figure 3-11e). However, this proportion increased with infection in young mice whereas in elderly mice it remained unchanged. The total numbers of GC B cells in all three tissues was not significantly different between young and elderly mice at any time point. There may be a trend towards higher numbers of GC B cells in elderly lymph nodes both before and after infection, but in-group variability was high. This data suggests that elderly mice are not affected by a defect in B cell recruitment to secondary lymphoid tissues, or differentiation to GC B cells.

CD4⁺ T cells were a smaller proportion of all lymphocytes in elderly mice both at day 0 and at day 18 in lungs and lymph nodes (Figure 3-12a,b). In the lung, this did not translate to smaller numbers of CD4⁺ T cells in elderly mice and is likely due to higher overall cell numbers in elderly mice. In the lymph nodes, CD4⁺ T cell numbers increased significantly with infection in young mice, but a similar increase in the elderly mice was not

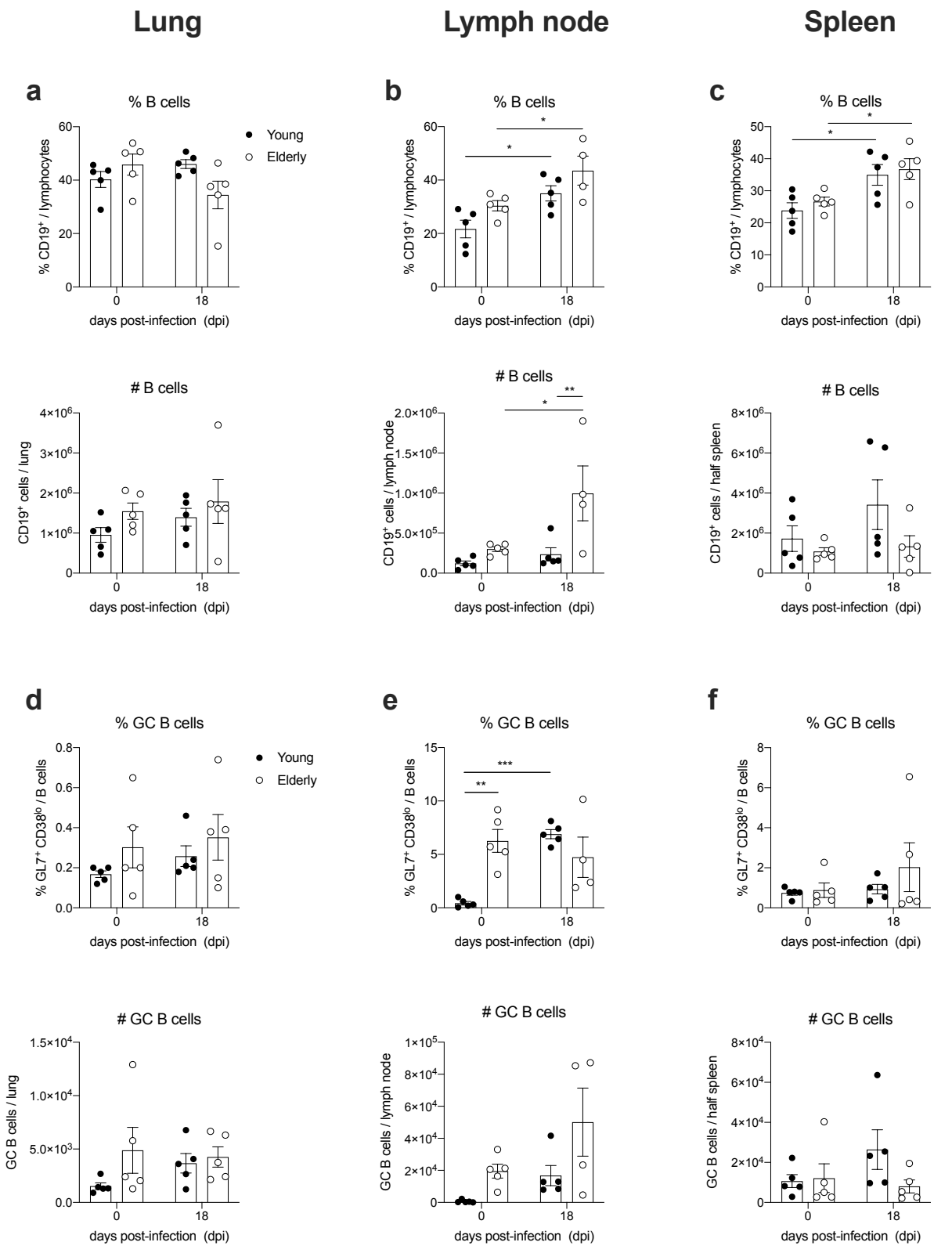

Figure 3-11 Germinal centre B cells young and elderly mice with RSV

a-c. B cells as a proportion of lymphocytes (top panels) and absolute numbers (bottom panels). **d-f.** Germinal centre (GC) B cells as a proportion of B cells (top panels) and absolute numbers (bottom panels). **a+d.** Results from lung tissue. **b+e.** Results from lymph nodes. **c+f.** Results from spleen tissue.Two-way ANOVA with Bonferroni's multiple comparison test. One experiments at n=4-5.

significant. In the spleen at baseline, elderly mice had significantly lower $CD4^+$ T cells as a proportion of lymphocytes compared to young mice, but much like in the lung, this did not cause lower total numbers of $CD4^+$ T cells in the elderly mice (Figure 3-12c). Tfh cells were unexpectedly highly abundant in elderly mice compared to young mice (Figure 3-12d-f). The proportion of Tfh cells out of all $CD4^+$ T cells was significantly higher in elderly mice in all three tissues tested, both at baseline and after 18 days of RSV infection. The lungs and spleens of elderly mice contained significantly more Tfh cells than those of young mice at both time points (Figure 3-12d,f). Tfh cells in the lymph nodes of elderly mice increased significantly in number between baseline and day 18, at which point there were also significantly more Tfh cells in the lymph nodes of elderly mice compared to young mice (Figure 3-12e). This suggests that elderly mice do not have a defect in the generation of Tfh cells. The increased abundance of Tfh cells in elderly mice at baseline may be due to on-going immune responses to commensals or autoantigens.

Since Tfh cells were already elevated in elderly mice prior to RSV infection, not all Tfh cells found in elderly mice are likely to be specific to RSV. Hence, cells were stained with an MHC class II tetramer loaded with an RSV peptide to stain for RSV-specific $CD4^+$ T cells. 18 days after infection, the lymph nodes of elderly mice contained significantly more RSV-specific $CD4^+$ T cells, both as a proportion of $CD4^+$ T cells and in absolute numbers (Figure 3-13a-c). There was no significant difference in RSV-specific $CD4^+$ T cells between young and elderly mice in lungs and spleens. On the other hand, the proportion of Tfh cells that stained positive for the RSV tetramer was significantly lower in elderly mice than in young mice in all three tissues tested (Figure 3-13d-f). This may be because elderly mice had such large numbers of Tfh cells to begin with, since the absolute number of RSV-specific Tfh cells was not different between young and elderly mice. RSV tetramer staining was also carried out in a separate experiment at 8 days post-infection. At this point, the RSV-specific adaptive immune response peaks in terms of inflammatory response in the lungs. Among cells in BAL fluid, fewer $CD4^+$ T cells were RSV-specific in the elderly mice than the young, and a similar trend was not significant

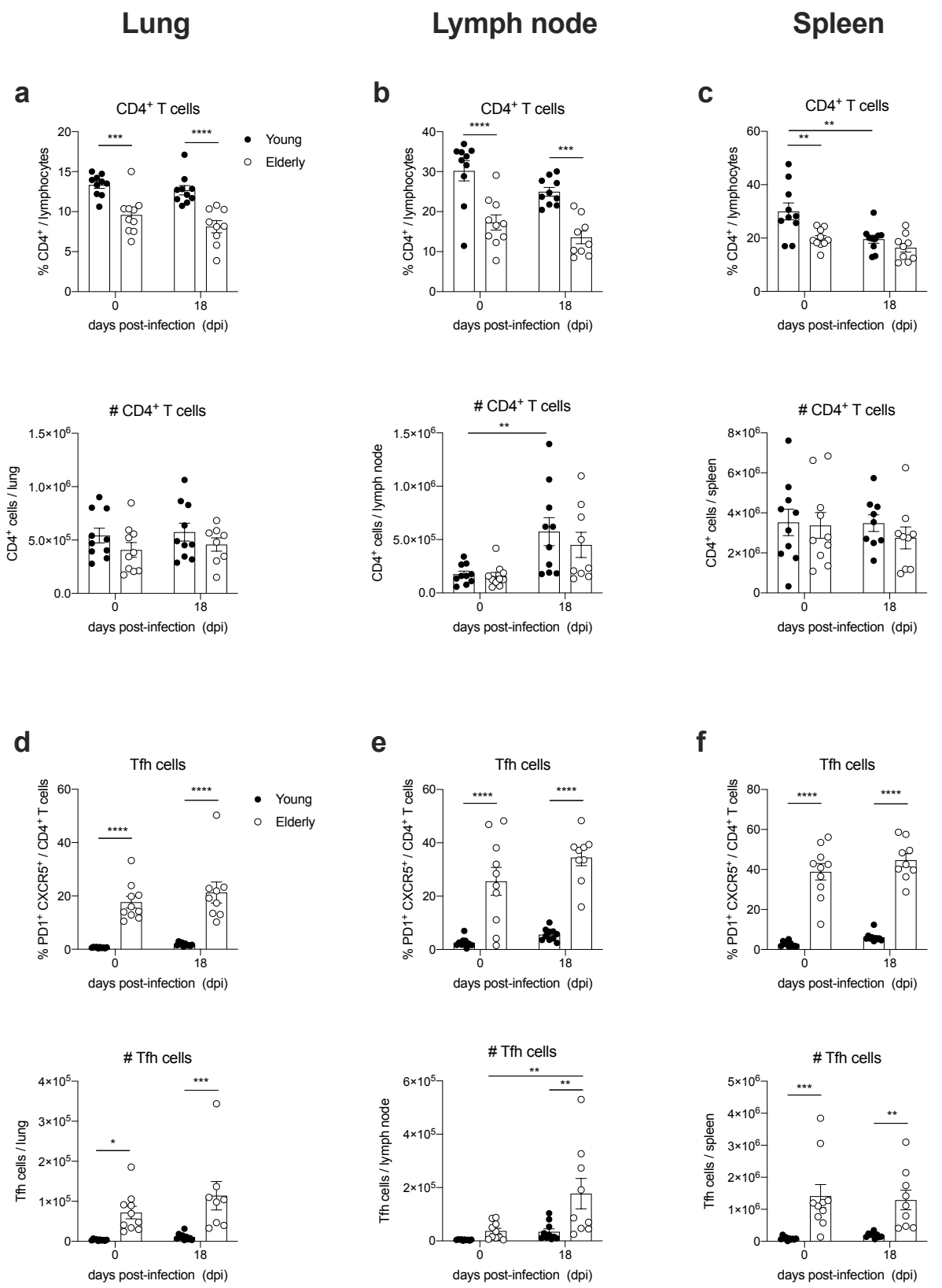

Figure 3-12 Tfh cells in young and elderly mice after RSV infection

a-c. CD4+ T cells as a proportion of lymphocytes (top panels) and absolute numbers (bottom panels). **d-f.** T follicular helper (Tfh) cells as a proportion of CD4+ T cells (top panels) and absolute numbers (bottom panels). **a+d.** Lung tissue. **b+e.** Lymph nodes. **c+f.** Spleen tissue.Two-way ANOVA with Bonferroni's multiple comparison test. Pooled from two independent experiments at n=4-5 each.

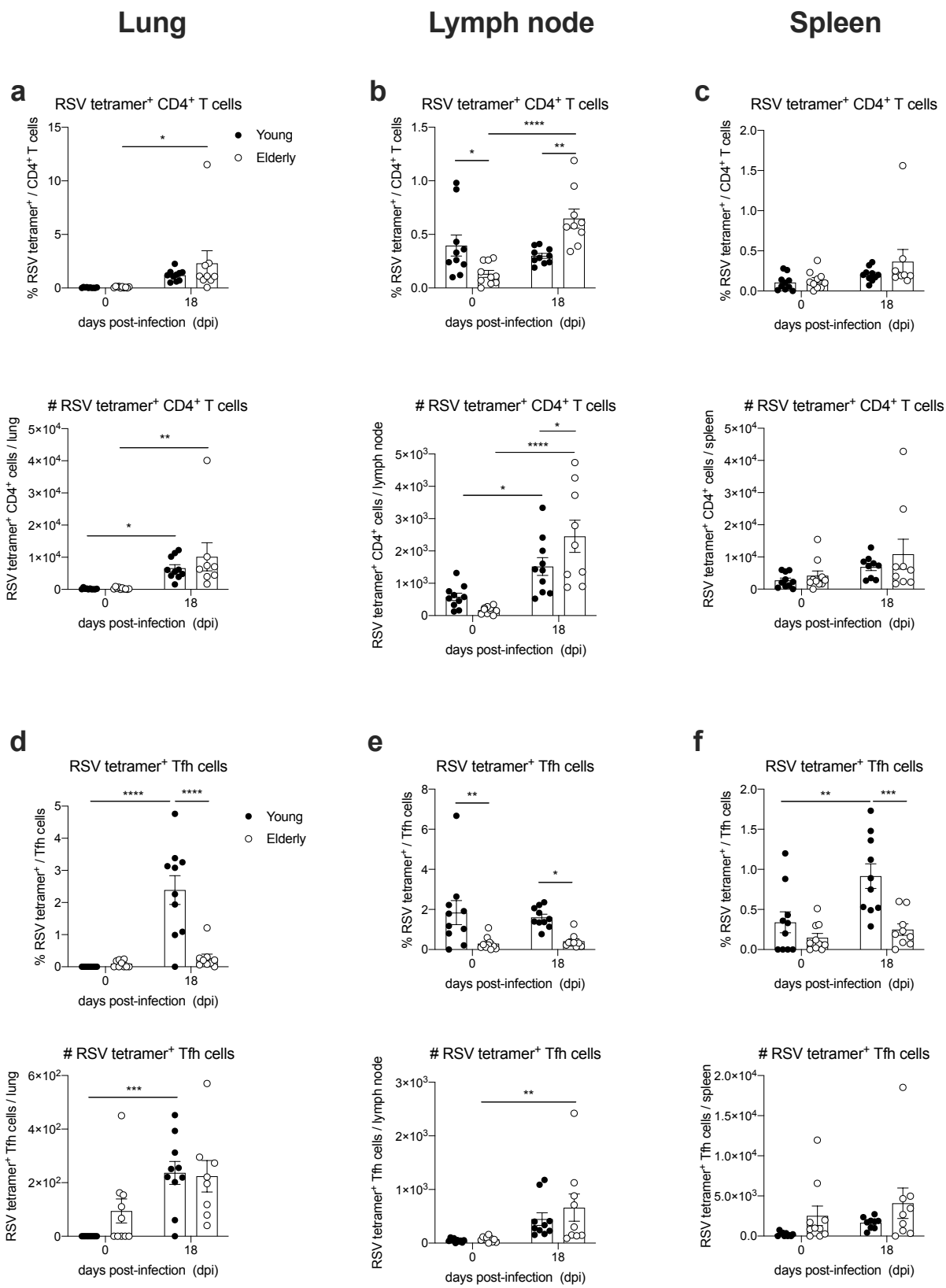

Figure 3-13 RSV tetramer staining in young and elderly mice after RSV infection

a-c. RSV tetramer+ CD4+ T cells as a proportion of CD4+ T cells (top panels) and absolute numbers (bottom panels). **d-f.** RSV tetramer+ T follicular helper (Tfh) cells as a proportion of Tfh cells (top) and absolute numbers (bottom). **a+d.** Lung tissue. **b+e.** Lymph nodes. **c+f.** Spleen tissue.Two-way ANOVA with Bonferroni's multiple comparison test. Pooled from two independent experiments at n=4-5 each per timepoint.

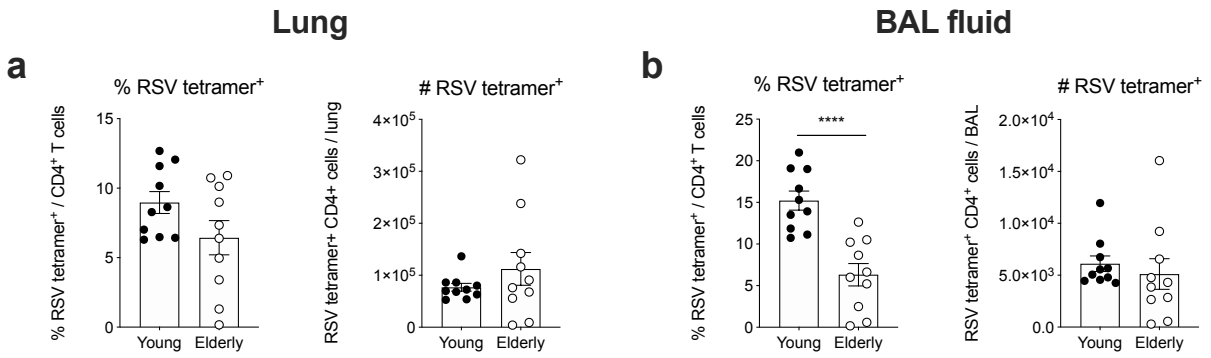

Figure 3-14 RSV tetramer staining at the peak of RSV infection

a. Lung tissue stained for RSV tetramer. RSV tetramer$^+$ CD4$^+$ T cells as a proportion of CD4$^+$ T cells (left panel) and absolute numbers (right panel). **b.** BAL fluid cells stained for RSV tetramer. RSV tetramer$^+$ CD4$^+$ T cells as a proportion of CD4$^+$ T cells (left panel) and absolute numbers (right panel). Student's two-tailed unpaired t test. One experiment at n=10.

in lung cells (Figure 3-14). However, total numbers of RSV-specific CD4$^+$ T cells were not different between young and elderly mice in either tissue.

The ability of immune cells to mount an effective response against pathogens is highly dependent on their ability to secrete cytokines. Cells from lung tissue and BAL fluid were stained for IFN-γ and IL-10 using intracellular cytokine staining. This was carried out at day 8 at the peak of infection. The gating strategy is shown in Figure 3-15. Gates were set using FMO controls and using samples of cells that were not stimulated so should not be producing large amounts of either cytokine. The cell types investigated for their ability to produce IFN-γ and IL-10 were CD8$^+$ T cells, CD4$^+$ T cells, and RSV tetramer-positive CD4$^+$ T cells. A higher proportion of CD8$^+$ T cells stained positive for IFN-γ in the lungs and BAL fluid of elderly mice compared to young mice (Figure 3-16a,b). There were also more IFN-γ$^+$ CD8$^+$ T cells in total in the lungs and BAL fluid of elderly mice. CD4$^+$ IFN-γ$^+$ T cells were equally more frequent and more abundant in the lungs of elderly mice (Figure 3-16c). There was no difference in the frequency or abundance of IFN-γ$^+$ CD4$^+$ T cells in BAL fluid between young and elderly mice (Figure 3-16d). In contrast to all CD4$^+$ T cells, RSV-specific CD4$^+$ T cells in the lungs of elderly mice were less frequently IFN-γ$^+$ (Figure 3-16e). In BAL fluid, IFN-γ$^+$ RSV-specific CD4$^+$ T cells were more frequent in elderly mice

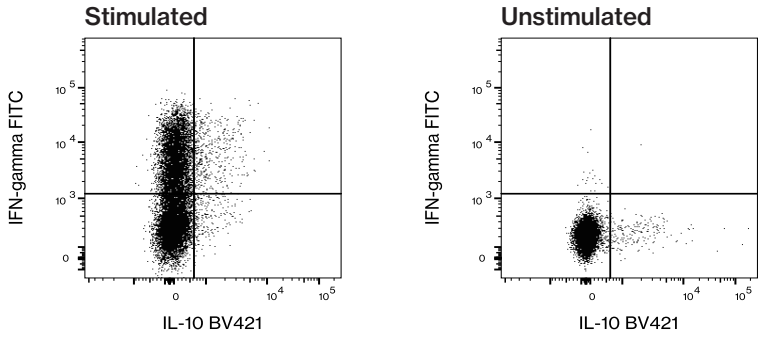

Figure 3-15 Gating strategy for cytokine response of young and elderly mice to RSV

Gating strategy to determine production of the cytokines IL-10 and IFN-gamma in immune cell subsets using intracellular flow cytometric staining. This set of gates was applied to $CD4^+$, $CD8^+$ T cells, and RSV $tetramer^+$ $CD4^+$ T cells, which were gated according to Figure 3-9. Left panel, lung cells derived from RSV-infected mice stimulated with PMA and ionomycin for one hour. Right panel, lung cells mock-stimulated with complete RPMI medium for the same amount of time. After the stimulation, cells were incubated for two hours with Golgi Stop export inhibitor to retain cytokines inside cells.

than in young mice (Figure 3-16f). However, IFN-γ^+ RSV-specific $CD4^+$ T cells were no more or less abundant in the lungs and BAL fluid of elderly mice.

More $CD8^+$ T cells stained positive for IL-10 in the lungs of elderly mice compared to young mice (Figure 3-17a,b). There were also more IL-10^+ $CD8^+$ T cells in total in the lungs and BAL fluid of elderly mice (Figure 3-17a,b). $CD4^+$ IL-10^+ T cells were equally more frequent and more abundant in the lungs of elderly mice (Figure 3-17c). In BAL fluid, $CD4^+$ IL-10^+ T cells were less frequent as a proportion of $CD4^+$ T cells, but more abundant in total compared with young mice (Figure 3-17d). Like IFN-γ, RSV-specific $CD4^+$ T cells in the lungs of elderly mice were less frequently IL-10^+ rather than more frequently like all $CD4^+$ T cells (Figure 3-17e). In BAL fluid, there was no difference in the frequency of IL-10^+ staining of RSV-specific $CD4^+$ T cells between young and elderly mice (Figure 3-17f). There was no difference between young and elderly mice in the abundance of IL-10^+ RSV-specific $CD4^+$ T cells in lungs and BAL fluid. These results do not support the hypothesis of elderly T cells being impaired in their ability to secrete cytokines during an RSV infection.

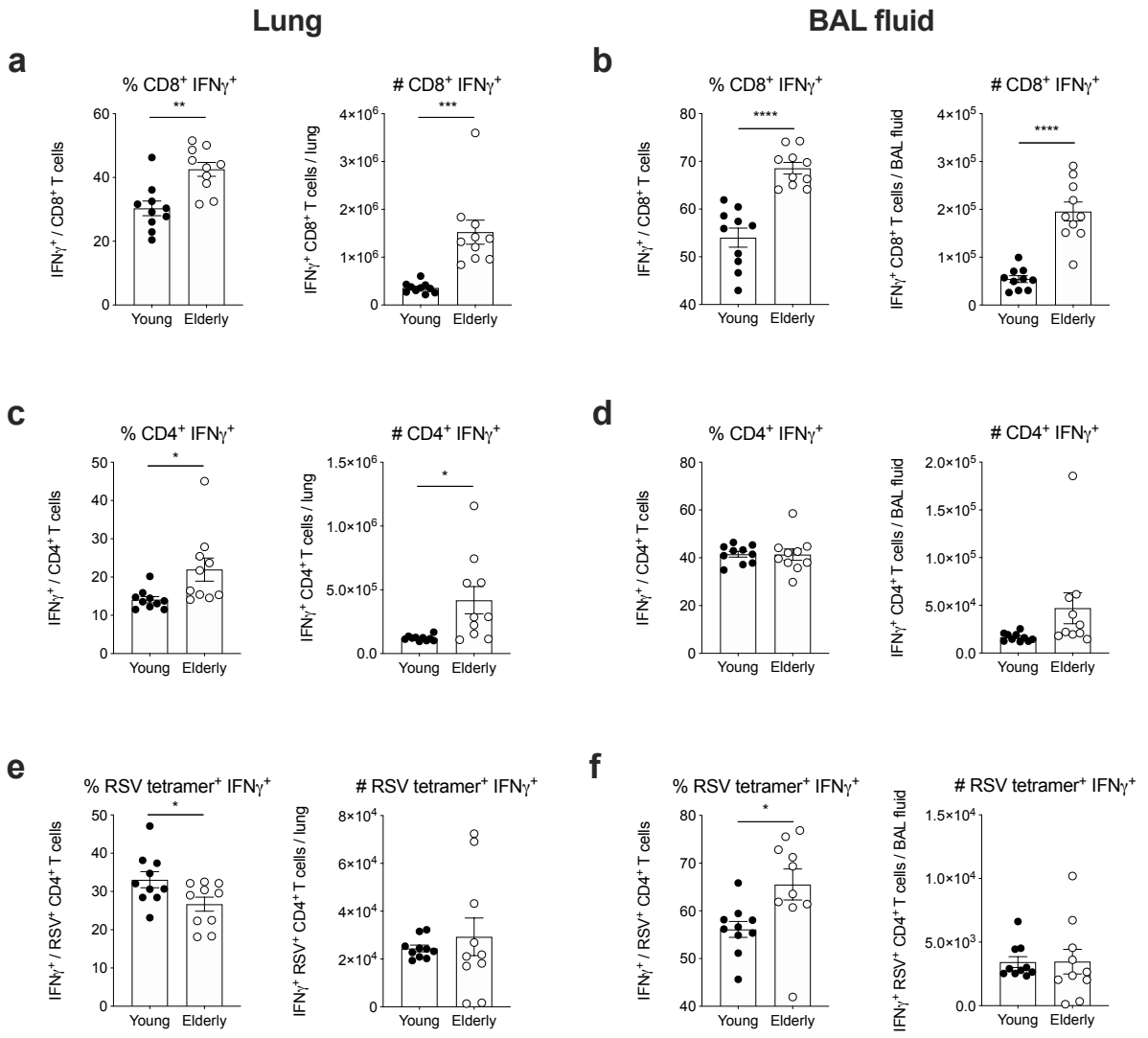

Figure 3-16 IFNγ production by immune cells of young and elderly mice infected with RSV

Lung cells and BAL fluid cells were harvested from young and elderly mice 8 days after RSV infection. Populations were gated according to Figure 3-9 and Figure 3-15. One experiment at n=10. Student's unpaired two-tailed t test. **a.,c.,e.** Results from lung cells. **b.,d.,f.** Results from BAL fluid cells. **a.-b.** $CD8^+$ T cells. **c.-d.** $CD4^+$ T cells. **e.-f.** RSV tetramer-positive $CD4^+$ T cells.

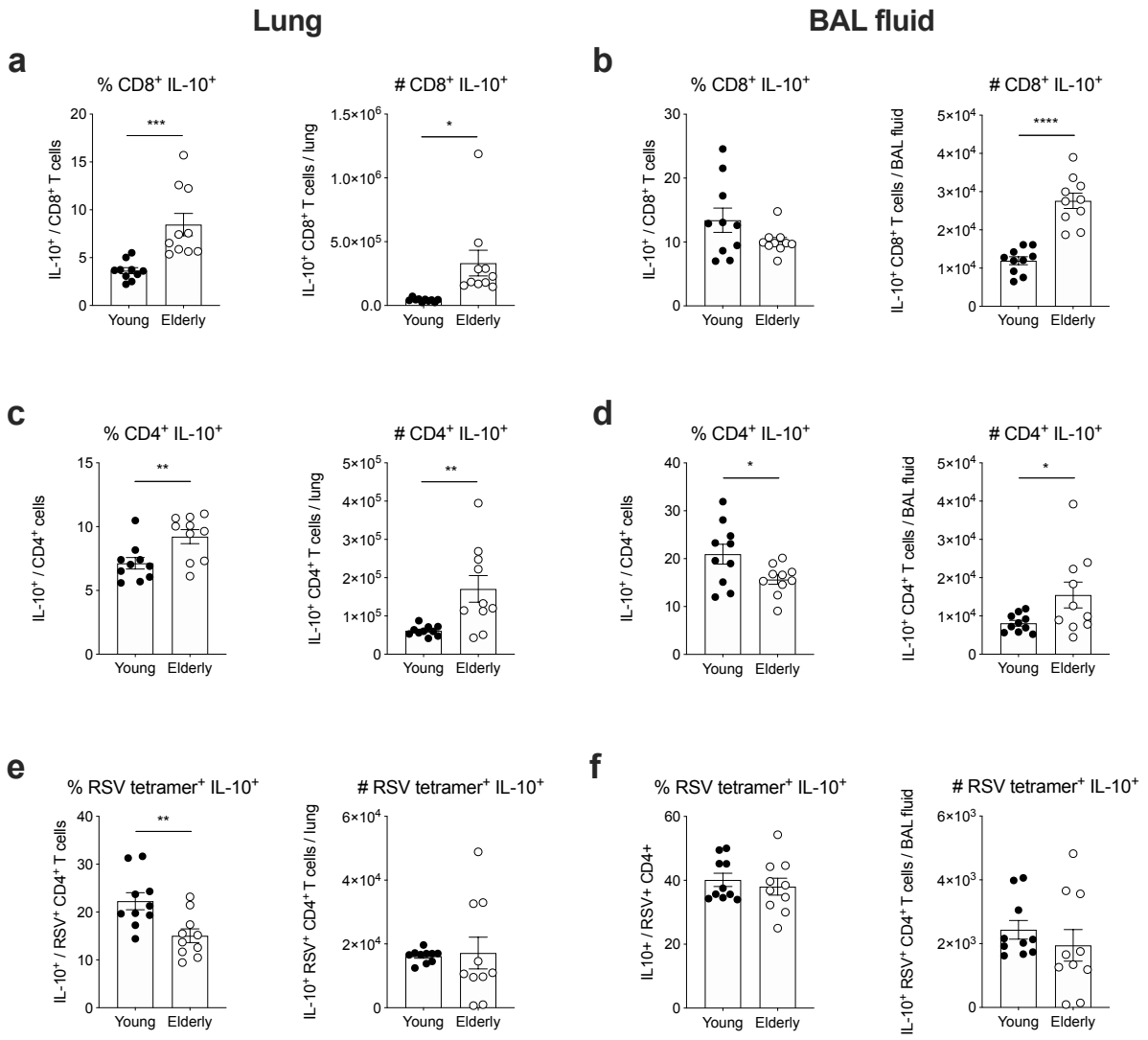

Figure 3-17 IL-10 production by immune cells of young and elderly mice infected with RSV

Lung cells and BAL fluid cells were harvested from young and elderly mice 8 days after RSV infection. Populations were gated according to Figure 3-9 and Figure 3-15. One experiment at n=10. Student's unpaired two-tailed t test. **a.,c.,e.** Results from lung cells. **b.,d.,f.** Results from BAL fluid cells. **a.-b.** $CD8^+$ T cells. **c.-d.** $CD4^+$ T cells. **e.-f.** RSV tetramer-positive $CD4^+$ T cells.

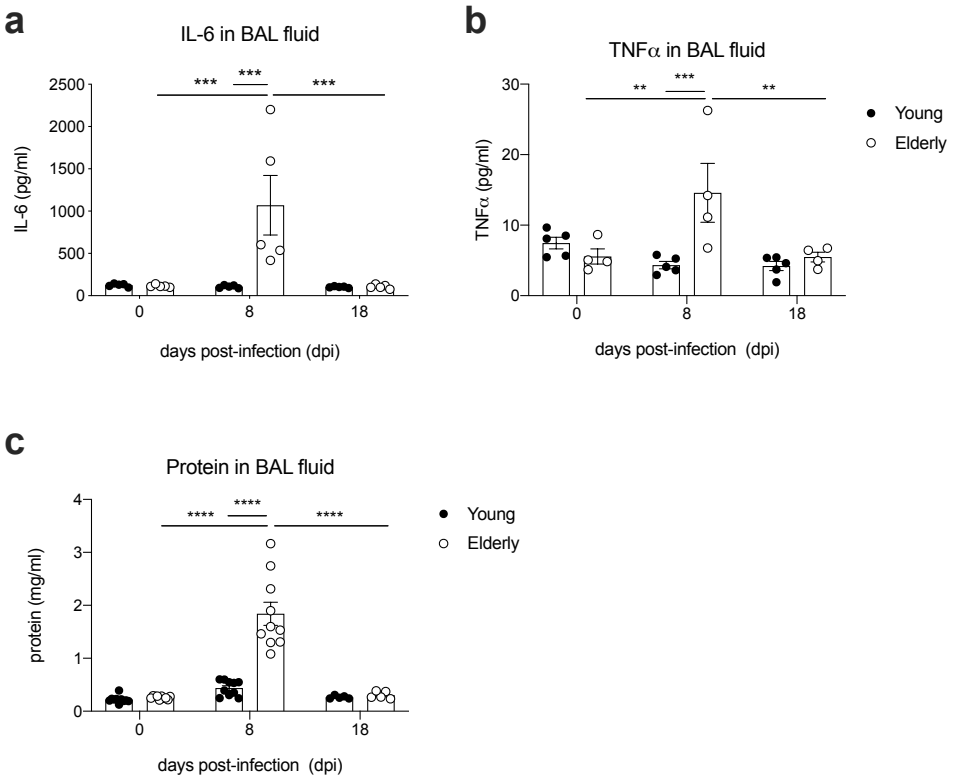

Figure 3-18 Cytokines in the airways of young and elderly mice infected with RSV

Cytokine levels were assayed using ELISA. Total protein content was assessed by Bradford assay. **a.** IL-6 protein in BAL fluid. n=5 per age group and time point **b.** TNF-α protein in BAL fluid. n=4-5 per age group and time point. This assay was carried out by Tasneem Oubira. **c.** Total protein content in BAL fluid. n=10 per age group and per time point. Two-way ANOVA with Bonferroni's multiple comparison test.

3.3.2.6. Elevated pro-inflammatory cytokines in the airways of RSV-infected elderly mice

During an RSV infection, immune cells in the airways produce cytokines. The protein levels of interleukin 6 (IL-6) and tumor necrosis factor alpha (TNF-α) were assayed in the BAL fluid of young and elderly mice infected with RSV (Figure 3-18a,b). Additionally, total protein levels in the BAL fluid were measured with a Bradford assay (Figure 3-18c). Total protein in BAL fluid reflects the amount of vascular permeability and is thereby another measure of inflammation. IL-6 increased significantly in the BAL fluid of elderly mice from baseline to day 8 post-infection. At this time point, the peak of infection, IL-6 levels were significantly higher in elderly mice than in young mice. IL-6 levels decreased back

to baseline again in elderly mice by day 18. TNF-α levels also increased significantly in the BAL fluid of elderly mice with RSV infection (Figure 3-18b). At day 8 post-infection, TNF-α levels were significantly higher in the BAL fluid of elderly mice than in young mice. TNF-α levels at day 18 post-infection were not significantly different to baseline levels in either young or old mice. Total protein in the BAL fluid increased significantly in elderly mice with infection, and was significantly higher in elderly mice than young mice at day 8 (Figure 3-18c). If tested in a separate t-test, total BAL protein levels at baseline were also significantly higher in elderly mice than young mice, but this was not significant in the two-way ANOVA employed to test multiple time points. These results add further evidence to the theory that elderly mice have higher levels of inflammation than young mice after RSV infection.

3.3.3. Elderly mice display muscle wasting after RSV infection

3.3.3.1. Gross and relative muscle weight decreases in elderly mice during RSV infection

The weight lost by elderly mice during RSV infection likely includes muscle mass, fat mass, and water weight. The aim of this study was to interrogate the effect of infection on the loss of muscle mass specifically. Therefore, the tibialis anterior (TA) muscle was extracted from young and elderly mice infected with RSV. The TA is a large leg muscle used for locomotion. After euthanasia, the TA from both legs of each animal was removed and weighed before further processing. Prior to infection, elderly mice had heavier TA muscles than young mice, consistent with their higher baseline bodyweight (Figure 3-19a). At the peak of infection at day 8, the TA weight of elderly mice had decreased significantly from baseline. The mean TA weight of elderly mice at this point was below that of young mice, but this was not statistically significant. From day 8 to day 18, the TA weights of elderly mice increased again. At day 18, elderly mice had significantly heavier TA muscles than young mice again, although this difference was not as pronounced as at baseline. 18 days after infection, the average TA weight of elderly mice remained significantly lower than at day 0. The TA weight of young mice remained almost unchanged

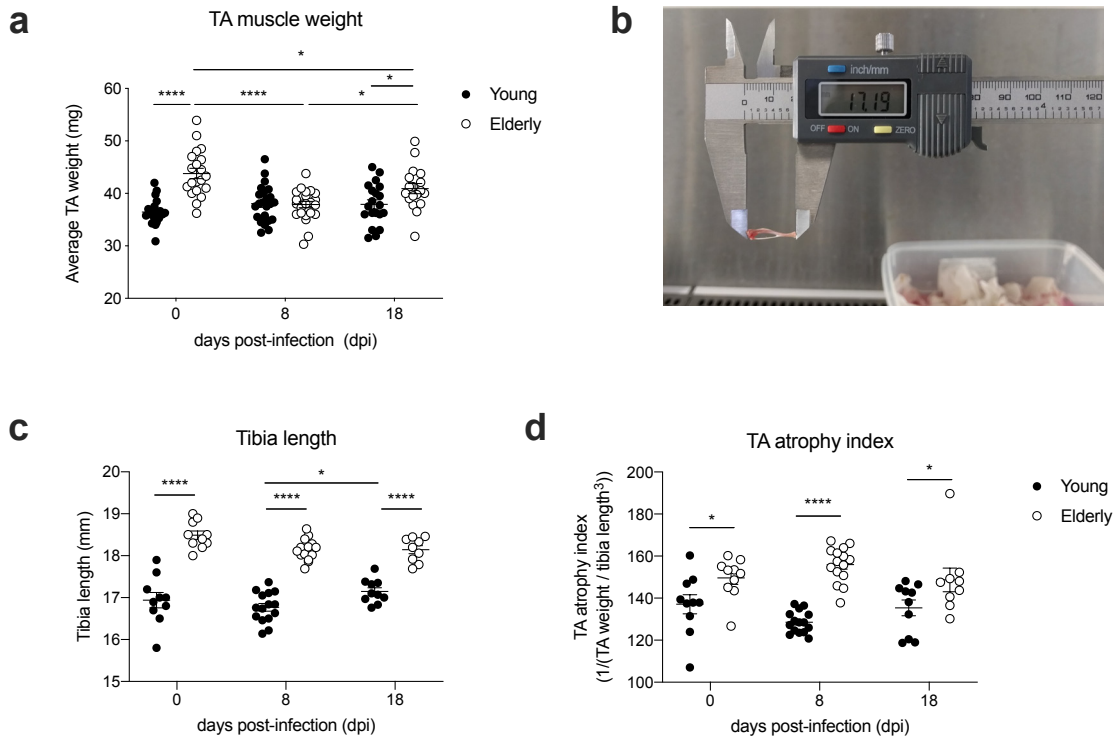

Figure 3-19 Elderly mice lose skeletal muscle mass during RSV infection

a. Tibialis anterior (TA) muscle weight of young and elderly mice before RSV infection, 8 days post-infection, and 18 days post-infection (average of both legs per mouse). Pooled from 11 independent experiments at n=4-10 each per timepoint. **b.** Example of how tibia length was measured using calipers. **c.** Tibia length of young and elderly mice before and during RSV infection. Pooled from 6 independent experiments at n=4-10 each per timepoint. **d.** TA atrophy index of young and elderly mice before and during RSV infection. Pooled from 6 independent experiments at n=4-10 each per timepoint. Two-way ANOVA with Bonferroni's multiple comparison test.

throughout infection.

Applying statistical tests to compare the raw muscle weights of young and elderly mice may not be useful because young and elderly mice had different body compositions at baseline. For example, elderly mice had a significantly higher baseline bodyweight. In addition, the data displayed considerable individual variation in elderly mice. Therefore, I sought to normalise TA weight to better account for individual variability and the different starting conditions of young and elderly mice before infection. A "TA atrophy index" was calculated as follows (Patel *et al*., 2016):

$$\text{TA atrophy index} = \frac{1}{\left(\frac{\text{TA weight}}{\text{tibia length}^3}\right)}$$

The TA atrophy index normalises an individual animal's TA muscle weight to the length of its tibia cubed (Figure 3-19b,c). In contrast to bodyweight, which was known to change with infection, tibia size should remain unchanged. The length of the tibia was cubed to obtain a measure of the same dimension as weight. The reciprocal was taken so that high levels of atrophy (small TA weight in relation to tibia) would yield high values. This atrophy index yielded an output of muscle mass in relation to the size of the mouse (Figure 3-19d). The TA atrophy index of elderly mice was significantly higher than that of young mice at all three time points. However, this relationship was most significant 8 days post-infection. This suggests that at the peak of infection, elderly mice had significantly smaller TA muscles in relation to their body size than young mice.

3.3.3.2. The muscles of elderly mice have an atrogenic gene signature

Muscle mass is maintained in a balance of synthesis and breakdown. Weighing the TA muscle only measures the net outcome of this balance, which may be disturbed on either side. Gene expression in the muscle can determine muscle mass and function. The expression of several genes in TA muscle was measured by qPCR. The expression of three genes encoding products promoting muscle atrophy were assayed: *Fbxo32* (encoding Atrogin-1), *Trim63* (encoding MuRF-1), and *Mstn* (encdoing myostatin). The expression of five genes encoding products promoting muscle growth were assayed: *Myog* (encoding myogenin), *Pax7* (encoding Paired box 7 (Pax7)), *Myod1* (encoding Myogenic Differentiation 1 (MyoD1)), *Mef2c* (Myocyte enhancer factor 2 c (Mef2c)) and *Igf1* (encoding insulin-like growth factor 1 (IGF-1)). IGF-1 is a key coordinator of systemic growth and cellular proliferation via activation of mTOR, and promotes muscle protein synthesis. Myogenin, Pax7, MyoD1 and Mef2c are key determinants of the differentiation

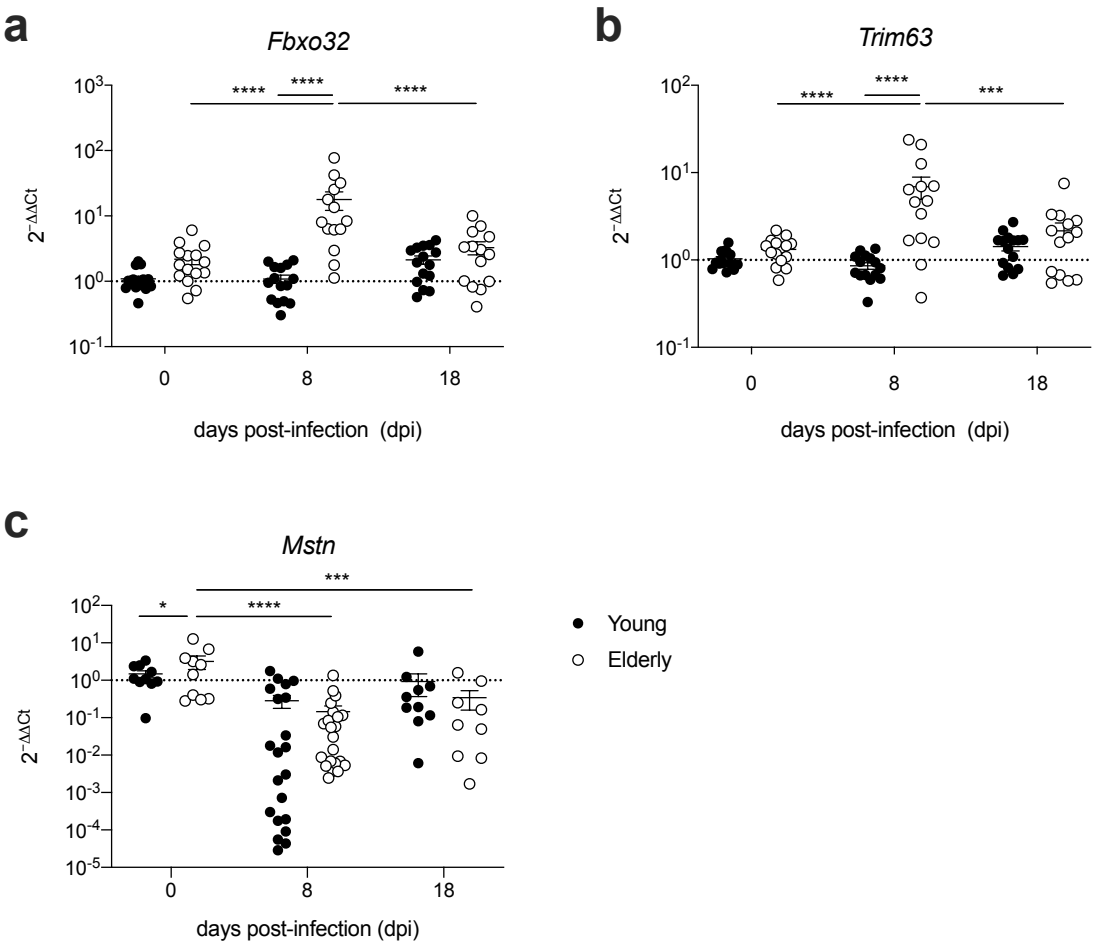

Figure 3-20 Expression of negative regulators of muscle mass during RSV infection

qPCR assays of gene expression in the TA muscle of young and elderly mice before RSV infection, 8 days post-infection, and 18 days post-infection. Pooled from 6 independent experiments at n=4-10 each. Two-way ANOVA with Bonferroni's multiple comparison test. **a.** *Fbxo32* encoding Atrogin-1 **b.** *Trim63* encoding MuRF-1. **c.** *Mstn* encoding Myostatin.

and maturation of muscle fibres, both during embryogenesis and during regeneration after damage. Atrogin-1 and MuRF-1 are both E3 ubiquitin ligases that are expressed exclusively in muscle tissue. In concert with other enzymes, they link ubiquitin groups to target proteins, causing the target protein to be directed towards 26S proteasomes for degradation. They are therefore important negative regulators of muscle mass. Myostatin is a key negative regulator of muscle mass, signalling through Activin receptor IIB to promote muscle atrophy, partially by inducing the expression of Atrogin-1 and MuRF-1.

The expression of Atrogin-1 and MuRF-1 was not significantly different between young

and elderly mice at baseline (Figure 3-20a,b). 8 days after infection, Atrogin-1 and MuRF-1 expression remained constant in the muscles of young mice, but increased significantly in the muscles of elderly mice. At this time point, expression of both Atrogin-1 and MuRF-1 was significantly higher in the muscle of elderly mice than in young mice. The expression of both Atrogin-1 and MuRF-1in the muscles of elderly mice significantly decreased from day 8 to day 18 post-infection, and was not signifcantly different to that of young mice at 18 days post-infection.

The muscles of elderly mice expressed significantly more Myostatin at baseline than young mice (Figure 3-20c). Curiously, Myostatin expression decreased from baseline to day 8 of RSV infection in the muscles of elderly mice, and remained significantly lower at day 18 than at baseline. The expression of Myostatin in the muscles of young mice did not change with infection, but expression was generally very low.

The effect of RSV infection on the expression of genes promoting muscle growth and repair was mixed. Myogenin expression was significantly higher in the muscles of elderly mice than the muscles of young mice at the peak of RSV infection (Figure 3-21a), but there were no differences between young and elderly mice at baseline or 18 days post-infection.

Pax7 expression was significantly lower at baseline in the muscles of elderly mice compared to young mice (Figure 3-21b). Pax7 expression decreased significantly in the muscles of young mice from baseline to day 8 of infection, and remained significantly lower at day 18 compared to baseline. These trends were also evident in the muscles of elderly mice, but did not reach statistical significance, possibly due to the large variability in the data from elderly mice. At the peak of RSV infection, Pax7 expression was significantly lower in the muscles of elderly mice than in the muscles of young mice, suggesting a defect in muscle regeneration stemming from a lack of satellite cells in elderly mice.

MyoD1 expression was not significantly different between young and elderly mouse muscles at any time point of RSV infection (Figure 3-21c). Expression of MyoD1 decreased

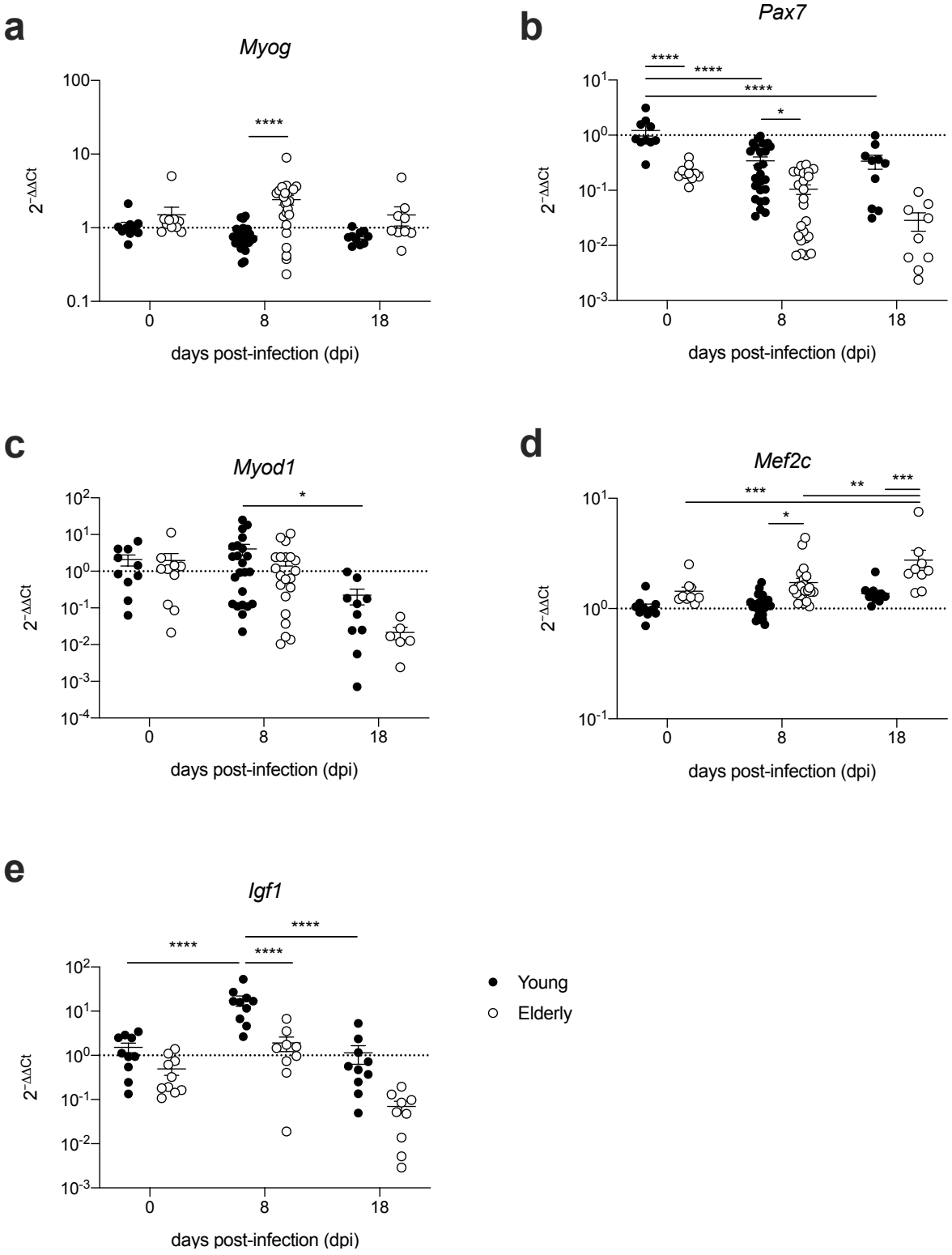

Figure 3-21 Expression of positive regulators of muscle mass during RSV infection

qPCR assays of gene expression in the TA muscle of young and elderly mice before RSV infection, 8 days post-infection, and 18 days post-infection. Pooled from 6 independent experiments at n=4-10 each. Two-way ANOVA with Bonferroni's multiple comparison test. **a.** *Myog* encoding Myogenin. **b.** *Pax7* encoding Pax7. **c.** *Myod1* encoding MyoD1. **d.** *Mef2c* encoding Mef2c. **e.** *Igf1* encoding IGF-1.

significantly in the muscles of young mice from day 8 to day 18 of infection. A similar trend was seen in the muscles of elderly mice, but this was not statistically significant.

Counterintuitively, the expression of Mef2c was significantly higher in the muscles of elderly mice at the peak of RSV infection than in the muscles of young mice (Figure 3-21d). Expression of Mef2c further increased significantly from day 8 to day 18 in the muscles of elderly mice, and was significantly elevated at day 18 compared to baseline.

IGF-1 expression increased significantly in the muscles of young mice from baseline to day 8 of infection, and returned to baseline at day 18 of infection (Figure 3-21e). At day 8, the muscles of young mice expressed significantly more IGF-1 than the muscles of elderly mice. The expression of IGF-1 in the muscles of elderly mice was not changed significantly by infection.

3.3.3.3. A novel assay for measuring polypeptide turnover

Puromycin is an aminonucleoside compound produced naturally by the bacterium *Streptomyces alboniger*. It is a structural analogue of tyrosyl-tRNA (Figure 3-22a). Puromycin functions as an antibiotic by terminating ribosome translation. Puromycin can insert into the A site of a ribosome and be linked to the nascent amino acid chain. However, the amide bond at the 3' position of the ribofuranose ring is more resistant to hydrolysis than the ester bond created by an aminoacyl tRNA. Translation cannot progress and the truncated peptide chain is released. At low doses, puromycin is non-toxic and its incorporation can be used as a correlate of the rate of protein synthesis (Nakano & Hara, 1979). Utilising puromycin incorporation as a measure of protein synthesis in cultured cells was first described by Schmidt *et al.* (Schmidt *et al.*, 2009), and developed further for *in vivo* use by Goodman *et al.* (Goodman *et al.*, 2011, 2012). The protocol used here for assaying puromycin incorporation into murine muscle was adapted and optimised from Goodman *et al.* (Goodman *et al.*, 2012, 2011) and in discussion with Paul Kemp (personal discussion). Mice were injected intraperitoneally with 0.8µmol puromycin dihydrochloride suspended in sterile PBS and sacrificed 30 minutes later. TA muscles were homogenised, centrifuged, and the clear, protein-containing supernatant aliquoted.

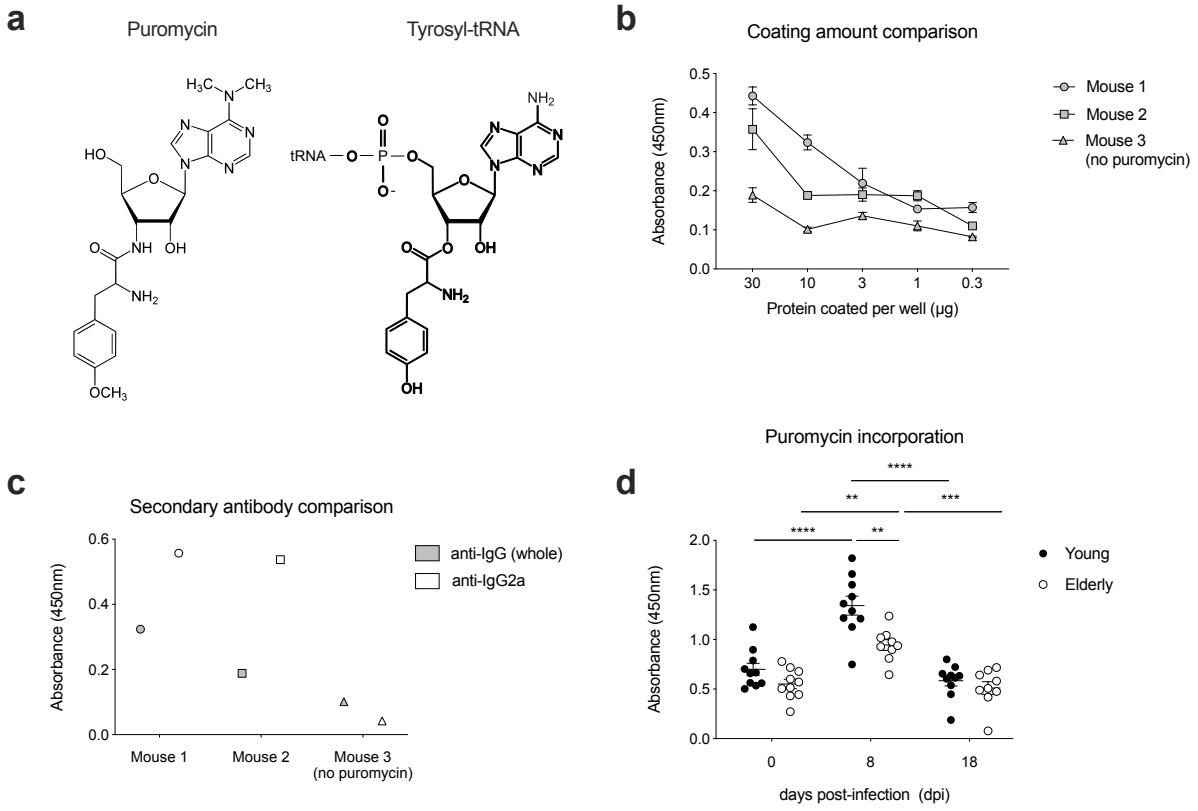

Figure 3-22 Optimisation and results of puromycin incorporation assay

a. Chemical structure of puromycin (left) compared to the structure of tyrosyl-tRNA (right). **b.** Titration of amount of TA protein supernatant to coat on ELISA plates to achieve an acceptable signal/noise ratio. **c.** Comparison of two peroxidase-conjugated secondary antibodies on the same samples shown in b, coated at 10µg/well. Closed symbols: anti-IgG (whole), open symbols: anti-IgG2a. **d.** Incorporation of puromycin into TA muscle of young and elderly mice before and after RSV infection. Pooled from 5 independent experiments, n=4-10. Two-way ANOVA with Bonferroni's multiple comparison test.

Firstly, the amount of TA protein supernatant with which to coat ELISA plates was established in a titration experiment (Figure 3-22b). Samples from two mice injected with puromycin were compared to a sample from a mouse that had not been injected with puromycin. The titration suggested that plates should be coated with at least 10µg protein suspension per well to allow for discrimination of samples from background (the sample with no puromycin). Coating with 30µg protein per well may have yielded even clearer results, however, this would have used up a large amount of sample for each assay. For sample conservation purposes, wells were coated with 10µg protein and diluted

in coating buffer.

The background signal in the muscle homogenate of a mouse not injected with puromycin was relatively high. Options for improving signal strength were explored. The peroxidase-conjugated secondary antibody used to detect the anti-puromycin antibody was raised against murine whole IgG. The high background may have been due to non-specific binding of this secondary antibody to other epitopes found in the muscle homogenate. Previous publications had also encountered this problem and solved it by using a secondary antibody specific to the isotype of the anti-puromycin antibody (IgG2a) (Goodman & Hornberger, 2013). To test this, the secondary antibody was substituted with an IgG2a-specific secondary antibody. This led to an increase in absorbance in samples treated with puromycin, and to a decrease in absorbance in the sample not treated with puromycin (Figure 3-22c). Using an isotype-specific secondary antibody thus increased both sensitivity and specificity. The IgG2a-specific secondary antibody was used in all other puromycin incorporation assays.

This optimised method was applied to samples from the RSV infection time course in young and elderly mice (Figure 3-22d). At baseline, there was a trend towards elderly mice having slightly lower levels of puromycin incorporation, however this was not significant. Unexpectedly, levels of puromycin incorporation increased significantly with infection in both young and elderly mice. This suggests that protein synthesis activity in skeletal muscle actually increases during respiratory infection. At the peak of infection at day 8, puromycin incorporation, and by extension overall protein synthesis, was significantly lower in elderly mice than in young mice. By day 18, levels had returned to baseline in both young and elderly mice. This discrepancy in upregulation of protein synthesis at the peak of infection may contribute towards the higher loss of muscle mass observed in elderly mice.

3.3.3.4. Elderly mice display smaller muscle fibre sizes after RSV infection

The methods of assessing muscle wasting implemented so far have included weighing a muscle, measuring protein synthesis in the muscle, and measuring the expression of

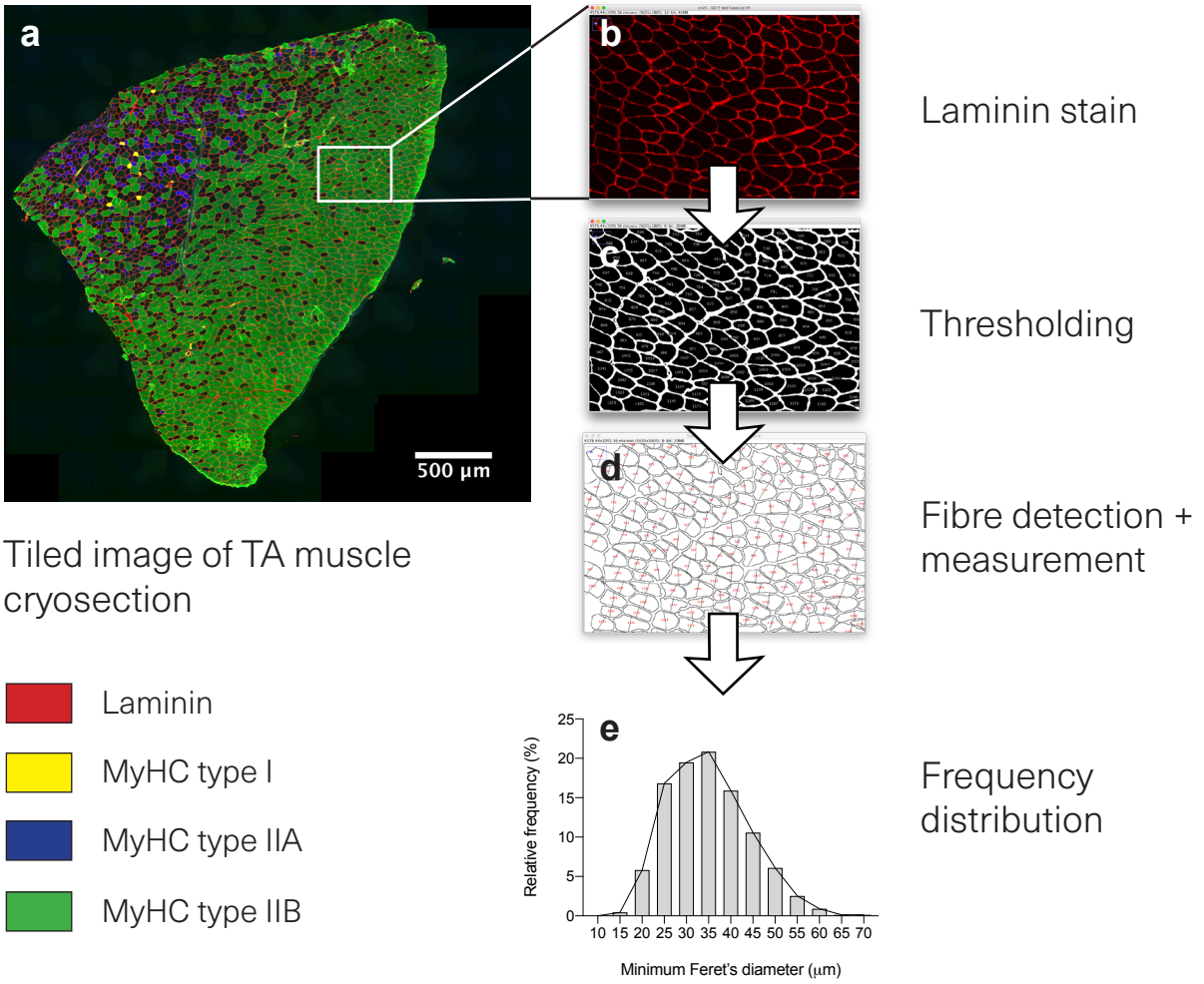

Figure 3-23 Fibre size macro steps

a. Example of a tiled light microscopy image of a TA muscle cryosection stained for laminin (red), and various myosin heavy chain (MHC) isotypes: MHC type I (yellow), MHC type IIA (blue), and MHC type IIB (green). **b.-e.** Illustrated steps of the macro script used to automatically detect muscle fibres and measure muscle fibre size. For the full code of the macro see Figure 2-1. **b.** Isolation of the image channel with the laminin stain. **c.** Thresholding of the laminin image creating a binary mask that distinguishes muscle fibre from extracellular matrix **d.** Detection of the individual muscle fibres using the binary mask and measurement of minimum Feret's diameter. **e.** Frequency distribution of the fibre minimum Feret's diameters measured in a given image.

genes promoting either muscle hypertrophy or atrophy. A different approach would be measuring the size and type of muscle fibres directly. To do this, the TA muscle of young and elderly mice at different stages of RSV infection was embedded in OCT compound and frozen. TA muscles were cryosectioned and the sections stained by immunohistochemistry. Sections were stained for laminin and three different myosin heavy chain (MyHC) isotypes. Laminin is part of the basal lamina in the extracellular matrix surround-

ing the bundles of muscle fibres. Myosin heavy chain (MyHC) forms part of the myosin/actin complex which generates force during muscle contraction. The different MyHC isotypes confer different biophysical properties onto a muscle fibre. Four different types of MyHC are found in mammalian skeletal muscle, MyHC type I, type IIA, type IIB, and type IIX. Muscle fibres expressing MyHC type I, also known as "type I fibres" or "slow twitch" fibres have a slow contraction time and do not generate a lot of power, but they are highly resistant to fatigue (Schiaffino & Reggiani, 2011). Type I fibres have a high oxidative capacity but low glycolytic capacity which makes them suited to aerobic activities. The "fast twitch" fibres include those expressing MyHC type IIA, IIB, and IIX. These fibres generally produce more power than type I fibres but are more prone to fatigue. Type IIA fibres contract moderately fast, generate a moderate amount of power, and have a fairly high resistance to fatigue. They have both a high oxidative capacity and a high glycolytic capacity. Type IIB fibres by contrast contract very fast and can generate a large amount of power. However, this power can only be sustained for a very short amount of time, and the fibres fatigue quickly. Type IIB fibres have a low oxidative capacity and a high glycolytic capacity which makes them suitable to short-term anaerobic activities that require quick bursts of power. Type IIX fibres have properties intermediate between type IIA and IIB. MyHC type IIX fibres were not specifically stained. Instead, fibres that did not stain for any other MyHC isotype were considered to be type IIX.

For previous work in the lab, muscle fibre sizes had been measured by hand. This process was highly inefficient, as well as prone to human error and sampling bias. Since each TA cross-section contains ~2500 fibres, it was not possible to count all fibres in a section when measuring by hand. Moreover, use of a standard light microscope did not allow for capture of the entire muscle cross-section, necessitating manual selection of regions to image and analyse. The method was optimised to improve efficiency and remove sources of error and bias. Sections were imaged on a Widefield microscope with a motorised stage at FILM Imperial, which allowed for tiling of multiple images to capture an entire cross-section. To automate analysis, a macro script was written using the ImageJ image

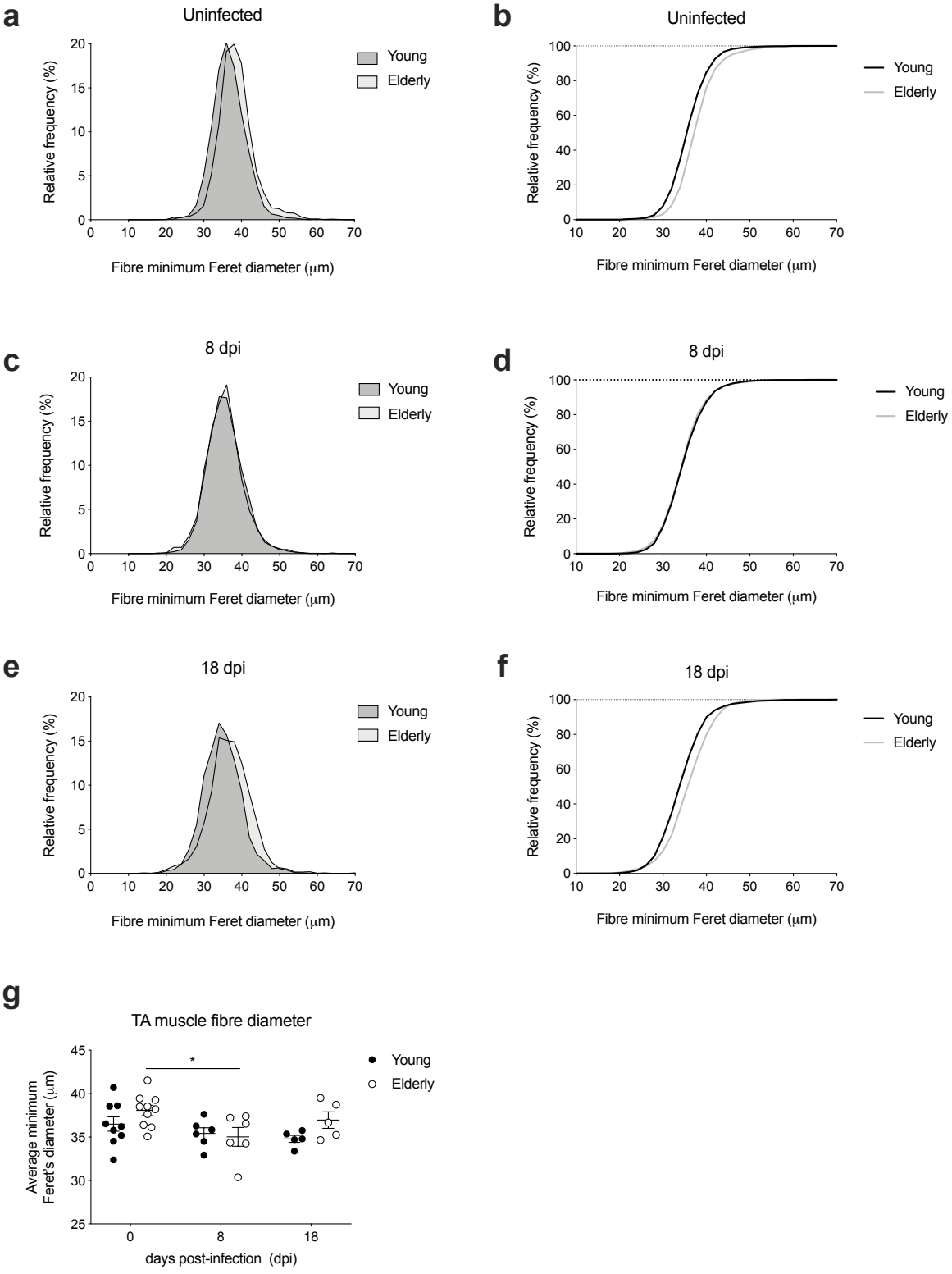

Figure 3-24 TA muscle fibre minimum Feret's diameter during RSV infection

a.+c.+e. Relative frequency histograms. **b.+d.+f.** Cumulative frequency histograms. **a.+b.** Uninfected young and elderly mice. **c.+d.** Young and elderly mice after 8 days of RSV infection. **e.+f.** Young and elderly mice after 18 days of RSV infection. **g.** Average minimum Feret's diameter of TA muscle fibres in young and elderly mice before, and during RSV infection. Pooled from 5 independent experiments, n=4-5. Two-way ANOVA with Bonferroni's multiple comparison test.

analysis software package. The macro semi-automatically detected muscle fibres and measured a range of outputs, including minimum Feret's diameter. The full code of the macro is shown in Figure 2-1. The steps of the macro are exemplified in Figure 3-23. The macro started with a tiled image covering the entire TA muscle cross-section, stained for laminin (red), MyHC type I (yellow), MyHC type IIA (blue), and MyHC type IIB (green) (Figure 3-23a). The channel containing only the laminin staining was isolated (Figure 3-23b). The laminin image was "thresholded" and converted to a binary image distinguishing extracellular matrix from individual muscle fibres (Figure 3-23c). This separated muscle fibres sufficiently to allow for automatic object (fibre) detection and batch measurement (Figure 3-23d). The frequency distribution of the fibre minimum Feret's diameter was calculated and averaged in each experimental group (Figure 3-23e). Additionally, the mean minimum Feret's diameter for each mouse was calculated. Minimum Feret's diameter was chosen as the most appropriate measure of fibre size, since it is less prone to distortion by irregular cutting angles than maximum diameter or cross-sectional area. The distribution of fibre sizes would be expected to skew smaller in the infected elderly mice as compared to the uninfected.

Figure 3-24 shows average relative frequency distributions and average cumulative frequency distributions of TA muscle fibre minimum Feret's diameter in young and elderly mice at baseline, and after 8 and 18 days of RSV infection. Using the cumulative frequency distribution can make it easier to visualise changes in the mean. At baseline, there was a trend towards elderly mice displaying larger muscle fibre sizes, consistent with their higher gross muscle weight (Figure 3-24a,b). 8 days after RSV infection, the frequency distributions of TA fibre size of young and elderly mice were virtually identical, suggesting a downwards shift of the elderly mice (Figure 3-24c,d). 18 days after RSV infection, there was once again a trend towards elderly mice displaying larger muscle fibres, similar to baseline measurements (Figure 3-24e,f). Figure 3-24g shows the mean fibre minimum Feret's diameter of each mouse in the different experimental groups. The mean fibre minimum Feret's diameter of young and elderly mice was not significant-

ly different at any time point. As suggested by the frequency distributions, there was a trend towards a higher fibre minimum Feret's diameter in elderly mice at baseline and at day 18. Fibre minimum Feret's diameter decreased significantly in elderly mice between baseline and day 8. This adds to the evidence collected so far that elderly mice exhibit muscle wasting during RSV infection, whereas young mice do not.

3.4. Discussion

3.4.1. RSV infection of elderly mice as model to study infection-associated muscle wasting in the elderly

The ageing population of the world is growing rapidly, and the incidence of age-related diseases grows with it (Office for National Statistics, 2018). There is an urgent need to expand our understanding our knowledge of the fundamental processes of ageing, and how age interacts with conditions like infection and muscle wasting. Respiratory Syncytial Virus (RSV) is a well-known cause of bronchiolitis and hospitalisation in young children, but it is also emerging as an important pathogen in the elderly population, both as a cause of severe disease and as an exacerbating factor for age-associated conditions like chronic obstructive pulmonary disease (COPD) (Falsey & Walsh, 2005). Loss of muscle mass occurs naturally with age (sarcopenia) but can be exacerbated by inflammation or inactivity. Decreased muscle mass in elderly persons is associated with frailty, leading to increased risk of mortality and decreased quality of life (Landi *et al.*, 2013; Arango-Lopera *et al.*, 2013). The effect of respiratory viral infection on skeletal muscle has not been investigated in-depth. This chapter has described a mouse model of RSV infection in elderly mice with a number of methods for measuring mass, composition and dynamics of skeletal muscle. The chapter has additionally characterised basic features of the adaptive immune response to RSV infection in elderly mice and compared them to that of young mice.

3.4.2. Elderly mice display enhanced inflammation after RSV infection

Compared to young mice, elderly mice lost significantly more weight than young mice during RSV infection, peaking around day 8 of infection. Interestingly, weight recovery

was still incomplete 18 days after infection. Elderly mice also displayed significantly elevated viral load as measured by the expression of viral L gene in their lung tissue, and increased and prolonged cellular infiltrates in the airways and lungs. These findings are consistent with previous models of RSV infection in elderly mice (Graham *et al.*, 1988; Zhang *et al.*, 2002b; Fulton *et al.*, 2013; Wong *et al.*, 2014).

To my knowledge, the individual components of the immune response of elderly mice to RSV have not been fully characterised. Therefore, the frequency and absolute number of various immune cell types, including lymphocytes, T cells, $CD4^+$ T cells, $CD8^+$ T cells, B cells, NK cells, and granulocytes were measured in the lung tissue and BAL fluid of young and elderly mice after 8 days of RSV infection. Consistently with their stronger weight loss and cellular infiltration, elderly mice displayed significantly increased numbers of lymphocytes in their lung tissue and BAL fluid. The number of T cells in general, $CD4^+$ T cells and $CD8^+$ T cells was significantly elevated in the lungs and airways of elderly mice compared to young mice. This contrasts with previous findings of Fulton *et al.*, who did not find a statistically significant difference in the number of $CD8^+$ T cells in lung and BAL fluid between young and elderly mice 8 days after RSV infection. On the contrary, Fulton *et al.* suggest that the $CD8^+$ T cell response of elderly mice to RSV is blunted, as evidenced by reduced numbers of RSV-specific $CD8^+$ T cells in lung, BAL fluid, and peripheral blood. The RSV specificity of $CD8^+$ T cells was not tested in this study so a comparison cannot be made. There were also crucial differences between the two studies, for example, Fulton *et al.* used BALB/c mice, which are known to be more susceptible to RSV, and the young mice used were up to 6 weeks younger than the ones used in the present study. There are known to be strong differences in the response of different mouse strains to RSV, which may account for the differences observed in the $CD8^+$ T cell response of elderly mice to RSV (Stark *et al.*, 2002).

Curiously, NK cell numbers were decreased in lung tissue compared to young mice, but elevated in BAL fluid, suggesting that in elderly mice, NK cells are preferentially recruited out of the lungs and into the airways, presumably to combat the active infection. The

number of granulocytes was also significantly elevated in lungs and airways of elderly mice compared to young. Unfortunately, more detailed investigation of different types of granulocytes was not undertaken. It is likely that the increased number of granulocytes in elderly mice includes a large number of neutrophils. Aged neutrophils are known have reduced chemotactic ability, leading to inefficient migration through tissues that causes increased tissue damage due to prolonged protease secretion (Sapey *et al.*, 2014; Hazeldine *et al.*, 2014). This may contribute to the enhanced inflammation seen in the lungs of elderly mice after RSV infection. Future studies may want to investigate differences in the innate immune response to RSV between young and elderly mice.

3.4.3. The RSV serum antibody response of elderly mice

The antibody response of elderly mice to RSV has not been investigated in detail. Since there is some evidence that serum antibodies to RSV can be protective in humans, characterising the differences in antibody response to RSV with age is important (Hall *et al.*, 1991). Serum IgG is also often used as a correlate of protection in vaccine trials, and it is of high importance that a future vaccine protects the elderly as a highly vulnerable group. Serum titration showed that elderly mice produced significantly less RSV-specific IgG compared to young mice 18 days after infection, when the antibody response should have begun. This contrasts with observations that older humans tend to generate equally strong, or even stronger, serum antibody responses to RSV infection compared to adults (Agius *et al.*, 1990; Walsh & Falsey, 2004). However, it is important to consider that humans will have been exposed to RSV infection many times throughout life before, meaning that an infection in old age also recalls memory responses, which will be stronger and generated more rapidly than during a primary infection. The mice used in this study are an artificial model in the sense that they are specific-pathogen-free and should not have had any infections previously. This may explain the weak antibody response in the elderly mice as compared to observations in humans.

3.4.4. The germinal centre response of elderly mice infected with RSV

The lower serum IgG response suggested that the generation of antibodies was im-

paired in elderly mice. High-specificity antibodies are produced by plasma B cells which have undergone somatic hypermutation and affinity maturation in secondary lymphoid tissues, a process termed the germinal centre response. In germinal centres, B cells express GL7, and interact with cognate specialised $CD4^+$ T cells, T follicular helper (Tfh) cells, which express CXCR5 and PD1. The frequency and abundance of these cell populations was investigated in the lung tissue, lung-draining lymph nodes, and spleen tissue of young and elderly mice 18 days after RSV infection. Additionally, the RSV specificity of $CD4^+$ T cells and Tfh cells was investigated using an MHC class II tetramer presenting an RSV M2 protein peptide.

3.4.4.1. T follicular helper cells and germinal centre B cells in elderly mice

There were no large differences in B or germinal centre (GC) B cell frequency or abundance between young and elderly mice. In fact, the number of B cells in the lymph nodes of elderly mice was significantly higher 18 days after infection than in young mice, suggesting that a B cell trafficking defect may not be responsible for the impaired antibody response. The frequency of $CD4^+$ T cells was significantly lower in the lungs and lymph nodes of elderly mice both at baseline and 18 days after RSV infection, but the total number of $CD4^+$ T cells was not significantly different between young and elderly mice after infection. Interestingly, the frequency and total number of Tfh cells was strongly elevated in elderly mice compared to young mice in all three tissues tested, lung, lymph nodes, and spleen, both at baseline and 18 days after RSV infection. Up to 40% of $CD4^+$ T cells in the spleen tissue of elderly mice were Tfh cells, even prior to RSV infection. This was unexpected considering that, as stated above, these mice should not have been exposed to any infection prior to experiments, so should not have prior germinal centre activation leading to the retention of Tfh cells in these tissues. The increased abundance of Tfh cells in elderly mice may be due to on-going immune responses to commensals or autoantigens, and may reflect a latent inflammatory state associated with ageing, termed "inflammageing". Personal communication with other researchers suggested that the high occurrence of Tfh cells in elderly mice was indeed due to commensal or subclinical

infection, since stricter hygiene procedures in the animal facility could prevent it (Michelle Linterman, pers. comm.).

3.4.4.2. RSV specificity of the antibody response in elderly mice

The sheer abundance of Tfh cells in elderly mice does not guarantee their usefulness during RSV infection, so specificity of $CD4^+$ T cells was tested with an MHC class II tetramer. RSV infection induced the expansion of RSV-specific $CD4^+$ T cells in the lungs and lymph nodes of both young and elderly mice. In fact, there were significantly more RSV-specific $CD4^+$ T cells in the lymph nodes of elderly mice than young mice. However, the frequency of RSV-specific Tfh cells was significantly decreased in elderly mice compared to young mice in all tissues. This may be due to the very large number of pre-existing Tfh cells in the elderly mice. The total number of RSV-specific Tfh cells was not significantly different in young versus elderly mice. This suggests that elderly mice do not have a defect in the proliferation and recruitment of RSV-specific $CD4^+$ T cells or Tfh cells.

Curiously, a number of cells were detected with the RSV tetramer in baseline samples. None of these cells should bind an RSV peptide considering that the mice had never been exposed to RSV before. This is most likely the result of few cells falling within the gate set during flow cytometric analysis, which when multiplied up yields noticeable frequencies and abundances. In the future, the gating strategy could be relaxed to prevent this.

The M2 peptide presented by the MHC class II tetramer utilised in this panel is only one antigen and many other cells will recognise other RSV antigens. This study assumed that the reaction of immune cells in young and elderly mice to this peptide was representative of the true proportion of all RSV-specific cells. However, it is a possibility is that the epitopes that the elderly recognise are different to those recognised in the young. The M2 epitope used may not be immunodominant in the elderly and they may predominantly recognise different antigens. On the other hand, Fulton *et al.* trialled three different RSV MHC class I peptides and found a similar pattern between young and elderly mice for all

of them (Fulton *et al.*, 2013).

Although elderly mice did not display numerical impairments in B or T cell populations associated with the germinal centre response, protective immunity was clearly not generated, considering the high viral load and low serum IgG in elderly mice. Other aspects of the germinal centre response may be impaired, for example, in future studies, the interaction or functionality of Tfh and GC B cells could be investigated. Additionally, the functionality of the $CD8^+$ T cell response was not investigated, which is also known to contribute to control of RSV viral load, and which may be impaired in the elderly. A cell type in the germinal centre reaction that was not investigated was follicular dendritic cells (fDCs), which present antigen to B cells during affinity maturation. The microenvironment of the germinal centre is known to be crucial to proper antibody generation, and is known to be disturbed with age (Linterman, 2014; Celia Diaz, unpublished). A recent study found that dendritic cell maturation and cytokine secretion was inhibited by RSV *in vitro* (Le Nouën *et al.*, 2019). It is possible that this effect is magnified with age, further impairing initiation of the antibody response to RSV. This could be investigated in future studies.

3.4.4.3. The antibody response to RSV versus influenza A virus infection in elderly mice

To my knowledge the antibody response to RSV has not been previously interrogated in aged mice, but Lefebvre *et al.* conducted a similar study investigating the antibody response to influenza A virus (IAV) infection in aged mice (Lefebvre *et al.*, 2016). Even though RSV and IAV are clearly very different viral infections, comparing the results of these two studies may shed light on universal impairments in the antibody response with age. Lefebvre *et al.* suggest that impaired humoral responses in aged organisms are derived from disturbed B-T cell interactions. They used the same strain of mice (C57BL/6) and similarly aged mice to this study, but slightly different time points, 7 dpi and 14 dpi, as opposed to 8 dpi and 18 dpi. Lefebvre *et al.* found lower influenza-specific IgG serum titres in aged mice, similarly to the present findings of lower RSV-specific IgG in aged

mice. Like this study, they also found that Tfh cells were found in higher frequencies in the spleens of old mice, but that there was no large change over the course of infection. In contrast to the present findings however, Lefebvre *et al.* found significantly lower numbers of GC B cells in the spleens of aged mice, whereas this study did not find a significant difference. Using tetramer staining, Lefebvre *et al.* found that the total number of influenza-specific $CD4^+$ T cells and Tfh cells was not significantly altered in the spleens of aged mice, which was the same finding as the ones presented here.

A key finding of Lefebvre *et al.* was that $CD4^+$ T cells and Tfh cells in aged mice displayed a "regulatory-like" phenotype, as evidenced by increased frequency and numbers of Foxp3-expressing IAV-specific $CD4^+$ T and Tfh cells in aged mice. The authors suggest that this is indicative of impaired Tfh function and impaired interaction with cognate B cells. Foxp3 staining was attempted in the present study but was unsuccessful. Future experiments may want to repeat and optimise this to attempt to confirm this potential tolerogenic effect of age on $CD4^+$ T cells in RSV infection.

Lefebvre *et al.* found that more $CD4^+$ T cells from the spleens of aged mice produced IFN-γ and IL-10. Cytokine production was not measured in spleen tissue in this study, but increased IFN-γ and IL-10 production was also found in lung and BAL fluid $CD4^+$ T cells. This may suggest a more anti-inflammatory, inhibitory phenotype of $CD4^+$ T cells in aged mice that hinders the germinal centre response in both IAV and RSV infection. By contrast, Fulton *et al.* found that IFN-γ secretion was impaired in aged RSV-specific $CD8^+$ T cells in BAL fluid. However, $CD8^+$ T cells fulfil a very different function to $CD4^+$ T cells so the effect of a cytokine production impairment is not comparable in this case. Interestingly, Lefebvre *et al.* did not measure cytokine production in virus-specific cells specifically. The results from the current study suggest that while IFN-γ and IL-10 production by $CD4^+$ and $CD8^+$ T cells is generally increased in aged mice, the production of these cytokines in RSV-specific $CD4^+$ T cells is not affected by age. This may be due to a "bystander" effect of non-specific cells secreting inhibitory cytokines that hamper the development of the specific antibody response.

To visualise the spatial organisation of germinal centres, Lefebvre *et al.* carried out confocal microscopy of spleen sections of young and elderly mice after IAV infection. They found fewer, smaller, and more disorganised germinal centres in the spleens of elderly mice. Similar experiments were carried out on the elderly mice used in this study by Masters student Celia Diaz, and after RSV infection, splenic germinal centres of elderly mice were equally smaller, fewer in number, and visibly disorganised compared to young mice (not shown). Future studies may want to investigate the nature of the germinal centre disorganisation more closely, for example by analysis of the distribution of T vs B cells and perhaps DCs.

Lefebvre *et al.*'s conclusion of a more regulatory Tfh phenotype in elderly mice after IAV infection is based primarily on enhanced Foxp3 expression and decreased GL7 and CXCR5 expression. As mentioned, Foxp3 staining was not successful in this study, but GL7 and CXCR5 expression data was collected. MFI analysis was not conducted but the frequency and number of GL7-positive Tfh cells was not different in the lungs, lymph nodes or spleens of aged mice (not shown). Future studies may want to investigate the phenotype of Tfh cells of aged mice in RSV in more detail. A crucial difference between this study and the work by Lefebvre *et al.* is of course the use of two very different pathogens, RSV and IAV. Divergent findings in these two studies do not necessarily disqualify either, however, there was remarkable overlap in a number of results, particularly the blunted serum IgG response, increased IL-10 and IFN-γ production of $CD4^+$ T cells, and comparable numbers of virus-specific $CD4^+$ and Tfh cells in aged mice. Lefebvre *et al.* only investigated the splenic responses, whereas the present study found the most stark differences between young and elderly mice in the lung-draining lymph nodes, which presumably contain cells confronted most recently with the pathogen. This may explain part of the differences in the results.

3.4.5. Elderly mice display molecular and macroscopic signals of muscle wasting after RSV infection

Muscle is a highly dynamic tissue that is tightly regulated by multiple factors. The meth-

ods used in this chapter were designed to interrogate both factors promoting muscle growth and factors promoting muscle atrophy, as well as measuring the net outcome of the combination of these. The net outcome of infection on muscle was assessed by weighing the whole tibialis anterior (TA) muscle, and by measuring the minimum Feret's diameter of muscle fibres using immunohistochemistry of TA cryosections. Muscle synthesis was evaluated by measuring the expression of a number of genes promoting muscle growth and repair, and with a novel type of assay measuring the incorporation of puromycin into muscle polypeptide chains as a proxy for the rate of protein synthesis. Muscle atrophy was evaluated by measuring the expression of a number of genes promoting the breakdown of muscle proteins.

3.4.5.1. The muscle weight of elderly mice decreases significantly with RSV infection

The raw weight of TA muscles of elderly mice decreases significantly from baseline to the peak of weight loss at 8 dpi, whereas no such decrease was observed in the muscles of young mice. This was a strong indicator that RSV infection indeed induced muscle wasting in the elderly mice. However, comparing raw muscle weights between young and elderly mice may not be statistically appropriate since the muscles of elderly mice were already significantly heavier (in accordance with their higher body weight) at baseline. Therefore, it was attempted to normalise TA weight to overall body size in order to account for the differing starting conditions of young and elderly mice before infection. Normalisation to bodyweight was not appropriate since the bodyweight of elderly mice was known to change dramatically over the course of infection, in contrast to young mice. Instead, the tibia (shinbone) to which the TA is attached, was extracted and its length measured. The tibia length should not change over the course of infection and should be a consistent proxy for overall body size of an individual animal. A "TA atrophy index" was calculated by dividing the TA weight by the tibia length cubed. The TA atrophy index of elderly mice was significantly lower than that of young mice at the peak of infection, suggesting that during RSV infection, elderly mice had significantly less mus-

cle mass in relation to overall body size than young mice. No other studies so far appear to have measured muscle weight in elderly mice in response to RSV, so it is unclear how universal these results are. Bartley *et al.* (2016) infected young and elderly mice with influenza and observed signs of muscle wasting (discussed below), but did not weigh any muscles. It is plausible that they would have also observed lower muscle weights in the elderly mice after infection.

3.4.5.2. Elderly mice upregulate expression of muscle atrophy genes after RSV

The expression of genes encoding factors promoting both muscle growth and atrophy was measured by qPCR. The ubiquitin-proteasome pathway is a key regulator of protein homeostasis in the muscle. Atrogin-1 (encoded by the *Fbxo32* gene) and MuRF-1 (encoded by the *Trim63* gene) are the dominant muscle-specific E3 ubiquitin ligases responsible for breakdown of muscle proteins (Bodine & Baehr, 2014). The expression of both *Fbxo32* and *Trim63* was strongly upregulated in the TA muscles of elderly mice after 8 days of RSV infection, but not at all in the muscles of young mice. This is indicative of a strong atrogenic signal in the muscles of elderly mice.

Bartley *et al.* compared the expression of Atrogin-1 and MuRF-1 in the gastrocnemicus muscles of young and elderly mice after influenza A virus (IAV) infection (Bartley *et al.*, 2016). They equally observed increased expression of Atrogin-1 and MuRF-1 in the muscles of elderly mice after infection, although this was only significantly higher than in young mice at 11 dpi. Curiously, Bartley *et al.* found that expression of these genes was elevated in the muscles of both young and elderly mice at 7 dpi. It is possible that due to the choice of time points in this study, an increase in the expression of Atrogin-1 and MuRF-1 in the muscles of young mice was missed. It is conceivable that young mice simply downregulate the expression of these genes earlier in infection. More detailed time courses could be carried out to elucidate the kinetics of expression. However, a single experiment carried out at 5 dpi indicated that Atrogin-1 and MuRF-1 expression was only minorly elevated in the muscles of both young and elderly mice at this time point.

It is also important to remember that Bartley *et al.* investigated a different pathogen and a different muscle to the present study, which may account for the differences between this study and theirs. A different study observed increased baseline levels of Atrogin-1 and MuRF-1 mRNA in the muscles of aged rats, however, this was not the case in the present study.

Myostatin is a strong driver of muscle atrophy via inhibition of muscle synthesis pathways and induction of many atrophy-related genes, including Atrogin-1 and MuRF-1. At baseline, the expression of the *Mstn* gene encoding myostatin in the muscles of elderly mice was significantly higher, which may indicate a propensity towards muscle wasting. But curiously, the expression of myostatin decreased significantly in the muscles of elderly mice from baseline to 8 dpi. Even 18 days after infection, myostatin expression in the muscles of elderly mice remained significantly lower than baseline. This was unexpected considering that myostatin is considered a crucial driver of muscle atrophy that is induced by inflammation (McFarlane *et al.*, 2006). Interestingly, Bartley *et al.* (2016) found that myostatin expression increased in the gastrocnemicus muscles of both young and elderly mice after 7 days of IAV infection, but was no different between the two age groups. Perhaps IAV is simply a stronger atrogenic stimulus than RSV, considering that young mice also lost weight after IAV. These results suggest that muscle loss in elderly mice after RSV infection was not driven by myostatin signalling. Atrogin-1 and MuRF-1 expression may have been induced by other means, for example by TNFα signalling via NF-κB activation, although only very low amounts of circulating TNFα were detected in this study (not shown).

3.4.5.3. Expression of muscle growth-promoting genes in elderly mice after RSV

The expression of a number of genes involved in promoting muscle growth and repair was measured in the muscles of elderly and young mice after RSV infection. The expression of *Igf1*, encoding IGF-1, a key driver of cell proliferation, was increased in the muscles of young mice at the peak of infection. No such upregulation took place in the

muscles of elderly mice. It was unexpected that the muscles of young mice would up-regulate IGF-1 expression during an infection, when muscle growth is presumably not an organismal priority. It is possible that this constitutes a repair response to inflammatory injury to the muscle, which conversely was not observed in the elderly mice. This might contribute to the muscle wasting observed in the muscles of elderly mice.

The expression of Pax7, a key determinant of satellite cell (muscle stem cell) identity, was significantly decreased in the muscles of elderly mice compared to young mice, both at baseline and at day 8 post-infection. This, in combination with the impaired upregulation of IGF-1 in elderly mice, might suggest that there are fewer satellite cells in the muscles of elderly mice, hindering muscle regeneration after damage. Future studies may want to stain for and quantify satellite cells in histological images of muscles of young and elderly mice after RSV infection. It is well known that aged mice and rats have fewer satellite cells in their muscles (Snow, 1977; Schultz & Lipton, 1982; Brack, Bildsoe & Hughes, 2005; Day *et al.*, 2010). It would be interesting to see whether this is exacerbated by RSV infection in the long-term, since there was a non-significant trend towards persistently lower expression of Pax7 in the muscles of elderly mice after 18 days of infection. This might indicate a loss of regenerative potential in the muscles of elderly mice.

Counterintuitively, the expression of two other genes involved in promoting muscle growth, myogenin and Mef2c, was significantly increased in the muscles of elderly mice at 8 dpi compared to young mice. The reasons for this are unclear. It might be an example of a compensatory mechanisms attempting to regenerate muscle in the absence of sufficient Pax7 and IGF-1 expression. Myogenin and Mef2c synergistically promote the differentiation of committed muscle progenitor cells into myofibres, (Wright, Sassoon & Lin, 1989; Molkentin *et al.*, 1995). Perhaps an upregulation of myogenin and Mef2c indicates the necessity of elderly muscle to regenerate in the face of damage, which is made impossible by a lack of muscle progenitor cells derived from $Pax7^{+}$ satellite cells.

Mef2c is known to promote a switch towards a slow-twitch muscle fibre phenotype (Pot-

thoff *et al.*, 2007b). Myogenin is more highly expressed in slow-twitch muscle (Ekmark *et al.*, 2007), and promotes a switch in fast-twitch myofibres from glycolytic to more oxidative, and causes a reduction in fast-twitch fibre size (Hughes *et al.*, 1999).The increase in myogenin and Mef2c expression observed in the muscles of elderly mice may be an indicator of an age-associated transition away from high-power fast-twitch muscles, potentially accelerated by RSV infection. This study unfortunately did not assess muscle fibre type, but future experiments could measure whether the fibre type composition changes towards a more slow-twitch dominated one in the muscles of elderly mice after RSV infection.

On the other hand, one study suggests that myogenin, while important for muscle development, actually promotes the expression of Atrogin-1 and MuRF-1 in a mouse denervation model of muscle atrophy (Moresi *et al.*, 2010). The present study used an inflammatory stimulus in the form of a live viral infection to induce muscle atrophy, so muscle atrophy was likely not caused by the exact same pathways as in a pure denervation model. However, it is possible that the increased expression of myogenin observed in the muscles of elderly mice after RSV infection contributed to the high expression of Atrogin-1 and MuRF-1 and thus increased muscle atrophy.

3.4.5.4. Elderly mice fail to upregulate protein synthesis in skeletal muscle after RSV infection

Puromycin is a natural antibiotic produced by the bacterium *Streptomyces alboniger*. It is a structural analogue of tyrosyl-tRNA and is readily incorporated into nascent polypeptide chains (Nathans, 1964). Because puromycin lacks a hydrolysable ester bond, it terminates peptide elongation. In high concentrations, this inhibits protein translation and constitutes its antibiotic effect. In lower doses, puromycin incorporation into nascent peptides correlates approximately to the overall rate of protein synthesis in a given tissue (Goodman & Hornberger, 2013). Wool and Kurihara were first to devise a ^{3}H-puromycin-based technique for estimating the number of active ribosomes in a cell-free preparation from rat skeletal muscle (Wool & Kurihara, 1967). Nakano and Hara adapted this

method to measure protein synthetic activity in the tissues of rats *in vivo*, and found that puromycin incorporation was significantly reduced by a 24-hour fast or a low-protein diet (Nakano & Hara, 1979). Since, the puromycin method has been adapted to various contexts, being detected by radiographic, ELISA, or fluorescent methods, *in vitro*, *in vivo*, and immunohistochemically (Schmidt *et al.*, 2009; Kawahashi *et al.*, 2006; Goodman *et al.*, 2011, 2012; Liu *et al.*, 2012; David *et al.*, 2012; Signer *et al.*, 2014; Pekkala *et al.*, 2015; Henrich, 2016). In this study, a puromycin ELISA method was optimised for measuring protein turnover in the muscles of young and elderly mice. Mice were injected intraperitoneally with 0.8µmol puromycin dihydrochloride, a dose based on Goodman *et al.* (2011, 2012) and culled 30 minutes later. TA muscles were extracted and homogenised and the protein-containing supernatant assayed.

Surprisingly, the puromycin incorporation assay revealed an increase in the rate of protein synthesis in the TA muscles of young mice at the peak of infection (day 8). This increase was not observed in the muscles of the elderly mice. This finding might imply that a repair response in the muscle is impaired in the elderly mice. This data is consistent with the finding that IGF-1 expression was upregulated in the muscles of young, but not elderly mice, at 8 dpi. The reasons for this increase in protein synthesis in the muscles of young mice, which fails to occur in the elderly mice, are unclear. It is conceivable that skeletal muscle is broken down for metabolic demands of the immune response, and elderly mice fail to replenish this reservoir. However, the expression of Atrogin-1 and MuRF-1 was not increased in the muscles of young mice, and total TA weight did not change significantly, suggesting that their muscles did not experience notable breakdown.

Quy *et al.* found that in a denervation model of muscle atrophy in mice, muscle wasting in the denervated muscle was accompanied by constitutively activated mTORC1 and elevated protein synthesis as determined by increased puromycin incorporation (Quy *et al.*, 2013). Rapamycin treatment (blocking mTOR activity) reduced puromycin incorporation and exacerbated muscle loss. The authors conclude that amino acids freed by pro-

teasome-mediated proteolysis activated mTORC1 in denervated muscle. Denervation is clearly a different type of stressor causing muscle wasting compared to the RSV infection used in this study. It is conceivable that a similar mechanism to Quy *et al.*'s observations was seen in the muscles of young mice in this study. An inflammatory insult to the muscle, was counteracted by increased IGF-1 expression (which promotes mTOR activity) and protein synthesis inferred from puromycin incorporation. Perhaps this mechanism is fundamentally disturbed in elderly mice, leading to pronounced muscle wasting. To investigate whether amino acids from muscle are incorporated into immune cells during RSV infection, future studies could conduct amino acid tracing experiments. Free amino acids could be measured in the muscle samples like in Quy *et al.* (2013). Rather than intraperitoneal injection, puromycin could also be injected into the TA muscle directly and then incorporation measured in lung tissue. Rates of protein synthesis are closely correlated to the last time of feeding, so to decrease the variability in the data, mice could be fasted and/or given a defined nutrient bolus prior to the puromycin injection (Paul Kemp, pers. comm. 2017).

Baehr *et al.* studied the effects of hindlimb unloading on adult and elderly rats to investigate muscle wasting after disuse (Baehr *et al.*, 2016, 2017). Since by visual observation, elderly mice infected with RSV did move around less, it is likely that disuse contributed to muscle wasting to some extent.

Hindlimb unloading in rats induced muscle atrophy in both adult and elderly rats, from which the adult rats recovered 14 days after reloading, but elderly rats did not. Baehr *et al.* (2017) found that hindlimb unloading did not affect TA puromycin incorporation in the elderly rats. They observed a boost in protein synthesis after reloading, but this was not impaired in the elderly rats (Baehr *et al.*, 2016). A key finding of Baehr *et al.* was that changes in protein synthesis and proteolysis were highly muscle-specific. For example, while hindlimb unloading did not decrease puromycin incorporation in the TA of elderly rats, it did decrease in the soleus and gastrocnemicus muscle. Additionaly, even though Atrogin-1/MuRF-1 expression was increased in all muscles tested, actual proteasome

activity was only increased in the soleus of adult rats. This suggests that some puzzling findings in the present study, such as the fact that protein synthesis was unchanged in the TA muscle of elderly mice after RSV infection, may be due to highly muscle-specific effects. Other muscles, such as the soleus and gastrocnemicus, could be extracted in future studies and measured with the methods developed here. Moreover, the Baehr *et al.* studies emphasise that expression data does not always correlate with function. This study assumed that the increased expression of Atrogin-1 and MuRF-1 and the decrease in muscle mass observed in elderly mice were causally connected, but future studies may want to measure actual proteasome activity or ubiquitylated proteins to confirm that proteolysis is indeed increased.

Caution is still warranted in comparing this study and the studies of Baehr *et al.*. Muscle wasting induced by RSV infection is probably not exclusively attributable to disuse. Different stressors may well induce different pathways including upregulation of proteolysis and/or downregulation of protein synthesis. Also, Baehr *et al.* used male rats whereas the present study used female mice. Muscle and ageing responses among rodents should be relatively well conserved, but nevertheless there may be differences.

3.4.5.5. RSV infection decreases muscle fibre size in elderly mice

The size of individual muscle fibres in the TA muscles of young and elderly mice after RSV infection was measured by immunohistochemistry. Previously, muscle fibre size had been measured by hand, a process that was labour-intensive and prone to sampling bias. A pipeline was developed where complete muscle sections were imaged and tiled, and fibre size automatically measured using a script. To correct for variations in cutting angle, the measurement taken was minimum Feret's diameter rather than maximum diameter or cross-sectional area. To my knowledge, muscle fibre size has not been previously measured in mice after RSV infection. Consistently with their decreased TA weight, elderly mice displayed a significant decrease in the average TA minimum Feret's diameter from baseline to 8 days post-RSV infection. The size of muscle fibres in young mice was not affected, consistent with their unchanged TA weight over the course of

RSV infection.

The most directly comparable study to the present work, Bartley *et al*. (2016), did not measure the muscle fibre size of young and elderly mice after influenza A virus (IAV) infection. It would be interesting to investigate whether a similar effect would be seen with influenza, a similar inflammatory stimulus to RSV infection. Radigan *et al.* investigated the effect of IAV infection on the muscle fibre size of adult C57BL/6 mice (Radigan *et al.*, 2019). The dose of IAV administered was sufficient to induce 20% weight loss, comparable to what was achieved with RSV infection in elderly mice in the present study. Radigan *et al*. assayed the soleus and extensor digitorum longus (EDL) muscles, of which the EDL is most similar in fibre type profile to the TA. EDL weight was significantly reduced, as was EDL fibre cross-sectional area. Although elderly mice were not assessed by Radigan *et al*., this appears to confirm the present data that respiratory viral infection is capable of inducing muscle wasting in mice.

3.4.6. Limitations and future work

The results presented here have a number of limitations. Firstly, data from the elderly mice was highly variable. This is likely due to increased variability accumulated over the longer lifespan of the elderly animals, and is difficult to eliminate. Mice were bought as littermates and kept under the same conditions. Ideally, data should be collected longitudinally from the same animals to minimise this inter-animal variability. This is possible for outputs like bodyweight, but clearly not for other outputs necessitating euthanasia such as TA weight. Methods for measuring muscle wasting longitudinally should be considered, such as NMR or MRI scanning.

Secondly, only static outputs of muscle mass were measured, which are not necessarily correlated with strength or function. A number of methods could be applied to additionally measure muscle function in mice after RSV infection. Simple tests could include wire hang tests (timing how long a mouse can suspend its own weight) or grip strength meters. More advanced methods could include measuring gait changes on specialised equipment or measuring overall activity in the home cage with beam breaks similarly to

Bartley *et al.* (2016).

The data for muscle fibre type composition was collected as part of immunohistochemical staining, but could not be analysed comprehensively for technical reasons. This should be a priority for future studies to evaluate whether fibres of different types were differentially affected by infection-induced atrophy in aged muscle. Ageing is generally accompanied by a shift from fast to slow-twitch type fibres (Ciciliot et al., 2013; Holloszy et al., 1991), in addition to a general decrase in the number of muscle fibres (Lexell, 1995) and a decrase in size in fast-twitch fibres (Frontera et al., 2000; Janssen et al., 2000). Disuse, on the other hand, is associated with a shift from slow- to fast-twitch fibres, in both spaceflight-induced unloading in humans and hindlimb unloading in rats (Caiozzo et al., 1994; Zhou et al., 1995; Baehr et al., 2017). Investigating the effect of infection of muscle fibre type composition would clarify which is the case in this model.

As already mentioned, analysis of muscle in this study was limited to the TA. The TA was chosen because it is a large, predominantly fast-twitch muscle used for locomotion, which was likely to be affected by atrophy. As other studies have shown, the effect of an atrogenic stimulus can have highly variable effects on different muscles (Baehr *et al.*, 2017). Future studies should take this into account and investigate other muscles, including other fast-twitch muscles like the gastrocnemicus, and slow-twitch muscles like the soleus.

3.4.7. Summary

This chapter has investigated the fundamental immune response to RSV by young and elderly mice, and the effects on skeletal muscle. Elderly mice display pronounced weight loss, enhanced lung and airway inflammation, and higher viral load after RSV infection. Despite lower serum IgG titres, the RSV-specific $CD4^+$ T cell response and Tfh response of elderly mice was not impaired in terms of number of cells. The TA muscle weight and muscle fiber size of elderly mice decreased significantly from baseline to the peak of infection, but was not changed in young mice. Elderly mice displayed an increased expression of muscle-specific E3 ubiquitin ligases in their muscles after RSV, suggesting

increased protein breakdown. Elderly mice also displayed reduced expression of muscle satellite cell marker Pax7 and growth promoter IGF-1 after RSV infection, suggesting impaired muscle repair responses. This was confirmed by measuring protein synthesis using puromycin incorporation. Young mice upregulated protein synthesis in their TA muscles after RSV infection, whereas elderly mice did not. Together, these results demonstrate that age is an important determinant of RSV infection outcome, and that RSV infection can cause muscle wasting in elderly mice. The same infectious insult can cause dramatically different outcomes in muscle atrophy depending on age. Muscle wasting should be considered as a potential clinical outcome of RSV infection in the elderly.

4.

The role of GDF-15 in the elderly during respiratory infection

Chapter 4. The role of GDF-15 in the elderly during respiratory infection

4.1. Introduction

4.1.1. Background

GDF-15 is a hormone of the TGF-β cytokine superfamily. Since its discovery, it has been found to be elevated in a range of medical conditions, including diabetes, heart failure, COPD, and cancer cachexia; and high levels are often predictive of a poor outcome (Carstensen *et al*., 2010; Cotter *et al.*, 2015; Bloch *et al.*, 2015). However, until recently, its mechanism of action was unknown. In 2017, four groups simultaneously identified the receptor for GDF-15 (Mullican *et al.*, 2017; Hsu *et al.*, 2017; Yang *et al.*, 2017; Emmerson *et al.*, 2017). The only target that bound GDF-15 in a high-throughput screen was GFRAL, an orphan neuronal brain stem receptor. Further studies by the authors suggested that GFRAL was essential to the ability of GDF-15 to suppress appetite. On the other hand, *in vitro* studies have suggested that GDF-15 can directly promote muscle wasting in cultured myotubes by upregulating the expression of atrophy-promoting genes like *Fbox32* (Bloch *et al.*, 2013; Patel *et al.*, 2016). This implies the existence of a GFRAL-independent, direct method of action of GDF-15 on muscle. Serum GDF-15 levels are also known to rise with age (Fujita *et al*., 2017; Brown *et al*., 2002). The role of GDF-15 in viral infectious disease has not been clearly defined.

4.1.2. Purpose of chapter

This chapter aims to elucidate the role of GDF-15 in the elderly mouse model of RSV infection developed in the previous chapter. The effects of GDF-15 were blocked with a monoclonal antibody to GDF-15 during RSV infection of elderly mice. The results compare the effect of GDF-15 blockade on general features of the immune response to RSV (markers of inflammation, cellular airway infiltration, viral load) and on muscle wasting using the methodologies developed in the previous chapter (TA muscle weight, fibre size, protein turnover, and gene expression profile).

4.1.3. Aims

- To determine the effects of GDF-15 blockade on the outcome of RSV infection in elderly mice
- To determine the effects of GDF-15 blockade on muscle wasting after RSV infection in elderly mice

4.2. Experimental Design

The results in this chapter describe an interventional study of the effects of blocking GDF-15 using a monoclonal antibody to GDF-15. All mice used in this chapter were "elderly" (±80 weeks) mice. One day before RSV infection, mice were injected intraperitoneally with 250µg anti-GDF-15 antibody or isotype control antibody, suspended in 100µl PBS (kindly provided by Bernard Allan and Harding Luan (NGM Biopharmaceuticals, San Francisco, CA, USA)). Groups were assigned randomly, and experimenters were blinded to treatment. The next day, mice were infected with $2.3x10^5$ PFU of RSV strain A2 and weighed daily. Tissues were collected 8 days post-infection (Figure 4-1). Tissues collected were blood, BAL fluid, lung tissue, tibia, and tibialis anterior (TA) muscle. Flow cytom-

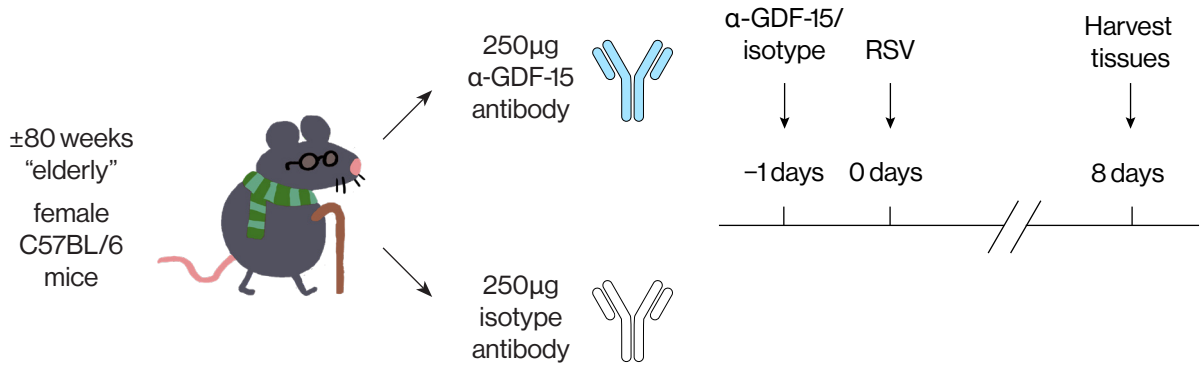

Figure 4-1 Timeline of GDF-15 blockade in elderly mice during RSV infection

Elderly (±80 week-old) female C57BL/6 mice were injected intraperitoneally with 250µg of either α-GDF-15 antibody or isotype control (keyhole limpet hemocyanin) antibody suspended in PBS. The following day, mice were intranasally inoculated with $2.3x10^5$ PFU of RSV strain A2 in a volume of 75µl. Mice were euthanised and tissues harvested 8 days post-infection. Illustration by Michael Barrett.

etry of lung cells and BAL fluid cells was used to quantify cell numbers and determine changes in the frequency of various immune cell types. Copy number of RSV L gene was measured in lung tissue by qPCR. Cytokines in BAL fluid were measured by ELISA. The TA muscle was weighed, and tibia length measured. The expression of various genes controlling muscle mass was determined by qPCR. Protein turnover in the TA was determined with a novel assay measuring puromycin incorporation by ELISA technology. Muscle fibre size and fibre type composition was determined by immunohistochemistry of muscle cryosections.

4.3. Results

4.3.1. GDF-15 is elevated in elderly mice and increases with RSV infection

A collaborator's lab had previously found evidence suggesting that GDF-15 promoted skeletal muscle wasting (Patel *et al.*, 2016). Assays conducted during the time course experiments shown in Chapter 3 showed that elderly mice had significantly higher circulating levels of GDF-15 compared to young mice (Figure 4-2a). Levels of GDF-15 protein in serum remained constant in both young and elderly mice throughout the course of infection. In the BAL fluid however, GDF-15 protein increased markedly in elderly mice between baseline and day 8 of RSV infection (Figure 4-2b). At day 8, GDF-15 protein was significantly higher in the BAL fluid of elderly mice than in young mice. At baseline and at day 18, BAL fluid levels of GDF-15 were not significantly different between young and elderly mice (analysed by Two-way ANOVA), although this did reach statistical significance in separate t-tests (not shown).

The expression of the gene encoding the GDF-15 protein, *Gdf15*, in lung tissue was measured by qPCR. Expression was measured at the time points of RSV infection used previously, and additionally at day 5, for which samples were available. *Gdf15* was significantly more highly expressed in the lung tissue of elderly mice at day 5 compared to young mice (Figure 4-2c). At day 8 on the other hand, *Gdf15* was more highly expressed in the lung tissue of young mice. 18 days after RSV infection, *Gdf15* expression remained elevated in the lung tissue of elderly mice. *Gdf15* expression was not detectable in TA

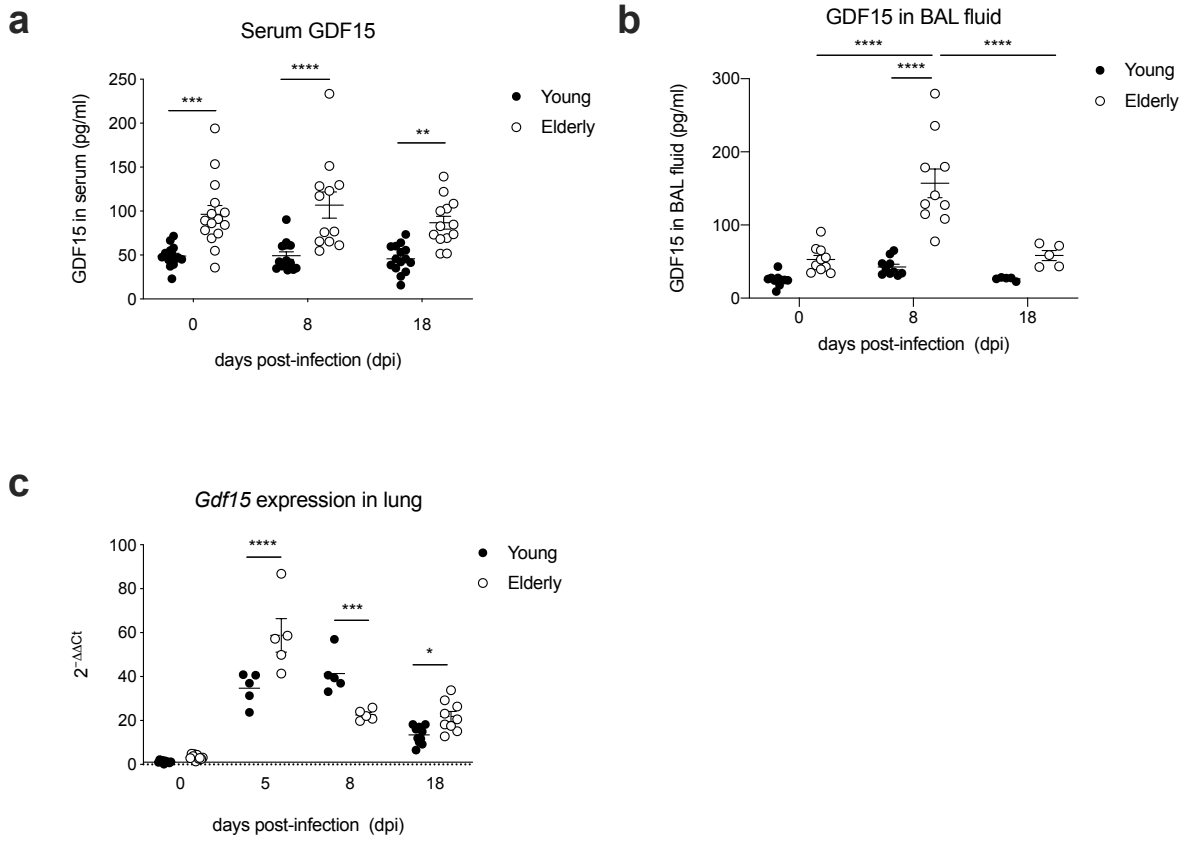

Figure 4-2 GDF-15 protein levels in serum and BAL fluid

a. Serum GDF-15 levels in young and elderly mice during RSV infection. Pooled from 5 independent experiments at n=4-10. 2-way ANOVA with Bonferroni's multiple comparisons test. **b.** BAL fluid GDF-15 levels in young and elderly mice during RSV infection. Pooled from 4 independent experiments at n=4-5. 2-way ANOVA with Bonferroni's multiple comparisons test. **c.** Expression of the *Gdf15* gene in lung tissue of young and elderly mice during RSV infection. Pooled from 5 independent experiments at n=4-5. 2-way ANOVA with Bonferroni's multiple comparisons test.

muscle (not shown).

4.3.2. GDF-15 blockade in RSV infection of elderly mice

4.3.2.1. Blocking GDF-15 does not affect weight loss or appetite during RSV infection

Elderly mice were given αGDF-15 antibody or isotype control antibody intraperitoneally one day before RSV infection and euthanised 8 days after infection. Blocking GDF-15 did not affect weight loss compared to the isotype control antibody (Figure 4-3a). The isotype-treated group lost on average 15.97% of their original bodyweight (SD ±5.61) and the αGDF-15-treated group lost an average of 17.40% of their original bodyweight (SD

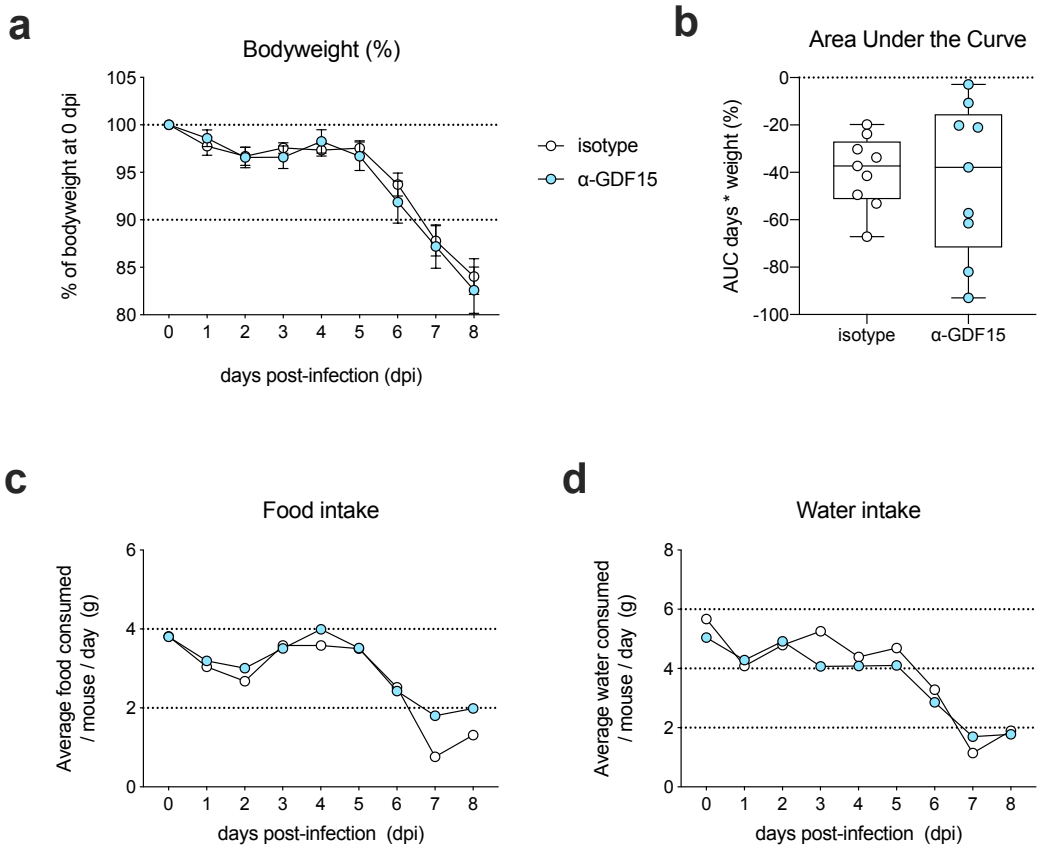

Figure 4-3 Weight loss, food and water intake after GDF-15 blockade

Pooled from two independent experiments n=4-5. **a.** Bodyweight as a percentage of weight at day 0 (the day of infection). Shown are group means with the standard error of the mean. **b.** Area under the curve of weight loss as a percentage of starting weight. **c.** and **d.** Food and water intake per mouse over the course of RSV infection. Open circles: Mice given isotype control antibody. Blue filled circles: Mice given α-GDF-15 antibody. Pooled from two experiments of one cage for each treatment group.

±7.314). This was also evident in the Area Under the Curve, as the two groups were not significantly different (Figure 4-3b). Food and water intake was likewise not significantly different between the αGDF-15-treated group and the isotype-treated group (Figure 4-3c,d).

4.3.2.2. Blocking GDF-15 increases viral load but does not affect lung infiltration

The αGDF-15-treated mice displayed higher RSV L gene copy number in their lungs compared to the isotype-treated mice (Figure 4-4a). However, this increased viral exposure did not translate to enhanced cellular infiltration of the airways or lungs, since total

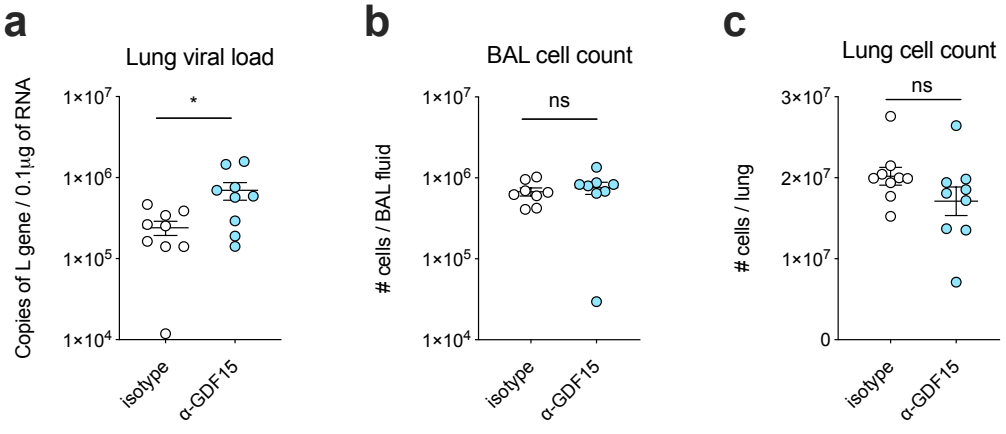

Figure 4-4 Lung viral load and cell counts in BAL fluid and lung tissue after GDF-15 blockade

Pooled from two independent experiments n=4-5. Student's unpaired two-tailed t test. **a.** RSV viral load expressed as copies of RSV L gene detected per ug of RNA extracted from lung tissue. **b.** Live cells in bronchoalveolar lavage (BAL) fluid of young and elderly mice infected with RSV. **c.** Live cells in homogenised lung tissue of young and elderly mice infected with RSV.

cell counts in the BAL fluid and lung tissue were not significantly different between the two groups (Figure 4-4b,c).

4.3.2.3. Lung inflammation and GDF-15 levels during GDF-15 blockade

The cell counts in BAL fluid and lung tissue suggested that GDF-15 blockade did not affect inflammation in the lung during RSV infection. To confirm this, levels of total protein and of IL-6 protein were measured in BAL fluid. Elderly mice like the ones used in this experiment were previously found to have very high levels of total protein and of IL-6 in their BAL fluid, a signal of high RSV-induced inflammation. αGDF-15-treated mice had neither more total protein nor more IL-6 in their BAL fluid than isotype-treated mice (Figure 4-5a,c). This was consistent with the previous evidence that αGDF-15 treatment did not promote or inhibit RSV-driven inflammation. Curiously, the αGDF-15-treated group was found to have significantly more GDF-15 protein in their BAL fluid than the isotype-treated group, although this may be an artefact caused by antibody-bound protein interacting with the ELISA (Figure 4-5b).

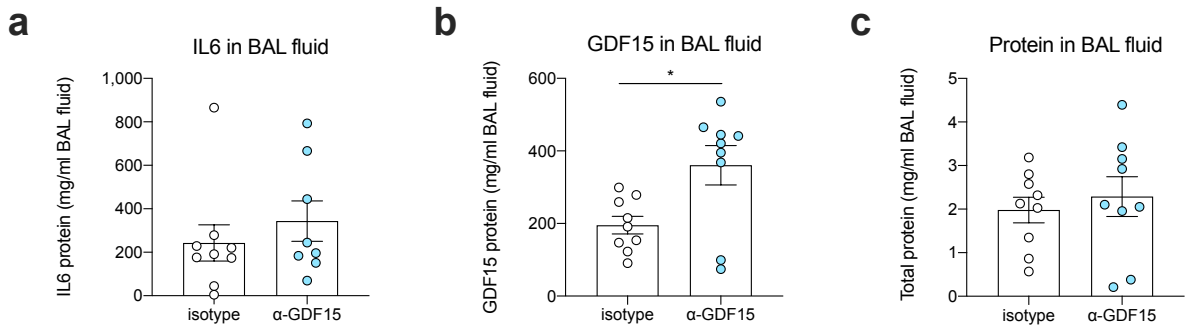

Figure 4-5 Airway cytokines and inflammation during GDF-15 blockade in RSV infection

Cytokine levels were assayed using ELISA. Total protein content was assessed by Bradford assay. Pooled from two independent experiments n=4-5. Student's unpaired two-tailed t test. **a.** IL-6 protein in BAL fluid. **b.** GDF-15 in BAL fluid. **c.** Total protein content in BAL fluid.

4.3.2.4. GDF-15 blockade during RSV infection in elderly mice does not affect immune cell populations

Based on the unchanged levels of cellular infiltration and pro-inflammatory cytokines in the two experimental groups, it may be that GDF-15 blockade did not affect inflammation. However, the increase in viral load in the lungs of elderly mice treated with αGDF-15 suggests there may be subtle differences in the immune response to RSV in this model. Multicolour flow cytometry experiments were employed to identify the different immune cell populations in BAL fluid and lung tissue. Cells from homogenised lung tissue and from BAL fluid were stained for surface markers of Natural Killer (NK) cells, B cells, and T cells, including CD4+ and CD8+ subsets. $CD4^+$ T cells were stained with an MHC class II tetramer displaying an RSV peptide to determine RSV specificity of the response. Additionally, intracellular cytokine staining was carried out to measure production of IFNγ and IL-10. The gating strategy is shown in Figure 4-6. Lymphocytes were defined as live, singlet, $CD45^+$ cells that had characteristically small forward and side scatter. T cells were defined as $CD3^+$ lymphocytes. $CD4^+$ and $CD8^+$ T cells were defined as $CD3^+$ cells staining positive for $CD4^+$ and $CD8^+$, respectively. NK cells were defined as $NK1.1^+$ lymphocytes and B cells were defined as $CD19^+$ lymphocytes.

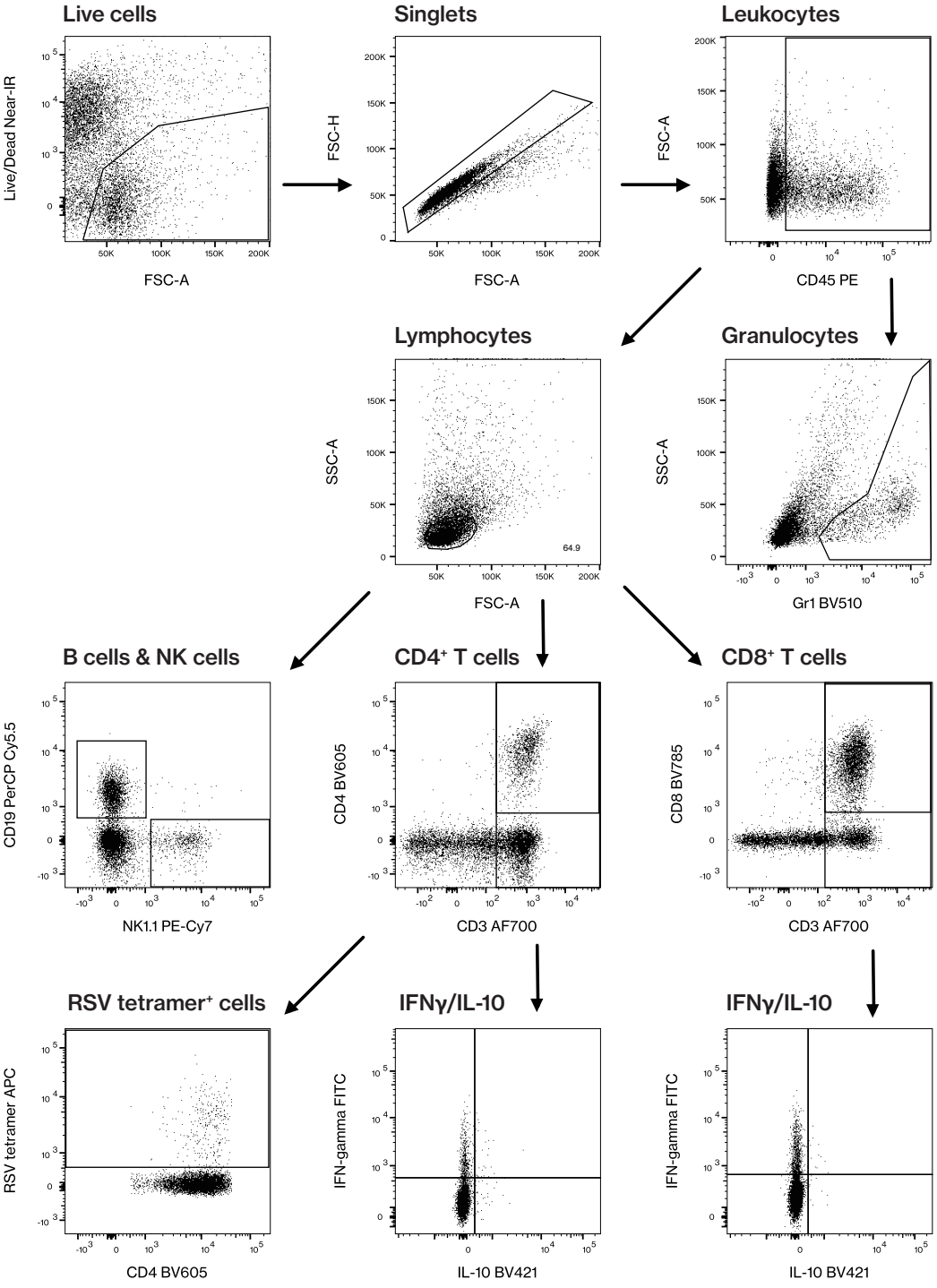

Figure 4-6 Gating strategy for immune response to RSV during GDF-15 blockade

Gating strategy shown as an example on a lung sample from an elderly mouse at 8 dpi. Lung and BAL cells were gated to remove debris and dead cells using Live/Dead fixable cell stain. Single cells were defined using forward scatter area and forward scatter height. Leukocytes were defined as CD45⁺ cells and all other cell populations gated on it. Granulocytes were determined with Gr1 staining. Lymphocytes were identified using forward and side scatter area. Lymphocytes were then gated for B cells (CD19⁺), NK cells (NK1.1⁺), T cells (CD3⁺) and CD4⁺ and CD8⁺ T cells. RSV specificity of CD4⁺ T cells was determined with an MHC class II tetramer. The production of IFNγ and IL-10 by CD4⁺ and CD8⁺ T cells was determined by intracellular cytokine staining.

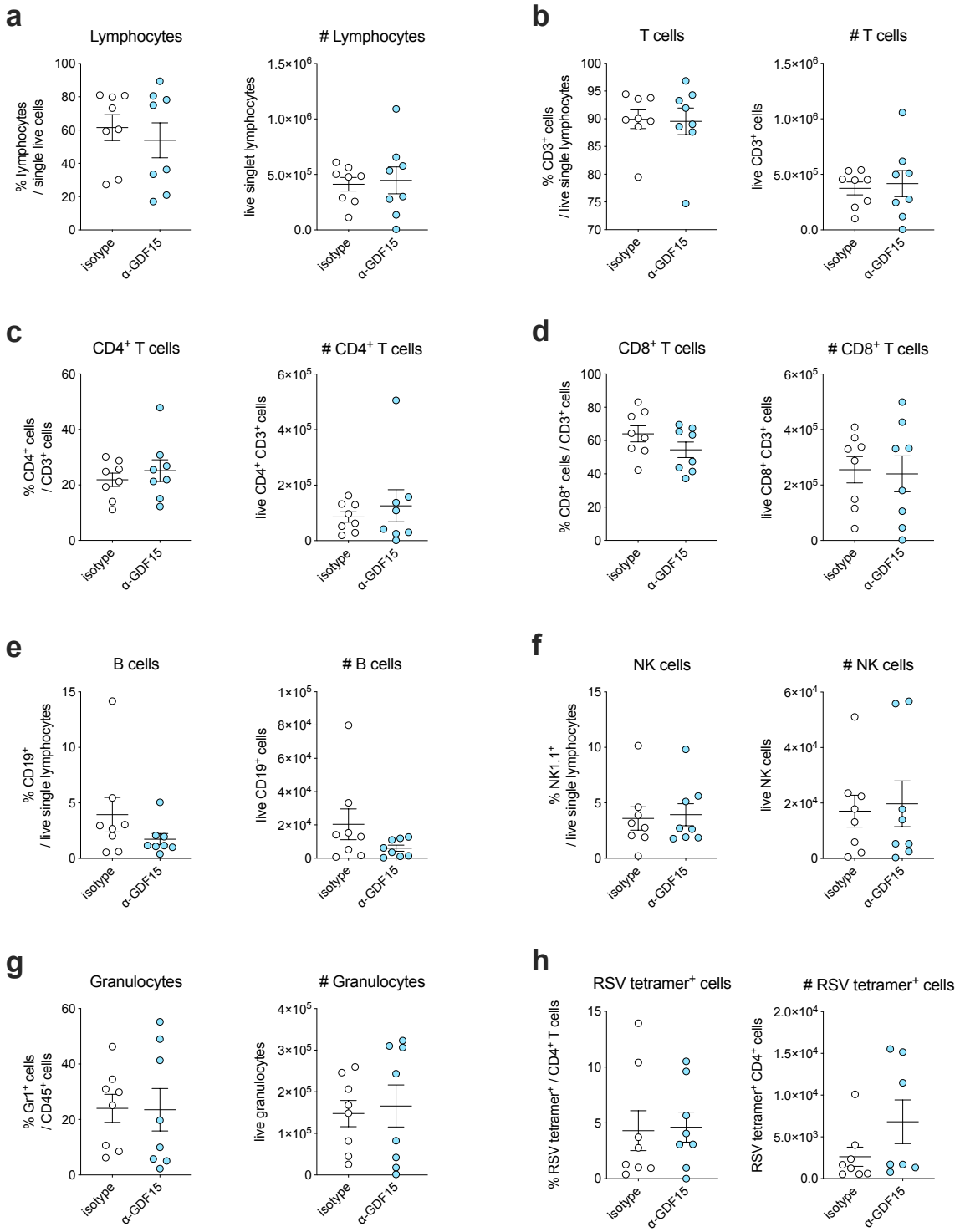

Figure 4-7 The effect of GDF-15 blockade on immune responses to RSV in lung tissue

Immune cell populations in lung tissue of elderly mice after 8 days of RSV infection, treated with either isotype control antibody or α-GDF-15 antibody. **a.** Lymphocytes. **b.** T cells. **c.** CD4$^+$ T cells. **d.** CD8$^+$ T cells. **e.** B cells. **f.** NK cells. **g.** Granulocytes. **h.** RSV tetramer-staining CD4$^+$ T cells. Student's unpaired two-tailed t-test. Pooled from two independent experiments at n=4-5. Left panels: proportion of population out of parent population. Right panels: Total number of cells of the given population in tissue.

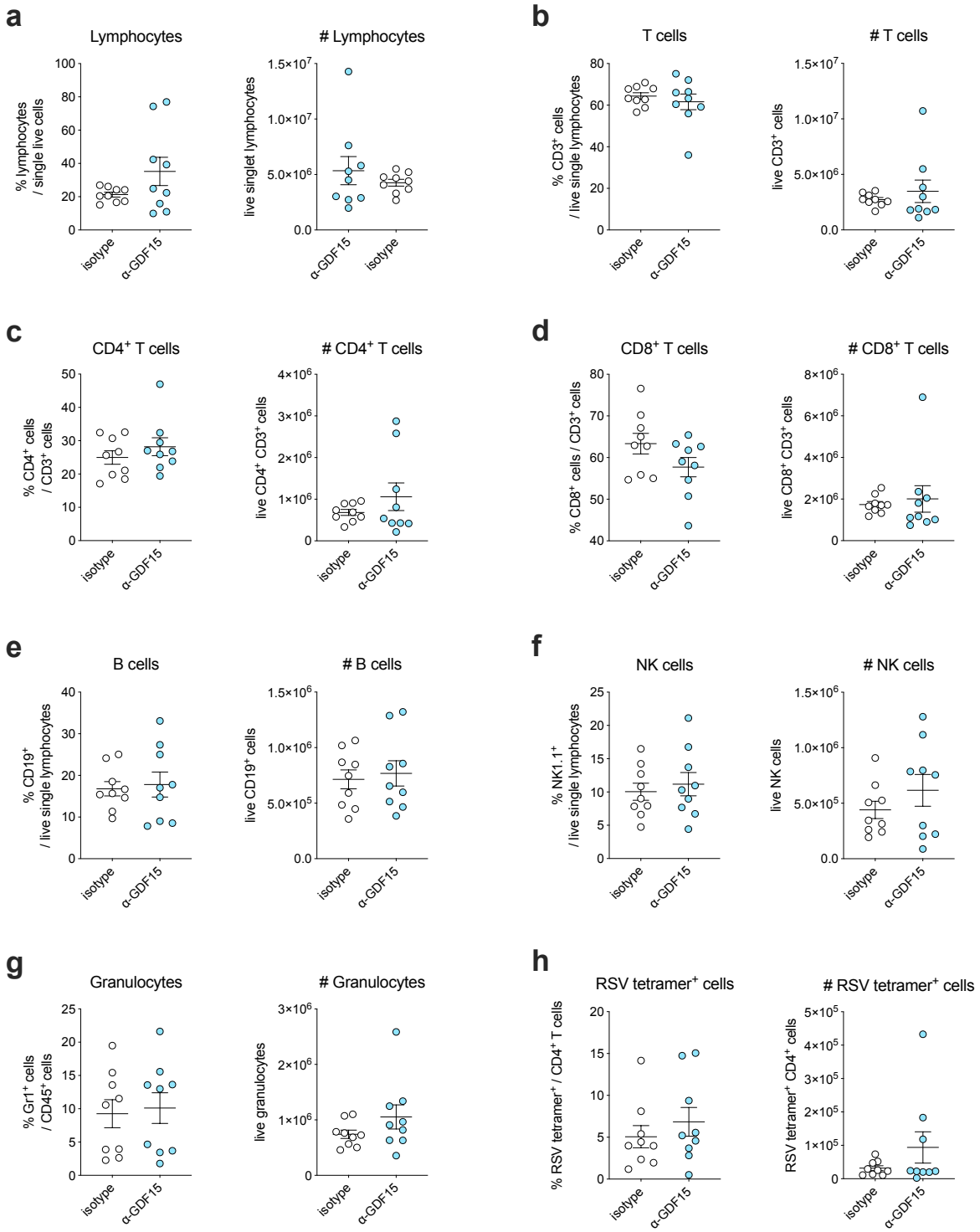

Figure 4-8 The effect of GDF-15 blockade on immune responses to RSV in BAL fluid cells

Immune cell populations in lung tissue of elderly mice after 8 days of RSV infection, treated with either isotype control antibody or α-GDF-15 antibody. **a.** Lymphocytes. **b.** T cells. **c.** CD4$^+$ T cells. **d.** CD8$^+$ T cells. **e.** B cells. **f.** NK cells. **g.** Granulocytes. **h.** RSV tetramer-staining CD4$^+$ T cells. Student's unpaired two-tailed t-test. Pooled from two independent experiments at n=4-5. Left panels: proportion of population out of parent population. Right panels: Total number of cells of the given population in tissue.

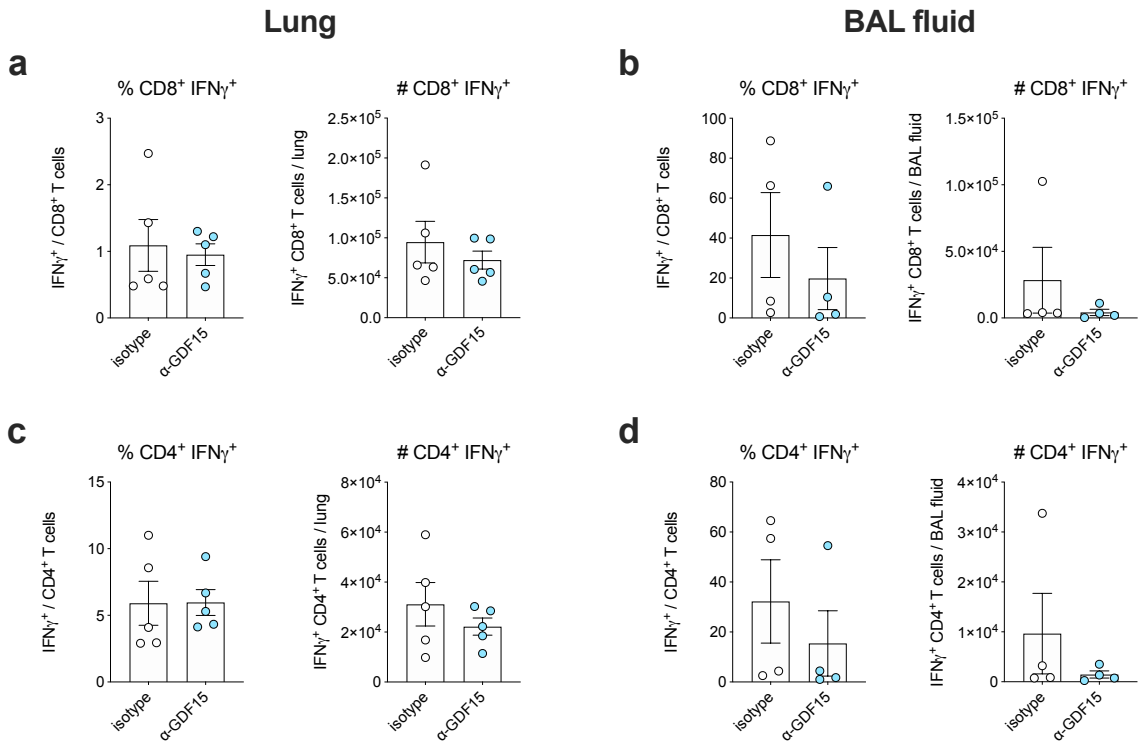

Figure 4-9 IFNγ production by immune cells in RSV during GDF-15 blockade

Lung cells and BAL fluid cells were harvested from elderly mice after 8 days of RSV infection, treated with either isotype control antibody or α-GDF-15 antibody. Populations were gated according to Figure 4-6. One experiment at n=4-5. Student's unpaired two-tailed t test. **a.,c.** Results from lung cells. **b.,d.** Results from BAL fluid cells. **a.-b.** $CD8^+$ T cells. **c.-d.** $CD4^+$ T cells. Left panels: proportion of population out of parent population. Right panels: Total number of cells of the given population in tissue.

There were no significant differences between mice treated with αGDF-15 antibody and mice treated with isotype antibody in any immune cell population measured in lung tissue or BAL fluid cells (Figure 4-7, Figure 4-8). There was high individual variability between the mice, as observed previously in elderly mice. There was no detectable difference in IL-10 or IFNγ production between the two groups either, however, intracellular cytokine staining was only done in one experiment (Figure 4-9, Figure 4-10).

4.3.2.5. The effect of GDF-15 blockade on skeletal muscle mass during RSV infection

At this point, GDF-15 blockade had not shown any clear effect on airway or lung inflammation during RSV infection. The muscles of elderly mice treated with αGDF-15 anti-

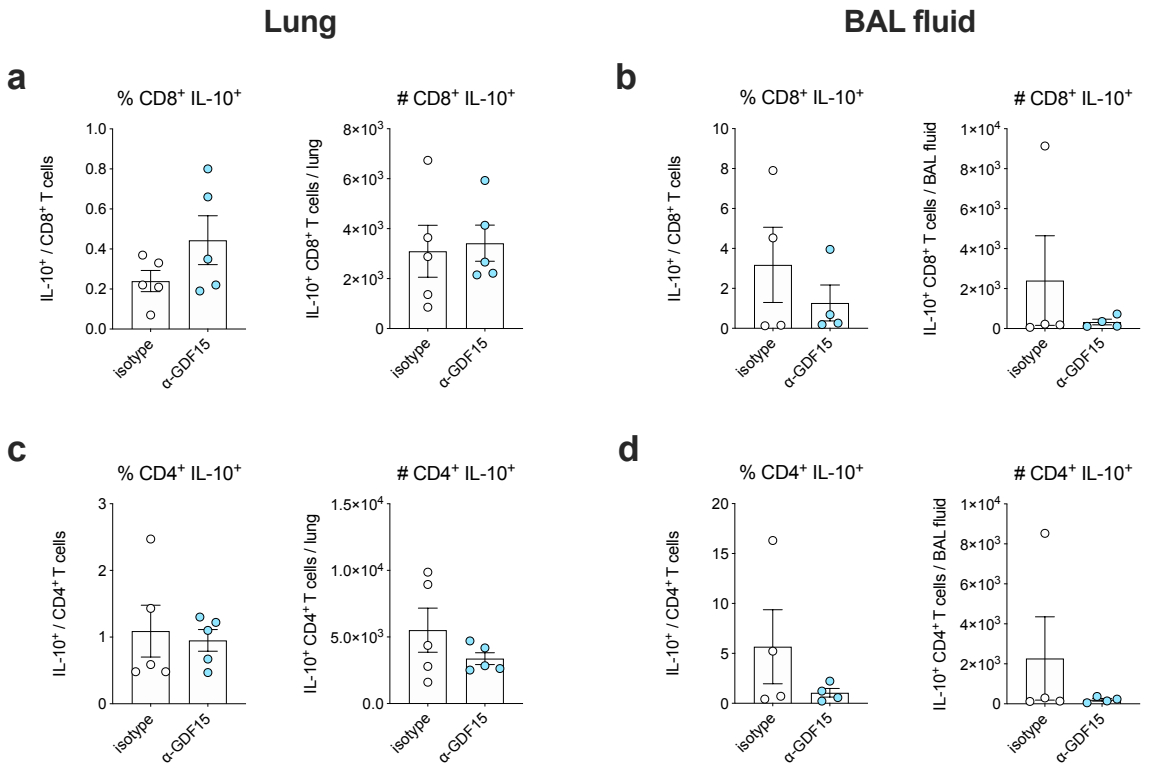

Figure 4-10 IL-10 production by immune cells in RSV during GDF-15 blockade

Lung cells and BAL fluid cells were harvested from elderly mice after 8 days of RSV infection, treated with either isotype control antibody or α-GDF-15 antibody. Populations were gated according to Figure 4-6. One experiment at n=4-5. Student's unpaired two-tailed t test. **a.,c.** Results from lung cells. **b.,d.** Results from BAL fluid cells. **a.-b.** $CD8^+$ T cells. **c.-d.** $CD4^+$ T cells. Left panels: proportion of population out of parent population. Right panels: Total number of cells of the given population in tissue.

body or with isotype antibody were analysed to determine any potential effect of GDF-15 blockade on muscle wasting during RSV infection. The TA muscle was extracted from both legs of each animal after euthanasia. Mice treated with αGDF-15 antibody trended towards having lighter TA muscles than those treated with isotype antibody, but this trend was not statistically significant, probably due to inadequate sample size (Figure 4-11a). However, when expressed as the TA atrophy index, which normalises muscle weight to the tibia length of the animal, αGDF-15-treated mice had significantly lower relative TA muscle mass than isotype-treated animals (Figure 4-11c). The tibia length used to calculate this atrophy index was not significantly different between the two groups (Figure 4-11b).

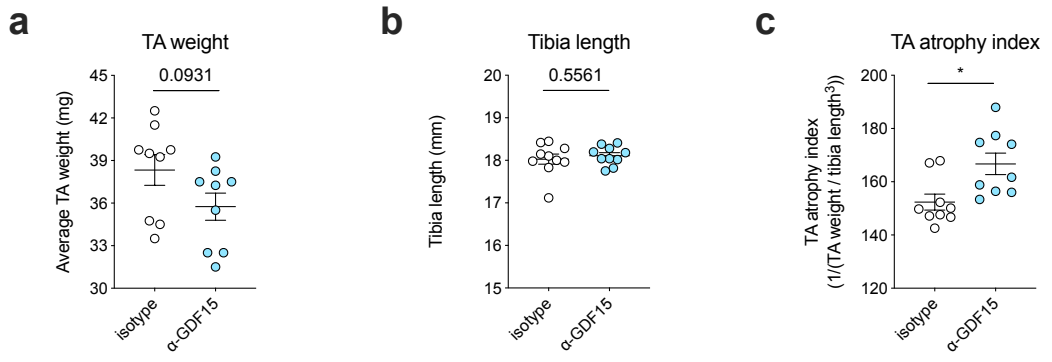

Figure 4-11 Gross and relative skeletal muscle mass during GDF-15 blockade

a. Tibialis anterior (TA) muscle weight of elderly mice 8 days after RSV infection treated with either isotype control antibody or α-GDF-15 antibody (average of both legs per mouse). Pooled from two independent experiments at n=4-5. Student's unpaired two-tailed t test. **b.** Tibia length. **c.** TA atrophy index.

4.3.2.6. Expression of positive and negative regulators of muscle during GDF-15 blockade

After measuring raw muscle weight, muscle wasting was interrogated on a molecular level by qPCR. The expression of the atrophy-promoting gene *Fbox32* (encoding Atrogin-1) was upregulated significantly in the TA muscles of elderly mice treated with αGDF-15 antibody compared to isotype-treated mice (Figure 4-12a). There was a similar trend towards increased expression of *Trim63* (MuRF-1), but this did not reach statistical significance (Figure 4-12b). There was no statistically significant difference in the expression of myostatin, or in the expression of the growth-promoting factors myogenin, Pax7, Myod1, and Mef2c, between isotype- and anti-GDF-15-treated groups (Figure 4-12c-g). Interestingly, there was a trend towards upregulation of the *Gdf15* gene itself in the lung tissue of elderly mice treated with αGDF-15 antibody (Figure 4-12h). This may represent a positive feedback loop induced by the systemic blockade of GDF-15 signalling.

4.3.2.7. Muscle fibre size and protein synthesis during GDF-15 blockade

The minimum Feret's diameter of TA muscle fibres in elderly RSV-infected mice treated with either isotype or αGDF-15 antibody was measured. Mice treated with αGDF-15 antibody trended towards having smaller TA muscle fibres compared to mice treated

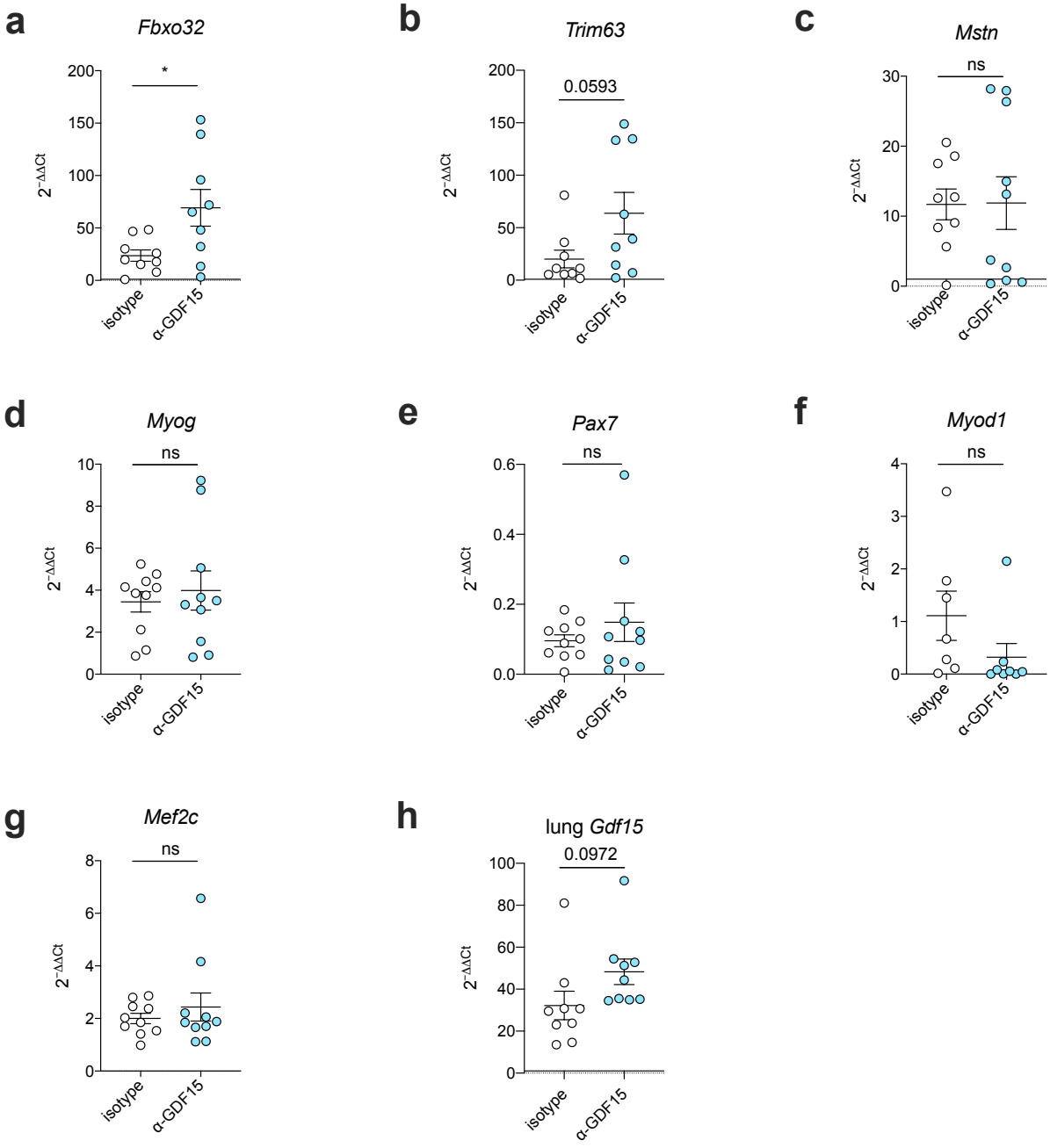

Figure 4-12 Expression of negative regulators of muscle mass during RSV infection

qPCR assays of gene expression in TA muscle (**a.-h.**) or lung tissue (**i.**) of elderly mice 8 days after RSV infection, treated with either isotype control antibody or α-GDF-15 antibody. Pooled from two independent experiments at n=4-5. Student's unpaired two-tailed t test. **a.** *Fbxo32* encoding Atrogin-1 **b.** *Trim63* encoding MuRF-1. **c.** *Mstn* encoding Myostatin. **d.** *Myog* encoding Myogenin. **e.** *Pax7* encoding Pax7. **f.** *Myod1* encoding MyoD1. **g.** *Mef2c* encoding Mef2c. **h.** *Igf1* encoding IGF-1. **i.** Expression of GDF-15 in lung tissue.

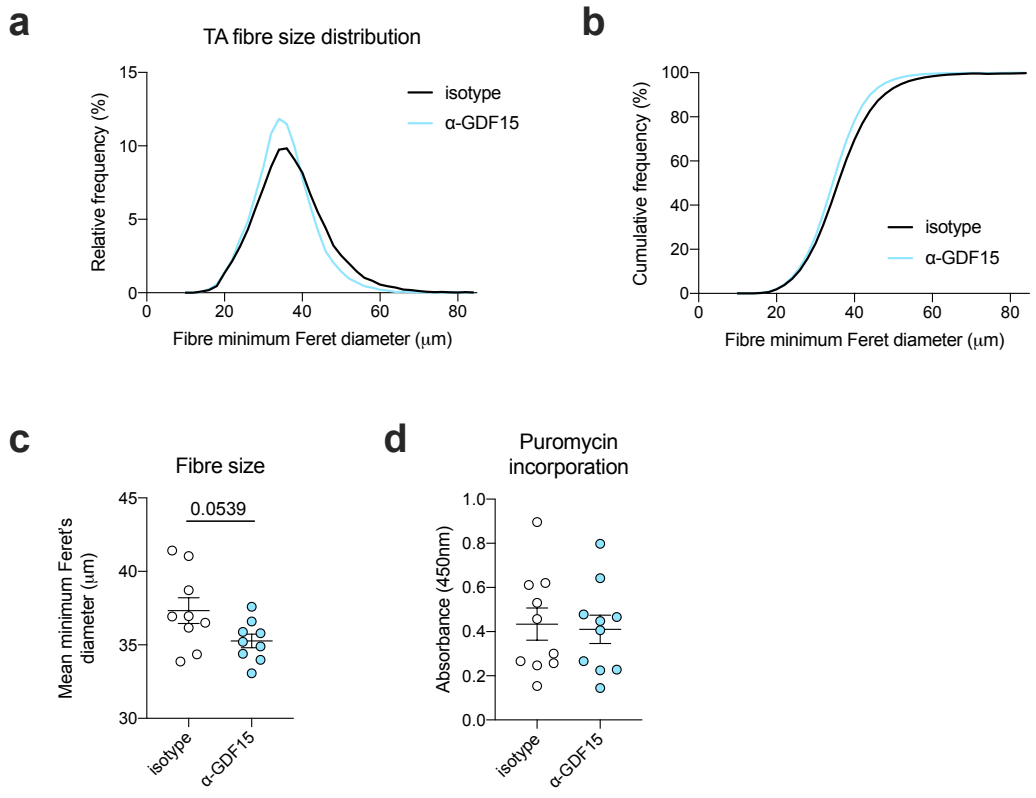

Figure 4-13 Muscle fibre size and puromycin incorporation during GDF-15 blockade

a.-c. TA muscle fibre minimum Feret's diameter measurement in elderly mice 8 days after RSV infection, treated with either α-GDF-15 antibody or isotype antibody. **a.** Relative frequency histogram of TA muscle fibre minimum Feret's diameter. **b.** Cumulative frequency histogram of a. **c.** Average minimum Feret's diameter of TA muscle fibres in elderly mice 8 days after RSV infection treated with either α-GDF-15 antibody or isotype antibody. **d.** Incorporation of puromycin into TA muscle of elderly mice 8 days after RSV infection treated with either α-GDF-15 antibody or isotype antibody. Pooled from 2 independent experiments at n=4-5. Student's unpaired two-tailed t test.

with isotype antibody, although this did not quite reach statistical significance (Figure 4-13a-c). Protein synthesis as measured with the puromycin incorporation assay was unchanged between isotype-treated and αGDF-15-treated mice (Figure 4-13d).

4.3.3. GDF-15 in samples from elderly human RSV challenge

Chris Chiu and Stephanie Ascough kindly provided plasma and BAL fluid samples from the INFLAMMAGE study, in which healthy elderly adults (age 65-75 years) were challenged with RSV. Young healthy volunteers (age 18-45 years) were also challenged and served as comparison. The individuals included in these results had cold-like symptoms

	"Young"	"Elderly"	*P* value
n =	3	7	—
Median age (range), years	26 (24-38)	66 (61-71)	0.0167
Sex, M:F (%M)	3:0 (100%)	4:3 (57%)	—
Ethnicity			
White	1	7	—
Asian	1	0	—
Mixed	1	0	—
Mean cumulative symptom score (IQR)	11 (NA)	29 (41)	0.3314
Mean cumulative viral load (IQR), log_{10} copies/ml	21.32 (NA)	30.79 (11.89)	0.3196

Table 4-1 Demographic and clinical information from participants of the INFLAMMAGE study whose samples were analysed for GDF-15

All participants listed here were infected with RSV strain X, were qPCR-confirmed to have been productively infected, and had cold-like symptoms. IQR = interquartile range; NA = not applicable; ns = not significant. P values for unpaired, two-tailed Student's t test.

and had been confirmed to be infected with RSV by qPCR of nasal swabs for RSV L gene (by Stephanie Ascough). Viral load data and symptom score data was provided by Stephanie Ascough (Figure 4-14c-f). The basic information about the participants whose samples were analysed here is shown in Table 4-1.

Plasma samples were available for baseline (day 0, before infection) and 3, 6, 14, and 28 days after RSV infection. GDF-15 protein was assayed in plasma samples by ELISA. Like in mice, plasma GDF-15 levels were elevated in the elderly participants compared to the young participants (Figure 4-14a). This difference was statistically significant at baseline (before RSV infection) and 3 days after infection. Similarly to what was found in mice, the time point of infection did not appear to affect circulating levels of GDF-15 in either young or elderly participants. Baseline plasma levels of GDF-15 were not correlated with cumulative viral load (Figure 4-14g) or symptom score (Figure 4-14h) over the course of

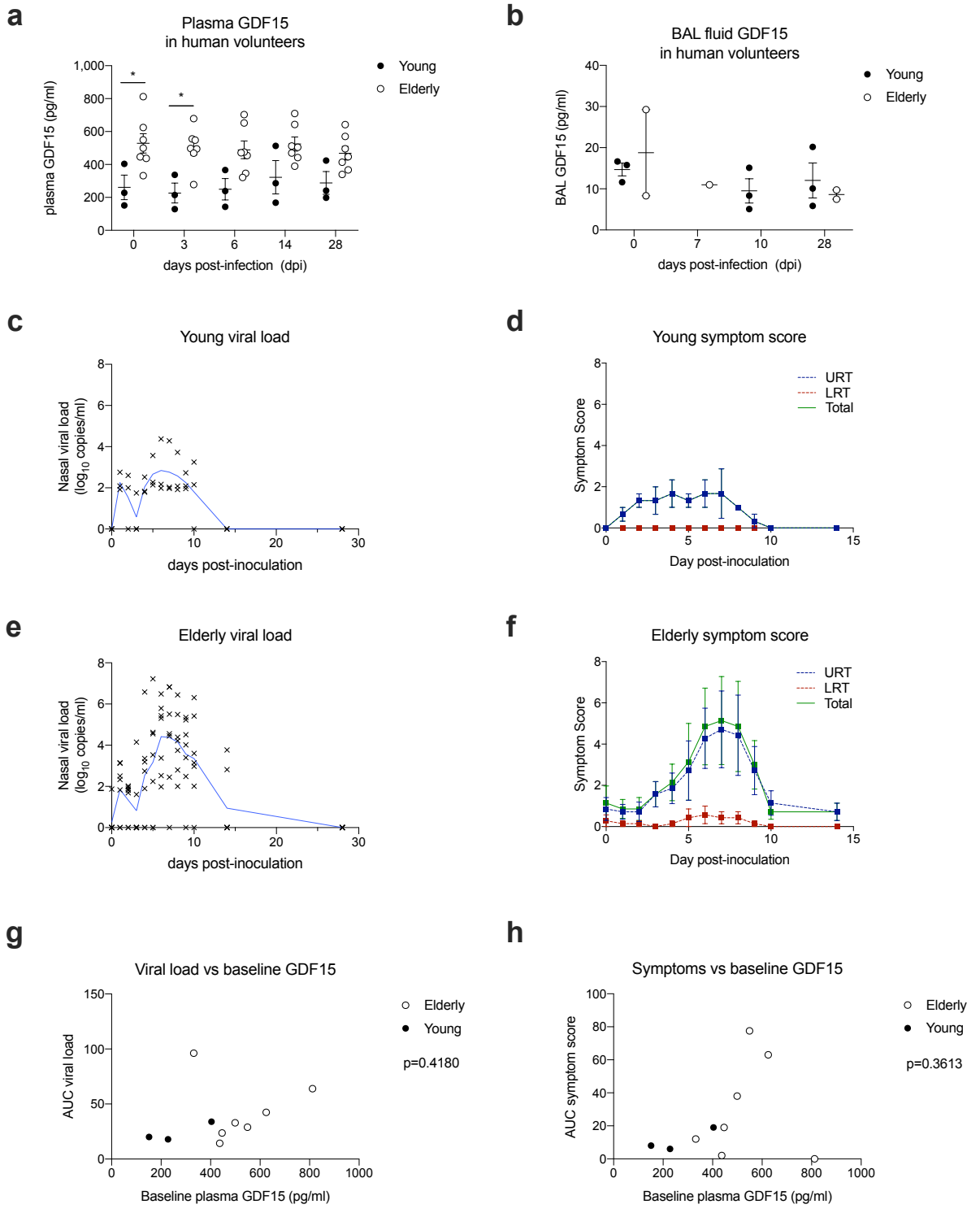

Figure 4-14 GDF-15 in young and elderly human volunteers experimentally infected with RSV

Young (age 18-55) and elderly (age 60-78) volunteers were intranasally infected with RSV as part of the INFLAMMAGE study. **a.** GDF-15 protein in plasma of RSV-infected young (n=3) and elderly (n=7) human volunteers. Two-way ANOVA with Bonferroni's post-test for multiple comparisons. **b.** GDF-15 protein in BAL fluid of RSV-infected young (n=3) and elderly (n=2) human volunteers **c.+e.** Nasal wash viral load determined by qPCR in young (**c.**) and elderly (**e.**) participants. **d.+f.** Daily self-reported symptom score in young (**d.**) and elderly (**f.**) participants. **g.+h.** Correlation of plasma GDF-15 with RSV cumulative viral load (**g.**) and cumulative symptoms score (**h.**) of experimentally RSV-challenged young and elderly volunteers.

RSV infection, but this may be due to the small number of samples.

The largest difference in GDF-15 protein levels between young and elderly mice had been found in BAL fluid. Hence, GDF-15 levels were tested in BAL fluid samples from INFLAMMAGE participants. Samples were only available from three young volunteers and two elderly volunteers, and only for some time points. Baseline samples and samples from 28 days after infection were available from all five participants. BAL fluid samples for day 10 were available from the young participants. There was one BAL fluid sample from an elderly volunteer for day 7. As expected, data was fairly variable. There was no difference in BAL fluid GDF-15 levels between young and elderly volunteers at any time point, and also there was no significant change in GDF-15 levels with the course of infection (Figure 4-14b). However, due to the small sample size, no conclusions should be drawn from this data other than that GDF-15 is detectable in the BAL fluid of humans both before and after RSV challenge.

4.4. Discussion

This chapter has explored the role of GDF-15 in the elderly mouse model of RSV infection using a GDF-15-blocking antibody. GDF-15 is a cytokine of the TGF-beta cytokine superfamily. GDF-15 levels are known to be elevated in many conditions and higher levels are commonly prognostic of a poor outcome (Carstensen *et al*., 2010; Cotter *et al*., 2015; Bloch *et al*., 2015). Until recently, its receptor and mode of action were unknown. High levels of GDF-15 being associated with poor outcomes may suggest that GDF-15 is causatively involved in these conditions, and that blocking its signalling may improve the conditions. Time course experiments comparing young and elderly mice suggested that GDF-15 was generally elevated in the serum of elderly mice and was more strongly increased in the BAL fluid and lungs of elderly mice during RSV infection. The discovery of the receptor of GDF-15, GFRAL, has suggested a role as an appetite suppressor (Mullican *et al*., 2017; Hsu *et al*., 2017; Yang *et al*., 2017; Emmerson *et al*., 2017). Since time course experiments had found that elderly mice consumed less food and water during

RSV infection than young mice, it was hypothesised that GDF-15 blockade may alleviate anorexia and subsequently ameliorate RSV weight loss. Additionally, previous *in vitro* studies had suggested that GDF-15 may possess a direct activity on muscle to promote atrophy, potentially by enhancing expression of the muscle-specific E3 ubiquitin ligases *Fbox32* and *Trim63* (Bloch *et al*., 2015), which I sought to confirm in this study.

4.4.1. GDF-15 does not influence inflammation during RSV infection

Contrary to expectations, elderly mice treated with αGDF-15 antibody did not lose more or less weight after 8 days of RSV infection than mice treated with an isotype control antibody. Blocking GDF-15 also did not affect food or water intake, unlike other studies that found it was a strong appetite suppressor. These results may suggest that not enough antibody was administered to achieve full suppression of GDF-15 signalling, or that the appetite suppression observed in elderly mice as compared to young mice was not primarily driven by GDF-15-mediated mechanisms.

Anti-GDF-15 treated mice also did not display changed levels of cellular infiltration in either BAL fluid or lung tissue. The frequency and total abundance of various immune cell subsets in BAL fluid and lung tissue, including T cells, B cells, NK cells, granulocytes, $CD8^+$ T cells, $CD4^+$ T cells, and RSV-specific $CD4^+$ T cells was likewise unchanged by GDF-15 blockade. A small preliminary experiment into cytokine production also suggested that GDF-15 blockade did not significantly affect the ability of immune cells to produce either IL-10 or IFNγ.

There was a slight increase in the viral load detected in the lungs of αGDF-15-treated mice compared to isotype-treated mice. However, the spread in the data was fairly broad so this may not have been caused by the antibody intervention. Contrary to this study, Wu *et al.* found increased rhinovirus viral load in mice overexpressing human GDF-15 (Wu et al., 2018). Knockdown of GDF-15 reduced rhinovirus load in human airway epithelial cells. Wu *et al*. also found increased airway inflammation after rhinovirus infection in GDF-15 transgenic mice, whereas the present study did not detect a change in inflammation after GDF-15 blockade during viral infection. Differences between this study and

Wu *et al*.'s study may be related to the differences between RSV and rhinovirus, and the differing experimental models. Wu *et al*. did not carry out the converse experiment in their model, blocking GDF-15 signalling either in transgenic or wild-type mice with rhinovirus infection. Similarly, this study did not test whether administration of recombinant GDF-15 exacerbated the response of elderly mice during RSV infection. This experiment could be of considerable interest to future studies because of the known strong correlation between elevated GDF-15 levels and poor health outcomes in many medical conditions.

There was a non-significant trend towards T cells particularly in the BAL fluid producing less IFNγ in mice treated with αGDF-15. This may be related to the increased viral load, as IFNγ is known to promote antiviral responses. Blocking GDF-15 may cause T cells to secrete less IFNγ, impairing protection against RSV, and leading to higher viral replication. The mechanism of GDF-15 signalling on T cells cytokine secretion is unclear and may be indirect.

4.4.2. The effect of GDF-15 blockade on muscle wasting during RSV infection

Patel *et al*. applied recombinant GDF-15 to myotube culture and observed an increase in expression of *Fbxo32* (Atrogin-1) and a decrease in minimum Feret's diameter of the myotubules (Patel et al., 2016). The authors concluded that GDF-15 may be a promoter of muscle atrophy. Counterintuitively, in the present study, the opposite appeared to be the case. There was a trend towards αGDF-15-treated elderly mice having lighter TA muscles proportionally to overall body size 8 days after RSV infection. There was also a non-significant trend towards smaller TA fibre size with GDF-15 blockade. Blocking GDF-15 caused significant upregulation of *Fbxo32* expression in TA muscle, the gene encoding the atrophy-promoting ubiquitin ligase Atrogin-1. There was a non-significant trend towards upregulation of another ubiquitin ligase, MuRF-1. These results may suggest that contrary to the findings of Patel *et al*., GDF-15 in fact fulfils a muscle-protective role in the context of RSV infection. Future studies with larger sample sizes are needed to confirm these trends.

Considering that GFRAL, the receptor for GDF-15, is exclusively expressed in the brain stem, it is unclear how GDF-15 administration to myotubes *in vitro* could have yielded the effects observed by Patel *et al*. There have been reports of commercially available recombinant GDF-15 being contaminated with TGF-β, which could explain these effects (Okamura, 2015; Olsen et al., 2017). A simple way of testing this would be to repeat the experiment and attempt to block the effects of the recombinant GDF-15 preparation with anti-GDF-15 and anti-TGF-β antibodies, respectively.

On the other hand, there is still a large body of work suggesting that GDF-15 has immunomodulatory effects (such as the original finding that it inhibits macrophage function) that cannot be explained by its interaction with GFRAL. Many *in vitro* studies using cell models that do not express GFRAL have found effects of GDF-15 (Fairlie et al., 1999; De Jager et al., 2011; Kempf et al., 2011). How can the results of these studies be reconciled with the apparent finding that GFRAL is the only receptor that binds GDF-15 (Mullican et al., 2017; Hsu et al., 2017; Yang et al., 2017; Emmerson et al., 2017)? There may still be other receptors or modes of action of GDF-15 to be discovered. For example, Patel *et al*. and Bloch *et al*. claim that in myotubes, GDF-15 downregulated the expression of miRNAs that positively regulate muscle mass, which led to an upregulation of Atrogin-1 (Bloch *et al.*, 2015). The authors hypothesise that GDF-15 may make muscles more sensitive to TGFβ-driven muscle wasting by inhibiting the expression of muscle-protective miRNAs like miR-181a. However, this experiment was not controlled for example by attempting to block the effect with an anti-GDF-15 antibody, or by replicating this *in vivo*. Non-canonical modes of signalling of GDF-15 remain to be elucidated. This could include administering anti-GFRAL antibodies or ablating the area postrema before administering GDF-15 in an elderly RSV mouse model.

The exact mechanism of how GDF-15 blockade would promote muscle wasting in this model was not investigated. It appears that effects were mediated by an upregulation in atrophic signals, such as increased expression of Atrogin-1, but not by a decrease in protein synthesis, since puromycin incorporation was unchanged. It is interesting that

the muscle wasting response appears to be uncoupled from inflammation, which was not significantly increased with GDF-15 blockade.

4.4.3. GDF-15 as a systemic regulator of stress responses

The findings that GDF-15 blockade did not affect weight loss, appetite, or inflammation caused by RSV infection may appear disappointing considering the strong association of GDF-15 with anorexia and poor outcome in numerous medical conditions. However, this may simply indicate that GDF-15 is not causative of a poor outcome, at least in the context of RSV infection in elderly mice.

Luan *et al*. recently conducted a study investigating the role of GDF-15 in mouse models of lethal IAV infection or bacterial sepsis (Luan et al., 2019). In this study, survival was significantly lower in mice treated with αGDF-15 antibody, despite unchanged systemic inflammation and viral/bacterial loads. Conversely, treating wild-type mice with recombinant GDF-15 improved sepsis survival. These results are intriguing because they contradict the widespread assumption that GDF-15 is associated with poor outcomes. It is also consistent with the findings of the present study that viral load and inflammation was not majorly changed by GDF-15 blockade. Luan *et al*. suggest that GDF-15 signalling induces sympathetic neural signalling that promotes the release of cardioprotective lipid species from the liver. In this theory, GDF-15 is a regulator of systemic stress responses, which would explain its high production during conditions as varied as cancer, COPD, and ageing.

The effect of GDF-15 on cardiac function was not investigated in this study, but there is evidence that muscle mass and function are also regulated by lipids (Lipina & Hundal, 2017). The application of saturated fatty acids decreases C2C12 myotube diameter and increases expression of Atrogin-1, an effect that can be prevented by co-administration of unsaturated fatty acids (Bryner et al., 2012; Woodworth-Hobbs et al., 2014). Supplementing the diet of experimental animals with unsaturated fatty acids can prevent or ameliorate muscle wasting in a number of *in vivo* models, including colon adenocarcinoma, muscle dystrophy, and adjuvant-induced arthritis (Whitehouse et al., 2001; Graves

et al., 2005; Langen et al., 2006; Castillero et al., 2009; Fiaccavento et al., 2010). This protective effect of unsaturated fatty acids was associated with reduced TNF-α signalling and improved mitochondrial function. Impaired mitochondrial function, such as reduced oxidative capacity, has been suggested to contribute to both diet- and age-associated muscle wasting (Gouspillou et al., 2014; Jang et al., 2010; Roseno et al., 2015). Luan *et al*. did not investigate the effect of GDF-15-mediated triglyceride release on skeletal muscle, but it is conceivable that the same mechanism is responsible for the effects observed in this study. A metabolomic screen of lipid species in the serum of elderly mice treated with isotype antibody and anti-GDF-15 antibody was initiated but not completed at this time.

4.4.4. Human challenge studies confirm higher but constant GDF-15 levels in the elderly during RSV infection

Chris Chiu and Stephanie Ascough kindly provided plasma and BAL fluid samples from the INFLAMMAGE study, in which healthy elderly adults (age 60-78 years) and young adults (age 18-55 years) were challenged intranasally with RSV. Consistent with the results from the mouse model, circulating GDF-15 levels were elevated in elderly volunteers compared to young volunteers, but did not change significantly over the course of RSV infection.

Since the largest change in GDF-15 was observed in the BAL fluid of elderly mice over the course of RSV infection, GDF-15 levels were also assayed in the BAL fluid of some INFLAMMAGE volunteers. Unfortunately, only few BAL fluid samples were available. There was no discernible pattern of GDF-15 levels changing in the BAL fluid of young or elderly volunteers over RSV infection. BAL fluid levels of GDF-15 were also not different between young and elderly volunteers at any time point. However, this may be due to the fact that only one sample from an elderly volunteer was available for the peak of infection (day 7). Moreover, BAL is conducted with a fairly large volume of liquid in humans and only a small branch of the lung is lavaged. This increased dilution may be the cause for the fairly low concentration of GDF-15 found in BAL fluid, and may make it more difficult in

the future to detect small amounts of GDF-15. Baseline plasma GDF-15 levels were not predictive of viral load or symptom score in either age group or collectively, but this may be due to the small number of samples.

Overall, the number of patients tested in this preliminary study was too small to draw firm conclusions on the role of GDF-15 in RSV infection of young vs elderly humans. Unfortunately, the INFLAMMAGE study is currently indefinitely suspended due to the COVID-19 pandemic, so obtaining additional samples will prove difficult. However, these results confirm the findings of the mouse model that GDF-15 is elevated with age, but does not necessarily change in circulation over the course of RSV infection.

4.4.5. Limitations

4.4.5.1. Anti-GDF-15 antibody dosing effects

Considering the modest effects of blocking GDF-15 in this model, it is possible that not enough of the antibody was administered to prevent all GDF-15 signalling. To address this, one experiment was conducted that included a second dose of αGDF-15 four days after the initial dose (3 dpi). However, results from that experiment did not show larger differences between the two groups than the experiments using a single dose (not shown). Personal communication with Harding Luan of NGM Pharmaceuticals, who provided the antibodies, indicated that a single dose should be sufficient to block GDF-15 signalling in the time frame of these experiments (8 days).

4.4.5.2. Existence of potential feedback loops

Elevated levels of GDF-15 protein were found in the BAL fluid of mice given αGDF-15 antibody. Mice treated with anti-GDF-15 antibody also displayed signs of increased expression of GDF-15 in lung tissue. Finding elevated GDF-15 protein and expression with αGDF-15 treatment may seem counterintuitive. It is possible that remnants of the αGDF-15 antibody in the BAL fluid interacted with the ELISA assay to produce this result. However, it may also be due to a feedback loop where the absence of GDF-15 triggers increased production, suggesting an important function of GDF-15 in the response to stress. Future experiments may wish to establish if the increased amount of GDF-15

protein detected in BAL fluid is biologically active. If this is found to be the case, then the effects seen when administering the antibody might not be due to the absence of GDF-15, but in fact an increase in GDF-15.

4.4.6. Future work

Future studies using this model may want to focus on elucidating the exact pathway through which GDF-15 signalling affects muscle mass. It is possible that this includes systemic lipid signalling, but other, non-canonical modes of action should also be considered.

This study blocked GDF-15 with a monoclonal antibody, but did not attempt the converse experiment, i.e. the administration of recombinant GDF-15 to elderly mice during RSV infection. In future studies it would be interesting to determine if recombinant GDF-15 may protect elderly mice from muscle wasting during RSV infection, and whether this is dose-dependent. In high doses, GDF-15 is well-known to induce anorexia and subsequent body and muscle weight loss (Harding Luan, pers. comm. 2019), but at lower doses it might have beneficial effects. It may also be of interest to determine the kinetics of this response, for example, if late or early GDF-15 blockade/signalling during an infection have differential effects. Another avenue includes the effect of route of administration. Antibodies were administered intraperitoneally in this study, but since RSV is a respiratory infection, perhaps intranasal administration of recombinant GDF-15 may yield stronger effects.

It might be informative to compare the results of these experiments with experiments blocking GFRAL, for example with an anti-GFRAL antibody. This could shed light on potential non-canonical, non-GFRAL-mediated modes of action of GDF-15.

To avoid antibody interactions and achieve a “clean” phenotype without any active protein, future studies may also use genetically modified mice, such as GDF-15$^{-/-}$ or GFRAL$^{-/-}$ mice. However, investigating the role of age presents the additional complication of having to wait for these mice to achieve the right age, a substantial cost. As CRISPR-Cas9

technology and other precision genetic manipulation tools become more widely available, this may present an opportunity for future experiments to study the role of GDF-15 in aged mouse models with various genetic modifications.

This study was primarily concerned with the effect of GDF-15 in an aged model, due to the strong associations of GDF-15 with age and age-associated diseases. However, it might also be of interest to repeat this study with young mice to establish effects of GDF-15 in the absence of systemic inflammation as may be found in elderly mice. To induce muscle wasting in young mice, a stronger stimulus will have to be used, for example IAV infection or a higher dose of RSV.

The study by Luan *et al*. (2019) suggested a potential role of GDF-15 in the regulation of circulating triglycerides with a cardioprotective effect. This pathway may also be responsible for the non-significant trends observed of GDF-15 blockade on skeletal muscle mass. A metabolomic screen of lipid species was initiated but not completed at time of writing. Evaluation of the other potential metabolic effects of GDF-15, particularly in the context of age and immunometabolism, may be of substantial interest. Investigation of the role of lipids in the regulation of muscle with age should focus on the role of mitochondria, which are known to be dysregulated with age.

The few experiments using human plasma and BAL fluid samples from the INFLAMMAGE study obviously suffered from a small sample number, making statistical analysis difficult. As the INFLAMMAGE study progresses, more samples should become available to consolidate those results, which may shed light on the dynamics of GDF-15 production with age over RSV infection.

Another potential avenue involves the potential role of GDF-15 in cardiac protection. Cardiovascular complications, including congestive heart failure, acute coronary syndrome, and cardiac arrhythmias, develop in approximately a fifth of immunocompetent elderly adults infected with RSV, and the risk of acute myocardial infarction increases significantly in the week after hospitalisation for influenza infection (Anderson et al., 2016;

Kwong et al., 2018). This suggests a connection between systemic inflammation and cardiac events.

The current limited data does not suggest that high baseline GDF-15 levels predispose to more severe acute RSV infection as measured by symptoms and viral load, in contrast to many other conditions. However, lower GDF-15 may predispose for future cardiac events in the longer term. Adding outputs measuring cardiac function and damage, such as plasma troponin, to the INFLAMMAGE study, may be able to indicate if this is the case.

4.4.7. Summary

The TGF-β superfamily cytokine GDF-15 is associated with a poor outcome in many medical conditions, and was found to be elevated in the serum of elderly mice, and increased in the BAL fluid of elderly mice infected with RSV. GDF-15 was also elevated in the plasma of elderly volunteers experimentally infected with RSV, regardless of time point. The recent discovery of the receptor for GDF-15, the brain stem receptor GFRAL, implies that the detrimental effects of GDF-15 are driven by anorexia. This chapter has investigated if RSV-driven anorexia, body- and muscle weight loss in elderly mice could be rescued by blockade of GDF-15 using a monoclonal antibody. Contrary to expectations, GDF-15 blockade did not affect weight loss or lung inflammation. However, an increase in the expression of the atrogenic enzyme Atrogin-1, and non-significant trends towards a decrease in proportional TA muscle mass were observed in αGDF-15-treated mice. This provides tentative evidence that GDF-15 may not promote muscle wasting as previously assumed. The pathways through which GDF-15 may act on skeletal muscle remain to be elucidated but could include promotion of the release of certain lipid species. The commercial development of drugs blocking GDF-15 should be approached with great caution. The results of this study suggest that these drugs may have unintended side effects on skeletal muscle. On the other hand, increasing GDF-15 may present an interesting avenue for increasing resilience to infection-induced muscle wasting in aged organisms.

5.

The role of IL-6 in the elderly during respiratory infection

Chapter 5. The role of IL-6 in the elderly during respiratory infection

5.1. Introduction

5.1.1. Background

IL-6 is a pleiotropic cytokine that can have both pro-inflammatory and anti-inflammatory effects. Assays conducted during the time course experiments showed that IL-6 protein was strongly elevated in the BAL fluid of elderly mice at the peak of RSV infection (see Figure 3-18). IL-6 has been implicated in "inflammageing", a state of detrimental chronic inflammation sometimes observed in aged organisms (Franceschi *et al.,* 2006). Blocking IL-6 signalling may remove excess inflammation and thus improve the outcome of RSV infection in elderly mice. On the other hand, Pyle *et al.* previously found that in young mice, IL-6 signalling early during RSV infection was essential to preventing excessive immunopathology, so it is also possible that blocking IL-6 signalling may cause more severe disease in elderly mice (Pyle *et al.*, 2017). IL-6 is a myokine, a cytokine produced by skeletal muscle and released into circulation in response to exercise (Steensberg *et al.*, 2000). The effect of IL-6 signalling on muscle itself is controversial. Studies with IL-6-knockout mice have demonstrated that IL-6 promotes muscle growth (hypertrophy) by stimulating proliferation of satellite cells (Serrano *et al.*, 2008). However, prolonged exposure to IL-6 such as may be found in chronic inflammatory conditions has been associated with increased muscle atrophy, although its method of action in this context may be indirect (Muñoz-Cánoves *et al.*, 2013). In cancer cachexia mouse models, blocking IL-6 suppresses cachexia, and transgenic mice overexpressing IL-6 display profound muscle wasting, a phenotype which can be reversed by blockade of the IL-6 receptor, IL-6R (Strassmann *et al.*, 1992; Tsujinaka *et al.*, 1995, 1996). Lastly, IL-6 plays an important role in the germinal centre response, driving the differentiation of B cells into antibody-producing plasma cells, and of T cells into Tfh cells (Suematsu *et al.*, 1989; Nurieva *et al.*, 2008). IL-6-deficient mice mount weaker IgG and IgA responses, which can be rescued

with recombinant IL-6 (Kopf *et al.*, 1994; Ramsay *et al.*, 1994). In this context, blocking IL-6 signalling may be detrimental to the germinal centre response to RSV infection in the elderly mouse model.

5.1.2. Purpose of chapter

This chapter aims to elucidate the role of IL-6 in the elderly mouse model of RSV infection. The effects of IL-6 signalling were blocked with a monoclonal antibody to the IL-6 receptor (IL-6R) during RSV infection of elderly mice. The results compare the effect of IL-6 signalling blockade on general features of the immune response to RSV (markers of inflammation, cellular airway infiltration, viral load) and on muscle wasting using the methodologies developed previously (TA muscle weight, fibre size, protein turnover, and gene expression profile).

5.1.3. Aims

- To determine the effects of IL-6 blockade on the immune response to RSV infection in elderly mice
- To determine the effects of IL-6 blockade on muscle wasting after RSV infection in elderly mice

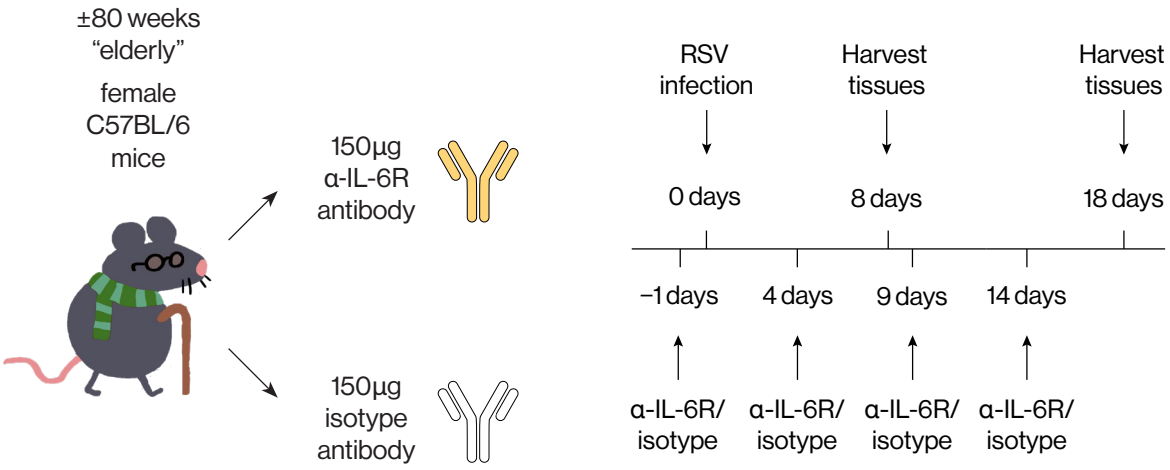

Figure 5-1 Timeline of IL-6R blockade in elderly mice during RSV infection

Elderly (±80 week-old) female C57BL/6 mice were injected intraperitoneally with 150µg of either α-IL-6R antibody or isotype control (keyhole limpet hemocyanin) antibody suspended in 200µl PBS every five days, beginning one day before RSV infection. Mice were intranasally inoculated with $2.3x10^5$ PFU of RSV strain A2 in a volume of 75µl. Mice were euthanised and tissues harvested 8 days or 18 days post-infection. Illustration by Michael Barrett.

5.2. Experimental Design

The results in this chapter describe an interventional study of the effects of blocking IL-6 signalling using a monoclonal antibody to IL-6R. All mice used in this chapter were "elderly" (±80 weeks) mice. Mice were injected intraperitoneally with 150µg αIL-6R antibody or isotype control antibody, suspended in 200µl PBS, one day before RSV infection, and every five days thereafter (Figure 5-1). Groups were assigned randomly, and experimenters were blinded to treatment. Mice were infected with $2.3x10^5$ PFU of RSV strain A2 and weighed daily. Tissues were collected 8 days post-infection or 18 days post-infection. Tissues collected were blood, BAL fluid, lung tissue, tibia, and tibialis anterior (TA) muscle. Flow cytometry of lung cells and BAL fluid cells was used to quantify cell numbers and determine changes in the frequency of various immune cell types. Copy number of RSV L gene was measured in lung tissue by qPCR. Cytokines in BAL fluid were measured by ELISA. The TA muscle was weighed, and tibia length measured. The expression of various genes controlling muscle mass was determined by qPCR. Protein turnover in the TA was determined with a novel assay measuring puromycin incorporation by ELISA technology. Muscle fibre size was determined by immunohistochemistry of muscle cryosections.

5.3. Results

5.3.1. IL-6R blockade in elderly mice at baseline

Prior to commencing experiments with RSV infection, the baseline effect of IL-6R blockade in elderly mouse was determined. Every five days, elderly mice were injected intraperitoneally with αIL-6R antibody or isotype control antibody. Mice were observed for 17 days which covered a total of four antibody injections. Mice were weighed daily and their food hoppers and water bottles were weighed to calculate the average daily intake of food and water per mouse.

Over the course of 17 days, the two groups of mice did not diverge significantly in weight (Figure 5-2a). Towards the end of the experiment, the isotype-treated group trended to-

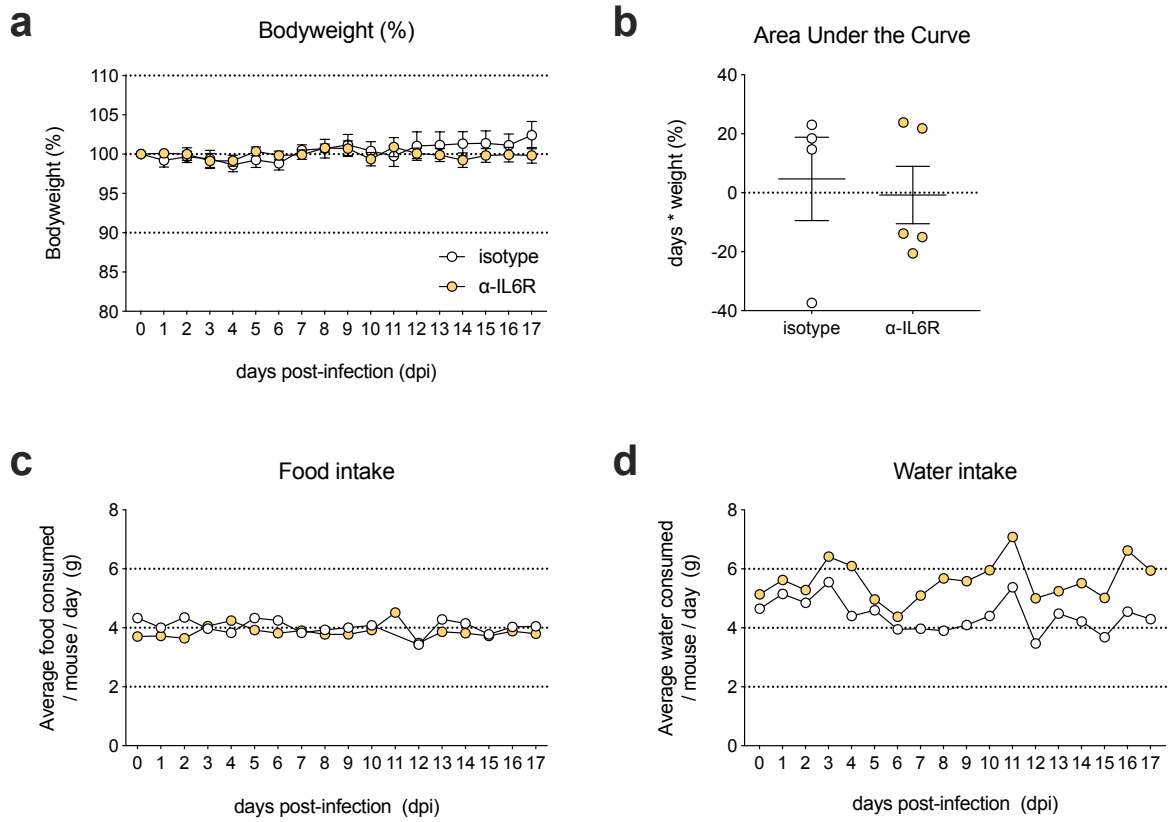

Figure 5-2 Weight, food and water intake at baseline while blocking IL-6R

One experiment n=4-5. Open circles: Mice given isotype control antibody. Yellow filled circles: Mice given α-IL-6R antibody. **a.** Bodyweight as a percentage of weight at day 0. Shown are group means with the standard error of the mean. **b.** Area under the curve of weight change as a percentage of starting weight. **c.** Food intake and **d.** Water intake per mouse over the course of 17 days.

wards an increasing bodyweight compared to the starting weight, but this may be unrelated to the antibody treatment. Calculating the Area Under the Curve (AUC) confirmed that neither group had lost or gained significantly more weight than the other (Figure 5-2b). The food intake of both groups was very similar and very consistent over 17 days (Figure 5-3c). Water intake trended towards being higher in the αIL-6R-treated group, but since only two cages were compared, this was not statistically significant (Figure 5-2d). This experiment suggested that blocking IL-6R signalling would not have effects in elderly mice independent of RSV infection.

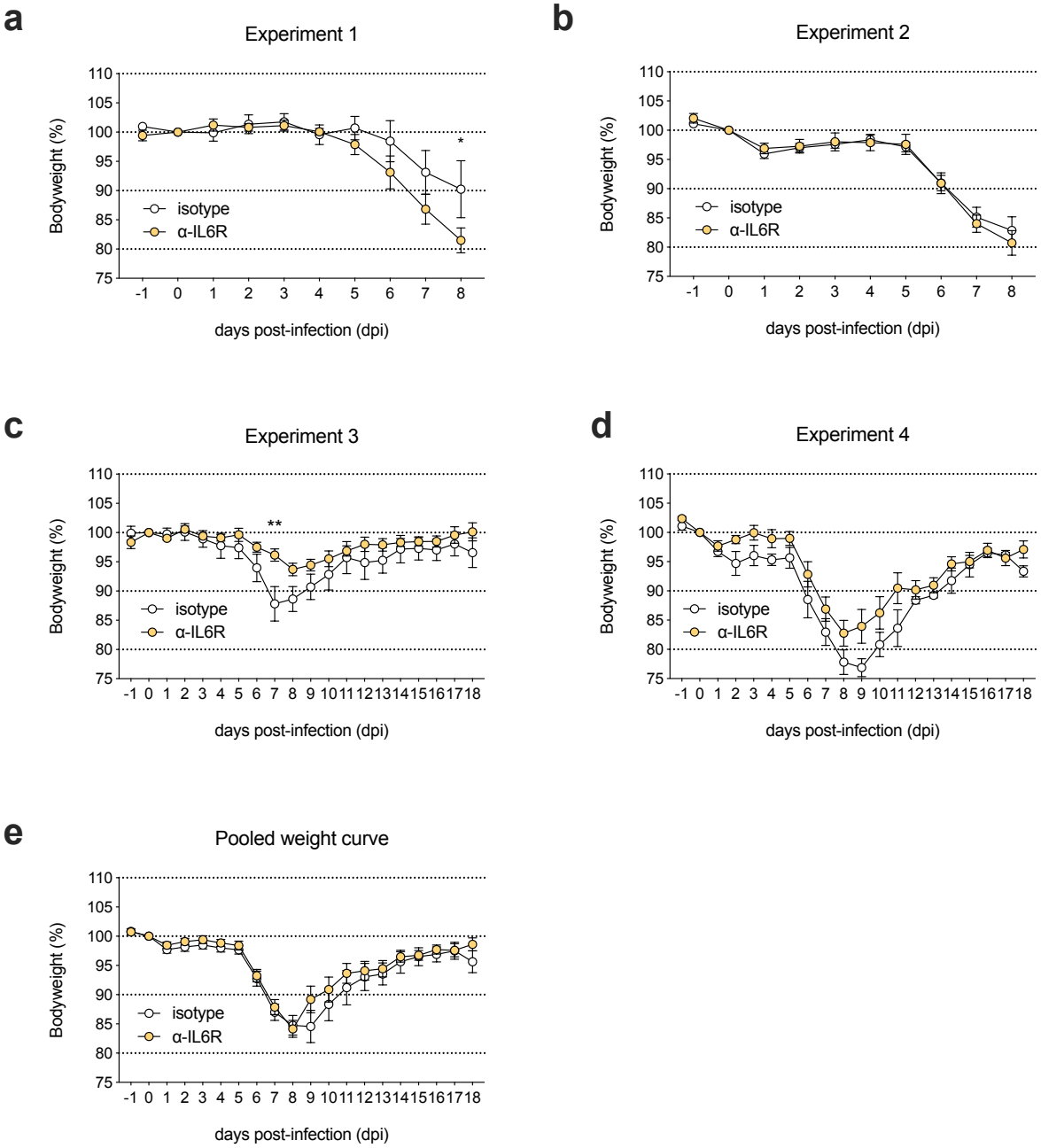

Figure 5-3 Weight loss of elderly mice during RSV infection after IL-6R blockade

Elderly mice were given α-IL-6R antibody or isotype control antibody intraperitoneally one day before RSV infection and every five days, and euthanised either 8 days or 18 days after infection. Two experiments each were conducted at a day 8 (**a.** and **b.**) and a day 18 (**c.** and **d.**) time point, n=2-10. Bodyweight is shown as a percentage of weight at day 0 (the day of infection). Shown are group means with the standard error of the mean. **e.** Experiments shown in a-d pooled.

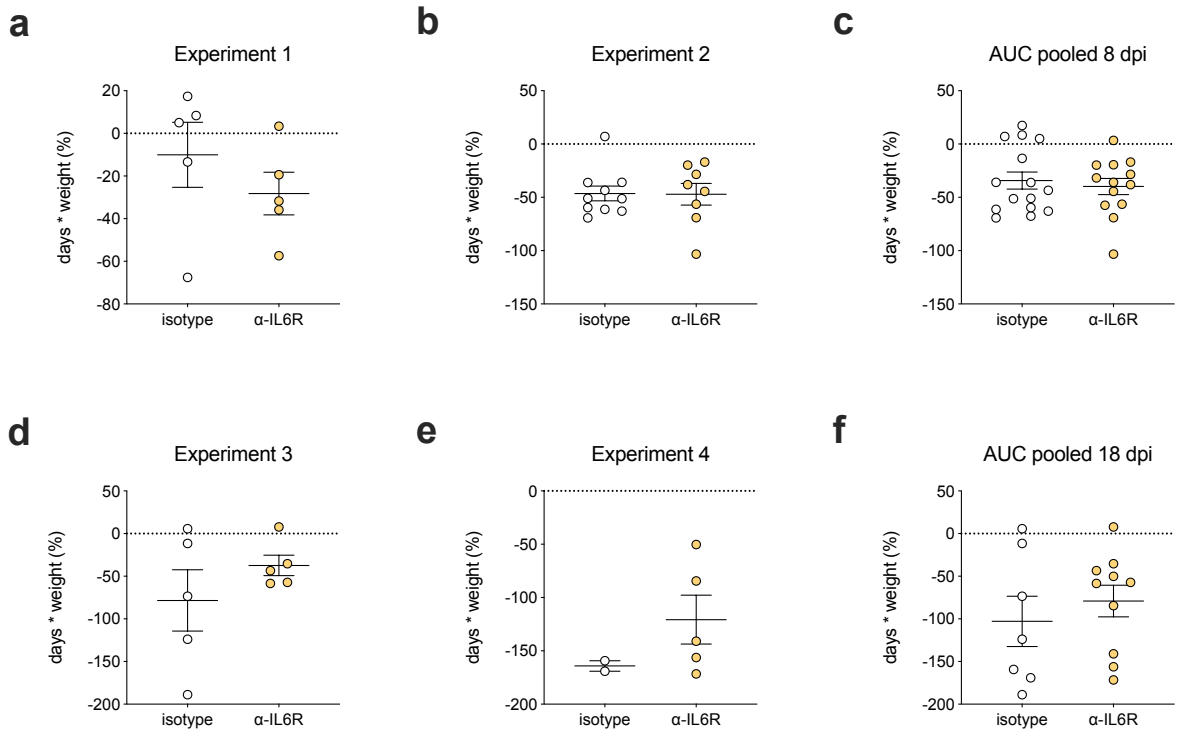

Figure 5-4 Area Under the Curve during RSV infection and IL-6R blockade

Area Under the Curve as a measure of total weight loss over the course of RSV infection of elderly mice while blocking IL-6R (yellow filled circles) or isotype antibody (open circles), n=2-10. **a.-c.** RSV infection over 8 days. **d.-f.** RSV infection over 18 days. **c.** and **f.** represent pooled data from **a. + b.** and **d. + e.**, respectively.

5.3.2. Blocking IL-6R does not affect weight loss during RSV infection

Elderly mice were given αIL-6R antibody or isotype control antibody intraperitoneally one day before RSV infection and every five days, and euthanised either 8 days or 18 days after infection. Two experiments were conducted at each time point.

Contrary to expectations, blocking IL-6R signalling in this model did not yield a consistent weight loss phenotype (Figure 5-3). In the two experiments that were concluded at day 18 after RSV infection, Experiments 3 and 4, there was a strong trend towards the αIL-6R-treated group losing less weight than the isotype-treated group (Figure 5-c,d). In one of these experiments, αIL-6R-treated mice had lost significantly less weight than

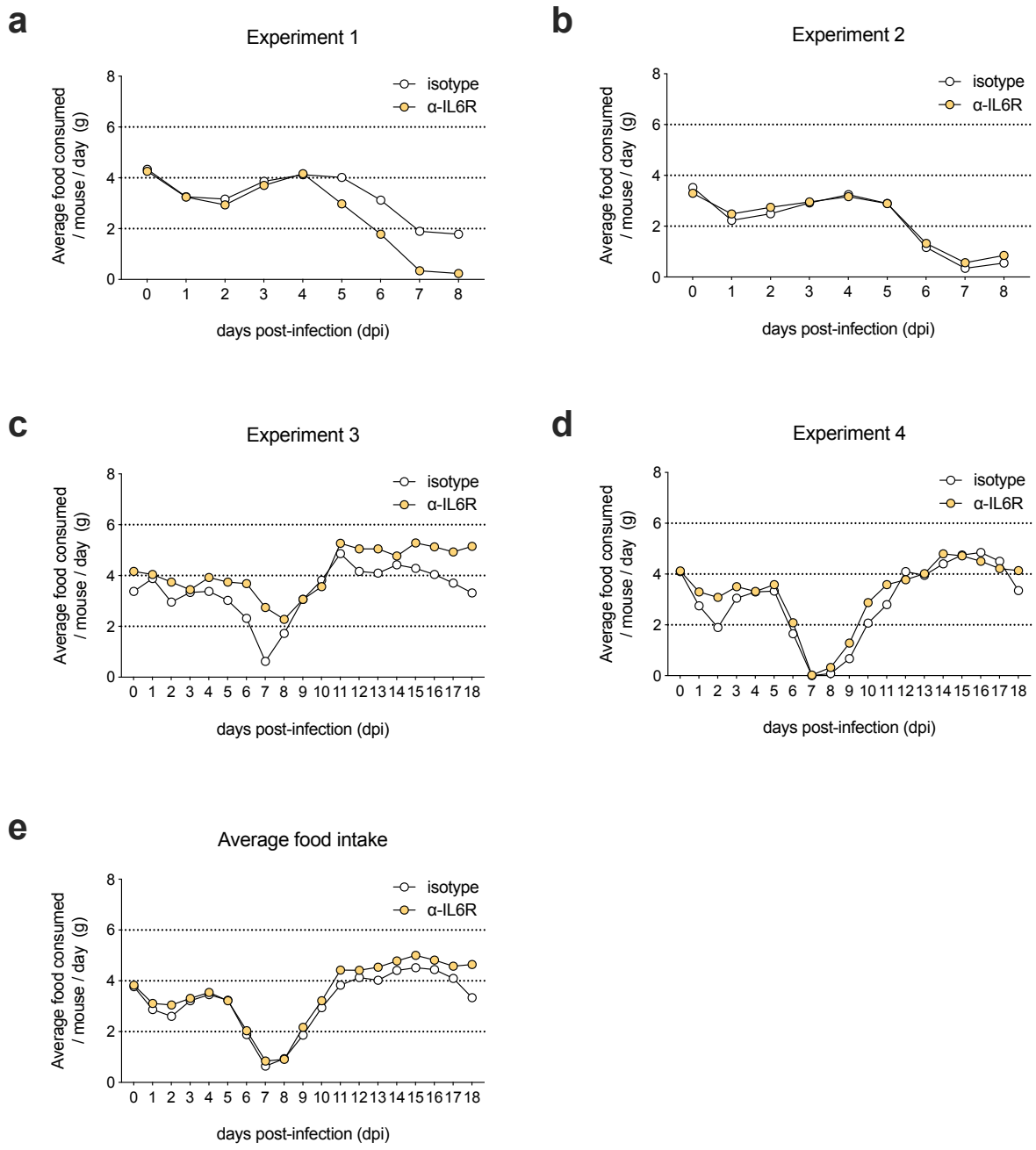

Figure 5-5 Food intake of elderly mice during RSV infection after IL-6R blockade

Food intake in grams of food consumed by each mouse per day (on average). Elderly mice were given α-IL-6R antibody or isotype control antibody intraperitoneally one day before RSV infection and every five days, and euthanised either 8 days or 18 days after infection. Two experiments each were conducted at a day 8 (**a.** and **b.**) and a day 18 (**c.** and **d.**) time point, n=2-10. **e.** All four experiments pooled.

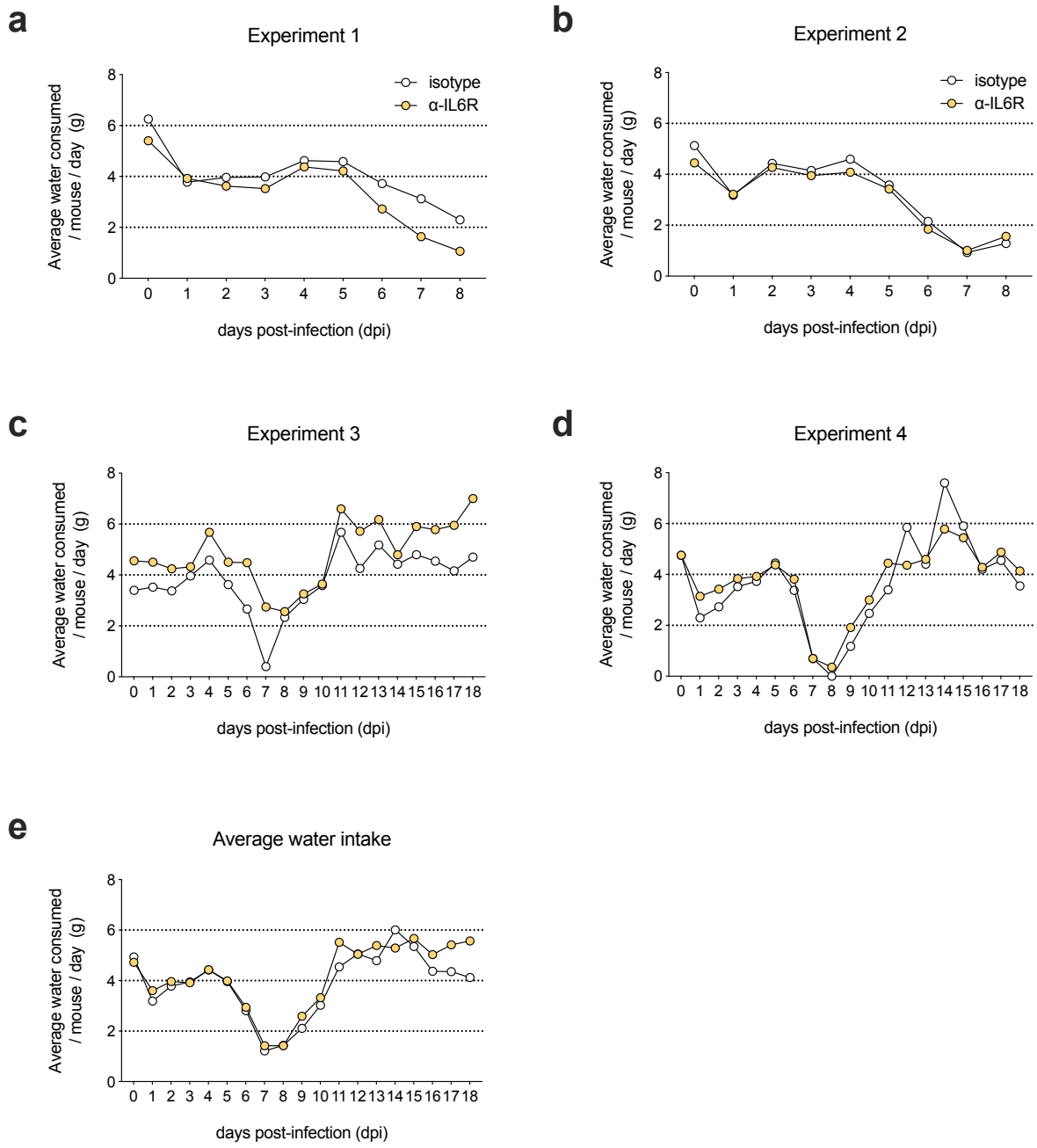

Figure 5-6 Water intake of elderly mice during RSV infection after IL-6R blockade

Water intake in grams of water consumed by each mouse per day (on average). Elderly mice were given α-IL-6R antibody or isotype control antibody intraperitoneally one day before RSV infection and every five days, and euthanised either 8 days or 18 days after infection. Two experiments each were conducted at a day 8 (**a.** and **b.**) and a day 18 (**c.** and **d.**) time point, n=2-10. **e.** All four experiments pooled.

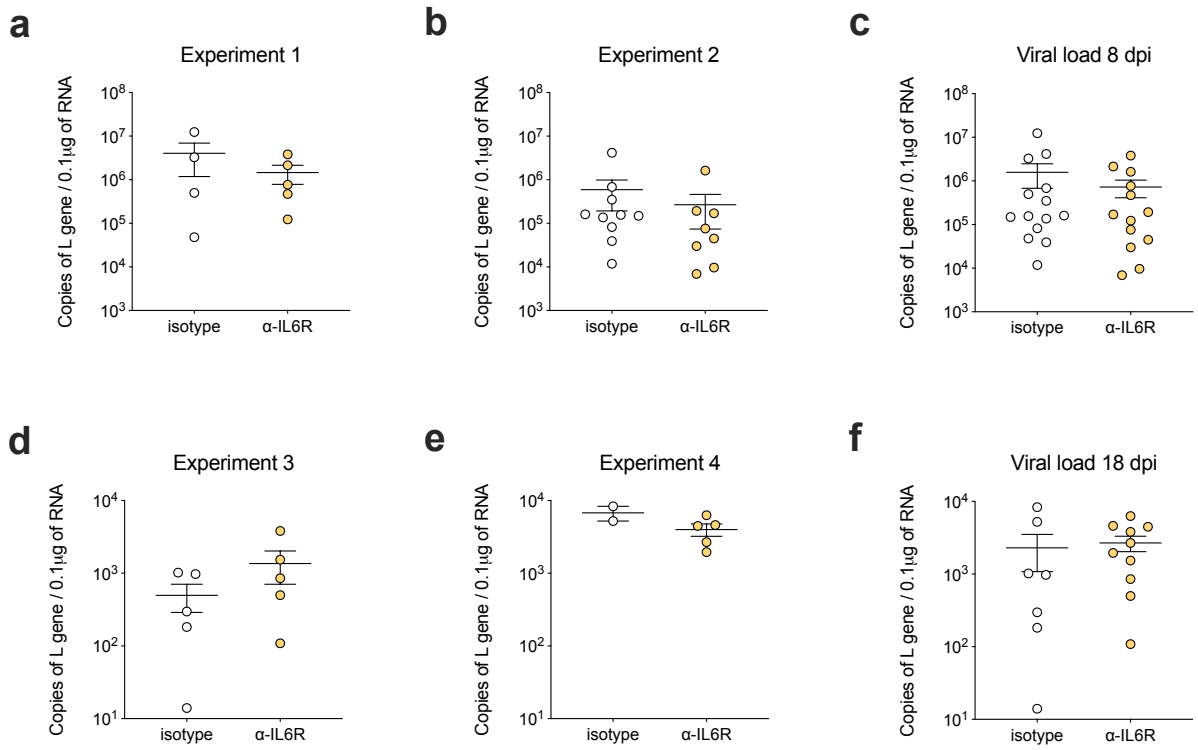

Figure 5-7 RSV viral load during IL-6R blockade

RSV viral load expressed as copies of RSV L gene detected per ug of RNA extracted from lung tissue. Open circles: Mice given isotype control antibody. Yellow filled circles: Mice given α-IL-6R antibody. **a.-c.** RSV infection over 8 days. **d.-f.** RSV infection over 18 days, n=2-10. **c.** and **f.** represent pooled data from **a. + b.** and **d. + e.**, respectively.

isotype-treated mice at day 7, at the peak of weight loss (Figure 5-3c). The shape of the weight loss curve was not changed, i.e. mice did not lose weight less rapidly or recover weight quicker. Instead, the entire weight loss curve appeared to be shifted upwards (less weight loss) in the αIL-6R-treated mice. By contrast, in one of the two experiments concluded at day 8 post-infection, Experiment 2, there was no significant difference in weight loss between the groups, and in the other, Experiment 1, mice treated with αIL-6R antibody lost significantly *more* weight at day 8 than the isotype-treated mice (Figure 5-3a,b). When these four experiments were pooled together, there was no statistical difference in weight loss between mice treated with αIL-6R antibody and mice treated with isotype control antibody (Figure 5-3e). When weight loss was quantified as Area Under

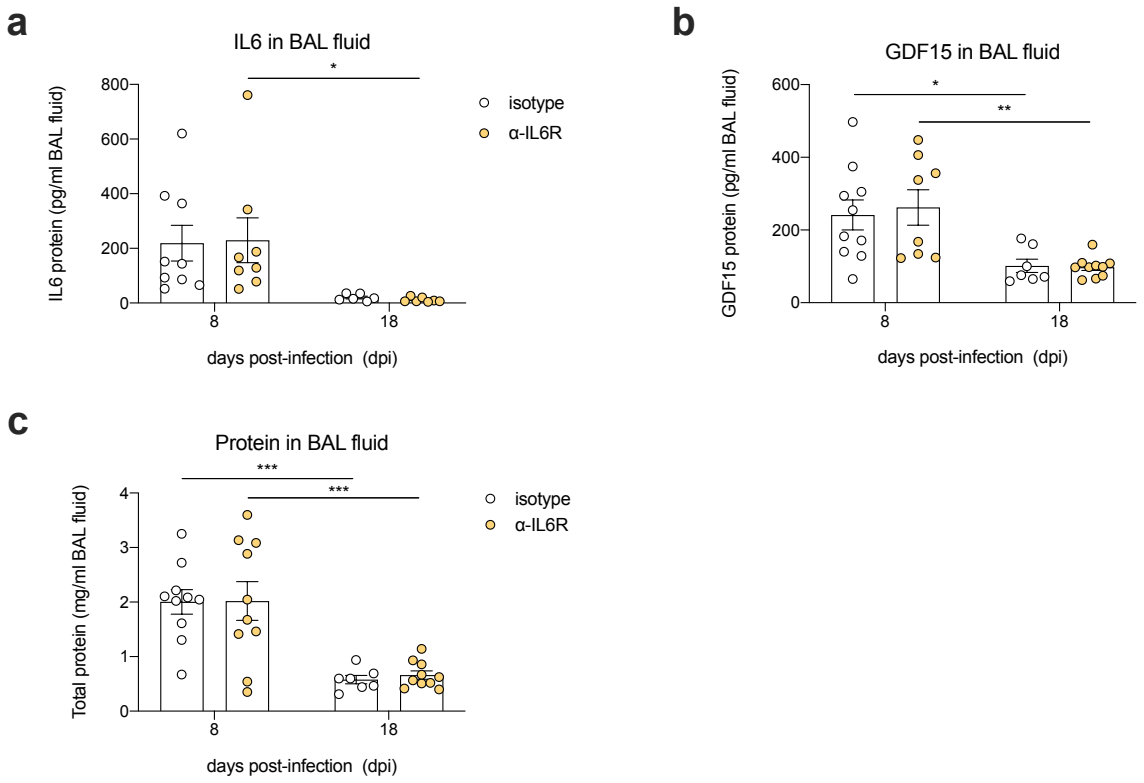

Figure 5-8 Airway cytokines and total protein during IL-6R blockade in RSV infection

Cytokine levels were assayed using ELISA. Total protein content was assessed by Bradford assay. Pooled from two independent experiments for each time point at n=2-5. Open circles: Mice given isotype control antibody. Yellow filled circles: Mice given α-IL-6R antibody. **a.** IL-6 protein in BAL fluid. **b.** GDF-15 in BAL fluid. **c.** Total protein content in BAL fluid.

the Curve (AUC), the antibody treatment also did not cause significant differences (Figure 5-4).

5.3.3. Blocking IL-6R does not affect appetite during RSV infection

Food and water intake largely followed the weight loss phenotype of the individual experiment. In Experiment 1, where αIL-6R-treated mice lost more weight than isotype-treated mice, they likewise tended to consume less food and water (Figure 5-5a, Figure 5-6a). In Experiment 2, where there was no differential weight loss between the groups, food and water intake were not different between groups (Figure 5-5b, Figure 5-6b). In Experiment 3, where IL-6R blockade led to lower weight loss, food and water intake tended to be higher in that group (Figure 5-5c, Figure 5-6c). In the final experiment, where there was

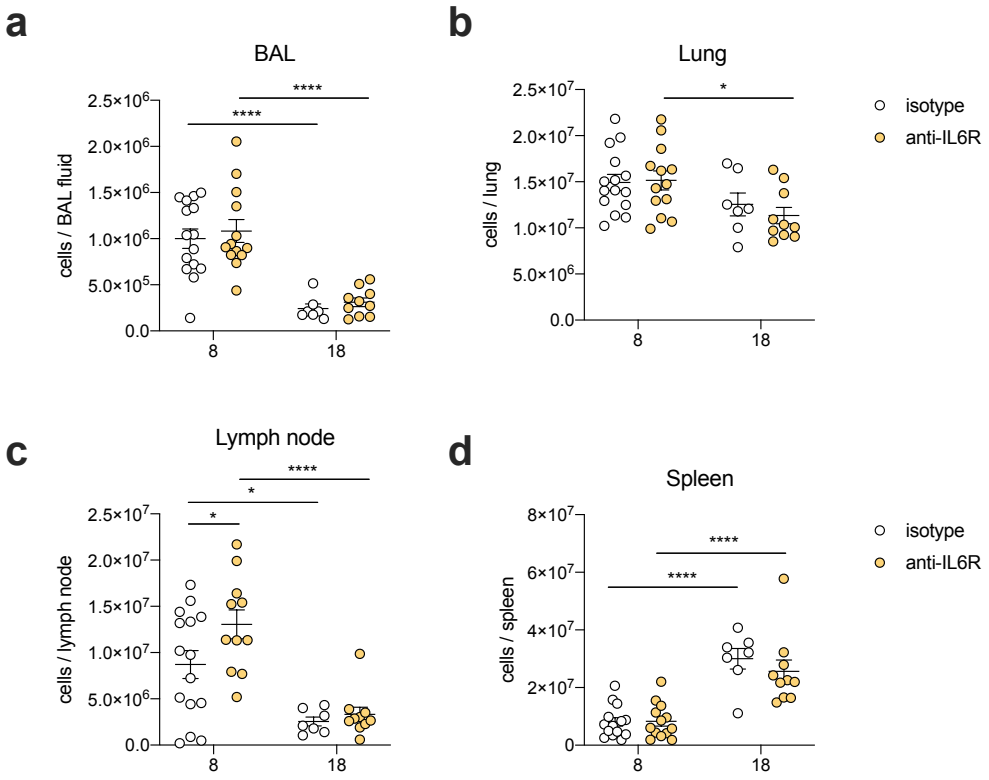

Figure 5-9 Total cell count in airways, lung, lung-draining lymph node and spleen of elderly mice during IL-6R blockade in RSV infection

Elderly mice were injected with isotype control antibody (open circles) or α-IL-6R antibody (yellow filled circles) one day before RSV infection and every five days. Tissues were harvested either 8 days or 18 days after RSV infection. Pooled from two independent experiments for each time point at n=2-10. **a.** Live cells in bronchoalveolar lavage (BAL) fluid. **b.** Live cells in homogenised lung tissue. **c.** Live cells in homogenised lung-draining lymph node. **d.** Live cells in homogenised spleen tissue.

a non-significant trend towards IL-6R blockade to reduce weight loss during RSV infection, there was no difference in food or water intake between groups (Figure 5-5d, Figure 5-6d). When pooled, these results suggested that IL-6R blockade did not affect food or water consumption of elderly mice during RSV infection (Figure 5-5e, Figure 5-6e).

5.3.4. Blocking IL-6R does not affect RSV viral load in elderly mice

The copy number of RSV L gene in lung tissue was not significantly different between mice treated with isotype antibody and mice treated with αIL-6R antibody in any experiment (Figure 5-7). There may have been a trend towards lower viral load in αIL-6R-treated mice 8 days after RSV infection, but this was not statistically significant (Figure 5-7c).

5.3.5. Lung inflammation is unchanged by IL-6R blockade during RSV infection

So far, IL-6R blockade in elderly mice during RSV infection had not yielded a consistent phenotype in terms of either enhancing or reducing inflammation. Levels of total protein and of IL-6 protein were measured in BAL fluid. Elderly mice were previously found to have very high levels of total protein and of IL-6 in their BAL fluid, a sign of high RSV-induced inflammation. Levels of IL-6 in BAL fluid were not different between αIL-6R-treated mice and isotype-treated mice at either 8 or 18 days after RSV infection (Figure 5-8a,c). IL-6 protein and total BAL fluid protein decreased significantly in αIL-6R-treated mice between day 8 and day 18 (Figure 5-8a,c). Total BAL fluid protein also decreased significantly in isotype-treated mice between day 8 and day 18 (Figure 5-8c). Since GDF-15 was implicated in the reaction of elderly mice to RSV infection in the previous chapter, GDF-15 protein was measured in BAL fluid. GDF-15 protein levels were no different between αIL-6R-treated mice and isotype-treated mice at either 8 or 18 days after RSV infection, but levels were significantly higher in both groups at day 8 compared to day 18 (Figure 5-8b).

5.3.6. Cellular infiltration of lung-draining lymph nodes may be enhanced by IL-6R blockade

Inflammation caused by RSV infection was further quantified by measuring the cellular infiltration of BAL fluid and lung tissue – the location of infection – and additionally in lung-draining lymph nodes and spleen tissue. The spleen and lymph nodes are secondary lymphoid tissues where the germinal centre response to RSV is likely to take place. IL-6 is an important cytokine to the germinal centre response, contributing to the differentiation and maintenance of germinal centre cells such as Tfh cells. It was hypothesised that blocking IL-6 signalling may inhibit the germinal centre responses of elderly mice. Total cell numbers in BAL fluid did not differ between isotype-treated and αIL-6R-treated mice at either 8 or 18 days after RSV infection, but cell numbers decreased significantly in both groups between day 8 and day 18 (Figure 5-9a). Total cell numbers in homogenised lung tissue also did not differ between isotype-treated and αIL-6R-treated mice at either 8 or

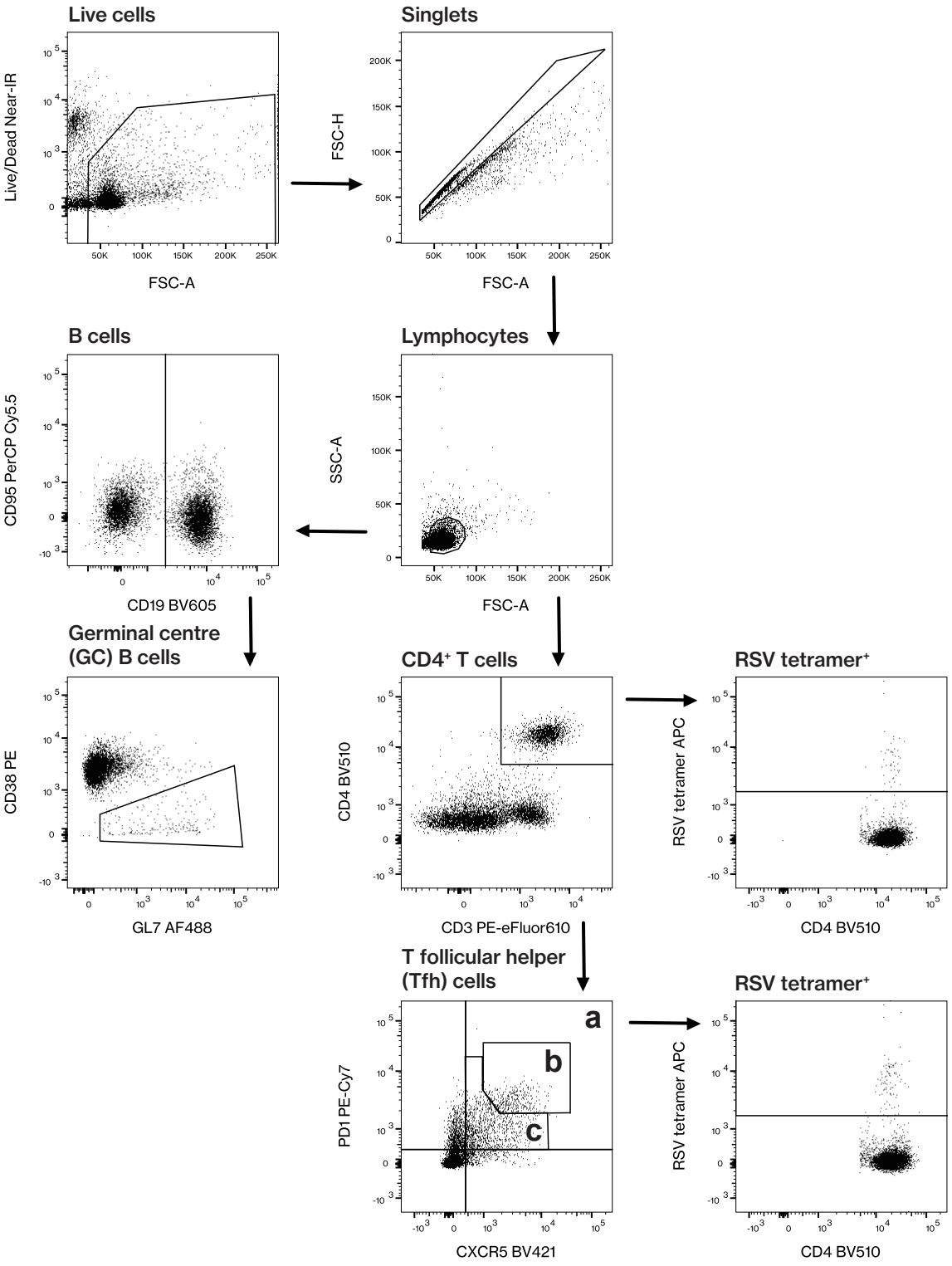

Figure 5-10 Gating strategy for immune response to RSV during IL-6R blockade

Gating strategy shown as an example on a lymph node sample from an elderly mouse at 18 dpi. Lymph node and spleen cells were gated to remove debris and dead cells using Live/Dead fixable cell stain. Single cells were defined using forward scatter area and forward scatter height. Lymphocytes were identified using forward and side scatter area. Lymphocytes were gated for B cells ($CD19^+$) and $CD4^+$ T cells ($CD3^+$ $CD4^+$). RSV specificity of $CD4^+$ T cells was determined with an MHC class II tetramer. Germinal centre B cells were defined as $GL7^+$ and $CD38^{lo}$. **a.** All T follicular helper (Tfh) cells ($CXCR5^+$ $PD1^+$ $CD4^+$ T cells). **b.** "High" Tfh cells staining strongly for CXCR5 and PD1. **c.** "Low" Tfh cells staining less strongly for CXCR5 and PD1.

18 days after RSV infection, and cell numbers decreased significantly in αIL-6R-treated mice between day 8 and day 18 (Figure 5-9b). But αIL-6R-treated mice had significantly more cells in their lymph nodes at the 8 day time point compared to isotype-treated mice (Figure 5-9c). Lymph node cell numbers decreased significantly in both groups between day 8 and day 18. There was no significant difference in the number of spleen cells between isotype-treated and αIL-6R-treated mice at time point, but there was a significant increase in spleen cell numbers from day 8 to day 18 in both groups (Figure 5-9d). This may suggest the formation of a germinal centre response.

5.3.7. IL-6R blockade and the germinal centre response to RSV in elderly mice

Multicolour flow cytometry experiments were employed to identify general immune cell populations and the germinal centre response in lung-draining lymph nodes and spleen tissue. Figure 5-10 shows the gating strategy used. Cells from homogenised spleen tissue and from lung-draining lymph nodes were stained for surface markers of B cells, including germinal centre B cells, and $CD4^+$,T cells, and T follicular helper cells. Lymphocytes were defined as live (Live/Dead Near-IR^-), single cells that had characteristically low forward and side scatter. Germinal centre B cells were defined as $GL7^+$ $CD38^{lo}$ $CD19^+$ lymphocytes. $CD4^+$ T cells were defined as $CD4^+$ $CD3^+$ lymphocytes. T follicular helper (Tfh) cells were defined as PD-1^+ $CXCR5^+$ $CD4^+$ T cells. Tfh cells were further divided into Tfh “low” and Tfh “high” populations depending on the intensity of their staining for PD-1 and CXCR5. Cells were additionally stained with an MHC class II tetramer displaying an RSV peptide to determine RSV specificity of the $CD4^+$ T cell response. Positive staining of $CD4^+$ T cells with the RSV tetramer was determined by comparison to staining with a control tetramer that was ligated to the same fluorophore but loaded with CLIP, a fragment of the MHC class II invariant chain that should not be bound. B cells were defined as $CD19^+$ lymphocytes. Germinal centre (GC) B cells were defined as $GL7^+$ $CD38^{lo}$ $CD19^+$ cells.

There was no difference between the two antibody treatment groups in the proportion of lymphocytes out of live single cells at either time point in either the lymph nodes or

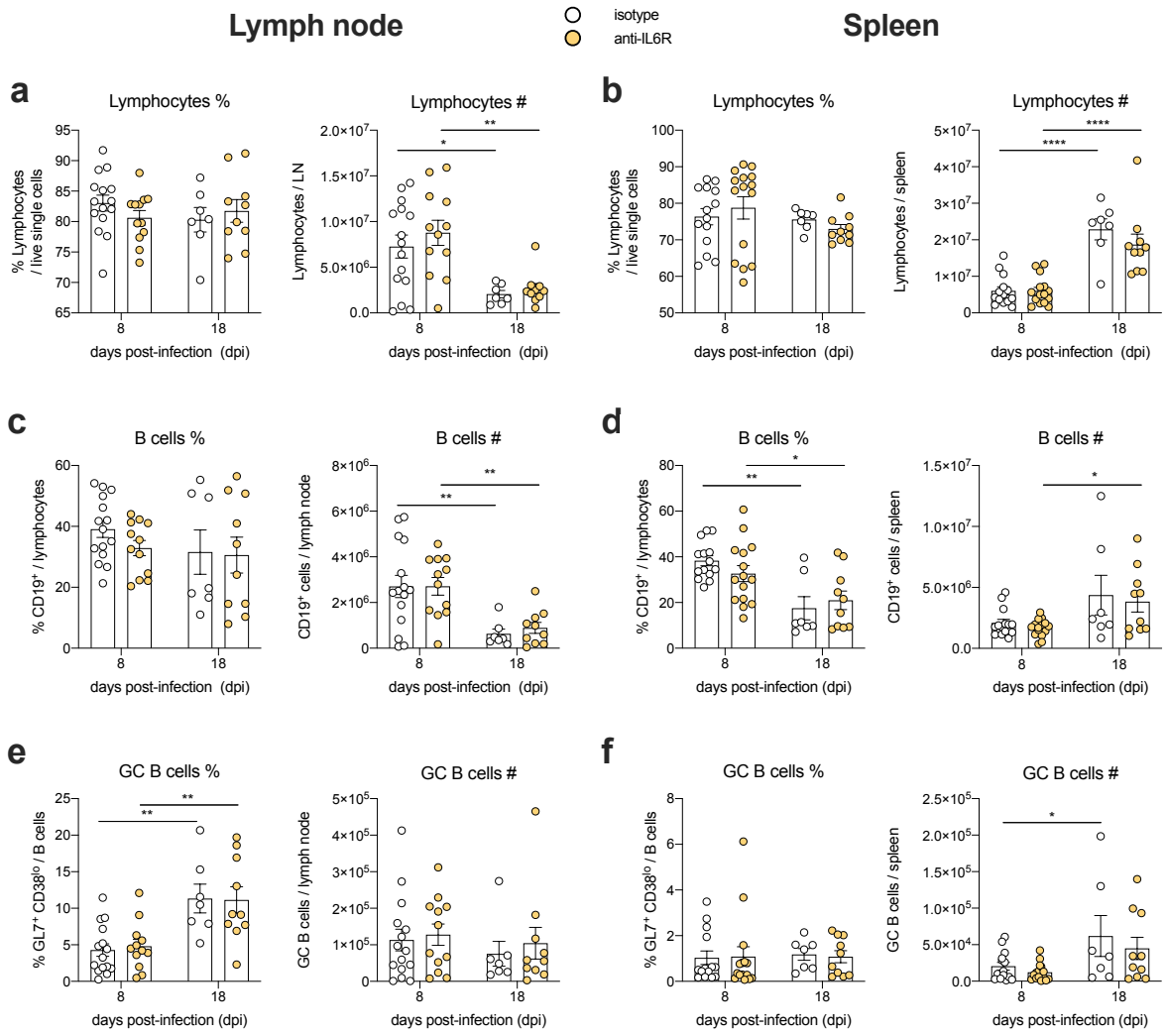

Figure 5-11 The effect of IL-6R blockade on B cell responses to RSV in elderly mice

Immune cell populations in lymph node or spleen tissue of elderly mice after 8 or 18 days of RSV infection, treated with either isotype control antibody or α-IL-6R antibody. Left panels: proportion of population out of parent population. Right panels: Total number of cells of the given population in tissue. Pooled from four experiments, n=2-10. **a.+b.** Lymphocytes. **c.+d.** B cells. **e.+f.** Germinal centre (GC) B cells. Two-way ANOVA with Bonferroni's multiple comparison test. **a.,c.,e.** Populations in lymph nodes. **b.,d.,f.** Populations in spleen cells.

the spleen (Figure 5-11a,b). However, when expressed as total cell numbers, there were significantly more lymphocytes in the lymph nodes in both groups at day 8 compared to day 18. On the other hand, total lymphocyte numbers increased from day 8 to day 18 in spleen in both groups (Figure 5-11a,b). The proportion of B cells out of lymphocytes was not different between isotype and αIL-6R-treated mice in lymph nodes, and no different between the two time points (Figure 5-11c). Total B cell numbers in the lymph node

decreased significantly from day 8 to day 18 in both groups (Figure 5-11c). In spleen cells, the proportion of B cells out of lymphocytes decreased significantly in both groups from day 8 to day 18 (Figure 5-11d). In terms of total cell numbers, B cells increased significantly from day 8 to day 18 in αIL-6R-treated mice (Figure 5-11d). The frequency of germinal centre (GC) B cells increased significantly between day 8 and day 18 in both groups in the lymph nodes, but total GC B cell numbers were not different between either the groups or the timepoints (Figure 5-11e). In the spleen, there was no difference in frequency of GC B cells between the two groups or the two time points tested, but the total number of GC B cells increased from day 8 to day 18 in isotype-treated mice (Figure 5-11f). Both the frequency and total abundance of $CD4^+$ T cells decreased from day 8 to day 18 in the lymph nodes of both isotype- and αIL-6R-treated mice (Figure 5-12a). In spleen cells, the frequency of $CD4^+$ T cells decreased between day 8 and day 18 in both groups, but the total number of $CD4^+$ T cells was no different between either the two time points or the two groups (Figure 5-12b). There was no difference in the frequency of RSV $tetramer^+$ $CD4^+$ T cells between the groups or time points in either lymph nodes or spleen cells except that in the lymph nodes of both isotype and αIL-6R-treated mice, there were significantly more $tetramer^+$ $CD4^+$ T cells at day 8 compared to day 18. (Figure 5-12c,d). There was a trend for lower frequency and abundance of RSV $tetramer^+$ cells in αIL-6R-treated mice at day 8 in both lymph node and spleen. This was statistically significant in one of the experiments (Experiment 2, no differential weight loss). The frequency of Tfh cells increased in the lymph nodes of isotype-treated mice from day 8 to day 18, and was significantly higher than the frequency of Tfh cells in αIL-6R-treated mice at day 18 (Figure 5-12e). However, total Tfh numbers were not different. Total Tfh cell numbers decreased significantly from day 8 to day 18 in both groups. The frequency and abundance of Tfh cells in spleen tissue was unchanged by either time point or antibody treatment (Figure 5-12f). The proportion of RSV $tetramer^+$ Tfh cells in lymph nodes decreased significantly from day 8 to day 18 in isotype-treated mice (Figure 5-12g). The total number of $tetramer^+$ Tfh cells decreased from day 8 to day 18 in both antibody-treated groups.

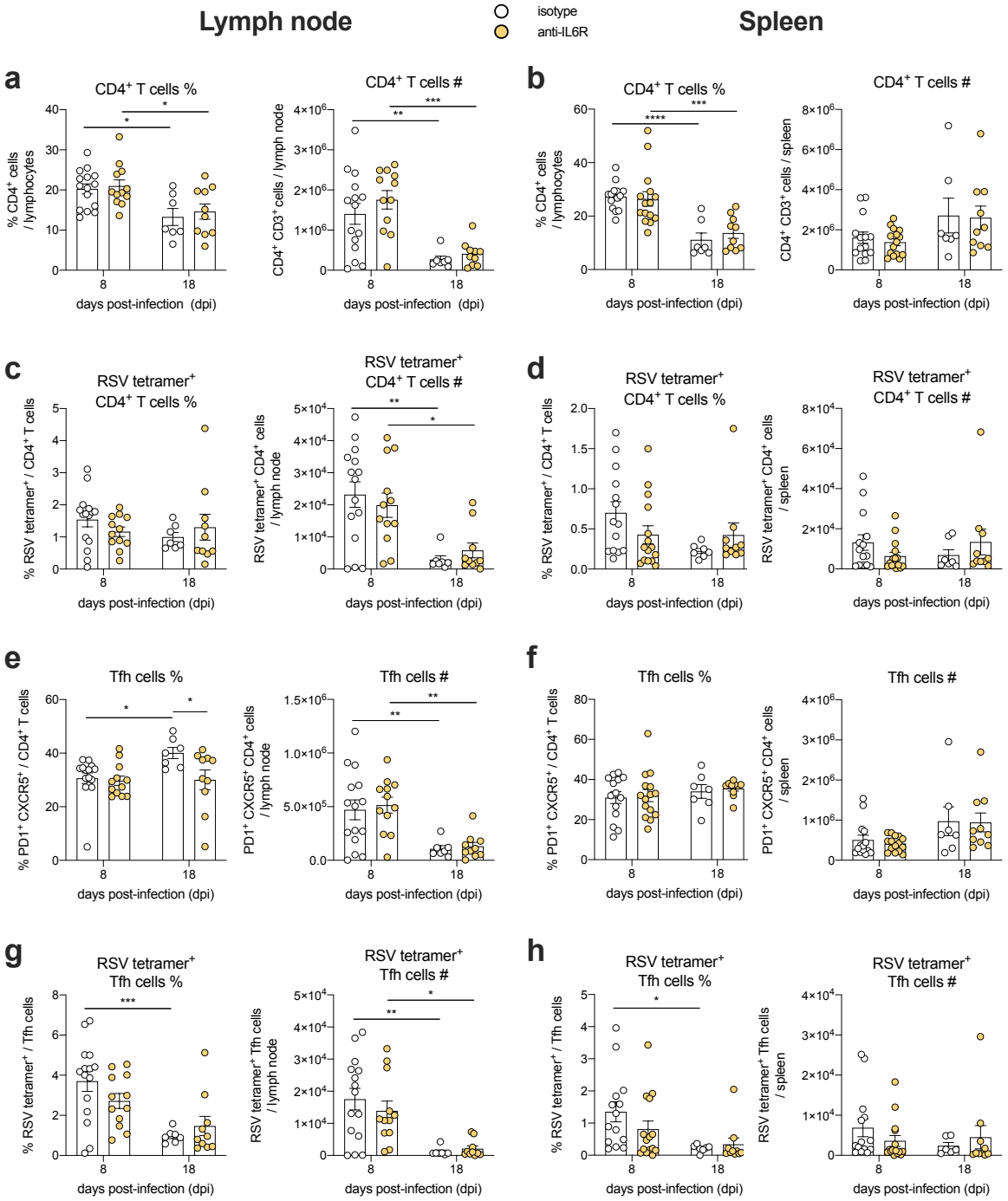

Figure 5-12 The effect of IL-6R blockade on T cell responses to RSV in elderly mice

Immune cell populations in lymph node or spleen tissue of elderly mice after 8 or 18 days of RSV infection, treated with either isotype control antibody or α-IL-6R antibody. Left panels: proportion of population out of parent population. Right panels: Total number of cells of the given population in tissue. Pooled from four independent experiments (two per time point), n=2-10. **a.+b.** $CD4^+$ T cells. **c.+d.** RSV $tetramer^+$ $CD4^+$ T cells. **e.+f.** T follicular helper (Tfh) cells. **g.+h.** RSV $tetramer^+$ Tfh cells. **a.,c.,e.,g.** Populations in lymph nodes. **b.,d.,f.,h.** Populations in spleen cells. Two-way ANOVA with Bonferroni's multiple comparison test.

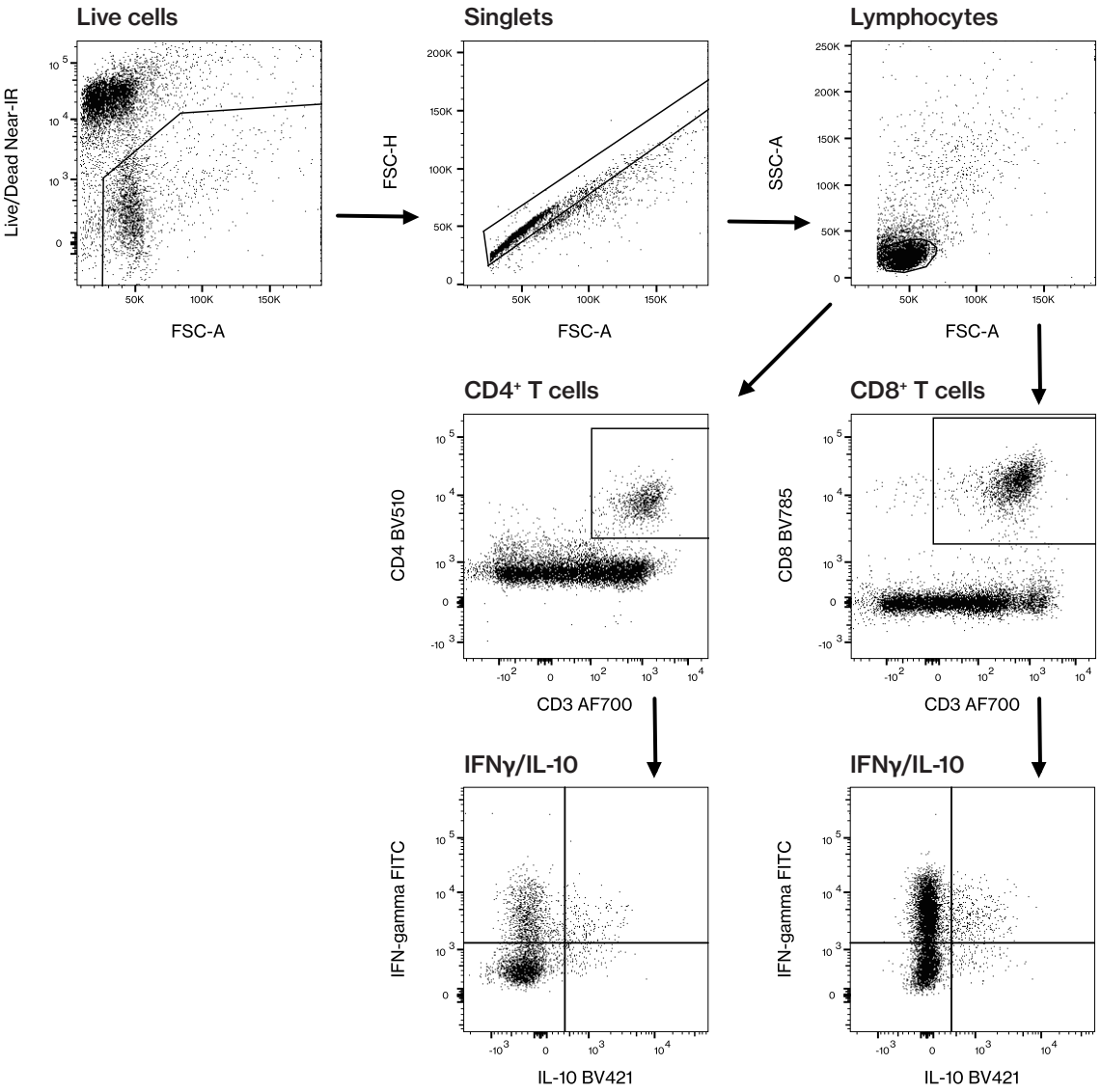

Figure 5-13 Gating strategy for intracellular cytokine response in RSV during IL-6R blockade

Lung cells and BAL fluid cells were harvested from elderly mice treated with either isotype control antibody or α-IL-6R antibody after 8 or 18 days of RSV infection. The production of IFNγ and IL-10 by $CD4^+$ and $CD8^+$ T cells was determined by intracellular cytokine staining. Lung and BAL fluid cells were gated to remove debris and dead cells using Live/Dead fixable cell stain. Single cells were defined using forward scatter area and forward scatter height. Lymphocytes were identified using forward and side scatter area. Lymphocytes were gated for $CD4^+$ T cells ($CD3^+$ $CD4^+$) and $CD8^+$ T cells ($CD3^+$ $CD8^+$). $CD4^+$ and $CD8^+$ T cells were gated for IFNγ and IL-10 production using unstimulated controls and fluorescence-minus-one controls (not shown).

In spleen tissue, the proportion of RSV tetramer$^+$ Tfh cells decreased significantly from day 8 to day 18 in isotype-treated mice, but total abundance was not different in either group or either time point (Figure 5-12h). Like among $CD4^+$ T cells, there was a trend

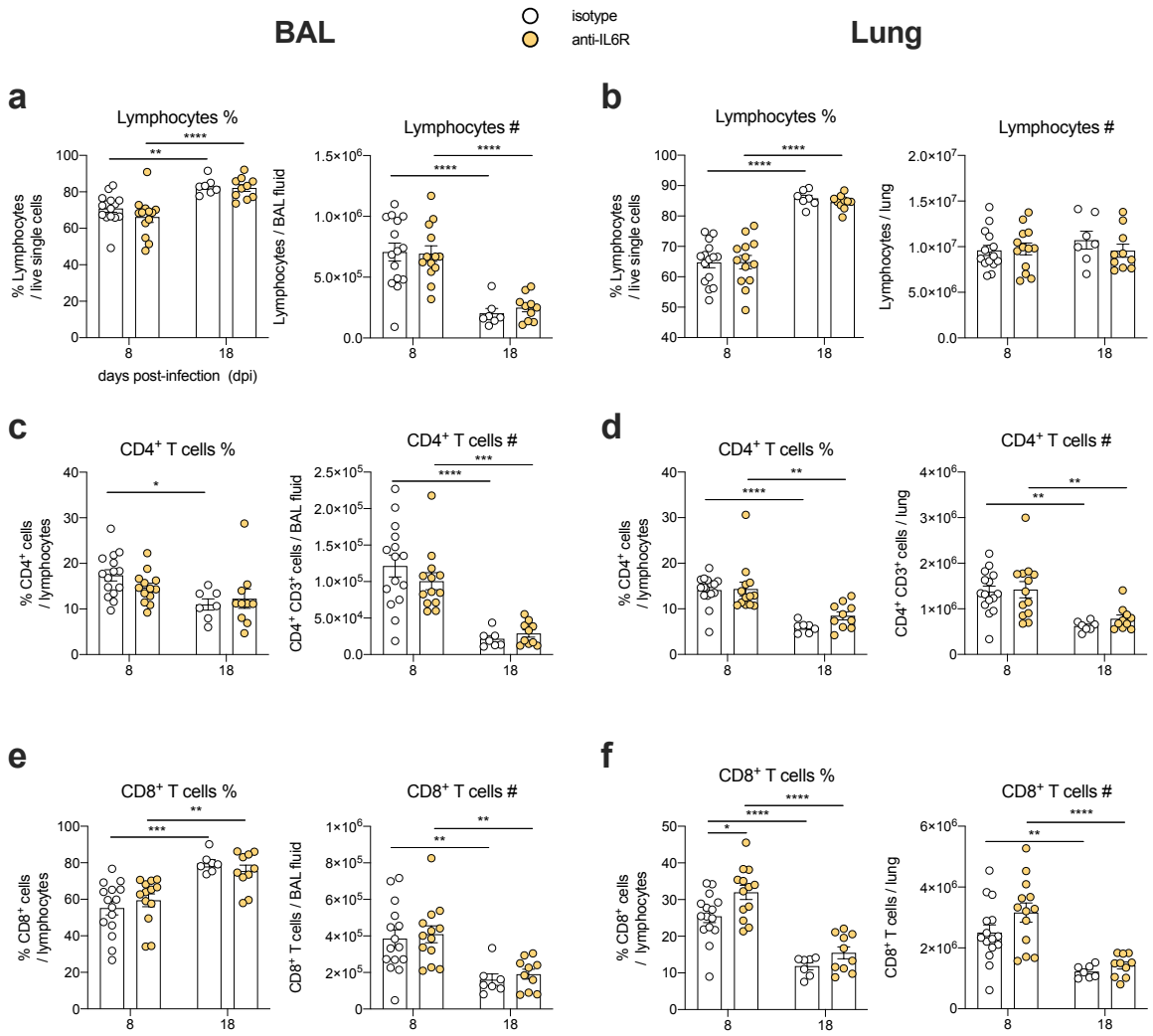

Figure 5-14 Immune cell populations in lung and airways during IL-6R blockade in RSV infection

Immune cell populations in lung cells or BAL fluid cells of elderly mice treated with either isotype control antibody or α-IL-6R antibody, after 8 or 18 days of RSV infection. Populations were gated according to Figure 5-13 Left panels: proportion of population out of parent population. Right panels: Total number of cells of the given population in tissue. Pooled from four independent experiments (two per time point), n=2-10. **a.+b.** Lymphocytes. **c.+d.** CD4⁺ T cells. **e.+f.** CD8⁺ T cells. **a.,c.,e.** Populations in BAL fluid cells. **b.,d.,f.** Populations in lung cells. Two-way ANOVA with Bonferroni's multiple comparison test.

towards lower frequency and abundance of RSV tetramer⁺ Tfh cells in the lymph nodes and spleen cells of the αIL-6R-treated mice, which reached statistical significance in one experiment when analysed separately (not shown). When pooled, there was no statistically significant difference in the frequency or abundance of any cell type between the two antibody-treated groups, except for a reduced frequency of Tfh cells in the lymph

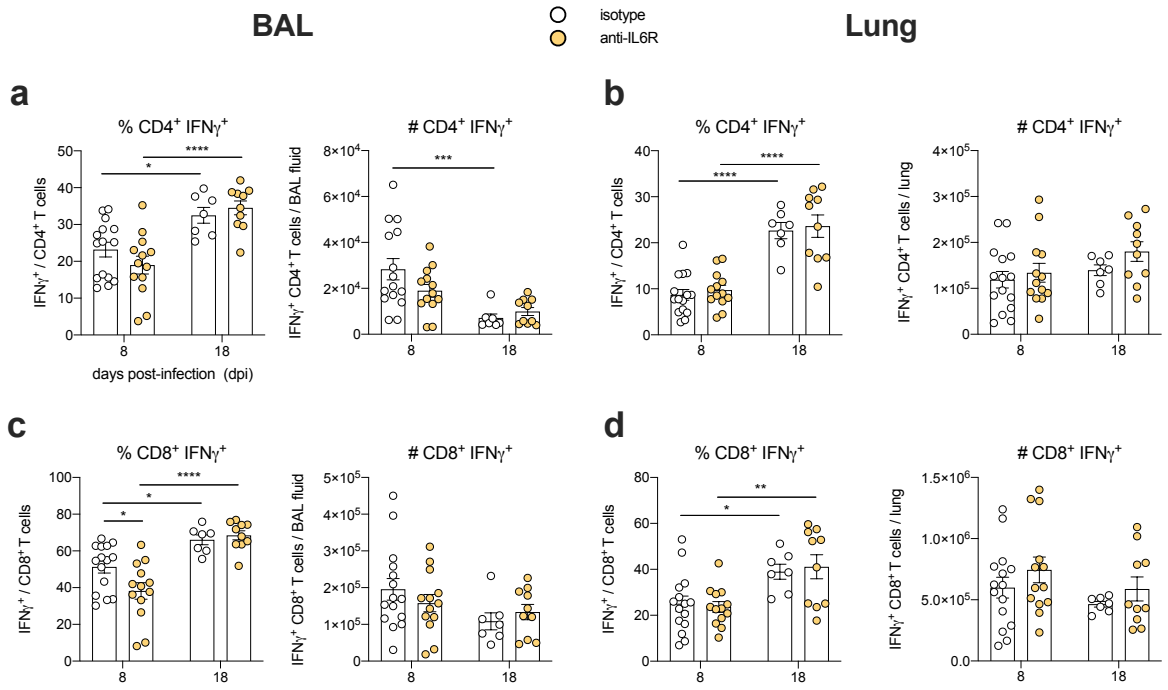

Figure 5-15 IFNγ production by immune cells in RSV during IL-6R blockade

Lung cells and BAL fluid cells were harvested from elderly mice treated with either isotype control antibody or α-IL-6R antibody after 8 or 18 days of RSV infection. Populations were gated according to Figure 5-13. Pooled from four independent experiments (two per time point), n=2-10. **a.,c.** Results from BAL fluid cells. **b.,d.** Results from lung cells. **a.-b.** CD4+ T cells. **c.-d.** CD8+ T cells. Left panels: proportion of population out of parent population. Right panels: Total number of cells of the given population in tissue. Two-way ANOVA with Bonferroni's multiple comparison test.

nodes of αIL-6R-treated mice after 18 days of RSV infection.

5.3.8. Intracellular cytokine production during IL-6R blockade in RSV infection

Intracellular cytokine staining was carried out to measure production of IFNγ and IL-10 by CD4+ and CD8+ T cells in BAL fluid and lungs. The gating strategy is shown in Figure 5-13. Live single-celled lymphocytes were gated as in Figure 5-10. CD4+ and CD8+ T cells were defined as CD3+ lymphocytes staining positive for CD4+ and CD8+, respectively. IFNγ and IL-10 gating was determined with unstimulated cells and fluorescence-minus-one controls (not shown). The proportion of lymphocytes out of live single cells increased in both antibody-treated groups from day 8 to day 18 in both BAL fluid cells and

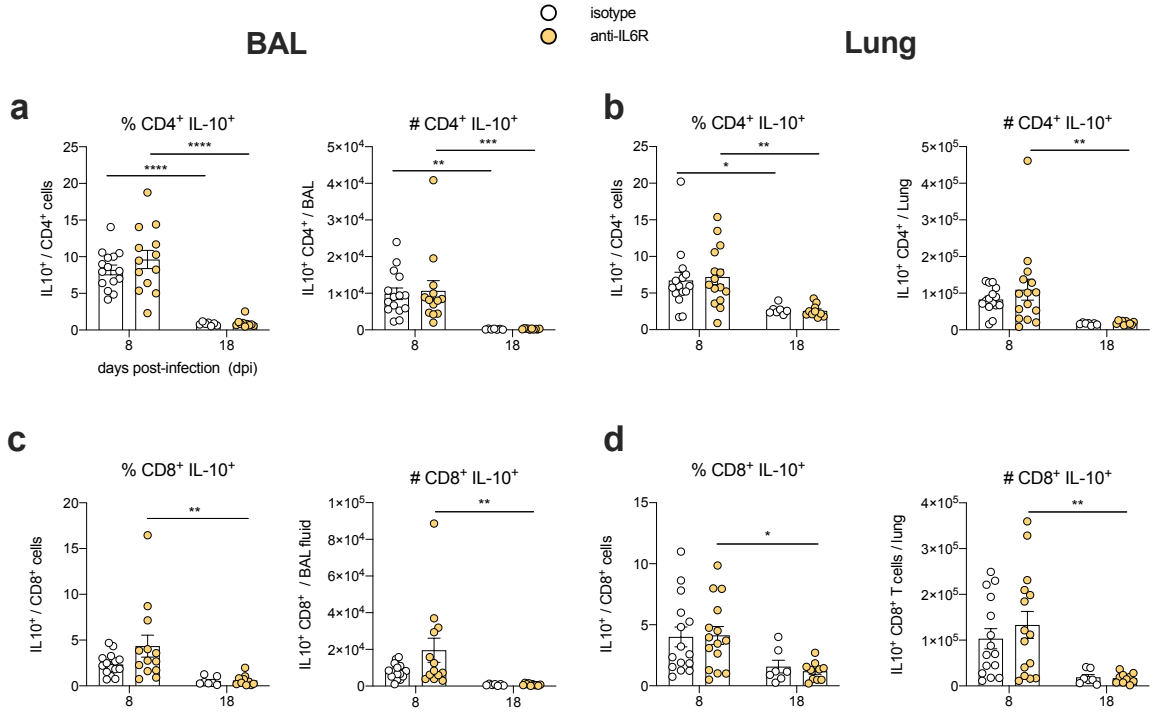

Figure 5-16 IL-10 production by immune cells in RSV during IL-6R blockade

Lung cells and BAL fluid cells were harvested from elderly mice treated with either isotype control antibody or α-IL-6R antibody after 8 or 18 days of RSV infection. Populations were gated according to Figure 5-13. Pooled from four independent experiments (two per time point), n=2-10. **a.,c.** Results from BAL fluid cells. **b.,d.** Results from lung cells. **a.-b.** CD4+ T cells. **c.-d.** CD8+ T cells. Left panels: proportion of population out of parent population. Right panels: Total number of cells of the given population in tissue. Two-way ANOVA with Bonferroni's multiple comparison test.

lung cells (Figure 5-14a,b). The total number of lymphocytes was not different between groups or time points in lung tissue, whereas it fell between day 8 and day 18 in both groups. This may be expected since day 8 represents the peak of inflammation when there is high recruitment of immune cells into the airways. CD4+ T cells as a proportion of lymphocytes in the BAL fluid decreased in isotype-treated mice from day 8 to day 18 (Figure 5-14c). The total number of CD4+ T cells in BAL fluid decreased significantly in both groups from day 8 to day 18. The frequency and abundance of CD4+ T cells among lung tissue cells decreased significantly in both groups from day 8 to 18, but there was no difference between the two groups (Figure 5-14d). The frequency of CD8+ T cells in BAL fluid cells increased in both groups between day 8 and day 18, but the total number of CD8+ T cells decreased in both groups between day 8 and day 18 (Figure 5-14e). At

day 8, a higher proportion of lymphocytes in the lung tissue of αIL-6R-treated mice were $CD8^+$ T cells compared to isotype-treated mice (Figure 5-14f). The frequency and abundance of $CD8^+$ T cells in lung tissue decreased in both groups between day 8 and day 18.

The frequency of $IFN\gamma^+$ $CD4^+$ T cells increased in both groups from day 8 to day 18 in both BAL fluid cells and lung cells (Figure 5-15a,b). The total number of $IFN\gamma^+$ $CD4^+$ T cells decreased significantly in the BAL fluid of isotype-treated mice from day 8 to day 18 (Figure 5-15a). The total number of $IFN\gamma^+$ $CD4^+$ T cells in lung tissue was unchanged by time point or antibody treatment (Figure 5-15b). A lower proportion of $CD8^+$ T cells in the BAL fluid of αIL-6R-treated mice were $IFN\gamma^+$ compared to isotype-treated mice (Figure 5-15c). This almost reached statistical significance when expressed as cell numbers. The proportion of $IFN\gamma^+$ $CD8^+$ T cells increased from day 8 to day 18 in both groups in both BAL cells and lung tissue (Figure 5-15c,d). Total abundance of $CD8^+$ $IFN\gamma^+$ T cells was not significantly different with either antibody treatment or time point of infection in either BAL cells or lung tissue.

The frequency and abundance of IL-10^+ $CD4^+$ T cells decreased in both groups between day 8 and day 18 in BAL fluid and lung tissue (Figure 5-16a,b). The total abundance of IL-10^+ $CD4^+$ T cells also decreased in both groups from day 8 to day 18 in BAL fluid, and in αIL-6R-treated mice in lung tissue. The frequency and abundance of IL-10^+ $CD8^+$ T cells decreased significantly between day 8 and day 18 in αIL-6R-treated mice in both BAL fluid and lung tissue (Figure 5-16c,d). There was a small trend towards higher frequency and abundance of IL-10^+ $CD8^+$ T cells in αIL-6R-treated mice at day 8 post-infection in BAL fluid and lung cells.

When analysed separately, in one of the day 8 experiments (Experiment 2, no differential weight loss), a significantly higher proportion of BAL $CD8^+$ T cells from αIL-6R-treated mice were IL-10^+ and a significantly lower proportion of the same cells were $IFN\gamma^+$ (not shown). This almost reached statistical significance when expressed as total cell numbers. BAL $CD4^+$ cells from αIL-6R-treated mice were also more frequently IL-10^+ in this

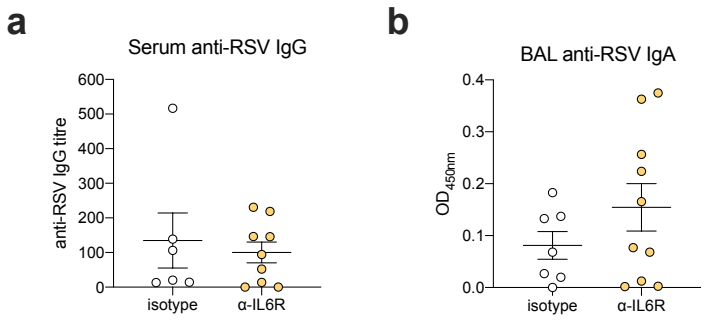

Figure 5-17 RSV-specific antibody response during IL-6R blockade

a. RSV-specific IgG titres in serum of elderly mice 18 days after RSV infection treated with either anti-IL-6R antibody or isotype antibody were calculated from dilution curves. Pooled from two independent experiments, n=1-5 **b.** RSV-specific IgA in BAL fluid of elderly mice 18 days after RSV infection treated with either anti-IL-6R antibody or isotype antibody. BAL fluid was coated neat and the OD was read at 450 nm.

experiment. This trend towards $CD8^+$ T cells in the BAL fluid of αIL-6R-treated mice producing less IFNγ and more IL-10 could be a sign of a less inflammatory response when blocking IL-6 signalling. However, in the experiment in which these differences were most pronounced, these differences did not translate into differences in weight loss.

5.3.9. Blocking IL-6R does not affect RSV IgG or IgA response in the elderly

IL-6 is a key cytokine for the generation of a germinal centre response. This then leads to the production of high-affinity immunoglobulins. Blocking IL-6 signalling may lead to lower levels of RSV-specific antibodies. RSV-specific IgG was measured in serum and RSV-specific IgA was measured in the BAL fluid of elderly mice treated with either αIL-6R antibody or isotype antibody after 18 days of RSV infection. RSV-specific serum IgG and BAL IgA levels were not different between isotype and αIL-6R-treated mice (Figure 5-17). There was a non-significant trend towards higher levels of RSV-specific IgA in the BAL fluid of αIL-6R-treated mice, but the spread of the data was very broad.

To summarise at this point, IL-6R blockade did not appear to strongly impact the immune response to RSV. Weight loss from RSV infection was very variable, and RSV viral load was not different between isotype- and αIL-6R-treated groups. There was a small signif-

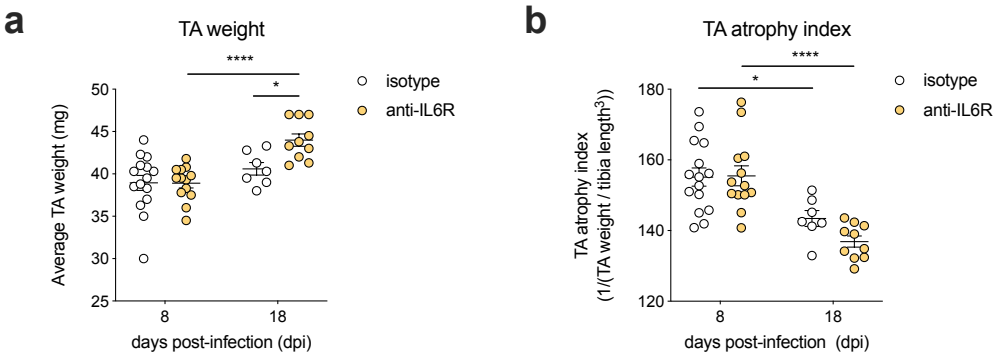

Figure 5-18 Gross and relative skeletal muscle mass during IL-6R blockade

a. Tibialis anterior (TA) muscle weight of elderly mice treated with either isotype control antibody or α-IL-6R antibody 8 or 18 days after RSV infection (average of both legs per mouse). **b.** TA atrophy index. Pooled from two independent experiments at n=4-10. Student's unpaired two-tailed t test. Two-way ANOVA with Bonferroni's multiple comparison test.

icant increase in lymph node cell count when blocking IL-6R, but only few differences in the types of immune cells found. There was a small non-significant trend towards a lower RSV-tetramer $CD4^+$ and Tfh response in αIL-6R-treated mice. αIL-6R-treated mice also tended to have more $CD8^+$ T cells in their lungs at the peak of infection. In the lungs and the BAL fluid of αIL-6R-treated mice, there was a slight trend towards $CD8^+$ T cells producing less IFNγ and more IL-10.

5.3.10. Skeletal muscle mass during IL-6R blockade in RSV infection of elderly mice

TA muscle was extracted from euthanised mice and weighed. At the peak of infection at day 8, TA weight was not different between isotype- and αIL-6R-treated mice (Figure 5-18a). Interestingly, TA weight was not different between the two groups in Experiment 1 either, despite differences in the pattern of weight loss (not shown). This suggests that bodyweight lost likely includes loss of body components other than muscle, such as fat and water. TA weight increased significantly in αIL-6R-treated mice from day 8 to day 18, and at day 18, αIL-6R-treated mice had significantly heavier TA muscles than isotype-treated mice. The TA atrophy index, normalising TA weight to the overall size of an individual mice using tibia length, decreased significantly from day 8 to day 18 in both

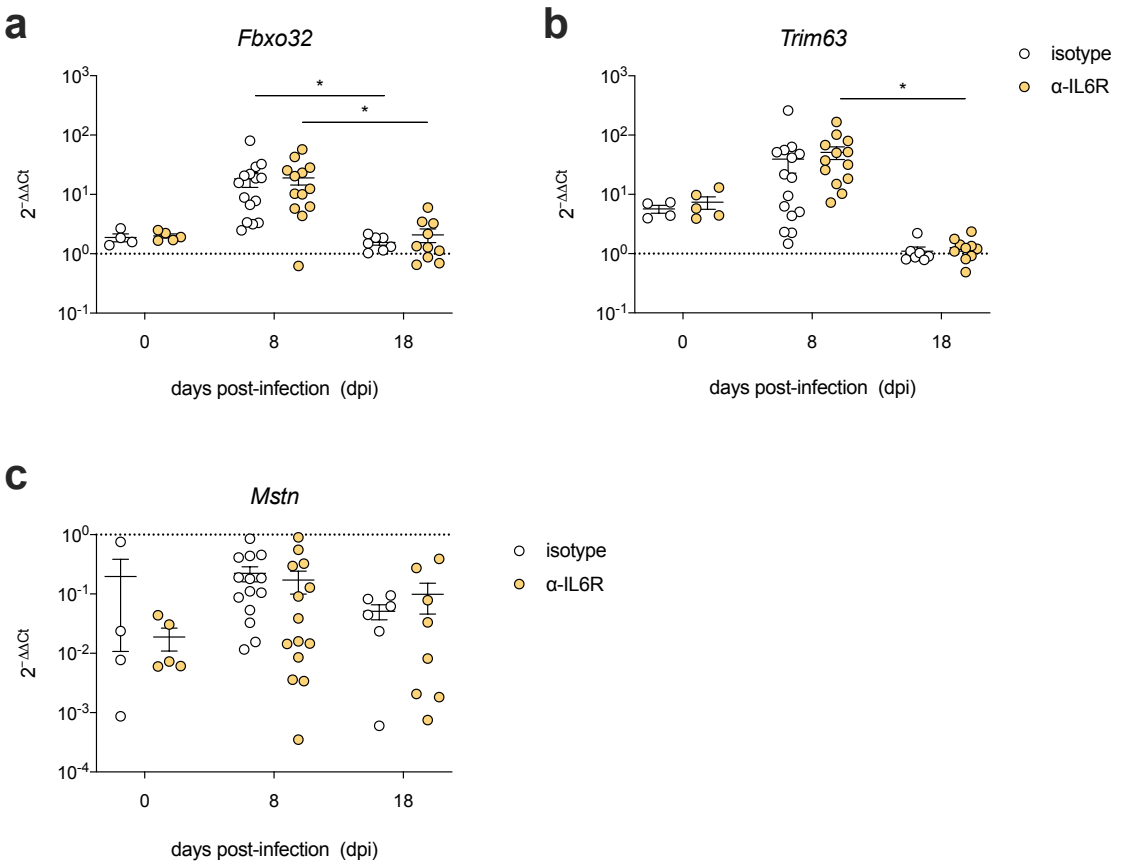

Figure 5-19 Expression of negative regulators of muscle mass during IL-6R infection

qPCR assays of gene expression in the TA muscle of elderly mice treated with either anti-IL-6R antibody or isotype antibody before RSV infection, 8 days post-infection, and 18 days post-infection. Pooled from 4 independent experiments at n=4-10 each. Two-way ANOVA with Bonferroni's multiple comparison test. **a.** *Fbxo32* encoding Atrogin-1 **b.** *Trim63* encoding MuRF-1. **c.** *Mstn* encoding Myostatin.

groups, but was not significantly different between the groups at either time point (Figure 5-18b).

5.3.11. Expression of positive and negative regulators of muscle during IL-6R blockade

Muscle wasting was interrogated on a molecular level by qPCR. Figure 5-19 shows the expression of genes promoting muscle wasting in TA muscle of elderly mice infected with RSV and treated with either isotype or αIL-6R antibody. Expression of the target

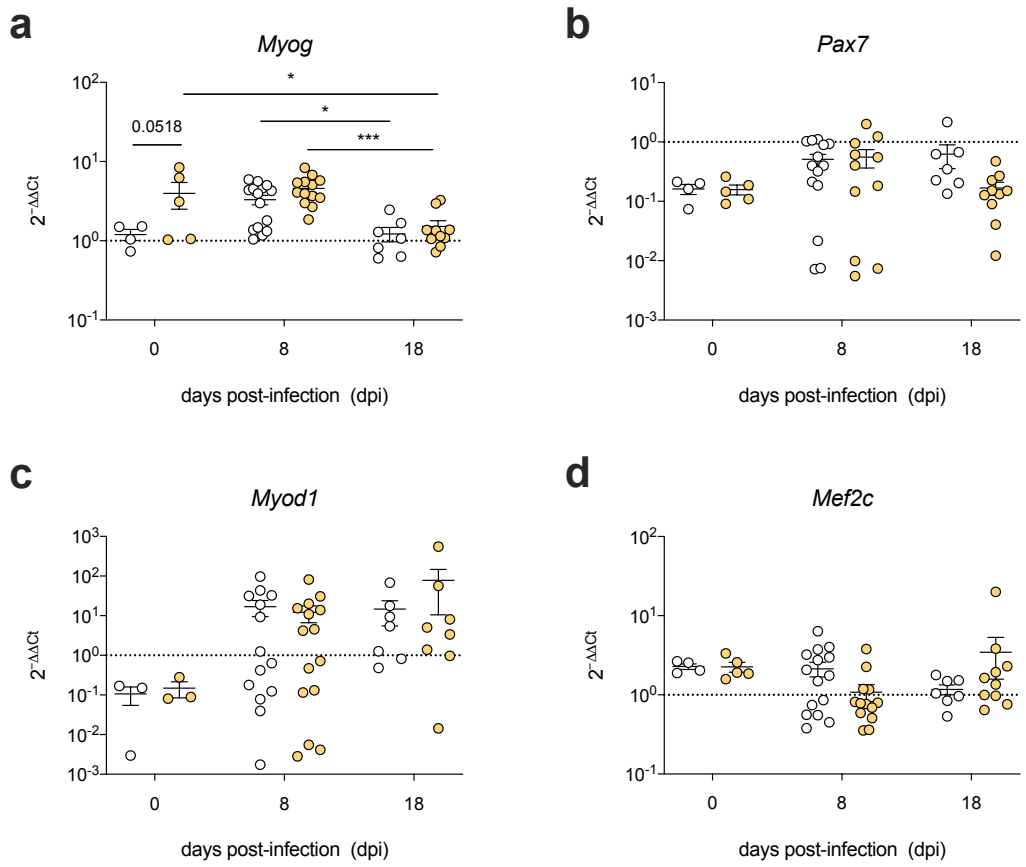

Figure 5-20 Expression of positive regulators of muscle mass during IL-6R infection

qPCR assays of gene expression in the TA muscle of elderly mice treated with either anti-IL-6R antibody or isotype antibody before RSV infection, 8 days post-infection, and 18 days post-infection. Pooled from 4 independent experiments at n=4-10 each. Two-way ANOVA with Bonferroni's multiple comparison test. **a.** *Myog* encoding Myogenin. **b.** *Pax7* encoding Pax7. **c.** *Myod1* encoding MyoD1. **d.** *Mef2c* encoding Mef2c.

gene was normalised to expression of GAPDH.

The expression of *Fbox32* (encoding Atrogin-1) followed a similar pattern in both antibody-treated groups (Figure 5-19a). There was a non-significant trend towards an increase in *Fbxo32* expression from day 0 to day 8 of infection, followed by a significant decrease from day 8 to day 18 in both groups. There was no significant difference in *Fbox32* expression between isotype and αIL-6R-treated mice at any timepoint.

There was a similar trend in *Trim63* (MuRF-1) of an increase from day 0 to day 8, and a decrease from day 8 to day 18 (Figure 5-19b). This only reached statistical significance

in the αIL-6R-treated group for the decrease from day 8 to day 18. There was no significant difference in *Trim63* expression between isotype and αIL-6R-treated mice at any timepoint.

The expression of *Mstn* (myostatin) in TA was very low overall (Figure 5-19c). Expression did not change significantly over the course of infection in either group. There was no significant difference in *Mstn* expression between isotype and αIL-6R-treated mice at any timepoint.

These results suggested an upregulation of atrophy-promoting genes in the TA of elderly mice during RSV infection in general, consistent with the results of Chapter 3, but no effect of blocking IL-6R signalling.

Figure 5-20 shows the expression of a number of growth-promoting genes in TA muscle of elderly mice infected with RSV and treated with either isotype or αIL-6R antibody. The expression of *Myog* (Myogenin) was elevated in αIL-6R-treated mice at baseline, although this did not quite reach statistical significance (Figure 5-20a). The expression of *Myog* decreased significantly in both antibody-treated groups from day 8 to day 18, and remained significantly lower at day 18 than at baseline in the αIL-6R-treated group.

The expression of *Pax7* in TA was very low overall (Figure 5-20b). There was a non-significant trend towards an increase in *Pax7* expression from day 0 to day 8 of infection in both groups. Expression did not change significantly over the course of infection in either group. There was no significant difference in *Pax7* expression between isotype and αIL-6R-treated mice at any timepoint.

There was a non-significant trend towards an increase in *MyoD1* expression from day 0 to day 8 of infection in both groups, although data was highly variable (Figure 5-20c). There was no significant difference in *MyoD1* expression between isotype and αIL-6R-treated mice at any timepoint. The high level of variability in the data may indicate a technical issue.

The expression of *Mef2c* in TA muscle did not change significantly with either timepoint

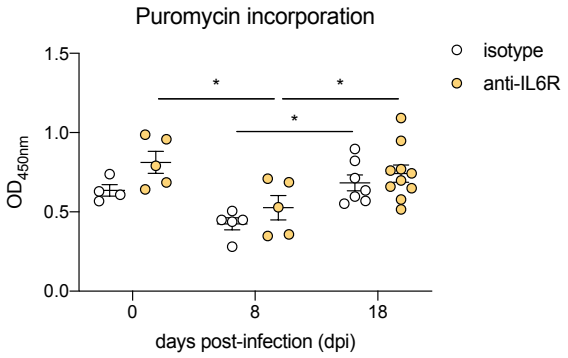

Figure 5-21 Puromycin incorporation during IL-6R blockade

Incorporation of puromycin into TA muscle of elderly mice treated with either α-IL-6R antibody or isotype antibody; 8 days or 18 days after RSV infection. Pooled from 2 independent experiments at each time point at n=2-5. Two-way ANOVA with Bonferroni's multiple comparison test.

of infection or antibody treatment (Figure 5-20d).

5.3.12. Protein synthesis during IL-6R blockade

Protein synthesis in TA muscle was measured using the puromycin incorporation assay developed previously. There was no difference in puromycin incorporation between isotype and αIL-6R-treated groups at baseline, although there was a small non-significant trend towards higher incorporation in the αIL-6R-treated mice (Figure 5-21). Puromycin incorporation decreased significantly in αIL-6R-treated mice from baseline to day 8 of infection, but increased again from day 8 to day 18, to levels that were not significantly different to baseline. The puromycin incorporation in the TA muscles of isotype-treated mice increased significantly from day 8 to day 18. There was no significant difference in the puromycin incorporation into TA muscle between the two antibody-treated groups at any time point.

5.3.13. Muscle fibre size during IL-6R blockade

Results from raw TA muscle weight, expression of muscle-regulating genes, and puromycin incorporation indicated that IL-6R blockade did not have an effect on the muscle

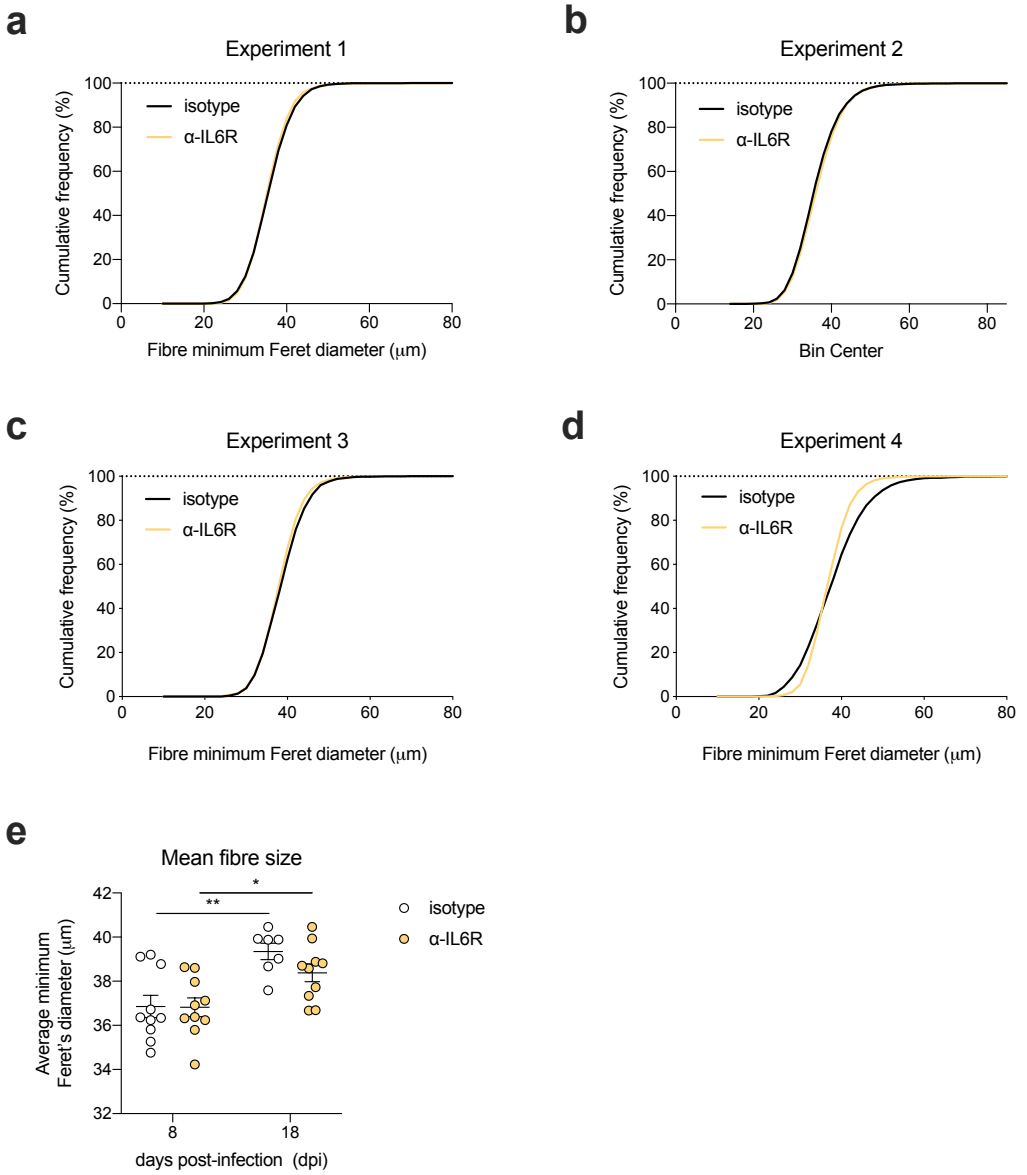

Figure 5-22 Muscle fibre size of elderly mice infected with RSV during IL-6R blockade

TA muscle fibre minimum Feret's diameter measurement in elderly mice 8 days (**a.+b.**) or 18 days (**c.+d.**) after RSV infection, treated with either α-IL-6R antibody or isotype antibody. **a.-d.** Cumulative frequency histogram of TA muscle fibre minimum Feret's diameter in four independent experiments. **e.** Average minimum Feret's diameter of TA muscle fibres in elderly mice 8 or 18 days after RSV infection treated with either α-IL-6R antibody or isotype antibody. Pooled from 4 independent experiments at n=2-5. Two-way ANOVA with Bonferroni's multiple comparison test.

of elderly mice during RSV infection. This was confirmed by measuring the minimum Feret's diameter of TA muscle fibres in elderly RSV-infected mice treated with either isotype or αIL-6R antibody. Mice treated with αIL-6R antibody did not exhibit a change in size of TA muscle fibres compared to mice treated with isotype antibody in any experiment or at any point of RSV infection (Figure 5-22). The distribution of fibre sizes was slightly different in Experiment 4 (Figure 5-22d). The fibre sizes of mice treated with αIL-6R antibody exhibited a narrower spread, i.e. smaller standard deviation, than those of isotype-treated mice. However, this was not statistically significant, and may be due to the fact that there were only two mice in the isotype-treated group. The TA muscle fibre size interestingly did not differ even in experiments where the two groups exhibited significantly different weight loss (Experiments 1, 3, 4). Isotype-treated mice in Experiment 1 exhibited lower weight loss but unchanged TA weight compared to αIL-6R-treated mice, which may help to explain why their muscle fibre size was unchanged (Figure 5-22a). But in Experiments 3 and 4, αIL-6R-treated mice lost significantly less weight than isotype-treated mice, and also had significantly heavier TA muscles. In spite of this, muscle fibre size in these experiments was not significantly different between the two antibody-treated groups (Figure 5-22c,d). In fact, there was a slight trend towards αIL-6R-treated mice having smaller muscle fibres at day 18. This suggests that TA muscle weight is not always driven by an increase in size of the individual muscle fibre.

5.4. Discussion

This chapter has explored the role of IL-6 signalling in the elderly mouse model of RSV infection using an IL-6 receptor-blocking antibody. Time course experiments comparing young and elderly mice showed that elderly mice strongly upregulated the production of IL-6 in their airways at the peak of RSV infection (See Chapter 3). IL-6 is a multifunctional cytokine that has been implicated in various contexts relevant to the elderly mouse model of RSV infection, including predicting morbidity and mortality with age (Puzianowska-Kuźnicka *et al*., 2016) but also protection from pathological inflammation during RSV infection (Pyle *et al*., 2017), promotion of or protection from muscle wasting depending

on the context (Serrano *et al.*, 2008; Muñoz-Cánoves *et al.*, 2013), and promotion of the germinal centre response (Kopf *et al.*, 1994; Ramsay *et al.*, 1994). Based on this, it was hypothesised that blocking IL-6 signalling may improve the outcome of RSV infection in elderly mice by removing excess inflammation. However, due to the pleiotropic nature of IL-6, effects on the muscle and on the germinal centre response were also expected. Elderly mice were treated with αIL-6R antibody or isotype control antibody one day before RSV infection and every five days.

5.4.1. IL-6 blockade may not affect weight loss in elderly mice with RSV

Throughout multiple experiments, IL-6R blockade did not have a clear effect on RSV infection-induced weight loss. In one experiment, αIL-6R-treated mice lost more weight than isotype-treated mice, in another, there was no difference in weight loss, and in two experiments, αIL-6R-treated mice lost less weight than isotype-treated mice. The cause for this disparity is unknown. As found previously, elderly mice were highly variable, both in their response to RSV infection, and also when followed in the absence of infection during an experiment testing the effect of the αIL-6R antibody at steady state. The variability in the weight curves could be due in part to cage effects such as differences in microbiota and grooming hierarchies that might affect the access of individual mice to food and water. To reduce the strength of cage effects, mice were reallocated between cages prior to an experiment commencing. Mice were reallocated on the basis of weight to achieve a similar average starting weight across cages.

Due to the variations in weight loss caused, the effect of IL-6R blockade on other aspects of the model was difficult to discern. Some outputs were clear corollaries of weight loss. For example, there was no significant difference in TA weight at day 8 after infection, probably because the experiments concluded at this time point exhibited little difference in weight loss between isotype and αIL-6R-treated mice. However, both experiments that concluded at day 18 showed decreased weight loss of the αIL-6R-treated mice, which may help to explain their significantly heavier TA muscles compared to isotype-treated mice that lost more weight. The amount of food and water consumed also close-

ly tracked with weight loss, which implies that the weight loss during RSV infection is caused mostly by anorexia (loss of appetite). To summarise, some differences observed between isotype and αIL-6R-treated groups in these experiments may not be specific to antibody treatment, but caused simply by the variable levels of weight loss.

5.4.2. IL-6R blockade may not influence inflammation during RSV infection of elderly mice

Contrary to the hypothesis that removing excess IL-6 from elderly mice would improve their markers of inflammation during RSV infection, there were very few differences in inflammation and immune cell populations between the isotype and αIL-6R-treated groups of mice. Viral load, and IL-6, GDF-15, or total protein in BAL fluid were not significantly different between isotype and αIL-6R-treated mice either at day 8 or at day 18. They also did not display changed levels of cellular infiltration in either BAL fluid, spleen or lung tissue. There were significantly more cells in the lymph nodes of αIL-6R-treated mice compared to isotype-treated mice at day 8. However, this was primarily due to the single experiment at day 8 in which αIL-6R-treated mice lost more weight than isotype-treated mice, so this increase in cellular infiltration was probably driven by stronger inflammation in this one particular experiment.

There were very few differences in the frequency and total abundance of various immune cell subsets, including T cells, B cells, $CD8^+$ T cells, $CD4^+$ T cells, and RSV-specific $CD4^+$ T cells, between mice treated with αIL-6R antibody and mice treated with isotype antibody. The frequency of Tfh cells at day 18 was lower in the lymph nodes of αIL-6R-treated mice compared to isotype-treated mice, but the total abundance was not significantly different. The reduction in the proportion of Tfh cells in the αIL-6R-treated mice may imply that Tfh differentiation was impaired due to the lack of IL-6 signalling, which is consistent with knowledge that IL-6 is a key driver of the Tfh fate in $CD4^+$ T cells (Nurieva et al., 2008, 2009).

$CD8^+$ T cells were more frequent in the lungs of αIL-6R-treated mice, but $IFN\gamma^+$ $CD8^+$ T cells were less frequent in the BAL fluid of αIL-6R-treated mice at day 8. However, none

of these differences translated into significant differences in the total number of these cell populations between the two antibody-treated groups. Curiously, in Experiment 2, there were differences in the ability of BAL fluid $CD8^+$ T cells to produce IFNγ and IL-10. The BAL fluid $CD8^+$ T cells derived from αIL-6R-treated mice produced proportionately less IFNγ and more IL-10 (not shown). This almost reached statistical significance when expressed as total cell abundance. This was notable due to the lack of a difference in weight loss induced by RSV, meaning this was likely an effect that was independent of inflammation induced by higher weight loss. This implies that IL-6 is required to promote an inflammatory profile in elderly $CD8^+$ T cells recruited to the BAL fluid. This contrasts with the known ability of IL-6 to promote IL10 production (Stumhofer et al., 2007; McGeachy et al., 2007). Pyle *et al*. observed the opposite effect in young BALB/c mice with RSV infection. IL10 production was reduced with αIL-6R treatment whereas IFNγ production by $CD4^+$ T cells was increased. This may suggest that IL-6 plays a fundamentally different role during RSV infection in young vs aged mice (pro-inflammatory in the elderly vs anti-inflammatory in the young). However, it is important to bear in mind that this phenotype was only observed in one experiment, which had very different patterns of RSV-induced weight loss compared to the other experiments.

The amounts of RSV-specific IgG and IgA antibodies produced did not differ between isotype and αIL-6R-treated mice, despite the literature suggesting that IL-6 is crucial for promoting antibody responses (Kopf et al., 1994; Ramsay et al., 1994). This may suggest that IL-6 signalling blockade was not complete in this study, since the ability to produce antibodies was no different in mice treated with αIL-6R antibody.

5.4.3. IL-6R blockade may not influence muscle wasting of elderly mice during RSV infection

Muscle wasting was assessed in elderly mice infected with RSV and treated with either αIL-6R antibody or isotype control antibody. Raw TA weight or the TA atrophy index was not significantly different between groups at day 8, which was likely related to the fact that there was no significantly different weight loss in the experiments concluded at this

time point. On the other hand, both experiments that concluded at day 18 showed reduced weight loss of the αIL-6R-treated mice, and had significantly heavier TA muscles than isotype-treated mice. In this context, it is probable that muscle weight was driven primarily by RSV-induced weight loss rather than the effect of the antibody treatment. The expression of genes related to the control of muscle mass, either positive or negative, was not significantly different between αIL-6R and isotype-treated mice at any time point.

Radigan *et al*. (2019) carried out a similar study, studying the effect of IL-6 signalling on muscle wasting of mice after IAV infection. Radigan *et al*. claim that IL-6 signalling contributes to infection-induced skeletal muscle wasting via the upregulation of Atrogin-1. Treatment with tocilizumab, an αIL-6R antibody, improved grip strength and decreased Atrogin-1 expression in mice infected with IAV, but did not affect weight loss or EDL or soleus muscle weight or fibre size. IL-6 treatment of myotubes promoted a decrease in myotube diameter which was dependent on the upregulation of STAT3, FoxO3a, and Atrogin-1. This implies that part of respiratory infection-induced skeletal muscle wasting is due to systemic IL-6 signalling upregulating Atrogin-1.

Some of these results were mirrored in the present study. For example, overall, this study also did not find changed weight loss or changed muscle weight or fibre size with αIL-6R antibody treatment at the peak of infection. However, in the present study, αIL-6R antibody treatment did not affect the expression of Atrogin-1 in TA muscle. This could be due to the fact that expression was measured in a different muscle (TA as opposed to EDL or soleus in Radigan *et al*.). Grip strength was not measured in this study but this output would be a simple addition to the protocol to additionally measure the muscle function of mice in this model. Unlike this study, Radigan *et al*. did not assess the effects of IL-6R blockade on the rest of the immune response to IAV, or the effects in elderly mice, so only limited comparisons can be made.

5.4.4. Limitations and Future Work

A major limitation of the work presented in this chapter is the inconsistent phenotype

in RSV-induced weight loss after IL-6R blockade. Considering the inconsistent effects of blocking IL-6 signalling in this model, it is possible that the antibody treatment given did not prevent all IL-6 signalling. BAL fluid IL-6 protein levels were not different between the two treatment groups, however this is not necessarily indicative of the antibody not working. These experiments used the exact antibodies and dosing schedule used successfully by Pyle *et al.* (2017) in young mice. It is possible that using an IL-6R-blocking antibody produced different results than what might have been found using an antibody against IL-6 directly. Pyle *et al*. also successfully employed an IL-6-blocking antibody, which in their studies did not behave differently to the IL-6R-blocking antibody (James Harker, pers. comm. 2019). An IL-6-blocking antibody was not used in these experiments for cost and animal welfare reasons. The αIL-6 antibody has a shorter half-life and must be administered daily compared to every 5 days for the αIL-6R antibody. Apart from higher expenses, this would also have caused additional stress for the animals, which was to be avoided.

Pyle *et al*. found that in young mice, blocking IL-6 resulted in increased weight loss from RSV. Their findings suggested that IL-6 signalling early during infection stimulates macrophages to secrete IL27, which is crucial to induce T regulatory cells (Tregs), thus preventing immunopathology. This effect was not detected in elderly mice in this study. Treg detection was attempted by staining for Foxp3 in flow cytometry assays. However, technical issues precluded the reliable quantification of Tregs in these experiments. Future studies should urgently address this.

One crucial difference between this study and Pyle *et al.*'s experiments was that they used the BALB/c strain of mice while this study used the C57BL/6 strain. There are known differences between mouse strains in their susceptibility and response to RSV infection, for example, BALB/c mice are known to be more susceptible to RSV infection than C57BL/6 mice and exhibit a type-2-skewed response (Stark *et al*., 2002). C57BL/6 mice were chosen for this study because of concerns that elderly BALB/c mice, additionally susceptible to RSV infection due to their age, may meet their humane endpoint

too early for the planned experiments to be conducted. It is possible that repeating this study with aged BALB/c mice may yield data more consistent with Pyle *et al*., however it is also conceivable that elderly mice respond fundamentally differently to RSV and IL-6 blockade, irrespective of strain.

It is imperative for future studies to identify the source of variability in this model of IL-6R blockade to be able to discern the role of IL-6 signalling blockade in the elderly in RSV infection. Repeating the experiments in elderly mice with an anti-IL-6 antibody may show a if there was a problem with the anti-IL-6R antibody, and experiments in young C57BL/6 mice could determine if differences compared to Pyle *et al*. were due to mouse strain.

5.4.5. Summary

IL-6 is strongly upregulated in RSV-infected elderly mice. IL-6 has well-known roles in inflammation, muscle regulation, and the germinal centre response. On this basis, it was hypothesised that IL-6R blockade in elderly RSV-infected mice would have a noticeable effect in at least one of these aspects. If any, effects were obscured by high variability in RSV-induced weight loss in elderly mice. It is also possible that the multiple roles of IL-6 cancelled out each other's effects to various degrees in different experiments, leading to a variable phenotype. Future studies should urgently address the source of variability in order to determine with higher reliability the role of IL-6 signalling in the elderly during RSV infection.

6.

Discussion

Chapter 6. Discussion

6.1. Introduction

The population of the world is ageing rapidly, increasing the incidence of age-associated diseases. Infection with respiratory viruses is a major cause of morbidity and mortality in the elderly population. Respiratory Syncytial Virus (RSV) is emerging as a prevalent cause of severe illness in the elderly, which is all the more salient because of a lack of vaccines and treatments, and the ability of the virus to re-infect throughout life (Troeger *et al.*, 2017; Shi *et al.*, 2019). Muscle weakness is a common outcome of respiratory infections in the elderly, and predisposes to a downward spiral of decreased activity, and higher risk of frailty and mortality (Spruit *et al.*, 2003; Swallow *et al.*, 2007; Vilaró *et al.*, 2010; Landi *et al.*, 2013). How RSV infection affects muscle wasting in the elderly is not known. In this study, muscle wasting and the immune response were investigated in an aged mouse model of RSV infection. The aim of the study was to determine if and to what extent RSV infection caused muscle wasting in elderly mice, and whether this could be prevented. Severe RSV disease disproportionately affects elderly people, partially due to impaired innate responses, but also due to impaired antibody responses (Falsey & Walsh, 1998; Walsh, Peterson & Falsey, 2004). Antibody is to some extent protective against future RSV infection. Therefore, this study also investigated the antibody response of aged mice to RSV infection. There is an urgent need to understand how ageing interacts with commonly occurring conditions like respiratory infections and muscle wasting.

6.2. An elderly mouse model of RSV infection

6.2.1. Key findings

6.2.1.1. Elderly mice develop more severe RSV disease

This study has developed a mouse model of RSV infection in the elderly for additionally evaluating the degree and type of muscle wasting. Young (10-12 weeks old) and Elderly (18 months old) mice were infected with the same dose of RSV A2 and followed over the course of the infection. The two primary time points observed were 8 days post-infection

(dpi) and 18 dpi, which represent the peak of weight loss and the recovery phase, respectively. Elderly mice developed more severe disease than young mice. Elderly mice displayed enhanced weight loss, viral load, lung and airway infiltration of lymphocytes, and higher serum markers of inflammation. This is consistent with previous models utilising elderly mice in RSV infection models (Graham *et al.*, 1988; Zhang *et al.*, 2002b; Fulton *et al.*, 2013; Wong *et al.*, 2014). There were minor differences in the extent of inflammation caused in elderly mice, compared to some of the existing literature, which may be attributable to different mouse and virus strains used.

6.2.2. Key methods

Other studies have already used elderly mice in RSV infection models (Graham *et al.*, 1988; Zhang *et al.*, 2002b; Fulton *et al.*, 2013; Wong *et al.*, 2014), but this study has characterised the immune response, including the germinal centre response, in more depth, and for the first time, describes the skeletal muscle response of elderly mice to RSV infection.

In infectious disease research, it is crucial to consider the effect of infection on the entire organism, something that can only be done in *in vivo* models like the mouse. Many studies still focus only on the site of infection, such as the lung in the case of respiratory viral infection. However, local infection can have systemic effects, particularly in organisms that are already systemically dysregulated as is the case with progressive ageing. The aged mouse model presented here is an appropriate model to study the systemic impact of ageing when exposed to stressors such as infection.

6.2.3. Limitations

6.2.3.1. High variability in elderly mice

A key feature of the elderly mice in this model was a high individual variability in almost all outputs, compared to young mice. This is likely due to the accumulation of small differences over the total lifetime of the mice. There were also noticeable cage effects within the elderly mice. These may be due to grooming hierarchies or differences in microbiota. The microbiota is known to have a strong effect on the germinal centre response

(Stebegg *et al.*, 2019). Precautions were taken to keep elderly mice as comparable as possible, for example, mice were of the same strain, gender, and purchased from the same supplier. Mice were also re-distributed between cages to achieve a similar average starting weight for the GDF-15 and IL-6R antibody intervention experiments. In future studies, the high individual variability of elderly mice must be an important consideration. Power calculations should be carried out to ensure that biologically relevant effects can be reliably detected.

6.2.3.2. Mouse models in ageing and RSV research

The mouse (*Mus musculus*) is a widely-used model animal in biological and medical research. Mice are easy to handle, cheap to maintain, and as mammals bear higher resemblance to humans than fish or insect models. Their lifespan of approximately two years is longer than some animals models of ageing, such as the African kilifish, but short enough to observe and study ageing in a cost-effective manner. Since the ageing process is highly conserved, using mice as an animal model for ageing research is likely appropriate in many contexts.

Early descriptions of mouse models to study RSV already found that older were more susceptible to RSV infection and had higher lung virus titres (Graham *et al.*, 1988). Older mice manifested enhanced disease with reduced activity, weight loss, and increased cellular lung infiltration. This is very similar to how RSV disease manifests in older humans, making mice an appropriate model for RSV research. However, in some aspects, mice are known to react to RSV infection differently to humans.

For example, RSV infection can induce protective immunity from repeated infection in mice, whereas humans experience repeated infection with RSV throughout life, a phenomenon termed “immune amnesia” (Habibi *et al.*, 2015; Openshaw *et al.*, 2017). Mice are also usually kept under specific pathogen-free conditions and most RSV research describes primary infection. This is clearly not representative of older humans having been infected with RSV many times throughout life. These factors are highly relevant to considerations about vaccine development for which the elderly are a key target group.

The ability to extrapolate from mouse data to humans is limited. Hence clinical studies such as INFLAMMAGE are crucial additions to pre-clinical work using mouse models. Experimental pathogen challenge in humans yields invaluable information about baseline predispositions and immune responses at defined times of infection.

6.2.4. Relevance

As of 15th November 2020, the Severe Acute Respiratory Syndrome Coronavirus 2 (SARS-CoV2) pandemic has caused over 53.7 million confirmed cases of Coronavirus infectious disease 2019 (COVID-19) and 1.3 million deaths (World Health Organization, 2020). SARS-CoV2 is a novel coronavirus that emerged in the Wuhan region of China in late 2019. The virus is spread primarily by droplets and infects human airway epithelial cells by binding the receptor ACE2 (Hoffmann *et al.*, 2020). Infection can be asymptomatic or entail a variety of symptoms, classically fever, dry cough, shortness of breath, and loss of the sense of smell or taste (Song *et al.*, 2020). In severe cases, COVID-19 can lead to cytokine storm, multiple organ failure and/or respiratory failure, and death. In the United Kingdom, 56.3% of deaths from COVID-19 were in the 80+ age group, and those over the age of 80 with confirmed COVID-19 diagnosis were 70 times more likely to die than those under the age of 40 (Public Health England, 2020). Comorbities such as chronic cardiac disease, liver disease, malignancy, and dementia, which are more common in the elderly, are associated with higher mortality in hospital-admitted COVID-19 patients (Docherty *et al.*, 2020). Older patients are also more likely to require supplemental oxygen or mechanical ventilation when hospitalised (Chen *et al.*, 2020; Wu *et al.*, 2020). The emergence of SARS-CoV2 and the particular risks it poses to older people underscore the importance of considering age and age-associated conditions in the context of respiratory infections. Especially reports that antibody-mediated protection against COVID-19 (Ward *et al.*, 2020) may wane faster than anticipated warrant a comparison of SARS-CoV2 with RSV, since similar immunological mechanisms may underlie the waning of antibodies. Just like with RSV, it will be a key consideration to ensure that future vaccines and treatments for COVID-19 are effective in older age groups.

6.3. The germinal centre response of elderly mice to RSV infection

6.3.1. Key findings

6.3.1.1. Elderly mice produce less RSV-specific IgG but GC B cells and RSV-specific Tfh cells are not impaired in frequency or number

The germinal centre (GC) response is crucial to generating high-affinity antibodies. Since there is some evidence that serum antibodies to RSV can be protective in humans, characterising the differences in antibody response to RSV with age is important, particularly considering the aim of achieving high IgG levels in vaccine development (Hall *et al.*, 1991). The germinal centre response to RSV in elderly mice has not been investigated in detail. Elderly mice produced a lower RSV-specific IgG titre compared to young mice, which may have contributed to their enhanced RSV disease. This contrasts with observations that older humans tend to generate equally strong serum antibody responses to RSV infection compared to adults (Agius *et al.*, 1990; Walsh & Falsey, 2004). These differences may be due to the fact that this infection was a primary infection in the mice whereas an elderly human will have been infected with RSV many times throughout life, so generating an additional memory response.

There were no differences in B or GC B cell (marked by $GL7^+$) frequency or abundance between young and elderly mice. The frequency and total number of Tfh cells, specialised $CXCR5^+$ $PD1^+$ $CD4^+$ T cells that mediate GC B cell interactions, was strongly elevated in the secondary lymphoid tissues and the lungs of elderly mice. The number of RSV-specific Tfh cells was not different between young and elderly mice. These results suggest that elderly mice do not have a defect in the proliferation or recruitment of B cells or RSV-specific Tfh cells. The unexpectedly high abundance of Tfh cells in elderly mice may be due to on-going immune responses to commensals or autoantigens, and may reflect a latent inflammatory state associated with ageing, termed “inflammageing” (Franceschi *et al.*, 2006).

Lefebvre *et al.* (2016) carried out a similar study investigating the antibody response to influenza A virus (IAV) infection in elderly mice. Despite the different infectious agent,

there were striking similarities, including higher viral load, lower IgG serum titres, and high Tfh numbers in elderly mice. This suggests universal age-related impairments in the antiviral immune response. Lefebvre *et al.* posit that aged Tfh cells exhibit a less mature, more regulatory-like phenotype, characterised by reduced CXCR5 and GL7 expression and enhanced Foxp3 expression. CXCR5 and GL7 expression were not reduced on aged RSV-specific Tfh cells in this study, but Foxp3 expression could be characterised in future studies.

6.3.2. Key methods

The methodology developed here to study the germinal centre response of elderly mice could be applied to different infectious disease models and could be used for testing vaccines for RSV. There is currently no licenced vaccine for RSV. Older humans are more susceptible to severe RSV infection, meaning they are an important target group for vaccine development. Most pre-clinical research is still conducted in young animal models. This is not representative of older people as a main target group, and does not take into account that vaccines are often less effective in the elderly. Using a well-characterised aged mouse model like the one presented here may be an appropriate model for development of treatments and vaccines for age-related conditions.

6.3.3. Future work

This study focused mostly on the frequency and total number of certain immune cell populations. Many immune cell populations were present in equal or higher numbers in elderly mice. This may suggest that these populations are not responsible for the observed defect in immunity leading to increased RSV disease in elderly mice. On the other hand, pure abundance does not necessarily reflect the functionality of these cells.

The production of some cytokines was measured in this study, but others could be easily studied by expanding and modifying the flow cytometry panels given. Other surface markers on cells reflecting maturity or functionality may equally be added to the panels, for example to determine ICOS expression on Tfh cells.

Lefebvre *et al.* (2016) suggest that the antibody response in elderly mice is impaired due to Tfh cells developing a more "regulatory-like" phenotype. This could be easily interrogated in the short term by addition of Foxp3 and other markers to the flow cytometry panels. Foxp3 staining was attempted in this study, but was unsuccessful for unknown reasons. Further optimisation may be necessary.

In the long term, future studies may want to investigate the spatial interactions in the germinal centre. Preliminary experiments carried out by Masters students Celia Diaz and Lucy Petagine found that the splenic GC microenvironment structure was highly disorganised in elderly mice compared to young mice. This may suggest that Tfh and GC B cells do not interact properly to promote antibody production. These spatial interactions may be studied using immunohistochemistry with more markers, perhaps even live imaging of spleen sections to determine defects in chemotaxis.

6.4. Skeletal muscle wasting in elderly mice after RSV infection

6.4.1. Key findings

6.4.1.1. Elderly mice display muscle wasting after RSV infection

Muscle wasting is a natural component of ageing but can be exacerbated by inactivity, chronic disease, and infectious disease, and promotes frailty and increased risk of mortality. To my knowledge, this is the first study to quantify muscle wasting in response to RSV infection and its interaction with age. Elderly mice infected with RSV had significantly decreased TA muscle weight, decreased TA muscle fibre size, increased expression of E3 ubiquitin ligases contributing to muscle breakdown, and failed to upregulate protein synthesis in the muscle. The expression of IGF-1, a key regulator of muscle growth, and Pax7, the marker for muscle stem satellite cells, was downregulated at the peak of RSV infection in the muscles of elderly mice compared to young mice. These results together suggest that RSV infection induced muscle wasting in elderly mice by both upregulating muscle breakdown processes and downregulating muscle growth processes.

Although muscle wasting in elderly mice in response to RSV infection has not been previously studied, other studies utilising other models of muscle wasting largely support

these findings. Bartley *et al.* (2016) observed enhanced weight loss, viral load, increased expression of E3 ubiquitin ligases, and decreased expression of some muscle growth promoting genes in elderly mice infected with IAV. The expression patterns of some muscle-associated genes differed slightly between Bartley *et al.* and this study, but this may be due to differences in virus used, muscle assayed, or mouse age and sex. Generally, this confirms the findings of this study that respiratory viral infection can promote muscle wasting in elderly mice.

An overview of the potential pathways through which RSV infection may promote muscle wasting in the elderly is shown in Figure 6-1. The key pathways are likely to include inactivity, inflammation, and metabolic pathways such as anorexia. These pathways are not separate and there is strong interaction between them, for example, high levels of inflammation can promote both anorexia and inactivity as parts of sickness behaviour.

6.4.2. Key methods

The methods developed here interrogate both the net outcome of muscle gain/loss as well as the individual factors promoting either muscle growth or muscle atrophy. They utilise common laboratory methods (qPCR, ELISA, immunohistochemistry) that are relatively cheap and easily adaptable for other users. The puromycin incorporation assay has been adapted to measure rates of protein synthesis in muscle homogenate from young and elderly mice. This yields valuable information on the ability of the muscle to grow and repair, and could be further developed to interrogate other aspects, for example fluorescent tagging of puromycin could be used to measure protein synthesis in different muscle fibre types or to determine rates of protein synthesis in different immune cell populations. The macro developed to automatically measure muscle fibre size in section images saves labour and time, and is flexible to adaptation by modifying the code.

6.4.3. Limitations

6.4.3.1. The respective contributions of anorexia, inactivity, and inflammation to muscle wasting

The muscle wasting observed in elderly mice after RSV infection in this study was likely

contributed to by a number of factors, including anorexia, inactivity, and potentially the direct effect of inflammatory cytokines. It is difficult to determine the exact relative contributions of these factors to the muscle wasting observed. It is unclear to what extent elderly mice would experience the same phenotype of muscle wasting when immobilised, for example by hindlimb unloading, compared to the effects induced by RSV infection in this study. Decreased activity and anorexia are characteristic components of sickness behaviour, which are also evident in humans with severe respiratory infections. This study therefore did not aim to discern the exact contributions of inactivity or anorexia to muscle wasting observed after RSV infection.

6.4.4. Future work

6.4.4.1. Measuring muscle strength and function

Muscle mass is not equivalent to muscle strength or function. It is well known that in humans, the relationship between muscle mass and strength is not linear. With age, strength declines quicker than mass (Goodpaster *et al.*, 2006). This reduced quality of muscle observed over age is probably attributable to the loss of fast twitch type II fibres, reduced mitochondrial mass and increased intramuscular fat (Narici & Maffulli, 2010).

Future studies could expand the model presented here with simple measures of muscle strength. In the short term, mice in this model could be tested fairly easily with a grip strength meter (commercially available) or by a wire hang test (Wilson *et al.*, 2017). More specialised measures of activity and muscle stability could be measuring gait and locomotion using beam breaks and specialised treadmills as employed by Bartley *et al.* (2016).

A drawback of the outputs used in this study was that most measures of muscle were not longitudinal and required euthanasia. This increases the noise-to-signal ratio due to inter-mouse variability. In the longer term, studies like this could be repeated with longitudinal measurements of muscle mass using for example repeated MRI, NMR, or DEXA scanning methods.

6.5. The role of GDF-15 in RSV infection of elderly mice

6.5.1. Key findings

GDF-15 is a TGF-β superfamily cytokine which increases with age and is associated with poor prognosis in a number of medical conditions, including diabetes, cancer, COPD, and cardiovascular disease (Carstensen *et al.*, 2010; Cotter *et al.*, 2015; Bloch *et al.*, 2015). Four groups recently identified GFRAL as the receptor for GDF-15. GFRAL expression is highly restricted to a cluster of neurons in the brain stem, leading to the hypothesis that GDF-15 exerts its effects by promoting anorexia during periods of systemic stress (Mullican *et al.*, 2017; Hsu *et al.*, 2017; Yang *et al.*, 2017; Emmerson *et al.*, 2017). Elderly mice exhibited elevated serum levels of GDF-15 at all time points, and increased expression of GDF-15 in lung tissue and increased levels of GDF-15 in the BAL fluid when infected with RSV. GDF-15 signalling was blocked in elderly mice using a monoclonal antibody. The hypothesis was that GDF-15 blockade may alleviate RSV-induced anorexia and weight loss in elderly mice.

Contrary to expectations, GDF-15 blockade did not affect RSV-induced anorexia, weight loss or inflammation, but led to enhanced muscle wasting in elderly mice compared to treatment with an isotype control antibody. Anti-GDF-15-treated mice had a significantly lower TA atrophy index, increased expression of the atrophy-promoting E3 ligase Atrogin-1, and a trend towards decreased TA muscle fibre size. These results may appear counterintuitive in the face of a large volume of literature associating high GDF-15 with worse disease. However, the results are cast into an interesting light by a recent study by Luan *et al.* (2019). Luan *et al.* found that GDF-15 blockade did not affect inflammation or viral load during lethal IAV challenge of mice, but did enhance mortality by a mechanism of reduced hepatic secretion of cardioprotective triglycerides. The authors hypothesise that GDF-15 is a systemic regulator of stress. It is conceivable that the blockade of GDF-15 in elderly RSV-infected mice led to decreased circulating triglycerides. In mice, medium-chain triglycerides have been associated with increased mitochondrial biogenesis, activation of Akt, and suppression of TGF-β signalling, suggesting that triglycerides could contribute to muscle growth (Wang *et al.*, 2018b). Dietary supplementation

with medium-chain triglycerides improved body weight and muscle strength in nursing home residents (Abe, Ezaki & Suzuki, 2016). This hypothesis may explain how GDF-15 blockade led to muscle wasting in RSV-infected elderly mice. Future studies may want to investigate this.

Samples were available from the INFLAMMAGE study in which young and older human volunteers are challenged with RSV. Similarly to the findings in the mouse model, plasma GDF-15 levels were elevated in older participants, but not affected by RSV infection. Not enough BAL fluid samples were available at the time to determine GDF-15 production in the airways of human volunteers. There was no detectable correlation between baseline GDF-15 and peak viral load or cumulative symptom score.

6.5.2. Future work

6.5.2.1. Therapeutic applications of GDF-15 signalling modification

The GDF-15 blocking experiments unexpectedly yielded the result of a potentially muscle protective effect of GDF-15. This presents an opportunity for future studies to evaluate the role of GDF-15 in muscle wasting. The discovery of GFRAL, the receptor for GDF-15, in the area of the brain stem responsible for promoting anorexia suggested that GDF-15 exerts its effects primarily by appetite regulation. However, in the present study, GDF-15 blockade did not affect food or water intake of elderly mice during RSV infection, suggesting the existence of an anorexia-independent signalling mechanism.

Luan *et al.* (2019) propose that GDF-15 is a systemic stress regulator that induces the secretion of cardioprotective triglycerides from the liver. It is conceivable that triglycerides are also protective of muscle mass since they can be used as fuel, particularly during an otherwise food-restricted period such as anorectic RSV-infected elderly mice.

In the short term, this hypothesis could be tested by measuring triglycerides in archived serum samples from elderly mice treated with anti-GDF-15 antibody. This could take the form a simple kit test or more comprehensive lipidomic/metabolomic studies. The connection of GDF-15 to cardiac muscle could also be further investigated since hearts

were collected from the mice in this experiment. For example, the extent of cardiac damage could be assayed by measuring troponin levels in the serum.

In the long term, the exact mechanism behind GDF-15 signalling on the muscle should be elucidated. This may take the form of screens for interaction partners, particularly miRNAs, as Bloch *et al.* (2015) suggest that GDF-15 may promote certain muscle regulatory miRNAs (Bloch *et al.*, 2015). Since it takes prohibitively long to let genetically modified mice age for use as elderly mice, other techniques may be necessary, such as CRISPR-Cas9, or the use of progeroid animal models.

This study only evaluated the GDF-15 levels in a very small number of samples from a human RSV challenge cohort, INFLAMMAGE. As the cohort progresses and more samples become available, this would be an excellent extension and confirmation of the mouse model to determine the role of GDF-15 in the predisposition and outcome of RSV infection. Measures of muscle mass and function may be added to the study, such as grip strength or thigh circumference, to additionally investigate the effect of GDF-15 levels on muscle in humans during and after RSV challenge.

6.6. The role of IL-6 in RSV infection of elderly mice

6.6.1. Key findings

IL-6 was strongly upregulated in the BAL fluid of elderly mice infected with RSV. IL-6 has well-known roles in inflammation, muscle regulation, and the germinal centre response. For example, IL-6 in the elderly is associated with detrimental “inflammageing” (Franceschi *et al.*, 2006) and a higher risk of mortality (Puzianowska-Kuźnicka *et al.*, 2016). IL-6 is a “myokine” that is secreted in response to exercise to promote muscle growth and repair, however chronic IL-6 exposure can contribute to muscle wasting (Serrano *et al.*, 2008; Muñoz-Cánoves *et al.*, 2013). Finally, IL-6 is a key cytokine for the development of a functional germinal centre response via its promotion of Tfh cell and plasma cell differentiation (Hirano *et al.*, 1986; Nurieva *et al.*, 2008, 2009). On this basis, it was hypothesised that IL-6 signalling blockade in elderly mice may rescue detrimental inflammation during

RSV infection, or prevent the generation of an antibody response, or ameliorate muscle wasting. RSV-induced weight loss was highly variable in elderly mice treated with anti-IL-6R antibody and no distinct phenotype in comparison to isotype-treated mice could be established. It is possible that the multiple roles of IL-6 cancelled out each other's effects to various degrees in different experiments. The source of the variability should be identified in future experiments for example by varying mouse strain, housing conditions, or using an anti-IL-6 antibody instead of anti-IL-6R.

IL-6 signalling has been suggested to be crucial during early stages of RSV infection to promote maturation of Treg cells that prevent excessive immunopathology (Pyle *et al.*, 2017). This seemingly contradicts with the finding that elderly mice produce large amounts of IL-6 in response to RSV infection, but still experience substantial immunopathology. This may suggest that IL-6 plays a fundamentally different role during RSV infection with advancing age (pro-inflammatory in the elderly vs anti-inflammatory in the young). One study claims that IAV-induced IL-6 signalling causes muscle wasting in young mice by upregulation of Atrogin-1 (Radigan *et al.*, 2019). However, this study did not observe a noticeable change in Atrogin-1 expression with IL-6R blockade. This may be attributable to the highly variable weight loss phenotype in elderly mice.

6.6.2. Key methods

The intervention studies using anti-GDF-15 and anti-IL-6R monoclonal antibodies demonstrate that this model is suitable to conduct mechanistic studies, although the inherent higher variability in the elderly mice may necessitate an increased sample size.

6.7. Summary

Respiratory Syncytial Virus (RSV) is emerging as a common cause of severe respiratory infection in the elderly. Muscle weakness occurs naturally with age but can be exacerbated by inflammation or bedrest, and predisposes to a downward spiral of decreased activity, and higher risk of frailty and mortality. These observations suggest that respiratory viral infections are important in promoting frailty in the elderly. Despite its clinical im-

portance, the relationship between respiratory viral infection and muscle wasting in the elderly is not well understood. In this study, muscle wasting and the immune response were investigated in an aged mouse model of RSV infection. The study has demonstrated that elderly mice develop more severe RSV disease and experience muscle wasting. The loss of muscle mass was attributable to both an increase in atrophy-promoting processes and a decrease in muscle protein synthesis relative to young mice. Elderly mice produced lower titres of RSV-specific IgG, but had no defect in the numbers of germinal centre B cells or RSV-specific Tfh cells produced in response to the infection. The pharmacological inhibition of IL-6 signalling did not reliably affect the outcome of RSV infection or muscle wasting in elderly mice. Unexpectedly, the blockade of GDF-15, a TGF-β superfamily cytokine associated with poor prognosis in many diseases, led to enhanced muscle wasting in elderly mice infected with RSV, suggesting a metabolic protective effect of GDF-15 during increased systemic stress. These findings posit the elderly mouse RSV model as an appropriate choice for the investigation of a range of issues, including the antibody response, muscle wasting, and the mechanistics of age-related differences in antiviral responses.

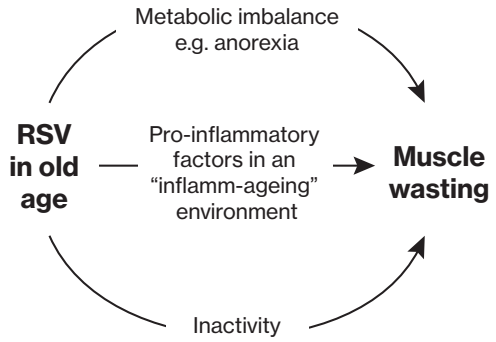

Figure 6-1 Overview of factors through which RSV may influence muscle wasting in the elderly

RSV infection in the elderly may lead to muscle wasting through various mechanisms, which may not all be present or contribute equally in every case. Anorexia was observed in elderly, but not young mice, after RSV infection. Due to the negative energy balance, it is likely that this contributed to muscle wasting in the model. Unexpectedly, blocking the known appetite suppressor GDF-15 did not alter food intake in elderly mice with RSV, suggesting that anorexia is not mediated by GDF-15 in this model. However, there was tentative evidence that blockade of GDF-15 promoted muscle wasting, which warrants further study. Although the influence of the pro-inflammatory cytokine IL-6 on muscle wasting could not be proven in this study, existing literature strongly suggests that a pro-inflammatory environment as is commonly found in the elderly is conducive to muscle wasting (Cesari et al., 2012; Muñoz-Cánoves et al., 2013). Inactivity was not separately interrogated in this study, but it is highly likely that sickness behaviour induced by RSV may lead to a downwards spiral of muscle wasting in the elderly (Kortebein et al., 2007; Tanner et al., 2015).

7.

References

Chapter 7. References

References are listed in alphabetical order.

Abe, S., Ezaki, O. & Suzuki, M. (2016) Medium-Chain Triglycerides in Combination with Leucine and Vitamin D Increase Muscle Strength and Function in Frail Elderly Adults in a Randomized Controlled Trial. *The Journal of Nutrition*. [Online] Available from: doi:10.3945/jn.115.228965.

Abulizi, P., Loganathan, N., Zhao, D., Mele, T., et al. (2017) Growth Differentiation Factor-15 Deficiency Augments Inflammatory Response and Exacerbates Septic Heart and Renal Injury Induced by Lipopolysaccharide. *Scientific Reports*. [Online] Available from: doi:10.1038/s41598-017-00902-5.

Ackerson, B., Tseng, H.F., Sy, L.S., Solano, Z., et al. (2018) Severe Morbidity and Mortality Associated With Respiratory Syncytial Virus Versus Influenza Infection in Hospitalized Older Adults. *Clinical Infectious Diseases*. [Online] Available from: doi:10.1093/cid/ciy991 [Accessed: 30 November 2018].

Acosta-Rodriguez, E. V., Napolitani, G., Lanzavecchia, A. & Sallusto, F. (2007) Interleukins 1β and 6 but not transforming growth factor-β are essential for the differentiation of interleukin 17-producing human T helper cells. *Nature Immunology*. [Online] Available from: doi:10.1038/ni1496.

Adler, A.S., Sinha, S., Kawahara, T.L.A., Zhang, J.Y., et al. (2007) Motif module map reveals enforcement of aging by continual NF-κB activity. *Genes and Development*. [Online] 21 (24), 3244–3257. Available from: doi:10.1101/gad.1588507 [Accessed: 20 November 2020].

Agius, E., Lacy, K.E., Vukmanovic-Stejic, M., Jagger, A.L., et al. (2009) Decreased TNF-α synthesis by macrophages restricts cutaneous immunosurveillance by memory CD4+ T cells during aging. *Journal of Experimental Medicine*. [Online] Available from: doi:10.1084/jem.20090896.

Agius, G., Dindinaud, G., Biggar, R.J., Peyre, R., et al. (1990) An epidemic of respiratory syncytial virus in elderly people: Clinical and serological findings. *Journal of Medical Virology*. [Online] Available from: doi:10.1002/jmv.1890300208.

Akbar, A.N., Henson, S.M. & Lanna, A. (2016) Senescence of T Lymphocytes: Implications for Enhancing Human Immunity. *Trends in Immunology*. [Online]. 37 (12) pp.866–876. Available from: doi:10.1016/j.it.2016.09.002 [Accessed: 24 November 2020].

Alers, S., Loffler, A.S., Wesselborg, S. & Stork, B. (2012) Role of AMPK-mTOR-Ulk1/2 in the Regulation of Autophagy: Cross Talk, Shortcuts, and Feedbacks. *Molecular and Cellular Biology*. [Online] 32 (1), 2–11. Available from: doi:10.1128/mcb.06159-11.

De Alvaro, C., Teruel, T., Hernandez, R. & Lorenzo, M. (2004) Tumor Necrosis Factor α Produces Insulin Resistance in Skeletal Muscle by Activation of Inhibitor κB Kinase in a p38 MAPK-dependent Manner. *Journal of Biological Chemistry*. [Online] Available from: doi:10.1074/jbc.M312021200.

Anderson, L.J., Hierholzer, J.C., Tsou, C., Michael Hendry, R., et al. (1985) Antigenic characterization of respiratory syncytial virus strains with monoclonal antibodies. *Journal of Infectious Diseases*. [Online] 151 (4), 626–633. Available from: doi:10.1093/infdis/151.4.626.

Anderson, N.W., Binnicker, M.J., Harris, D.M., Chirila, R.M., et al. (2016) Morbidity and mortality among patients with respiratory syncytial virus infection: a 2-year retrospective review. *Diagnostic Microbiology and Infectious Disease*. [Online] Available from: doi:10.1016/j.diagmicrobio.2016.02.025.

Ando, K., Takahashi, F., Kato, M., Kaneko, N., et al. (2014) Tocilizumab, a proposed therapy for the cachexia of interleukin6-expressing lung cancer. *PLoS ONE*. [Online] 9 (7). Available from: doi:10.1371/journal.pone.0102436.

Ando, K., Takahashi, F., Motojima, S., Nakashima, K., et al. (2013) Possible role for tocilizumab, an anti-interleukin-6 receptor antibody, in treating cancer cachexia. *Journal of clinical oncology : official journal of the American Society of Clinical Oncology*. [Online] 31 (6), e69-72. Available from: doi:10.1200/JCO.2012.44.2020 [Accessed: 9 April 2020].

Andres, V., Cervera, M. & Mahdavi, V. (1995) Determination of the consensus binding site for MEF2 expressed in muscle and brain reveals tissue-specific sequence constraints. *Journal of Biological Chemistry*. [Online] Available from: doi:10.1074/jbc.270.40.23246.

Anisimov, V.N., Berstein, L.M., Popovich, I.G., Zabezhinski, M.A., et al. (2011) If started early in life, metformin treatment increases life span and postpones tumors in female SHR mice. *Aging*. [Online] 3 (2), 148–157. Available from: doi:10.18632/aging.100273 [Accessed: 16 November 2020].

Anon (2016) Siltuximab (Sylvant). Castleman's disease: good symptomatic efficacy in some patients. [Online] 25 (169), 61–64. Available from: http://www.ncbi.nlm.nih.gov/pubmed/27152394 [Accessed: 7 April 2020].

Arango-Lopera, V.E., Arroyo, P., Gutierrez-Robledo, L.M., Perez-Zepeda, M.U., et al. (2013) Mortality as an adverse outcome of sarcopenia. *Journal of Nutrition, Health and Aging*. [Online] 17 (3), 259–262. Available from: doi:10.1007/s12603-012-0434-0.

Armanios, M., Alder, J.K., Parry, E.M., Karim, B., et al. (2009) Short Telomeres are Sufficient to Cause the Degenerative Defects Associated with Aging. *American Journal of Human Genetics*. [Online] 85 (6), 823–832. Available from: doi:10.1016/j.ajhg.2009.10.028.

Armanios, M. & Blackburn, E.H. (2012) The telomere syndromes. *Nature reviews. Genetics*. [Online]. Available from: doi:10.1038/nrg3246.

Atreya, R., Mudter, J., Finotto, S., Müllberg, J., et al. (2000) Blockade of interleukin 6 trans signaling suppresses T-cell resistance against apoptosis in chronic intestinal inflammation: Evidence in Crohn disease and experimental colitis in vivo. *Nature Medicine*. [Online] Available from: doi:10.1038/75068.

Aw, D., Hilliard, L., Nishikawa, Y., Cadman, E.T., et al. (2016) Disorganization of the splenic microanatomy in ageing mice. *Immunology*. [Online] 148 (1), 92–101. Available from: doi:10.1111/imm.12590.

Aw, D., Silva, A.B. & Palmer, D.B. (2007) Immunosenescence: Emerging challenges for an ageing population. *Immunology*. [Online]. 120 (4) pp.435–446. Available from: doi:10.1111/j.1365-2567.2007.02555.x [Accessed: 23 November 2020].

Aydar, Y., Balogh, P., Tew, J.G. & Szakal, A.K. (2004) Follicular dendritic cells in aging, a 'bottle-neck' in the humoral immune response. *Ageing Research Reviews*. [Online]. Available from: doi:10.1016/j.arr.2003.08.002.

Le Bacquer, O., Petroulakis, E., Paglialunga, S., Poulin, F., et al. (2007) Elevated sensitivity to diet-induced obesity and insulin resistance in mice lacking 4E-BP1 and 4E-BP2. *Journal of Clinical Investigation*. [Online] Available from: doi:10.1172/JCI29528.

Baek, S.J., Kim, K.S., Nixon, J.B., Wilson, L.C., et al. (2001) Cyclooxygenase inhibitors regulate the expression of a TGF-β superfamily member that has proapoptotic and antitumorigenic activities. *Molecular Pharmacology*. [Online] 59 (4), 901–908. Available from: doi:10.1124/mol.59.4.901.

Baek, S.J., Okazaki, R., Lee, S.H., Martinez, J., et al. (2006) Nonsteroidal Anti-Inflammatory Drug-Activated Gene-1 Over Expression in Transgenic Mice Suppresses Intestinal Neoplasia. *Gastroenterology*. [Online] Available from: doi:10.1053/j.gastro.2006.09.015.

Bahar, R., Hartmann, C.H., Rodriguez, K.A., Denny, A.D., et al. (2006) Increased cell-to-cell variation in gene expression in ageing mouse heart. *Nature*. [Online] 441 (7096), 1011–1014. Available from: doi:10.1038/nature04844 [Accessed: 15 November 2020].

Baker, D.J., Childs, B.G., Durik, M., Wijers, M.E., et al. (2016) Naturally occurring p16 Ink4a-positive cells shorten healthy lifespan. *Nature*. [Online] 530 (7589), 184–189. Available from: doi:10.1038/nature16932 [Accessed: 18 November 2020].

Baker, D.J., Wijshake, T., Tchkonia, T., Lebrasseur, N.K., et al. (2011) Clearance of p16 Ink4a-positive senescent cells delays ageing-associated disorders. *Nature*. [Online] 479 (7372), 232–236. Available from: doi:10.1038/nature10600 [Accessed: 18 November 2020].

Bär, E., Whitney, P.G., Moor, K., ReiseSousa, C., et al. (2014) IL-17 regulates systemic fungal immunity by controlling the functional competence of NK Cells. *Immunity*. [Online] 40 (1), 117–127. Available from: doi:10.1016/j.immuni.2013.12.002 [Accessed: 7 April 2020].

Baran, P., Nitz, R., Grötzinger, J., Scheller, J., et al. (2013) Minimal Interleukin 6 (IL-6) receptor stalk composition for IL-6 receptor shedding and IL-6 classic signaling. *Journal of Biological Chemistry*. [Online] Available from: doi:10.1074/jbc.M113.466169.

Barbieri, M., Ferrucci, L., Ragno, E., Corsi, A., et al. (2003) Chronic inflammation and the effect of IGF-I on muscle strength and power in older persons. *American Journal of Physiology - Endocrinology and Metabolism*. [Online] 284 (3 47-3). Available from: doi:10.1152/ajpendo.00319.2002.

Barkhausen, T., Tschernig, T., Rosenstiel, P., Van Griensven, M., et al. (2011) Selective blockade of interleukin-6 trans-signaling improves survival in a murine polymicrobial sepsis model. *Critical Care Medicine*. [Online] Available from: doi:10.1097/CCM.0b013e318211ff56.

Bartley, J., Hopkins, J. & Haynes, L. (2015) Influenza infection results in upregulation of inflammatory and atrophy genes in murine skeletal muscle (VIR5P.1146). *The Journal of Immunology*. 194 (1 Supplement).

Bartley, J.M., Pan, S.J., Keilich, S.R., Hopkins, J.W., et al. (2016) Aging augments the impact of influenza respiratory tract infection on mobility impairments, muscle-localized inflammation, and muscle atrophy. *Aging*. [Online] 8 (4), 620–635. Available from: doi:10.18632/aging.100882 [Accessed: 11 January 2018].

Barzilai, N., Huffman, D.M., Muzumdar, R.H. & Bartke, A. (2012) The critical role of metabolic pathways in aging. *Diabetes*. [Online]. Available from: doi:10.2337/db11-1300.

Basisty, N., Kale, A., Jeon, O.H., Kuehnemann, C., et al. (2020) A proteomic atlas of senescence-associated secretomes for aging biomarker development. *PLoS biology*. [Online] 18 (1), e3000599. Available from: doi:10.1371/journal.pbio.3000599 [Accessed: 18 November 2020].

Battles, M.B. & McLellan, J.S. (2019) Respiratory syncytial virus entry and how to block it. *Nature Reviews Microbiology*. [Online]. 17 (4) pp.233–245. Available from: doi:10.1038/s41579-019-0149-x.

Becklund, B.R., Purton, J.F., Ramsey, C., Favre, S., et al. (2016) The aged lymphoid tissue environment fails to support naive T cell homeostasis. *Scientific Reports*. [Online] Available from: doi:10.1038/srep30842.

Beekman, M., Blanché, H., Perola, M., Hervonen, A., et al. (2013) Genome-wide linkage analysis for human longevity: Genetics of healthy aging study. *Aging Cell*. [Online] 12 (2), 184–193. Available from: doi:10.1111/acel.12039 [Accessed: 21 November 2020].

Beerman, I., Bhattacharya, D., Zandi, S., Sigvardsson, M., et al. (2010) Functionally distinct hematopoietic stem cells modulate hematopoietic lineage potential during aging by a mechanism of clonal expansion. *Proceedings of the National Academy of Sciences of the United States of America*. [Online] Available from: doi:10.1073/pnas.1000834107.

Belsky, D.W., Huffman, K.M., Pieper, C.F., Shalev, I., et al. (2018) Change in the rate of biological aging in response to caloric restriction: Calerie Biobank analysis. *Journals of Gerontology - Series A Biological Sciences and Medical Sciences*. [Online] 73 (1), 4–10. Available from: doi:10.1093/gerona/glx096 [Accessed: 21 November 2020].

De Benedetti, F., Alonzi, T., Moretta, A., Lazzaro, D., et al. (1997) Interleukin 6 causes growth impairment in transgenic mice through a decrease in insulin-like growth factor-I. A model for stunted growth in children with chronic inflammation. *The Journal of clinical investigation*. [Online] 99 (4), 643–650. Available from: doi:10.1172/JCI119207 [Accessed: 7 May 2019].

Bermingham, A. & Collins, P.L. (1999) The M2-2 protein of human respiratory syncytial virus is a regulatory factor involved in the balance between RNA replication and transcription. *Proceedings of the National Academy of Sciences of the United States of America*. [Online] 96 (20), 11259–11264. Available from: doi:10.1073/pnas.96.20.11259.

Bernardes de Jesus, B., Vera, E., Schneeberger, K., Tejera, A.M., et al. (2012) Telomerase gene therapy in adult and old mice delays aging and increases longevity without increasing cancer. *EMBO Molecular Medicine*. [Online] 4 (8), 691–704. Available from: doi:10.1002/emmm.201200245 [Accessed: 15 November 2020].

Bhoj, V.G., Sun, Q., Bhoj, E.J., Somers, C., et al. (2008) MAVS and MyD88 are essential for innate immunity but not cytotoxic T lymphocyte response against respiratory syncytial virus. *Proceedings of the National Academy of Sciences of the United States of America*. [Online] Available from: doi:10.1073/pnas.0804717105.

Biressi, S. & Rando, T.A. (2010) Heterogeneity in the muscle satellite cell population. *Seminars in Cell and Developmental Biology*. [Online]. Available from: doi:10.1016/j.semcdb.2010.09.003.

Bitko, V. & Barik, S. (2001) An endoplasmic reticulum-specific stress-activated caspase (caspase-12) is implicated in the apoptosis of A549 epithelial cells by respiratory syncytial virus. *Journal of Cellular Biochemistry*. [Online] Available from: doi:10.1002/1097-4644(20010301)80:3<441::AID-JCB170>3.0.CO;2-C.

Bitko, V., Shulyayeva, O., Mazumder, B., Musiyenko, A., et al. (2007) Nonstructural Proteins of Respiratory Syncytial Virus Suppress Premature Apoptosis by an NF- B-Dependent, Interferon-Independent Mechanism and Facilitate Virus Growth. *Journal of Virology*. [Online] 81 (4), 1786–1795. Available from: doi:10.1128/jvi.01420-06.

Blaauw, B., Canato, M., Agatea, L., Toniolo, L., et al. (2009) Inducible activation of Akt increases skeletal muscle mass and force without satellite cell activation. *The FASEB Journal*. [Online] Available from: doi:10.1096/fj.09-131870.
Blackburn, E.H., Greider, C.W. & Szostak, J.W. (2006) Telomeres and telomerase: The path from maize, Tetrahymena and yeast to human cancer and aging. *Nature Medicine*. [Online]. 12 (10) pp.1133–1138. Available from: doi:10.1038/nm1006-1133.
Blasco, M.A. (2007) Telomere length, stem cells and aging. *Nature Chemical Biology*. [Online]. Available from: doi:10.1038/nchembio.2007.38.
Bleier, J.I., Pillarisetty, V.G., Shah, A.B. & DeMatteo, R.P. (2004) Increased and Long-Term Generation of Dendritic Cells with Reduced Function from IL-6-Deficient Bone Marrow. *The Journal of Immunology*. [Online] Available from: doi:10.4049/jimmunol.172.12.7408.
Bloch, S.A.A., Lee, J.Y., Syburra, T., Rosendahl, U., et al. (2015) Increased expression of GDF-15 may mediate ICU-acquired weakness by down-regulating muscle micrornas. *Thorax*. [Online] 70 (3), 219–228. Available from: doi:10.1136/thoraxjnl-2014-206225 [Accessed: 11 January 2018].
Bloch, S.A.A., Lee, J.Y., Wort, S.J., Polkey, M.I., et al. (2013) Sustained Elevation of Circulating Growth and Differentiation Factor-15 and a Dynamic Imbalance in Mediators of Muscle Homeostasis Are Associated With the Development of Acute Muscle Wasting Following Cardiac Surgery*. *Critical Care Medicine*. [Online] 41 (4), 982–989. Available from: doi:10.1097/CCM.0b013e318274671b [Accessed: 11 January 2018].
Blomberg, B.B. & Frasca, D. (2013) Age effects on mouse and human B cells. *Immunologic Research*. [Online] Available from: doi:10.1007/s12026-013-8440-9.
Bodine, S.C. & Baehr, L.M. (2014) Skeletal muscle atrophy and the E3 ubiquitin ligases MuRF1 and MAFbx/atrogin-1. *American Journal of Physiology - Endocrinology and Metabolism*. [Online] 307 (6). Available from: doi:10.1152/ajpendo.00204.2014 [Accessed: 11 January 2018].
Bodine, S.C., Latres, E., Baumhueter, S., Lai, V.K., et al. (2001a) Identification of Ubiquitin Ligases Required for Skeletal Muscle Atrophy. *Science*. [Online] 294 (5547), 1704–1708. Available from: doi:10.1126/science.1065874 [Accessed: 11 January 2018].
Bodine, S.C., Stitt, T.N., Gonzalez, M., Kline, W.O., et al. (2001b) Akt/mTOR pathway is a crucial regulator of skeletal muscle hypertrophy and can prevent muscle atrophy in vivo. *Nature Cell Biology*. [Online] Available from: doi:10.1038/ncb1101-1014.
Bodnar, A.G., Ouellette, M., Frolkis, M., Holt, S.E., et al. (1998) Extension of life-span by introduction of telomerase into normal human cells. *Science*. [Online] 279 (5349), 349–352. Available from: doi:10.1126/science.279.5349.349.
Boehmer, E.D., Goral, J., Faunce, D.E. & Kovacs, E.J. (2004) Age-dependent decrease in Toll-like receptor 4-mediated proinflammatory cytokine production and mitogen-activated protein kinase expression. *Journal of Leukocyte Biology*. [Online] Available from: doi:10.1189/jlb.0803389.
Boehmer, E.D., Meehan, M.J., Cutro, B.T. & Kovacs, E.J. (2005) Aging negatively skews macrophage TLR2- and TLR4-mediated pro-inflammatory responses without affecting the IL-2-stimulated pathway. *Mechanisms of Ageing and Development*. [Online] Available from: doi:10.1016/j.mad.2005.07.009.
Bootcov, M.R., Bauskin, A.R., Valenzuela, S.M., Moore, A.G., et al. (1997) MIC-1, a novel macrophage inhibitory cytokine, is a divergent member of the TGF-β superfamily. *Proceedings of the National Academy of Sciences of the United States of America*. [Online] 94 (21), 11514–11519. Available from: doi:10.1073/pnas.94.21.11514.
Boraschi, D., Aguado, M.T., Dutel, C., Goronzy, J., et al. (2013) The gracefully aging immune system. *Science Translational Medicine*. [Online]. 5 (185). Available from: doi:10.1126/scitranslmed.3005624.
Böttner, M., Suter-Crazzolara, C., Schober, A. & Unsicker, K. (1999) Expression of a novel member of the TGF-β superfamily, growth/differentiation factor-15/macrophage-inhibiting cytokine-1 (GDF-15/MIC-1) in adult rat tissues. *Cell and Tissue Research*. [Online] 297 (1), 103–110. Available from: doi:10.1007/s004410051337.
Boukhvalova, M.S., Yim, K.C., Kuhn, K.H., Hemming, J.P., et al. (2007) Age-related differences in pulmonary cytokine response to respiratory syncytial virus infection: Modulation by anti-inflammatory and antiviral treatment. *Journal of Infectious Diseases*. [Online] Available from: doi:10.1086/510628.
Brack, A.S., Bildsoe, H. & Hughes, S.M. (2005) Evidence that satellite cell decrement contributes to preferential decline in nuclear number from large fibres during murine age-related muscle atrophy. *Journal of Cell Science*. [Online] 118 (20), 4813–4821. Available from: doi:10.1242/jcs.02602.
Bratic, A. & Larsson, N.G. (2013) The role of mitochondria in aging. *Journal of Clinical Investigation*. [Online]. 123 (3) pp.951–957. Available from: doi:10.1172/JCI64125 [Accessed: 17 November 2020].
de Bree, G.J., Heidema, J., van Leeuwen, E.M.M., van Bleek, G.M., et al. (2005) Respiratory Syncytial Virus–Specific CD8 + Memory T Cell Responses in Elderly Persons . *The Journal of Infectious Diseases*. [Online] Available from: doi:10.1086/429695.
Breit, S.N., Carrero, J.J., Tsai, V.W.W., Yagoutifam, N., et al. (2012) Macrophage inhibitory cytokine-1 (MIC-1/GDF15) and mortality in end-stage renal disease. *Nephrology Dialysis Transplantation*. [Online] Available from: doi:10.1093/ndt/gfr575.
Breit, S.N., Tsai, V.W.-W. & Brown, D.A. (2017) Targeting Obesity and Cachexia: Identification of the GFRAL Receptor-MIC-1/GDF15 Pathway. *Trends in molecular medicine*. [Online] 23 (12), 1065–1067. Available from: doi:10.1016/j.molmed.2017.10.005 [Accessed: 8 August 2018].
Bret-Dibat, J.L., Bluthe, R.M., Kent, S., Kelley, K.W., et al. (1995) Lipopolysaccharide and interleukin-1 depress food-motivated behavior in mice by a vagal-mediated mechanism. *Brain Behavior and Immunity*. [Online] Available from: doi:10.1006/brbi.1995.1023.
Briguet, A., Courdier-Fruh, I., Foster, M., Meier, T., et al. (2004) Histological parameters for the quantitative assessment of muscular dystrophy in the mdx-mouse. *Neuromuscular Disorders*. [Online] Available from: doi:10.1016/j.nmd.2004.06.008.
Brinkmann, V., Reichard, U., Goosmann, C., Fauler, B., et al. (2004) Neutrophil Extracellular Traps Kill Bacteria. *Science*. [Online] Available from: doi:10.1126/science.1092385.
Briso, E.M., Dienz, O. & Rincon, M. (2008) Cutting Edge: Soluble IL-6R Is Produced by IL-6R Ectodomain Shedding in Activated CD4 T Cells. *The Journal of Immunology*. [Online] Available from: doi:10.4049/jimmunol.180.11.7102.
Bronikowski, A.M. & Flatt, T. (2010) Aging and Its Demographic Measurement How do we Define Aging Demographically? *Nature Education Knowledge*. [Online]. 1 (12). Available from: http://www.nature.com/scitable/knowledge/library/aging-and-i... [Accessed: 8 November 2020].
Brown, D.A., Breit, S.N., Buring, J., Fairlie, W.D., et al. (2002) Concentration in plasma of macrophage inhibitory cytokine-1 and risk of cardiovascular events in women: A nested case-control study. *Lancet*. [Online] Available from: doi:10.1016/S0140-

6736(02)09093-1.
Brown, D.A., Hance, K.W., Rogers, C.J., Sansbury, L.B., et al. (2012) Serum macrophage inhibitory cytokine-1 (MIC-1/GDF15): A potential screening tool for the prevention of colon cancer? *Cancer Epidemiology Biomarkers and Prevention*. [Online] Available from: doi:10.1158/1055-9965.EPI-11-0786.
Brown, D.A., Moore, J., Johnen, H., Smeets, T.J., et al. (2007) Serum macrophage inhibitory cytokine 1 in rheumatoid arthritis: A potential marker of erosive joint destruction. *Arthritis and Rheumatism*. [Online] Available from: doi:10.1002/art.22410.
Brown, D.A., Ward, R.L., Buckhaults, P., Liu, T., et al. (2003) MIC-1 serum level and genotype: Associations with progress and prognosis of colorectal carcinoma. *Clinical Cancer Research*.
Brown, K.L., Wathne, G.J., Sales, J., Bruce, M.E., et al. (2009) The Effects of Host Age on Follicular Dendritic Cell Status Dramatically Impair Scrapie Agent Neuroinvasion in Aged Mice. *The Journal of Immunology*. [Online] Available from: doi:10.4049/jimmunol.0802695.
Bryner, R.W., Woodworth-Hobbs, M.E., Williamson, D.L. & Alway, S.E. (2012) Docosahexaenoic Acid Protects Muscle Cells from Palmitate-Induced Atrophy. *ISRN Obesity*. [Online] Available from: doi:10.5402/2012/647348.
Buchberger, A., Ragge, K. & Arnold, H.H. (1994) The myogenin gene is activated during myocyte differentiation by pre- existing, not newly synthesized transcription factor MEF-2. *Journal of Biological Chemistry*.
Bulati, M., Buffa, S., Candore, G., Caruso, C., et al. (2011) B cells and immunosenescence: A focus on IgG+IgD-CD27- (DN) B cells in aged humans. *Ageing Research Reviews*. [Online]. Available from: doi:10.1016/j.arr.2010.12.002.
Burtner, C.R. & Kennedy, B.K. (2010) Progeria syndromes and ageing: What is the connection? *Nature Reviews Molecular Cell Biology*. [Online]. 11 (8) pp.567–578. Available from: doi:10.1038/nrm2944.
Cai, D., Frantz, J.D., Tawa, N.E., Melendez, P.A., et al. (2004) IKKβ/NF-κB activation causes severe muscle wasting in mice. *Cell*. [Online] Available from: doi:10.1016/j.cell.2004.09.027.
Calabrese, V., Cornelius, C., Cuzzocrea, S., Iavicoli, I., et al. (2011) Hormesis, cellular stress response and vitagenes as critical determinants in aging and longevity. *Molecular Aspects of Medicine*. [Online] 32 (4–6), 279–304. Available from: doi:10.1016/j.mam.2011.10.007.
Caldeira Da Silva, C.C., Cerqueira, F.M., Barbosa, L.F., Medeiros, M.H.G., et al. (2008) Mild mitochondrial uncoupling in mice affects energy metabolism, redox balance and longevity. *Aging Cell*. [Online] 7 (4), 552–560. Available from: doi:10.1111/j.1474-9726.2008.00407.x [Accessed: 17 November 2020].
Campbell, I.L., Abraham, C.R., Masliah, E., Kemper, P., et al. (1993) Neurologic disease induced in transgenic mice by cerebral overexpression of interleukin 6. *Proceedings of the National Academy of Sciences of the United States of America*. [Online] Available from: doi:10.1073/pnas.90.21.10061.
Campbell, I.L., Erta, M., Lim, S.L., Frausto, R., et al. (2014) Trans-signaling is a dominant mechanism for the pathogenic actions of interleukin-6 in the brain. *Journal of Neuroscience*. [Online] Available from: doi:10.1523/JNEUROSCI.2830-13.2014.
Cao, L., Li, W., Kim, S., Brodie, S.G., et al. (2003) Senescence, aging, and malignant transformation mediated by p53 in mice lacking the brca1 full-length isoform. *Genes and Development*. [Online] 17 (2), 201–213. Available from: doi:10.1101/gad.1050003 [Accessed: 18 November 2020].
Carey, A.L., Steinberg, G.R., Macaulay, S.L., Thomas, W.G., et al. (2006) Interleukin-6 increases insulin-stimulated glucose disposal in humans and glucose uptake and fatty acid oxidation in vitro via AMP-activated protein kinase. *Diabetes*. [Online] Available from: doi:10.2337/db05-1404.
Carstensen, M., Herder, C., Brunner, E.J., Strassburger, K., et al. (2010) Macrophage inhibitory cytokine-1 is increased in individuals before type 2 diabetes diagnosis but is not an independent predictor of type 2 diabetes: the Whitehall II study. *European journal of endocrinology*. [Online] 162 (5), 913–917. Available from: doi:10.1530/EJE-09-1066 [Accessed: 13 January 2018].
Casanovas, G., Spasić, M.V., Casu, C., Rivella, S., et al. (2013) The murine growth differentiation factor 15 is not essential for systemic iron homeostasis in phlebotomized mice. *Haematologica*. [Online] Available from: doi:10.3324/haematol.2012.069807.
Castilho, R.M., Squarize, C.H., Chodosh, L.A., Williams, B.O., et al. (2009) mTOR Mediates Wnt-Induced Epidermal Stem Cell Exhaustion and Aging. *Cell Stem Cell*. [Online] Available from: doi:10.1016/j.stem.2009.06.017.
Castillero, E., Martín, A.I., López-Menduiña, M., Villanúa, M.A., et al. (2009) Eicosapentaenoic acid attenuates arthritis-induced muscle wasting acting on atrogin-1 and on myogenic regulatory factors. *American Journal of Physiology - Regulatory Integrative and Comparative Physiology*. [Online] Available from: doi:10.1152/ajpregu.00388.2009.
Castilow, E.M., Olson, M.R., Meyerholz, D.K. & Varga, S.M. (2008) Differential Role of Gamma Interferon in Inhibiting Pulmonary Eosinophilia and Exacerbating Systemic Disease in Fusion Protein-Immunized Mice Undergoing Challenge Infection with Respiratory Syncytial Virus. *Journal of Virology*. [Online] 82 (5), 2196–2207. Available from: doi:10.1128/jvi.01949-07 [Accessed: 22 November 2020].
Cerletti, M., Jang, Y.C., Finley, L.W.S., Haigis, M.C., et al. (2012) Short-term calorie restriction enhances skeletal muscle stem cell function. *Cell Stem Cell*. [Online] Available from: doi:10.1016/j.stem.2012.04.002.
Cervantes-Ortiz, S.L., Cuervo, N.Z. & Grandvaux, N. (2016) Respiratory syncytial virus and cellular stress responses: Impact on replication and physiopathology. *Viruses*. [Online]. Available from: doi:10.3390/v8050124.
Cesari, M., Kritchevsky, S.B., Nicklas, B., Kanaya, A.M., et al. (2012) Oxidative damage, platelet activation, and inflammation to predict mobility disability and mortality in older persons: Results from the health aging and body composition study. *Journals of Gerontology - Series A Biological Sciences and Medical Sciences*. [Online] Available from: doi:10.1093/gerona/glr246.
Chanock, R. & Finberg, L. (1957) Recovery from Infants with Respiratory Illness of a Virus related to Chimpanzee Coryza Agent (CCA). II. Epidemiologic Aspects of Infection in Infants and Young Children. *American Journal of Hygiene*. [Online] 66 (3), 291–300. Available from: https://www.cabdirect.org/cabdirect/abstract/19582701408 [Accessed: 5 March 2020].
Chanock, R., Roizman, B. & Myers, R. (1957) Recovery from infants with respiratory illness of a virus related to chimpanzee coryza agent (CCA): Isolation, properties and characterization. *American Journal of Hygiene*. [Online] 66 (3), 281–290. Available from: doi:10.1093/oxfordjournals.aje.a119901.
Chelvarajan, R.L., Collins, S.M., Van Willigen, J.M. & Bondada, S. (2005) The unresponsiveness of aged mice to polysaccharide antigens is a result of a defect in macrophage function. *Journal of Leukocyte Biology*. [Online] Available from: doi:10.1189/jlb.0804449.
Chen, C., Liu, Y., Liu, Y. & Zheng, P. (2009) MTOR regulation and therapeutic rejuvenation of aging hematopoietic stem cells. *Science Signaling*. [Online] Available from: doi:10.1126/scisignal.2000559.

Chen, T.L., Dai, Z., Mo, P., Li, X., et al. (2020) Clinical Characteristics and Outcomes of Older Patients with Coronavirus Disease 2019 (COVID-19) in Wuhan, China: A Single-Centered, Retrospective Study. *Journals of Gerontology - Series A Biological Sciences and Medical Sciences*. [Online] Available from: doi:10.1093/gerona/glaa089.
Cheng, T., Rodrigues, N., Shen, H., Yang, Y.G., et al. (2000) Hematopoietic stem cell quiescence maintained by p21(cip1/waf1). *Science*. [Online] Available from: doi:10.1126/science.287.5459.1804.
Cherukuri, A., Patton, K., Gasser, R.A., Zuo, F., et al. (2013) Adults 65 years old and older have reduced numbers of functional memory T cells to respiratory syncytial virus fusion protein. *Clinical and vaccine immunology : CVI*. [Online] 20 (2), 239–247. Available from: doi:10.1128/CVI.00580-12 [Accessed: 12 February 2019].
Chiu, C. & Openshaw, P.J. (2015) Antiviral B cell and T cell immunity in the lungs. *Nature Immunology*. [Online]. 16 (1) pp.18–26. Available from: doi:10.1038/ni.3056.
Chomarat, P., Banchereau, J., Davoust, J. & Palucka, A.K. (2000) IL-6 switches the differentiation of monocytes from dendritic cells to macrophages. *Nature Immunology*. [Online] Available from: doi:10.1038/82763.
Chrysovergis, K., Wang, X., Kosak, J., Lee, S.-H., et al. (2014) NAG-1/GDF-15 prevents obesity by increasing thermogenesis, lipolysis and oxidative metabolism. *International Journal of Obesity*. [Online] 38 (12), 1555–1564. Available from: doi:10.1038/ijo.2014.27 [Accessed: 6 August 2018].
Chu, H.Y., Steinhoff, M.C., Magaret, A., Zaman, K., et al. (2014) Respiratory Syncytial Virus Transplacental Antibody Transfer and Kinetics in Mother-Infant Pairs in Bangladesh. *Journal of Infectious Diseases*. [Online] Available from: doi:10.1093/infdis/jiu316.
Clarke, B.A., Drujan, D., Willis, M.S., Murphy, L.O., et al. (2007) The E3 Ligase MuRF1 Degrades Myosin Heavy Chain Protein in Dexamethasone-Treated Skeletal Muscle. *Cell Metabolism*. [Online] 6 (5), 376–385. Available from: doi:10.1016/j.cmet.2007.09.009.
Clavel, S., Coldefy, A.S., Kurkdjian, E., Salles, J., et al. (2006) Atrophy-related ubiquitin ligases, atrogin-1 and MuRF1 are up-regulated in aged rat Tibialis Anterior muscle. *Mechanisms of Ageing and Development*. [Online] Available from: doi:10.1016/j.mad.2006.07.005.
Clop, A., Marcq, F., Takeda, H., Pirottin, D., et al. (2006) A mutation creating a potential illegitimate microRNA target site in the myostatin gene affects muscularity in sheep. *Nature Genetics*. [Online] Available from: doi:10.1038/ng1810.
Cohen, S., Brault, J.J., Gygi, S.P., Glass, D.J., et al. (2009) During muscle atrophy, thick, but not thin, filament components are degraded by MuRF1-dependent ubiquitylation. *Journal of Cell Biology*. [Online] 185 (6), 1083–1095. Available from: doi:10.1083/jcb.200901052.
Collado, M., Blasco, M.A. & Serrano, M. (2007) Cellular Senescence in Cancer and Aging. *Cell*. [Online]. 130 (2) pp.223–233. Available from: doi:10.1016/j.cell.2007.07.003.
Collins, C.A., Olsen, I., Zammit, P.S., Heslop, L., et al. (2005) Stem cell function, self-renewal, and behavioral heterogeneity of cells from the adult muscle satellite cell niche. *Cell*. [Online] Available from: doi:10.1016/j.cell.2005.05.010.
Colman, R.J., Anderson, R.M., Johnson, S.C., Kastman, E.K., et al. (2009) Caloric restriction delays disease onset and mortality in rhesus monkeys. *Science*. [Online] 325 (5937), 201–204. Available from: doi:10.1126/science.1173635 [Accessed: 16 November 2020].
Colonna-Romano, G., Aquino, A., Bulati, M., Di Lorenzo, G., et al. (2006) Memory B cell subpopulations in the aged. In: *Rejuvenation Research*. [Online]. 2006 p. Available from: doi:10.1089/rej.2006.9.149.
Conboy, I.M., Conboy, M.J., Wagers, A.J., Girma, E.R., et al. (2005) Rejuvenation of aged progenitor cells by exposure to a young systemic environment. *Nature*. [Online] Available from: doi:10.1038/nature03260.
Conboy, I.M. & Rando, T.A. (2012) Heterochronic parabiosis for the study of the effects of aging on stem cells and their niches. *Cell Cycle*. [Online]. Available from: doi:10.4161/cc.20437.
Conery, A.R., Cao, Y., Thompson, E.A., Townsend, C.M., et al. (2004) Akt interacts directly with Smad3 to regulate the sensitivity to TGF-β-induced apoptosis. *Nature Cell Biology*. [Online] Available from: doi:10.1038/ncb1117.
Cong, H., Sun, L., Liu, C. & Tien, P. (2011) Inhibition of atrogin-1/MAFbx expression by adenovirus-delivered small hairpin RNAs attenuates muscle atrophy in fasting mice. *Human Gene Therapy*. [Online] Available from: doi:10.1089/hum.2010.057.
Connor, E.M. (1998) Palivizumab, a humanized respiratory syncytial virus monoclonal antibody, reduces hospitalization from respiratory syncytial virus infection in high-risk infants. *Pediatrics*. [Online] Available from: doi:10.1542/peds.102.3.531.
Cornelison, D.D.W., Olwin, B.B., Rudnicki, M.A. & Wold, B.J. (2000) MyoD(-/-) satellite cells in single-fiber culture are differentiation defective and MRF4 deficient. *Developmental Biology*. [Online] Available from: doi:10.1006/dbio.2000.9682.
Cotter, G., Voors, A., Prescott, M., Felker, G., et al. (2015) Growth differentiation factor 15 (GDF-15) in patients admitted for acute heart failure: results from the RELAX-AHF study. *European journal of heart failure*. [Online]. 17 (11) pp.1133–1143. Available from: doi:10.1002/ejhf.331.
Coulie, P.G., Vink, A. & Van Snick, J. (1990) A monoclonal antibody specific for the murine IL-6-receptor inhibits the growth of a mouse plasmacytoma in vivo. In: *Current Topics in Microbiology and Immunology*. [Online]. 1990 pp. 43–46. Available from: doi:10.1007/978-3-642-75889-8_6.
Cruz-Jentoft, A.J. & Sayer, A.A. (2019) Sarcopenia. *The Lancet*. [Online]. 393 (10191) pp.2636–2646. Available from: doi:10.1016/S0140-6736(19)31138-9.
Curtis, S.J., Ottolini, M.G., Porter, D.D. & Prince, G.A. (2002) Age-dependent replication of respiratory syncytial virus in the cotton rat. *Experimental Biology and Medicine*. [Online] 227 (9), 799–802. Available from: doi:10.1177/153537020222700912 [Accessed: 25 November 2020].
Cusella-De Angelis, M.G., Lyons, G., Sonnino, C., De Angelis, L., et al. (1992) MyoD, myogenin independent differentiation of primordial myoblasts in mouse somites. *Journal of Cell Biology*. [Online] Available from: doi:10.1083/jcb.116.5.1243.
Cusi, M.G., Martorelli, B., Di Genova, G., Terrosi, C., et al. (2010) Age related changes in T cell mediated immune response and effector memory to Respiratory Syncytial Virus (RSV) in healthy subjects. *Immunity and Ageing*. [Online] Available from: doi:10.1186/1742-4933-7-14.
Daste, A., Domblides, C., Gross-goupil, M., Chakiba, C., et al. (2017) Immune checkpoint inhibitors and elderly people: A review. *European Journal of Cancer*. [Online]. Available from: doi:10.1016/j.ejca.2017.05.044.
David, A., Dolan, B.P., Hickman, H.D., Knowlton, J.J., et al. (2012) Nuclear translation visualized by ribosome-bound nascent chain puromycylation. *Journal of Cell Biology*. [Online] 197 (1), 45–57. Available from: doi:10.1083/jcb.201112145 [Accessed: 6

February 2018].
Davis, R.L., Weintraub, H. & Lassar, A.B. (1987) Expression of a single transfected cDNA converts fibroblasts to myoblasts. *Cell*. [Online] Available from: doi:10.1016/0092-8674(87)90585-X.
Day, K., Shefer, G., Shearer, A. & Yablonka-Reuveni, Z. (2010) The depletion of skeletal muscle satellite cells with age is concomitant with reduced capacity of single progenitors to produce reserve progeny. *Developmental Biology*. [Online] 340 (2), 330–343. Available from: doi:10.1016/j.ydbio.2010.01.006.
Debrabant, B., Soerensen, M., Flachsbart, F., Dato, S., et al. (2014) Human longevity and variation in DNA damage response and repair: Study of the contribution of sub-processes using competitive gene-set analysis. *European Journal of Human Genetics*. [Online] 22 (9), 1131–1136. Available from: doi:10.1038/ejhg.2013.299 [Accessed: 21 November 2020].
Deelen, J., Beekman, M., Uh, H.W., Broer, L., et al. (2014) Genome-wide association meta-analysis of human longevity identifies a novel locus conferring survival beyond 90 years of age. *Human Molecular Genetics*. [Online] 23 (16), 4420–4432. Available from: doi:10.1093/hmg/ddu139 [Accessed: 21 November 2020].
Diamant, M., Rieneck, K., Mechti, N., Zhang, X.G., et al. (1997) Cloning and expression of an alternatively spliced mRNA encoding a soluble form of the human interleukin-6 signal transducer gp130. *FEBS Letters*. [Online] Available from: doi:10.1016/S0014-5793(97)00750-3.
DiCosmo, B.F., Geba, G.P., Picarella, D., Elias, J.A., et al. (1994) Airway epithelial cell expression of interleukin-6 in transgenic mice. Uncoupling of airway inflammation and bronchial hyperreactivity. *Journal of Clinical Investigation*. [Online] Available from: doi:10.1172/JCI117556.
Dienz, O., Eaton, S.M., Bond, J.P., Neveu, W., et al. (2009) The induction of antibody production by IL-6 is indirectly mediated by IL-21 produced by CD4 $^{+}$ T cells. *The Journal of Experimental Medicine*. [Online] 206 (1), 69–78. Available from: doi:10.1084/jem.20081571 [Accessed: 29 January 2019].
Dienz, O., Rud, J.G., Eaton, S.M., Lanthier, P.A., et al. (2012) Essential role of IL-6 in protection against H1N1 influenza virus by promoting neutrophil survival in the lung. *Mucosal Immunology*. [Online] Available from: doi:10.1038/mi.2012.2.
Ding, Q., Mracek, T., Gonzalez-Muniesa, P., Kos, K., et al. (2009) Identification of macrophage inhibitory cytokine-1 in adipose tissue and its secretion as an adipokine by human adipocytes. *Endocrinology*. [Online] Available from: doi:10.1210/en.2008-0952.
Ditt, V., Lüsebrink, J., Tillmann, R.L., Schildgen, V., et al. (2011) Respiratory infections by HMPV and RSV are clinically indistinguishable but induce different host response in aged individuals. *PLoS ONE*. [Online] Available from: doi:10.1371/journal.pone.0016314.
Docherty, A.B., Harrison, E.M., Green, C.A., Hardwick, H.E., et al. (2020) Features of 20 133 UK patients in hospital with covid-19 using the ISARIC WHO Clinical Characterisation Protocol: Prospective observational cohort study. *The BMJ*. [Online] 369. Available from: doi:10.1136/bmj.m1985 [Accessed: 22 November 2020].
Doonan, R., McElwee, J.J., Matthijssens, F., Walker, G.A., et al. (2008) Against the oxidative damage theory of aging: Superoxide dismutases protect against oxidative stress but have little or no effect on life span in Caenorhabditis elegans. *Genes and Development*. [Online] 22 (23), 3236–3241. Available from: doi:10.1101/gad.504808 [Accessed: 17 November 2020].
Dostálová, I., Kaválková, P., Papeová, H., Domluvilová, D., et al. (2010) Association of macrophage inhibitory cytokine-1 with nutritional status, body composition and bone mineral density in patients with anorexia nervosa: The influence of partial realimentation. *Nutrition and Metabolism*. [Online] Available from: doi:10.1186/1743-7075-7-34.
Dostálová, I., Roubíček, T., Bártlová, M., Mráz, M., et al. (2009) Increased serum concentrations of macrophage inhibitory cytokine-1 in patients with obesity and type 2 diabetes mellitus: The influence of very low calorie diet. *European Journal of Endocrinology*. [Online] Available from: doi:10.1530/EJE-09-0417.
Duggal, N.A., Pollock, R.D., Lazarus, N.R., Harridge, S., et al. (2018) Major features of immunesenescence, including reduced thymic output, are ameliorated by high levels of physical activity in adulthood. *Aging Cell*. [Online] 17 (2), e12750. Available from: doi:10.1111/acel.12750 [Accessed: 21 November 2020].
van Duin, D., Allore, H.G., Mohanty, S., Ginter, S., et al. (2007a) Prevaccine determination of the expression of costimulatoiy B7 molecules in activated monocytes predicts influenza vaccine responses in young and older adults. *Journal of Infectious Diseases*. [Online] Available from: doi:10.1086/516788.
van Duin, D., Mohanty, S., Thomas, V., Ginter, S., et al. (2007b) Age-Associated Defect in Human TLR-1/2 Function. *The Journal of Immunology*. [Online] 178 (2), 970–975. Available from: doi:10.4049/jimmunol.178.2.970 [Accessed: 23 November 2020].
Dunston, C.R. & Griffiths, H.R. (2010) The effect of ageing on macrophage Toll-like receptor-mediated responses in the fight against pathogens. *Clinical and Experimental Immunology*. [Online]. Available from: doi:10.1111/j.1365-2249.2010.04213.x.
Ebisui, C., Tsujinaka, T., Morimoto, T., Kan, K., et al. (1995) Interleukin-6 induces proteolysis by activating intracellular proteases (cathepsins B and L, proteasome) in C2C12 myotubes. *Clinical Science*. [Online] Available from: doi:10.1042/cs0890431.
Edmondson, D.G., Cheng, T.C., Cserjesi, P., Chakraborty, T., et al. (1992) Analysis of the myogenin promoter reveals an indirect pathway for positive autoregulation mediated by the muscle-specific enhancer factor MEF-2. *Molecular and Cellular Biology*. [Online] Available from: doi:10.1128/mcb.12.9.3665.
Edström, E., Altun, M., Hägglund, M. & Ulfhake, B. (2006) Atrogin-1/MAFbx and MuRF1 are downregulated in aging-related loss of skeletal muscle. *Journals of Gerontology - Series A Biological Sciences and Medical Sciences*. [Online] Available from: doi:10.1093/gerona/61.7.663.
Eichinger, K.M., Egaña, L., Orend, J.G., Resetar, E., et al. (2015) Alveolar macrophages support interferon gamma-mediated viral clearance in RSVinfected neonatal mice. *Respiratory Research*. [Online] 16 (1). Available from: doi:10.1186/s12931-015-0282-7 [Accessed: 22 November 2020].
Eichinger, K.M., Resetar, E., Orend, J., Anderson, K., et al. (2017) Age predicts cytokine kinetics and innate immune cell activation following intranasal delivery of IFNγ and GM-CSF in a mouse model of RSV infection. *Cytokine*. [Online] 97, 25–37. Available from: doi:10.1016/j.cyto.2017.05.019 [Accessed: 22 November 2020].
Eisenberg, T., Knauer, H., Schauer, A., Büttner, S., et al. (2009) Induction of autophagy by spermidine promotes longevity. *Nature Cell Biology*. [Online] 11 (11), 1305–1314. Available from: doi:10.1038/ncb1975 [Accessed: 15 November 2020].
Ek, M., Kurosawa, M., Lundeberg, T. & Ericsson, A. (1998) Activation of vagal afferents after intravenous injection of interleukin-1β: Role of endogenous prostaglandins. *Journal of Neuroscience*. [Online] Available from: doi:10.1523/jneurosci.18-22-09471.1998.
Ekmark, M., Rana, Z.A., Stewart, G., Hardie, D.G., et al. (2007) De-phosphorylation of MyoD is linking nerve-evoked activity to fast

myosin heavy chain expression in rodent adult skeletal muscle. *Journal of Physiology*. [Online] Available from: doi:10.1113/jphysiol.2007.141457.
Elander, L., Engström, L., Hallbeck, M. & Blomqvist, A. (2007) IL-1β and LPS induce anorexia by distinct mechanisms differentially dependent on microsomal prostaglandin E synthase-1. *American Journal of Physiology - Regulatory Integrative and Comparative Physiology*. [Online] Available from: doi:10.1152/ajpregu.00511.2006.
Emery, P., Keystone, E., Tony, H.P., Cantagrel, A., et al. (2008) IL-6 receptor inhibition with tocilizumab improves treatment outcomes in patients with rheumatoid arthritis refractory to anti-tumour necrosis factor biologicals: Results from a 24-week multicentre randomised placebo-controlled trial. *Annals of the Rheumatic Diseases*. [Online] 67 (11), 1516–1523. Available from: doi:10.1136/ard.2008.092932.
Emmerson, P.J., Wang, F., Du, Y., Liu, Q., et al. (2017) The metabolic effects of GDF15 are mediated by the orphan receptor GFRAL. *Nature Medicine*. [Online] 23 (10), 1215–1219. Available from: doi:10.1038/nm.4393 [Accessed: 11 January 2018].
Fairlie, W.D., Moore, A.G., Bauskin, A.R., Russell, P.K., et al. (1999) MIC-1 is a novel TGF-β superfamily cytokine associated with macrophage activation. *Journal of Leukocyte Biology*. [Online] 65 (1), 2–5. Available from: doi:10.1002/jlb.65.1.2 [Accessed: 27 March 2020].
Falsey, A.R. & Walsh, E.E. (1998) Relationship of serum antibody to risk of respiratory syncytial virus infection in elderly adults. *The Journal of infectious diseases*. 177 (2), 463–466.
Falsey, A.R. & Walsh, E.E. (2005) Respiratory Syncytial Virus Infection in Elderly Adults. *Drugs & Aging*. [Online] 22 (7), 577–587. Available from: doi:10.2165/00002512-200522070-00004.
Faralli, H. & Dilworth, F.J. (2012) Turning on Myogenin in Muscle: A Paradigm for Understanding Mechanisms of Tissue-Specific Gene Expression. *Comparative and Functional Genomics*. [Online] 2012. Available from: doi:10.1155/2012/836374.
Faunce, D.E., Palmer, J.L., Paskowicz, K.K., Witte, P.L., et al. (2005) CD1d-Restricted NKT Cells Contribute to the Age-Associated Decline of T Cell Immunity. *The Journal of Immunology*. [Online] Available from: doi:10.4049/jimmunol.175.5.3102.
Fearns, R., Peeples, M.E. & Collins, P.L. (2002) Mapping the Transcription and Replication Promoters of Respiratory Syncytial Virus. *Journal of Virology*. [Online] Available from: doi:10.1128/jvi.76.4.1663-1672.2002.
Febbraio, M.A. & Pedersen, B.K. (2005) Contraction-induced myokine production and release: Is skeletal muscle an endocrine organ? *Exercise and Sport Sciences Reviews*. [Online]. Available from: doi:10.1097/00003677-200507000-00003.
Fejzo, M.S., Sazonova, O. V., Sathirapongsasuti, J.F., Hallgrímsdóttir, I.B., et al. (2018) Placenta and appetite genes GDF15 and IGFBP7 are associated with hyperemesis gravidarum. *Nature Communications*. [Online] Available from: doi:10.1038/s41467-018-03258-0.
Fernández-Celemín, L. & Thissen, J.P. (2001) Interleukin-6 stimulates hepatic insulin-like growth factor binding protein-4 messenger ribonucleic acid and protein. *Endocrinology*. [Online] 142 (1), 241–248. Available from: doi:10.1210/endo.142.1.7903 [Accessed: 10 April 2020].
Ferreira, G., Ferry, B., Meurisse, M. & Lévy, F. (2006) Forebrain structures specifically activated by conditioned taste aversion. *Behavioral Neuroscience*. [Online] Available from: doi:10.1037/0735-7044.120.4.952.
Fiaccavento, R., Carotenuto, F., Vecchini, A., Binaglia, L., et al. (2010) An omega-3 fatty acid-enriched diet prevents skeletal muscle lesions in a hamster model of dystrophy. *American Journal of Pathology*. [Online] Available from: doi:10.2353/ajpath.2010.100174.
Fielitz, J., Kim, M.S., Shelton, J.M., Latif, S., et al. (2007) Myosin accumulation and striated muscle myopathy result from the loss of muscle RING finger 1 and 3. *Journal of Clinical Investigation*. [Online] Available from: doi:10.1172/JCI32827.
Flatt, T. (2012) A new definition of aging? *Frontiers in Genetics*. [Online]. 3 (AUG). Available from: doi:10.3389/fgene.2012.00148 [Accessed: 8 November 2020].
Flores, I., Cayuela, M.L. & Blasco, M.A. (2005) Molecular biology: Effects of telomerase and telomere length on epidermal stem cell behavior. *Science*. [Online] Available from: doi:10.1126/science.1115025.
Flynn, J.M., Meadows, E., Fiorotto, M. & Klein, W.H. (2010) Myogenin regulates exercise capacity and skeletal muscle metabolism in the adult mouse. *PLoS ONE*. [Online] Available from: doi:10.1371/journal.pone.0013535.
Fraga, M.F. & Esteller, M. (2007) Epigenetics and aging: the targets and the marks. *Trends in Genetics*. [Online]. 23 (8) pp.413–418. Available from: doi:10.1016/j.tig.2007.05.008.
Franceschi, C., Bonafè, M., Valensin, S., Olivieri, F., et al. (2006) Inflamm-aging: An Evolutionary Perspective on Immunosenescence. *Annals of the New York Academy of Sciences*. [Online] 908 (1), 244–254. Available from: doi:10.1111/j.1749-6632.2000.tb06651.x.
Franceschi, C., Capri, M., Monti, D., Giunta, S., et al. (2007) Inflammaging and anti-inflammaging: A systemic perspective on aging and longevity emerged from studies in humans. *Mechanisms of Ageing and Development*. [Online] 128 (1), 92–105. Available from: doi:10.1016/j.mad.2006.11.016.
Frasca, D., Van der Put, E., Riley, R.L. & Blomberg, B.B. (2004) Reduced Ig Class Switch in Aged Mice Correlates with Decreased E47 and Activation-Induced Cytidine Deaminase. *The Journal of Immunology*. [Online] Available from: doi:10.4049/jimmunol.172.4.2155.
Fraunberger, P., Wang, Y., Holler, E., Parhofer, K.G., et al. (2006) Prognostic value of interleukin 6, procalcitonin, and C-reactive protein levels in intensive care unit patients during first increase of fever. *Shock*. [Online] Available from: doi:10.1097/01.shk.0000215319.06866.bd.
Freeman, A.F. & Holland, S.M. (2010) Clinical manifestations of hyper IgE syndromes. *Disease Markers*. [Online] Available from: doi:10.3233/DMA-2010-0734.
Füchtbauer, E. -M & Westphal, H. (1992) MyoD and myogenin are coexpressed in regenerating skeletal muscle of the mouse. *Developmental Dynamics*. [Online] Available from: doi:10.1002/aja.1001930106.
Fuentes, S., Tran, K.C., Luthra, P., Teng, M.N., et al. (2007) Function of the Respiratory Syncytial Virus Small Hydrophobic Protein. *Journal of Virology*. [Online] 81 (15), 8361–8366. Available from: doi:10.1128/jvi.02717-06.
Fujimoto, M., Nakano, M., Terabe, F., Kawahata, H., et al. (2011) The Influence of Excessive IL-6 Production In Vivo on the Development and Function of Foxp3 + Regulatory T Cells . *The Journal of Immunology*. [Online] Available from: doi:10.4049/jimmunol.0903314.
Fujita, Y., Taniguchi, Y., Tanaka, M., Shinkai, S., et al. (2017) Serum GDF15 predicts all-cause mortality in a general population of Japanese elderly. *Innovation in Aging*. [Online] Available from: doi:10.1093/geroni/igx004.2901.

Fulop, T., Larbi, A., Dupuis, G., Page, A. Le, et al. (2018) Immunosenescence and inflamm-aging as two sides of the same coin: Friends or Foes? *Frontiers in Immunology*. [Online]. 8 (JAN). Available from: doi:10.3389/fimmu.2017.01960 [Accessed: 24 November 2020].

Fulop, T., Le Page, A., Fortin, C., Witkowski, J.M., et al. (2014) Cellular signaling in the aging immune system. *Current Opinion in Immunology*. [Online]. Available from: doi:10.1016/j.coi.2014.05.007.

Fulton, R.B., Weiss, K.A., Pewe, L.L., Harty, J.T., et al. (2013) Aged Mice Exhibit a Severely Diminished CD8 T Cell Response following Respiratory Syncytial Virus Infection. *Journal of Virology*. [Online] 87 (23), 12694–12700. Available from: doi:10.1128/jvi.02282-12 [Accessed: 26 June 2019].

Gabay, C. & Kushner, I. (1999) Acute-Phase Proteins and Other Systemic Responses to Inflammation. *New England Journal of Medicine*. [Online] Available from: doi:10.1056/nejm199902113400607.

Gaigé, S., Abou, E., Abysique, A. & Bouvier, M. (2004) Effects of interactions between interleukin-1β and leptin on cat intestinal vagal mechanoreceptors. *Journal of Physiology*. [Online]. Available from: doi:10.1113/jphysiol.2003.054379.

Gan, S.W., Ng, L., Lin, X., Gong, X., et al. (2008) Structure and ion channel activity of the human respiratory syncytial virus (hRSV) small hydrophobic protein transmembrane domain. *Protein Science*. [Online] 17 (5), 813–820. Available from: doi:10.1110/ps.073366208.

Gan, S.W., Tan, E., Lin, X., Yu, D., et al. (2012) The small hydrophobic protein of the human respiratory syncytial virus forms pentameric ion channels. *Journal of Biological Chemistry*. [Online] 287 (29), 24671–24689. Available from: doi:10.1074/jbc.M111.332791 [Accessed: 12 October 2020].

Garbers, C., Jänner, N., Chalaris, A., Moss, M.L., et al. (2011) Species specificity of ADAM10 and ADAM17 proteins in interleukin-6 (IL-6) trans-signaling and novel role of ADAM10 in inducible IL-6 receptor shedding. *Journal of Biological Chemistry*. [Online] Available from: doi:10.1074/jbc.M111.229393.

Garinis, G.A., van der Horst, G.T.J., Vijg, J. & Hoeijmakers, J.H.J. (2008) DNA damage and ageing: New-age ideas for an age-old problem. *Nature Cell Biology*. [Online]. Available from: doi:10.1038/ncb1108-1241.

Gates, A.C., Bernal-Mizrachi, C., Chinault, S.L., Feng, C., et al. (2007) Respiratory Uncoupling in Skeletal Muscle Delays Death and Diminishes Age-Related Disease. *Cell Metabolism*. [Online] 6 (6), 497–505. Available from: doi:10.1016/j.cmet.2007.10.010.

Gaugler, M., Brown, A., Merrell, E., DiSanto-Rose, M., et al. (2011) PKB signaling and atrogene expression in skeletal muscle of aged mice. *Journal of Applied Physiology*. [Online] Available from: doi:10.1152/japplphysiol.00175.2011.

Gaykema, R.P.A., Chen, C.C. & Goehler, L.E. (2007) Organization of immune-responsive medullary projections to the bed nucleus of the stria terminalis, central amygdala, and paraventricular nucleus of the hypothalamus: Evidence for parallel viscerosensory pathways in the rat brain. *Brain Research*. [Online] Available from: doi:10.1016/j.brainres.2006.10.084.

van der Geest, K.S.M., Abdulahad, W.H., Tete, S.M., Lorencetti, P.G., et al. (2014) Aging disturbs the balance between effector and regulatory CD4+ T cells. *Experimental Gerontology*. [Online] Available from: doi:10.1016/j.exger.2014.11.005.

Gehrig, S.M., Van Der Poel, C., Sayer, T.A., Schertzer, J.D., et al. (2012) Hsp72 preserves muscle function and slows progression of severe muscular dystrophy. *Nature*. [Online] 484 (7394), 394–398. Available from: doi:10.1038/nature10980 [Accessed: 15 November 2020].

Gibson, K.L., Wu, Y.C., Barnett, Y., Duggan, O., et al. (2009) B-cell diversity decreases in old age and is correlated with poor health status. *Aging Cell*. [Online] Available from: doi:10.1111/j.1474-9726.2008.00443.x.

Gilca, R., De Serres, G., Tremblay, M., Vachon, M., et al. (2006) Distribution and Clinical Impact of Human Respiratory Syncytial Virus Genotypes in Hospitalized Children over 2 Winter Seasons. *The Journal of Infectious Diseases*. [Online] 193 (1), 54–58. Available from: doi:10.1086/498526 [Accessed: 10 March 2020].

Giralt, A. & Villarroya, F. (2012) SIRT3, a pivotal actor in mitochondrial functions: Metabolism, cell death and aging. *Biochemical Journal*. [Online]. Available from: doi:10.1042/BJ20120030.

Gitlin, L., Benoit, L., Song, C., Cella, M., et al. (2010) Melanoma differentiation-associated gene 5 (MDA5) is involved in the innate immune response to Paramyxoviridae infection in vivo. *PLoS Pathogens*. [Online] Available from: doi:10.1371/journal.ppat.1000734.

Glezen, W.P., Paredes, A., Allison, J.E., Taber, L.H., et al. (1981) Risk of respiratory syncytial virus infection for infants from low-income families in relationship to age, sex, ethnic group, and maternal antibody level. *Journal of Pediatrics*. [Online] 98 (5), 708–715. Available from: doi:10.1016/S0022-3476(81)80829-3.

Glick, D., Barth, S. & Macleod, K.F. (2010) Autophagy: Cellular and molecular mechanisms. *Journal of Pathology*. [Online]. Available from: doi:10.1002/path.2697.

Gomes, M.D., Lecker, S.H., Jagoe, R.T., Navon, A., et al. (2001) Atrogin-1, a muscle-specific F-box protein highly expressed during muscle atrophy. *Proceedings of the National Academy of Sciences of the United States of America*. [Online] Available from: doi:10.1073/pnas.251541198.

Goodman, C.A. & Hornberger, T.A. (2013) Measuring protein synthesis with SUnSET: A valid alternative to traditional techniques? *Exercise and Sport Sciences Reviews*. [Online] 41 (2), 107–115. Available from: doi:10.1097/JES.0b013e3182798a95 [Accessed: 17 September 2016].

Goodman, C.A., Kotecki, J.A., Jacobs, B.L. & Hornberger, T.A. (2012) Muscle fiber type-dependent differences in the regulation of protein synthesis. *PLoS ONE*. [Online] 7 (5). Available from: doi:10.1371/journal.pone.0037890.

Goodman, C.A., Mabrey, D.M., Frey, J.W., Miu, M.H., et al. (2011) Novel insights into the regulation of skeletal muscle protein synthesis as revealed by a new nonradioactive in vivo technique. *FASEB Journal*. [Online] 25 (3), 1028–1039. Available from: doi:10.1096/fj.10-168799.

Goodman, C.A., McNally, R.M., Hoffmann, F.M. & Hornberger, T.A. (2013) Smad3 induces atrogin-1, inhibits mTOR and protein synthesis, and promotes muscle atrophy in vivo. *Molecular Endocrinology*. [Online] Available from: doi:10.1210/me.2013-1194.

Goodpaster, B.H., Park, S.W., Harris, T.B., Kritchevsky, S.B., et al. (2006) The loss of skeletal muscle strength, mass, and quality in older adults: The Health, Aging and Body Composition Study. *Journals of Gerontology - Series A Biological Sciences and Medical Sciences*. [Online] Available from: doi:10.1093/gerona/61.10.1059.

Goritzka, M., Durant, L.R., Pereira, C., Salek-Ardakani, S., et al. (2014) Alpha/Beta Interferon Receptor Signaling Amplifies Early Proinflammatory Cytokine Production in the Lung during Respiratory Syncytial Virus Infection. *Journal of Virology*. [Online] Available from: doi:10.1128/jvi.00333-14.

Goronzy, J.J., Fang, F., Cavanagh, M.M., Qi, Q., et al. (2015) Naive T Cell Maintenance and Function in Human Aging. *The Journal of*

Immunology. [Online] 194 (9), 4073–4080. Available from: doi:10.4049/jimmunol.1500046 [Accessed: 24 November 2020].
Gouspillou, G., Sgarioto, N., Kapchinsky, S., Purves-Smith, F., et al. (2014) Increased sensitivity to mitochondrial permeability transition and myonuclear translocation of endonuclease G in atrophied muscle of physically active older humans. *FASEB Journal*. [Online] Available from: doi:10.1096/fj.13-242750.
Gower, T.L., Pastey, M.K., Peeples, M.E., Collins, P.L., et al. (2005) RhoA Signaling Is Required for Respiratory Syncytial Virus-Induced Syncytium Formation and Filamentous Virion Morphology. *Journal of Virology*. [Online] 79 (9), 5326–5336. Available from: doi:10.1128/jvi.79.9.5326-5336.2005.
Graham, B.S., Bunton, L.A., Wright, P.F. & Karzon, D.T. (1991) Role of T lymphocyte subsets in the pathogenesis of primary infection and rechallenge with respiratory syncytial virus in mice. *Journal of Clinical Investigation*. [Online] Available from: doi:10.1172/JCI115362.
Graham, B.S., Perkins, M.D., Wright, P.F. & Karzon, D.T. (1988) Primary respiratory syncytial virus infection in mice. *Journal of Medical Virology*. [Online] Available from: doi:10.1002/jmv.1890260207.
Grandvaux, N., Guan, X., Yoboua, F., Zucchini, N., et al. (2014) Sustained activation of interferon regulatory factor 3 during infection by paramyxoviruses requires MDA5. *Journal of Innate Immunity*. [Online] Available from: doi:10.1159/000360764.
Graves, E., Hitt, A., Pariza, M.W., Cook, M.E., et al. (2005) Conjugated linoleic acid preserves gastrocnemius muscle mass in mice bearing the colon-26 adenocarcinoma. *Research in Nursing and Health*. [Online] Available from: doi:10.1002/nur.20052.
Green, D.R., Galluzzi, L. & Kroemer, G. (2011) Mitochondria and the autophagy-inflammation-cell death axis in organismal aging. *Science*. [Online]. 333 (6046) pp.1109–1112. Available from: doi:10.1126/science.1201940 [Accessed: 17 November 2020].
Grivennikov, S., Karin, E., Terzic, J., Mucida, D., et al. (2009) IL-6 and Stat3 Are Required for Survival of Intestinal Epithelial Cells and Development of Colitis-Associated Cancer. *Cancer Cell*. [Online] Available from: doi:10.1016/j.ccr.2009.01.001.
Grolleau-Julius, A., Garg, M.R., Mo, R.R., Stoolman, L.L., et al. (2006) Effect of aging on bone marrow-derived murine CD11c+CD4 -CD8α- dendritic cell function. *Journals of Gerontology - Series A Biological Sciences and Medical Sciences*. [Online] Available from: doi:10.1093/gerona/61.10.1039.
Grolleau-Julius, A., Harning, E.K., Abernathy, L.M. & Yung, R.L. (2008) Impaired dendritic cell function in aging leads to defective antitumor immunity. *Cancer Research*. [Online] Available from: doi:10.1158/0008-5472.CAN-07-5769.
Grosfeld, H., Hill, M.G. & Collins, P.L. (1995) RNA replication by respiratory syncytial virus (RSV) is directed by the N, P, and L proteins; transcription also occurs under these conditions but requires RSV superinfection for efficient synthesis of full-length mRNA. *Journal of virology*. [Online] 69 (9), 5677–5686. Available from: doi:10.1128/jvi.69.9.5677-5686.1995.
Grounds, M.D., Garrett, K.L., Lai, M.C., Wright, W.E., et al. (1992) Identification of skeletal muscle precursor cells in vivo by use of MyoD1 and myogenin probes. *Cell & Tissue Research*. [Online] Available from: doi:10.1007/BF00318695.
Gruber, R., Koch, H., Doll, B.A., Tegtmeier, F., et al. (2006) Fracture healing in the elderly patient. *Experimental Gerontology*. [Online]. Available from: doi:10.1016/j.exger.2006.09.008.
de Guia, R.M., Agerholm, M., Nielsen, T.S., Consitt, L.A., et al. (2019) Aerobic and resistance exercise training reverses age-dependent decline in NAD $^+$ salvage capacity in human skeletal muscle. *Physiological Reports*. [Online] 7 (12). Available from: doi:10.14814/phy2.14139 [Accessed: 22 November 2020].
Guiraud, S. & Davies, K. (2019) Regenerative biomarkers for Duchenne muscular dystrophy. *Neural Regeneration Research*. [Online] 14 (8), 1317. Available from: doi:10.4103/1673-5374.253534 [Accessed: 15 November 2020].
Guttridge, D.C., Mayo, M.W., Madrid, L. V., Wang, C.Y., et al. (2000) NF-κB-induced loss of MyoD messenger RNA: Possible role in muscle decay and cachexia. *Science*. [Online] Available from: doi:10.1126/science.289.5488.2363.
Habibi, M.S., Jozwik, A., Makris, S., Dunning, J., et al. (2015) Impaired Antibody-mediated Protection and Defective IgA B-Cell Memory in Experimental Infection of Adults with Respiratory Syncytial Virus. *American journal of respiratory and critical care medicine*. [Online] 191 (9), 1040–1049. Available from: doi:10.1164/rccm.201412-2256OC [Accessed: 12 January 2018].
Haddad, F., Zaldivar, F., Cooper, D.M. & Adams, G.R. (2005) IL-6-induced skeletal muscle atrophy. *Journal of Applied Physiology*. [Online] Available from: doi:10.1152/japplphysiol.01026.2004.
Hall, C.B., Powell, K.R., Macdonald, N.E., Gala, C.L., et al. (1986) Respiratory Syncytial Viral Infection in Children with Compromised Immune Function. *New England Journal of Medicine*. [Online] Available from: doi:10.1056/NEJM198607103150201.
Hall, C.B., Walsh, E.E., Long, C.E. & Schnabel, K.C. (1991) Immunity to and frequency of reinfection with respiratory syncytial virus. *Journal of Infectious Diseases*. [Online] 163 (4), 693–698. Available from: doi:10.1093/infdis/163.4.693.
Hall, C.B., Walsh, E.E., Schnabel, K.C., Long, C.E., et al. (1990) Occurrence of groups A and B of respiratory syncytial virus over 15 years: associated epidemiologic and clinical characteristics in hospitalized and ambulatory children. *The Journal of infectious diseases*. [Online] 162 (6), 1283–1290. Available from: doi:10.1093/infdis/162.6.1283 [Accessed: 10 March 2020].
Van Hall, G., Steensberg, A., Sacchetti, M., Fischer, C., et al. (2003) Interleukin-6 stimulates lipolysis and fat oxidation in humans. *Journal of Clinical Endocrinology and Metabolism*. [Online] Available from: doi:10.1210/jc.2002-021687.
Han, S. & Brunet, A. (2012) Histone methylation makes its mark on longevity. *Trends in Cell Biology*. [Online]. 22 (1) pp.42–49. Available from: doi:10.1016/j.tcb.2011.11.001.
Hao, Y., O'Neill, P., Naradikian, M.S., Scholz, J.L., et al. (2011) A B-cell subset uniquely responsive to innate stimuli accumulates in aged mice. *Blood*. [Online] Available from: doi:10.1182/blood-2011-01-330530.
Harker, J.A., Lewis, G.M., Mack, L. & Zuniga, E.I. (2011) Late interleukin-6 escalates T follicular helper cell responses and controls a chronic viral infection. *Science*. [Online] Available from: doi:10.1126/science.1208421.
Harman, D. (1965) The Free Radical Theory Of Aging: Effect Of Age On Serum Copper Levels. *Journal of gerontology*. [Online] 20 (2), 151–153. Available from: doi:10.1093/geronj/20.2.151 [Accessed: 17 November 2020].
Harries, L.W., Hernandez, D., Henley, W., Wood, A.R., et al. (2011) Human aging is characterized by focused changes in gene expression and deregulation of alternative splicing. *Aging Cell*. [Online] 10 (5), 868–878. Available from: doi:10.1111/j.1474-9726.2011.00726.x [Accessed: 15 November 2020].
Harrison, D.E., Strong, R., Sharp, Z.D., Nelson, J.F., et al. (2009) Rapamycin fed late in life extends lifespan in genetically heterogeneous mice. *Nature*. [Online] 460 (7253), 392–395. Available from: doi:10.1038/nature08221 [Accessed: 15 November 2020].
Hartl, F.U., Bracher, A. & Hayer-Hartl, M. (2011) Molecular chaperones in protein folding and proteostasis. *Nature*. [Online]. 475 (7356) pp.324–332. Available from: doi:10.1038/nature10317 [Accessed: 15 November 2020].
Hasty, P., Bradley, A., Morris, J.H., Edmondson, D.G., et al. (1993) Muscle deficiency and neonatal death in mice with a targeted mutation in the myogenin gene. *Nature*. [Online] Available from: doi:10.1038/364501a0.

Hayflick, L. & Moorhead, P.S. (1961) The serial cultivation of human diploid cell strains. *Experimental Cell Research*. [Online] 25 (3), 585–621. Available from: doi:10.1016/0014-4827(61)90192-6.
Hazeldine, J., Harris, P., Chapple, I.L., Grant, M., et al. (2014) Impaired neutrophil extracellular trap formation: a novel defect in the innate immune system of aged individuals. *Aging Cell*. [Online] 13 (4), 690–698. Available from: doi:10.1111/acel.12222 [Accessed: 14 April 2020].
Heesters, B.A., Myers, R.C. & Carroll, M.C. (2014) Follicular dendritic cells: Dynamic antigen libraries. *Nature Reviews Immunology*. [Online]. 14 (7) pp.495–504. Available from: doi:10.1038/nri3689.
Heinrich, P.C., Behrmann, I., Haan, S., Hermanns, H.M., et al. (2003) Principles of interleukin (IL)-6-type cytokine signalling and its regulation. *Biochemical Journal*. [Online]. Available from: doi:10.1042/BJ20030407.
Henrich, C.J. (2016) A microplate-based nonradioactive protein synthesis assay: Application to TRAIL sensitization by protein synthesis inhibitors. *PLoS ONE*. [Online] 11 (10). Available from: doi:10.1371/journal.pone.0165192.
Henry, C.J., Casás-Selves, M., Kim, J., Zaberezhnyy, V., et al. (2015) Aging-associated inflammation promotes selection for adaptive oncogenic events in B cell progenitors. *Journal of Clinical Investigation*. [Online] Available from: doi:10.1172/JCI83024.
Herranz, D., Muñoz-Martin, M., Cañamero, M., Mulero, F., et al. (2010) Sirt1 improves healthy ageing and protects from metabolic syndrome-associated cancer. *Nature Communications*. [Online] 1 (1), 1–8. Available from: doi:10.1038/ncomms1001 [Accessed: 15 November 2020].
Herrero, C., Marqués, L., Lloberas, J. & Celada, A. (2001) IFN-γ-dependent transcription of MHC class II IA is impaired in macrophages from aged mice. *Journal of Clinical Investigation*. [Online] Available from: doi:10.1172/JCI11696.
Herskind, A.M., McGue, M., Holm, N. V., Sørensen, T.I.A., et al. (1996) The heritability of human longevity: A population-based study of 2872 Danish twin pairs born 1870-1900. *Human Genetics*. [Online] 97 (3), 319–323. Available from: doi:10.1007/BF02185763 [Accessed: 21 November 2020].
Hibi, M., Murakami, M., Saito, M., Hirano, T., et al. (1990) Molecular cloning and expression of an IL-6 signal transducer, gp130. *Cell*. [Online] Available from: doi:10.1016/0092-8674(90)90411-7.
Higgins, D., Trujillo, C. & Keech, C. (2016) Advances in RSV vaccine research and development - A global agenda. *Vaccine*. [Online] 34 (26), 2870–2875. Available from: doi:10.1016/j.vaccine.2016.03.109.
Hinojosa, C.A., Akula Suresh Babu, R., Rahman, M.M., Fernandes, G., et al. (2014) Elevated A20 contributes to age-dependent macrophage dysfunction in the lungs. *Experimental Gerontology*. [Online] 54, 58–66. Available from: doi:10.1016/j.exger.2014.01.007 [Accessed: 26 November 2020].
Hinojosa, E., Boyd, A.R. & Orihuela, C. (2009) Age-associated inflammation and Toll-like receptor dysfunction prime the lungs for pneumococcal pneumonia. *Journal of Infectious Diseases*. [Online] 200 (4), 546–554. Available from: doi:10.1086/600870 [Accessed: 26 November 2020].
Hiona, A., Sanz, A., Kujoth, G.C., Pamplona, R., et al. (2010) Mitochondrial DNA Mutations Induce Mitochondrial Dysfunction, Apoptosis and Sarcopenia in Skeletal Muscle of Mitochondrial DNA Mutator Mice Mark A. Tarnopolsky (ed.). *PLoS ONE*. [Online] 5 (7), e11468. Available from: doi:10.1371/journal.pone.0011468 [Accessed: 17 November 2020].
Hirano, T., Yasukawa, K., Harada, H., Taga, T., et al. (1986) Complementary DNA for a novel human interleukin (BSF-2) that induces B lymphocytes to produce immunoglobulin. *Nature*. [Online] Available from: doi:10.1038/324073a0.
Hirner, S., Krohne, C., Schuster, A., Hoffmann, S., et al. (2008) MuRF1-dependent Regulation of Systemic Carbohydrate Metabolism as Revealed from Transgenic Mouse Studies. *Journal of Molecular Biology*. [Online] 379 (4), 666–677. Available from: doi:10.1016/j.jmb.2008.03.049 [Accessed: 7 August 2019].
Hoffmann, M., Kleine-Weber, H., Krüger, N., Müller, M., et al. (2020) The novel coronavirus 2019 (2019-nCoV) uses the SARS-coronavirus receptor ACE2 and the cellular protease TMPRSS2 for entry into target cells. *bioRxiv*. [Online] 2020.01.31.929042. Available from: doi:10.1101/2020.01.31.929042 [Accessed: 22 November 2020].
Holloszy, J.O. (2000) The biology of aging. *Mayo Clin Proc*. 75 Suppl, S3–S8.
Hou, W., Kang, H.S. & Kim, B.S. (2009) Th17 cells enhance viral persistence and inhibit T cell cytotoxicity in a model of chronic virus infection. *Journal of Experimental Medicine*. [Online] Available from: doi:10.1084/jem.20082030.
Howard, W.A., Gibson, K.L. & Dunn-Walters, D.K. (2006) Antibody quality in old age. In: *Rejuvenation Research*. [Online]. 2006 p. Available from: doi:10.1089/rej.2006.9.117.
Hromas, R., Hufford, M., Sutton, J., Xu, D., et al. (1997) PLAB, a novel placental bone morphogenetic protein. *Biochimica et Biophysica Acta - Gene Structure and Expression*. [Online] 1354 (1), 40–44. Available from: doi:10.1016/S0167-4781(97)00122-X.
Hsu, A.L., Murphy, C.T. & Kenyon, C. (2003) Regulation of aging and age-related disease by DAF-16 and heat-shock factor. *Science*. [Online] 300 (5622), 1142–1145. Available from: doi:10.1126/science.1083701.
Hsu, J.-Y., Crawley, S., Chen, M., Ayupova, D.A., et al. (2017) Non-homeostatic body weight regulation through a brainstem-restricted receptor for GDF15. *Nature*. [Online] 550 (7675), 255–259. Available from: doi:10.1038/nature24042 [Accessed: 11 January 2018].
Hughes, S.M., Chi, M.M.Y., Lowry, O.H. & Gundersen, K. (1999) Myogenin induces a shift of enzyme activity from glycolytic to oxidative metabolism in muscles of transgenic mice. *Journal of Cell Biology*. [Online] Available from: doi:10.1083/jcb.145.3.633.
Hughes, S.M., Taylor, J.M., Tapscott, S.J., Gurley, C.M., et al. (1993) Selective accumulation of MyoD and myogenin mRNAs in fast and slow adult skeletal muscle is controlled by innervation and hormones. *Development*.
Hunter, C.A. & Jones, S.A. (2015) IL-6 as a keystone cytokine in health and disease. *Nature Immunology*. [Online]. Available from: doi:10.1038/ni.3153.
Hunter, R.B. & Kandarian, S.C. (2004) Disruption of either the Nfkb1 or the Bcl3 gene inhibits skeletal muscle atrophy. *Journal of Clinical Investigation*. [Online] Available from: doi:10.1172/JCI200421696.
Hurst, S.M., Wilkinson, T.S., McLoughlin, R.M., Jones, S., et al. (2001) IL-6 and its soluble receptor orchestrate a temporal switch in the pattern of leukocyte recruitment seen during acute inflammation. *Immunity*. [Online] Available from: doi:10.1016/S1074-7613(01)00151-0.
Husebø, G.R., Grønseth, R., Lerner, L., Gyuris, J., et al. (2017) Growth differentiation factor-15 is a predictor of important disease outcomes in patients with COPD. *European Respiratory Journal*. [Online] 49 (3). Available from: doi:10.1183/13993003.01298-2016.
Hwee, D.T., Baehr, L.M., Philp, A., Baar, K., et al. (2014) Maintenance of muscle mass and load-induced growth in Muscle RING Finger 1 null mice with age. *Aging Cell*. [Online] Available from: doi:10.1111/acel.12150.

Imaz, M.S., Sequeira, M.D., Videla, C., Veronessi, I., et al. (2000) Clinical and epidemiologic characteristics of respiratory syncytial virus subgroups A and B infections in Santa Fe, Argentina. *Journal of Medical Virology*. [Online] 61 (1), 76–80. Available from: doi:10.1002/(SICI)1096-9071(200005)61:1<76::AID-JMV12>3.0.CO;2-P [Accessed: 10 March 2020].
In, H.L., Cao, L., Mostoslavsky, R., Lombard, D.B., et al. (2008) A role for the NAD-dependent deacetylase Sirt1 in the regulation of autophagy. *Proceedings of the National Academy of Sciences of the United States of America*. [Online] 105 (9), 3374–3379. Available from: doi:10.1073/pnas.0712145105 [Accessed: 17 November 2020].
Inui, T., Nakagawa, R., Ohkura, S., Habu, Y., et al. (2002) Age-Associated Augmentation of the Synthetic Ligand- Mediated Function of Mouse NK1.1 Ag + T Cells: Their Cytokine Production and Hepatotoxicity In Vivo and In Vitro . *The Journal of Immunology*. [Online] Available from: doi:10.4049/jimmunol.169.11.6127.
Ito, H., Takazoe, M., Fukuda, Y., Hibi, T., et al. (2004) A Pilot Randomized Trial of a Human Anti-Interleukin-6 Receptor Monoclonal Antibody in Active Crohn's Disease. *Gastroenterology*. [Online] Available from: doi:10.1053/j.gastro.2004.01.012.
Ivanov, I.I., McKenzie, B.S., Zhou, L., Tadokoro, C.E., et al. (2006) The Orphan Nuclear Receptor RORγt Directs the Differentiation Program of Proinflammatory IL-17+ T Helper Cells. *Cell*. [Online] Available from: doi:10.1016/j.cell.2006.07.035.
Jackson, G.G., Dowling, H.F., Spiesman, I.G. & Boand, A. V. (1958) Transmission of the Common Cold to Volunteers Under Controlled Conditions: I. The Common Cold as a Clinical Entity. *A.M.A Archives of Internal Medicine*. [Online] Available from: doi:10.1001/archinte.1958.00260140099015.
De Jager, S.C.A., Bermúdez, B., Bot, I., Koenen, R.R., et al. (2011) Growth differentiation factor 15 deficiency protects against atherosclerosis by attenuating CCR2-mediated macrophage chemotaxis. *Journal of Experimental Medicine*. [Online] Available from: doi:10.1084/jem.20100370.
Jang, Y.C., Lustgarten, M.S., Liu, Y., Muller, F.L., et al. (2010) Increased superoxide in vivo accelerates age-associated muscle atrophy through mitochondrial dysfunction and neuromuscular junction degeneration . *The FASEB Journal*. [Online] Available from: doi:10.1096/fj.09-146308.
Janssen, I., Heymsfield, S.B., Wang, Z. & Ross, R. (2000) Skeletal muscle mass and distribution in 468 men and women aged 18–88 yr. *Journal of Applied Physiology*. [Online] 89 (1), 81–88. Available from: doi:10.1093/oxfordjournals.aje.a009520.
Janzen, V., Forkert, R., Fleming, H.E., Saito, Y., et al. (2006) Stem-cell ageing modified by the cyclin-dependent kinase inhibitor p16 INK4a. *Nature*. [Online] Available from: doi:10.1038/nature05159.
Jaskelioff, M., Muller, F.L., Paik, J.H., Thomas, E., et al. (2011) Telomerase reactivation reverses tissue degeneration in aged telomerase-deficient mice. *Nature*. [Online] 469 (7328), 102–107. Available from: doi:10.1038/nature09603 [Accessed: 15 November 2020].
Jeck, W.R., Siebold, A.P. & Sharpless, N.E. (2012) Review: A meta-analysis of GWAS and age-associated diseases. *Aging Cell*. [Online]. 11 (5) pp.727–731. Available from: doi:10.1111/j.1474-9726.2012.00871.x.
Jenks, S.A., Cashman, K.S., Zumaquero, E., Marigorta, U.M., et al. (2018) Distinct Effector B Cells Induced by Unregulated Toll-like Receptor 7 Contribute to Pathogenic Responses in Systemic Lupus Erythematosus. *Immunity*. [Online] Available from: doi:10.1016/j.immuni.2018.08.015.
Jeon, O.H., Kim, C., Laberge, R.M., Demaria, M., et al. (2017) Local clearance of senescent cells attenuates the development of post-traumatic osteoarthritis and creates a pro-regenerative environment. *Nature Medicine*. [Online] Available from: doi:10.1038/nm.4324.
Jiang, N., He, J., Weinstein, J.A., Penland, L., et al. (2013) Lineage structure of the human antibody repertoire in response to influenza vaccination. *Science Translational Medicine*. [Online] Available from: doi:10.1126/scitranslmed.3004794.
Jin, C., Li, J., Green, C.D., Yu, X., et al. (2011) Histone demethylase UTX-1 regulates C. elegans life span by targeting the insulin/IGF-1 signaling pathway. *Cell Metabolism*. [Online] 14 (2), 161–172. Available from: doi:10.1016/j.cmet.2011.07.001.
Jin, H., Cheng, X., Zhou, H.Z.Y., Li, S., et al. (2000a) Respiratory Syncytial Virus That Lacks Open Reading Frame 2 of the M2 Gene (M2-2) Has Altered Growth Characteristics and Is Attenuated in Rodents. *Journal of Virology*. [Online] 74 (1), 74–82. Available from: doi:10.1128/jvi.74.1.74-82.2000.
Jin, H., Zhou, H., Cheng, X., Tang, R., et al. (2000b) Recombinant respiratory syncytial viruses with deletions in the NS1, NS2, SH, and M2-2 genes are attenuated in vitro and in vivo. *Virology*. [Online] Available from: doi:10.1006/viro.2000.0393.
Jing, Y., Shaheen, E., Drake, R.R., Chen, N., et al. (2009) Aging is associated with a numerical and functional decline in plasmacytoid dendritic cells, whereas myeloid dendritic cells are relatively unaltered in human peripheral blood. *Human Immunology*. [Online] Available from: doi:10.1016/j.humimm.2009.07.005.
Johnen, H., Lin, S., Kuffner, T., Brown, D.A., et al. (2007) Tumor-induced anorexia and weight loss are mediated by the TGF-b superfamily cytokine MIC-1. *NATURE MEDICINE VOLUME*. [Online] 13. Available from: doi:10.1038/nm1677 [Accessed: 9 August 2018].
Johnson, A.M., Vogt, S.K., Burney, M.W. & Muglia, L.J. (2002) COX-2 inhibition attenuates anorexia during systemic inflammation without impairing cytokine production. *American Journal of Physiology - Endocrinology and Metabolism*. [Online] Available from: doi:10.1152/ajpendo.00388.2001.
Johnson, J.E., Gonzales, R.A., Olson, S.J., Wright, P.F., et al. (2007) The histopathology of fatal untreated human respiratory syncytial virus infection. *Modern Pathology*. [Online] Available from: doi:10.1038/modpathol.3800725.
Johnson, S.M., McNally, B.A., Ioannidis, I., Flano, E., et al. (2015) Respiratory Syncytial Virus Uses CX3CR1 as a Receptor on Primary Human Airway Epithelial Cultures. *PLoS Pathogens*. [Online] Available from: doi:10.1371/journal.ppat.1005318.
Jones, G.W., McLoughlin, R.M., Hammond, V.J., Parker, C.R., et al. (2010) Loss of CD4 + T Cell IL-6R Expression during Inflammation Underlines a Role for IL-6 Trans Signaling in the Local Maintenance of Th17 Cells . *The Journal of Immunology*. [Online] Available from: doi:10.4049/jimmunol.0901528.
Jones, J.E., Cadena, S.M., Gong, C., Wang, X., et al. (2018) Supraphysiologic Administration of GDF11 Induces Cachexia in Part by Upregulating GDF15. *Cell Reports*. [Online] Available from: doi:10.1016/j.celrep.2018.01.044.
Jones, S.A. (2005) Directing Transition from Innate to Acquired Immunity: Defining a Role for IL-6. *The Journal of Immunology*. [Online] Available from: doi:10.4049/jimmunol.175.6.3463.
Jones, S.A., Horiuchi, S., Topley, N., Yamamoto, N., et al. (2001) The soluble interleukin 6 receptor: mechanisms of production and implications in disease. *The FASEB Journal*. [Online] Available from: doi:10.1096/fj.99-1003rev.
Jones, S.A., Scheller, J. & Rose-John, S. (2011) Therapeutic strategies for the clinical blockade of IL-6/gp130 signaling. *Journal of Clinical Investigation*. [Online]. Available from: doi:10.1172/JCI57158.

Jones, S.E., Maddocks, M., Kon, S.S.C., Canavan, J.L., et al. (2015) Sarcopenia in copd: Prevalence, clinical correlates and response to pulmonary rehabilitation. *Thorax*. [Online] Available from: doi:10.1136/thoraxjnl-2014-206440.

Jostock, T., Müllberg, J., Özbek, S., Atreya, R., et al. (2001) Soluble gp130 is the natural inhibitor of soluble interleukin-6 receptor transsignaling responses. *European Journal of Biochemistry*. [Online] Available from: doi:10.1046/j.1432-1327.2001.01867.x.

Jourdan, M., Cren, M., Robert, N., Bolloré, K., et al. (2014) IL-6 supports the generation of human long-lived plasma cells in combination with either APRIL or stromal cell-soluble factors. *Leukemia*. [Online] 28 (8), 1647–1656. Available from: doi:10.1038/leu.2014.61.

Jozwik, A., Habibi, M.S., Paras, A., Zhu, J., et al. (2015) RSV-specific airway resident memory CD8+ T cells and differential disease severity after experimental human infection. *Nature Communications*. [Online] Available from: doi:10.1038/ncomms10224.

Judge, A.R., Koncarevic, A., Hunter, R.B., Liou, H.C., et al. (2007) Role for IκBα, but not c-Rel, in skeletal muscle atrophy. *American Journal of Physiology - Cell Physiology*. [Online] Available from: doi:10.1152/ajpcell.00293.2006.

Juhász, G., Érdi, B., Sass, M. & Neufeld, T.P. (2007) Atg7-dependent autophagy promotes neuronal health, stress tolerance, and longevity but is dispensable for metamorphosis in Drosophila. *Genes and Development*. [Online] 21 (23), 3061–3066. Available from: doi:10.1101/gad.1600707 [Accessed: 17 November 2020].

Kadowaki, N. (2009) The divergence and interplay between pDC and mDC in humans. *Frontiers in Bioscience*. [Online] Available from: doi:10.2741/3279.

Kanfi, Y., Naiman, S., Amir, G., Peshti, V., et al. (2012) The sirtuin SIRT6 regulates lifespan in male mice. *Nature*. [Online] 483 (7388), 218–221. Available from: doi:10.1038/nature10815 [Accessed: 15 November 2020].

Kanfi, Y., Peshti, V., Gil, R., Naiman, S., et al. (2010) SIRT6 protects against pathological damage caused by diet-induced obesity. *Aging Cell*. [Online] 9 (2), 162–173. Available from: doi:10.1111/j.1474-9726.2009.00544.x [Accessed: 15 November 2020].

Kang, S., Moser, V.A., Svendsen, C.N. & Goodridge, H.S. (2020) Rejuvenating the blood and bone marrow to slow aging-associated cognitive decline and Alzheimer's disease. *Communications Biology*. [Online]. Available from: doi:10.1038/s42003-020-0797-4.

Kapikian, A.Z., Mitchell, R.H., Chanock, R.M., Shvedoff, R.A., et al. (1969) An epidemiologic study of altered clinical reactivity to Respiratory Syncytial (RS) virus infection in children previously vaccinated with an inactivated RS virus vaccine. *American Journal of Epidemiology*. [Online] Available from: doi:10.1093/oxfordjournals.aje.a120954.

Kassar-Duchossoy, L., Giacone, E., Gayraud-Morel, B., Jory, A., et al. (2005) Pax3/Pax7 mark a novel population of primitive myogenic cells during development. *Genes and Development*. [Online] Available from: doi:10.1101/gad.345505.

Katsimpardi, L., Litterman, N.K., Schein, P.A., Miller, C.M., et al. (2014) Vascular and neurogenic rejuvenation of the aging mouse brain by young systemic factors. *Science*. [Online] 344 (6184), 630–634. Available from: doi:10.1126/science.1251141 [Accessed: 19 November 2020].

Kawahara, T.L.A., Michishita, E., Adler, A.S., Damian, M., et al. (2009) SIRT6 Links Histone H3 Lysine 9 Deacetylation to NF-κB-Dependent Gene Expression and Organismal Life Span. *Cell*. [Online] 136 (1), 62–74. Available from: doi:10.1016/j.cell.2008.10.052.

Kawahashi, Y., Doi, N., Oishi, Y., Tsuda, C., et al. (2006) *High-throughput Fluorescence Labelling of Full-length cDNA Products Based on a Reconstituted Translation System*. [Online] Available from: doi:10.1093/jb/mvm003.

Kawano, M.M., Mihara, K., Huang, N., Tsujimoto, T., et al. (1995) Differentiation of early plasma cells on bone marrow stromal cells requires interleukin-6 for escaping from apoptosis. *Blood*. [Online] Available from: doi:10.1182/blood.v85.2.487.bloodjournal852487.

Ke, Z., Dillard, R.S., Chirkova, T., Leon, F., et al. (2018) The morphology and assembly of respiratory syncytial virus revealed by cryo-electron tomography. *Viruses*. [Online] Available from: doi:10.3390/v10080446.

Kedar, V., McDonough, H., Arya, R., Li, H.H., et al. (2004) Muscle-specific RING finger 1 is a bona fide ubiquitin ligase that degrades cardiac troponin I. *Proceedings of the National Academy of Sciences of the United States of America*. [Online] Available from: doi:10.1073/pnas.0404341102.

Kempf, T. & Wollert, K.C. (2009) Growth-Differentiation Factor-15 in Heart Failure. *Heart Failure Clinics*. [Online]. Available from: doi:10.1016/j.hfc.2009.04.006.

Kempf, T., Zarbock, A., Widera, C., Butz, S., et al. (2011) GDF-15 is an inhibitor of leukocyte integrin activation required for survival after myocardial infarction in mice. *Nature Medicine*. [Online] Available from: doi:10.1038/nm.2354.

Kennedy, B.K., Berger, S.L., Brunet, A., Campisi, J., et al. (2014) Geroscience: Linking aging to chronic disease. *Cell*. [Online]. 159 (4) pp.709–713. Available from: doi:10.1016/j.cell.2014.10.039 [Accessed: 17 September 2016].

Kent, S., Bluthe, R.-M., Dantzer, R., Hardwickt, A.J., et al. (1992) Different receptor mechanisms mediate the pyrogenic and behavioral effects of interleukin 1 (interleukin 1 receptor antagonist/sickness/food-motivated behavior/social behavior/fever). *Proceedings of the National Academy of Sciences*.

Kent, S., Bret-Dibat, J.L., Kelley, K.W. & Dantzer, R. (1996) Mechanisms of sickness-induced decreases in food-motivated behavior. *Neuroscience and Biobehavioral Reviews*. [Online] Available from: doi:10.1016/0149-7634(95)00037-F.

Kenyon, C.J. (2010) The genetics of ageing. *Nature*. [Online]. Available from: doi:10.1038/nature08980.

Khan, N., Shariff, N., Cobbold, M., Bruton, R., et al. (2002) Cytomegalovirus Seropositivity Drives the CD8 T Cell Repertoire Toward Greater Clonality in Healthy Elderly Individuals. *The Journal of Immunology*. [Online] 169 (4), 1984–1992. Available from: doi:10.4049/jimmunol.169.4.1984 [Accessed: 24 November 2020].

Khurana, S., Frasca, D., Blomberg, B. & Golding, H. (2012) AID Activity in B Cells Strongly Correlates with Polyclonal Antibody Affinity Maturation in-vivo Following Pandemic 2009-H1N1 Vaccination in Humans Patrick Wilson (ed.). *PLoS Pathogens*. [Online] 8 (9), e1002920. Available from: doi:10.1371/journal.ppat.1002920 [Accessed: 24 November 2020].

Kim, H.W., Canchola, J.G., Brandt, C.D., Pyles, G., et al. (1969) Respiratory Syncytial Virus Disease in Infants Despite Prior Administration of Antigenic Inactivated Vaccine. *American Journal of Epidemiology*. [Online] 89 (4), 422–434. Available from: doi:10.1093/oxfordjournals.aje.a120955 [Accessed: 28 February 2020].

Kim, K.H., Kim, S.H., Han, D.H., Jo, Y.S., et al. (2018) Growth differentiation factor 15 ameliorates nonalcoholic steatohepatitis and related metabolic disorders in mice. *Scientific Reports*. [Online] 8 (1), 6789. Available from: doi:10.1038/s41598-018-25098-0 [Accessed: 6 August 2018].

Kim, W.K., Jain, D., Sánchez, M.D., Koziol-White, C.J., et al. (2014) Deficiency of melanoma differentiation-associated protein 5 results in exacerbated chronic postviral lung inflammation. *American Journal of Respiratory and Critical Care Medicine*. [Online]

Available from: doi:10.1164/rccm.201307-1338OC.
King, A.M., Keating, P., Prabhu, A., Blomberg, B.B., et al. (2009) NK cells in the CD19- B220+ bone marrow fraction are increased in senescence and reduce E2A and surrogate light chain proteins in B cell precursors. *Mechanisms of Ageing and Development*. [Online] 130 (6), 384–392. Available from: doi:10.1016/j.mad.2009.03.002.
Kinnear, E., Lambert, L., McDonald, J.U., Cheeseman, H.M., et al. (2018) Airway T cells protect against RSV infection in the absence of antibody. *Mucosal Immunology*. [Online] 11 (1), 249–256. Available from: doi:10.1038/mi.2017.46.
Kippin, T.E., Martens, D.J. & Van Der Kooy, D. (2005) p21 loss compromises the relative quiescence of forebrain stem cell proliferation leading to exhaustion of their proliferation capacity. *Genes and Development*. [Online] 19 (6), 756–767. Available from: doi:10.1101/gad.1272305 [Accessed: 19 November 2020].
Kiss, G., Holl, J.M., Williams, G.M., Alonas, E., et al. (2014) Structural Analysis of Respiratory Syncytial Virus Reveals the Position of M2-1 between the Matrix Protein and the Ribonucleoprotein Complex. *Journal of Virology*. [Online] 88 (13), 7602–7617. Available from: doi:10.1128/jvi.00256-14.
Klimpel, G.R. (1980) Soluble factor(s) from LPS-activated macrophages induce cytotoxic T cell differentiation from alloantigen-primed spleen cells. *Journal of immunology (Baltimore, Md. : 1950)*.
Knapp, J.R., Davie, J.K., Myer, A., Meadows, E., et al. (2006) Loss of myogenin in postnatal life leads to normal skeletal muscle but reduced body size. *Development*. [Online] Available from: doi:10.1242/dev.02249.
Knox, J.J., Buggert, M., Kardava, L., Seaton, K.E., et al. (2017) T-bet+ B cells are induced by human viral infections and dominate the HIV gp140 response. *JCI insight*. [Online] Available from: doi:10.1172/jci.insight.92943.
Koch, S., Larbi, A., Derhovanessian, E., Özcelik, D., et al. (2008) Multiparameter flow cytometric analysis of CD4 and CD8 T cell subsets in young and old people. *Immunity and Ageing*. [Online] Available from: doi:10.1186/1742-4933-5-6.
Koga, H., Kaushik, S. & Cuervo, A.M. (2011) Protein homeostasis and aging: The importance of exquisite quality control. *Ageing Research Reviews*. [Online]. 10 (2) pp.205–215. Available from: doi:10.1016/j.arr.2010.02.001.
Koishi, K., Zhang, M., McLennan, I.S. & Harris, A.J. (1995) MyoD protein accumulates in satellite cells and is neurally regulated in regenerating myotubes and skeletal muscle fibers. *Developmental Dynamics*. [Online] Available from: doi:10.1002/aja.1002020304.
Kopf, M., Baumann, H., Freer, G., Freudenberg, M., et al. (1994) Impaired immune and acute-phase responses in interleukin-6-deficient mice. *Nature*. [Online] 368 (6469), 339–342. Available from: doi:10.1038/368339a0.
Korn, T., Mitsdoerffer, M., Croxford, A.L., Awasthi, A., et al. (2008) IL-6 controls Th17 immunity in vivo by inhibiting the conversion of conventional T cells into Foxp3+ regulatory T cells. *Proceedings of the National Academy of Sciences of the United States of America*. [Online] Available from: doi:10.1073/pnas.0809850105.
Kortebein, P., Ferrando, A., Lombeida, J., Wolfe, R., et al. (2007) Effect of 10 days of bed rest on skeletal muscle in healthy older adults. *Journal of the American Medical Association*. [Online]. Available from: doi:10.1001/jama.297.16.1772-b.
Kotas, M.E. & Medzhitov, R. (2015) Homeostasis, Inflammation, and Disease Susceptibility. *Cell*. [Online]. Available from: doi:10.1016/j.cell.2015.02.010.
Kotelkin, A., Prikhod'ko, E.A., Cohen, J.I., Collins, P.L., et al. (2003) Respiratory Syncytial Virus Infection Sensitizes Cells to Apoptosis Mediated by Tumor Necrosis Factor-Related Apoptosis-Inducing Ligand. *Journal of Virology*. [Online] Available from: doi:10.1128/jvi.77.17.9156-9172.2003.
Kraus, W.E., Bhapkar, M., Huffman, K.M., Pieper, C.F., et al. (2019) 2 years of calorie restriction and cardiometabolic risk (CALERIE): exploratory outcomes of a multicentre, phase 2, randomised controlled trial. *The Lancet Diabetes and Endocrinology*. [Online] 7 (9), 673–683. Available from: doi:10.1016/S2213-8587(19)30151-2 [Accessed: 21 November 2020].
Krishnamurthy, J., Torrice, C., Ramsey, M.R., Kovalev, G.I., et al. (2004) Ink4a/Arf expression is a biomarker of aging. *Journal of Clinical Investigation*. [Online] Available from: doi:10.1172/JCI22475.
Krishnan, V., Chow, M.Z.Y., Wang, Z., Zhang, L., et al. (2011) Histone H4 lysine 16 hypoacetylation is associated with defective DNA repair and premature senescence in Zmpste24-deficient mice. *Proceedings of the National Academy of Sciences of the United States of America*. [Online] 108 (30), 12325–12330. Available from: doi:10.1073/pnas.1102789108 [Accessed: 15 November 2020].
Kroemer, G., Galluzzi, L. & Brenner, C. (2007) Mitochondrial membrane permeabilization in cell death. *Physiological Reviews*. [Online]. 87 (1) pp.99–163. Available from: doi:10.1152/physrev.00013.2006 [Accessed: 17 November 2020].
Krusat, T. & Streckert, H.-J. (1997) Heparin-dependent attachment of respiratory syncytial virus (RSV) to host cells Brief Report. *Arch Virol*.142.
Kuang, S., Chargé, S.B., Seale, P., Huh, M., et al. (2006) Distinct roles for Pax7 and Pax3 in adult regenerative myogenesis. *Journal of Cell Biology*. [Online] Available from: doi:10.1083/jcb.200508001.
Kuang, S., Kuroda, K., Le Grand, F. & Rudnicki, M.A. (2007) Asymmetric Self-Renewal and Commitment of Satellite Stem Cells in Muscle. *Cell*. [Online] Available from: doi:10.1016/j.cell.2007.03.044.
Kulkarni, P.S., Hurwitz, J.L., Simões, E.A.F. & Piedra, P.A. (2018) Establishing Correlates of Protection for Vaccine Development: Considerations for the Respiratory Syncytial Virus Vaccine Field. *Viral Immunology*. [Online] 31 (2), 195–203. Available from: doi:10.1089/vim.2017.0147.
Kwong, J.C., Schwartz, K.L., Campitelli, M.A., Chung, H., et al. (2018) Acute myocardial infarction after laboratory-confirmed influenza infection. *New England Journal of Medicine*. [Online] Available from: doi:10.1056/NEJMoa1702090.
Lagirand-Cantaloube, J., Offner, N., Csibi, A., Leibovitch, M.P., et al. (2008) The initiation factor eIF3-f is a major target for Atrogin1/MAFbx function in skeletal muscle atrophy. *EMBO Journal*. [Online] Available from: doi:10.1038/emboj.2008.52.
Landi, F., Cruz-Jentoft, A.J., Liperoti, R., Russo, A., et al. (2013) Sarcopenia and mortality risk in frail older persons aged 80 years and older: results from ilSIRENTE study. *Age and ageing*. [Online] 42 (2), 203–209. Available from: doi:10.1093/ageing/afs194 [Accessed: 20 September 2016].
Langen, R.C.J., Schols, A.M.W.J., Kelders, M.C.J.M., Van Der Velden, J.L.J., et al. (2006) Muscle wasting and impaired muscle regeneration in a murine model of chronic pulmonary inflammation. *American Journal of Respiratory Cell and Molecular Biology*. [Online] Available from: doi:10.1165/rcmb.2006-0103OC.
Langhans, W., Savoldelli, D. & Weingarten, S. (1993) Comparison of the feeding responses to bacterial lipopolysaccharide and interleukin-1β. *Physiology and Behavior*. [Online] Available from: doi:10.1016/0031-9384(93)90168-F.
Langrish, C.L., Chen, Y., Blumenschein, W.M., Mattson, J., et al. (2005) IL-23 drives a pathogenic T cell population that induces auto-

immune inflammation. *Journal of Experimental Medicine*. [Online] Available from: doi:10.1084/jem.20041257.
Laplante, M. & Sabatini, D.M. (2012) MTOR signaling in growth control and disease. *Cell*. [Online]. 149 (2) pp.274–293. Available from: doi:10.1016/j.cell.2012.03.017.
Larson, K., Yan, S.-J., Tsurumi, A., Liu, J., et al. (2012) Heterochromatin Formation Promotes Longevity and Represses Ribosomal RNA Synthesis Stuart K. Kim (ed.). *PLoS Genetics*. [Online] 8 (1), e1002473. Available from: doi:10.1371/journal.pgen.1002473 [Accessed: 15 November 2020].
Lauder, S.N., Jones, E., Smart, K., Bloom, A., et al. (2013) Interleukin-6 limits influenza-induced inflammation and protects against fatal lung pathology. *European Journal of Immunology*. [Online] Available from: doi:10.1002/eji.201243018.
Lavasani, M., Robinson, A.R., Lu, A., Song, M., et al. (2012) Muscle-derived stem/progenitor cell dysfunction limits healthspan and lifespan in a murine progeria model. *Nature Communications*. [Online] Available from: doi:10.1038/ncomms1611.
Lawton, L.N., Bonaldo, M.D.F., Jelenc, P.C., Qiu, L., et al. (1997) Identification of a novel member of the TGF-beta superfamily highly expressed in human placenta. *Gene*. [Online] 203 (1), 17–26. Available from: doi:10.1016/S0378-1119(97)00485-X.
Laye, S., Bluthe, R.M., Kent, S., Combe, C., et al. (1995) Subdiaphragmatic vagotomy blocks induction of IL-1β mRNA in mice brain in response to peripheral LPS. *American Journal of Physiology - Regulatory Integrative and Comparative Physiology*. [Online] Available from: doi:10.1152/ajpregu.1995.268.5.r1327.
Lazarus, N.R. & Harridge, S.D.R. (2018) The Inherent Human Aging Process and the Facilitating Role of Exercise. *Frontiers in Physiology*. [Online] 9 (OCT), 1135. Available from: doi:10.3389/fphys.2018.01135 [Accessed: 22 November 2020].
Lee, D.C.P., Harker, J.A.E., Tregoning, J.S., Atabani, S.F., et al. (2010) CD25+ natural regulatory T cells are critical in limiting innate and adaptive immunity and resolving disease following respiratory syncytial virus infection. *Journal of virology*. [Online] 84 (17), 8790–8798. Available from: doi:10.1128/JVI.00796-10 [Accessed: 7 October 2019].
Lee, N., Lui, G.C.Y., Wong, K.T., Li, T.C.M., et al. (2013) High morbidity and mortality in adults hospitalized for respiratory syncytial virus infections. *Clinical infectious diseases : an official publication of the Infectious Diseases Society of America*. [Online] 57 (8), 1069–1077. Available from: doi:10.1093/cid/cit471 [Accessed: 17 September 2016].
Lee, N., Walsh, E.E., Sander, I., Stolper, R., et al. (2017) *Delayed Diagnosis of Respiratory Syncytial Virus Infections in Hospitalized Adults: Individual Patient Data, Record Review Analysis and Physician Survey in the United States*. [Online] 4–8. Available from: doi:10.1093/infdis/jiz236 [Accessed: 3 September 2019].
Lee, S.J., Reed, L.A., Davies, M. V., Girgenrath, S., et al. (2005) Regulation of muscle growth by multiple ligands signaling through activin type II receptors. *Proceedings of the National Academy of Sciences of the United States of America*. [Online] Available from: doi:10.1073/pnas.0505996102.
Lefebvre, J.S., Masters, A.R., Hopkins, J.W. & Haynes, L. (2016) Age-related impairment of humoral response to influenza is associated with changes in antigen specific T follicular helper cell responses. *Scientific Reports*. [Online] 6. Available from: doi:10.1038/srep25051.
Lepper, C., Partridge, T.A. & Fan, C.M. (2011) An absolute requirement for pax7-positive satellite cells in acute injury-induced skeletal muscle regeneration. *Development*. [Online] Available from: doi:10.1242/dev.067595.
Levine, S., Kaliaber-Franco, R. & Paradiso, P.R. (1987) Demonstration that glycoprotein G is the attachment protein of respiratory syncytial virus. *Journal of General Virology*. [Online] 68 (9), 2521–2524. Available from: doi:10.1099/0022-1317-68-9-2521.
Lexell, J. (1995) Human aging, muscle mass, and fiber type composition. *The journals of gerontology. Series A, Biological sciences and medical sciences*. [Online] 50 Spec No, 11–16. Available from: doi:10.1093/gerona/50A.Special_Issue.11.
Li, D., Jans, D.A., Bardin, P.G., Meanger, J., et al. (2008) Association of Respiratory Syncytial Virus M Protein with Viral Nucleocapsids Is Mediated by the M2-1 Protein. *Journal of Virology*. [Online] Available from: doi:10.1128/jvi.00343-08.
Li, G., Yu, M., Lee, W.W., Tsang, M., et al. (2012) Decline in miR-181a expression with age impairs T cell receptor sensitivity by increasing DUSP6 activity. *Nature Medicine*. [Online] Available from: doi:10.1038/nm.2963.
Li, J., Casanova, J.L. & Puel, A. (2018) Mucocutaneous IL-17 immunity in mice and humans: Host defense vs. excessive inflammation. *Mucosal Immunology*. [Online]. Available from: doi:10.1038/mi.2017.97.
Li, P.X., Wong, J., Ayed, A., Ngo, D., et al. (2000) Placental transforming growth factor-β is a downstream mediator of the growth arrest and apoptotic response of tumor cells to DNA damage and p53 overexpression. *Journal of Biological Chemistry*. [Online] Available from: doi:10.1074/jbc.M909580199.
Li, Z., Wang, B., Wu, X., Cheng, S.Y., et al. (2005) Identification, expression and functional characterization of the GRAL gene. *Journal of Neurochemistry*. [Online] Available from: doi:10.1111/j.1471-4159.2005.03372.x.
Liljeroos, L., Krzyzaniak, M.A., Helenius, A. & Butcher, S.J. (2013) Architecture of respiratory syncytial virus revealed by electron cryotomography. *Proceedings of the National Academy of Sciences of the United States of America*. [Online] 110 (27), 11133–11138. Available from: doi:10.1073/pnas.1309070110.
Lin, Q., Lu, J., Yanagisawa, H., Webb, R., et al. (1998) Requirement of the MADS-box transcription factor MEF2C for vascular development. *Development*.
Lin, Q., Schwarz, J., Bucana, C. & Olson, E.N. (1997) Control of mouse cardiac morphogenesis and myogenesis by transcription factor MEF2C. *Science*. [Online] Available from: doi:10.1126/science.276.5317.1404.
Lin, Y., Kim, J., Metter, E.J., Nguyen, H., et al. (2016) Changes in blood lymphocyte numbers with age in vivo and their association with the levels of cytokines/cytokine receptors. *Immunity and Ageing*. [Online] Available from: doi:10.1186/s12979-016-0079-7.
Lindquist, M.E., Lifland, A.W., Utley, T.J., Santangelo, P.J., et al. (2010) Respiratory Syncytial Virus Induces Host RNA Stress Granules To Facilitate Viral Replication. *Journal of Virology*. [Online] Available from: doi:10.1128/jvi.00260-10.
Linterman, M.A. (2014) How T follicular helper cells and the germinal centre response change with age. *Immunology and Cell Biology*. [Online]. 92 (1) pp.72–79. Available from: doi:10.1038/icb.2013.77.
Lipina, C. & Hundal, H.S. (2017) Lipid modulation of skeletal muscle mass and function. *Journal of Cachexia, Sarcopenia and Muscle*. [Online]. 8 (2) pp.190–201. Available from: doi:10.1002/jcsm.12144.
Listì, F., Candore, G., Modica, M.A., Russo, M., et al. (2006) A study of serum immunoglobulin levels in elderly persons that provides new insights into B cell immunosenescence. In: *Annals of the New York Academy of Sciences*. [Online]. 2006 p. Available from: doi:10.1196/annals.1386.013.
Liu, B. & Kimura, Y. (2007) Local immune response to respiratory syncytial virus infection is diminished in senescence-accelerated mice. *Journal of General Virology*. [Online] Available from: doi:10.1099/vir.0.83089-0.

Liu, F., Poursine-Laurent, J., Wu, H.Y. & Link, D.C. (1997) Interleukin-6 and the granulocyte colony-stimulating factor receptor are major independent regulators of granulopoiesis in vivo but are not required for lineage commitment or terminal differentiation. *Blood*. [Online] Available from: doi:10.1182/blood.v90.7.2583.2583_2583_2590.

Liu, J., Xu, Y., Stoleru, D. & Salic, A. (2012) Imaging protein synthesis in cells and tissues with an alkyne analog of puromycin. *Proceedings of the National Academy of Sciences*. [Online] 109 (2), 413–418. Available from: doi:10.1073/pnas.1111561108.

Liu, N., Nelson, B.R., Bezprozvannaya, S., Shelton, J.M., et al. (2014) Requirement of MEF2A, C, and D for skeletal muscle regeneration. *Proceedings of the National Academy of Sciences of the United States of America*. [Online] Available from: doi:10.1073/pnas.1401732111.

Liu, P., Jamaluddin, M., Li, K., Garofalo, R.P., et al. (2007) Retinoic Acid-Inducible Gene I Mediates Early Antiviral Response and Toll-Like Receptor 3 Expression in Respiratory Syncytial Virus-Infected Airway Epithelial Cells. *Journal of Virology*. [Online] 81 (3), 1401–1411. Available from: doi:10.1128/jvi.01740-06 [Accessed: 26 November 2020].

Lokireddy, S., McFarlane, C., Ge, X., Zhang, H., et al. (2011) Myostatin induces degradation of sarcomeric proteins through a Smad3 signaling mechanism during skeletal muscle wasting. *Molecular Endocrinology*. [Online] Available from: doi:10.1210/me.2011-1124.

Lokireddy, S., Wijesoma, I.W., Sze, S.K., McFarlane, C., et al. (2012) Identification of atrogin-1-targeted proteinsθδ during the myostatin-induced skeletal muscle wasting. *American Journal of Physiology - Cell Physiology*. [Online] Available from: doi:10.1152/ajpcell.00402.2011.

Looney, R.J., Falsey, A.R., Walsh, E. & Campbell, D. (2002) Effect of Aging on Cytokine Production in Response to Respiratory Syncytial Virus Infection. *The Journal of Infectious Diseases*. [Online] Available from: doi:10.1086/339008.

López-Otín, C., Blasco, M.A., Partridge, L., Serrano, M., et al. (2013) The hallmarks of aging. *Cell*. [Online]. Available from: doi:10.1016/j.cell.2013.05.039.

López, C.B. & Hermesh, T. (2011) Systemic responses during local viral infections: Type I IFNs sound the alarm. *Current Opinion in Immunology*. [Online]. Available from: doi:10.1016/j.coi.2011.06.003.

Lord, C.J. & Ashworth, A. (2012) The DNA damage response and cancer therapy. *Nature*. [Online]. Available from: doi:10.1038/nature10760.

Luan, H.H., Wang, A., Hilliard, B.K., Carvalho, F., et al. (2019) GDF15 Is an Inflammation-Induced Central Mediator of Tissue Tolerance. *Cell*. [Online] 178 (5), 1231-1244.e11. Available from: doi:10.1016/j.cell.2019.07.033 [Accessed: 7 October 2019].

Lukacs, N.W., Smit, J.J., Mukherjee, S., Morris, S.B., et al. (2010) Respiratory Virus-Induced TLR7 Activation Controls IL-17–Associated Increased Mucus via IL-23 Regulation. *The Journal of Immunology*. [Online] 185 (4), 2231–2239. Available from: doi:10.4049/jimmunol.1000733 [Accessed: 26 November 2020].

Macia, L., Tsai, V.W.W., Nguyen, A.D., Johnen, H., et al. (2012) Macrophage inhibitory cytokine 1 (MIC-1/GDF15) decreases food intake, body weight and improves glucose tolerance in mice on normal & obesogenic diets. *PLoS ONE*. [Online] Available from: doi:10.1371/journal.pone.0034868.

Maegawa, S., Hinkal, G., Kim, H.S., Shen, L., et al. (2010) Widespread and tissue specific age-related DNA methylation changes in mice. *Genome Research*. [Online] 20 (3), 332–340. Available from: doi:10.1101/gr.096826.109 [Accessed: 15 November 2020].

de Magalhães, J.P., Curado, J. & Church, G.M. (2009) Meta-analysis of age-related gene expression profiles identifies common signatures of aging. *Bioinformatics*. [Online] 25 (7), 875–881. Available from: doi:10.1093/bioinformatics/btp073 [Accessed: 15 November 2020].

Von Maltzahn, J., Jones, A.E., Parks, R.J. & Rudnicki, M.A. (2013) Pax7 is critical for the normal function of satellite cells in adult skeletal muscle. *Proceedings of the National Academy of Sciences of the United States of America*. [Online] Available from: doi:10.1073/pnas.1307680110.

Mansouri, A., Stoykova, A., Torres, M. & Gruss, P. (1996) Dysgenesis of cephalic neural crest derivatives in Pax7-/-mutant mice. *Development*.

Marjono, A.B., Brown, D.A., Horton, K.E., Wallace, E.M., et al. (2003) Macrophage inhibitory cytokine-1 in gestational tissues and maternal serum in normal and pre-eclamptic pregnancy. *Placenta*. [Online] Available from: doi:10.1053/plac.2002.0881.

Martin, J.F., Schwarz, J.J. & Olson, E.N. (1993) Myocyte enhancer factor (MEF) 2C: A tissue-restricted member of the MEF-2 family of transcription factors. *Proceedings of the National Academy of Sciences of the United States of America*. [Online] Available from: doi:10.1073/pnas.90.11.5282.

Masiero, E., Agatea, L., Mammucari, C., Blaauw, B., et al. (2009) Autophagy Is Required to Maintain Muscle Mass. *Cell Metabolism*. [Online] Available from: doi:10.1016/j.cmet.2009.10.008.

Masuda, K., Ripley, B., Nishimura, R., Mino, T., et al. (2013) Arid5a controls IL-6 mRNA stability, which contributes to elevation of IL-6 level in vivo. *Proceedings of the National Academy of Sciences of the United States of America*. [Online] Available from: doi:10.1073/pnas.1307419110.

Matheu, A., Maraver, A., Collado, M., Garcia-Cao, I., et al. (2009) Anti-aging activity of the *Ink4/Arf* locus. *Aging Cell*. [Online] 8 (2), 152–161. Available from: doi:10.1111/j.1474-9726.2009.00458.x [Accessed: 18 November 2020].

Matheu, A., Maraver, A., Klatt, P., Flores, I., et al. (2007) Delayed ageing through damage protection by the Arf/p53 pathway. *Nature*. [Online] 448 (7151), 375–379. Available from: doi:10.1038/nature05949 [Accessed: 18 November 2020].

Matthews, V.B., Allen, T.L., Risis, S., Chan, M.H.S., et al. (2010) Interleukin-6-deficient mice develop hepatic inflammation and systemic insulin resistance. *Diabetologia*. [Online] Available from: doi:10.1007/s00125-010-1865-y.

Mattison, J.A., Roth, G.S., Mark Beasley, T., Tilmont, E.M., et al. (2012) Impact of caloric restriction on health and survival in rhesus monkeys from the NIA study. *Nature*. [Online] 489 (7415), 318–321. Available from: doi:10.1038/nature11432 [Accessed: 16 November 2020].

Mauer, J., Chaurasia, B., Goldau, J., Vogt, M.C., et al. (2014) Signaling by IL-6 promotes alternative activation of macrophages to limit endotoxemia and obesity-associated resistance to insulin. *Nature Immunology*. [Online] Available from: doi:10.1038/ni.2865.

Mavalli, M.D., DiGirolamo, D.J., Fan, Y., Riddle, R.C., et al. (2010) Distinct growth hormone receptor signaling modes regulate skeletal muscle development and insulin sensitivity in mice. *Journal of Clinical Investigation*. [Online] Available from: doi:10.1172/JCI42447.

McElhaney, J.E., Zhou, X., Talbot, H.K., Soethout, E., et al. (2012) The unmet need in the elderly: How immunosenescence, CMV infection, co-morbidities and frailty are a challenge for the development of more effective influenza vaccines. *Vaccine*. [Online].

30 (12) pp.2060–2067. Available from: doi:10.1016/j.vaccine.2012.01.015.
McFarland-Mancini, M.M., Funk, H.M., Paluch, A.M., Zhou, M., et al. (2010) Differences in Wound Healing in Mice with Deficiency of IL-6 versus IL-6 Receptor. *The Journal of Immunology*. [Online] Available from: doi:10.4049/jimmunol.0901929.
McFarlane, C., Plummer, E., Thomas, M., Hennebry, A., et al. (2006) Myostatin induces cachexia by activating the ubiquitin proteolytic system through an NF-κB-independent, FoxO1-dependent mechanism. *Journal of Cellular Physiology*. [Online] Available from: doi:10.1002/jcp.20757.
McGeachy, M.J., Bak-Jensen, K.S., Chen, Y., Tato, C.M., et al. (2007) TGF-β and IL-6 drive the production of IL-17 and IL-10 by T cells and restrain TH-17 cell-mediated pathology. *Nature Immunology*. [Online] Available from: doi:10.1038/ni1539.
McLellan, J.S., Chen, M., Leung, S., Graepel, K.W., et al. (2013) Structure of RSV fusion glycoprotein trimer bound to a prefusion-specific neutralizing antibody. *Science*. [Online] Available from: doi:10.1126/science.1234914.
McLellan, J.S., Yang, Y., Graham, B.S. & Kwong, P.D. (2011) Structure of Respiratory Syncytial Virus Fusion Glycoprotein in the Postfusion Conformation Reveals Preservation of Neutralizing Epitopes. *Journal of Virology*. [Online] Available from: doi:10.1128/jvi.00555-11.
McLoughlin, R.M., Hurst, S.M., Nowell, M.A., Harris, D.A., et al. (2004) Differential Regulation of Neutrophil-Activating Chemokines by IL-6 and Its Soluble Receptor Isoforms. *The Journal of Immunology*. [Online] Available from: doi:10.4049/jimmunol.172.9.5676.
McNamara, P.S., Flanagan, B.F., Hart, C.A. & Smyth, R.L. (2005) Production of Chemokines in the Lungs of Infants with Severe Respiratory Syncytial Virus Bronchiolitis. *The Journal of Infectious Diseases*. [Online] Available from: doi:10.1086/428855.
McNamara, P.S., Flanagan, B.F., Selby, A.M., Hart, C.A., et al. (2004) Pro- and anti-inflammatory responses in respiratory syncytial virus bronchiolitis. *European Respiratory Journal*. [Online] Available from: doi:10.1183/09031936.03.00048103.
McPherron, A.C., Lawler, A.M. & Lee, S.J. (1997) Regulation of skeletal muscle mass in mice by a new TGF-β superfamily member. *Nature*. [Online] Available from: doi:10.1038/387083a0.
McPherron, A.C. & Lee, S.J. (1997) Double muscling in cattle due to mutations in the myostatin gene. *Proceedings of the National Academy of Sciences of the United States of America*. [Online] Available from: doi:10.1073/pnas.94.23.12457.
Meadows, E., Flynn, J.M. & Klein, W.H. (2011) Myogenin regulates exercise capacity but is dispensable for skeletal muscle regeneration in adult mdx mice. *PLoS ONE*. [Online] Available from: doi:10.1371/journal.pone.0016184.
Megeney, L.A., Kablar, B., Garrett, K., Anderson, J.E., et al. (1996) MyoD is required for myogenic stem cell function in adult skeletal muscle. *Genes and Development*. [Online] Available from: doi:10.1101/gad.10.10.1173.
Meléndez, A., Tallóczy, Z., Seaman, M., Eskelinen, E.L., et al. (2003) Autophagy genes are essential for dauer development and lifespan extension in C. elegans. *Science*. [Online] Available from: doi:10.1126/science.1087782.
Melov, S., Tamopolsky, M.A., Bechman, K., Felkey, K., et al. (2007) Resistance exercise reverses aging in human skeletal muscle. *PLoS ONE*. [Online] Available from: doi:10.1371/journal.pone.0000465.
Min, J.-N., Whaley, R.A., Sharpless, N.E., Lockyer, P., et al. (2008) CHIP Deficiency Decreases Longevity, with Accelerated Aging Phenotypes Accompanied by Altered Protein Quality Control. *Molecular and Cellular Biology*. [Online] 28 (12), 4018–4025. Available from: doi:10.1128/mcb.00296-08.
Min, K.W., Liggett, J.L., Silva, G., Wu, W.W., et al. (2016) NAG-1/GDF15 accumulates in the nucleus and modulates transcriptional regulation of the Smad pathway. *Oncogene*. [Online] Available from: doi:10.1038/onc.2015.95.
Minetti, G.C., Feige, J.N., Rosenstiel, A., Bombard, F., et al. (2011) Gαi2 signaling promotes skeletal muscle hypertrophy, myoblast differentiation, and muscle regeneration. *Science Signaling*. [Online] Available from: doi:10.1126/scisignal.2002038.
Mitra, R., Baviskar, P., Duncan-Decocq, R.R., Patel, D., et al. (2012) The Human Respiratory Syncytial Virus Matrix Protein Is Required for Maturation of Viral Filaments. *Journal of Virology*. [Online] Available from: doi:10.1128/jvi.06744-11.
Mizushima, N., Levine, B., Cuervo, A.M. & Klionsky, D.J. (2008) Autophagy fights disease through cellular self-digestion. *Nature*. [Online]. 451 (7182) pp.1069–1075. Available from: doi:10.1038/nature06639 [Accessed: 15 November 2020].
Mocchegiani, E., Giacconi, R., Cipriano, C. & Malavolta, M. (2009) NK and NKT cells in aging and longevity: Role of zinc and metallothioneins. *Journal of Clinical Immunology*. [Online]. 29 (4) pp.416–425. Available from: doi:10.1007/s10875-009-9298-4 [Accessed: 23 November 2020].
Modur, V., Li, Y., Zimmerman, G.A., Prescott, S.M., et al. (1997) Retrograde inflammatory signaling from neutrophils to endothelial cells by soluble interleukin-6 receptor alpha. *Journal of Clinical Investigation*. [Online] Available from: doi:10.1172/JCI119821.
Mofarrahi, M., Sigala, I., Guo, Y., Godin, R., et al. (2012) Autophagy and Skeletal Muscles in Sepsis. *PLoS ONE*. [Online] Available from: doi:10.1371/journal.pone.0047265.
Molkentin, J.D., Black, B.L., Martin, J.F. & Olson, E.N. (1995) Cooperative activation of muscle gene expression by MEF2 and myogenic bHLH proteins. *Cell*. [Online] Available from: doi:10.1016/0092-8674(95)90139-6.
Molkentin, J.D., Black, B.L., Martin, J.F. & Olson, E.N. (1996) Mutational analysis of the DNA binding, dimerization, and transcriptional activation domains of MEF2C. *Molecular and Cellular Biology*. [Online] Available from: doi:10.1128/mcb.16.6.2627.
Molofsky, A. V., Slutsky, S.G., Joseph, N.M., He, S., et al. (2006) Increasing p16INK4a expression decreases forebrain progenitors and neurogenesis during ageing. *Nature*. [Online] Available from: doi:10.1038/nature05091.
Monier, S., Le Cam, A. & Le Marchand Brustel, Y. (1983) Insulin and insulin-like growth factor I. Effects on protein synthesis in isolated muscles from lean and goldthioglucose-obese mice. *Diabetes*. [Online] Available from: doi:10.2337/diabetes.32.5.392.
Moore, A.G., Brown, D.A., Fairlie, W.D., Bauskin, A.R., et al. (2000) The transforming growth factor-β superfamily cytokine macrophage inhibitory cytokine-1 is present in high concentrations in the serum of pregnant women. *Journal of Clinical Endocrinology and Metabolism*. [Online] Available from: doi:10.1210/jc.85.12.4781.
Moresi, V., Williams, A.H., Meadows, E., Flynn, J.M., et al. (2010) Myogenin and class II HDACs control neurogenic muscle atrophy by inducing E3 ubiquitin ligases. *Cell*. [Online] Available from: doi:10.1016/j.cell.2010.09.004.
Moretti, I., Ciciliot, S., Dyar, K.A., Abraham, R., et al. (2016) MRF4 negatively regulates adult skeletal muscle growth by repressing MEF2 activity. *Nature Communications*. [Online] Available from: doi:10.1038/ncomms12397.
Morris, J.A., Blount, R.E. & Savage, R.E. (1956) Recovery of Cytopathogenic Agent from Chimpanzees with Coryza. *Experimental Biology and Medicine*. [Online] 92 (3), 544–549. Available from: doi:10.3181/00379727-92-22538 [Accessed: 5 March 2020].
Mosher, D.S., Quignon, P., Bustamante, C.D., Sutter, N.B., et al. (2007) A mutation in the myostatin gene increases muscle mass and enhances racing performance in heterozygote dogs. *PLoS Genetics*. [Online] Available from: doi:10.1371/journal.pgen.0030079.

Moskalev, A.A., Shaposhnikov, M. V., Plyusnina, E.N., Zhavoronkov, A., et al. (2013) The role of DNA damage and repair in aging through the prism of Koch-like criteria. *Ageing Research Reviews*. [Online]. Available from: doi:10.1016/j.arr.2012.02.001.
Mostoslavsky, R., Chua, K.F., Lombard, D.B., Pang, W.W., et al. (2006) Genomic instability and aging-like phenotype in the absence of mammalian SIRT6. *Cell*. [Online] 124 (2), 315–329. Available from: doi:10.1016/j.cell.2005.11.044.
Mourkioti, F., Kratsios, P., Luedde, T., Song, Y.H., et al. (2006) Targeted ablation of IKK2 improves skeletal muscle strength, maintains mass, and promotes regeneration. *Journal of Clinical Investigation*. [Online] Available from: doi:10.1172/JCI28721.
Mroczko, B., Groblewska, M., Gryko, M., Kedra, B., et al. (2010) Diagnostic usefulness of serum Interleukin 6 (IL-6) and C-Reactive Protein (CRP) in the differentiation between pancreatic cancer and chronic pancreatitis. *Journal of Clinical Laboratory Analysis*. [Online] Available from: doi:10.1002/jcla.20395.
Mufson, M.A., Orvell, C., Rafnar, B. & Norrby, E. (1985) Two distinct subtypes of human respiratory syncytial virus. *Journal of General Virology*. [Online] Available from: doi:10.1099/0022-1317-66-10-2111.
Mullican, S.E., Lin-Schmidt, X., Chin, C.-N., Chavez, J.A., et al. (2017) GFRAL is the receptor for GDF15 and the ligand promotes weight loss in mice and nonhuman primates. *Nature Medicine*. [Online] 23 (10), 1150–1157. Available from: doi:10.1038/nm.4392 [Accessed: 11 January 2018].
Mullican, S.E. & Rangwala, S.M. (2018) Uniting GDF15 and GFRAL: Therapeutic Opportunities in Obesity and Beyond. *Trends in Endocrinology & Metabolism*. [Online] 29 (8), 560–570. Available from: doi:10.1016/J.TEM.2018.05.002 [Accessed: 8 August 2018].
Muñoz-Cánoves, P., Scheele, C., Pedersen, B.K. & Serrano, A.L. (2013) Interleukin-6 myokine signaling in skeletal muscle: A double-edged sword? *FEBS Journal*. [Online]. 280 (17) pp.4131–4148. Available from: doi:10.1111/febs.12338.
Murawski, M.R., Bowen, G.N., Cerny, A.M., Anderson, L.J., et al. (2009) Respiratory Syncytial Virus Activates Innate Immunity through Toll-Like Receptor 2. *Journal of Virology*. [Online] Available from: doi:10.1128/jvi.00671-08.
Murphy, M.M., Lawson, J.A., Mathew, S.J., Hutcheson, D.A., et al. (2011) Satellite cells, connective tissue fibroblasts and their interactions are crucial for muscle regeneration. *Development*. [Online] Available from: doi:10.1242/dev.064162.
Musarò, A., McCullagh, K., Paul, A., Houghton, L., et al. (2001) Localized Igf-1 transgene expression sustains hypertrophy and regeneration in senescent skeletal muscle. *Nature Genetics*. [Online] 27 (2), 195–200. Available from: doi:10.1038/84839.
Muscaritoli, M., Anker, S.D., Argilés, J., Aversa, Z., et al. (2010) Consensus definition of sarcopenia, cachexia and pre-cachexia: Joint document elaborated by Special Interest Groups (SIG) ' cachexia-anorexia in chronic wasting diseases' and ' nutrition in geriatrics'. *Clinical Nutrition*. [Online] Available from: doi:10.1016/j.clnu.2009.12.004.
Nagabhushanam, V., Solache, A., Ting, L.-M., Escaron, C.J., et al. (2003) Innate Inhibition of Adaptive Immunity: Mycobacterium tuberculosis -Induced IL-6 Inhibits Macrophage Responses to IFN-γ . *The Journal of Immunology*. [Online] Available from: doi:10.4049/jimmunol.171.9.4750.
Nakagawa, S., Lagisz, M., Hector, K.L. & Spencer, H.G. (2012) Comparative and meta-analytic insights into life extension via dietary restriction. *Aging Cell*. [Online] 11 (3), 401–409. Available from: doi:10.1111/j.1474-9726.2012.00798.x [Accessed: 22 November 2020].
Nakamura-Lopez, Y., Villegas-Sepúlveda, N. & Gómez, B. (2015) RSV P-protein impairs extrinsic apoptosis pathway in a macrophage-like cell line persistently infected with respiratory syncytial virus. *Virus Research*. [Online] Available from: doi:10.1016/j.virusres.2015.04.018.
Nakano, K. & Hara, H. (1979) Measurement of the Protein-Synthetic Activity in vivo of Various Tissues in Rats by using I3HIPuromycin. *Biochem. J*. 184, 663–668.
Narici, M. V. & Maffulli, N. (2010) Sarcopenia: Characteristics, mechanisms and functional significance. *British Medical Bulletin*. [Online]. Available from: doi:10.1093/bmb/ldq008.
Nathans, D. (1964) Puromycin inhibition of protein synthesis: Incorporation of puromycin into peptide chains. *Proceedings of the National Academy of Sciences of the United States of America*. [Online] 51 (1963), 585–592. Available from: http://www.ncbi.nlm.nih.gov/pubmed/14166766 [Accessed: 4 January 2018].
Navarini, A.A., French, L.E. & Hofbauer, G.F.L. (2011) Interrupting IL-6-receptor signaling improves atopic dermatitis but associates with bacterial superinfection. *Journal of Allergy and Clinical Immunology*. [Online] Available from: doi:10.1016/j.jaci.2011.09.009.
Nicholas, A., de Magalhaes, J.P., Kraytsberg, Y., Richfield, E.K., et al. (2010) Age-related gene-specific changes of A-to-I mRNA editing in the human brain. *Mechanisms of Ageing and Development*. [Online] 131 (6), 445–447. Available from: doi:10.1016/j.mad.2010.06.001.
Nicholson, K.G. (1996) Impact of influenza and respiratory syncytial virus on mortality in England and Wales from January 1975 to. *Epidemiol. Infect*.116.
Nickel, N., Kempf, T., Tapken, H., Tongers, J., et al. (2008) Growth differentiation factor-15 in idiopathic pulmonary arterial hypertension. *American journal of respiratory and critical care medicine*. [Online] 178 (5), 534–541. Available from: doi:10.1164/rccm.200802-235OC.
Nogueiras, R., Habegger, K.M., Chaudhary, N., Finan, B., et al. (2012) Sirtuin 1 and sirtuin 3: Physiological modulators of metabolism. *Physiological Reviews*. [Online] 92 (3), 1479–1514. Available from: doi:10.1152/physrev.00022.2011 [Accessed: 15 November 2020].
Nomellini, V., Brubaker, A.L., Mahbub, S., Palmer, J.L., et al. (2012) Dysregulation of neutrophil CXCR2 and pulmonary endothelial ICAM-1 promotes age-related pulmonary inflammation. *Aging and Disease*.
Nomellini, V., Faunce, D.E., Gomez, C.R. & Kovacs, E.J. (2008) An age-associated increase in pulmonary inflammation after burn injury is abrogated by CXCR2 inhibition. *Journal of Leukocyte Biology*. [Online] 83 (6), 1493–1501. Available from: doi:10.1189/jlb.1007672 [Accessed: 23 November 2020].
Le Nouën, C., Hillyer, P., Levenson, E., Martens, C., et al. (2019) Lack of Activation Marker Induction and Chemokine Receptor Switch in Human Neonatal Myeloid Dendritic Cells in Response to Human Respiratory Syncytial Virus. *Journal of virology*. [Online] 93 (22). Available from: doi:10.1128/JVI.01216-19 [Accessed: 11 March 2020].
Nowell, M.A., Williams, A.S., Carty, S.A., Scheller, J., et al. (2009) Therapeutic Targeting of IL-6 Trans Signaling Counteracts STAT3 Control of Experimental Inflammatory Arthritis . *The Journal of Immunology*. [Online] Available from: doi:10.4049/jimmunol.182.1.613.
Nurieva, R.I., Chung, Y., Hwang, D., Yang, X.O., et al. (2008) Generation of T Follicular Helper Cells Is Mediated by Interleukin-21 but

Independent of T Helper 1, 2, or 17 Cell Lineages. *Immunity*. [Online] 29 (1), 138–149. Available from: doi:10.1016/j.immuni.2008.05.009 [Accessed: 26 February 2020].
Nurieva, R.I., Chung, Y., Martinez, G.J., Yang, X.O., et al. (2009) Bcl6 mediates the development of T follicular helper cells. *Science*. [Online] Available from: doi:10.1126/science.1176676.
Nutt, S.L., Hodgkin, P.D., Tarlinton, D.M. & Corcoran, L.M. (2015) The generation of antibody-secreting plasma cells. *Nature Reviews Immunology*. [Online] 15 (3), 160–171. Available from: doi:10.1038/nri3795.
Nyugen, J., Agrawal, S., Gollapudi, S. & Gupta, S. (2010) Impaired functions of peripheral blood monocyte subpopulations in aged humans. *Journal of Clinical Immunology*. [Online] Available from: doi:10.1007/s10875-010-9448-8.
O'Leary, M.F., Vainshtein, A., Iqbal, S., Ostojic, O., et al. (2013) Adaptive plasticity of autophagic proteins to denervation in aging skeletal muscle. *American Journal of Physiology - Cell Physiology*. [Online] Available from: doi:10.1152/ajpcell.00240.2012.
O'Rahilly, S. (2017) GDF15—From Biomarker to Allostatic Hormone. *Cell Metabolism*. [Online]. 26 (6) pp.807–808. Available from: doi:10.1016/j.cmet.2017.10.017 [Accessed: 8 March 2018].
Oberdoerffer, P. & Sinclair, D.A. (2007) The role of nuclear architecture in genomic instability and ageing. *Nature Reviews Molecular Cell Biology*. [Online]. 8 (9) pp.692–702. Available from: doi:10.1038/nrm2238 [Accessed: 15 November 2020].
Ochola, R., Sande, C., Fegan, G., Scott, P.D., et al. (2009) The Level and Duration of RSV-Specific Maternal IgG in Infants in Kilifi Kenya Lisa F. P. Ng (ed.). *PLoS ONE*. [Online] 4 (12), e8088. Available from: doi:10.1371/journal.pone.0008088 [Accessed: 13 April 2020].
Office for National Statistics (2018) Health state life expectancies, UK: 2015 to 2017. *Office for National Statistics*.
Ogilvie, M.M., Santhire Vathenen, A., Radford, M., Codd, J., et al. (1981) Maternal antibody and respiratory syncytial virus infection in infancy. *Journal of Medical Virology*. [Online] 7 (4), 263–271. Available from: doi:10.1002/jmv.1890070403 [Accessed: 13 April 2020].
Ohler, K.H. & Pham, J.T. (2013) Comparison of the timing of initial prophylactic palivizumab dosing on hospitalization of neonates for respiratory syncytial virus. *American Journal of Health-System Pharmacy*. [Online] Available from: doi:10.2146/ajhp120526.
Okamura, H. (2015) Lack of canonical SMAD2 pathway activation by recombinant GDF15 in vitro. *Journal of Cachexia, Sarcopenia and Muscle*. [Online] 6 (1), 25. Available from: https://onlinelibrary.wiley.com/doi/10.1002/jcsm.12004.
Olguin, H.C. & Olwin, B.B. (2004) Pax-7 up-regulation inhibits myogenesis and cell cycle progression in satellite cells: A potential mechanism for self-renewal. *Developmental Biology*. [Online] Available from: doi:10.1016/j.ydbio.2004.08.015.
Olsen, O.E., Skjærvik, A., Størdal, B.F., Sundan, A., et al. (2017) TGF-β contamination of purified recombinant GDF15 Marie Jose Goumans (ed.). *PLOS ONE*. [Online] 12 (11), e0187349. Available from: doi:10.1371/journal.pone.0187349 [Accessed: 27 March 2020].
Onken, B. & Driscoll, M. (2010) Metformin Induces a Dietary Restriction–Like State and the Oxidative Stress Response to Extend C. elegans Healthspan via AMPK, LKB1, and SKN-1 Anne C. Hart (ed.). *PLoS ONE*. [Online] 5 (1), e8758. Available from: doi:10.1371/journal.pone.0008758 [Accessed: 16 November 2020].
Openshaw, P.J.M., Chiu, C., Culley, F.J. & Johansson, C. (2017) Protective and Harmful Immunity to RSV Infection. *Annual Review of Immunology*. [Online] 35 (1), 501–532. Available from: doi:10.1146/annurev-immunol-051116-052206 [Accessed: 13 January 2018].
Orlich, M.J., Singh, P.N., Sabaté, J., Jaceldo-Siegl, K., et al. (2013) Vegetarian dietary patterns and mortality in adventist health study 2. *JAMA Internal Medicine*. [Online] 173 (13), 1230–1238. Available from: doi:10.1001/jamainternmed.2013.6473 [Accessed: 22 November 2020].
Osorio, F.G., Bárcena, C., Soria-Valles, C., Ramsay, A.J., et al. (2012) Nuclear lamina defects cause ATM-dependent NF-κB activation and link accelerated aging to a systemic inflammatory response. *Genes and Development*. [Online] 26 (20), 2311–2324. Available from: doi:10.1101/gad.197954.112 [Accessed: 20 November 2020].
Ostler, T., Davidson, W. & Ehl, S. (2002) Virus clearance and immunopathology by CD8+ T cells during infection with respiratory syncytial virus are mediated by IFN-γ. *European Journal of Immunology*. [Online] 32 (8), 2117–2123. Available from: doi:10.1002/1521-4141(200208)32:8<2117::AID-IMMU2117>3.0.CO;2-C [Accessed: 22 November 2020].
Pallafacchina, G., Calabria, E., Serrano, A.L., Kalhovde, J.M., et al. (2002) A protein kinase B-dependent and rapamycin-sensitive pathway controls skeletal muscle growth but not fiber type specification. *Proceedings of the National Academy of Sciences of the United States of America*. [Online] Available from: doi:10.1073/pnas.142166599.
Panda, A., Qian, F., Mohanty, S., van Duin, D., et al. (2010) Age-Associated Decrease in TLR Function in Primary Human Dendritic Cells Predicts Influenza Vaccine Response. *The Journal of Immunology*. [Online] Available from: doi:10.4049/jimmunol.0901022.
Pang, W.W., Price, E.A., Sahoo, D., Beerman, I., et al. (2011) Human bone marrow hematopoietic stem cells are increased in frequency and myeloid-biased with age. *Proceedings of the National Academy of Sciences of the United States of America*. [Online] 108 (50), 20012–20017. Available from: doi:10.1073/pnas.1116110108 [Accessed: 24 November 2020].
Panichi, V., Maggiore, U., Taccola, D., Migliori, M., et al. (2004) Interleukin-6 is a stronger predictor of total and cardiovascular mortality than C-reactive protein in haemodialysis patients. *Nephrology Dialysis Transplantation*. [Online] Available from: doi:10.1093/ndt/gfh052.
Paralkar, V.M., Vail, A.L., Grasser, W.A., Brown, T.A., et al. (1998) Cloning and characterization of a novel member of the transforming growth factor-β/bone morphogenetic protein family. *Journal of Biological Chemistry*. [Online] 273 (22), 13760–13767. Available from: doi:10.1074/jbc.273.22.13760.
Pasare, C. & Medzhitov, R. (2003) Toll pathway-dependent blockade of CD4+CD25+ T cell-mediated suppression by dendritic cells. *Science*. [Online] Available from: doi:10.1126/science.1078231.
Passarino, G., De Rango, F. & Montesanto, A. (2016) Human longevity: Genetics or Lifestyle? It takes two to tango. *Immunity and Ageing*. [Online]. Available from: doi:10.1186/s12979-016-0066-z.
Patel, M.S., Lee, J., Baz, M., Wells, C.E., et al. (2016) Growth differentiation factor-15 is associated with muscle mass in chronic obstructive pulmonary disease and promotes muscle wasting in vivo. *Journal of Cachexia, Sarcopenia and Muscle*. [Online] 7 (4), 436–448. Available from: doi:10.1002/jcsm.12096 [Accessed: 17 September 2016].
Paton, N.I. & Ng, Y.-M. (2006) Body composition studies in patients with wasting associated with tuberculosis. *Nutrition (Burbank, Los Angeles County, Calif.)*. [Online] 22 (3), 245–251. Available from: doi:10.1016/j.nut.2005.06.009.
Pawar, A., Desai, R.J., Solomon, D.H., Santiago Ortiz, A.J., et al. (2019) Risk of serious infections in tocilizumab versus other biologic

drugs in patients with rheumatoid arthritis: A multidatabase cohort study. *Annals of the Rheumatic Diseases*. [Online] Available from: doi:10.1136/annrheumdis-2018-214367.
Pawelec, G. (2014) Immunosenenescence: Role of cytomegalovirus. *Experimental Gerontology*. [Online]. 54 pp.1–5. Available from: doi:10.1016/j.exger.2013.11.010.
Pawelec, G. (2017) Immunosenescence and cancer. *Biogerontology*. [Online] 18 (4), 717–721. Available from: doi:10.1007/s10522-017-9682-z [Accessed: 24 November 2020].
Pawelec, G., McElhaney, J.E., Aiello, A.E. & Derhovanessian, E. (2012) The impact of CMV infection on survival in older humans. *Current Opinion in Immunology*. [Online]. Available from: doi:10.1016/j.coi.2012.04.002.
Payette, H., Roubenoff, R., Jacques, P.F., Dinarello, C.A., et al. (2003) Insulin-like growth factor-1 and interleukin 6 predict sarcopenia in very old community-living men and women: The Framingham heart study. *Journal of the American Geriatrics Society*. [Online] Available from: doi:10.1046/j.1532-5415.2003.51407.x.
Pedersen, B.K., Akerström, T.C.A., Nielsen, A.R. & Fischer, C.P. (2007) Role of myokines in exercise and metabolism. *Journal of applied physiology (Bethesda, Md. : 1985)*. [Online] 103 (3), 1093–1098. Available from: doi:10.1152/japplphysiol.00080.2007 [Accessed: 18 October 2017].
Pedersen, B.K. & Saltin, B. (2015) Exercise as medicine - Evidence for prescribing exercise as therapy in 26 different chronic diseases. *Scandinavian Journal of Medicine and Science in Sports*. [Online] 25, 1–72. Available from: doi:10.1111/sms.12581 [Accessed: 22 November 2020].
Pegoraro, G., Kubben, N., Wickert, U., Göhler, H., et al. (2009) Ageing-related chromatin defects through loss of the NURD complex. *Nature Cell Biology*. [Online] 11 (10), 1261–1267. Available from: doi:10.1038/ncb1971 [Accessed: 15 November 2020].
Pekkala, S., Wiklund, P., Hulmi, J.J., Pöllänen, E., et al. (2015) Cannabinoid receptor 1 and acute resistance exercise – In vivo and in vitro studies in human skeletal muscle. *Peptides*. [Online] 67, 55–63. Available from: doi:10.1016/j.peptides.2015.03.007.
Peleg, S., Sananbenesi, F., Zovoilis, A., Burkhardt, S., et al. (2010) Altered histone acetylation is associated with age-dependent memory impairment in mice. *Science*. [Online] 328 (5979), 753–756. Available from: doi:10.1126/science.1186088 [Accessed: 15 November 2020].
Pennings, J.L.A., Mariman, R., Hodemaekers, H.M., Reemers, S.S.N., et al. (2018) Transcriptomics in lung tissue upon respiratory syncytial virus infection reveals aging as important modulator of immune activation and matrix maintenance. *Scientific Reports*. [Online] 8 (1), 1–13. Available from: doi:10.1038/s41598-018-35180-2.
Pérez, V.I., Van Remmen, H., Bokov, A., Epstein, C.J., et al. (2009) The overexpression of major antioxidant enzymes does not extend the lifespan of mice. *Aging Cell*. [Online] 8 (1), 73–75. Available from: doi:10.1111/j.1474-9726.2008.00449.x.
Peters, M., Jacobs, S., Ehlers, M., Vollmer, P., et al. (1996) The function of the soluble interleukin 6 (IL-6) receptor in vivo: Sensitization of human soluble IL-6 receptor transgenic mice towards IL-6 and prolongation of the plasma half-life of IL-6. *Journal of Experimental Medicine*. [Online] Available from: doi:10.1084/jem.183.4.1399.
Peterson, J.M., Bakkar, N. & Guttridge, D.C. (2011) Chapter four – NF-κB Signaling in Skeletal Muscle Health and Disease. In: *Current Topics in Developmental Biology*. [Online]. pp. 85–119. Available from: doi:10.1016/B978-0-12-385940-2.00004-8.
Petry, C.J., Ong, K.K., Burling, K.A., Barker, P., et al. (2017) GDF15 Concentrations in Maternal Serum Associated with Vomiting in Pregnancy: the Cambridge Baby Growth Study. *bioRxiv*. [Online] Available from: doi:10.1101/221267.
Pillai, P.S., Molony, R.D., Martinod, K., Dong, H., et al. (2016) Mx1 reveals innate pathways to antiviral resistance and lethal influenza disease. *Science*. [Online] Available from: doi:10.1126/science.aaf3926.
Pitta, F., Troosters, T., Probst, V.S., Spruit, M.A., et al. (2006) Physical activity and hospitalization for exacerbation of COPD. *Chest*. [Online] Available from: doi:10.1378/chest.129.3.536.
Plata-Salamán, C.R. (1996) Anorexia induced by activators of the signal transducer gp 130. *NeuroReport*. [Online] Available from: doi:10.1097/00001756-199602290-00038.
Plata-Salamán, C.R., Sonti, G., Borkoski, J.P., Wilson, C.D., et al. (1996) Anorexia induced by chronic central administration of cytokines at estimated pathophysiological concentrations. *Physiology and Behavior*. [Online] Available from: doi:10.1016/S0031-9384(96)00148-5.
Polge, C., Heng, A.-E., Jarzaguet, M., Ventadour, S., et al. (2011) Muscle actin is polyubiquitinylated in vitro and in vivo and targeted for breakdown by the E3 ligase MuRF1 . *The FASEB Journal*. [Online] Available from: doi:10.1096/fj.11-180968.
Pollina, E.A. & Brunet, A. (2011) Epigenetic regulation of aging stem cells. *Oncogene*. [Online]. 30 (28) pp.3105–3126. Available from: doi:10.1038/onc.2011.45 [Accessed: 15 November 2020].
Potthoff, M.J., Arnold, M.A., McAnally, J., Richardson, J.A., et al. (2007a) Regulation of Skeletal Muscle Sarcomere Integrity and Postnatal Muscle Function by Mef2c. *Molecular and Cellular Biology*. [Online] Available from: doi:10.1128/mcb.01187-07.
Potthoff, M.J., Wu, H., Arnold, M.A., Shelton, J.M., et al. (2007b) Histone deacetylase degradation and MEF2 activation promote the formation of slow-twitch myofibers. *Journal of Clinical Investigation*. [Online] Available from: doi:10.1172/JCI31960.
Poulain, M., Herm, A. & Pes, G. (2014) The Blue Zones: areas of exceptional longevity around the world. *Vienna Yearbook of Population Research*. [Online] Volume 11 (1), 87–108. Available from: doi:10.1553/populationyearbook2013s87 [Accessed: 22 November 2020].
Powers, E.T., Morimoto, R.I., Dillin, A., Kelly, J.W., et al. (2009) Biological and Chemical Approaches to Diseases of Proteostasis Deficiency. *Annual Review of Biochemistry*. [Online] 78 (1), 959–991. Available from: doi:10.1146/annurev.biochem.052308.114844 [Accessed: 15 November 2020].
Pritz, T., Lair, J., Ban, M., Keller, M., et al. (2015) Plasma cell numbers decrease in bone marrow of old patients. *European Journal of Immunology*. [Online] Available from: doi:10.1002/eji.201444878.
Public Health England (2020) *Disparities in the risk and outcomes of COVID-19*. [Online]. Available from: www.facebook.com/PublicHealthEngland [Accessed: 22 November 2020].
Puel, A., Picard, C., Lorrot, M., Pons, C., et al. (2008) Recurrent Staphylococcal Cellulitis and Subcutaneous Abscesses in a Child with Autoantibodies against IL-6. *The Journal of Immunology*. [Online] Available from: doi:10.4049/jimmunol.180.1.647.
Puzianowska-Kuźnicka, M., Owczarz, M., Wieczorowska-Tobis, K., Nadrowski, P., et al. (2016) Interleukin-6 and C-reactive protein, successful aging, and mortality: The PolSenior study. *Immunity and Ageing*. [Online] 13 (1). Available from: doi:10.1186/s12979-016-0076-x.
Pyle, C.J., Uwadiae, F.I., Swieboda, D.P. & Harker, J.A. (2017) Early IL-6 signalling promotes IL-27 dependent maturation of regulatory T cells in the lungs and resolution of viral immunopathology. *PLoS Pathogens*. [Online] 13 (9). Available from: doi:10.1371/

journal.ppat.1006640.
Quy, P.N., Kuma, A., Pierres, P. & Mizushima, N. (2013) Proteasome-dependent activation of mammalian target of rapamycin complex 1 (mTORC1) is essential for autophagy suppression and muscle remodeling following denervation. *Journal of Biological Chemistry*. [Online] Available from: doi:10.1074/jbc.M112.399949.
Raben, N., Hill, V., Shea, L., Takikita, S., et al. (2008) Suppression of autophagy in skeletal muscle uncovers the accumulation of ubiquitinated proteins and their potential role in muscle damage in Pompe disease. *Human Molecular Genetics*. [Online] Available from: doi:10.1093/hmg/ddn292.
Radigan, K.A., Nicholson, T.T., Welch, L.C., Chi, M., et al. (2019) Influenza A Virus Infection Induces Muscle Wasting via IL-6 Regulation of the E3 Ubiquitin Ligase Atrogin-1. *The Journal of Immunology*. [Online] Available from: doi:10.4049/jimmunol.1701433.
Ramsay, A.J., Husband, A.J., Ramshaw, I.A., Bao, S., et al. (1994) The role of interleukin-6 in mucosal IgA antibody responses in vivo. *Science*. [Online] 264 (5158), 561–563. Available from: doi:10.1126/science.8160012.
Rantanen, J., Hurme, T., Lukka, R., Heino, J., et al. (1995) Satellite cell proliferation and the expression of myogenin and desmin in regenerating skeletal muscle: Evidence for two different populations of satellite cells. *Laboratory Investigation*.
Raule, N., Sevini, F., Li, S., Barbieri, A., et al. (2014) The co-occurrence of mtDNA mutations on different oxidative phosphorylation subunits, not detected by haplogroup analysis, affects human longevity and is population specific. *Aging Cell*. [Online] 13 (3), 401–407. Available from: doi:10.1111/acel.12186 [Accessed: 21 November 2020].
Ravussin, E., Redman, L.M., Rochon, J., Das, S.K., et al. (2015) A 2-year randomized controlled trial of human caloric restriction: Feasibility and effects on predictors of health span and longevity. *Journals of Gerontology - Series A Biological Sciences and Medical Sciences*. [Online] 70 (9), 1097–1104. Available from: doi:10.1093/gerona/glv057 [Accessed: 21 November 2020].
Reeves, R.M., Hardelid, P., Panagiotopoulos, N., Minaji, M., et al. (2019) Burden of hospital admissions caused by respiratory syncytial virus (RSV) in infants in England: A data linkage modelling study. *Journal of Infection*. [Online] Available from: doi:10.1016/j.jinf.2019.02.012.
Remy, I., Montmarquette, A. & Michnick, S.W. (2004) PKB/Akt modulates TGF-β signalling through a direct interaction with Smad3. *Nature Cell Biology*. [Online] Available from: doi:10.1038/ncb1113.
Renshaw, M., Rockwell, J., Engleman, C., Gewirtz, A., et al. (2002) Cutting Edge: Impaired Toll-Like Receptor Expression and Function in Aging. *The Journal of Immunology*. [Online] Available from: doi:10.4049/jimmunol.169.9.4697.
Richards, P.J., Nowell, M.A., Horiuchi, S., McLoughlin, R.M., et al. (2006) Functional characterization of a soluble gp130 isoform and its therapeutic capacity in an experimental model of inflammatory arthritis. *Arthritis and Rheumatism*. [Online] Available from: doi:10.1002/art.21818.
Richner, J.M., Gmyrek, G.B., Govero, J., Tu, Y., et al. (2015) Age-Dependent Cell Trafficking Defects in Draining Lymph Nodes Impair Adaptive Immunity and Control of West Nile Virus Infection Luis J. Sigal (ed.). *PLOS Pathogens*. [Online] 11 (7), e1005027. Available from: doi:10.1371/journal.ppat.1005027 [Accessed: 24 November 2020].
Rigas, J.R., Schuster, M., Orlov, S. V., Milovanovic, B., et al. (2010) Effect of ALD518, a humanized anti-IL-6 antibody, on lean body mass loss and symptoms in patients with advanced non-small cell lung cancer (NSCLC): Results of a phase II randomized, double-blind safety and efficacy trial. *Journal of Clinical Oncology*. [Online] 28 (15_suppl), 7622–7622. Available from: doi:10.1200/jco.2010.28.15_suppl.7622.
Rima, B., Collins, P., Easton, A., Fouchier, R., et al. (2017) ICTV virus taxonomy profile: Pneumoviridae. *Journal of General Virology*. [Online] 98 (12), 2912–2913. Available from: doi:10.1099/jgv.0.000959.
Risson, V., Mazelin, L., Roceri, M., Sanchez, H., et al. (2009) Muscle inactivation of mTOR causes metabolic and dystrophin defects leading to severe myopathy. *Journal of Cell Biology*. [Online] Available from: doi:10.1083/jcb.200903131.
Rivest, S. (1999) Activation of the nuclear factor kappa b (NF-kB) and cyclooxygenase-2 (COX-2) genes in cerebral blood vessels in response to systemic inflammation. *Molecular Psychiatry*. [Online]. Available from: doi:10.1038/sj.mp.4000679.
Rivest, S. (2003) Molecular insights on the cerebral innate immune system. *Brain, Behavior, and Immunity*. [Online]. Available from: doi:10.1016/S0889-1591(02)00055-7.
Rixon, H.W.M.L., Brown, G., Aitken, J., McDonald, T., et al. (2004) The small hydrophobic (SH) protein accumulates within lipid-raft structures of the Golgi complex during respiratory syncytial virus infection. *Journal of General Virology*. [Online] 85 (5), 1153–1165. Available from: doi:10.1099/vir.0.19769-0.
Romanello, V., Guadagnin, E., Gomes, L., Roder, I., et al. (2010) Mitochondrial fission and remodelling contributes to muscle atrophy. *EMBO Journal*. [Online] Available from: doi:10.1038/emboj.2010.60.
Romano, M., Sironi, M., Toniatti, C., Polentarutti, N., et al. (1997) Role of IL-6 and its soluble receptor in induction of chemokines and leukocyte recruitment. *Immunity*. [Online] Available from: doi:10.1016/S1074-7613(00)80334-9.
Rommel, C., Bodine, S.C., Clarke, B.A., Rossman, R., et al. (2001) Mediation of IGF-1-induced skeletal myotube hypertrophy by PI(3)K/Alt/mTOR and PI(3)K/Akt/GSK3 pathways. *Nature Cell Biology*. [Online] Available from: doi:10.1038/ncb1101-1009.
Rose, M.R. (1991) *Evolutionary Biology of Aging*. New York, Oxford University Press.
Roseno, S.L., Davis, P.R., Bollinger, L.M., Powell, J.J.S., et al. (2015) Short-term, high-fat diet accelerates disuse atrophy and protein degradation in a muscle-specific manner in mice. *Nutrition and Metabolism*. [Online] Available from: doi:10.1186/s12986-015-0037-y.
Rossaint, J., Vestweber, D. & Zarbock, A. (2013) GDF-15 prevents platelet integrin activation and thrombus formation. *Journal of Thrombosis and Haemostasis*. [Online] Available from: doi:10.1111/jth.12100.
Rossi, D.J., Bryder, D., Seita, J., Nussenzweig, A., et al. (2007) Deficiencies in DNA damage repair limit the function of haematopoietic stem cells with age. *Nature*. [Online] Available from: doi:10.1038/nature05862.
Rubinsztein, D.C., Mariño, G. & Kroemer, G. (2011) Autophagy and aging. *Cell*. [Online]. 146 (5) pp.682–695. Available from: doi:10.1016/j.cell.2011.07.030.
Rubtsov, A. V., Rubtsova, K., Fischer, A., Meehan, R.T., et al. (2011) Toll-like receptor 7 (TLR7)-driven accumulation of a novel CD11c+ B-cell population is important for the development of autoimmunity. *Blood*. [Online] Available from: doi:10.1182/blood-2011-01-331462.
Rubtsova, K., Rubtsov, A. V., Van Dyk, L.F., Kappler, J.W., et al. (2013) T-box transcription factor T-bet, a key player in a unique type of B-cell activation essential for effective viral clearance. *Proceedings of the National Academy of Sciences of the United States of America*. [Online] Available from: doi:10.1073/pnas.1312348110.

Rudd, B.D., Smit, J.J., Flavell, R.A., Alexopoulou, L., et al. (2006) Deletion of TLR3 Alters the Pulmonary Immune Environment and Mucus Production during Respiratory Syncytial Virus Infection. *The Journal of Immunology*. [Online] Available from: doi:10.4049/jimmunol.176.3.1937.
Rudolph, K.L., Chang, S., Lee, H.W., Blasco, M., et al. (1999) Longevity, stress response, and cancer in aging telomerase-deficient mice. *Cell*. [Online] 96 (5), 701–712. Available from: doi:10.1016/S0092-8674(00)80580-2.
Rullman, E., Fernandez-Gonzalo, R., Mekjavić, I.B., Gustafsson, T., et al. (2018) MEF2 as upstream regulator of the transcriptome signature in human skeletal muscle during unloading. *American Journal of Physiology - Regulatory Integrative and Comparative Physiology*. [Online] Available from: doi:10.1152/ajpregu.00452.2017.
Sabbah, A., Chang, T.H., Harnack, R., Frohlich, V., et al. (2009) Activation of innate immune antiviral responses by Nod2. *Nature Immunology*. [Online] 10 (10), 1073–1080. Available from: doi:10.1038/ni.1782 [Accessed: 26 November 2020].
Sacheck, J.M., Ohtsuka, A., McLary, S.C. & Goldberg, A.L. (2004) IGF-I stimulates muscle growth by suppressing protein breakdown and expression of atrophy-related ubiquitin ligases, atrogin-1 and MuRF1. *American Journal of Physiology - Endocrinology and Metabolism*. [Online] Available from: doi:10.1152/ajpendo.00073.2004.
Salminen, A., Kaarniranta, K. & Kauppinen, A. (2012) Inflammaging: Disturbed interplay between autophagy and inflammasomes. *Aging*. [Online] 4 (3), 166–175. Available from: doi:10.18632/aging.100444 [Accessed: 20 November 2020].
Sambasivan, R., Yao, R., Kissenpfennig, A., van Wittenberghe, L., et al. (2011) Pax7-expressing satellite cells are indispensable for adult skeletal muscle regeneration. *Development*. [Online] Available from: doi:10.1242/dev.067587.
Sapey, E., Greenwood, H., Walton, G., Mann, E., et al. (2014) Phosphoinositide 3-kinase inhibition restores neutrophil accuracy in the elderly: Toward targeted treatments for immunosenescence. *Blood*. [Online] 123 (2), 239–248. Available from: doi:10.1182/blood-2013-08-519520 [Accessed: 23 November 2020].
Sapey, E., Patel, J.M., Greenwood, H., Walton, G.M., et al. (2019) Simvastatin improves neutrophil function and clinical outcomes in pneumonia a pilot randomized controlled clinical trial. *American Journal of Respiratory and Critical Care Medicine*. [Online] 200 (10), 1282–1293. Available from: doi:10.1164/rccm.201812-2328OC [Accessed: 23 November 2020].
Sarosiek, S., Shah, R. & Munshi, N.C. (2016) Review of siltuximab in the treatment of multicentric Castleman's disease. *Therapeutic Advances in Hematology*. [Online] 7 (6), 360–366. Available from: doi:10.1177/2040620716653745.
Sartori, R., Milan, G., Patron, M., Mammucari, C., et al. (2009) Smad2 and 3 transcription factors control muscle mass in adulthood. *American Journal of Physiology - Cell Physiology*. [Online] Available from: doi:10.1152/ajpcell.00104.2009.
Sassoon, D., Lyons, G., Wright, W.E., Lin, V., et al. (1989) Expression of two myogenic regulatory factors myogenin and MyoDl during mouse embryogenesis. *Nature*. [Online] Available from: doi:10.1038/341303a0.
Sawyer, M.B., Casper, C., Munshi, N.C., Wong, R., et al. (2014) Effect of siltuximab on lean body mass (LBM) in multicentric Castleman's disease (MCD) patients (pts). *Journal of Clinical Oncology*. [Online] 32 (15_suppl), 8576–8576. Available from: doi:10.1200/jco.2014.32.15_suppl.8576.
Schaap, L.A., Pluijm, S.M.F., Deeg, D.J.H. & Visser, M. (2006) Inflammatory Markers and Loss of Muscle Mass (Sarcopenia) and Strength. *American Journal of Medicine*. [Online] Available from: doi:10.1016/j.amjmed.2005.10.049.
van Schaik, S.M., Obot, N., Enhorning, G., Hintz, K., et al. (2000) Role of interferon gamma in the pathogenesis of primary respiratory syncytial virus infection in BALB/c mice. *Journal of Medical Virology*. [Online] Available from: doi:10.1002/1096-9071(200010)62:23.0.CO;2-M.
Schiaffino, S., Dyar, K.A., Ciciliot, S., Blaauw, B., et al. (2013) Mechanisms regulating skeletal muscle growth and atrophy. *FEBS Journal*. [Online]. 280 (17) pp.4294–4314. Available from: doi:10.1111/febs.12253.
Schiaffino, S. & Reggiani, C. (2011) Fiber Types in Mammalian Skeletal Muscles. *Physiological Reviews*. [Online] 91 (4), 1447–1531. Available from: doi:10.1152/physrev.00031.2010 [Accessed: 24 February 2017].
Schindelin, J., Arganda-Carreras, I., Frise, E., Kaynig, V., et al. (2012) Fiji: An open-source platform for biological-image analysis. *Nature Methods*. [Online]. Available from: doi:10.1038/nmeth.2019.
Schmidt, E.K., Clavarino, G., Ceppi, M. & Pierre, P. (2009) SUnSET, a nonradioactive method to monitor protein synthesis. *Nature Methods*. [Online] 6 (4), 275–277. Available from: doi:10.1038/nmeth.1314 [Accessed: 17 September 2016].
Schmidt, M.E., Knudson, C.J., Hartwig, S.M., Pewe, L.L., et al. (2018) Memory CD8 T cells mediate severe immunopathology following respiratory syncytial virus infection. *PLoS Pathogens*. [Online] Available from: doi:10.1371/journal.ppat.1006810.
Schmidt, M.E. & Varga, S.M. (2018) Cytokines and CD8 T cell immunity during respiratory syncytial virus infection. *Cytokine*. [Online] Available from: doi:10.1016/j.cyto.2018.07.012 [Accessed: 20 April 2020].
Schöbitz, B., Pezeshki, G., Pohl, T., Hemmann, U., et al. (1995) Soluble interleukin-6 (IL-6) receptor augments central effects of IL-6 in vivo. *The FASEB Journal*. [Online] Available from: doi:10.1096/fasebj.9.8.7768358.
Schuelke, M., Wagner, K.R., Stolz, L.E., Hübner, C., et al. (2004) Myostatin mutation associated with gross muscle hypertrophy in a child. *New England Journal of Medicine*. [Online] Available from: doi:10.1056/NEJMoa040933.
Schultz, E. & Lipton, B.H. (1982) Skeletal muscle satellite cells: Changes in proliferation potential as a function of age. *Mechanisms of Ageing and Development*. [Online] 20 (4), 377–383. Available from: doi:10.1016/0047-6374(82)90105-1.
Schumacher, B., van der Pluijm, I., Moorhouse, M.J., Kosteas, T., et al. (2008) Delayed and Accelerated Aging Share Common Longevity Assurance Mechanisms Stuart K. Kim (ed.). *PLoS Genetics*. [Online] 4 (8), e1000161. Available from: doi:10.1371/journal.pgen.1000161 [Accessed: 16 November 2020].
Schütze, S., Potthoff, K., Machleidt, T., Berkovic, D., et al. (1992) TNF activates NF-**κ**B by phosphatidylcholine-specific phospholipase C-induced 'Acidic' sphingomyelin breakdown. *Cell*. [Online] Available from: doi:10.1016/0092-8674(92)90553-O.
Schwartz, G.J. (2000) The role of gastrointestinal vagal afferents in the control of food intake: Current prospects. In: *Nutrition*. [Online]. 2000 p. Available from: doi:10.1016/S0899-9007(00)00464-0.
Schwartz, G.J., Plata-Salaman, C.R. & Langhans, W. (1997) Subdiaphragmatic vagal deafferentation fails to block feeding- suppressive effects of LPS and IL-1β in rats. *American Journal of Physiology - Regulatory Integrative and Comparative Physiology*. [Online] Available from: doi:10.1152/ajpregu.1997.273.3.r1193.
Schwarze, J., Cieslewicz, G., Joetham, A., Ikemura, T., et al. (1999) CD8 T cells are essential in the development of respiratory syncytial virus-induced lung eosinophilia and airway hyperresponsiveness. *Journal of immunology (Baltimore, Md. : 1950)*. [Online] 162 (7), 4207–4211. Available from: http://www.ncbi.nlm.nih.gov/pubmed/10201948 [Accessed: 13 April 2020].
Seale, P., Sabourin, L.A., Girgis-Gabardo, A., Mansouri, A., et al. (2000) Pax7 is required for the specification of myogenic satellite

cells. *Cell*. [Online] Available from: doi:10.1016/S0092-8674(00)00066-0.
Sebastiani, P., Solovieff, N., DeWan, A.T., Walsh, K.M., et al. (2012) Genetic signatures of exceptional longevity in humans. *PLoS ONE*. [Online] 7 (1), 29848. Available from: doi:10.1371/journal.pone.0029848 [Accessed: 21 November 2020].
Segovia, J., Sabbah, A., Mgbemena, V., Tsai, S.Y., et al. (2012) TLR2/MyD88/NF-κB pathway, reactive oxygen species, potassium efflux activates NLRP3/ASC inflammasome during respiratory syncytial virus infection. *PLoS ONE*. [Online] Available from: doi:10.1371/journal.pone.0029695.
Selman, C., Tullet, J.M.A., Wieser, D., Irvine, E., et al. (2009) Ribosomal protein S6 kinase 1 signaling regulates mammalian life span. *Science*. [Online] 326 (5949), 140–144. Available from: doi:10.1126/science.1177221 [Accessed: 15 November 2020].
Serrano, A.L., Baeza-Raja, B., Perdiguero, E., Jardí, M., et al. (2008) Interleukin-6 Is an Essential Regulator of Satellite Cell-Mediated Skeletal Muscle Hypertrophy. *Cell Metabolism*. [Online] 7 (1), 33–44. Available from: doi:10.1016/j.cmet.2007.11.011 [Accessed: 25 February 2020].
Sestan, M., Marinovi, S., Kavazovi, I., Konrad, D., et al. (2018) Virus-Induced Interferon-γ Causes Insulin Resistance in Skeletal Muscle and Derails Glycemic Control in Obesity. *Immunity*. [Online] 49, 164-177.e6. Available from: doi:10.1016/j.immuni.2018.05.005 [Accessed: 23 July 2018].
Seymour, J.M., Spruit, M.A., Hopkinson, N.S., Natanek, S.A., et al. (2010) The prevalence of quadriceps weakness in COPD and the relationship with disease severity. *European Respiratory Journal*. [Online] Available from: doi:10.1183/09031936.00104909.
Shaw, A.C., Joshi, S., Greenwood, H., Panda, A., et al. (2010) Aging of the innate immune system. *Current Opinion in Immunology*. [Online]. Available from: doi:10.1016/j.coi.2010.05.003.
Shaw, A.C., Panda, A., Joshi, S.R., Qian, F., et al. (2011) Dysregulation of human Toll-like receptor function in aging. *Ageing Research Reviews*. [Online]. 10 (3) pp.346–353. Available from: doi:10.1016/j.arr.2010.10.007 [Accessed: 26 November 2020].
Shi, T., Denouel, A., Tietjen, A.K., Campbell, I., et al. (2019) Global Disease Burden Estimates of Respiratory Syncytial Virus–Associated Acute Respiratory Infection in Older Adults in 2015: A Systematic Review and Meta-Analysis. *The Journal of Infectious Diseases*. [Online] Available from: doi:10.1093/infdis/jiz059.
Shi, T., McAllister, D.A., O'Brien, K.L., Simoes, E.A.F., et al. (2017) Global, regional, and national disease burden estimates of acute lower respiratory infections due to respiratory syncytial virus in young children in 2015: a systematic review and modelling study. *The Lancet*. [Online] Available from: doi:10.1016/S0140-6736(17)30938-8.
Short, K.R., Bigelow, M.L., Kahl, J., Singh, R., et al. (2005) Decline in skeletal muscle mitochondrial function with aging in humans. *Proceedings of the National Academy of Sciences of the United States of America*. [Online] 102 (15), 5618–5623. Available from: doi:10.1073/pnas.0501559102 [Accessed: 17 November 2020].
Signer, R.A.J., Magee, J.A., Salic, A. & Morrison, S.J. (2014) Haematopoietic stem cells require a highly regulated protein synthesis rate. *Nature*. [Online] 508. Available from: doi:10.1038/nature13035.
Silver, J.S., Stumhofer, J.S., Passos, S., Ernst, M., et al. (2011) IL-6 Mediates the Susceptibility of Glycoprotein 130 Hypermorphs to Toxoplasma gondii . *The Journal of Immunology*. [Online] Available from: doi:10.4049/jimmunol.1004144.
Simpson, S.J. & Raubenheimer, D. (2009) Macronutrient balance and lifespan. *Aging*. [Online] 1 (10), 875–880. Available from: doi:10.18632/aging.100098 [Accessed: 22 November 2020].
Skytthe, A., Pedersen, N.L., Kaprio, J., Stazi, M.A., et al. (2003) Longevity Studies in GenomEUtwin. *Twin Research*. [Online]. 6 (5) pp.448–454. Available from: doi:10.1375/136905203770326457 [Accessed: 21 November 2020].
Slaats, J., ten Oever, J., van de Veerdonk, F.L. & Netea, M.G. (2016) IL-1β/IL-6/CRP and IL-18/ferritin: Distinct Inflammatory Programs in Infections James B. Bliska (ed.). *PLOS Pathogens*. [Online] 12 (12), e1005973. Available from: doi:10.1371/journal.ppat.1005973 [Accessed: 7 February 2017].
Smolen, J.S., Beaulieu, A., Rubbert-Roth, A., Ramos-Remus, C., et al. (2008) Effect of interleukin-6 receptor inhibition with tocilizumab in patients with rheumatoid arthritis (OPTION study): a double-blind, placebo-controlled, randomised trial. *The Lancet*. [Online] 371 (9617), 987–997. Available from: doi:10.1016/S0140-6736(08)60453-5 [Accessed: 9 April 2020].
Snell, N., Strachan, D., Hubbard, R., Gibson, J., et al. (2016) Burden of lung disease in the UK; findings from the British Lung Foundation's 'respiratory health of the nation' project. In: *6.1 Epidemiology*. [Online]. 8 September 2016 European Respiratory Society. p. PA4913. Available from: doi:10.1183/13993003.congress-2016.PA4913 [Accessed: 31 August 2018].
Snow, M.H. (1977) The effects of aging on satellite cells in skeletal muscles of mice and rats. *Cell and Tissue Research*. [Online] 185 (3), 399–408. Available from: doi:10.1007/BF00220299.
Soerensen, M., Thinggaard, M., Nygaard, M., Dato, S., et al. (2012) Genetic variation in TERT and TERC and human leukocyte telomere length and longevity: A cross-sectional and longitudinal analysis. *Aging Cell*. [Online] 11 (2), 223–227. Available from: doi:10.1111/j.1474-9726.2011.00775.x [Accessed: 21 November 2020].
Solana, R., Tarazona, R., Aiello, A.E., Akbar, A.N., et al. (2012a) CMV and Immunosenescence: From basics to clinics. *Immunity and Ageing*. [Online] Available from: doi:10.1186/1742-4933-9-23.
Solana, R., Tarazona, R., Gayoso, I., Lesur, O., et al. (2012b) Innate immunosenescence: Effect of aging on cells and receptors of the innate immune system in humans. *Seminars in Immunology*. [Online]. Available from: doi:10.1016/j.smim.2012.04.008.
Soleimani, V.D., Punch, V.G., Kawabe, Y. ichi, Jones, A.E., et al. (2012) Transcriptional Dominance of Pax7 in Adult Myogenesis Is Due to High-Affinity Recognition of Homeodomain Motifs. *Developmental Cell*. [Online] Available from: doi:10.1016/j.devcel.2012.03.014.
Song, P., Li, W., Xie, J., Hou, Y., et al. (2020) Cytokine storm induced by SARS-CoV-2. *Clinica Chimica Acta*. [Online]. 509 pp.280–287. Available from: doi:10.1016/j.cca.2020.06.017 [Accessed: 22 November 2020].
Soucy-Faulkner, A., Mukawera, E., Fink, K., Martel, A., et al. (2010) Requirement of NOX2 and reactive oxygen species for efficient RIG-I-mediated antiviral response through regulation of MAVS expression. *PLoS Pathogens*. [Online] Available from: doi:10.1371/journal.ppat.1000930.
Spann, K.M., Tran, K.-C., Chi, B., Rabin, R.L., et al. (2004) Suppression of the Induction of Alpha, Beta, and Gamma Interferons by the NS1 and NS2 Proteins of Human Respiratory Syncytial Virus in Human Epithelial Cells and Macrophages. *Journal of Virology*. [Online] Available from: doi:10.1128/jvi.78.8.4363-4369.2004.
Spann, K.M., Tran, K.C. & Collins, P.L. (2005) Effects of Nonstructural Proteins NS1 and NS2 of Human Respiratory Syncytial Virus on Interferon Regulatory Factor 3, NF- B, and Proinflammatory Cytokines. *Journal of Virology*. [Online] 79 (9), 5353–5362. Available from: doi:10.1128/jvi.79.9.5353-5362.2005.
Spehlmann, M.E., Manthey, C.F., Dann, S.M., Hanson, E., et al. (2013) Trp53 Deficiency Protects against Acute Intestinal Inflamma-

tion . *The Journal of Immunology*. [Online] Available from: doi:10.4049/jimmunol.1201716.
Spruit, M.A., Gosselink, R., Troosters, T., Kasran, A., et al. (2003) Muscle force during an acute exacerbation in hospitalised patients with COPD and its relationship with CXCL8 and IGF-I. *Thorax*. [Online] Available from: doi:10.1136/thorax.58.9.752.
Stark, J.M., McDowell, S.A., Koenigsknecht, V., Prows, D.R., et al. (2002) Genetic susceptibility to respiratory syncytial virus infection in inbred mice. *Journal of Medical Virology*. [Online] 67 (1), 92–100. Available from: doi:10.1002/jmv.2196 [Accessed: 4 March 2020].
Stebegg, M., Silva-Cayetano, A., Innocentin, S., Jenkins, T.P., et al. (2019) Heterochronic faecal transplantation boosts gut germinal centres in aged mice. *Nature Communications*. [Online] Available from: doi:10.1038/s41467-019-10430-7.
Steensberg, A., Van Hall, G., Osada, T., Sacchetti, M., et al. (2000) Production of interleukin-6 in contracting human skeletal muscles can account for the exercise-induced increase in plasma interleukin-6. *Journal of Physiology*. [Online] 529 (1), 237–242. Available from: doi:10.1111/j.1469-7793.2000.00237.x [Accessed: 25 February 2020].
Steiner, M.K., Syrkina, O.L., Kolliputi, N., Mark, E.J., et al. (2009) Interleukin-6 overexpression induces pulmonary hypertension. *Circulation Research*. [Online] Available from: doi:10.1161/CIRCRESAHA.108.182014.
Stensballe, L.G., Ravn, H., Kristensen, K., Agerskov, K., et al. (2009) Respiratory syncytial virus neutralizing antibodies in cord blood, respiratory syncytial virus hospitalization, and recurrent wheeze. *Journal of Allergy and Clinical Immunology*. [Online] 123 (2), 398–403. Available from: doi:10.1016/j.jaci.2008.10.043.
Stephan, R.P., Sanders, V.M. & Witte, P.L. (1996) Stage-specific alterations in murine B lymphopoiesis with age. *International Immunology*. [Online] Available from: doi:10.1093/intimm/8.4.509.
Stout-Delgado, H.W., Du, W., Shirali, A.C., Booth, C.J., et al. (2009) Aging Promotes Neutrophil-Induced Mortality by Augmenting IL-17 Production during Viral Infection. *Cell Host and Microbe*. [Online] Available from: doi:10.1016/j.chom.2009.09.011.
Stout-Delgado, H.W., Yang, X., Walker, W.E., Tesar, B.M., et al. (2008) Aging Impairs IFN Regulatory Factor 7 Up-Regulation in Plasmacytoid Dendritic Cells during TLR9 Activation. *The Journal of Immunology*. [Online] Available from: doi:10.4049/jimmunol.181.10.6747.
Strassmann, G., Fong, M., Kenney, J.S. & Jacob, C.O. (1992) Evidence for the involvement of interleukin 6 in experimental cancer cachexia. *Journal of Clinical Investigation*. [Online] 89 (5), 1681–1684. Available from: doi:10.1172/JCI115767.
Strelau, J., Strzelczyk, A., Rusu, P., Bendner, G., et al. (2009) Progressive postnatal motoneuron loss in mice lacking GDF-15. *Journal of Neuroscience*. [Online] Available from: doi:10.1523/JNEUROSCI.1133-09.2009.
Stumhofer, J.S., Silver, J.S., Laurence, A., Porrett, P.M., et al. (2007) Interleukins 27 and 6 induce STAT3-mediated T cell production of interleukin 10. *Nature Immunology*. [Online] Available from: doi:10.1038/ni1537.
Suematsu, S., Matsuda, T., Aozasa, K., Akira, S., et al. (1989) IgG1 plasmacytosis in interleukin 6 transgenic mice. *Proceedings of the National Academy of Sciences of the United States of America*. [Online] 86 (19), 7547–7551. Available from: doi:10.1073/pnas.86.19.7547.
Sugimoto, T., Morioka, N., Zhang, F.F., Sato, K., et al. (2014) Clock gene Per1 regulates the production of CCL2 and interleukin-6 through p38, JNK1 and NF-κB activation in spinal astrocytes. *Molecular and Cellular Neuroscience*. [Online] Available from: doi:10.1016/j.mcn.2014.01.003.
Sun, Y. & López, C.B. (2017) The innate immune response to RSV: Advances in our understanding of critical viral and host factors. *Vaccine*. [Online] 35 (3), 481–488. Available from: doi:10.1016/j.vaccine.2016.09.030 [Accessed: 26 November 2020].
Swallow, E.B., Reyes, D., Hopkinson, N.S., Man, W.D.C., et al. (2007) Quadriceps strength predicts mortality in patients with moderate to severe chronic obstructive pulmonary disease. *Thorax*. [Online] 62 (2), 115–120. Available from: doi:10.1136/thx.2006.062026.
Swedan, S., Musiyenko, A. & Barik, S. (2009) Respiratory Syncytial Virus Nonstructural Proteins Decrease Levels of Multiple Members of the Cellular Interferon Pathways. *Journal of Virology*. [Online] Available from: doi:10.1128/jvi.00715-09.
Tabas, I. (2010) Macrophage death and defective inflammation resolution in atherosclerosis. *Nature Reviews Immunology*. [Online]. 10 (1) pp.36–46. Available from: doi:10.1038/nri2675 [Accessed: 20 November 2020].
Taga, T., Hibi, M., Hirata, Y., Yamasaki, K., et al. (1989) Interleukin-6 triggers the association of its receptor with a possible signal transducer, gp130. *Cell*. [Online] Available from: doi:10.1016/0092-8674(89)90438-8.
Tanner, R.E., Brunker, L.B., Agergaard, J., Barrows, K.M., et al. (2015) Age-related differences in lean mass, protein synthesis and skeletal muscle markers of proteolysis after bed rest and exercise rehabilitation. *Journal of Physiology*. [Online] Available from: doi:10.1113/JP270699.
Tawar, R.G., Duquerroy, S., Vonrhein, C., Varela, P.F., et al. (2009) Crystal structure of a nucleocapsid-like nucleoprotein-RNA complex of respiratory syncytial virus. *Science*. [Online] 326 (5957), 1279–1283. Available from: doi:10.1126/science.1177634.
Teng, M.N. & Collins, P.L. (1999) Altered Growth Characteristics of Recombinant Respiratory Syncytial Viruses Which Do Not Produce NS2 Protein. *Journal of Virology*. [Online] Available from: doi:10.1128/jvi.73.1.466-473.1999.
Thompson, H.L., Smithey, M.J., Surh, C.D. & Nikolich-Žugich, J. (2017) Functional and homeostatic impact of age-related changes in lymph node stroma. *Frontiers in Immunology*. [Online]. 8 (JUN) p.14. Available from: doi:10.3389/fimmu.2017.00706 [Accessed: 24 November 2020].
Thompson, W.W. (2003) Mortality Associated With Influenza and Respiratory Syncytial Virus in the United States. *JAMA: The Journal of the American Medical Association*. [Online] 289 (2), 179–186. Available from: doi:10.1001/jama.289.2.179.
Tilstra, J.S., Robinson, A.R., Wang, J., Gregg, S.Q., et al. (2012) NF-κB inhibition delays DNA damage - Induced senescence and aging in mice. *Journal of Clinical Investigation*. [Online] Available from: doi:10.1172/JCI45785.
Tintignac, L.A., Lagirand, J., Batonnet, S., Sirri, V., et al. (2005) Degradation of MyoD mediated by the SCF (MAFbx) ubiquitin ligase. *Journal of Biological Chemistry*. [Online] Available from: doi:10.1074/jbc.M411346200.
Tomaru, U., Takahashi, S., Ishizu, A., Miyatake, Y., et al. (2012) Decreased proteasomal activity causes age-related phenotypes and promotes the development of metabolic abnormalities. *American Journal of Pathology*. [Online] 180 (3), 963–972. Available from: doi:10.1016/j.ajpath.2011.11.012.
Tomás-Loba, A., Flores, I., Fernández-Marcos, P.J., Cayuela, M.L., et al. (2008) Telomerase Reverse Transcriptase Delays Aging in Cancer-Resistant Mice. *Cell*. [Online] 135 (4), 609–622. Available from: doi:10.1016/j.cell.2008.09.034.
Tregoning, J.S., Wang, B.L., McDonald, J.U., Yamaguchi, Y., et al. (2013) Neonatal antibody responses are attenuated by interferon-γ produced by NK and T cells during RSV infection. *Proceedings of the National Academy of Sciences of the United States of America*. [Online] 110 (14), 5576–5581. Available from: doi:10.1073/pnas.1214247110 [Accessed: 22 November 2020].

Tregoning, J.S., Yamaguchi, Y., Harker, J., Wang, B., et al. (2008) The Role of T Cells in the Enhancement of Respiratory Syncytial Virus Infection Severity during Adult Reinfection of Neonatally Sensitized Mice. *Journal of Virology*. [Online] 82 (8), 4115–4124. Available from: doi:10.1128/jvi.02313-07.

Trendelenburg, A.U., Meyer, A., Rohner, D., Boyle, J., et al. (2009) Myostatin reduces Akt/TORC1/p70S6K signaling, inhibiting myoblast differentiation and myotube size. *American Journal of Physiology - Cell Physiology*. [Online] Available from: doi:10.1152/ajpcell.00105.2009.

Triantafilou, K., Kar, S., Vakakis, E., Kotecha, S., et al. (2013) Human respiratory syncytial virus viroporin SH: A viral recognition pathway used by the host to signal inflammasome activation. *Thorax*. [Online] 68 (1), 66–75. Available from: doi:10.1136/thoraxjnl-2012-202182.

Trifunovic, A., Wredenberg, A., Falkenberg, M., Spelbrink, J.N., et al. (2004) Premature ageing in mice expressing defective mitochondrial DNA polymerase. *Nature*. [Online] 429 (6990), 417–423. Available from: doi:10.1038/nature02517.

Troeger, C., Forouzanfar, M., Rao, P.C., Khalil, I., et al. (2017) Estimates of the global, regional, and national morbidity, mortality, and aetiologies of lower respiratory tract infections in 195 countries: a systematic analysis for the Global Burden of Disease Study 2015. *The Lancet Infectious Diseases*. [Online] 17 (11), 1133–1161. Available from: doi:10.1016/S1473-3099(17)30396-1.

Tsai, V.W.-W., Manandhar, R., Jørgensen, S.B., Lee-Ng, K.K.M., et al. (2014) The Anorectic Actions of the TGFβ Cytokine MIC-1/GDF15 Require an Intact Brainstem Area Postrema and Nucleus of the Solitary Tract Mihai Covasa (ed.). *PLoS ONE*. [Online] 9 (6), e100370. Available from: doi:10.1371/journal.pone.0100370 [Accessed: 8 August 2018].

Tsai, V.W., Zhang, H.P., Manandhar, R., Lee-Ng, K.K.M., et al. (2018) Treatment with the TGF-b superfamily cytokine MIC-1/GDF15 reduces the adiposity and corrects the metabolic dysfunction of mice with diet-induced obesity. *International Journal of Obesity*. [Online] Available from: doi:10.1038/ijo.2017.258.

Tsai, V.W.W., Macia, L., Johnen, H., Kuffner, T., et al. (2013) TGF-b Superfamily Cytokine MIC-1/GDF15 Is a Physiological Appetite and Body Weight Regulator. *PLoS ONE*. [Online] Available from: doi:10.1371/journal.pone.0055174.

Tsujinaka, T., Ebisui, C., Fujita, J., Kishibuchi, M., et al. (1995) Muscle undergoes atrophy in association with increase of lysosomal cathepsin activity in interleukin-6 transgenic mouse. *Biochemical and Biophysical Research Communications*. [Online] 207 (1), 168–174. Available from: doi:10.1006/bbrc.1995.1168 [Accessed: 25 February 2020].

Tsujinaka, T., Fujita, J., Ebisui, C., Yano, M., et al. (1996) Interleukin 6 receptor antibody inhibits muscle atrophy and modulates proteolytic systems in interleukin 6 transgenic mice. *Journal of Clinical Investigation*. [Online] 97 (1), 244–249. Available from: doi:10.1172/JCI118398.

Tu, W. & Rao, S. (2016) Mechanisms underlying T cell immunosenescence: Aging and cytomegalovirus infection. *Frontiers in Microbiology*. [Online]. 7 (DEC) p.2111. Available from: doi:10.3389/fmicb.2016.02111 [Accessed: 24 November 2020].

United Nations (2017) World Population Prospects: The 2017 Revision, Key Findings and Advance Tables ESA/P/WP/248. *World Population Prospects The 2017 revision*. [Online]. Available from: doi:10.1017/CBO9781107415324.004.

Varela, I., Cadiñanos, J., Pendás, A.M., Gutiérrez-Fernández, A., et al. (2005) Accelerated ageing in mice deficient in Zmpste24 protease is linked to p53 signalling activation. *Nature*. [Online] 437 (7058), 564–568. Available from: doi:10.1038/nature04019 [Accessed: 18 November 2020].

Varga, S.M., Wang, X., Welsh, R.M. & Braciale, T.J. (2001) Immunopathology in RSV infection is mediated by a discrete oligoclonal subset of antigen-specific CD4+ T cells. *Immunity*. [Online] 15 (4), 637–646. Available from: doi:10.1016/S1074-7613(01)00209-6.

Veldhoen, M., Hocking, R.J., Atkins, C.J., Locksley, R.M., et al. (2006) TGFβ in the context of an inflammatory cytokine milieu supports de novo differentiation of IL-17-producing T cells. *Immunity*. [Online] Available from: doi:10.1016/j.immuni.2006.01.001.

Venuti, J.M., Morris, J.H., Vivian, J.L., Olson, E.N., et al. (1995) Myogenin is required for late but not early aspects of myogenesis during mouse development. *Journal of Cell Biology*. [Online] Available from: doi:10.1083/jcb.128.4.563.

Vermulst, M., Wanagat, J., Kujoth, G.C., Bielas, J.H., et al. (2008) DNA deletions and clonal mutations drive premature aging in mitochondrial mutator mice. *Nature Genetics*. [Online] Available from: doi:10.1038/ng.95.

Vilaró, J., Ramirez-Sarmiento, A., Martínez-Llorens, J.M., Mendoza, T., et al. (2010) Global muscle dysfunction as a risk factor of readmission to hospital due to COPD exacerbations. *Respiratory Medicine*. [Online] Available from: doi:10.1016/j.rmed.2010.05.001.

Villanueva, J.L., Solana, R., Alonsa, M.C. & Pena, J. (1990) Changes in the expression of HLA-class II antigens on peripheral blood monocytes from aged humans. *Disease Markers*.

Viswanathan, S.R., Powers, J.T., Einhorn, W., Hoshida, Y., et al. (2009) Lin28 promotes transformation and is associated with advanced human malignancies. *Nature Genetics*. [Online] Available from: doi:10.1038/ng.392.

Volkova, M., Zhang, Y., Shaw, A.C. & Lee, P.J. (2012) The role of toll-like receptors in age-associated lung diseases. *Journals of Gerontology - Series A Biological Sciences and Medical Sciences*. [Online] Available from: doi:10.1093/gerona/glr226.

Waage, A., Brandtzaeg, P., Halstensen, A., Kierulf, P., et al. (1989) The complex pattern of cytokines in serum from patients with meningococcal septic shock. Association between interleukin 6, interleukin 1, and fatal outcome. *Journal of Experimental Medicine*. [Online] Available from: doi:10.1084/jem.169.1.333.

Wallenius, V., Wallenius, K., Ahrén, B., Rudling, M., et al. (2002) Interleukin-6-deficient mice develop mature-onset obesity. *Nature Medicine*. [Online] Available from: doi:10.1038/nm0102-75.

Walsh, E.E. & Falsey, A.R. (2004) Age Related Differences in Humoral Immune Response to Respiratory Syncytial Virus Infection in Adults. *Journal of Medical Virology*. [Online] 73 (2), 295–299. Available from: doi:10.1002/jmv.20090.

Walsh, E.E. & Hruska, J. (1983) Monoclonal antibodies to respiratory syncytial virus proteins: identification of the fusion protein. *Journal of Virology*. [Online] 47 (1), 171–177. Available from: doi:10.1128/jvi.47.1.171-177.1983.

Walsh, E.E., Peterson, D.R. & Falsey, A.R. (2004) Risk Factors for Severe Respiratory Syncytial Virus Infection in Elderly Persons. *The Journal of Infectious Diseases*. [Online] Available from: doi:10.1086/380907.

Walsh, E.E., Peterson, D.R., Kalkanoglu, A.E., Lee, F.E.H., et al. (2013) Viral shedding and immune responses to respiratory syncytial virus infection in older adults. *Journal of Infectious Diseases*. [Online] Available from: doi:10.1093/infdis/jit038.

Wang, C., Jurk, D., Maddick, M., Nelson, G., et al. (2009) DNA damage response and cellular senescence in tissues of aging mice. *Aging Cell*. [Online] 8 (3), 311–323. Available from: doi:10.1111/j.1474-9726.2009.00481.x.

Wang, D., Cummins, C., Bayliss, S., Sandercock, J., et al. (2008) Immunoprophylaxis against respiratory syncytial virus (RSV) with palivizumab in children: A systematic review and economic evaluation. *Health Technology Assessment*. [Online]. Available

from: doi:10.3310/hta12360.
Wang, D.Z., Renee Valdez, M., McAnally, J., Richardson, J., et al. (2001) The Mef2c gene is a direct transcriptional target of myogenic bHLH and MEF2 proteins during skeletal muscle development. *Development*.
Wang, S., Wang, J., Kumar, V., Karnell, J.L., et al. (2018a) IL-21 drives expansion and plasma cell differentiation of autoreactive CD-11chiT-bet+ B cells in SLE. *Nature Communications*. [Online] Available from: doi:10.1038/s41467-018-03750-7.
Wang, X., Chrysovergis, K., Kosak, J., Kissling, G., et al. (2014) hNAG-1 increases lifespan by regulating energy metabolism and insulin/IGF-1/mTOR signaling. *Aging*. [Online] Available from: doi:10.18632/aging.100687.
Wang, Y., Liu, Z., Han, Y., Xu, J., et al. (2018b) Medium Chain Triglycerides enhances exercise endurance through the increased mitochondrial biogenesis and metabolism. *PLoS ONE*. [Online] Available from: doi:10.1371/journal.pone.0191182.
Wanke, C.A., Silva, M., Knox, T.A., Forrester, J., et al. (2000) Weight Loss and Wasting Remain Common Complications in Individuals Infected with Human Immunodeficiency Virus in the Era of Highly Active Antiretroviral Therapy. *Clinical Infectious Diseases*. [Online] 31 (3), 803–805. Available from: doi:10.1086/314027.
Ward, H., Cooke, G., Atchison, C., Whitaker, M., et al. (2020) Declining prevalence of antibody positivity to SARS-CoV-2: a community study of 365,000 adults. *medRxiv*. [Online] 2020.10.26.20219725. Available from: doi:10.1101/2020.10.26.20219725 [Accessed: 22 November 2020].
Weiland, T.J., Anthony-Harvey-Beavis, D., Voudouris, N.J. & Kent, S. (2006) Metabotropic glutamate receptors mediate lipopolysaccharide-induced fever and sickness behavior. *Brain, Behavior, and Immunity*. [Online] Available from: doi:10.1016/j.bbi.2005.08.007.
Weintraub, H., Davis, R., Tapscott, S., Thayer, M., et al. (1991) The myoD gene family: Nodal point during specification of the muscle cell lineage. *Science*. [Online] Available from: doi:10.1126/science.1846704.
Welsh, J.B., Sapinoso, L.M., Kern, S.G., Brown, D.A., et al. (2003) Large-scale delineation of secreted protein biomarkers overexpressed in cancer tissue and serum. *Proceedings of the National Academy of Sciences of the United States of America*. [Online] Available from: doi:10.1073/pnas.0530278100.
Wenisch, C., Patruta, S., Daxböck, F., Krause, R., et al. (2000) Effect of age on human neutrophil function. *Journal of Leukocyte Biology*. [Online] Available from: doi:10.1002/jlb.67.1.40.
Westerheide, S.D., Anckar, J., Stevens, S.M., Sistonen, L., et al. (2009) Stress-inducible regulation of heat shock factor 1 by the deacetylase SIRT. *Science*. [Online] 323 (5917), 1063–1066. Available from: doi:10.1126/science.1165946 [Accessed: 15 November 2020].
Weyand, C.M. & Goronzy, J.J. (2016) Aging of the immune system: Mechanisms and therapeutic targets. In: *Annals of the American Thoracic Society*. [Online]. 2016 p. Available from: doi:10.1513/AnnalsATS.201602-095AW.
Wheeler, D. a, Gibert, C.L., Launer, C. a, Muurahainen, N., et al. (1998) Weight loss as a predictor of survival and disease progression in HIV infection. Terry Beirn Community Programs for Clinical Research on AIDS. *Journal of acquired immune deficiency syndromes and human retrovirology : official publication of the International Retrovirology Association*.18 (1) pp.80–85.
White, J.D., Scaffidi, A., Davies, M., McGeachie, J., et al. (2000) Myotube formation is delayed but not prevented in MyoD-deficient skeletal muscle: Studies in regenerating whole muscle grafts of adult mice. *Journal of Histochemistry and Cytochemistry*. [Online] Available from: doi:10.1177/002215540004801110.
White, J.P., Puppa, M.J., Sato, S., Gao, S., et al. (2012) IL-6 regulation on skeletal muscle mitochondrial remodeling during cancer cachexia in the ApcMin/+ mouse. *Skeletal Muscle*. [Online] Available from: doi:10.1186/2044-5040-2-14.
Whitehouse, A.S., Smith, H.J., Drake, J.L. & Tisdale, M.J. (2001) Mechanism of attenuation of skeletal muscle protein catabolism in cancer cachexia by eicosapentaenoic acid. *Cancer Research*.
Wieczorek, M., Swiergiel, A.H., Pournajafi-Nazarloo, H. & Dunn, A.J. (2005) Physiological and behavioral responses to interleukin-1β and LPS in vagotomized mice. *Physiology and Behavior*. [Online] Available from: doi:10.1016/j.physbeh.2005.05.012.
Wiklund, F.E., Bennet, A.M., Magnusson, P.K.E., Eriksson, U.K., et al. (2010) Macrophage inhibitory cytokine-1 (MIC-1/GDF15): A new marker of all-cause mortality. *Aging Cell*. [Online] Available from: doi:10.1111/j.1474-9726.2010.00629.x.
Wilkinson, J.E., Burmeister, L., Brooks, S. V., Chan, C.C., et al. (2012) Rapamycin slows aging in mice. *Aging Cell*. [Online] Available from: doi:10.1111/j.1474-9726.2012.00832.x.
Willcox, B.J., Willcox, D.C., Todoriki, H., Fujiyoshi, A., et al. (2007) Caloric restriction, the traditional okinawan diet, and healthy aging: The diet of the world's longest-lived people and its potential impact on morbidity and life span. In: *Annals of the New York Academy of Sciences*. [Online]. 2007 Blackwell Publishing Inc. pp. 434–455. Available from: doi:10.1196/annals.1396.037 [Accessed: 22 November 2020].
Wilson, D., Drew, W., Jasper, A., Crisford, H., et al. (2020) Frailty Is Associated With Neutrophil Dysfunction Which Is Correctable With Phosphoinositol-3-Kinase Inhibitors. *The Journals of Gerontology: Series A*. [Online] 75 (12), 2320. Available from: doi:10.1093/gerona/glaa216 [Accessed: 23 November 2020].
Wilson, D., Jackson, T., Sapey, E. & Lord, J.M. (2017) Frailty and sarcopenia: The potential role of an aged immune system. *Ageing Research Reviews*. [Online]. Available from: doi:10.1016/j.arr.2017.01.006.
Winbanks, C.E., Weeks, K.L., Thomson, R.E., Sepulveda, P. V., et al. (2012) Follistatin-mediated skeletal muscle hypertrophy is regulated by Smad3 and mTOR independently of myostatin. *Journal of Cell Biology*. [Online] Available from: doi:10.1083/jcb.201109091.
Wolsk, E., Mygind, H., Grøndahl, T.S., Pedersen, B.K., et al. (2010) IL-6 selectively stimulates fat metabolism in human skeletal muscle. *American Journal of Physiology - Endocrinology and Metabolism*. [Online] Available from: doi:10.1152/ajpendo.00328.2010.
Wong, T.M., Boyapalle, S., Sampayo, V., Nguyen, H.D., et al. (2014) Respiratory syncytial virus (RSV) infection in elderly mice results in altered antiviral gene expression and enhanced pathology. *PloS one*. [Online] 9 (2), e88764. Available from: doi:10.1371/journal.pone.0088764 [Accessed: 12 February 2019].
Woodworth-Hobbs, M.E., Hudson, M.B., Rahnert, J.A., Zheng, B., et al. (2014) Docosahexaenoic acid prevents palmitate-induced activation of proteolytic systems in C2C12 myotubes. *Journal of Nutritional Biochemistry*. [Online] Available from: doi:10.1016/j.jnutbio.2014.03.017.
Wool, I.G. & Kurihara, K. (1967) Determination of the number of active muscle ribosomes: effect of diabetes and insulin. *Proceedings of the National Academy of Sciences of the United States of America*. [Online] Available from: doi:10.1073/pnas.58.6.2401.

World Health Organization (2020) *Weekly epidemiological update - 17 November 2020*. [Online]. 2020. Available from: https://www.who.int/publications/m/item/weekly-epidemiological-update---17-november-2020 [Accessed: 22 November 2020].
Wright, W.E., Sassoon, D.A. & Lin, V.K. (1989) Myogenin, a factor regulating myogenesis, has a domain homologous to MyoD. *Cell*. [Online] Available from: doi:10.1016/0092-8674(89)90583-7.
Wu, C., Chen, X., Cai, Y., Xia, J., et al. (2020) Risk Factors Associated with Acute Respiratory Distress Syndrome and Death in Patients with Coronavirus Disease 2019 Pneumonia in Wuhan, China. *JAMA Internal Medicine*. [Online] Available from: doi:10.1001/jamainternmed.2020.0994.
Wu, Q., Jiang, D., Schaefer, N.R., Harmacek, L., et al. (2018) Overproduction of growth differentiation factor 15 promotes human rhinovirus infection and virus-induced inflammation in the lung. *American Journal of Physiology-Lung Cellular and Molecular Physiology*. [Online] 314 (3), L514–L527. Available from: doi:10.1152/ajplung.00324.2017 [Accessed: 7 August 2018].
Xie, J., Zhang, X. & Zhang, L. (2013) Negative regulation of inflammation by SIRT1. *Pharmacological Research*. [Online]. Available from: doi:10.1016/j.phrs.2012.10.010.
Yamaguchi, K., Lee, S.H., Eling, T.E. & Seung, J.B. (2004) Identification of nonsteroidal anti-inflammatory drug-activated gene (NAG-1) as a novel downstream target of phosphatidylinositol 3-kinase/AKT/GSK-3β pathway. *Journal of Biological Chemistry*. [Online] Available from: doi:10.1074/jbc.M408796200.
Yamasaki, K., Taga, T., Hirata, Y., Yawata, H., et al. (1988) Cloning and expression of the human interleukin-6 (BSF-2/IFNβ 2) receptor. *Science*. [Online] Available from: doi:10.1126/science.3136546.
Yanes, R.E., Gustafson, C.E., Weyand, C.M. & Goronzy, J.J. (2017) Lymphocyte generation and population homeostasis throughout life. *Seminars in Hematology*. [Online]. 54 (1) pp.33–38. Available from: doi:10.1053/j.seminhematol.2016.10.003.
Yang, H., Filipovic, Z., Brown, D., Breit, S.N., et al. (2003) Macrophage inhibitory cytokine-1: A novel biomarker for p53 pathway activation. *Molecular Cancer Therapeutics*.
Yang, L., Chang, C.-C., Sun, Z., Madsen, D., et al. (2017) GFRAL is the receptor for GDF15 and is required for the anti-obesity effects of the ligand. *Nature Medicine*. [Online] 23 (10), 1158–1166. Available from: doi:10.1038/nm.4394 [Accessed: 11 January 2018].
Yang, S.B., Tien, A.C., Boddupalli, G., Xu, A.W., et al. (2012) Rapamycin ameliorates age-dependent obesity associated with increased mTOR signaling in hypothalamic POMC neurons. *Neuron*. [Online] 75 (3), 425–436. Available from: doi:10.1016/j.neuron.2012.03.043.
Yao, H., Chung, S., Hwang, J.W., Rajendrasozhan, S., et al. (2012) SIRT1 protects against emphysema via FOXO3-mediated reduction of premature senescence in mice. *Journal of Clinical Investigation*. [Online] Available from: doi:10.1172/JCI60132.
Yao, J.H., Ye, S.M., Burgess, W., Zachary, J.F., et al. (1999) Mice deficient in interleukin-1β converting enzyme resist anorexia induced by central lipopolysaccharide. *American Journal of Physiology - Regulatory Integrative and Comparative Physiology*. [Online] Available from: doi:10.1152/ajpregu.1999.277.5.r1435.
Yen, W.L. & Klionsky, D.J. (2008) How to live long and prosper: Autophagy, mitochondria, and aging. *Physiology*. [Online]. 23 (5) pp.248–262. Available from: doi:10.1152/physiol.00013.2008 [Accessed: 17 November 2020].
Yilmaz, Ö.H., Katajisto, P., Lamming, D.W., Gültekin, Y., et al. (2012) MTORC1 in the Paneth cell niche couples intestinal stem-cell function to calorie intake. *Nature*. [Online] Available from: doi:10.1038/nature11163.
Yoboua, F., Martel, A., Duval, A., Mukawera, E., et al. (2010) Respiratory Syncytial Virus-Mediated NF-κB p65 Phosphorylation at Serine 536 Is Dependent on RIG-I, TRAF6, and IKKβ. *Journal of Virology*. [Online] Available from: doi:10.1128/jvi.00142-10.
Yoshida, K., Taga, T., Saito, M., Suematsu, S., et al. (1996) Targeted disruption of gp130, a common signal transducer for the interleukin 6 family of cytokines, leads to myocardial and hematological disorders. *Proceedings of the National Academy of Sciences of the United States of America*. [Online] Available from: doi:10.1073/pnas.93.1.407.
Yoshizaki, K., Nakagawa, T., Fukunaga, K., Tseng, L.T., et al. (1984) Isolation and characterization of B cell differentiation factor (BCDF) secreted from a human B lymphoblastoid cell line. *Journal of immunology (Baltimore, Md. : 1950)*.
Yu, M., Li, G., Lee, W.W., Yuan, M., et al. (2012) Signal inhibition by the dual-specific phosphatase 4 impairs T cell-dependent B-cell responses with age. *Proceedings of the National Academy of Sciences of the United States of America*. [Online] Available from: doi:10.1073/pnas.1109797109.
Yu, Y.T., Breitbart, R.E., Smoot, L.B., Lee, Y., et al. (1992) Human myocyte-specific enhancer factor 2 comprises a group of tissue-restricted MADS box transcription factors. *Genes and Development*. [Online] Available from: doi:10.1101/gad.6.9.1783.
Yuan, R., Tsaih, S.W., Petkova, S.B., de Evsikova, C.M., et al. (2009) Aging in inbred strains of mice: Study design and interim report on median lifespans and circulating IGF1 levels. *Aging Cell*. [Online] Available from: doi:10.1111/j.1474-9726.2009.00478.x.
Zammit, P.S. (2017) Function of the myogenic regulatory factors Myf5, MyoD, Myogenin and MRF4 in skeletal muscle, satellite cells and regenerative myogenesis. *Seminars in Cell and Developmental Biology*. [Online]. Available from: doi:10.1016/j.semcdb.2017.11.011.
Zammit, P.S., Relaix, F., Nagata, Y., Ruiz, A.P., et al. (2006) Pax7 and myogenic progression in skeletal muscle satellite cells. *Journal of Cell Science*. [Online] Available from: doi:10.1242/jcs.02908.
Zhang, C. & Cuervo, A.M. (2008) Restoration of chaperone-mediated autophagy in aging liver improves cellular maintenance and hepatic function. *Nature Medicine*. [Online] Available from: doi:10.1038/nm.1851.
Zhang, J. & Rivest, S. (1999) Distribution, regulation and colocalization of the genes encoding the EP2- and EP4-PGE2 receptors in the rat brain and neuronal responses to systemic inflammation. *European Journal of Neuroscience*. [Online] Available from: doi:10.1046/j.1460-9568.1999.00682.x.
Zhang, L., Pan, J., Dong, Y., Tweardy, D.J., et al. (2013) Stat3 activation links a C/EBPδ to myostatin pathway to stimulate loss of muscle mass. *Cell Metabolism*. [Online] 18 (3), 368–379. Available from: doi:10.1016/j.cmet.2013.07.012.
Zhang, L., Peeples, M.E., Boucher, R.C., Collins, P.L., et al. (2002a) Respiratory Syncytial Virus Infection of Human Airway Epithelial Cells Is Polarized, Specific to Ciliated Cells, and without Obvious Cytopathology. *Journal of Virology*. [Online] Available from: doi:10.1128/jvi.76.11.5654-5666.2002.
Zhang, Y., Ikeno, Y., Qi, W., Chaudhuri, A., et al. (2009) Mice deficient in both Mn superoxide dismutase and glutathione peroxidase-1 have increased oxidative damage and a greater incidence of pathology but no reduction in longevity. *Journals of Gerontology - Series A Biological Sciences and Medical Sciences*. [Online] 64 (12), 1212–1220. Available from: doi:10.1093/gerona/glp132 [Accessed: 17 November 2020].
Zhang, Y., Wang, Y., Gilmore, X., Xu, K., et al. (2002b) An aged mouse model for RSV infection and diminished CD8+ CTL responses.

Experimental Biology and Medicine. [Online] 227 (2), 133–140. Available from: doi:10.1177/153537020222700208 [Accessed: 17 September 2016].
Zhao, J., Zhao, J., Legge, K. & Perlman, S. (2011) Age-related increases in PGD 2 expression impair respiratory DC migration, resulting in diminished T cell responses upon respiratory virus infection in mice. *Journal of Clinical Investigation*. [Online] Available from: doi:10.1172/JCI59777.
Zhong, L., D'Urso, A., Toiber, D., Sebastian, C., et al. (2010) The Histone Deacetylase Sirt6 Regulates Glucose Homeostasis via Hif1α. *Cell*. [Online] 140 (2), 280–293. Available from: doi:10.1016/j.cell.2009.12.041.
Zhou, L., Ivanov, I.I., Spolski, R., Min, R., et al. (2007) IL-6 programs TH-17 cell differentiation by promoting sequential engagement of the IL-21 and IL-23 pathways. *Nature Immunology*. [Online] Available from: doi:10.1038/ni1488.
Zhu, N., Zhang, D., Wang, W., Li, X., et al. (2020) A Novel Coronavirus from Patients with Pneumonia in China, 2019. *New England Journal of Medicine*. [Online] 382 (8), 727–733. Available from: doi:10.1056/nejmoa2001017 [Accessed: 22 November 2020].

8.

Appendix

Chapter 8. Appendix

8.1. Abbreviations

A	
7-AAD	7-amino-actinomycin
ABC	Age-associated B cell
ACK	Ammonium chloride potassium
AF	Alexa Fluor™
ALRI	Acute lower respiratory tract infection
AP	Area postrema
APC	Antigen-presenting cell / Allophycocyanin
ATCC	American Type Culture Collection
ATP	Adenosine triphosphate
B	
BAL	Broncho-alveolar lavage
BSA	Bovine serum albumin
BV	Brilliant Violet™
C	
CCA	Chimpanzee coryza agent
CCL	Chemokine ligand (C-C motif)
CD	Cluster of differentiation
cDC	Conventional dendritic cell
cDNA	Complementary DNA
CMV	Cytomegalovirus
COPD	Chronic obstructive pulmonary disease
COVID-19	Coronavirus infectious disease 2019
CSR	Class-switch recombination
CTL	Cytotoxic T lymphocyte
CTLA-4	Cytotoxic T lymphocyte-associated protein 4
CXCL	Chemokine ligand (C-X-C motif)
D	
DAMP	Danger-associated molecular pattern
DAPI	4’6-diamidino-2-phenylindole
DC	Dendritic cell
DMEM	Dulbecco’s modified Eagle’s medium
DNA	Deoxyribonucleic acid

dpi	Days post-infection
E	
ECM	Extracellular matrix
EDTA	Ethylene-diamine-tetraacetic acid
ELISA	Enzyme-linked immunosorbent assay
EtOH	Ethanol
F	
FCS	Foetal calf serum
fDC	follicular dendritic cell
FITC	Fluorescein isothiocyanate
FMO	Fluorescence minus-one
G	
g	Gram
GC	Germinal centre
GDF	Growth and differentiation factor
GH	Growth hormone
GPCR	G-protein coupled receptor
H	
H & E	Haematoxylin and eosin
HDM	House dust mite
HEp-2	Human larynx epidermoid carcinoma
HP 1α	Heterochromatin protein 1 alpha
HRP	Horseradish peroxidase
hr(s)	Hour(s)
HSC	Haematopoietic stem cell
HSP	Heat shock protein
I	
IAV	Influenza A virus
ICAM-1	Intercellular adhesion molecule 1
IFN	Interferon
IFNAR	Interferon alpha/beta receptor
Ig	Immunoglobulin
IGF	Insulin-like growth factor
IL	Interleukin
ILC	Innate lymphoid cell
i.n.	Intranasal

IR	Infrared
IRF	Interferon-regulated factor
IκB	Inhibitor of kappa B
IKK	Inhibitor of kappa B kinase
IRF	Interferon regulatory factor
ISG	Interferon-stimulated gene

K

kg	Kilogram
KO	Knock-out

L

LMIC	Low and middle-income countries
LN	Lymph node
LPS	Lipopolysaccharide
LRTI	Lower respiratory tract infection
LTA	Lipoteichoic acid
Ly	Lymphocytes

M

MAPK	Mitogen-activated protein kinase
mDC	Myeloid dendritic cell
mg	Milligram
MHC	Major histocompatibility complex
MyHC	Myosin heavy chain
min	Minute(s)
MIP-1α	Macrophage inhibitory protein 1 α
ml	Millilitre
µl	Microlitre
MLN	Mediastinal lymph node
mRNA	Messenger RNA
mtDNA	mitochondrial DNA
mTOR	mammalian target of rapamycin
MuRF	Muscle ring finger protein

N

ns	Not significant
ND	Not detected
NF-κB	Nuclear factor kappa B
ng	Nanogram

NK	Natural killer
NLR	Nod-like receptor
NTS	Nucleus of the solitary tract

O

OCT	Optimal cutting temperature
O/N	Overnight
OD	Optical density

P

PAMP	Pathogen-associated molecular pattern
PBMC	Peripheral blood mononuclear cell
PBS	Phosphate-buffered saline
PCR	Polymerase chain reaction
pDC	plasmacytoid dendritic cell
PD-1	Programmed death 1
PE	Phycoerythrin
PFU	Plaque-forming unit
PMA	Phorbol 12-myristate 13-acetate
PRR	Pattern recognition receptor

Q

qPCR	quantitative PCR

R

RIG-I	Retinoic acid-inducible gene I
RNA	Ribonucleic acid
RNP	Ribonucleoprotein
ROS	Reactive oxygen species
rpm	Revolutions per minute
RPMI	Roswell Park Memorial Institute
RSV	Respiratory syncytial virus
RT	Room temperature
RV	Rhinovirus

S

SARS-CoV2	Severe Acute Respiratory Syndrome Coronavirus 2
SASP	Senescence-associated secretory phenotype
SD	Standard deviation
SEM	Standard error of the mean
SIRT	Sirtuin

SNP	Single nucleotide polymorphism
ss	Single-stranded
STAT	Signal transducer and activator of transcription

T

TA	Tibialis anterior
TCR	T cell receptor
TF	Transcription factor
Tfh	T follicular helper
TGF	Transforming growth factor
Th	T helper
Th1	Type 1 T helper
Th2	Type 2 T helper
TIR	Toll-interleukin 1 receptor
TLR	Toll-like receptor
TMB	3,3',5,5'-Tetramethylbenzidine
TNF	Tumor necrosis factor
Treg	T regulatory
Trm	T resident memory
TRIM	Tripartite motif

U

URTI	Upper respiratory tract infection

W

wk	Week(s)
WT	Wild type

8.2. Licence statement for Figure 1-1

Open Government Licence
for public sector information

delivered by
THE NATIONAL ARCHIVES

Back to The National Archives

You are encouraged to use and re-use the Information that is available under this licence freely and flexibly, with only a few conditions.

Using Information under this licence

Use of copyright and database right material expressly made available under this licence (the 'Information') indicates your acceptance of the terms and conditions below.

The Licensor grants you a worldwide, royalty-free, perpetual, non-exclusive licence to use the Information subject to the conditions below.

This licence does not affect your freedom under fair dealing or fair use or any other copyright or database right exceptions and limitations.

You are free to:

copy, publish, distribute and transmit the Information;

adapt the Information;

exploit the Information commercially and non-commercially for example, by combining it with other Information, or by including it in your own product or application.

You must (where you do any of the above):

acknowledge the source of the Information in your product or application by including or linking to any attribution statement specified by the Information Provider(s) and, where possible, provide a link to this licence;

If the Information Provider does not provide a specific attribution statement, you must use the following:

Contains public sector information licensed under the Open Government Licence v3.0.

If you are using Information from several Information Providers and listing multiple attributions is not practical in your product or application, you may include a URI or hyperlink to a resource that contains the required attribution statements.

These are important conditions of this licence and if you fail to comply with them the rights granted to you under this licence, or any similar licence granted by the Licensor, will end automatically.

Exemptions

This licence does not cover:

- personal data in the Information;
- Information that has not been accessed by way of publication or disclosure under information access legislation (including the Freedom of Information Acts for the UK and Scotland) by or with the consent of the Information Provider;
- departmental or public sector organisation logos, crests and the Royal Arms except where they form an integral part of a document or dataset;
- military insignia;
- third party rights the Information Provider is not authorised to license;
- other intellectual property rights, including patents, trade marks, and design rights; and
- identity documents such as the British Passport

Non-endorsement

This licence does not grant you any right to use the Information in a way that suggests any official status or that the Information Provider and/or Licensor endorse you or your use of the Information.

No warranty

The Information is licensed 'as is' and the Information Provider and/or Licensor excludes all representations, warranties, obligations and liabilities in relation to the Information to the maximum extent permitted by law.

The Information Provider and/or Licensor are not liable for any errors or omissions in the Information and shall not be liable for any loss, injury or damage of any kind caused by its use. The Information Provider does not guarantee the continued supply of the Information.

Governing Law

This licence is governed by the laws of the jurisdiction in which the Information Provider has its principal place of business, unless otherwise specified by the Information Provider.

Definitions

In this licence, the terms below have the following meanings:

'Information' means information protected by copyright or by database right (for example, literary and artistic works, content, data and source code) offered for use under the terms of this licence.

'Information Provider' means the person or organisation providing the Information under this licence.

'Licensor' means any Information Provider which has the authority to offer Information under the terms of this licence or the Keeper of Public Records, who has the authority to offer Information subject to Crown copyright and Crown database rights and Information subject to copyright and database right that has been assigned to or acquired by the Crown, under the terms of this licence.

'Use' means doing any act which is restricted by copyright or database right, whether in the original medium or in any other medium, and includes without limitation distributing, copying, adapting, modifying as may be technically necessary to use it in a different mode or format.

'You', 'you' and 'your' means the natural or legal person, or body of persons corporate or incorporate, acquiring rights in the Information (whether the Information is obtained directly from the Licensor or otherwise) under this licence.

About the Open Government Licence

The National Archives has developed this licence as a tool to enable Information Providers in the public sector to license the use and re-use of their Information under a common open licence. The National Archives invites public sector bodies owning their own copyright and database rights to permit the use of their Information under this licence.

The Keeper of the Public Records has authority to license Information subject to copyright and database right owned by the Crown. The extent of the offer to license this Information under the terms of this licence is set out in the UK Government Licensing Framework.

This is version 3.0 of the Open Government Licence. The National Archives may, from time to time, issue new versions of the Open Government Licence. If you are already using Information under a previous version of the Open Government Licence, the terms of that licence will continue to apply.

These terms are compatible with the Creative Commons Attribution License 4.0 and the Open Data Commons Attribution License, both of which license copyright and database rights. This means that when the Information is adapted and licensed under either of those licences, you automatically satisfy the conditions of the OGL when you comply with the other licence. The OGLv3.0 is Open Definition compliant.

Further context, best practice and guidance can be found in the UK Government Licensing Framework section on The National Archives website.

Go to the version 1 of the licence.
Go to the version 2 of the licence.
Go to the Welsh version of the licence.

8.3. Licence statement for Figure 1-2

SPRINGER NATURE LICENSE
TERMS AND CONDITIONS

Mar 09, 2020

This Agreement between Imperial College London -- Johanna Sophie Sagawe ("You") and Springer Nature ("Springer Nature") consists of your license details and the terms and conditions provided by Springer Nature and Copyright Clearance Center.

License Number	4784820885489
License date	Mar 09, 2020
Licensed Content Publisher	Springer Nature
Licensed Content Publication	Nature Reviews Microbiology
Licensed Content Title	Respiratory syncytial virus entry and how to block it
Licensed Content Author	Michael B. Battles et al
Licensed Content Date	Feb 5, 2019
Type of Use	Thesis/Dissertation
Requestor type	academic/university or research institute
Format	print and electronic
Portion	figures/tables/illustrations
Number of figures/tables/illustrations	1
High-res required	no

Will you be translating?	no
Circulation/distribution	1 - 29
Author of this Springer Nature content	no
Title	The interaction of the immune system with skeletal muscle during respiratory viral infection of the elderly
Institution name	Imperial College London
Expected presentation date	May 2020
Portions	Figure 1
Requestor Location	Imperial College London Respiratory Diseases Section, National H St Mary's Hospital, Norfolk Place London, W2 1NY United Kingdom Attn: Imperial College London
Total	0.00 GBP

Terms and Conditions

Springer Nature Customer Service Centre GmbH
Terms and Conditions

This agreement sets out the terms and conditions of the licence (the **Licence**) between you and **Springer Nature Customer Service Centre GmbH** (the **Licensor**). By clicking 'accept' and completing the transaction for the material (**Licensed Material**), you also confirm your acceptance of these terms and conditions.

1. Grant of License

1. 1. The Licensor grants you a personal, non-exclusive, non-transferable, world-wide licence to reproduce the Licensed Material for the purpose specified in your order only. Licences are granted for the specific use requested in the order and for no other use, subject to the conditions below.

1. 2. The Licensor warrants that it has, to the best of its knowledge, the rights to license reuse of the Licensed Material. However, you should ensure that the material you are requesting is original to the Licensor and does not carry the copyright of

another entity (as credited in the published version).

1. 3. If the credit line on any part of the material you have requested indicates that it was reprinted or adapted with permission from another source, then you should also seek permission from that source to reuse the material.

2. Scope of Licence

2. 1. You may only use the Licensed Content in the manner and to the extent permitted by these Ts&Cs and any applicable laws.

2. 2. A separate licence may be required for any additional use of the Licensed Material, e.g. where a licence has been purchased for print only use, separate permission must be obtained for electronic re-use. Similarly, a licence is only valid in the language selected and does not apply for editions in other languages unless additional translation rights have been granted separately in the licence. Any content owned by third parties are expressly excluded from the licence.

2. 3. Similarly, rights for additional components such as custom editions and derivatives require additional permission and may be subject to an additional fee. Please apply to Journalpermissions@springernature.com/bookpermissions@springernature.com for these rights.

2. 4. Where permission has been granted **free of charge** for material in print, permission may also be granted for any electronic version of that work, provided that the material is incidental to your work as a whole and that the electronic version is essentially equivalent to, or substitutes for, the print version.

2. 5. An alternative scope of licence may apply to signatories of the STM Permissions Guidelines, as amended from time to time.

3. Duration of Licence

3. 1. A licence for is valid from the date of purchase ('Licence Date') at the end of the relevant period in the below table:

Scope of Licence	Duration of Licence
Post on a website	12 months
Presentations	12 months
Books and journals	Lifetime of the edition in the language purchased

4. Acknowledgement

4. 1. The Licensor's permission must be acknowledged next to the Licenced Material in print. In electronic form, this acknowledgement must be visible at the same time as the figures/tables/illustrations or abstract, and must be hyperlinked to the journal/book's homepage. Our required acknowledgement format is in the Appendix below.

5. Restrictions on use

5. 1. Use of the Licensed Material may be permitted for incidental promotional use and minor editing privileges e.g. minor adaptations of single figures, changes of format, colour and/or style where the adaptation is credited as set out in Appendix 1 below. Any other changes including but not limited to, cropping, adapting, omitting material that affect the meaning, intention or moral rights of the author are strictly prohibited.

5. 2. You must not use any Licensed Material as part of any design or trademark.

5. 3. Licensed Material may be used in Open Access Publications (OAP) before publication by Springer Nature, but any Licensed Material must be removed from OAP sites prior to final publication.

6. Ownership of Rights

6. 1. Licensed Material remains the property of either Licensor or the relevant third party and any rights not explicitly granted herein are expressly reserved.

7. Warranty

IN NO EVENT SHALL LICENSOR BE LIABLE TO YOU OR ANY OTHER PARTY OR ANY OTHER PERSON OR FOR ANY SPECIAL, CONSEQUENTIAL, INCIDENTAL OR INDIRECT DAMAGES, HOWEVER CAUSED, ARISING OUT OF OR IN CONNECTION WITH THE DOWNLOADING, VIEWING OR USE OF THE MATERIALS REGARDLESS OF THE FORM OF ACTION, WHETHER FOR BREACH OF CONTRACT, BREACH OF WARRANTY, TORT, NEGLIGENCE, INFRINGEMENT OR OTHERWISE (INCLUDING, WITHOUT LIMITATION, DAMAGES BASED ON LOSS OF PROFITS, DATA, FILES, USE, BUSINESS OPPORTUNITY OR CLAIMS OF THIRD PARTIES), AND
WHETHER OR NOT THE PARTY HAS BEEN ADVISED OF THE POSSIBILITY OF SUCH DAMAGES. THIS LIMITATION SHALL APPLY NOTWITHSTANDING ANY FAILURE OF ESSENTIAL PURPOSE OF ANY LIMITED REMEDY PROVIDED HEREIN.

8. Limitations

8. 1. ***BOOKS ONLY:*** Where **'reuse in a dissertation/thesis'** has been selected the following terms apply: Print rights of the final author's accepted manuscript (for clarity, NOT the published version) for up to 100 copies, electronic rights for use only on a personal website or institutional repository as defined by the Sherpa guideline (www.sherpa.ac.uk/romeo/).

9. Termination and Cancellation

9. 1. Licences will expire after the period shown in Clause 3 (above).

9. 2. Licensee reserves the right to terminate the Licence in the event that payment is not received in full or if there has been a breach of this agreement by you.

Appendix 1 — Acknowledgements:

For Journal Content:
Reprinted by permission from [**the Licensor**]: [**Journal Publisher** (e.g. Nature/Springer/Palgrave)] [**JOURNAL NAME**] [**REFERENCE CITATION** (Article name, Author(s) Name), [**COPYRIGHT**] (year of publication)

For **Advance Online Publication papers:**
Reprinted by permission from [**the Licensor**]: [**Journal Publisher** (e.g. Nature/Springer/Palgrave)] [**JOURNAL NAME**] [**REFERENCE CITATION** (Article name, Author(s) Name), [**COPYRIGHT**] (year of publication), advance online publication, day month year (doi: 10.1038/sj.[JOURNAL ACRONYM].)

For Adaptations/Translations:
Adapted/Translated by permission from [**the Licensor**]: [**Journal Publisher** (e.g. Nature/Springer/Palgrave)] [**JOURNAL NAME**] [**REFERENCE CITATION** (Article name, Author(s) Name), [**COPYRIGHT**] (year of publication)

Note: For any republication from the British Journal of Cancer, the following credit line style applies:

Reprinted/adapted/translated by permission from [**the Licensor**]: on behalf of Cancer Research UK: : [**Journal Publisher** (e.g. Nature/Springer/Palgrave)] [**JOURNAL NAME**] [**REFERENCE CITATION** (Article name, Author(s) Name), [**COPYRIGHT**] (year of publication)

For **Advance Online Publication** papers:
Reprinted by permission from The [**the Licensor**]: on behalf of Cancer Research UK: [**Journal Publisher** (e.g. Nature/Springer/Palgrave)] [**JOURNAL NAME**] [**REFERENCE CITATION** (Article name, Author(s) Name), [**COPYRIGHT**] (year of publication), advance online publication, day month year (doi: 10.1038/sj.[JOURNAL ACRONYM])

For Book content:
Reprinted/adapted by permission from [**the Licensor**]: [**Book Publisher** (e.g. Palgrave Macmillan, Springer etc) [**Book Title**] by [**Book author**(s)] [**COPYRIGHT**] (year of publication)

Other Conditions:

Version 1.2

Questions? customercare@copyright.com or +1-855-239-3415 (toll free in the US) or +1-978-646-2777.

8.4. Permission for Figure 1-4

Wednesday, May 13, 2020 at 5:13:27 PM British Summer Time

Subject: RE: Figure adaptation in PhD thesis
Date: Wednesday, 13 May 2020 at 17:02:37 British Summer Time
From: ATS Permission Requests
To: Sagawe, Sophie

Dear Sophie,

You are very welcome! Best of luck with your thesis.

Best regards,

Megan

Megan Murphy
Production Coordinator
American Thoracic Society
25 Broadway, 4th Floor
New York, NY 10004
212-315-8643
mmurphy@thoracic.org

From: Sagawe, Sophie <johanna.sagawe11@imperial.ac.uk>
Sent: Wednesday, May 13, 2020 12:00 PM
To: ATS Permission Requests <permissions@thoracic.org>
Subject: Re: Figure adaptation in PhD thesis

Dear Megan,

Thank you so much! That was quicker than I anticipated.

Best regards
Sophie

From: ATS Permission Requests <permissions@thoracic.org>
Date: Wednesday, 13 May 2020 at 16:56
To: "Sagawe, Sophie" <johanna.sagawe11@imperial.ac.uk>
Subject: RE: Figure adaptation in PhD thesis

Dear Sophie,

Thank you so much for your patience. I have heard from the original authors of the article, who have approved your intended use of the figure and informed us that we can proceed.
Permission is granted at no charge. Please complete the below and use it beneath the material. Thank you.

Adapted with permission of the American Thoracic Society.

Best regards,

Megan

Megan Murphy
Production Coordinator
American Thoracic Society
25 Broadway, 4th Floor
New York, NY 10004
212-315-8643
mmurphy@thoracic.org

From: Sagawe, Sophie <johanna.sagawe11@imperial.ac.uk>
Sent: Friday, May 8, 2020 2:52 PM
To: ATS Permission Requests <permissions@thoracic.org>
Subject: Re: Figure adaptation in PhD thesis

Dear Megan,
Yes please!
Thank you
Sophie

From: ATS Permission Requests <permissions@thoracic.org>
Sent: 08 May 2020 19:11
To: Sagawe, Sophie <johanna.sagawe11@imperial.ac.uk>
Subject: RE: Figure adaptation in PhD thesis

Dear Sophie,

Thank you very much for sending! Because you are requesting to adapt the figure, I must reach out to the

authors of the original article for approval before we can move forward with this request. This may take some time. Would you like to proceed?

Best regards,

Megan

Megan Murphy
Production Coordinator
American Thoracic Society
25 Broadway, 4th Floor
New York, NY 10004
212-315-8643
mmurphy@thoracic.org

Please donate to the ATS to make COVID-19 resources accessible and support respiratory health professionals worldwide. Wishing you, your community, and all health care professionals safety during this difficult time.

From: Sagawe, Sophie <johanna.sagawe11@imperial.ac.uk>
Sent: Friday, May 8, 2020 12:01 PM
To: ATS Permission Requests <permissions@thoracic.org>
Subject: Re: Figure adaptation in PhD thesis

Dear Megan,

Thank you for your quick reply. I have attached my figure and the original version.

Best regards
Sophie

From: ATS Permission Requests <permissions@thoracic.org>
Date: Friday, 8 May 2020 at 16:55
To: "Sagawe, Sophie" <johanna.sagawe11@imperial.ac.uk>
Subject: RE: Figure adaptation in PhD thesis

Dear Sophie,

Thank you for your request, and your interest in ATS. Can you kindly send your adaption of the figure for our review?

Best regards,

Megan

Megan Murphy
Production Coordinator
American Thoracic Society
25 Broadway, 4th Floor
New York, NY 10004
212-315-8643
mmurphy@thoracic.org

Please donate to the ATS to make COVID-19 resources accessible and support respiratory health professionals worldwide. Wishing you, your community, and all health care professionals safety during this difficult time.

From: Sagawe, Sophie <johanna.sagawe11@imperial.ac.uk>
Sent: Friday, May 8, 2020 11:40 AM
To: ATS Permission Requests <permissions@thoracic.org>
Subject: Figure adaptation in PhD thesis

Dear Mrs Gern,

I would like to include an adapted version of Figure 1 from the following publication in my PhD thesis:

Deterioration of Limb Muscle Function during Acute Exacerbation of Chronic Obstructive Pulmonary Disease
By Raolat M. Abdulai, Tina Jellesmark Jensen, Naimish R. Patel, Michael I. Polkey, Paul Jansson, Bartolomé R. Celli, and Stephen I. Rennard
Page 433–449 in volume 197 issue 4 of AJRCCM (15 February 2018). doi: 10.1164/rccm.201703-0615CI

The figure will not be reprinted in its published form. Instead I have adapted it to omit some parts of the pathway and added more details in other parts. This figure will be part of the introduction to my PhD thesis to illustrate mechanisms of muscle growth and atrophy.

Kind regards
Sophie Sagawe